

# Degradable Poly(ethylene glycol) Nanocarriers for Encapsulation of Therapeutic Proteins, Directed Transport and Controlled Release

Dissertation zur Erlangung des Grades

“Doktor der Naturwissenschaften” im Promotionsfach Chemie

am Fachbereich Chemie, Pharmazie und Geowissenschaften  
der Johannes Gutenberg-Universität Mainz

Hannah Sarah Pohlit (geb. Köhring)

geboren in Frankfurt am Main

Mainz 2016

JOHANNES GUTENBERG  
UNIVERSITÄT MAINZ



UNIVERSITÄTSmedizin.  
MAINZ



Max Planck Graduate Center  
mit der Johannes Gutenberg-Universität Mainz



Dekan:

1. Berichterstatter:
2. Berichterstatter:

Tag der mündlichen Prüfung: 14. November 2016

Die als Dissertation vorgelegte Arbeit wurde in der Zeit von Oktober 2012 bis September 2016 am Institut für Organische Chemie der Johannes Gutenberg-Universität Mainz im Arbeitskreis von Herrn Univ.-Prof. Dr. Holger Frey sowie an der Hautklinik der Universitätsmedizin der Johannes Gutenberg-Universität Mainz im Arbeitskreis von Herrn Prof. Dr. Joachim Saloga angefertigt.



Für meine Familie

*„Nur wenige wissen, wie viel man wissen muss, um zu wissen, wie wenig man weiß.“*

Werner Heisenberg

## Danksagung (Acknowledgements)

In den letzten fast 4 Jahren habe ich während meiner Doktorarbeit eine sehr spannende, abwechslungsreiche, von Neugier erfüllte, ereignisreiche und manchmal auch anstrengende Zeit erlebt. Ohne die Unterstützung vieler verschiedener Menschen hätte ich diese Arbeit niemals so erfolgreich abschließen können! Deshalb möchte ich die Gelegenheit ergreifen und an dieser Stelle „Danke“ sagen.







## Table of Contents

Danksagung (Acknowledgements).....	6
Table of Contents .....	9
Abstract .....	11
Zusammenfassung .....	13
Graphical Abstract.....	17
Motivation and Objectives.....	20
Chapter 1. Introduction.....	23
1.1 Could allergen-specific immunotherapy benefit from the use of nanocarriers? .....	24
1.2 Nanoparticles for Allergen-specific Immunotherapy.....	30
1.3 Polyethers Bearing Cleavable Moieties.....	87
Chapter 2. Biodegradable pH-Sensitive Poly(ethylene glycol) Nanocarriers for Allergen Encapsulation and Controlled Release.....	93
Chapter 3. PEG Dimethacrylates with Cleavable Ketal Sites: A Precursor for Cleavable Hydrogels .....	120
Chapter 4. A Magic Effect of Silver Oxide on the Monotosylation of PEG? A Facile and General Route to Heterobifunctional PEG via Polymer Desymmetrization .....	152
Chapter 5. Transformation of vaterite nanoparticles to hydroxycarbonate apatite in a hydrogel scaffold: Relevance to bone formation.....	203
Appendix .....	231
A1. Polyethylenglykol-(PEG)-Nanopartikel zur Verkapselung und pH-abhängigen intrazellulären Freisetzung von Allergenen.....	233
A2. Polymerization of Ethylene Oxide, Propylene Oxide, and Other Alkylene Oxides: Synthesis, Novel Polymer Architectures, and Bioconjugation .....	241
Resume (CV).....	317
Declaration .....	321



## Abstract

This thesis aims at the synthesis of acid-labile poly(ethylene glycol) (PEG) building blocks suitable for nanogel formation by radical polymerization, as well as the synthesis of heterobifunctional PEGs for the functionalization of nanocarrier systems to obtain polymer networks for transportation and controlled release of therapeutic proteins. The thesis was motivated both by principal synthetic challenges and the potential future application of the nanocarriers in allergen-specific immunotherapy. A special feature of this thesis is the interdisciplinary approach through the fact that it was carried out in two laboratories; hence polymer synthesis, nanocarrier preparation and cellular tests are performed by the same person.

**Chapter 1** serves as an introduction to this thesis. In **chapter 1.1**, the benefit of using polymer-nanocarriers for protection, transport and release of allergens as therapeutic proteins is discussed in an editorial article. The underlying mechanism of allergen-specific immunotherapy (AIT) in general as well as nanoparticle supported AIT are explained. Different biodegradable and non-biodegradable polymers, synthetic or nature-derived nanostructures and inorganic nanoparticles that were investigated for AIT are summarized in a comprehensive review in **chapter 1.2** that gives the state of the art in this field. **Chapter 1.3** focuses on the synthesis of poly(ethylene glycol)s with cleavable moieties in the polymer backbone, as they represent interesting candidates for reversible bioconjugation or as stimuli-responsive, degradable building blocks for e.g. nanocarriers.

The synthesis and characterization of an acid-labile PEG-acetal-dimethacrylate building block is presented in **chapter 2**. A quantitative acid-catalyzed addition reaction of the hydroxyl function of PEG to a vinyl ether methacrylate yields an acetal-containing macromonomer that degrades under mildly acidic conditions (hydrolysis half-life time at pH 5 is 48 hours). The protein cargo and the PEG macromonomer are encapsulated inside of the liposomes prepared by dual centrifugation. The loaded liposomes function as templates for UV-induced crosslinking. *In vitro* studies investigate cellular uptake, cytotoxicity and the absence of cell maturation. The shielding of the protein cargo from detection by antibodies and immune cells as well as the release of the therapeutic proteins inside of the cell and its capability to induce T cell responses are demonstrated in proof of principle experiments.

**Chapter 3** expands the scope of available building blocks for nanocarrier formation by presenting a synthetic concept for PEG with acid-labile ketal units in the polymer backbone. A ketal-initiator

is used for anionic ring-opening polymerization of ethylene oxide. Methacrylate units are attached by a post-polymerization reaction with *Candida Antarctica* lipase B to enable three-dimensional crosslinking *via* radical polymerization. The degradation kinetics is analyzed by *in-situ*  $^1\text{H}$  NMR studies, revealing faster degradation of PEG-ketal-dimethacrylates compared to PEG-ketal-diols. The novel PEG-ketal-dimethacrylate macromonomer is used to synthesize hydrogels composed of non-degradable PEG-dimethacrylate and PEG-ketal-dimethacrylate. The degradation kinetics of the hydrogels was studied at pH 5 and 7.4. Since nanogels feature a much higher surface to volume ratio compared to macroscopic hydrogels, they are likely to disintegrate ever faster. Thus, the use of PEG-ketal-dimethacrylates in protein loaded nanoparticles seems promising.

In **Chapter 4**, a simple, but effective method for polymer desymmetrization of PEG to heterobifunctional PEGs is presented. Low-cost symmetric PEG was transformed into monotosylated PEG with yields exceeding the expected ratios from statistical considerations upon addition of silver(I)-oxide as a heterogeneous catalyst. The reaction products of the catalyzed transformation and the non-catalyzed reaction were compared by using an analytical HPLC method that makes use of evaporative light scattering detection. Since the peaks of the different reaction products are base-line separated, the HPLC method is easily transferable to the semi-preparative scale to obtain pure heterobifunctional PEG in a one-step reaction following HPLC purification of 200 mg of crude product per injection. In the context of this thesis, the purified heterobifunctional PEG-synthons can be transformed into valuable components for the functionalization of nanocarriers.  $\alpha$ -4-( $\alpha$ -D-mannopyranosyloxymethylene)-1,2,3,4-tetrahydro-1H-benzotriazol-1-yl- $\omega$ -methacryloyl-PEG is exemplarily synthesized from symmetrical PEG-diol as one possible functionalization option to target CD11c-positive cells.

As one example for the wide range of possible applications of the molecular building block PEG-acetal-dimethacrylate, the preparation of vaterite nanoparticle-containing PEG-hydrogels is described in **Chapter 5**, which is the result of a close collaboration with Romina Schröder (Tremel group, Inorganic Chemistry, University of Mainz). These biodegradable PEG hydrogels serve as mineral storage that might be applied as bone biomaterial during bone regeneration. Vaterite nanoparticles incorporated into the polymer network show an accelerated transformation to hydroxycarbonate apatite when incubated in simulated body fluid at 37 °C compared to free vaterite nanoparticles.

## Zusammenfassung

Ziel dieser Arbeit war die Synthese von säurelabilen oligomeren Polyethylenglykol (PEG)-Bausteinen für die Herstellung von Nano-Hydrogelen durch radikalische Polymerisation, sowie die Synthese von heterobifunktionellen PEGs zur Funktionalisierung von Nanocarrier-Systemen, die polare und biokompatible Polymer-Netzwerke für den Transport und die gezielte Freisetzung von therapeutischen Proteinen enthalten. Die Untersuchungen sind sowohl durch die grundlegenden synthetischen Herausforderungen, als auch durch die mögliche zukünftige Anwendung der Nanocarrier-Systeme in der allergen-spezifischen Immuntherapie motiviert. Ein besonderes Merkmal dieser Doktorarbeit ist der interdisziplinäre Ansatz: Die Polymersynthese, die Nanocarrier-Herstellung und die Zelltests wurden in zwar in verschiedenen Laboren durchgeführt, jedoch von einer Person ausgeführt.

**Kapitel 1** stellt eine Einleitung zur allergen-spezifischen Immuntherapie (AIT) dar. Es wird auf die Anwendung von Nanocarrier-Systemen in der AIT und die bereits bekannten spaltbaren Gruppen in PEGs eingegangen. In **Unterkapitel 1.1** werden die Vorteile der Verwendung von Nanocarrier-Systemen zum Transport, zum Schutz vor vorzeitigem Abbau und zur gezielten Freisetzung von Allergenen beschrieben. Der zugrundeliegende Mechanismus der AIT mit freien Allergenen im Vergleich zur AIT mit Nanocarrier-Systemen wird erläutert. Einen vollständigen Überblick über den Stand der Technik im Gebiet der verschiedenen bioabbaubaren und nicht-bioabbaubaren Nanostrukturen (synthetischer oder natürlicher Abstammung), die für die Anwendung in der AIT untersucht wurden, gibt **Unterkapitel 1.2**. Eine Übersicht über die bekannten spaltbaren Gruppen in PEGs, welche als Sollbruchstellen im Polymer-Rückgrat eingebaut werden, gibt **Unterkapitel 1.3**. Die spaltbaren PEGs stellen vielversprechende Kandidaten für die reversible Biokonjugation oder für stimuli-responsive, abbaubare molekulare Bausteine für die Nanocarrier-Systeme dar.

Die Synthese und Charakterisierung des säurelabilen PEG-acetal-dimethacrylat Bausteins ist Gegenstand von **Kapitel 2**. Die quantitative säurekatalysierte Additionsreaktion der Hydroxylgruppe des PEG mit einem Vinylether-Methacrylat ergibt einen Acetal-haltigen Baustein der unter mild sauren Bedingungen hydrolysiert wird (die Halbwertszeit der Hydrolyse bei pH 5 beträgt 48 Stunden). Die zu transportierenden Proteine und der spaltbare PEG-Baustein werden in Liposomen, die als Template für die UV-induzierte Vernetzung der Bausteine dienen, eingeschlossen. Die Liposomen werden mittels dualer Zentrifugation hergestellt. Zellstudien zur Aufnahme der Nanocarrier-Systeme, zur Toxizität und zur Untersuchung der ausbleibenden

Zellreifung wurden durchgeführt. Um die Wirksamkeit der Verkapselung zu untersuchen, wurde die Abschirmung der Proteine vor Erkennung durch Antikörper und Zellen des Immunsystems, ebenso wie die Freisetzung des therapeutischen Proteins innerhalb der Zelle und dessen Fähigkeit, T-Zellantworten zu induzieren, nachgewiesen.

In **Kapitel 3** wird das Synthesekonzept für einen neuartigen säurelabilen Baustein vorgestellt, welcher Ketalgruppen im Polymerrückgrat enthält und somit die zur Verfügung stehenden molekularen Bausteine für die Nanocarrier-Herstellung erweitert. Ein Ketal-Initiator wird in der anionischen Ringöffnungspolymerisation von Ethylenoxid eingesetzt. Methacrylat-Einheiten werden in einer Post-Polymerisationsmodifikation mit dem Enzym *Candida antarctica* lipase B eingefügt um die dreidimensionale Vernetzung durch radikalische Polymerisation zu ermöglichen. Die Abbaukinetik wurde mittels *in-situ*  $^1\text{H}$ -NMR Spektroskopie-Studien untersucht, und offenbarte eine schnellere Spaltung der PEG-ketal-Dimethacrylate (DMA) im Vergleich mit der Vorstufe PEG-ketal-diol. Der neuartige Baustein wurde in verschiedenen Mischungsverhältnissen mit nicht-spaltbarem PEG-DMA für die Synthese makroskopischer Hydrogel-Proben eingesetzt. Der Zerfall der Hydrogele bei pH 5 und pH 7 wurde untersucht. Da Nano-Hydrogele im Vergleich zu makroskopischen Hydrogelen ein höheres Oberflächen-zu-Volumen-Verhältnis aufweisen und somit noch schneller gespalten werden sollten, ist die Verwendung von PEG-ketal-DMA in Protein-beladenen Nano-Hydrogelen sehr vielversprechend.

Der Schwerpunkt von **Kapitel 4** ist die Entwicklung einer einfachen, aber dennoch effektiven Methode zur Polymer Desymmetrisierung von PEG-Diolen zu heterobifunktionellen PEGs. Kostengünstiges, konventionelles PEG kann durch Zugabe von Silberoxid als heterogenem Katalysator mit Ausbeuten, welche die erwarteten statistischen Werte übertreffen, in monotosyliertes PEG transformiert werden. Die Reaktionsprodukte der katalysierten und der unkatalysierten Umsetzung werden durch die Verwendung einer analytischen HPLC-Methode mit integriertem Verdampfungs-Lichtstredetektor verglichen. Da die Signale der verschiedenen Reaktionsprodukte basisliniengetrennt sind, kann die HPLC-Methode leicht auf einen semi-präparativen Maßstab übertragen werden. Reines heterobifunktionelles PEG kann durch eine einstufige Synthese mit anschließender HPLC Aufreinigung mit 200 mg Rohprodukt pro Injektion erhalten werden. Monotosyliertes PEG kann als Ausgangsverbindung für die Synthese weiterer wertvoller heterobifunktioneller PEGs und für die Funktionalisierung der Nanocarrier-Systeme genutzt werden. Die Synthese von  $\alpha$ -4-( $\alpha$ -D-mannopyranosyloxymethylene)-1,2,3, triazol-1-yl- $\omega$ -

methacryloyl-PEG aus symmetrischem PEG-diol als Beispiel für eine mögliche Funktionalisierungsoption zur gezielten Wirkstoffabgabe in CD11c-positive Zellen wird gezeigt.

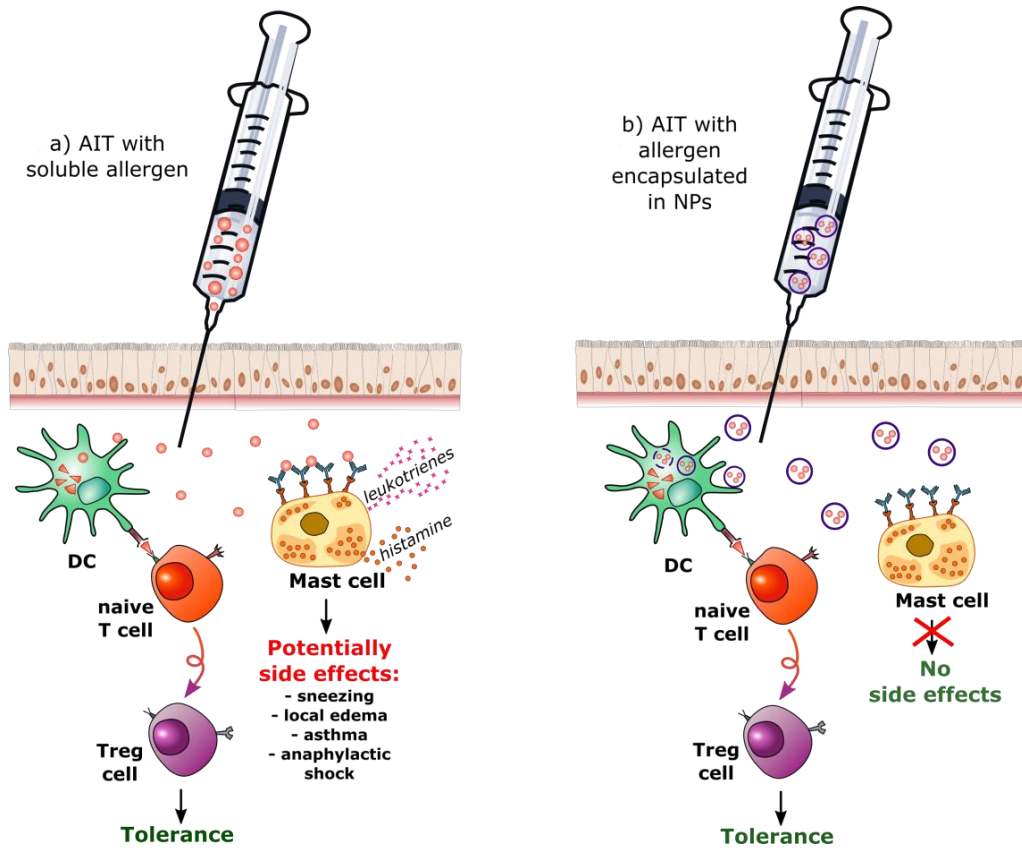
Als ein Beispiel für die große Vielfalt an möglichen Einsatzgebieten des PEG-acetal-DMA Bausteins wird die Synthese von mit Vaterit-Nanopartikeln beladenen PEG-Hydrogelen in **Kapitel 5** beschrieben. Dieses Kapitel ist in enger Kooperation mit Romina Schröder aus dem Arbeitskreis Prof. Tremel am Institut für Anorganische Chemie der Universität Mainz entstanden. Diese abbaubaren PEG-Hydrogele fungieren als Mineralspeicher für die Anwendung als Knochenersatzmaterial während der Knochenregeneration. Der Einschluss von Vaterit-Nanopartikeln in das Polymer-Netzwerk führt im Vergleich zu freien Vaterit-Nanopartikeln zu einer beschleunigten Transformation in carbonathaltigen Hydroxylapatit bei Inkubation in simulierter Körperflüssigkeit bei 37 °C.



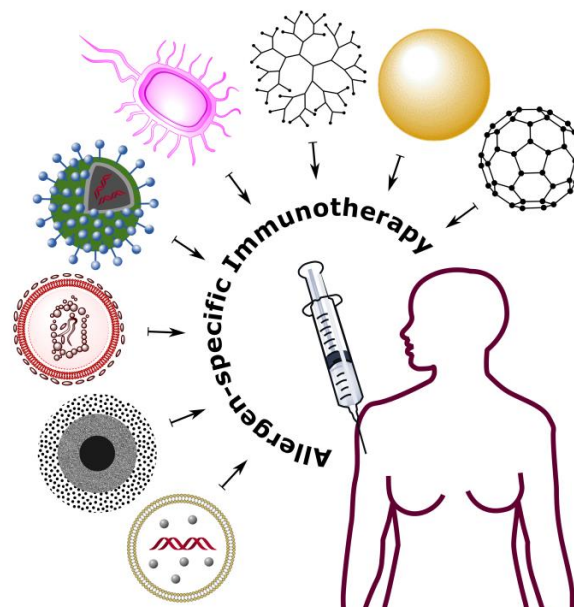


## Graphical Abstract

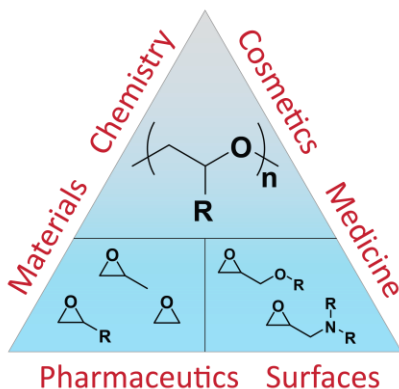
### 1.1 Could allergen-specific immunotherapy benefit from the use of nanocarriers?



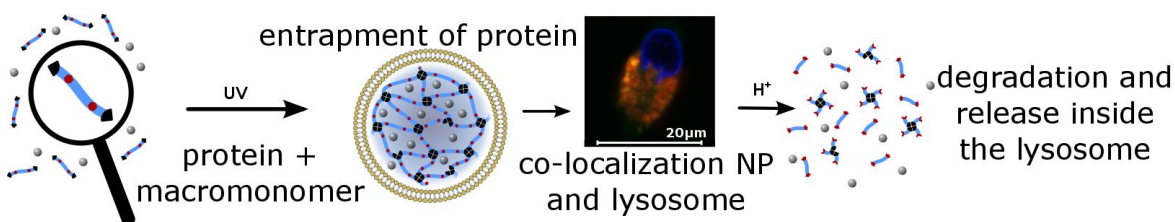
### 1.2 Nanoparticles for Allergen-specific Immunotherapy



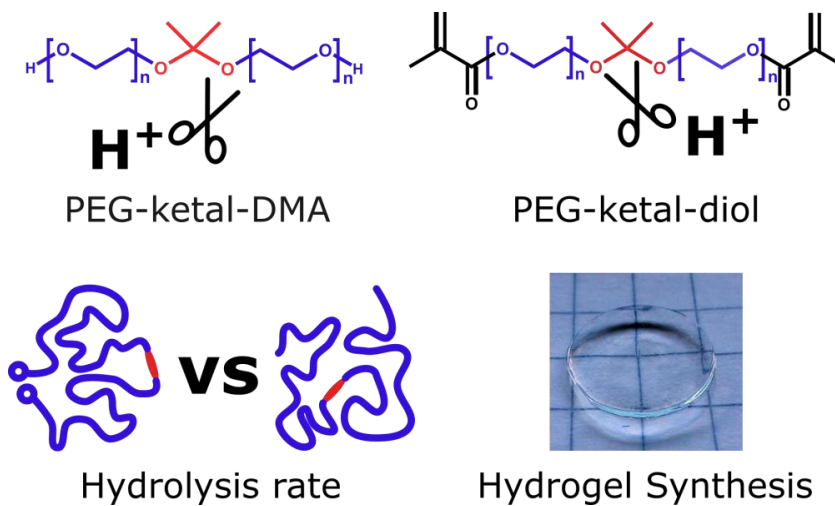
1.3 Polymerization of Ethylene Oxide, Propylene Oxide, and Other Alkylene Oxides: Synthesis, Novel Polymer Architectures, and Bioconjugation – Chapter 6.2 Cleavable Polyethers



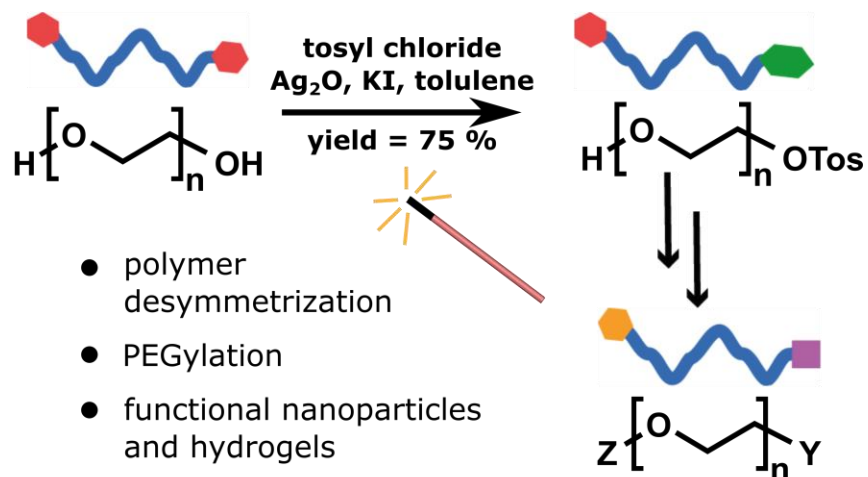
2. Biodegradable pH-Sensitive Poly(ethylene glycol) Nanocarriers for Allergen Encapsulation and Controlled Release



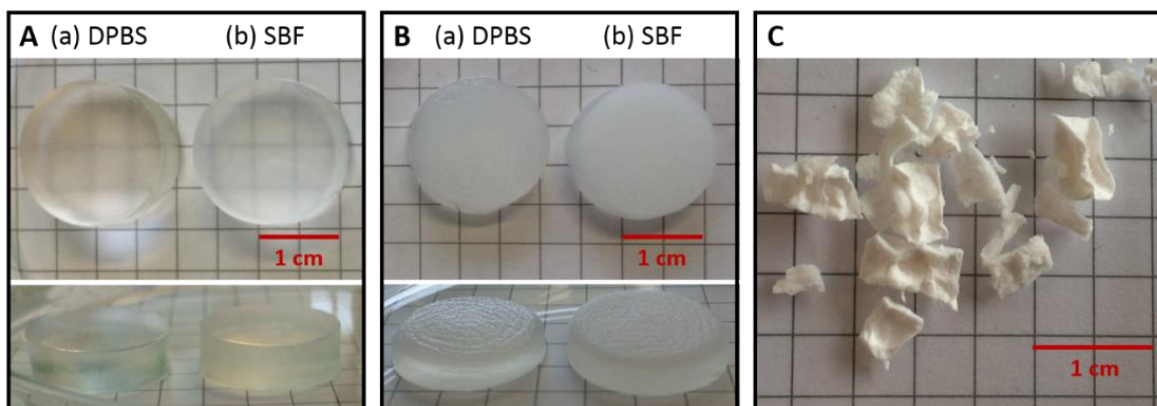
3. PEG Dimethacrylates with Cleavable Ketal Sites: A Precursor for Cleavable Hydrogels



4. A Magic Effect of Silver Oxide on the Monotosylation of PEG? A Facile and General Route to Heterobifunctional PEG via Polymer Desymmetrization



5. Transformation of vaterite nanoparticles to hydroxycarbonate apatite in a hydrogel scaffold: relevance to bone formation



## Motivation and Objectives

During the last decades, the number of patients suffering from allergic diseases has increased alarmingly. In 2008, there were about 8 million allergic patients worldwide. While avoidance of the allergen is the easiest and most successful strategy to circumvent suffering from allergies, it is merely impossible for numerous allergens in daily life. The only available disease-modifying treatment against allergies is allergen-specific immunotherapy (AIT), where an allergen is administered in increasing doses to induce immunological tolerance. Among the disadvantages of this therapy are long duration (3-5 years) and the risk of severe side effects. Currently, the application of high allergen doses during AIT is restricted because of adverse reactions like allergic symptoms or even anaphylactic shock. Several attempts have been made to reduce side effects, e.g. by chemical modification of the allergen to destroy the B cell epitopes under simultaneous preservation of the required T cell epitopes, to obtain so called “allergoids”. An alternative approach is the encapsulation of allergens in polymer nanoparticles. Polymer nanoparticles most likely possess great potential in the treatment of allergic diseases like hay-fever or asthma (among others). Through encapsulation of allergens (proteins and peptides) their delivery to antigen presenting cells, especially dendritic cells, might be realized without activation of other immune cells and recognition by antibodies, therefore avoiding severe side effects. Currently known carrier-structures, however, suffer from several disadvantages, such as poor water solubility and the intrinsic capability to mature and activate cells, or from the fact that they are not practicable because of long degradation times and slow release of the cargo.

In this work, we designed polymeric nanoparticles solely composed of poly(ethylene glycol) (PEG), a widely used polymer, which is FDA-approved in numerous formulations and has undergone broad clinical studies as well as several decades of application. A significant difference in pH/redox potential between the endolysosome and other cell compartments (i.e. the cytosol) and the extracellular fluid can be exploited for novel stimuli-responsive materials. Chemical design of the oligomer building blocks for the nanoparticles, so called “macromonomers” and subsequent crosslinking lead to PEG-nanoparticles that degrade at a predefined pH-value specifically inside the endolysosome of a cell. This degradation triggered by a certain stimulus is a major improvement over carrier systems that degrade through unspecific hydrolysis.

The specific objectives of this thesis are described in the following.

- i) The design of a carrier system for proteins is envisaged that encapsulates high amounts of protein, is stable in aqueous solutions under neutral conditions, but specifically degrades and releases its protein cargo upon acidification. The main topic of the first part of this thesis is the synthesis of an acid-labile macromonomer suitable for three-dimensional crosslinking in aqueous solution and subsequently the development of a synthetic route for nanogels from this macromonomer. Key-requirements for the created carrier system primarily imply water solubility, non-toxicity and prevention of cell maturation or activation.
- ii) The incorporation of acetal units into the poly(ethylene glycol) backbone resulted in degradation at pH 5 within several days. As nanocarriers with a burst release behavior upon acidification are desired for the application as an allergen delivery tool in allergen-specific immunotherapy, the acetal units were replaced with ketal units which are known for their higher acid-lability. The combination of a new ketal-containing initiator with epoxide chemistry aims at enlargement of the macromonomer toolbox for nanogel synthesis.
- iii) A targeted delivery in addition to the controlled release of the allergen into antigen-presenting cells is a key step in modulating the immune responses against harmless allergens towards tolerance or anergy. Furthermore, attachment of fluorescent dyes to track the fate of nanoparticles *in vitro* and *in vivo* is highly desirable. For both intended purposes, heterobifunctional poly(ethylene glycols) are essential bearing one end group that enables covalent incorporation into the polymer network of the nanogel and a second end group that allows for the attachment of a targeting moiety or a fluorescent dye. To obtain heterobifunctional PEGs from symmetric PEG-diol precursors, a maximum yield of the monofunctional polymer product in a “polymer desymmetrization” step is crucial. The purity of the monofunctional PEG-precursor is important to permit complete incorporation of the expensive, biologically active targeting molecule or the fluorescent dye into the nanoparticle network.
- iv) Motivated by the need for synthetic bone and tissue substitutes to promote bone healing *in vivo*, particular interest has been pronounced in the use of macromonomers from nanogel synthesis for the preparation of hydrogels. A new bone grafting material is developed by incorporating vaterite nanoparticles into hydrogel networks, in order to introduce flexibility and degradability, while retaining the nanoparticles’ bioactivity

and osteoconductivity. This work was carried out in close collaboration with Romina Schröder from the group of W. Tremel at the Institute of Inorganic Chemistry.

- v) An immediate evaluation of the designed carrier systems using blood cells of allergic human blood donors was one of the main goals of this work. The nanocarrier systems were tested with regard to cytotoxicity, endotoxin content, cell maturation, uptake into dendritic cells, release of the cargo protein inside of dendritic cells, and shielding of the cargo proteins by the nanocarriers from detection by immune cells. Depending on the results of the cellular tests, the reagents of the nanocarrier synthesis as well as the synthetic procedure for the nanocarrier formation could be adapted straight away, which is a clear advantage of the interdisciplinary research project handled by the same person. With detailed *in vitro* testings, problems for biological applications occurring during the nanocarrier synthesis could be eliminated prior to envisaged *in vivo* tests and the eventual clinical trials for application in humans.

## Chapter 1. Introduction

## 1.1 Could allergen-specific immunotherapy benefit from the use of nanocarriers?

Hannah Pohlit<sup>1,2,3</sup>, Holger Frey<sup>2</sup>, and Joachim Saloga<sup>1</sup>

<sup>1</sup>Department of Dermatology, University Medical Center Mainz, Langenbeckstr. 1, 55131 Mainz, Germany

<sup>2</sup>Institute of Organic Chemistry, Johannes Gutenberg University Mainz, Duesbergweg 10-14, 55128 Mainz, Germany

<sup>3</sup>Graduate School Materials Science in Mainz, Staudinger Weg 9, 55128 Mainz, Germany

Published in: *Nanomedicine*, **2016**, 11, 1329-1331. Reprinted with permission from Future medicine LTD.

**Keywords:** AIT (allergen- immunotherapy), nanoparticles, drug delivery, nanomedicine, antigen delivery

“Chemists, pharmacists and clinicians should work hand in hand to adapt the existing concepts of protein delivery into dendritic cells for the potential application in AIT.”

### Allergen-specific immunotherapy – Challenges

The total number of people suffering from allergic diseases increased dramatically during the last decades. Allergic reactions of the immediate type (type I hypersensitivity reactions according to classification by Coombs and Gell) involve an overreaction of the immune system and the formation of IgE antibodies, which act against environmental substances that are essentially harmless to the body. IgE binds to mast cells and basophilic leucocytes that release pro-inflammatory mediators upon contact (cross-presentation) with allergen responsible for symptoms like asthma, hay fever, or anaphylactic shock. So far, allergen-specific immunotherapy (AIT) treats the allergy by repeated subcutaneous injections or sublingual application of increasing doses of allergen which leads to the development of tolerance toward the specific allergen. The efficacy of AIT has been proven in a great number of clinical trials, but possible dangerous side effects and long-term treatment with insufficient adherence to therapy remain obstacles. On a cellular level, immunotherapy leads to a shift from a Th2 and Th17 towards a Th1 response and the induction of regulatory T cells.<sup>[1]</sup> This is characterized by reduced production of IgE, IL-4 and



IL-13 and an enhanced production of IFN  $\gamma$  and IgG subtypes, which act as blocking antibodies and capture the allergen before activating effector cells. The exact mechanisms of specific immunotherapy have been reviewed in detail.<sup>[2]</sup>

### **How can nanoparticles aid?**

Nanoparticles (NPs) can either serve as adjuvants<sup>[3]</sup> or as carrier systems for the allergen or DNA molecules,<sup>[4]</sup> or both.<sup>[5]</sup> The nanoparticles can encapsulate and thereby protect sensitive cargo from degradation by enzymes or changes in pH, enable high-density loading of cargo, and can deliver antigens and, if desired, co-deliver adjuvants to the desired location in the body. On the other hand, antigen shielding by nanoparticles can avoid detection of the cargo by IgE-antibodies on the surface of basophilic leucocytes or mast cells, and thereby prevent undesired side effects during AIT. Through “hiding” the allergen from detection by the immune system, undesired and sometimes severe side effects may be prevented. It is even conceivable that AIT may be facilitated where it is not yet routinely available (e.g. for food allergies like peanut allergy).<sup>[6]</sup> For oral immunotherapy, the design of nanoparticles resistant to acidic conditions in the stomach is feasible, which are capable of crossing the mucosa and epithelial barrier to deliver their cargo to dendritic cells in the intestine.<sup>[7]</sup> Furthermore, NPs can enhance uptake of allergen into dendritic cells and thereby may allow therapy with lower doses of allergen compared to conventional AIT. The AIT with allergen entrapped in nanoparticles could result in a more convenient therapy for the patient due to fewer injections and may thereby effect a decrease in the timeframe required for effective AIT and reduce harmful secondary effects, which may in turn result in higher patient compliance.

### **Which kinds of delivery systems do we know?**

Many concepts are known, have been tested and further developed for transportation of proteins and DNA molecules in preventive vaccination against infectious diseases or cancer.<sup>[8,9]</sup> Surprisingly, only a couple of dozen articles have been published on the utilization of nanoparticles in a therapeutic approach on established allergic diseases. These nanoparticles include allergen-loaded, allergen-coated, and empty NPs. Allergen-loaded NPs offer the advantages described in the section above. Nanoparticles coated with allergens facilitate cross-linking and activation of immunoglobulins on cell-surfaces and are more often used for preventive vaccination strategies. Nanoparticles that do not contain specific allergens utilize the materials capability of inducing Th1-

driven immune responses and thereby establish a balance between allergy-related Th2- and Th2-antagonizing Th1-responses.<sup>[10–12]</sup> Although this approach does not belong to immunotherapy treatment, the results are promising. However, extensive studies investigating mechanisms and effects on systemic Th1 activation are required.

Materials investigated for the delivery of allergens to date are based on biodegradable and/or biocompatible synthetic polymers like polyanhydride, poly(D,L-lactide-co-glycolide) (PLG) and poly(D,L-lactide-co-glycolic acid) (PLGA), poly(ethylene glycol)-dimethacrylate (PEG-acetal-DMA), poly(methyl vinyl ether-co-maleic anhydride) (Gantrez-NPs), poly- $\epsilon$ -caprolactone (PCL), polyvinylpyrrolidone, poly(propylene imine), and polymethacrylic acid co-polymers (i.e. Eudragit L-100). Some materials are obtained from nature as bacterial ghosts (emptied bacterial envelopes as a carrier) like lactic acid bacteria (LAB) or heat/phenol-killed *E. coli*. Biopolymers or bio-inspired polymers like sodium alginate, neoglycocomplexes, micro-sepharose, protamine-based nanoparticles (proticles), and liposomes serve as carrier structures as well as core-shell construction consisting of different materials like carbohydrate modified ultrafine ceramic core based nanoparticles (aquasomes), or enteric-coated NPs. For DNA delivery, chitosan, liposome-protamine-DNA nanoparticles (LPD), PLGA, and poly(ethylene imine) represent materials already tested for application in AIT.<sup>[4; 13–15]</sup>

By far, the most popular materials used for nanoparticle preparation are the rather apolar, water-insoluble PLG and PLGA in case of protein encapsulation, and chitosan regarding DNA entrapment. These materials all exhibit unspecific degradation behavior upon hydrolysis and enzymatic degradation. This property results in sustained release, which may be advantageous in terms of a depot effect, but also affects storage stability of synthesized nanoparticle formulations in solution (short shelf-life). Degradation of the carrier system and release of the cargo may take up to several weeks.<sup>[16]</sup> Many of the aforementioned materials are not susceptible to an external stimulus that enables particle degradation. This can result in cargo release before application or at undesired locations *in vivo*, i.e. in the extracellular matrix or blood. In turn, the immune system can be activated and side effects that one tries to circumvent by nanoparticle shielding may occur nevertheless.

### **Future prospects/Conclusion**

AIT today still is not free from undesired effects occurring during therapy, limiting its therapeutic scope. A key objective for the therapy development should be to decrease undesired effects,

thereby enhancing the patients' safety and clinical efficacy. Research during the last decades examined specific immunotherapy with allergoids (chemically modified allergens) or peptides (B cell epitopes are removed preventing cross-linking of IgE immunoglobulins), or co-administration of anti-IgE-antibody omalizumab or DARPins (prevent binding of free IgE to FcεRI).<sup>[17]</sup> Approaches aim on influencing the balance of T cell subtypes include synthetic CpG-oligodeoxynucleotides (unspecific induction of Th1 response), and sialic acid polyclonal IgG, Tregitopes or Lactobacillus rhamnoses (induction of regulatory T cells).<sup>[18]</sup> Nanoparticles, on the other hand, can combine the advantages of these approaches by acting as delivery systems (protection from degradation, avoidance of IgE cross-linking, targeting of dendritic cells, co-delivery of adjuvants), which show promising results for the improvement of safety and efficacy that should be beneficial to AIT. It is a safe bet that in the next decade nanoparticles will gain increasing influence in AIT because of these favorable features. The stage is set: We have now attained comprehensive knowledge regarding the influence of NPs on the immune system. However, further studies will be necessary to comprehend effects of nanoparticles on the immune system when applied in the way of repeated injections and to prove their long-term compatibility before widespread application can be considered.

Many NP systems with new capabilities and functionalities are known from recently developed drug delivery concepts, e.g. in cancer therapy.<sup>[8, 13, 19]</sup> The employment of biocompatible, non-toxic and non-immunogenic polymers bears promise, as they may combine the advantage of long-term stability and degradation only upon a certain stimulus, such as a pH difference inside the endolysosome.<sup>[20]</sup> The design of novel carrier systems should take advantage of the progress in nanoparticle engineering, i.e. by using NPs that can selectively target cells or organs, and contain predetermined degradation sites that facilitate drug delivery upon a certain stimulus. To this end, chemists, pharmacists and clinicians should work hand in hand to adapt the existing concepts of protein delivery into dendritic cells for the potential application in AIT.

### **Acknowledgements**

The author would like to thank Matthias Worm and Dr. Iris Bellinghausen for carefully proofreading the manuscript.

### Financial & competing interests' disclosure

HP is a recipient of a fellowship through funding of the Excellence Initiative (DFG/GSC 266) in the context of the graduate school of excellence "MAINZ" (Materials Science in Mainz) and the Max Planck Graduate Center with the Johannes Gutenberg-Universität Mainz (MPGC).

HP, HF and JS: One patent is pending on degradable PEG-nanocarriers "Spaltbare Polyethylenglykol-(PEG)-Makromoleküle zum Einschluss von (Glyko-) Proteinen/Antigenen/Allergenen in abbaubaren Polyethylenglykol-(PEG)-Nanopartikeln sowie Verfahren zu ihrer Herstellung" (application number: 10 2013 015 112.0). The author has no other relevant affiliations or financial interest in or financial conflict with the subject matter or materials discussed in the manuscript apart from the disclosed. No writing assistance was utilized in the production of this manuscript.

HP and JS received research funding or speaker fees from manufacturers of AIT products.

### References

- [1] Lambrecht BN, Hammad H., The immunology of asthma, *Nat. Immunol.*, **2014**, 16(1), 45–56.
- [2] Akdis M, Akdis CA., Mechanisms of allergen-specific immunotherapy, *J. Allergy Clin. Immunol.*, **2014**, 133(3), 621–631.
- [3] Di Felice G, Barletta B, Bonura A, Butteroni C, Corinti S, Colombo P., Nanoparticles Adjuvants in Allergology: New Challenges and Pitfalls, *Curr. Pharm. Des.*, **2015**, 21(29), 4229–4239.
- [4] De Souza Rebouças, Juliana, Esparza I, Ferrer M, Sanz ML, Irache JM, Gamazo C., Nanoparticulate adjuvants and delivery systems for allergen immunotherapy, *J. Biomed. Biotechnol.*, **2012**, 2012(474605), 1–13.
- [5] De Souza Rebouças, Juliana, Irache JM, Camacho AI, et al., Immunogenicity of peanut proteins containing poly(anhydride) nanoparticles, *Clin. Vaccine Immunol.*, **2014**, 21(8), 1106–1112.
- [6] Hayen SM, Kostadinova AI, Garssen J, Otten HG, Willemsen, Linette E M., Novel immunotherapy approaches to food allergy, *Curr. Opin. Allergy Clin. Immunol.*, **2014**, 14(6), 549–556.
- [7] Gamazo C, Gastaminza G, Ferrer M, Sanz ML, Irache JM., Nanoparticle based-immunotherapy against allergy, *Immunotherapy*, **2014**, 6(7), 885–897.
- [8] Irvine DJ, Hanson MC, Rakhra K, Tokatlian T., Synthetic Nanoparticles for Vaccines and Immunotherapy, *Chem. Rev.*, **2015**, 115(19), 11109–11146.
- [9] Shao K, Singha S, Clemente-Casares X, Tsai S, Yang Y, Santamaria P., Nanoparticle-Based Immunotherapy for Cancer, *ACS Nano*, **2015**, 9(1), 16–30.

- 
- [10] Shibata Y, Foster LA, Bradfield JF, Myrvik QN., Oral Administration of Chitin Down-Regulates Serum IgE Levels and Lung Eosinophilia in the Allergic Mouse, *J. Immunol.*, **2000**, 164(3), 1314–1321.
- [11] Strong P, Clark H, Reid K., Intranasal application of chitin microparticles down-regulates symptoms of allergic hypersensitivity to *Dermatophagoides pteronyssinus* and *Aspergillus fumigatus* in murine models of allergy, *Clin. Exp. Allergy*, **2002**, 32(12), 1794–1800.
- [12] Vo T, Kim S., Marine-derived polysaccharides for regulation of allergic responses, *Adv. Food Nutr. Res.*, **2014**, 731–13.
- [13] Schöll I, Boltz-Nitulescu G, Jensen-Jarolim E., Review of novel particulate antigen delivery systems with special focus on treatment of type I allergy, *J. Control. Release*, **2005**, 104(1), 1–27.
- [14] Craparo EF, Bondi ML., Application of polymeric nanoparticles in immunotherapy, *Curr. Opin. Allergy Clin. Immunol.*, **2012**, 12(6), 658–664.
- [15] Fraser C., Nanoparticle Therapy for Allergic and Inflammatory Disease, *Antiinflamm. Antiallergy Agents Med. Chem.*, **2010**, 9(1), 54–70.
- [16] Park TG., Degradation of poly(lactic-co-glycolic acid) microspheres, *Biomaterials*, **1995**, 16(15), 1123–1130.
- [17] Manohar M, Nadeau KC., The Potential of Anti-IgE in Food Allergy Therapy, *Curr. Treat. Options Allergy*, **2014**, 1(2), 145–156.
- [18] Francis JN, Durham SR., Adjuvants for allergen immunotherapy: experimental results and clinical perspectives, *Curr. Opin. Allergy Clin. Immunol.*, **2004**, 4(6), 543–548.
- [19] Zhao L, Seth A, Wibowo N, et al., Nanoparticle vaccines, *Vaccine*, **2014**, 32(3), 327–337.
- [20] Pohlit H, Bellinghausen I, Schömer M, Heydenreich B, Saloga J, Frey H., Biodegradable pH-Sensitive Poly(ethylene glycol) Nanocarriers for Allergen Encapsulation and Controlled Release, *Biomacromolecules*, **2015**, 16(10), 3103–3111.

## 1.2 Nanoparticles for Allergen-specific Immunotherapy

*Hannah Pohlit<sup>1,2,3</sup>, Iris Bellinghausen<sup>1</sup>, Holger Frey<sup>2</sup>, Joachim Saloga<sup>1</sup>*

1 Department of Dermatology, University Medical Center Mainz, Langenbeckstr. 1, 55131 Mainz, Germany

2 Institute of Organic Chemistry, Johannes Gutenberg University Mainz, Duesbergweg 10-14, 55128 Mainz, Germany

3 Graduate School Materials Science in Mainz, Staudinger Weg 9, 55128 Mainz, Germany

\* corresponding author: Joachim Saloga

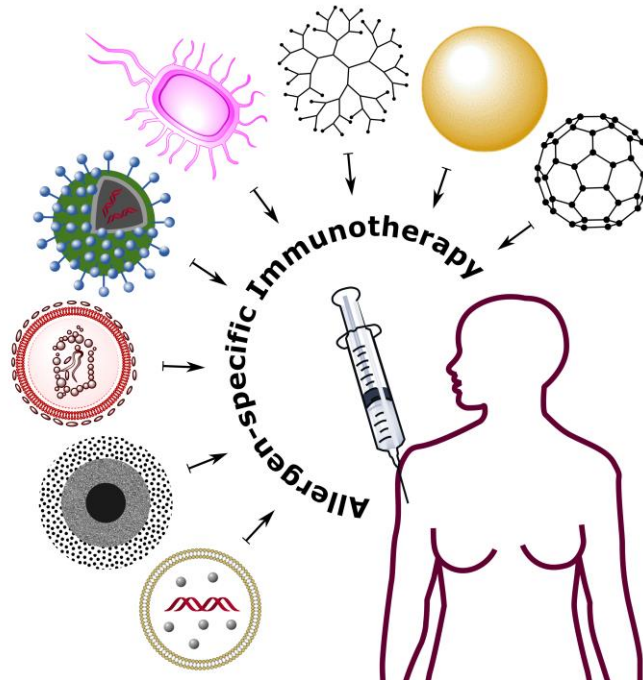
joachim.saloga@unimedizin-mainz.de, Tel.: 0049-6131-173751

To be submitted.

**Keywords:** Nanoparticles, Allergen-specific immunotherapy, drug delivery

### **Abstract**

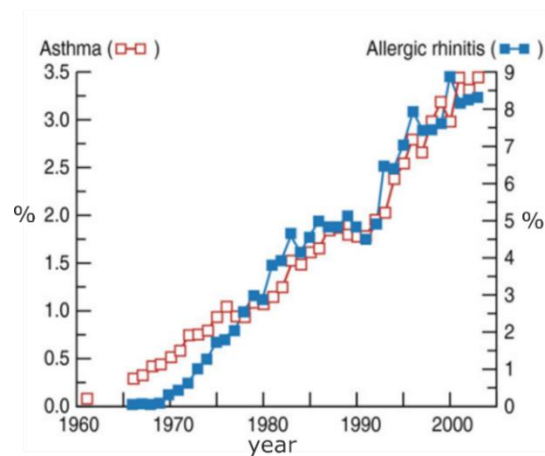
Within the last decades, the number of patients suffering from allergic asthma and rhinoconjunctivitis has increased dramatically. The only available cause-oriented therapy is allergen-specific immunotherapy (AIT). AIT reduces symptoms, but also has a disease modifying effect. Disadvantages are a long-lasting procedure, and in a few cases severe adverse effects like anaphylactic reaction. Encapsulation of allergens or DNA vaccines for AIT into nanostructures may provide advantages compared to the conventional AIT: The protein/DNA molecule can be protected from degradation, higher local concentrations and targeted delivery to the site of action appear possible and most importantly, recognition of encapsulated allergen by the immune system, especially by IgE antibodies is prevented. AIT with nanoparticles (NPs) offers a safer and potentially more efficient way of treatment for allergic diseases. In this review we summarize different approaches using NPs for AIT.



## 1. Introduction

### 1.1 Allergy and AIT

The prevalence of allergic diseases increased dramatically during the last century. Immediate hypersensitivity, also known as type I hypersensitivity reaction as classified by Coombs and Gell, is caused by an overreaction of the immune system to usually otherwise harmless environmental substances.<sup>[1]</sup>



*Figure 1.* Prevalence of asthma and allergic rhinitis among Finnish military conscripts in 1966-2003 in percent shows an increasing trend. Modified from Ref. <sup>[2]</sup>.

In the sensitization phase after first contact with the allergen, the allergen is internalized, degraded and presented on the cell surface by antigen-presenting cells, especially dendritic cells (DCs) resident in the epithelia of skin and mucosa. After migration to the lymph nodes, DCs can present the allergen-fragments on their cell surface especially to naïve T cells initiating the induction of a T cell response and further Th2 cell differentiation. Th2 cells can activate B cells to transform into plasma cells that secrete IgE antibodies against the allergen. IgE can bind to high-affinity membrane-bound receptors (FcεRI) on the surface of mast cells and basophilic leucocytes (see Figure 2a).

Upon further contact with the allergen, the IgE molecules bound to the mast cell surface are cross-linked by the specific allergen and trigger a signaling cascade resulting in degranulation of these cells and the release of preformed mediator molecules like histamine and leukotrienes. The release of these mediator molecules is responsible for the early inflammatory response and in this way for the symptoms of allergic patients. These symptoms include sneezing, oedema, wheezing and mucus congestion in hay fever and asthma and are created by bronchoconstriction, vasodilation, leucocyte recruitment and increased mucus production. In the most serious cases of allergy against insect stings, drugs, or food allergy like peanuts, the inflammatory responses affect many body systems simultaneously, and an anaphylactic shock can occur (see Figure 2b and c). Additionally, memory Th2 cells are activated by dendritic cells and release chemoattractant molecules that besides mast cells also attract further granulocytes, especially eosinophils leading to late inflammatory responses such as oedema, pain, warmth, erythema, airway narrowing, and mucus hypersecretion. A more detailed description of the mechanisms occurring during allergic inflammation is given by Galli et al.<sup>[3]</sup>



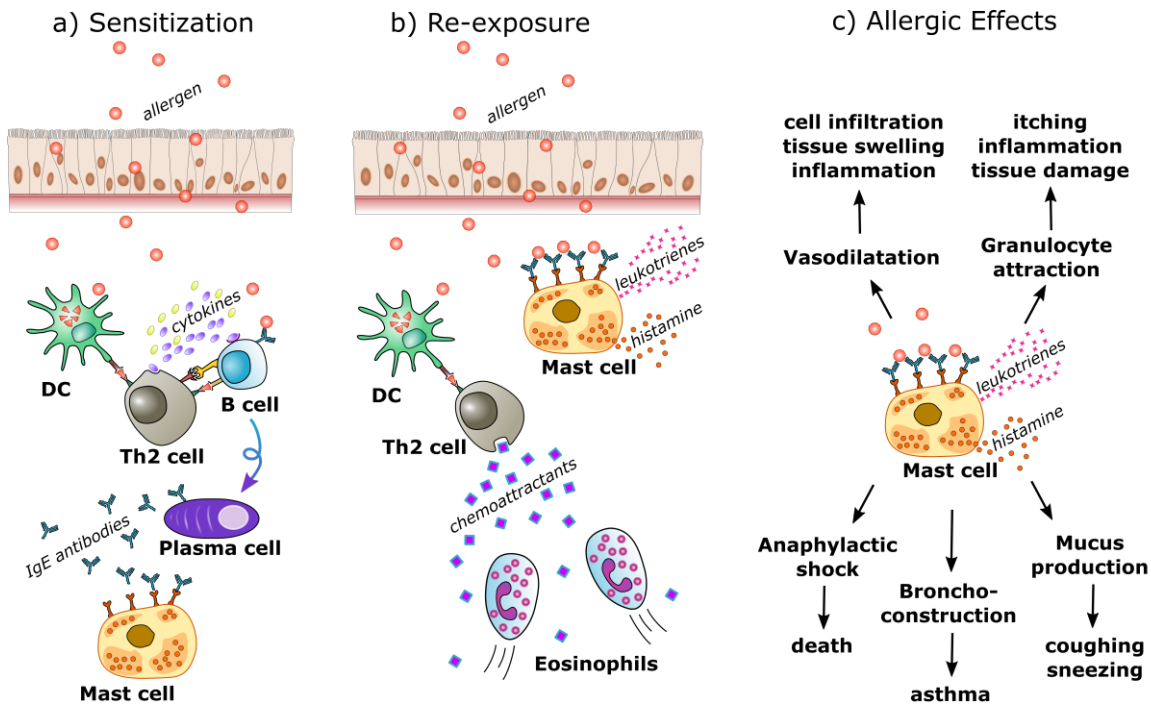


Figure 2. Schematic representation of a) sensitization against allergen, (b) re-exposure to the same allergen, and (c) allergic effects upon repeated contact with allergen.

To date, allergen-specific immunotherapy (AIT) is the only cause-oriented therapy for immediate hypersensitivity. Invented over 100 years ago by Leonhard Noon and John Freeman, AIT consists of repeated injections of the specific allergen in increasing doses, resulting in restored tolerance towards this specific allergen.<sup>[4]</sup> Applications in clinical use are restricted to subcutaneous injections or sublingual application (droplets or tablets).

The mechanisms underlying AIT are not fully elucidated, nonetheless it is known that allergen-specific memory T- and B-cell responses are modified, combined with an antibody class switch from IgE towards protective IgG antibodies. IgG antibodies can neutralize the allergen before it gets in contact with effector cells. Furthermore, infiltration and activation of eosinophils, mast cells, and basophilic leucocytes is reduced. AIT influences the reciprocal regulation of T cell subtypes Th1, Th2, Th9, Th17, Th22 and Treg. Successful AIT is characterized by a shift from Th2/Th17 immune response towards an induction of regulatory T cells sometimes along with a Th1 response. On the cytokine level, IL 4 and IL 13 are reduced while IL 10 and IFN  $\gamma$  levels are elevated (see Figure 3). The exact mechanisms of AIT have been reviewed elsewhere.<sup>[5; 6]</sup> Although effectiveness of AIT was confirmed in the majority of clinical trials, it still suffers from drawbacks like the potential induction of severe side effects, long treatment duration and sometimes limited

treatment effect, which all affect therapy safety and patient compliance. In the following section, different approaches for potential improvement of AIT will be discussed.

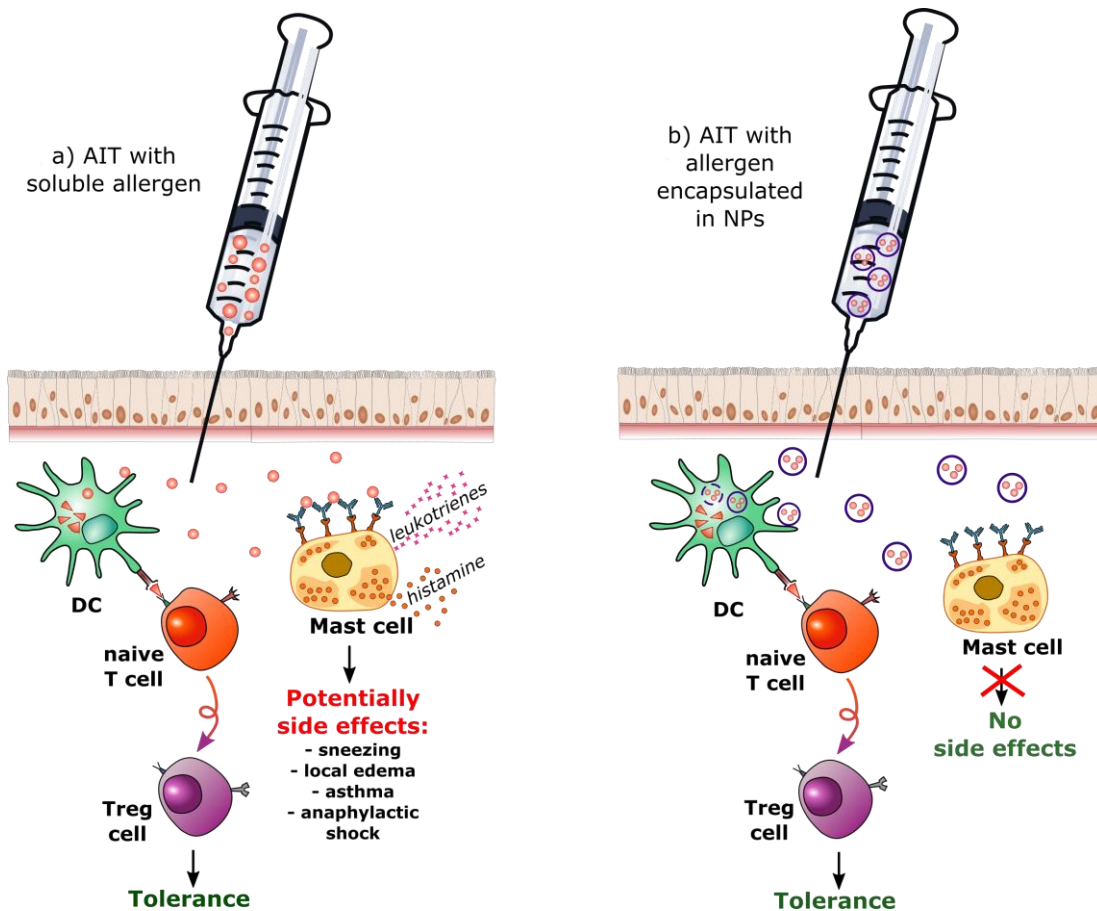


Figure 3. Comparison of allergen-specific immunotherapy with soluble allergen and with allergen encapsulated in nanoparticles.

### 1.2 Co-administration of antibodies or fusion proteins

Combination of anti-IgE (Omalizumab, Ligelizumab) and conventional AIT shows certain benefits compared to treatment without Omalizumab. Anti-IgE antibody may decrease the symptom load during AIT as well as increase the safety when during up-dosing in rush immunotherapy.<sup>[7; 8]</sup> The fusion protein DARPin (designed ankyrin repeat protein) may also be of great interest for co-administration in AIT. They do not only antagonize the interplay between FcεRI and unbound IgE, but also disrupt existing IgE-FcεRI interaction.<sup>[9–11]</sup>

### 1.3 Allergoids

One approach to improve safety and efficacy of AIT is the chemical modification of allergens. So-called allergoids are prepared by reaction with glutaraldehyde or formaldehyde and are characterized by destruction of B cell epitopes (reduced allergenicity) but maintenance of T cell epitopes (same immunogenicity). Glutaraldehyde (a bis-aldehyde) treatment of native allergens results in conjugation to the proteins and thus polymerization of the proteins.<sup>[12; 13]</sup> Inter-molecular cross-linking of allergens can also be achieved by through microbial transglutaminases.<sup>[14]</sup> Treatment with allergoids in clinical trials results in reduced side effects during AIT.<sup>[15; 16]</sup> Similar approaches are the use of peptides (fragmented allergens) for AIT<sup>[17]</sup> and recombinant and/or genetically modified allergens.<sup>[18; 19]</sup> Another advantage of recombinant allergens over natural extracts is better standardization due to non-seasonal shifts in allergen composition. Another approach is conjugation of allergens to polymers, e.g. to poly(ethylene glycol), so called PEGylation, leading to reduced allergenicity but retained immunogenicity, too.<sup>[20; 21]</sup>

### 1.4 Adjuvants

Approved and most commonly used adjuvant (agent that modifies the effects of antigens) in AIT is alum (aluminum hydroxide). The allergen is adsorbed to hardly soluble alum, which, in addition, strengthens the immunologic effect (functions as an allergen depot). However, alum also shows some disadvantages as it can cause sensitivity to aluminum, and due to its function as a Th2 cell inducer, it may also aggravate allergic reactions.<sup>[22]</sup> Therefore, the exploration of other adjuvants for AIT is desirable.

Adjuvant-allergen conjugates do not influence allergenicity but trigger the innate immune response and thereby shift it towards Th1. The conjugates may compose e.g. of CpG oligonucleotides, imidazoquinolines, adenine derivatives, or monophosphoryl lipid (MPL-A).<sup>[23–26]</sup>

### 1.5 Nanoparticles

Nanoparticulate structures may serve as carrier system for proteins, peptides, or DNA molecules and may also have adjuvant effects. There are two possible ways of transportation: encapsulation or surface coating of the cargo. Encapsulation offers protection from enzymatic or acidic degradation, delivery and co-delivery with other molecules to the targeted site of action, which enable high local concentrations, and prevent detection of the cargo molecule by the immune system. Especially in AIT, shielding of the allergen prevents recognition by IgE bound on the

surface of mast cells or basophilic leucocytes, which in turn should mitigate or even prevent side-effects (i.e. in the worst case anaphylactic shock) during AIT treatment. This property may be also useful for the realization of AIT against food allergies, where it is not yet routinely available.<sup>[27]</sup> An oral administration route for food AIT seems natural, but it brings along additional requirements for the nanocarrier; as the cargo needs to be delivered to the intestine, NPs have to be resistant to gastric acid and need to cross epithelial barrier and the mucosa to reach the lamina propria.<sup>[28]</sup> Another important feature of NPs depending on the design (size, charge, particle shape) is improved and accelerated cellular uptake, which might enable treatment during AIT with reduced doses of allergen. Reduced doses in turn may lead to fewer injections and in this way to a less unpleasant therapy for the patient. Allergen-coated NPs, on the other hand, facilitate cross-linking of IgE on the cellular surface and thereby activation of the immune cells and are usually used for investigation of prophylactic allergen vaccinations in mice. Non-loaded NPs have also been tested for allergen treatment, mostly in a prophylactic approach and show promising results due the ability to restore balanced Th1 and Th2 responses due to their adjuvant activity.

There are thousands of publications concerning NPs as carrier systems for drug delivery<sup>[29; 30]</sup> many of them with focus on vaccination strategies against cancer, infectious diseases or autoimmune diseases.<sup>[31-34]</sup> Considerably less research has been undertaken for NPs with focus on AIT. Some concepts investigate prophylactic vaccination strategies against allergies, others concentrate on a therapeutic approach in established allergic disease. Nanoparticle composition, structure and origin is manifold; the cargo (allergen or DNA) may be encapsulated or deposited on the surface. In the following sections, we will present the different NPs used for AIT sorted by their composition.<sup>[35-37; 31; 38]</sup>

## 2 Biodegradable Nanostructures

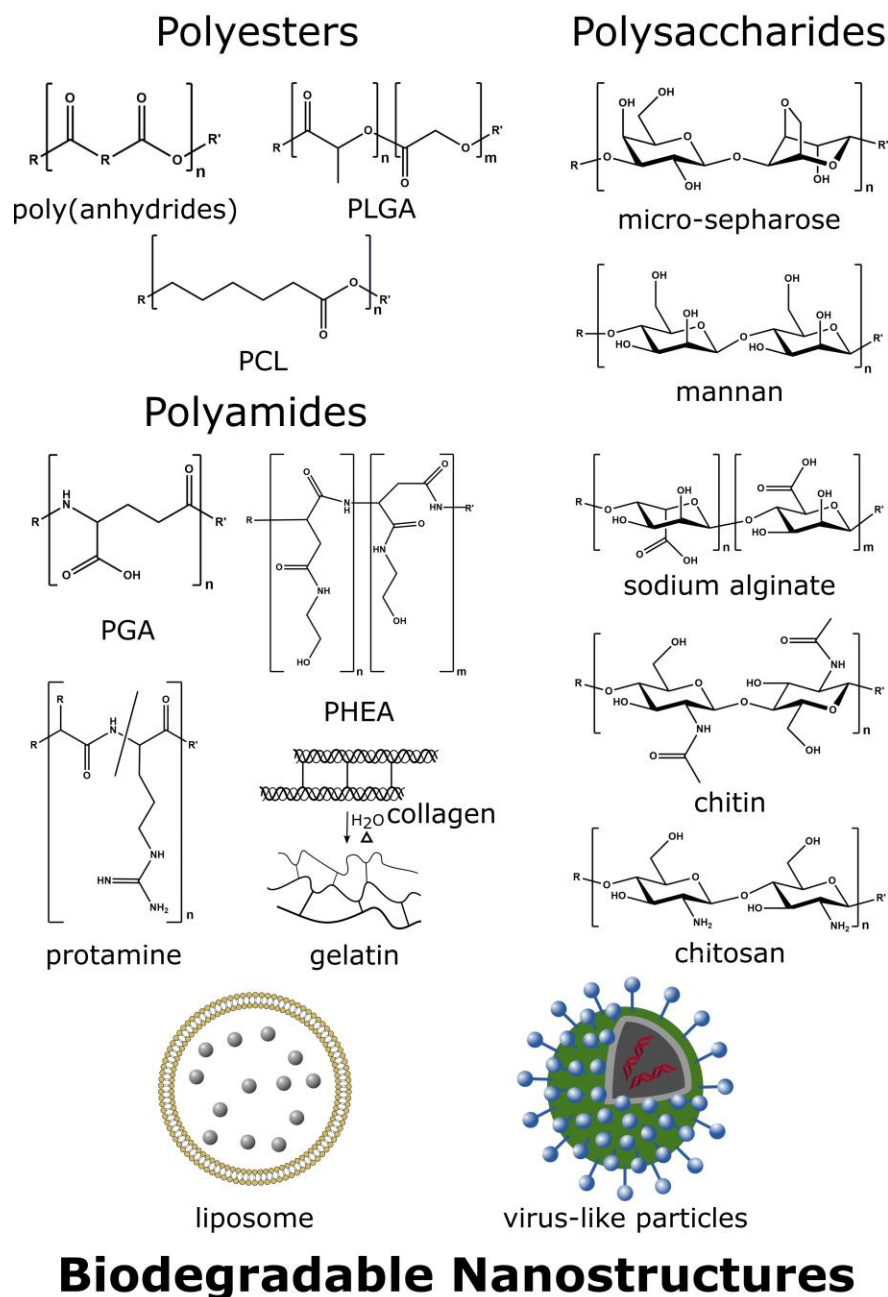


Figure 4. Overview of biodegradable nanostructures used in AIT.

### 2.1 Polymer Nanoparticles

#### 2.1.1 Polyesters

The most popular polyesters used in drug delivery are the polyesters poly(lactic acid) (PLA) and poly(lactic-co-glycolide) (PLGA, poly(lactic-co-glycolic acid)).<sup>[39]</sup> These biodegradable polymers

degrade under biological conditions via enzymatic hydrolysis. Degradation times can be adjusted from 2 weeks to 24 months.<sup>[40; 41]</sup> The rather long degradation times together with the acidic degradation products, which may result in inflammation at higher concentrations, and the difficulty of derivatization are the main drawbacks of these materials. To overcome these limitations, copolymers of basic character to neutralize generated acidity or copolymers to allow derivatization can be utilized.<sup>[41]</sup> Poly( $\epsilon$ -caprolactone) nanoparticles are distinguished by very low degradation rates by hydrolysis and enzymatic degradation, drug molecule release is dominated mainly by diffusion. This characteristic results in long term drug release, and sometimes incomplete drug release.<sup>[42]</sup> Here again, the limitations can be circumvented by copolymerization with suitable comonomers like other lactones. Poly(anhydrides) are applied in controlled-release coatings or temporary medical implants, as they degrade hydrolytically.

### 2.1.2 Poly(lactic-co-glycolic acid)

The copolymer poly(lactic-co-glycolide) (PLGA or poly(lactide-co-glycolide), PLG) combines many advantageous features like easy preparation, biocompatibility, inexpensive and commercially availability and degradation by hydrolysis.<sup>[42; 38]</sup>

The encapsulation of the major olive pollen allergen Ole e 1 in PLGA microparticles was investigated by Batanero *et al.* Interestingly, the microparticles showed a fast allergen release profile (about 45% release within 1 h).<sup>[43]</sup> Immunization of mice with these NPs resulted in a Th1-type immune response (enhanced IgG2a and IFN- $\gamma$  production, no IL-4 production).<sup>[44]</sup> Igartua *et al.* investigated their olive pollen loaded PLGA microspheres physicochemically as well as in mice concerning the induction of an immune response following sensitization with allergen-loaded microspheres. IgM antibodies were detected after sensitization and sustained for 28 weeks.<sup>[45]</sup> Marazuela *et al.* observed inhibited allergen-specific IgE and IgG1 antibody levels, and increased specific IgG2a upon preventive treatment of mice with Ole e 1-peptide loaded PLGA NPs. Furthermore they showed that IL-5 and IL-10 levels in spleen cell cultures were suppressed, as well as airway histopathologic parameters.<sup>[46]</sup>

Fattal *et al.* developed PLGA-microspheres loaded with milk protein  $\beta$ -lactoglobulin (BLG) for oral delivery. Treatment of mice with this carrier system tolerized mice to subsequent BLG challenge reducing both specific IgE and delayed type hypersensitivity responses.<sup>[47; 48]</sup>

Martínez Gómez *et al.* observed protection against an allergen challenge (exposure to the allergen) in PLA2-allergic mice treated with PLGA microspheres loaded with PLA2 (phospholipase

A2 from honey bee venom) and CpG. Consequently, the authors reported an increase of IgG2a. The therapeutic effect was even enhanced by co-encapsulating allergen, CpG and protamine.<sup>[49]</sup> Jilek *et al.* used PLGA microspheres to encapsulate PLA2-DNA. Mice that received these delivery systems showed T-cell hyporesponsiveness, increased PLA2-specific IgG1 and IgG2a, and reduced PLA2-specific IgE. Challenge with allergen resulted in balanced Th1 and Th2 cytokine expression as well as sustained expression of IL-10.<sup>[50]</sup>

PLGA as possible oral delivery platform for bee venom phospholipase A2 was analyzed by Guerin *et al.* The authors showed no *in vivo* data, but proved integrity of the entrapped PLA2 by PLA2-specific ELISA.<sup>[51]</sup> Detailed analyses of the physicochemical properties of bee venom,<sup>[52; 53]</sup> mellitin from bee venom,<sup>[54]</sup> and house dust mite allergen Der p 1<sup>[55]</sup> were performed investigating the influence of the reaction conditions necessary for PLGA NP preparation on the proteins.

Xiao *et al.* treated pre-sensitized mice with recombinant *Caryota mitis* profilin -loaded PLGA nanoparticles. The treatment resulted in conversion of Th2 to Th1 response, and evidently alleviated allergic symptoms.<sup>[56]</sup>

Joshi *et al.* described a preventive treatment with PLGA NPs co-administered during sensitization against Der p 2 allergen in mice. The authors found increased numbers of eosinophils in BAL fluids, increased IgE and IgG1 antibody levels, and increased airway hyperresponsiveness for Der p 2 NPs. However, when these NPs were loaded with CpG, airway hyperresponsiveness was prevented and IgG2a antibody levels elevated. Unfortunately, the effect of CpG alone was not compared to the results.<sup>[57]</sup> Upon treatment of pre-sensitized mice with recombinant Der p 2-loaded PLGA NPs, Yu *et al.* detected decreased lung inflammation and mucus secretion, the number of total cells and eosinophils decreased in BAL fluid, and a shift towards a Th1 response could be observed.<sup>[58]</sup>

Salari *et al.* treated pre-sensitized mice with PLGA-encapsulated rChe a 3. AIT with these NPs resulted in a shift from Th2 to Th1 as well as an upregulation of regulatory T cells.<sup>[59]</sup>

Takagi *et al.* presented a delivery system based on PLGA and loaded with OVA. AIT with these NPs in guinea pigs showed weaker local tissue reactions, increased in the threshold value of antigen inhalation test, and the amount of IgG2 blocking antibody.<sup>[60]</sup> Smarr *et al.* synthesized PLGA particles either conjugated to or loaded with ovalbumin. Particles with OVA conjugated to the surface could only partially inhibited Th2 responses in a therapeutic approach, although they worked well in prophylactic vaccination of mice. NPs with encapsulated OVA were able to inhibit

Th2 responses as well as airway inflammation both in a prophylactic and in a therapeutic approach in mice.<sup>[61]</sup>

The group of Jensen-Jarolim developed PLGA microspheres functionalized with lectin or wheat germ agglutinin to target  $\alpha$ -L-fucose residues on M-cells and enhance uptake in human enterocytes.<sup>[62]</sup> In a preventive immunization approach, mice treated with birch pollen-loaded microspheres showed higher levels of allergen-specific IgG.<sup>[63]</sup> Treatment of pre-sensitized mice with birch-pollen loaded microspheres resulted in a shift towards Th1 response. Functionalized microspheres showed better therapeutic effect than unfunctionalized ones.<sup>[64]</sup> Encapsulated protein was protected from gastric degradation. Immunization of mice with these PLGA microspheres resulted in an increase of specific IgG2a, but no increase of IgG1 antibodies.<sup>[65]</sup> In an *in vitro* experiment with human PBMCs, microspheres showed no cytotoxicity but immune stimulatory properties in general.<sup>[66]</sup> Schöll *et al.* investigated the benefit of a single-shot treatment of sensitized mice with Bet v 1-loaded PLGA nanospheres. Mice receiving the loaded nanospheres subcutaneously or orally with or without alum showed a decrease of IgG1 and increase of IFN- $\gamma$  and IL-10.<sup>[67; 68]</sup>

Zhang *et al.* entrapped OVA as model antigen together with CpG ODN (a TLR 9 agonist) in PLGA microparticles and compared the generation of immune response to an OVA-CpG ODN fusion molecule. OVA and CpG ODN loaded microparticles injected in mice showed higher IgG2a and IFN- $\gamma$  levels than CpG-ODN fusion molecules.<sup>[69]</sup> Dendritic cells that took up the microparticles matured and were more effective in T cell activation.<sup>[70]</sup> San Roman *et al.* treated pre-sensitized mice with PLGA microparticles loaded with OVA and CpG. The treatment protected mice from anaphylactic shock after allergen challenge. The presence of CpG shifted the immune response of mice with an established allergy towards Th1.<sup>[71]</sup> In a recent publication, Maldonado *et al.* demonstrated the use of PLGA as tolerogenic NPs with the capability to use as prophylactic or post-sensitization therapy. The model allergen ovalbumin was co-encapsulated with immunosuppressant rapamycin. Mice treated prophylactically with these PLGA-NPs exhibited an IgE response and suppressed recruitment of lymphocytes to the airways. Independent from the route of administration during sensitization (oral or nasal), treatment with PLGA-NPs induced regulatory B cells, T cell activation was inhibited. The quantity of lymphocytes and eosinophils in BAL fluid was reduced as well as antigen-specific hypersensitivity reactions.<sup>[72]</sup>



### 2.1.3 Poly( $\epsilon$ -caprolactone)

Poly( $\epsilon$ -caprolactone) is one of the most popular polymer for biodegradable drug delivery systems because of its characteristics like biocompatibility, high permeability, and low glass transition temperature.<sup>[42; 73]</sup> San Roman *et al.* found out that immunization of naïve mice with poly- $\epsilon$ -caprolactone (PCL) microparticles with a single shot by an intradermal route resulted in a Th2-type immune response. When the same microparticles were used in a therapeutic approach in mice, high OVA-specific IgG but low levels of IgE were found together with lower levels of serum histamine, leading to a higher survival rate after allergen challenge and induced anaphylactic shock.<sup>[74]</sup>

### 2.1.4 Poly(anhydride) nanoparticles

Poly(anhydrides) degrade within days to several months. This property in concert with biocompatibility, low melting points and solubility in organic solvents makes them interesting candidates for drug delivery.<sup>[42; 75]</sup> De Souza Rebouças *et al.* immunized naïve mice with peanut protein loaded poly(anhydride) nanoparticles. Depending on work-up procedure, the authors observed balanced Th1 and Th2 antibody and cytokine responses using lyophilized NPs, while spray-dried NPs additionally induced enhanced Th1 and Treg cytokines.<sup>[76; 77]</sup>

## 2.2 Natural biodegradable polymers

Natural biodegradable polymers are most often obtained from plants, e.g. chitosan, dextran, alginate, or cellulose derivatives. The source of origin is advantageous as there exists a low risk of unwanted immunological reactions due to the plant origin.<sup>[5]</sup> With regard to their composition, biodegradable natural polymers may consist of proteins (e.g. collagen, albumin, globulin, gelatin) or polysaccharides (e.g. starch, chitosan, alginate, dextran, hyaluronic acid).<sup>[78]</sup>

### 2.2.1 Polyamides

For drug delivery purposes, mostly natural poly(amino acids) or synthetic polyamides like polyhydroxyethylaspartamide are used due to their water-solubility and biodegradation. Natural water-soluble polymers have not only been used to encapsulate allergens but also DNA or activators of Th1 cells like CpG-ODN.

### 2.2.1.1 Protamine-based nanoparticles

Protamines are arginine-rich proteins derived from the sperm of different fish species. In nature protamin complexes DNA by electrostatic interaction, and for drug delivery it can bind nucleotides or peptides/proteins.<sup>[79]</sup> Pali-Schöll encapsulated peanut protein Ara h 2 together with CpG in protamine-based nanoparticles (proticles). Immunization of mice with Ara h 2-loaded proticles resulted in increased specific IgG2a antibodies whereas specific IgE was not detectable. On the cytokine level, they detected a low ratio of IL-5/IFN- $\gamma$ . Type I skin test reactivity to Ara h 2 was lower and granuloma formation was completely absent. Furthermore, stimulation of bone marrow-derived DC with Ara h 2-loaded proticles resulted in an upregulation of CD11c, CD80 and IL-6.<sup>[80; 81]</sup>

### 2.2.1.2 Poly( $\gamma$ -glutamic acid)

Poly( $\gamma$ -glutamic acid) ( $\gamma$ -PGA) is a poly(amino acid) showing water-soluble, biodegradable, edible, and non-toxic properties.  $\gamma$ -PGA is synthesized by gram positive bacilli and can be used as a carrier and adjuvant simultaneously.<sup>[82]</sup> Self-aggregated nanoparticles made of graft copolymers composed of hydrophilic  $\gamma$ -PGA and hydrophobic L-phenylalanine ethylester loaded with OVA as well as empty ones were prepared by Akagi *et al.*<sup>[83]</sup> Broos *et al.* investigated whether these NPs could serve as adjuvants in AIT. They could show that  $\gamma$ -PGA NPs were strong activators of human monocyte-derived DC and that stimulation of DC from allergic donors with a mixture of  $\gamma$ -PGA and grass pollen extract *in vitro* enhanced proliferation and IL-10 production of autologous memory T cells.<sup>[84]</sup>

Kunda *et al.* synthesized poly(glycerol adipate-co- $\omega$ -pentadecalactone) NPs which showed excellent BSA adsorption behavior. NPs were not suitable for direct inhalation because the majority of the inhaled dose would be exhaled due to their small size. The authors circumvented this problem by delivering the NPs inside of L-leucine microcarriers which might be promising for pulmonary vaccine delivery.<sup>[85]</sup>

Toita *et al.* investigated the biodistribution of s.c. injected fluorescent labelled poly( $\gamma$ -glutamic acid)-phenylalanine ( $\gamma$ -PGA-Phe-633) NPs in mice. The authors observed complete disappearance of the NPs at the injection site and major organs within 1 month after administration. When the NPs were administered systemically via the i.v. and i.p. route, the NPs mainly accumulated in the liver and were more rapidly cleared compared to non-biodegradable NPs.<sup>[86]</sup>

### 2.2.2 Polyhydroxyethylaspartamide

Polyhydroxyethylaspartamide (PHEA) is an artificial polymer adopting protein-like structure with high water solubility, multifunctionality, biocompatibility and low cost of production.<sup>[87]</sup> An allergen-copolymer nanoaggregate consisting of *Parietaria judaica* pollen allergens and poly(hydroxyethyl)-aspartamide with butyryl and succinyl side chains was prepared by Licciardi *et al.* The formation of the complex had no influence on allergenicity *in vitro*. Unfortunately, the authors do not show any immunological tests.<sup>[88]</sup>

### 2.2.3 Polysaccharides

Biodegradable natural polymers containing polysaccharides may be starch, chitosan, alginate, dextran, or hyaluronic acid.<sup>[61]</sup> Polysaccharides have not only been used to encapsulate allergens but also DNA or activators of Th1 cells like CpG-ODN.

#### 2.2.3.1 Neoglycocomplexes

Neoglycocomplexes were prepared by oxidizing mannan to obtain aldehyde groups that thereafter can react with proteins.<sup>[89]</sup> Weinberger *et al.* synthesized mannan-conjugates with OVA or papain that target dendritic cells *in vivo*. Both proteins induced elevated specific humoral immune responses and a shift from IgE to IgG in mice. Additionally, papain glycocomplexes combine the DC targeting and simultaneously mask B-cell epitopes revealing hypoallergenicity.<sup>[90]</sup>

#### 2.2.3.2 Carbohydrate-based particles (micro-Sepharose)

Proteins can be coupled to the surface of polysaccharides by cyanogen halide coupling.<sup>[91]</sup> Grönlund *et al.* coupled timothy grass pollen allergen to sepharose microbeads and treated mice with this formulation. The microbeads were more effective than conventional immunization with soluble allergen and induced a mixed allergen-specific Th1/Th2 immune response. Injection of the microbeads did not lead to granulomatous tissue reactions compared to the alum-adsorbed allergen.<sup>[92]</sup> The same micro sepharose beads were used for coupling of cat allergen protein and tested *in vitro* on human PBMCs. The microbeads got internalized by DCs leading to an upregulation of CD86, IL-8 and TNF- $\alpha$ .<sup>[93]</sup> In a pre-sensitized mouse model treatment with microbeads reduced airway hypersensitivity reactions and eosinophils in BAL fluid, and counterbalanced Th1/Th2 immunoglobulins.<sup>[94]</sup> If the microbeads were applied in a preventive vaccination strategy, airway inflammation was prevented, allergen-specific T cell anergy was induced, and Th1 immunoglobulins were preferentially produced. Concerning biodistribution, the

authors ascertained that microparticles were internalized by APCs and transported to the draining lymph nodes and spleen.<sup>[95]</sup>

### 2.2.3.3 Chitin particles

Chitin is a compound of the cell wall of fungi and upregulates Th1 immune responses. Shibata *et al.* investigated whether chitin can prevent Th2 responses during sensitization in allergy in mice. Chitin was administered orally 3 days before and 13 days during sensitization, which resulted in a decrease of IgE and lung eosinophil numbers. *In vitro* experiments showed an increase of Th1 cytokines and a decrease in Th2 and Treg cytokines.<sup>[96]</sup> Strong *et al.* tested chitin microparticles when directly applied i.n. of pre-sensitized mice during allergen challenge, and observed a reduction in serum IgE as well as peripheral blood eosinophilia, airway hyper-responsiveness and lung inflammation.<sup>[97]</sup>

### 2.2.3.4 Sodium alginate carrier

Alginate is received from the cell walls of brown algae and shows adjuvant activity, too. Taylor *et al.* compared the immunogenicity of grass pollen extract adsorbed on alum or conjugated to alginate and observed enhanced allergen-specific IgG and lower IgE in alginate-conjugate immunized mice.<sup>[98]</sup>

In clinical trials, immunotherapy with alginate-conjugated grass pollen extract leads to higher grass-specific IgG levels compared to alum-conjugation without changing the symptom scores.<sup>[99]</sup> Three placebo-controlled clinical trials were conducted with the same conjugate by Ortolani *et al.*<sup>[100]</sup>, Pastorello *et al.*<sup>[101]</sup>, and Corrado *et al.*<sup>[102]</sup>, where the clinical efficacy of AIT with alginate conjugates was demonstrated.

### 2.2.3.5 Gelatin nanoparticles

Gelatin consists of denatured and hydrated collagen is derived from animals. Klier *et al.* developed an aerosol formulation of gelatin nanoparticle-based CpG. Treatment of allergic horses increased IL-10 expression and partial remission of allergic symptoms.<sup>[103]</sup> In the subsequent Phase I and IIa study, Klier *et al.* could confirm their results.<sup>[104]</sup>

### 2.2.3.6 Chitosan NPs

Chitosan is a linear polysaccharide produced by crustacean and is known from different drug delivery approaches. It has been extensively reviewed concerning applications and features like

biodegradation, biodistribution and cytotoxicity.<sup>[105–108; 35]</sup> In several approaches, chitosan had been used to complex DNA via complex coacervation process and was investigated for vaccination efficacy as protection against allergic diseases. Chew *et al.* immunized naïve mice with house dust mite-chitosan NPs and observed a Th1-skewed immune responses against Der p 1.<sup>[109]</sup> Li *et al.* used the same approach and found in agreement with Chew *et al.* an induction of Th1 immune response and prevention from Th2 cell-regulated specific IgE responses subsequent to sensitization in mice.<sup>[110]</sup> Alike, Shi *et al.* used recombinant house dust mite pVAX1-Derp1 loaded chitosan NPs and achieved less allergic inflammation in nasal tissue in mice as well as an induction of Th1 immune response.<sup>[111]</sup> Ou *et al.* prevented inflammation of nasal mucosa in mice immunized with a DNA vaccine coexpressing Der p 1 allergen and murine ubiquitin by elicitation of a Th1-type response.<sup>[112]</sup>

Oral administration of peanut-allergen-DNA NPs transduced gene expression in the intestinal epithelium, as shown by Roy *et al.* Mice treated with the DNA NP produced secretory IgA and serum IgG2a, at the same time allergen-induced anaphylaxis was reduced.<sup>[113]</sup> Goldmann *et al.* used the model allergen OVA to show that mice treated with OVA-encoding DNA NPs had suppressed delayed-type hypersensitivity responses, anti-OVA antibodies, and spleen cell proliferation while Treg were induced.<sup>[114]</sup> Another approach is to induce the *in situ* production of IFN- $\gamma$  and thereby induce Th1 type reaction. Kumar *et al.* immunized mice with IFN- $\gamma$  DNA NPs and monitored a decrease in allergen-specific IgE, airway hypersensitivity reaction, and eosinophilia.<sup>[115]</sup> On a similar basis, Li *et al.* immunized mice orally with a TGF- $\beta$  expressing DNA chitosan NP to alleviate symptoms of food allergy.<sup>[116]</sup>

Chitosan NPs may also be suitable for encapsulation of proteins for classic AIT. In a preventive approach Hall *et al.* could show that treatment of mice with house dust mite peptide adsorbed to the chitosan prevented induction of airway inflammation by inducing allergen-specific IL-10 production.<sup>[117]</sup>

Chitosan can be cross-linked via ionotropic gelation with multivalent anions like tripolyphosphate. Li *et al.* treated Der f 2-sensitized mice with Der f 2-loaded cross-linked chitosan NP i.p. and demonstrated a decreased AHR, less eosinophils in the BAL fluid and mitigated lung inflammation and mucus production after i.n. allergen challenge. Furthermore, they found decreased allergen-specific IgE and increased allergen-specific IgG2a.<sup>[118]</sup> When administered intra nasally in mice, Liu *et al.* reported additionally to the above-mentioned parameters increased specific IgA, inhibited T cell proliferation and increased Tregs.<sup>[119; 120]</sup> The encapsulation of OVA into chitosan

triphosphate microparticles by Saint-Lu *et al.* increased uptake, processing and antigen-presentation as well as specific T cell proliferation *in vitro*, while *in vivo* tolerance induction was enhanced and Th2 responses reduced in mice.<sup>[121]</sup>

Another chemical modification of chitosan was applied by Jirawutthiwongchai *et al.* The authors exploited self-aggregation of chitosan-phenylalanine-mPEG for entrapment of house dust mite allergen extract. Upon stimulation of a human keratinocyte cell line or human PBMCs from allergic donors with these NPs they observed a reduction in reactive oxygen species, and a decreased IFN- $\gamma$  and IL-10 production, respectively.<sup>[122]</sup>

### 2.3 Liposomes

Liposomes consists of lipids that self-assemble to a vesicular system, in which a lipid double layer separates an aqueous core from the aqueous environment. Liposomes have been investigated as drug delivery platforms or as adjuvants for several decades and are extensively reviewed elsewhere.<sup>[123–127]</sup> Since 1984, liposomes arouse interest as delivery systems and adjuvants for AIT.<sup>[128; 129]</sup> In the following section, different types of liposomes are presented.

#### 2.3.1 Non-modified liposomes

The first report of liposomes as delivery vehicles for allergens in AIT was published 1984 by Wagner *et al.*<sup>[130]</sup> Allergen-loaded liposomes did avoid anaphylactic reactions in pre-sensitized guinea-pigs.<sup>[131]</sup>

The group of Olaguibel in cooperation with ALK-Abelló Spain synthesized liposomes by extrusion method consisting of dipalmitoylphosphatidylcholine (DPPC), cholesterol, and tocopheryl acid succinate which were loaded with house dust mite body extract (*D. pteronyssinus*, Der p 1 and Der p 2). A clinical trial in young, mono-sensitive, mild asthma patients revealed tolerance of higher allergen doses, and decreased bronchial immediate responses as well as eosinophilic inflammation.<sup>[132]</sup> Patients reported reduced symptom and medication scores by at least 60%, in addition organ sensitivity (skin prick test, intradermal testing, and bronchial challenge test) was reduced. Accordingly, in the humoral immune response specific IgG production was augmented during the therapy, whereas no change in specific IgE production was observed.<sup>[133]</sup>

Arora *et al.* published several studies reporting *Artemisia scoparia* pollen extract-loaded liposomes by ultra-sonication made from phosphatidylcholine, cholesterol, and phosphatidic acid. In a first study, they analyzed the tissue distribution. Allergen-loaded liposomes showed an

extended retention in all organs except kidneys compared to free allergen.<sup>[134]</sup> Intraperitoneal treatment of sensitized BALB/c mice with allergen-loaded liposomes resulted in a Th1-immune response and of Treg increase.<sup>[135; 136]</sup> The authors found higher survival rates after allergen challenge, and only a slight increase in plasma histamine levels in liposome-treated mice compared to mice which received free allergen or allergen adsorbed to alum.<sup>[137; 138]</sup> Unfortunately, the authors did not include untreated mice for comparison of immune responses.

Genin *et al.* introduced negatively-charged multilamellar liposomes, made from phosphatidylcholine, cholesterol, and L- $\alpha$ -tocopherol, where one third of the allergen is associated to the surface and two thirds were encapsulated. Immunogenicity was measured by basophil activation tests and skin tests in allergic patients.<sup>[139]</sup> Nigam *et al.* used the same liposome composition to encapsulate *A. fumigatus* glycoprotein, a fungal allergen. AIT with the liposomal formulation induced Th1 type response in humoral and cellular parameters.<sup>[140]</sup>

Audera *et al.* tested liposomes made from DPPC, cholesterol, and optional dicetylphosphate or stearylamine to obtain, neutral, positive, or negative charged liposomes. Neutral and positively charged liposomes seem to be more promising for AIT.<sup>[128]</sup> In a more recent study, Calderon *et al.* formulated liposomes from DPPC by dehydration/rehydration method which were loaded with purified allergen from *Dermatophagoides siboney*. Treatment of BALB/c mice resulted in high specific IgG levels, but in contrast to immunotherapy with allergen adsorbed on alum, IgE levels were not elevated. Furthermore, a reduced cellular infiltration was observed (especially eosinophils).<sup>[141]</sup>

Galvain and coworkers from Stallergènes compared 4 clinical trials with allergen-loaded liposomes. In the first two trials, they tested cutaneous tolerance of liposomes administered in skin prick tests and local and systemic safety of empty liposomes after s.c. injection. In the following two trials, AIT with allergen-loaded liposomes was conducted. They discovered that liposomal formulations were as effective as conventional AIT, but systemic safety was less affirmative and sophisticated manufacturing process leads to their conclusion that liposomes are not suited for AIT.<sup>[142]</sup>

The liposomes prepared by Tasaniyananda *et al.* consisting of didodecyldimethylammonium bromide, phosphatidylcholine, and cholesterol loaded with cat allergens were reported very recently. AIT with this liposomes resulted in reduced serum IgE and intranasal mucus and cytokine profile was shifted towards Th1 and Treg.<sup>[143]</sup>

Ouadahi *et al.* administered pre-sensitized mice with OVA-loaded liposomes intragastrically, and compared passive cutaneous anaphylaxis of OVA loaded liposomes and free OVA. In the mouse model they used, free OVA was able to decrease IgE levels, and liposomal preparations had no additional benefits.<sup>[144]</sup>

### 2.3.2 Oligomannose-coated liposomes

Ishii *et al.* prepared oligomannose-coated liposomes (OMLs) consisting of DPPC, DPPE, cholesterol, and Man3-DPPE. Preventive vaccination with OLMs lead to decreased IL-4 and IL-5, IgE and specific IgG1 levels in sera, but increased specific IgG2a and IFN-gamma production. Pre-sensitized mice treated with OMLs showed likewise suppressed IgE levels, as well as decreased IL-5 and increased IFN-gamma levels.<sup>[145]</sup> Oligomannose-coated liposomes were also used from Kawakita *et al.* to analyze the adjuvant activity of OMLs to induce CD8<sup>+</sup>-Treg that are able to suppress allergic diarrhea. *In vitro*, the number of Treg expanded, allergen-specific IgE was reduced and IL-10, IgG1, IgG2 and soluble IgA were elevated.<sup>[146]</sup>

Meechan *et al.* compared liposomes loaded with purified Per a 9 allergen to liposomes loaded with crude extract. Liposomes with Per a 9 were able to alleviate airway inflammation after allergen challenge and caused a shift of allergic Th2 to Th1 and Treg response, whereas crude-extract loaded liposomes merely resulted in a shift from Th2 to Th1 response, while airway inflammation and Treg response were not altered.<sup>[147]</sup>

### 2.3.3 DNA liposomes

To co-deliver plasmid-DNA of CpG and allergen extract, Mueller *et al.* introduced preformed liposomes consisting of DOTIM (octadecenoyloxy{ethyl-2-heptadecenyl-3-hydroxyethyl}imidazolium chloride) and cholesterol that were complexed with CpG-DNA and allergen by mixing before administration. The liposome formulation was administered to dogs with atopic dermatitis in a series of intradermal injections which resulted in an improvement of the pruritus score and a decrease in IL-4 mRNA expression in PBMCs compared to the pretreatment values while IFN- $\gamma$  and IL-10 mRNA as well as medication score did not change.<sup>[148]</sup>

The immunotherapy with feline IL-2 cDNA liposome complexes (immune stimulator of innate immunity and Th1 responses) prepared from DOTIM and cholesterol was investigated by Veir *et al.* Cats with chronic rhinitis that were treated with these liposome-IL-2 DNA complexes showed significant improvement in frequency of sneezing, but no differences in cytokine profile were



detected compared to placebo control. The authors infer that chronic rhinitis in cats is not a disease with a Th2 cytokine bias.<sup>[149]</sup>

Another transport system for DNA was described by Nouri *et al.* AIT of pre-sensitized mice with liposome-protamine-DNA nanoparticles shows a reduction in IgE as well as induction of IgG2a, IFN- $\gamma$ , and T-bet. Furthermore, the authors reported higher lymphoproliferative responses.<sup>[150]</sup>

#### 2.3.4 Allergen-coupled liposomes

A completely different approach is presented by Ichikawa *et al.* In their setup, OVA is covalently coupled to the DSPC-cholesterol liposome surface. When pre-sensitized mice were treated with OVA-coated liposomes, OVA-specific IgE was strongly suppressed whereas IgG levels increased during AIT but decreased after sensitization. A biodistribution study revealed accumulation of OVA-liposome in the liver and spleen.<sup>[151]</sup> Loading of these liposomes with doxorubicin (DOX) resulted in considerably less OVA-specific IgE, compared to unloaded OVA-coated liposomes. The authors assume targeted transport of DOX to the OVA-specific B cells in spleen, which were eradicated by DOX.<sup>[152]</sup>

#### 2.3.5 Potential platforms

Cabral *et al.* used the dehydration/rehydration method without further homogenization to prepare small unilamellar liposomes from phosphatidylcholine and cholesterol. For lyophilization and reconstitution they used trehalose as cryoprotectant and compared liposome characteristics before and after freeze-drying.<sup>[153]</sup>

Wojdani describes in his US patent liposomes with different lipid compositions that encapsulated or covalently bound allergen. The results shown indicate reduced specific IgE and elevated IgG serum levels in rabbits.<sup>[154]</sup>

McWilliam *et al.* described another potential delivery system for house dust mite allergens. The group compared the suitability of multilamellar, small unilamellar, and reversed phase vesicle liposomes regarding encapsulation efficiency and entrapment of allergens of different MW. Unfortunately, no cellular tests were performed.<sup>[155]</sup>

### 2.4 Virus-like particles

Virus-like particles have been applied as adjuvants or drug delivery systems.<sup>[156; 157]</sup> To test an allergen-free immunomodulator, a toll-like receptor 9 agonist was encapsulated into virus-like

particles (VLP). Klimek *et al.* treated house-dust mite allergic patients and six injections resulted in lower rhinoconjunctivitis symptoms and better quality of life score. Additionally, a 10-fold increase in allergen tolerance was demonstrated by conjunctival provocation test.<sup>[158–160]</sup>

Virus-like particles consisting of bacteriophage Q $\beta$  coat protein associated with CpG oligodeoxynucleotide were used as adjuvant for house dust mite allergen extract by Kündig *et al.* In a phase I clinical study, healthy volunteers developed allergen-specific IgG antibodies upon vaccination with this virus-like particle.<sup>[161]</sup> Symptoms of rhinitis and allergic asthma were significantly reduced and humoral response was shifted towards Th1 in a phase I/IIa clinical trial.<sup>[162]</sup> A single vaccination of Fel d 1 coupled to bacteriophage Q $\beta$ -derived virus-like particles induced protection against type I allergic reactions. No local or systemic reactions were observed in sensitized mice. *In vitro*, their allergen-coupled VLPs did not degranulate human basophils.<sup>[163]</sup>

The B cell epitope of OVA was inserted in the capsid sequence of adeno-associated virus-like particles used by Manzano-Szalai *et al.* After immunization with the VLP, high titers of OVA-specific IgG1 were observed while allergen-specific IgE was reduced compared to treatment with soluble OVA. No anaphylactic reaction was observed for VLP-treated mice upon OVA challenge.<sup>[164]</sup>

## 2.5 Conclusion Biodegradable Nanostructures

PLGA is by far the most intense investigated biodegradable polymer applied in AIT to date. Other polyester materials like polydioxanone, polycarbonates, poly(phosphate)s, poly(phosphazene)s, or poly(ortho esters) are well-known materials for biomedical applications and may be interesting candidates for materials in AIT drug delivery. Poly(alkyl cyanoacrylate) (PACA), which is degradable under acidic conditions, is also known in drug delivery.<sup>[165]</sup> Extensive studies regarding immune responses to the materials as well as metabolization products need to be performed in detail. Natural water-soluble polymers possess great potential as drug delivery systems in AIT. So far, chitosan has been extensively investigated as transport vehicle for DNA and protein delivery. Other materials like alginate or chitin are tested in the field just now, but there remains an elusive amount of possible materials. Possible materials may be xanthan gum, pectins, dextran, carrageenan, cellulose ethers, hyaluronic acid, starch, or starch-based derivatives, to name only a few of them.<sup>[166; 78]</sup> The employment of liposomes as allergen delivery vehicles was investigated by many researchers around the world. Many structural varieties of liposomes tested in other applications are promising but were not yet transferred to AIT, like stealth liposomes, liposomes

with targeting moieties, or liposomes with cross-linked core or shells to improve stability of liposomes until arrival at the targeted location.

VLP as delivery systems take advantage of manufacturing methods perfected by nature. Additionally, they often combine transport and adjuvant function. There is an increasing interest in these nanomaterials for immunotherapy applications.

Table 1. Overview of biodegradable nanostructures for allergen-specific immunotherapy.

Nanoparticle composition and manufacturing method	Cargo	Vaccination approach	Species/Route	Reference
poly(D,L-lactide-co-glycolide) microparticles	<i>Olea europaea</i> Ole e 1 peptide	prophylactic	BALB/c mice, i.p.	Batanero 2003 <sup>[43; 44]</sup>
poly(D,L-lactide-co-glycolide) microspheres double emulsion solvent evaporation/extraction method	<i>Olea europaea</i> pollen extracts	possible delivery platform	BALB/c mice, s.c.	Igartua 2002 <sup>[45]</sup>
poly(D,L-lactide-co-glycolide) microparticles double emulsion solvent evaporation method	Ole e 1 peptide	prophylactic	BALB/c mice, i.n.	Marazuela 2008 <sup>[46]</sup>
poly(D,L-lactide-co-glycolide) microspheres	$\beta$ lactoglobulin (BLG)	prophylactic	BALB/c mice, p.o. (orally)	Fattal 2002 <sup>[47]</sup> Pecquet 2000 <sup>[48]</sup>
poly(D,L-lactide-co-glycolide) microspheres solvent extraction method	bee venom phospholipase A2 (PLA2), oligodeoxynucleotide (CpG) and protamine	therapeutic	CBA/J mice, s.c.	Martínez-Gómez <sup>[49]</sup>
poly(D,L-lactide-co-glycolide) microspheres spray-drying method	bee venom PLA2 DNA	prophylactic	CBA/J mice, s.c.	Jilek 2004 <sup>[50]</sup>
poly(D,L-lactide-co-glycolide) NPs double emulsion solvent evaporation method	recombinant <i>Caryota mitis</i> profilin (rCmP)	therapeutic	BALB/c mice, s.c.	Xiao 2013 <sup>[56]</sup>
poly(D,L-lactide-co-glycolide) NPs double emulsion solvent evaporation method	Der p 2-coated, CpG motifs encapsulated	prophylactic	C3H/HeB FeJ mice, s.c.	Joshi 2014 <sup>[57]</sup>
poly(D,L-lactide-co-glycolide) NPs	recombinant Der p 2	therapeutic	BALB/c mice, s.c.	Yu 2006 <sup>[58]</sup>
poly(D,L-lactide-co-glycolide) nanoparticles double emulsion solvent evaporation method	<i>Chenopodium album</i> pollen rChe a 3	therapeutic	BALB/c mice, s.l.	Salari 2015 <sup>[59]</sup>

## 1.2 Nanoparticles for Allergen-specific Immunotherapy

poly(D,L-lactide-co-glycolide) microspheres double emulsion solvent evaporation method	ovalbumin (OVA)	therapeutic	guinea pigs	Takagi 1992 <sup>[60]</sup>
poly(D,L-lactide-co-glycolide) microspheres double emulsion solvent evaporation method	OVA-coated or encapsulated	prophylactic and therapeutic	BALB/c mice	Smarr 2016 <sup>[61]</sup>
poly(D,L-lactide-co-glycolide) microspheres functionalized with lectin from <i>Aleuria aurantia</i> (AAL) or wheat germ agglutinin (WGA)	birch pollen extract	prophylactic and therapeutic	<i>In vitro</i> BALB/c mice, p.o. (orally)	Diesner 2012 <sup>[62]</sup> Walter 2004 <sup>[63]</sup> Roth-Walter 2005 <sup>[64-66]</sup>
poly(D,L-lactide-co-glycolide) nanospheres double emulsion solvent evaporation method	Bet v 1	therapeutic	BALB/c mice, s.c. or p.o. (orally)	Schöll 2004 <sup>[67]</sup> , 2006 <sup>[68]</sup>
poly(D,L-lactide-co-glycolide) NPs double emulsion solvent evaporation method	OVA and CpG ODN	prophylactic	<i>In vitro</i> and C57BL/6 mice	Zhang 2007 <sup>[69; 70]</sup>
poly(D,L-lactide-co-glycolide) microparticles double emulsion solvent evaporation method	OVA and CpG ODN	therapeutic	BALB/c mice. i.d.	San Roman 2009 <sup>[71]</sup>
poly(D,L-lactide-co-glycolide) NPs double emulsion solvent evaporation method	OVA + rapamycin (tolerogenic immunomodulator)	therapeutic and prophylactic	BALB/c mice, i.v.	Maldonado 2015 <sup>[72]</sup>
poly(D,L-lactide-co-glycolide) microspheres double emulsion solvent evaporation method	bee-venom phospholipase A2 (PLA2)	possible delivery platform no cellular tests	<i>In vitro</i> ELISA	Guerin 2002 <sup>[51]</sup>
poly(D,L-lactide-co-glycolide) microspheres double emulsion solvent evaporation method	bee venom	possible delivery platform no cellular tests	Preformulation studies	Trindade 2012 <sup>[52]</sup>
poly(D,L-lactide-co-glycolide) microparticles double emulsion solvent evaporation method	<i>Dermatophagoides pteronyssinus</i> Der p 1	possible delivery platform no cellular tests	preformulation studies	Sharif 1995 <sup>[55]</sup>
poly(D,L-lactide-co-glycolide) NPs double emulsion solvent evaporation method	Melittin (bee venom)	possible delivery platform no cellular tests	preformulation studies	Park 2015 <sup>[54]</sup>
poly-ε-caprolactone (PCL) microparticles solvent extraction/evaporation method	ovalbumin (OVA)	prophylactic and therapeutic	BALB/c mice, i.d.	San Roman 2007 <sup>[74]</sup>

poly(anhydride) nanoparticles solvent displacement method	raw or roasted peanut proteins	prophylactic	C57BL/6 mice, p.o. (orally)	De Souza Rebouças 2012 <sup>[76]</sup> 2014 <sup>[77]</sup>
protamine-based nanoparticles (proticles) self-assembly in aqueous solution	CpG-oligodeoxynucleotides (ODNs), complexed with Ara h 2 extract (peanut)	prophylactic	BALB/c mice, s.c.	Pali-Schöll 2013 <sup>[80]</sup> Zimmer 2014 <sup>[81]</sup>
poly(gamma-glutamic acid) (gamma-PGA) nanoparticles self-assembly in aqueous solutions	mixture $\gamma$ -PGA NPs and <i>Phleum pretense</i> extract Phl p	prophylactic	<i>In vitro</i> human MoDCs	Akagi 2005 <sup>[83]</sup> Broos 2010 <sup>[84]</sup>
poly( $\gamma$ -glutamic acid)-phenylalanine ( $\gamma$ -PGA-Phe-633) self-assembly in aqueous solutions	ovalbumin	possible delivery platform no immunological tests	mice s.c., i.v. or i.p.	Toita 2013 <sup>[86]</sup>
PGA-co-PDL polymeric nanoparticles (NPs) within L-leucine (L-leu) microcarriers	BSA	possible delivery platform no cellular tests	for dry powder inhalation	Kunda 2015 <sup>[85]</sup>
poly(hydroxyethyl)-aspartamide (PHEA) allergen-copolymer nanoaggregate	Par j 1 and Par j 2	possible delivery platform no cellular tests	<i>in vitro</i> (murine and human)	Licciardi 2014 <sup>[88]</sup> Bondi 2011 <sup>[167]</sup>
neoglycoconjugates Mannan was oxidized and the reacted with proteins	ovalbumin and papain	prophylactic	BALB/c mice, i.d.	Weinberger 2013 <sup>[90]</sup>
carbohydrate-based particles (micro sepharose)	timothy grass pollen allergen, Phl p 5b	prophylactic	BALB/c mice, s.c.	Grönlund 2002 <sup>[92]</sup>
carbohydrate-based particles (micro sepharose)	rFel d 1 cat allergen protein	therapeutic	<i>in vitro</i> , human PBMCs	Andersson 2004 <sup>[93]</sup>
hydrate-based particles (micro sepharose)	recombinant cat allergen rFel d 1	therapeutic and prophylactic	BALB/c mice, i.n. or s.c.	Neimert-Andersson 2008 <sup>[94]</sup> Thunberg 2009 <sup>[95]</sup>
chitin particles Ultrasonication of chitin powder	empty	prophylactic	BALB/c and C57BL/6 mice, orally	Shibata 2000 <sup>[96]</sup> Strong 2002 <sup>[97]</sup>
sodium alginate carrier (Conjuvac®) purchased	grass pollen extract, <i>Parietaria judaica</i> extract or <i>D. pteronyssinus</i> extract	prophylactic and therapeutic	BALB/c mice, s.c., and clinical trial, s.c.	Taylor 1981 <sup>[98]</sup> Pegelow 1984 <sup>[99]</sup> Corrado 1989 <sup>[102]</sup> Pastorello 1990 <sup>[101]</sup> Ortolani 1994 <sup>[100]</sup>
gelatin nanoparticles	CpG-ODN	therapeutic	horses, inhalation therapy	Klier 2012 <sup>[103]</sup> 2015 <sup>[104]</sup>

## 1.2 Nanoparticles for Allergen-specific Immunotherapy

chitosan NPs complex coacervation	pDer p 1 and pDer p 1 DNA	prophylactic	BALB/c mice, orally	Chew 2003 <sup>[109]</sup>
chitosan NPs complex coacervation	plasmid DNA Der p 2	prophylactic	BALB/c mice, orally	Li Liu 2009 <sup>[110]</sup>
chitosan NPs complex coacervation	recombinant house dust mite pVAX1-Derp1	prophylactic	BALB/c mice, i.n.	Shi 2013 <sup>[111]</sup>
chitosan NPs complex coacervation	DNA vaccine coexpressing Der p 1 allergen and murine ubiquitin	prophylactic	BALB/c mice, i.n.	Ou 2014 <sup>[112]</sup>
chitosan-DNA NPs complex coacervation	peanut allergen DNA (pCMVArah2)	prophylactic	AKR/J mice, orally	Roy 1999 <sup>[113]</sup>
chitosan NPs complex coacervation	(OVA)-encoding DNA	prophylactic	BALB/c mice, orally	Goldmann 2012 <sup>[114]</sup>
chitosan NPs complex coacervation	IFN- $\gamma$ pDNA	prophylactic	STAT4-/- BALB/c mice, i.n.	Kumar 2003 <sup>[115]</sup>
chitosan NPs complex coacervation	TGF- $\beta$ expressing DNA vector	therapeutic	BALB/c mice, orally	Li Wang 2009 <sup>[116]</sup>
chitosan NPs Peptide adsorbed on chitosan	<i>D. pteronyssinus</i> Der p 1 allergen peptide	prophylactic	C57BL/6 mice, i.n.	Hall 2002 <sup>[117]</sup>
chitosan triphosphate microparticles ionotropic gelation	Der f 2 allergen peptide	therapeutic	BALB/c mice, i.p.	Li Liu 2008 <sup>[118]</sup>
chitosan-triphosphate NPs ionotropic gelation	Der f allergen	therapeutic	BALB/c mice i.n.	Liu 2009 <sup>[119]</sup> Yu 2011 <sup>[120]</sup>
chitosan triphosphate microparticles ionotropic gelation	OVA	therapeutic	mice, s.l.	Saint-Lu 2009 <sup>[121]</sup>
chitosan-phenylalanine-mPEG NPs Self-aggregation	house dust mite allergen extract	therapeutic	<i>in vitro</i> , human PBMCs	Jirawutthiwongcha i 2016 <sup>[122]</sup>

Table 2. Overview of liposomes investigated for allergen-specific immunotherapy.

Liposome composition and manufacturing method	Cargo	Vaccination approach	Species/ Route	Reference
not known	ragweed allergen		guinea pigs, i.p.	Wagner 1984 <sup>[130]</sup>
DPPC, cholesterol and tocopheryl acid succinate dehydration/rehydration+ extrusion	<i>Dermatophagoides pteronyssinus</i> extract (Der p 1 and Der p 2)	therapeutic	Clinical trial s.c.	Alvarez 2002 <sup>[132]</sup> Basomba 2002 <sup>[133]</sup>
phosphatidylcholine, cholesterol, and phosphatidic acid dehydration/rehydration + ultra-sonication	<i>Artemisia scoparia</i> pollen extract	therapeutic	BALB/c mice, i.p.	Arora 1990-1998 <sup>[134-137]</sup> Sehra 1998 <sup>[138]</sup>
phosphatidylcholine, cholesterol, and phosphatidic acid dehydration/rehydration method	<i>Aspergillus fumigatus</i> glycoprotein (Af-gp)	therapeutic	BALB/c mice, s.c.	Nigam 2002 <sup>[140]</sup>
phosphatidylcholine, cholesterol, and L- $\alpha$ -tocopherol dehydration/rehydration method	<i>Dactylis glomerata</i> , <i>Dermatophagoides pteronyssinus</i> , and cat hair and dander	therapeutic	<i>in vitro</i> (human) and skin prick test	Genin 1994 <sup>[139]</sup>
DPPC, DPPE and cholesterol, Man3-DPPE dehydration/rehydration + extrusion	<i>Cryptomeria japonica</i> (Cry j 1, japanese cedar pollen)	prophylactic and therapeutic	BALB/c mice, i.d.	Ishii 2010 <sup>[145]</sup>
DPPC, cholesterol and Man-DPPE purchased	ovalbumin (OVA)	therapeutic	BALB/c mice, i.n.	Kawakita 2012 <sup>[146]</sup>
phosphatidylcholine, cholesterol, and didecyldioctadecylammonium bromide dehydration/rehydration method	<i>Periplaneta americana</i> crude extract and Per a 9 (cockroach allergen)	therapeutic	BALB/c mice, i.n.	Meechan 2013 <sup>[147]</sup>
DPPC dehydration/rehydration method	<i>Dermatophagoides siboney</i> , Der s 1 and Der s 2	therapeutic	BALB/c mice, i.p.	Calderon 2006 <sup>[141]</sup>
DPPC, cholesterol, and optional dicetylphosphate or stearylamine dehydration/rehydration + extrusion	<i>Dermatophagoides pteronyssinus</i> , <i>Lolium perenne</i> , <i>Phleium pretense</i> , <i>Parietaria Judaica</i> , <i>Artemisia vulgaris</i> , and cat dander extract	therapeutic	BALB/c mice, s.c.	Audera 1991 <sup>[128]</sup>

## 1.2 Nanoparticles for Allergen-specific Immunotherapy

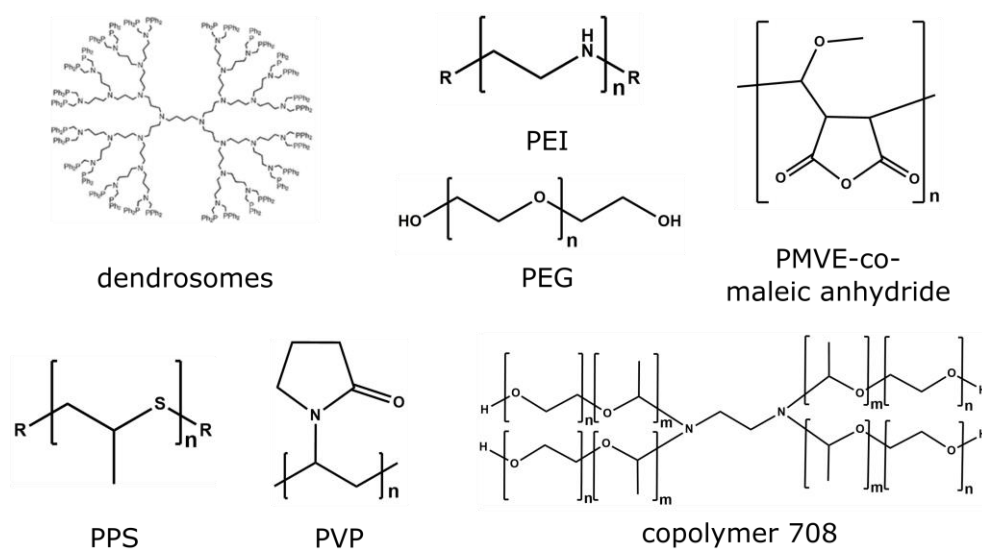
phosphatidylcholine, cholesterol, diacetylphosphate, and L- $\alpha$ -tocopherol dehydration/rehydration method	5 grass pollens (orchard, timothy, sweet vernal, rye, and meadow grasses) or Dermatophagoides pteronyssinus extract	therapeutic	clinical trial, skin prick test, s.c.	Galvain 1999 <sup>[142]</sup>
DOTIM (octadecenoyloxy [ethyl-2-heptadecenyl-3-hydroxyethyl] imidazolium chloride and cholesterol dehydration/rehydration + extrusion	feline IL-2 cDNA	therapeutic	cats, i.p.	Veir 2006 <sup>[149]</sup>
distearoylphosphatidylcholine (DSPC) and cholesterol dehydration/rehydration + extrusion	OVA coupled to the liposome surface, optionally DOX loaded	therapeutic	BALB/c mice, i.v.	Ichikawa 2007 <sup>[151]</sup> 2013 <sup>[152]</sup>
Didodecyldimethylammonium bromide, phosphatidylcholine, and cholesterol dehydration/rehydration method	native Fel d 1 or crude cat hair extract	therapeutic	BALB/c mice, i.n.	Tasaniyananda 2016 <sup>[143]</sup>
phosphatidylcholine or DSPC, cholesterol, and dicetylphosphate dehydration/rehydration method	OVA	therapeutic	BALB/c mice, i.g. (intragastric)	Ouadahi 1997 <sup>[144]</sup>
phosphatidylcholine and cholesterol dehydration/rehydration + extrusion	<i>Dreschlera (Helminthosporium) monoceras</i> extract	possible delivery platform		Cabral 2004 <sup>[153]</sup>
different lipids dehydration/rehydration method	different allergens covalently linked to lipids	possible delivery platform		Wojdani 1991 <sup>[154]</sup>
DPPC, phosphatidyl glycerol and cholesterol dehydration/rehydration method	<i>Dermatophagoides Pteronyssinus</i> extract	possible delivery platform		McWilliam 1989 <sup>[155]</sup>
DOTIM (octadecenoyloxy{ethyl-2-heptadecenyl-3-hydroxyethyl} imidazolium chloride) and cholesterol dehydration/rehydration + extrusion	CpG-DNA and several allergen extracts	therapeutic	dogs, i.d.	Mueller 2005 <sup>[148]</sup>
DOTAP, cholesterol, protamine, CpG dehydration/rehydration + sonication	recombinant hybrid molecule	therapeutic	BALB/c mice, s.c.	Nouri 2015 <sup>[150]</sup>



virus-like particles (bacteriophage Qb coat protein) spontaneous assembly	TLR9 ligands (CpG)	therapeutic	clinical trial, s.c.	Klimek 2011 <sup>[158]</sup>
virus-like particles (bacteriophage Qb coat protein) spontaneous assembly	Der p 1 allergen	prophylactic and therapeutic	clinical trial, i.m. or s.c.	Senti 2009 <sup>[162]</sup> Kündig 2006 <sup>[161]</sup>
virus-like particles (bacteriophage Qb coat protein) spontaneous assembly	Fel d 1	prophylactic	BALB/c mice, s.c.	Schmitz 2009 <sup>[163]</sup>
adeno-associated virus- like particles Spontaneous assembly	OVA	prophylactic	BALB/c mice, s.c.	Manzano- Szalai 2014 <sup>[164]</sup>

### 3 Non-biodegradable Nanostructures

Non-biodegradable polymers find wide application in everyday life as bottles, packaging materials, plastic films, toys, and hundreds of other applications. Only a few materials used for AIT are described in literature so far. Inorganic nanoparticles have physical and structural properties that can be tailored for the desired interactions with biological systems. Surface coating of inorganic NPs inaugurates pathways for diagnosis and as delivery systems.<sup>[168; 169]</sup> In AIT, most inorganic nanoparticles do not have an exclusive influence on the allergy but act in a rather general way immunomodulatory.



## Non-biodegradable Nanostructures

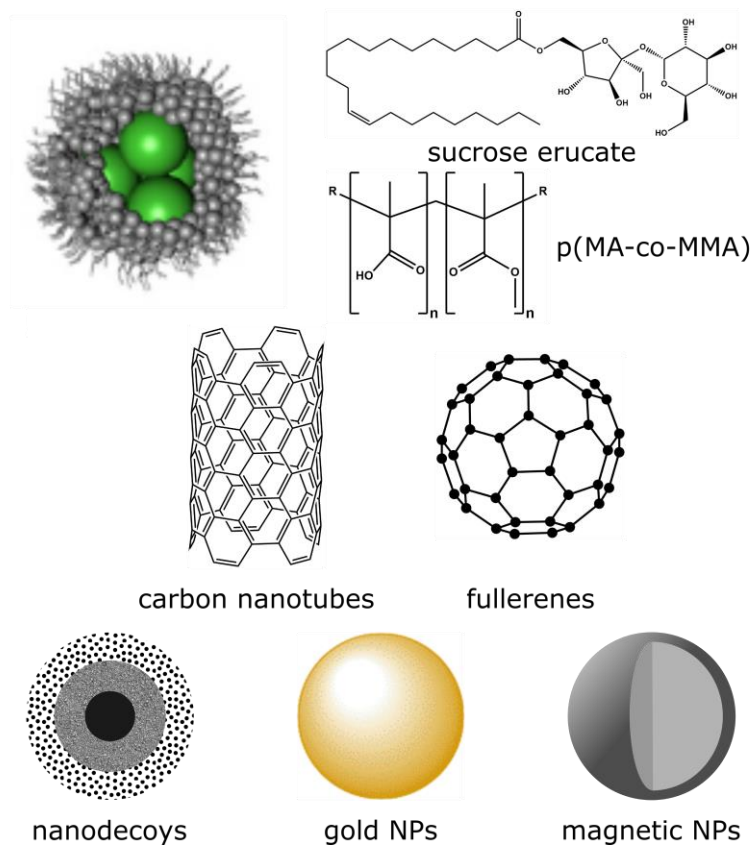


Figure 5. Overview of non-biodegradable polymers used in AIT. Enteric-coated nanoparticles, reprinted from Ref. <sup>[170]</sup> with permission from Elsevier.

### 3.1 Polymer Nanoparticles

#### 3.1.1 Poly(propylene imine) dendrosomes

Dendrimers, which are symmetrically branched polymer structures, were investigated as drug delivery systems.<sup>[171–173]</sup> Balenga *et al.* presented a dendrimer made from poly(propylene imine) loaded with Bet v 1a gene. Vaccination of mice with these nanotransporters resulted in plasmid release and thereby decreased specific IgE combined with balanced Th1/Th2 response.<sup>[174]</sup>

Another possible delivery platform made of guanidine-terminated dendrimers is presented by Kojima *et al.*<sup>[175]</sup> The dendrimer contains an amyloid-promoting peptide derived from the helix B region of OVA, which acts as an anchoring point for the OVA protein and is responsible for NP formation. The NPs effectively associate with RAW264 cells, but unfortunately no further immunological tests are shown. In both cases, it is likely that the cargo is transported by several molecules that assemble to form NPs, not by one dendrimer molecule itself.

#### 3.1.2 Poly(propylene sulfide) NPs

The therapy with allergen-unspecific CpG coupled in a poly(propylene sulfide) (PPS) NP was investigated by Ballester *et al.* Independent of a preventive or therapeutic experimental setup, they observed an enhanced recruitment of activated DCs and a shift towards Th1 immunity which was superior compared to free CpG.<sup>[176]</sup>

#### 3.1.3 Poly(ethylene imine)

Garaczi *et al.* assembled nanoparticles by mixing poly(ethylene imine) with OVA pDNA. The NPs migrated to the lymph nodes, cells that internalized the NPs express the antigens and present the epitopes to naïve T cells. In a preventive approach in a murine allergic rhinitis model, NPs were administered topically resulting in reduction of nasal symptoms of about 50% and a balanced Th1/Th2 response.<sup>[177]</sup>

#### 3.1.4 Poly(vinylpyrrolidone)

Madan *et al.* encapsulated fungal allergen *A. fumigatus* in poly(vinylpyrrolidone) (PVP) NPs. The authors could show intact integrity and immunoreactivity of the allergens after entrapment in nanoparticles, and a sustained allergen release in 9 weeks. Mice immunized with these NPs in a single dose showed decreased specific IgE as well as persisting IgG levels.<sup>[178]</sup>

### 3.1.5 Poly(methyl vinyl ether-co-maleic anhydride)

Gantrez® AN nanoparticles made from poly(methyl vinyl ether-(PMVE)-co-maleic anhydride) were loaded with OVA as model allergen and in some cases with LPS as immunomodulator. In the first publication, the authors compared OVA encapsulated vs. OVA-coated NPs and reported a shift towards Th1 cytokine response in mice mainly in the formulation that contained the antigen inside.<sup>[179]</sup> In further studies, they proved that immunization with their NPs protected mice from anaphylactic shock and observed increased IgG2a and IgG1 levels.<sup>[180]</sup> Although there was no strong difference with regard to the histamine release and temperature decrease between OVA and LPS encapsulated or coated NPs, full protection against anaphylaxis and survival of the mice was only achieved by OVA plus LPS entrapped NPs.<sup>[181]</sup> The authors confirmed the application of Gantrez® AN nanoparticles in AIT by encapsulating the clinical relevant allergen *L. perenne*, and treated pre-sensitized mice with this formulation. Likewise, the therapy resulted in induced Th1 responses and a decreased mortality rate following allergen challenge.<sup>[182]</sup>

### 3.1.6 Poly(ethylene oxide)-poly(propyleneoxide)-NHC2H4NH- poly(propyleneoxide)-poly(ethylene oxide)

Poloxamine nanospheres loaded with Der f 1 plasmid were tested by Beilvert *et al.* regarding therapeutic effect on asthmatic mice. The authors observed a reduction of airway hyperresponsiveness and a decrease in inflammatory cytokines.<sup>[183]</sup>

### 3.1.7 Enteric-coated NPS (solid-in-oil (S/O) nanodispersion)

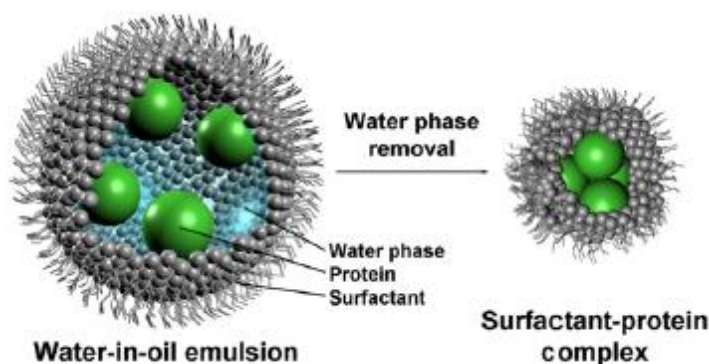


Figure 6. Synthesis of enteric-coated nanoparticles, reprinted from Ref. <sup>[170]</sup> with permission from Elsevier.

### 3.1.7.1 Sucrose erucate

An interesting method to prepare nano-sized peptide-surfactant complexes by solid-in-oil nanodispersions with proteins was reported by Tahara *et al.*<sup>[170]</sup> Kitaoka *et al.* prepared a nanodispersion with Japanese cedar allergen by the same method, which facilitates skin penetration of the allergen peptide and suppressed IgE levels in mice.<sup>[184]</sup>

### 3.1.7.2 Poly(methacrylate-methyl methacrylate) copolymer

Acrylamides and Methacrylamides are also widely used for drug delivery applications, e.g. Eudragit®, a copolymer of methacrylic acid and methylmethacrylate used as gastro-resistant capsules in drug delivery. Litwin *et al.* conducted several clinical studies with ragweed pollen encapsulated in polymethacrylic acid co-polymers NPs. For the NP preparation, the authors spray-coated a sugar starch core with allergen dissolved in poly(vinyl pyrrolidone) and enterocoated the NP with polymethacrylic acid co-polymers. Human volunteers treated with the encapsulated allergen in AIT produced high titers of allergen-specific IgG antibodies and showed no increase in specific IgE antibodies. The therapy was possible without side effects and decreased symptomatic medication.<sup>[185; 186]</sup> The same nanoparticle system was applied for encapsulation of timothy grass pollen by TePas *et al.* The authors discovered additionally to decreased medication and symptom scores in *in vitro* experiments with blood cells of the volunteers resulted in a reduced allergen-specific T cell proliferation and IL-5 mRNA production.<sup>[183]</sup>

The same method was applied 25 years earlier by Wheeler *et al.* The authors utilized methacrylic acid-methylmethacrylic acid copolymer as surfactant. The enteric coated grass pollen allergen induced increased secondary antibody responses upon oral treatment of pre-sensitized guinea pigs.<sup>[194]</sup> The authors annotated that this system required unacceptably high amounts of formulation for any benefit.<sup>[189; 190]</sup>

### 3.1.8 Poly(ethylene glycol) (PEG)

The most prominent synthetic water-soluble polymer is poly(ethylene glycol) (PEG), which is widely used in pharmaceutical applications. PEG is determined as the “gold standard” in biomedical applications and received this status because of its unique properties.<sup>[191]</sup> As PEG is considered a non-biodegradable polymer, cleavage sites needs to be introduced for controlled delivery of proteins in AIT. Acid-labile units were introduced into the PEG backbone by Pohlit *et al.* Nanogels prepared from PEG-acetal-dimethacrylate molecular building blocks showed

targeted delivery and the potential to induce T cell proliferation concurrently with allergen shielding from recognition by IgE antibodies in human *in vitro* experiments.<sup>[192]</sup>

### 3.2 Carbon-based NPs

#### 3.2.1 Carbon Nanotubes

Carbon nanotubes are extensively investigated in the field of drug delivery, especially in tumor-targeting and as biosensors. The toxicity and influence on the immune system is controversially discussed.<sup>[193]</sup> Laverny *et al.* incubated human PBMCs from allergic donors with allergen and with or without multi-walled carbon nanotubes (MWCNTs). Cytokine release was not altered by MWCNTs alone but in combination with allergen, IL-5 secretion was inhibited and differentiation of monocytes into functional DC was altered. The authors concluded that MWCNTs may either promote or suppress immune responses.<sup>[194]</sup> In another study Ronzani *et al.* investigated the effect of MWCNTs on asthma. The authors found a worsening effect of MWCNTs when co-administered with house dust mite allergen on allergen-induced systemic immune response and airway inflammation.<sup>[195]</sup> Whether the immune system is activated or not by MWCNTs depends on diameter and functionalization. Some MWCNTs are cell specific immunomodulatory systems, and may therefore be suitable adjuvants, as Pescatori *et al.* described.<sup>[196]</sup>

#### 3.2.2 Fullerenes

For several decades, fullerenes, a carbon allotrope, have been investigated for possible application in biotechnology and medicine. Ryan *et al.* described a negative regulator function of C60 fullerene on mast cells and basophils, which showed an inhibition of IgE dependent mediator release. Due to hindrance of signaling molecules and cytoplasmic reactive oxygen species levels, fullerenes prevented the *in vivo* release of histamine and anaphylaxis.<sup>[197]</sup> Norton *et al.* reported that pre-sensitized mice treated with tetraglycolate fullerenes show reduced airway inflammation, eosinophilia, and bronchoconstriction. The authors investigated the inhibition mechanism and found out that their fullerenes triggered the production of an anti-inflammatory P-450 eicosanoid metabolite.<sup>[198; 199]</sup> These two reports reveal the possibility to use fullerenes for allergic symptom alleviation.

Fullerenes have also been tested as immunomodulator as an alternative for AIT. Kaidashev *et al.* treated pre-sensitized mice with fullerenes or OVA-fullerenes and observed reduced specific IgE levels, eosinophilic infiltration, and pathological changes in the lungs.<sup>[200; 201]</sup> Another therapeutic

approach was described by Shershakova *et al.* Upon treatment of pre-sensitized mice with water-soluble form of C60 fullerene, the authors observed a shift in the cytokine production from Th2 to Th1. Additionally, Foxp3 and filaggrin mRNA expression was increased and eosinophil and leucocyte infiltration was reduced. The treatment was more effective with epicutaneous compared to subcutaneous application.<sup>[202]</sup>

### 3.3 Metal-based NPs

#### 3.3.1 Gold NPs

Gold NPs are known for their application as biosensors and gene delivery vehicles, and in general for their anti-inflammatory and anti-oxidant effects.<sup>[203; 204]</sup> Barreto *et al.* investigated the therapeutic effect of gold NPs administered to mice prior to allergen challenge. Gold NPs inhibited accumulation of inflammatory cells, mucus production, and production of pro-inflammatory cytokines and reactive oxygen species.<sup>[205]</sup>

#### 3.3.2 Dextran-coated magnetic NPs

Magnetic NPs combine the advantage of good detectability for imaging purposes and drug delivery and gained attention e.g. in hyperthermia-based therapy.<sup>[206; 207]</sup> Marengo *et al.* presented a possible delivery platform for AIT made of  $Mn_{0.8}Zn_{0.2}Fe_2O_4$  NPs coated with carboxymethyl dextran and bovine  $\beta$ -lactoglobulin (BLG) or ovomucoid. They observed higher uptake of the BLG-conjugated MNPs compared to non-conjugated MNPs and confirmed internalization by confocal laser scanning microscopy.<sup>[208]</sup>

#### 3.3.3 Calcium-phosphate-based NPs

##### 3.3.3.1 Nanodecoy

Nanodecoys consist of a solid core made of hydroxyl apatite which provides structural stability, and a carbohydrate coating to which peptides and proteins can adsorb.<sup>[209]</sup> Ultrafine nanodecoys coated with trehalose and adsorbed by ovalbumin were prepared by Pandey *et al.*, also called aquasomes. Pre-sensitized mice treated with aquasomes showed lower levels of IgE, serum histamine, higher survival rate and reduced symptoms during anaphylaxis induction.<sup>[210]</sup>

### 3.4 Conclusion non-biodegradable polymers

Non-biodegradable polymers as drug delivery systems for allergen or allergen-DNA possess potential but the whereabouts of the carrier needs to be thoroughly investigated. As these materials do not naturally degrade in the body, they are usually biocompatible and no possible toxic degradation products are formed. This advantage opens the way for applications in e.g. implants and catheters. Due to repeated NP application during AIT, discharging of nanoparticle remnants from the body is inevitable, and degradation may be promoted by artificially enclosed predefined degradation points. A polymer with great impact on drug delivery but not in AIT yet is poly(methyl methacrylate) PMMA.<sup>[211]</sup> Positively charged polymers, such as polyethylenimine (PEI) and poly(L-lysine) show a common draw back as drug delivery materials as they often show cell toxicity, which might explain the few reports of these materials in drug delivery.<sup>[212]</sup> In the last decades, the amount of water-soluble non-degradable synthesized polymers has expanded incredibly. Some of them are currently explored with regard to their potential as drug delivery systems. To name only a few of them, poly(vinyl alcohol),<sup>[213]</sup> with the advantage of high stability and many hydroxyl groups available, poly(vinyl pyrrolidone),<sup>[214]</sup> poly(acrylic acid), poly(acrylamides), N-(2-Hydroxypropyl) methacrylamide, poly(divinyl ether-co-maleic anhydride), and poly(oxazoline)s are possible materials for drug delivery systems.<sup>[166]</sup> Only few systems of inorganic NPs are described for AIT so far. Inorganic NPs may contribute with structural properties desirable during AIT like the intrinsic Th1 activating effect or the option for facile modification. The fate of inorganic nanostructure is of particular importance as a lack of elimination from the body may result in undesired side effects. Furthermore, the impact of highly anisotropic NPs on cells needs to be investigated in detail.

*Table 3.* Overview over nanoparticles made from non-biodegradable polymers for allergen-specific immunotherapy.

Nanoparticle composition and manufacturing method	Cargo	Vaccination approach	Species/ Route	Reference
dendrosome Den123 amphiphilic polymer Self-assembly	Bet v1 gene	prophylactic	BALB/c mice, s.c.	Balenga 2006 <sup>[174]</sup>
guanidine-terminated dendrimers	amyloid-promoting peptide derived from OVA	possible delivery platform	<i>in vitro</i> , no immunological readout	Kojima 2015 <sup>[175]</sup>



pluronic-stabilized poly(propylene sulfide) NPs, surface conjugation of CpG	CpG	prophylactic and therapeutic	C57BL/6 mice, injections i.n.	Ballester 2015 <sup>[176]</sup>
polyethylenimine containing 3% mannobiose NPs self-assembly	synthetic plasmid OVA pDNA	prophylactic	BALB/c mice, patch treatment (administered topically)	Garaczi 2013 <sup>[177]</sup>
poly(vinylpyrrolidone) NPs reverse micelles method	<i>A. fumigatus</i> allergen	prophylactic	BALB/c mice, s.c.	Madan 1997 <sup>[178]</sup>
poly(methyl vinyl ether-co-maleic anhydride) NPs (Gantrez® AN NPs) solvent displacement method	OVA and LPS (immune-modulator)	prophylactic and therapeutic	BALB/c mice, orally or i.d.	Gomez 2006 <sup>[179]</sup> 2007 <sup>[180]</sup> 2008 <sup>[181]</sup>
poly(methyl vinyl ether-co-maleic anhydride) NPs (Gantrez® AN NPs) solvent displacement method	<i>Lolium perenne</i> extract and LPS	therapeutic	BALB/c mice, i.d.	Gomez 2009 <sup>[182]</sup>
PEO-PPO-ethylene diamine-PPO-PEO (block copolymer 704) Self-assembly	Der f 1 plasmid	prophylactic and therapeutic	BALB/c mice, i.m.	Beilvert 2012 <sup>[183]</sup>
solid-in-oil (S/O) nanodispersion with sucrose erucate as surfactant	<i>Cryptomeria japonica</i> peptide	therapeutic	B10.S mice, transcutaneous administration	Kitaoka 2015 <sup>[184]</sup>
poly(vinyl pyrrolidone) on sugar starch core, enterocoated with polymethacrylic acid co-polymers	short ragweed pollen extracts or timothy grass pollen	therapeutic	clinical trial, orally	Litwin 1996 <sup>[185]</sup> 1997 <sup>[186]</sup> TePas 2004 <sup>[187]</sup>
solid-in-oil nanodispersion MA-MMA-copolymer (Eudragit L-100) as surfactant	grass pollen extract	therapeutic	guinea pigs, administered orally clinical trial	Wheeler 1987 <sup>[188]</sup> Horak 1987 <sup>[189]</sup>
PEG-acetal-DMA-NPs Liposomes as templates	OVA, grass pollen/ house dust mite allergen	possible delivery platform	<i>in vitro</i> human	Pohlitz 2015 <sup>[192]</sup>

## 1.2 Nanoparticles for Allergen-specific Immunotherapy

multi-walled carbon nanotubes	none	possible immunomodulatory nanostructure	<i>in vitro</i> , human PBMCs	Laverny 2013 <sup>[194]</sup>
multi-walled carbon nanotubes	mixed with house dust mite allergen	prophylactic	BALB/cByJ mice, injection	Ronzani 2014 <sup>[195]</sup>
multi-walled carbon nanotubes	none	possible immunomodulatory nanostructure	<i>in vitro</i> , cell lines and PBMCs	Pescatori 2013 <sup>[196]</sup>
C(60) fullerenes	none	blocking signalling for mediator release in mast cells and basophils	<i>in vitro</i> human, <i>in vivo</i> mice	Ryan 2007 <sup>[197]</sup>
C(70)-tetraglycolate fullerenes	none	blocking signalling for mediator release in mast cells and basophils	C57BL/6 and BALB/c mice, i.n. and human mast cells <i>in vitro</i>	Norton 2010 <sup>[198]</sup> 2012 <sup>[199]</sup>
C(60) fullerenes	OVA-coupled to the surface	therapeutic	mice, i.m.	Kaidashev 2010 <sup>[200]</sup> Bobrova 2012 <sup>[201]</sup>
C(60) fullerenes	none	therapeutic	BALB/c mice, s.c. or e.c.	Shershakova 2016 <sup>[202]</sup>
gold NPs	none	therapeutic	Swiss-Webster (outbred) and A/J (inbred) mice	Barreto 2015 <sup>[205]</sup>
dextran-coated magnetic nanoparticles (MNPs) chemical coprecipitation method	bovine $\beta$ -lactoglobulin (BLG) and ovomucoid (OM)	possible delivery platform	<i>in vitro</i> human monocytes	Marengo 2011 <sup>[208]</sup>
hydroxy apatite NPs, carbohydrate modified (aquasomes) Self-precipitation method	ovalbumin (OVA) adsorbed	prophylactic and therapeutic	BALB/c mice, i.d.	Pandey 2011 <sup>[210]</sup>

## Summary and Outlook

Although being the only disease modifying therapy for allergic rhino conjunctivitis and asthma so far, allergen-specific immunotherapy (AIT) suffers from potentially severe side effects occurring during treatment. Prevention of these side effects resulting in safer therapy as well as a more efficient treatment is a main goal for improving strategies in AIT. Approaches to achieve this goal tested so far include the therapy with modified allergens or peptides or co-administration of anti-IgE-antibodies.<sup>[10]</sup> Another concept as an alternative to AIT aims at shifting the imbalance of T cell subtypes towards a more balanced one by unspecific induction of Th1 cells with adjuvant moieties, e.g. immunostimulatory DNA, monophosphoryl lipid A, or lactic acid bacteria. Nanoparticles can provide delivery function and in some cases adjuvant function at once; they may prevent enzymatic degradation and IgE cross-linking of the cargo molecule, can act as or co-deliver adjuvants and may have an additional targeting function.

AIT with proteins and DNA molecules protected by a variety of polymer structures and nanomaterials has been investigated so far. The most intensively investigated materials for NPs are rather apolar, like water-insoluble PLGA and chitosan. Degradation of these materials and thereby cargo release depends on hydrolytic/enzymatic degradation and may last several weeks.<sup>[215]</sup> This timeframe may be suitable for a depot function with sustained release behavior, but due to the unspecific degradation behavior shelf-life in aqueous solutions is affected. The need for nanoparticle engineering of structures that show extended shelf-life, targeted drug delivery, as well as desired degradation behavior, exists. This can be achieved e.g. by designing materials susceptible to external stimuli like reducing conditions, enzymes, pH changes, or light.<sup>[216–222]</sup> Stimuli-responsive materials, possibly with attached target functions like antibodies, ensure delivery of the cargo at the targeted site of action with less cargo release in a non-specific way (i.e. before administration or at undesired sites, which can result in immune activation and side effects).<sup>[223]</sup> Only a nanoparticle that shields the cargo from detection by the immune system and that is stable until it reaches its destination could prevent side effects during AIT. Another field where improvements are required are the preparation of sterile and endotoxin-free formulations for testing in *in vivo* experiments. Sterilization of NPs may be problematic when implemented after the NP synthesis process as it may alter the properties of the NP and/or the cargo.<sup>[224]</sup> Storage of these formulations needs also to be taken into account considering applicability for patients. Moreover, characterization and understanding of protein corona formation is required to accomplish the desired delivery and targeting.

Certainly, research of nanoparticles in AIT will be intensified as motivated by the promising results obtained so far and the huge diversity of nanoparticle formulations already described for other drug delivery purposes. This is exemplified for the usage of self-assembly processes,<sup>[225–227]</sup> nature-mimicking structures,<sup>[228; 229]</sup> polymer nanogels,<sup>[230; 231]</sup> or multilayer capsules,<sup>[232–234]</sup> to name only a few possibilities.

Improvements from other fields of NP engineering may be exploited for targeting cells or organs, and degradation mechanisms for predetermined degradation. Findings concerning the effects of NPs on the immune system made in other contexts can be transferred to application in AIT and knowledge regarding possible effects of long-term compatibility and immunogenicity upon repeated injections need to be broadened.

### Acknowledgements

HP is a recipient of a fellowship through funding of the Excellence Initiative (DFG/GSC 266) in the context of the graduate school of excellence “MAINZ” (Materials Science in Mainz) and the Max Planck Graduate Center with the Johannes Gutenberg University Mainz (MPGC).

### Abbreviations

AIT, allergen-specific immunotherapy; APC, antigen-presenting cell; BAL, bronchoalveolar lavage; BLG,  $\beta$ -lactoglobulin; BSA, bovine serum albumin; CLSM, confocal laser scanning microscopy; DARPIs, designed ankyrin repeat proteins; DCs, dendritic cells; DNA, deoxyribonucleic acid; DOTAP, *N*-[1-(2,3-Dioleoyloxy)propyl]-*N,N,N*-trimethylammonium chloride; DOTIM, octadecenolyoxy[ethyl-2-heptadecenyl-3-hydroxyethyl] chloride; DOX, doxorubicin; DPPC, dipalmitoylphosphatidylcholine; DPPE, 1,2-dipalmitoyl-*sn*-glycero-3-phosphoethanolamine; e.c., epicutaneous; ELISA, Enzyme Linked Immunosorbent Assay; Fc $\epsilon$ RI, high-affinity IgE receptor; IFN, interferon; Ig, immunoglobulin; IL, interleukin; i.d., intradermal; i.g., intragastrical; i.m., intramuscular; i.n., intranasal; i.p., intraperitoneal; i.v., intravenous; LAB, lactic acid bacteria; LPS, lipopolysaccharide; mPEG, methyl-poly(ethylene glycol); MPL-A, monophosphoryl lipid A; MWCNTs, multi-walled carbon nanotubes; NP, nanoparticle; ODN, oligodeoxynucleotide; OML, oligomannose-coated liposome; OVA, ovalbumin; PBMCs, peripheral blood mononuclear cell; PCL, poly(caprolactone); PEG, poly(ethylene glycol); PEI, poly(ethylene imine); PGA, poly(glutamic acid); PHEA, Polyhydroxyethylaspartamide; PGA, poly(glutamic acid); PLA, phospholipase A; PLGA, poly(lactic-co-glycolic acid); P(MA-co-MMA), poly(methacrylate-methyl methacrylate) copolymer;

PMVE, poly(methyl vinyl ether); p.o., per os (orally); PPS, poly(propylene sulfide); PVP, poly(vinylpyrrolidone); s.c., subcutaneous; s.l., sublingual; TLR, toll-like receptor; TGF, transforming growth factor; Th, T helper cell; Treg, regulatory T cell; VLP, virus-like particle.

### Financial & competing interests' disclosure

HP, HF and JS: One patent is granted on degradable PEG-nanocarriers "Spaltbare Polyethylenglykol-(PEG)-Makromoleküle zum Einschluss von (Glyko-) Proteinen/Antigenen/Allergenen in abbaubaren Polyethylenglykol-(PEG)-Nanopartikeln sowie Verfahren zu ihrer Herstellung" (publication number: DE 10 2013 015 112 A1). The author has no other relevant affiliations or financial interest in or financial conflict with the subject matter or materials discussed in the manuscript apart from the disclosed. No writing assistance was utilized in the production of this manuscript.

HP and JS received research funding or speaker fees from manufacturers of AIT products.

### References

- [1] Coombs, R. R. A.; Gell, P. G. H., Clinical Aspects of Immunology, *Immunology*, **1975**, 3, 761–781.
- [2] Haahtela, T.; Holgate, S.; Pawankar, R.; Akdis, C. A.; Benjaponpitak, S.; Caraballo, L.; Demain, J.; Portnoy, J.; Hertzen, L. von, The biodiversity hypothesis and allergic disease, *World Allergy Organization J.*, **2013**, 6, 3–21.
- [3] Galli, S. J.; Tsai, M.; Piliponsky, A. M., The development of allergic inflammation, *Nature*, **2008**, 454, 445–454.
- [4] Ring, J.; Gutermuth, J., 100 years of hyposensitization, *Allergy*, **2011**, 66, 713–724.
- [5] Akdis, M.; Akdis, C. A., Mechanisms of allergen-specific immunotherapy, *J. Allergy Clin. Immunol.*, **2014**, 133, 621–631.
- [6] Lambrecht, B. N.; Hammad, H., The immunology of asthma, *Nat. Immunol.*, **2014**, 16, 45–56.
- [7] Ozdemir, C., Monoclonal antibodies in allergy; updated applications and promising trials, *Recent Pat. Inflamm. Allergy Drug Discov.*, **2015**, 9, 54–65.
- [8] Stokes, J. R.; Casale, T. B., The Use of Anti-IgE Therapy Beyond Allergic Asthma, *J. Allergy Clin. Immunol. Pract.*, **2015**, 3, 162–166.
- [9] Baumann, M. J.; Eggel, A.; Amstutz, P.; Stadler, B. M.; Vogel, M., DARPin against a functional IgE epitope, *Immunol. Lett.*, **2010**, 133, 78–84.

- [10] Manohar, M.; Nadeau, K. C., The Potential of Anti-IgE in Food Allergy Therapy, *Curr. Treat. Options Allergy*, **2014**, 1, 145–156.
- [11] Kim, B.; Eggel, A.; Tarchevskaya, S. S.; Vogel, M.; Prinz, H.; Jardetzky, T. S., Accelerated disassembly of IgE–receptor complexes by a disruptive macromolecular inhibitor, *Nature*, **2012**, 491, 613–617.
- [12] HayGlass, K. T.; Strejan, G. H., Antigen- and IgE Class-Specific Suppression Mediated by T Suppressor Cells of Mice Treated with Glutaraldehyde-Polymerized Ovalbumin, *Int. Arch. Allergy Immunol.*, **2004**, 71, 23–31.
- [13] Okuda, K.; Urabe, I.; Yamada, Y.; Okada, H., Reaction of glutaraldehyde with amino and thiol compounds, *J. Ferment. Bioeng.*, **1991**, 71, 100–105.
- [14] Olivier, C. E.; Lima, R. P.; Pinto, D. G.; Santos, R. A.; Silva, G. K.; Lorena, S. L.; Villas-Boas, M. B.; Netto, F. M.; Zollner, R. L., In search of a tolerance-induction strategy for cow's milk allergies, *Clinics*, **2012**, 67, 1171–1179.
- [15] Marth, K.; Focke-Tejkl, M.; Lupinek, C.; Valenta, R.; Niederberger, V., Allergen Peptides, Recombinant Allergens and Hypoallergens for Allergen-Specific Immunotherapy, *Curr. Treat. Options Allergy*, **2014**, 1, 91–106.
- [16] Focke-Tejkl, M.; Valenta, R., Safety of engineered allergen-specific immunotherapy vaccines, *Curr. Opin. Allergy Clin. Immunol.*, **2012**, 12, 555–583.
- [17] El-Qutob, D.; Reche, P.; Subiza, J. L.; Fernández-Caldas, E., Peptide-based allergen specific immunotherapy for the treatment of allergic disorders, *Recent Pat. Inflamm. Allergy Drug Discov.*, **2015**, 9, 16–22.
- [18] Valenta, R.; Campana, R.; Focke-Tejkl, M.; Niederberger, V., Vaccine development for allergen-specific immunotherapy based on recombinant allergens and synthetic allergen peptides, *J. Allergy Clin. Immunol.*, **2016**, 137, 351–357.
- [19] Jongejan, L.; van Ree, R., Modified Allergens and their Potential to Treat Allergic Disease, *Curr. Allergy Asthma Rep.*, **2014**, 14, 478–488.
- [20] Wie, S. I.; Wie, C. W.; Lee, W. Y.; Fillion, L. G.; Schon, A. H.; Akerblom, E., Suppression of reaginic antibodies with modified allergens. III. Preparation of tolerogenic conjugates of common allergens with monomethoxypolyethylene glycols of different molecular weights by the mixed anhydride method, *Int. Arch. Allergy Appl. Immunol.*, **1981**, 64, 84–99.
- [21] Butterfield, J. H.; Gleich, G. J.; Yunginger, J. W.; Zimmermann, E. M.; Reed, C. E., Immunotherapy with short ragweed fraction A:D-glutamic acid:D-lysine polymer in ragweed hay fever, *J. Allergy Clin. Immunol.*, **1981**, 67, 272–278.
- [22] Jensen-Jarolim, E., Aluminium in Allergies and Allergen immunotherapy, *World Allergy Organization J.*, **2015**, 8, 7–12.
- [23] Fili, L.; Cardilicchia, E.; Maggi, E.; Parronchi, P., Perspectives in vaccine adjuvants for allergen-specific immunotherapy, *Immunol. Lett.*, **2014**, 161, 207–210.

- [24] Aryan, Z.; Rezaei, N., Toll-like receptors as targets for allergen immunotherapy, *Curr. Opin. Allergy Clin. Immunol.*, **2015**, 15, 568–574.
- [25] Vo, T.-S.; Kim, S.-K., Marine-derived polysaccharides for regulation of allergic responses, *Adv. Food Nutr. Res.*, **2014**, 73, 1–13.
- [26] Wang, Y.; Yamamoto, Y.; Shigemori, S.; Watanabe, T.; Oshiro, K.; Wang, X.; Wang, P.; Sato, T.; Yonekura, S.; Tanaka, S.; Kitazawa, H.; Shimosato, T., Inhibitory/suppressive oligodeoxynucleotide nanocapsules as simple oral delivery devices for preventing atopic dermatitis in mice, *Mol. Ther.*, **2015**, 23, 297–309.
- [27] Hayen, S. M.; Kostadinova, A. I.; Garssen, J.; Otten, H. G.; Willemsen, Linette E M, Novel immunotherapy approaches to food allergy, *Curr. Opin. Allergy Clin. Immunol.*, **2014**, 14, 549–556.
- [28] Gamazo, C.; Gastaminza, G.; Ferrer, M.; Sanz, M. L.; Irache, J. M., Nanoparticle based-immunotherapy against allergy, *Immunotherapy*, **2014**, 6, 885–897.
- [29] Zhang, Y.; Chan, H. F.; Leong, K. W., Advanced materials and processing for drug delivery, *Adv. Drug Deliv. Rev.*, **2013**, 65, 104–120.
- [30] Couvreur, P., Nanoparticles in drug delivery, *Adv. Drug Deliv. Rev.*, **2013**, 65, 21–23.
- [31] Irvine, D. J.; Hanson, M. C.; Rakhra, K.; Tokatlian, T., Synthetic Nanoparticles for Vaccines and Immunotherapy, *Chem. Rev.*, **2015**, 115, 11109–11146.
- [32] Shao, K.; Singha, S.; Clemente-Casares, X.; Tsai, S.; Yang, Y.; Santamaria, P., Nanoparticle-Based Immunotherapy for Cancer, *ACS Nano*, **2015**, 9, 16–30.
- [33] Zhao, L.; Seth, A.; Wibowo, N.; Zhao, C.-X.; Mitter, N.; Yu, C.; Middelberg, A. P., Nanoparticle vaccines, *Vaccine*, **2014**, 32, 327–337.
- [34] Flemming, A., Autoimmunity, *Nat. Rev. Immunol.*, **2016**, 16, 204–205.
- [35] Buschmann, M. D.; Merzouki, A.; Lavertu, M.; Thibault, M.; Jean, M.; Darras, V., Chitosans for delivery of nucleic acids, *Adv. Drug Deliv. Rev.*, **2013**, 65, 1234–1270.
- [36] Cano-Garrido, O.; Seras-Franzoso, J.; Garcia-Fruitós, E., Lactic acid bacteria, *Microb. Cell Fact.*, **2015**, 14, 137–148.
- [37] Craparo, E. F.; Bondi, M. L., Application of polymeric nanoparticles in immunotherapy, *Curr. Opin. Allergy Clin. Immunol.*, **2012**, 12, 658–664.
- [38] Makadia, H. K.; Siegel, S. J., Poly Lactic-co-Glycolic Acid (PLGA) as Biodegradable Controlled Drug Delivery Carrier, *Polymers*, **2011**, 3, 1377–1397.
- [39] Panyam, J.; Labhasetwar, V., Biodegradable nanoparticles for drug and gene delivery to cells and tissue, *Adv. Drug Deliv. Rev.*, **2003**, 55, 329–347.
- [40] Niu, X.; Zou, W.; Liu, C.; Zhang, N.; Fu, C., Modified nanoprecipitation method to fabricate DNA-loaded PLGA nanoparticles, *Drug Dev. Ind. Pharm.*, **2009**, 35, 1375–1383.

- [41] Karewicz, A., Polymeric and liposomal nanocarriers for controlled drug delivery. In: Dubruel, Peter; van Vlierberghe, Sandra, *Biomaterials for bone regeneration : novel techniques and applications*, Elsevier, Amsterdam, **2014**.
- [42] Albertsson, Ann-Christine, *Degradable aliphatic polyesters*. Springer, Berlin, New York, **2002**.
- [43] Batanero, E.; Barral, P.; Villalba, M.; Rodríguez, R., Biodegradable poly (dl-lactide glycolide) microparticles as a vehicle for allergen-specific vaccines: a study performed with Ole e 1, the main allergen of olive pollen, *J. Immunol. Methods*, **2002**, 259, 87–94.
- [44] Batanero, E.; Barral, P.; Villalba Mayte; Rodrigues, R., Encapsulation of Ole e 1 in biodegradable microparticles induces Th1 response in mice: a potential vaccine for allergy, *J. Control. Release*, **2003**, 92, 395–398.
- [45] Igartua, M.; Hernández, R. M.; Gutierrez, I.; Gascón, A. R.; Pedraz, J. L., Preliminary Assessment of the Immune Response to Olea europaea Pollen Extracts Encapsulated into PLGA Microspheres, *Pharm. Dev. Technol.*, **2002**, 6, 621–627.
- [46] Marazuela, E. G.; Prado, N.; Moro, E.; Fernández-García, H.; Villalba, M.; Rodríguez, R.; Batanero, E., Intranasal vaccination with poly(lactide-co-glycolide) microparticles containing a peptide T of Ole e 1 prevents mice against sensitization, *Clin. Exp. Allergy*, **2008**, 38, 520–528.
- [47] Fattal, E.; Pecquet, S.; Couvreur, P.; Andremont, A., Biodegradable microparticles for the mucosal delivery of antibacterial and dietary antigens, *Int. J. Pharm.*, **2002**, 242, 15–24.
- [48] Pecquet, S.; Leo, E.; Fritsché, R.; Pfeifer, A.; Couvreur, P.; Fattal, E., Oral tolerance elicited in mice by  $\beta$ -lactoglobulin entrapped in biodegradable microspheres, *Vaccine*, **2000**, 18, 1196–1202.
- [49] Martínez Gómez, Julia M; Fischer, S.; Csaba, N.; Kündig, T. M.; Merkle, H. P.; Gander, B.; Johansen, P., A protective allergy vaccine based on CpG- and protamine-containing PLGA microparticles, *Pharm. Res.*, **2007**, 24, 1927–1935.
- [50] Jilek, S.; Walter, E.; Merkle, H. P.; Corthésy, B., Modulation of allergic responses in mice by using biodegradable poly(lactide-co-glycolide) microspheres, *J. Allergy Clin. Immunol.*, **2004**, 114, 943–950.
- [51] Guérin, V.; Dubarryr, M.; Robic, D.; Brachet, F.; Rautureau, M.; André, C.; Bourbouze, R.; Tomé, D., Microsphere entrapped bee-venom phospholipase A2 retains specific IgE binding capacity: a possible use for oral specific immunotherapy, *J. Microencapsul.*, **2002**, 19, 761–765.
- [52] Trindade, R. A.; Kiyohara, P. K.; de Araujo, Pedro S; Bueno da Costa, Maria H, PLGA microspheres containing bee venom proteins for preventive immunotherapy, *Int. J. Pharm.*, **2012**, 423, 124–133.
- [53] Da Trindade, A.; Reginaldo, S.; Araujo, P. de; Helena Bueno-Da-Costa, M., Hoffmeister Ion Series Protected Bee Venom Proteins from Damages Induced by Microencapsulation Process, *Drug Deliv. Lett.*, **2012**, 2, 54–59.



- [54] Park, M.-H.; Kim, J.-H.; Jeon, J.-W.; Park, J.-K.; Lee, B.-J.; Suh, G.-H.; Cho, C.-W., Preformulation Studies of Bee Venom for the Preparation of Bee Venom-Loaded PLGA Particles, *Molecules*, **2015**, *20*, 15072–15083.
- [55] Sharif, S.; Wheeler, A. W.; O'Hagan, D. T., Biodegradable microparticles as a delivery system for the allergens of *Dermatophagoides pteronyssinus* (house dust mite): I. Preparation and characterization of microparticles, *Int. J. Pharm.*, **1995**, *119*, 239–246.
- [56] Xiao, X.; Zeng, X.; Zhang, X.; Ma, L.; Liu, X.; Yu, H.; Mei, L.; Liu, Z., Effects of *Caryota mitis* profilin-loaded PLGA nanoparticles in a murine model of allergic asthma, *Int. J. Nanomedicine*, **2013**, *8*, 4553–4562.
- [57] Joshi, V. B.; Adamcakova-Dodd, A.; Jing, X.; Wongrakpanich, A.; Gibson-Corley, K. N.; Thorne, P. S.; Salem, A. K., Development of a poly (lactic-co-glycolic acid) particle vaccine to protect against house dust mite induced allergy, *AAPS J.*, **2014**, *16*, 975–985.
- [58] Yu, H.-q.; Liu, Z.-g.; Yu, K.-Y.; Xu, Z.-Q.; Qiu, J., [Immunotherapy with recombinant house dust mite group 2 allergen vaccine inhibits allergic airway inflammation in mice], *Zhongguo Ji Sheng Chong Xue Yu Ji Sheng Chong Bing Za Zhi*, **2006**, *24*, 414–419.
- [59] Salari, F.; Varasteh, A.-R.; Vahedi, F.; Hashemi, M.; Sankian, M., Down-regulation of Th2 immune responses by sublingual administration of poly (lactic-co-glycolic) acid (PLGA)-encapsulated allergen in BALB/c mice, *Int. Immunopharmacol.*, **2015**, *29*, 672–678.
- [60] Takagi, I.; Nishimura, J.; Itoh, H.; Baba, S.; Kunimatsu, M.; Sasaki, M., Poly (lactic/glycolic acid) microspheres containing antigen as a novel and potential agent of immunotherapy for allergic disorders, *Allergy*, **1992**, *41*, 1388–1397.
- [61] Smarr, C. B.; Yap, W. T.; Neef, T. P.; Pearson, R. M.; Hunter, Z. N.; Ifergan, I.; Getts, D. R.; Bryce, P. J.; Shea, L. D.; Miller, S. D., Biodegradable antigen-associated PLG nanoparticles tolerate Th2-mediated allergic airway inflammation pre- and postsensitization, *Proc. Natl. Acad. Sci. USA*, **2016**, *113*, 5059–5064.
- [62] Diesner, S. C.; Wang, X.-Y.; Jensen-Jarolim, E.; Untersmayr, E.; Gabor, F., Use of lectin-functionalized particles for oral immunotherapy, *Ther. Deliv.*, **2012**, *3*, 277–290.
- [63] Walter, F.; Schöll, I.; Untersmayr, E.; Ellinger, A.; Boltz-Nitulescu, G.; Scheiner, O.; Gabor, F.; Jensen-Jarolim, E., Functionalisation of allergen-loaded microspheres with wheat germ agglutinin for targeting enterocytes, *Biochem. Biophys. Res. Commun.*, **2004**, *315*, 281–287.
- [64] Roth-Walter, F.; Schöll, I.; Untersmayr, E.; Fuchs, R.; Boltz-Nitulescu, G.; Weissenböck, A.; Scheiner, O.; Gabor, F.; Jensen-Jarolim, E., M cell targeting with *Aleuria aurantia* lectin as a novel approach for oral allergen immunotherapy, *J. Allergy Clin. Immunol.*, **2004**, *114*, 1362–1368.
- [65] Roth-Walter, F.; Schöll, I.; Untersmayr, E.; Ellinger, A.; Boltz-Nitulescu, G.; Scheiner, O.; Gabor, F.; Jensen-Jarolim, E., Mucosal targeting of allergen-loaded microspheres by *Aleuria aurantia* lectin, *Vaccine*, **2005**, *23*, 2703–2710.

- [66] Roth-Walter, F.; Bohle, B.; Schöll, I.; Untersmayr, E.; Scheiner, O.; Boltz-Nitulescu, G.; Gabor, F.; Brayden, D. J.; Jensen-Jarolim, E., Targeting antigens to murine and human M-cells with Aleuria aurantia lectin-functionalized microparticles, *Immunol. Lett.*, **2005**, 100, 182–188.
- [67] Schöll, I.; Weissenböck, A.; Förster-Waldl, E.; Untersmayr, E.; Walter, F.; Willheim, M.; Boltz-Nitulescu, G.; Scheiner, O.; Gabor, F.; Jensen-Jarolim, E., Allergen-loaded biodegradable poly(D,L-lactic-co-glycolic) acid nanoparticles down-regulate an ongoing Th2 response in the BALB/c mouse model, *Clin. Exp. Allergy*, **2004**, 34, 315–321.
- [68] Schöll, I.; Kopp, T.; Bohle, B.; Jensen-Jarolim, E., Biodegradable PLGA particles for improved systemic and mucosal treatment of Type I allergy, *Immunol. Allergy Clin. North Am.*, **2006**, 26, 349–364.
- [69] Zhang, X.-Q.; Dahle, C. E.; Weiner, G. J.; Salem, A. K., A comparative study of the antigen-specific immune response induced by co-delivery of CpG ODN and antigen using fusion molecules or biodegradable microparticles, *J. Pharm. Sci.*, **2007**, 96, 3283–3292.
- [70] Zhang, X.-Q.; Dahle, C. E.; Baman, N. K.; Rich, N.; Weiner, G. J.; Salem, A. K., Potent antigen-specific immune responses stimulated by codelivery of CpG ODN and antigens in degradable microparticles, *J. Immunother.*, **2007**, 30, 469–478.
- [71] San Roman, B.; Irache, J. M.; Gómez, S.; Gamazo, C.; Espuelas, S., Co-Delivery of Ovalbumin and CpG Motifs into Microparticles Protected Sensitized Mice from Anaphylaxis, *Int. Arch. Allergy Immunol.*, **2009**, 149, 111–118.
- [72] Maldonado, R. A.; LaMothe, R. A.; Ferrari, J. D.; Zhang, A.-H.; Rossi, R. J.; Kolte, P. N.; Griset, A. P.; O'Neil, C.; Altreuter, D. H.; Browning, E.; Johnston, L.; Farokhzad, O. C.; Langer, R.; Scott, D. W.; von Andrian, Ulrich H; Kishimoto, T. K., Polymeric synthetic nanoparticles for the induction of antigen-specific immunological tolerance, *Proc. Natl. Acad. Sci. USA*, **2015**, 112, 156–165.
- [73] Xiao, Y.; Yuan, M.; Zhang, J.; Yan, J.; Lang, M., Functional poly( $\epsilon$ -caprolactone) based materials: preparation, self-assembly and application in drug delivery, *Curr. Top. Med. Chem.*, **2014**, 14, 781–818.
- [74] San Roman, B.; Espuelas, S.; Gómez, S.; Gamazo, C.; Sanz, M. L.; Ferrer, M.; Irache, J. M., Intradermal immunization with ovalbumin-loaded poly-epsilon-caprolactone microparticles conferred protection in ovalbumin-sensitized allergic mice, *Clin. Exp. Allergy*, **2007**, 37, 287–295.
- [75] Jain, J. P.; Chitkara, D.; Kumar, N., Polyanhydrides as localized drug delivery carrier: an update, *Expert Opin. Drug Deliv.*, **2008**, 5, 889–907.
- [76] De Souza Rebouças, Juliana; Esparza, I.; Ferrer, M.; Sanz, M. L.; Irache, J. M.; Gamazo, C., Nanoparticulate adjuvants and delivery systems for allergen immunotherapy, *J. Biomed. Biotechnol.*, **2012**, 2012, 1–13.

- [77] De Souza Rebouças, Juliana; Irache, J. M.; Camacho, A. I.; Gastaminza, G.; Sanz, M. L.; Ferrer, M.; Gamazo, C., Immunogenicity of peanut proteins containing poly(anhydride) nanoparticles, *Clin. Vaccine Immunol.*, **2014**, 21, 1106–1112.
- [78] Sinha, V. R.; Trehan, A., Biodegradable microspheres for protein delivery, *J. Control. Release*, **2003**, 90, 261–280.
- [79] Scheicher, B.; Schachner-Nedherer, A.-L.; Zimmer, A., Protamine–oligonucleotide-nanoparticles, *Eur. J. Pharm. Sci.*, **2015**, 75, 54–59.
- [80] Pali-Schöll, I.; Szöllösi, H.; Starkl, P.; Scheicher, B.; Stremnitzer, C.; Hofmeister, A.; Roth-Walter, F.; Lukschal, A.; Diesner, S. C.; Zimmer, A.; Jensen-Jarolim, E., Protamine nanoparticles with CpG-oligodeoxynucleotide prevent an allergen-induced Th2-response in BALB/c mice, *Eur. J. Pharm. Biopharm.*, **2013**, 85, 656–664.
- [81] Zimmer; H Szöllösi; P Starkl; B Scheicher; C Stremnitzer; A Hofmeister; F Roth-Walter; A Lukschal; S C Diesner; E Jensen-Jarolim; I Pali-Schöll, Protamine-nanoparticles with CpG-ODN prevent an allergen-induced Th2-response in Balb/c mice, Conference paper, DOI: 10.13140/2.1.4914.1765, **2014**.
- [82] Uto, T.; Akagi, T.; Toyama, M.; Nishi, Y.; Shima, F.; Akashi, M.; Baba, M., Comparative activity of biodegradable nanoparticles with aluminum adjuvants, *Immunol. Lett.*, **2011**, 140, 36–43.
- [83] Akagi, T.; Kaneko, T.; Kida, T.; Akashi, M., Preparation and characterization of biodegradable nanoparticles based on poly( $\gamma$ -glutamic acid) with l-phenylalanine as a protein carrier, *J. Control. Release*, **2005**, 108, 226–236.
- [84] Broos, S.; Lundberg, K.; Akagi, T.; Kadowaki, K.; Akashi, M.; Greiff, L.; Borrebaeck, Carl A K; Lindstedt, M., Immunomodulatory nanoparticles as adjuvants and allergen-delivery system to human dendritic cells: Implications for specific immunotherapy, *Vaccine*, **2010**, 28, 5075–5085.
- [85] Kunda, N. K.; Alfagih, I. M.; Dennison, S. R.; Tawfeek, H. M.; Somavarapu, S.; Hutcheon, G. A.; Saleem, I. Y., Bovine serum albumin adsorbed PGA-co-PDL nanocarriers for vaccine delivery via dry powder inhalation, *Pharm. Res.*, **2015**, 32, 1341–1353.
- [86] Toita, R.; Nakao, K.; Mahara, A.; Yamaoka, T.; Akashi, M., Biodistribution of vaccines comprised of hydrophobically-modified poly( $\gamma$ -glutamic acid) nanoparticles and antigen proteins using fluorescence imaging, *Bioorg. Med. Chem.*, **2013**, 21, 6608–6615.
- [87] Civile, C.; Licciardi, M.; Cavallaro, G.; Giammona, G.; Mazzone, M. G., Polyhydroxyethylaspartamide-based micelles for ocular drug delivery, *Int. J. Pharm.*, **2009**, 378, 177–186.
- [88] Licciardi, M.; Montana, G.; Bondi, M. L.; Bonura, A.; Scialabba, C.; Melis, M.; Fiorica, C.; Giammona, G.; Colombo, P., An allergen-polymeric nanoaggregate as a new tool for allergy vaccination, *Int. J. Pharm.*, **2014**, 465, 275–283.

- [89] Mislovicová, D.; Masárová, J.; Svitel, J.; Mendichi, R.; Soltés, L.; Gemeiner, P.; Danielsson, B., Neoglycoconjugates of mannan with bovine serum albumin and their interaction with lectin concanavalin A, *Bioconjug. Chem.*, **2002**, 13, 136–142.
- [90] Weinberger, E. E.; Himly, M.; Myschik, J.; Hauser, M.; Altmann, F.; Isakovic, A.; Scheiblhofer, S.; Thalhamer, J.; Weiss, R., Generation of hypoallergenic neoglycoconjugates for dendritic cell targeted vaccination: a novel tool for specific immunotherapy, *J. Control. Release*, **2013**, 165, 101–109.
- [91] Axén, R.; Porath, J.; Ernback, S., Chemical Coupling of Peptides and Proteins to Polysaccharides by Means of Cyanogen Halides, *Nature*, **1967**, 214, 1302–1304.
- [92] Grönlund, H.; Vrtala, S.; Wiedermann, U.; Dekan, G.; Kraft, D.; Valenta, R.; van Hage-Hamsten, M., Carbohydrate-based particles, *Immunology*, **2002**, 107, 523–529.
- [93] Andersson, T. N.; Ekman, G. J.; Grönlund, H.; Buentke, E.; Eriksson, Tove L J; Scheynius, A.; van Hage-Hamsten, M.; Gafvelin, G., A novel adjuvant-allergen complex, CBP-rFel d 1, induces up-regulation of CD86 expression and enhances cytokine release by human dendritic cells in vitro, *Immunology*, **2004**, 113, 253–259.
- [94] Neimert-Andersson, T.; Thunberg, S.; Swedin, L.; Wiedermann, U.; Jacobsson-Ekman, G.; Dahlén, S.-E.; Scheynius, A.; Grönlund, H.; van Hage, M.; Gafvelin, G., Carbohydrate-based particles reduce allergic inflammation in a mouse model for cat allergy, *Allergy*, **2008**, 63, 518–526.
- [95] Thunberg, S.; Neimert-Andersson, T.; Cheng, Q.; Wermeling, F.; Bergström, U.; Swedin, L.; Dahlén, S.-E.; Arnér, E.; Scheynius, A.; Karlsson, M. C. I.; Gafvelin, G.; van Hage, M.; Grönlund, H., Prolonged antigen-exposure with carbohydrate particle based vaccination prevents allergic immune responses in sensitized mice, *Allergy*, **2009**, 64, 919–926.
- [96] Shibata, Y.; Foster, L. A.; Bradfield, J. F.; Myrvik, Q. N., Oral Administration of Chitin Down-Regulates Serum IgE Levels and Lung Eosinophilia in the Allergic Mouse, *J. Immunol.*, **2000**, 164, 1314–1321.
- [97] Strong, P.; Clark, H.; Reid, K., Intranasal application of chitin microparticles down-regulates symptoms of allergic hypersensitivity to *Dermatophagoides pteronyssinus* and *Aspergillus fumigatus* in murine models of allergy, *Clin. Exp. Allergy*, **2002**, 32, 1794–1800.
- [98] Taylor, W. A.; Sheldon, D.; Spicer, J. W., Adjuvant and suppressive effects of Grass Conjuvac and other alginate conjugates on IgG and IgE antibody responses in mice, *Immunology*, **1981**, 44, 41–50.
- [99] Pegelow, K.-O.; Belin, L.; Broman, P.; Heilborn, H.; Sundin, B.; Watson, K., Immunotherapy with Alginate-Conjugated and Alum-Precipitated Grass Pollen Extracts in Patients with Allergic Rhinoconjunctivitis, *Allergy*, **1984**, 39, 275–290.
- [100] Ortolani, C.; Pastorello, E. A.; Incorvaia, C.; Ispano, M.; Farioli, L.; Zara, C.; Pravettoni, V.; Zanussi, C., A double-blind, placebo-controlled study of immunotherapy with an alginate-conjugated extract of *Parietaria judaica* in patients with *Parietaria* hay fever, *Allergy*, **1994**, 49, 13–21.

- [101] Pastorello, E. A.; Ortolani, C.; Incorvaia, C.; Farioli, L.; Italia, M.; Pravettoni, V.; Harris, R. J.; Watson, H. K.; Corrado, O. J.; Davies, R. J., A double-blind study of hyposensitization with an alginate-conjugated extract of *Dermatophagoides pteronyssinus* (Conjuvac) in patients with perennial rhinitis. II. Immunological aspects, *Allergy*, **1990**, 45, 505–514.
- [102] Corrado, O. J.; Pastorello, E.; Ollier, S.; Cresswell, L.; Zanussi, C.; Ortolani, C.; Incorvaia, A.; Fugazza, A.; Lovely, J. R.; Harris, R. I., A double-blind study of hyposensitization with an alginate conjugated extract of *D. pteronyssinus* (Conjuvac) in patients with perennial rhinitis. 1. Clinical aspects, *Allergy*, **1989**, 44, 108–115.
- [103] Klier, J.; Fuchs, S.; May, A.; Schillinger, U.; Plank, C.; Winter, G.; Coester, C.; Gehlen, H., A nebulized gelatin nanoparticle-based CpG formulation is effective in immunotherapy of allergic horses, *Pharm. Res.*, **2012**, 29, 1650–1657.
- [104] Klier, J.; Lehmann, B.; Fuchs, S.; Reese, S.; Hirschmann, A.; Coester, C.; Winter, G.; Gehlen, H., Nanoparticulate CpG immunotherapy in RAO-affected horses: phase I and IIa study, *J. Vet. Intern. Med.*, **2015**, 29, 286–293.
- [105] Amidi, M.; Mastrobattista, E.; Jiskoot, W.; Hennink, W. E., Chitosan-based delivery systems for protein therapeutics and antigens, *Adv. Drug Deliv. Rev.*, **2010**, 62, 59–82.
- [106] Mao, S.; Sun, W.; Kissel, T., Chitosan-based formulations for delivery of DNA and siRNA, *Adv. Drug Deliv. Rev.*, **2010**, 62, 12–27.
- [107] Kean, T.; Thanou, M., Biodegradation, biodistribution and toxicity of chitosan, *Adv. Drug Deliv. Rev.*, **2010**, 62, 3–11.
- [108] Chen, M.-C.; Mi, F.-L.; Liao, Z.-X.; Hsiao, C.-W.; Sonaje, K.; Chung, M.-F.; Hsu, L.-W.; Sung, H.-W., Recent advances in chitosan-based nanoparticles for oral delivery of macromolecules, *Adv. Drug Deliv. Rev.*, **2013**, 65, 865–879.
- [109] Chew, J. L.; Wolfowicz, C. B.; Mao, H.-Q.; Leong, K. W.; Chua, K. Y., Chitosan nanoparticles containing plasmid DNA encoding house dust mite allergen, Der p 1 for oral vaccination in mice, *Vaccine*, **2003**, 21, 2720–2729.
- [110] Li, G. P.; Liu, Z. G.; Liao, B.; Zhong, N. S., Induction of Th1-type immune response by chitosan nanoparticles containing plasmid DNA encoding house dust mite allergen Der p 2 for oral vaccination in mice, *Cell. Mol. Immunol.*, **2009**, 6, 45–50.
- [111] Shi, W.-d.; Cao, W.; Liu, Y.; Xu, Y.; Tao, Z.-z.; Dai, Q., [Construction of recombinant house dust mite group 1 allergen vaccine and study on immune response induced by nasal immunization], *Zhonghua Er Bi Yan Hou Tou Jing Wai Ke Za Zhi*, **2013**, 48, 26–31.
- [112] Ou, J.; Shi, W.; Xu, Y.; Tao, Z., Intranasal immunization with DNA vaccine coexpressing Der p 1 and ubiquitin in an allergic rhinitis mouse model, *Ann. Allergy Asthma Immunol.*, **2014**, 113, 658–665.
- [113] Roy, K.; Mao, H. Q.; Huang, S. K.; Leong, K. W., Oral gene delivery with chitosan--DNA nanoparticles generates immunologic protection in a murine model of peanut allergy, *Nat. Med.*, **1999**, 5, 387–391.

- [114] Goldmann, K.; Ensminger, S. M.; Spriewald, B. M., Oral gene application using chitosan-DNA nanoparticles induces transferable tolerance, *Clin. Vaccine Immunol.*, **2012**, 19, 1758–1764.
- [115] Kumar, M.; Kong, X.; Behera, A. K.; Hellermann, G. R.; Lockey, R. F.; Mohapatra, S. S., Chitosan IFN-gamma-pDNA Nanoparticle (CIN) Therapy for Allergic Asthma, *Genet. Vaccines Ther.*, **2003**, 1, 3–12.
- [116] Li, F.; Wang, L.; Jin, X.-M.; Yan, C.-H.; Jiang, S.; Shen, X.-M., The immunologic effect of TGF-beta1 chitosan nanoparticle plasmids on ovalbumin-induced allergic BALB/c mice, *Immunobiology*, **2009**, 214, 87–99.
- [117] Hall, G.; Lund, L.; Lamb, J. R.; Jarman, E. R., Kinetics and mode of peptide delivery via the respiratory mucosa determine the outcome of activation versus TH2 immunity in allergic inflammation of the airways, *J. Allergy Clin. Immunol.*, **2002**, 110, 883–890.
- [118] Li, J.; Liu, Z.; Wu, Y.; Wu, H.; Ran, P., Chitosan microparticles loaded with mite group 2 allergen Der f 2 alleviate asthma in mice, *J. Investig. Allergol. Clin. Immunol.*, **2008**, 18, 454–460.
- [119] Liu, Z.; Guo, H.; Wu, Y.; Yu, H.; Yang, H.; Li, J., Local nasal immunotherapy: efficacy of Dermatophagoides farinae-chitosan vaccine in murine asthma, *Int. Arch. Allergy Immunol.*, **2009**, 150, 221–228.
- [120] Yu, H.-q.; Liu, Z.-g.; Guo, H.; Zhou, Y.-p., [Therapeutic effect on murine asthma with sublingual use of Dermatophagoides farinae/chitosan nanoparticle vaccine], *Zhongguo Ji Sheng Chong Xue Yu Ji Sheng Chong Bing Za Zhi*, **2011**, 29, 4–9.
- [121] Saint-Lu, N.; Tourdot, S.; Razafindratsita, A.; Mascarell, L.; Berjont, N.; Chabre, H.; Louise, A.; van Overtvelt, L.; Moingeon, P., Targeting the allergen to oral dendritic cells with mucoadhesive chitosan particles enhances tolerance induction, *Allergy*, **2009**, 64, 1003–1013.
- [122] Jirawutthiwongchai, J.; Klaharn, I.-Y.; Hobang, N.; Mai-Ngam, K.; Klaewsongkram, J.; Sereemasapun, A.; Chirachanchai, S., Chitosan-phenylalanine-mPEG nanoparticles: From a single step water-based conjugation to the potential allergen delivery system, *Carbohydr. Polym.*, **2016**, 141, 41–53.
- [123] Madni, A.; Sarfraz, M.; Rehman, M.; Ahmad, M.; Akhtar, N.; Ahmad, S.; Tahir, N.; Ijaz, S.; Al-Kassas, R.; Löbenberg, R., Liposomal drug delivery: a versatile platform for challenging clinical applications, *J. Pharm. Pharm. Sci.*, **2014**, 17, 401–426.
- [124] Koudelka, S.; Mikulik, R.; Mašek, J.; Raška, M.; Turánek Knotigová, P.; Miller, A. D.; Turánek, J., Liposomal nanocarriers for plasminogen activators, *J. Control. Release*, **2016**, 227, 45–57.
- [125] Tan, M. L.; Choong, P.; Dass, C. R., Recent developments in liposomes, microparticles and nanoparticles for protein and peptide drug delivery, *Peptides*, **2010**, 31, 184–193.
- [126] Allen, T. M.; Cullis, P. R., Liposomal drug delivery systems, *Adv. Drug Deliv. Rev.*, **2013**, 65, 36–48.

- [127] Perrie, Y.; Crofts, F.; Devitt, A.; Griffiths, H. R.; Kastner, E.; Nadella, V., Designing liposomal adjuvants for the next generation of vaccines, *Adv. Drug Deliv. Rev.*, **2016**, 99, 85–96.
- [128] Audera, C.; Ramirez, J.; Soler, E.; Carreira, J., Liposomes as carriers for allergy immunotherapy, *Clin. Exp. Allergy*, **1991**, 21, 139–144.
- [129] Walls, A. F., Liposomes for allergy immunotherapy?, *Clin. Exp. Allergy*, **1992**, 22, 1–2.
- [130] Wagner, W., Immunotherapy with allergen sequestered in liposomes, *J. Allergy Clin. Immunol.*, **1984**, 118–119.
- [131] Khan, M. Z. I.; Opdebeeck, J. P.; Tucker, I. G., Immunopotential and Delivery Systems for Antigens for Single-Step Immunization: Recent Trends and Progress, *Pharm. Res.*, **1994**, 11, 2–11.
- [132] Alvarez, M. J.; Echechipía, S.; García, B.; Tabar, A. I.; Martín, S.; Rico, P.; Olaguibel, J. M., Liposome-entrapped D. pteronyssinus vaccination in mild asthma patients, *Clin. Exp. Allergy*, **2002**, 32, 1574–1582.
- [133] Basomba, A.; Tabar, A. I.; de Rojas, Dolores Hernández F; García, B. E.; Alamar, R.; Olaguibel, J. M.; del Prado, Jaime Moscoso; Martín, S.; Rico, P., Allergen vaccination with a liposome-encapsulated extract of *Dermatophagoides pteronyssinus*: a randomized, double-blind, placebo-controlled trial in asthmatic patients, *J. Allergy Clin. Immunol.*, **2002**, 109, 943–948.
- [134] Arora, N.; Gangal, S. V., Allergens entrapped in liposomes reduce allergenicity and induce immunogenicity on repeated injections in mice, *Int. Arch. Allergy Appl. Immunol.*, **1990**, 91, 22–29.
- [135] Arora, N.; Gangal, S. V., Liposomes as vehicle for allergen presentation in the immunotherapy of allergic diseases, *Allergy*, **1991**, 46, 386–392.
- [136] Arora, N.; Gangal, S. V., Efficacy of liposome entrapped allergen in down regulation of IgE response in mice, *Clin. Exp. Allergy*, **1992**, 22, 35–42.
- [137] Arora, N.; Gangal, S. V., Liposome entrapped allergen reduces plasma histamine in sensitized mice, *Asian Pac. J. Allergy Immunol.*, **1998**, 16, 87–91.
- [138] Sehra; Chugh; Gangal, Polarized TH1 responses by liposome-entrapped allergen and its potential in immunotherapy of allergic disorders, *Clin. Exp. Allergy*, **1998**, 28, 1530–1537.
- [139] Genin, I.; Barratt, G.; Thao, T. X.; Delattre, J.; Puisieux, F., Optimization and characterization of freeze-dried multilamellar liposomes incorporating different standardized allergen extracts, *Allergy*, **1994**, 49, 645–652.
- [140] Nigam, S.; Ghosh, P.; Sarma, P., Altered immune response to liposomal allergens of *Aspergillus fumigatus* in mice, *Int. J. Pharm.*, **2002**, 236, 97–109.
- [141] Calderón, L.; Facenda, E.; Machado, L.; Uyema, K.; Rodríguez, D.; Gomez, E.; Martínez, Y.; González, B.; Bourg, V.; Alvarez, C.; Otero, A.; Russo, M.; Labrada, A.; Lanio, M. E., Modulation of the specific allergic response by mite allergens encapsulated into liposomes, *Vaccine*, **2006**, 24, 38–39.

- [142] Galvain, S.; André, C.; Vatrinet, C.; Villet, B., Safety and efficacy studies of liposomes in specific immunotherapy, *Curr. Ther. Res. Clin. Exp.*, **1999**, 60, 278–294.
- [143] Tasaniyananda, N.; Chaisri, U.; Tungtrongchitr, A.; Chaicumpa, W.; Sookrung, N.; Lai, H.-C., Mouse Model of Cat Allergic Rhinitis and Intranasal Liposome-Adjuvanted Refined Fel d 1 Vaccine, *PLoS ONE*, *PLoS ONE*, **2016**, 11, e0150463-e0150577.
- [144] Ouadahi, S.; Paternostre, M.; André, C.; Genin, I.; Thao, T. X.; Puisieux, F.; Devissaguep, J. P.; Barratt, G., Liposomal Formulations for Oral Immunotherapy, *J. Drug Target.*, **1997**, 5, 365–378.
- [145] Ishii, M.; Koyama, A.; Iseki, H.; Narumi, H.; Yokoyama, N.; Kojima, N., Anti-allergic potential of oligomannose-coated liposome-entrapped Cry j 1 as immunotherapy for Japanese cedar pollinosis in mice, *Int. Immunopharmacol.*, **2010**, 10, 1041–1046.
- [146] Kawakita, A.; Shirasaki, H.; Yasutomi, M.; Tokuriki, S.; Mayumi, M.; Naiki, H.; Ohshima, Y., Immunotherapy with oligomannose-coated liposomes ameliorates allergic symptoms in a murine food allergy model, *Allergy*, **2012**, 67, 371–379.
- [147] Meechan, P.; Tungtrongchitr, A.; Chaisri, U.; Maklon, K.; Indrawattana, N.; Chaicumpa, W.; Sookrung, N., Intranasal, Liposome-Adjuvanted Cockroach Allergy Vaccines Made of Refined Major Allergen and Whole-Body Extract of *Periplaneta americana*, *Int. Arch. Allergy Immunol.*, **2013**, 161, 351–362.
- [148] Mueller, R. S.; Veir, J.; Fieseler, K. V.; Dow, S. W., Use of immunostimulatory liposome-nucleic acid complexes in allergen-specific immunotherapy of dogs with refractory atopic dermatitis - a pilot study, *Vet. Dermatol.*, **2005**, 16, 61–68.
- [149] Veir, J.; Lappin, M.; Dow, S., Evaluation of a novel immunotherapy for treatment of chronic rhinitis in cats, *J. Feline Med. Surg.*, **2006**, 8, 400–411.
- [150] Nouri, H. R.; Varasteh, A.; Jaafari, M. R.; Davies, J. M.; Sankian, M., Induction of a Th1 immune response and suppression of IgE via immunotherapy with a recombinant hybrid molecule encapsulated in liposome-protamine-DNA nanoparticles in a model of experimental allergy, *Immunol. Res.*, **2015**, 62, 280–291.
- [151] Ichikawa, K.; Urakami, T.; Yonezawa, S.; Miyauchi, H.; Shimizu, K.; Asai, T.; Oku, N., Enhanced desensitization efficacy by liposomal conjugation of a specific antigen, *Int. J. Pharm.*, **2007**, 336, 391–395.
- [152] Ichikawa, K.; Asai, T.; Shimizu, K.; Yonezawa, S.; Urakami, T.; Miyauchi, H.; Kawashima, H.; Ishida, T.; Kiwada, H.; Oku, N., Suppression of immune response by antigen-modified liposomes encapsulating model agents, *J. Control. Release*, **2013**, 167, 284–289.
- [153] Cabral, E. C. M.; Zollner, R. L.; Santana, M. H. A., Preparation and characterization of liposomes entrapping allergenic proteins, *Braz. J. Chem. Eng.*, **2004**, 21, 137–146.
- [154] Aristo Wojdani, Liposome containing immunotherapy agents for treating IgE mediated allergies, US5049390 A, **1987**.



- [155] McWilliam, A. S.; Stewart, G. A., Production of multilamellar, small unilamellar and reverse-phase liposomes containing house dust mite allergens, *J. Immunol. Methods*, **1989**, 121, 53–60.
- [156] Ma, Y.; Nolte, R. J.; Cornelissen, J. J., Virus-based nanocarriers for drug delivery, *Adv. Drug Deliv. Rev.*, **2012**, 64, 811–825.
- [157] Jain, N. K.; Sahni, N.; Kumru, O. S.; Joshi, S. B.; Volkin, D. B.; Russell Middaugh, C., Formulation and stabilization of recombinant protein based virus-like particle vaccines, *Adv. Drug Deliv. Rev.*, **2015**, 93, 42–55.
- [158] Klimek, L.; Willers, J.; Hammann-Haenni, A.; Pfaar, O.; Stocker, H.; Mueller, P.; Renner, W. A.; Bachmann, M. F., Assessment of clinical efficacy of CYT003-QbG10 in patients with allergic rhinoconjunctivitis: a phase IIb study, *Clin. Exp. Allergy*, **2011**, 41, 1305–1312.
- [159] Klimek, L.; Schendzielorz, P.; Mueller, P.; Saudan, P.; Willers, J., Immunotherapy of allergic rhinitis, *Am. J. Rhinol. allergy*, **2013**, 27, 206–212.
- [160] Klimek, L.; Bachmann, M. F.; Senti, G.; Kündig, T. M., Immunotherapy of type-1 allergies with virus-like particles and CpG-motifs, *Expert Rev. Clin. Immunol.*, **2014**, 10, 1059–1067.
- [161] Kündig, T. M.; Senti, G.; Schnetzler, G.; Wolf, C.; Prinz Vavricka, B. M.; Fulurija, A.; Hennecke, F.; Sladko, K.; Jennings, G. T.; Bachmann, M. F., Der p 1 peptide on virus-like particles is safe and highly immunogenic in healthy adults, *J. Allergy Clin. Immunol.*, **2006**, 117, 1470–1476.
- [162] Senti, G.; Johansen, P.; Haug, S.; Bull, C.; Gottschaller, C.; Müller, P.; Pfister, T.; Maurer, P.; Bachmann, M. F.; Graf, N.; Kündig, T. M., Use of A-type CpG oligodeoxynucleotides as an adjuvant in allergen-specific immunotherapy in humans: a phase I/IIa clinical trial, *Clin. Exp. Allergy*, **2009**, 39, 562–570.
- [163] Schmitz, N.; Dietmeier, K.; Bauer, M.; Maudrich, M.; Utzinger, S.; Muntwiler, S.; Saudan, P.; Bachmann, M. F., Displaying Fel d1 on virus-like particles prevents reactogenicity despite greatly enhanced immunogenicity, *J. Exp. Med.*, **2009**, 206, 1941–1955.
- [164] Manzano-Szalai, K.; Thell, K.; Willensdorfer, A.; Weghofer, M.; Pfanzagl, B.; Singer, J.; Ritter, M.; Stremnitzer, C.; Flaschberger, I.; Michaelis, U.; Jensen-Jarolim, E., Adeno-Associated Virus-Like Particles as New Carriers for B-Cell Vaccines, *Viral Immunol.*, **2014**, 27, 438–448.
- [165] Vauthier, C.; Labarre, D.; Ponchel, G., Design aspects of poly(alkylcyanoacrylate) nanoparticles for drug delivery, *J. Drug Target.*, **2007**, 15, 641–663.
- [166] Kadajji, V. G.; Betageri, G. V., Water Soluble Polymers for Pharmaceutical Applications, *Polymers*, **2011**, 3, 1972–2009.
- [167] Bondi, M. L.; Montana, G.; Craparo, E. F.; Di Gesù, R.; Giammona, G.; Bonura, A.; Colombo, P., Lipid nanoparticles as delivery vehicles for the Parietaria judaica major allergen Par j 2, *Int. J. Nanomedicine*, **2011**, 6, 2953–2962.

- [168] Nam, J.; Won, N.; Bang, J.; Jin, H.; Park, J.; Jung, S.; Jung, S.; Park, Y.; Kim, S., Surface engineering of inorganic nanoparticles for imaging and therapy, *Adv. Drug Deliv. Rev.*, **2013**, 65, 622–648.
- [169] Kim, C. S.; Tonga, G. Y.; Solfiell, D.; Rotello, V. M., Inorganic nanosystems for therapeutic delivery, *Adv. Drug Deliv. Rev.*, **2013**, 65, 93–99.
- [170] Tahara, Y.; Honda, S.; Kamiya, N.; Piao, H.; Hirata, A.; Hayakawa, E.; Fujii, T.; Goto, M., A solid-in-oil nanodispersion for transcutaneous protein delivery, *J. Control. Release*, **2008**, 131, 14–18.
- [171] Lim, J.; Simanek, E. E., Triazine dendrimers as drug delivery systems, *Adv. Drug Deliv. Rev.*, **2012**, 64, 826–835.
- [172] Kesharwani, P.; Jain, K.; Jain, N. K., Dendrimer as nanocarrier for drug delivery, *Prog. Polym. Sci.*, **2014**, 39, 268–307.
- [173] Zhu, J.; Shi, X., Dendrimer-based nanodevices for targeted drug delivery applications, *J. Mater. Chem. B*, **2013**, 1, 4199–4211.
- [174] Balenga, Nariman Aghaei Bandbon; Zahedifard, F.; Weiss, R.; Sarbolouki, M. N.; Thalhamer, J.; Rafati, S., Protective efficiency of dendrosomes as novel nano-sized adjuvants for DNA vaccination against birch pollen allergy, *J. Biotechnol.*, **2006**, 124, 602–614.
- [175] Kojima, C.; Kameyama, R.; Yamada, M.; Ichikawa, M.; Waku, T.; Handa, A.; Tanaka, N., Ovalbumin Delivery by Guanidine-Terminated Dendrimers Bearing an Amyloid-Promoting Peptide via Nanoparticle Formulation, *Bioconjug. Chem.*, **2015**, 26, 1804–1810.
- [176] Ballester, M.; Jeanbart, L.; Titta, A. de; Nembrini, C.; Marsland, B. J.; Hubbell, J. A.; Swartz, M. A., Nanoparticle conjugation enhances the immunomodulatory effects of intranasally delivered CpG in house dust mite-allergic mice, *Sci. Rep.*, **2015**, 5, 14274–14286.
- [177] Garaczi, E.; Szabó, K.; Franciszti, L.; Csiszovszki, Z.; Lőrincz, O.; Tóke, E. R.; Molnár, L.; Bitai, T.; Jánossy, T.; Bata-Csörgő, Z.; Kemény, L.; Lisziewicz, J., DermAll nanomedicine for allergen-specific immunotherapy, *Nanomedicine: NBM*, **2013**, 9, 1245–1254.
- [178] Madan, T.; Munshi, N.; De, T. K.; Maitra, A.; Usha Sarma, P.; Aggarwal, S. S., Biodegradable nanoparticles as a sustained release system for the antigens/allergens of *Aspergillus fumigatus*: preparation and characterisation, *Int. J. Pharm.*, **1997**, 159, 135–147.
- [179] Gómez, S.; Gamazo, C.; Roman, B. S.; Vauthier, C.; Ferrer, M.; Irache, J. M., Development of a Novel Vaccine Delivery System Based on Gantrez Nanoparticles, *J. Nanosci. Nanotech.*, **2006**, 6, 3283–3289.
- [180] Gómez, S.; Gamazo, C.; Roman, B. S.; Ferrer, M.; Sanz, M. L.; Irache, J. M., Gantrez AN nanoparticles as an adjuvant for oral immunotherapy with allergens, *Vaccine*, **2007**, 25, 5263–5271.

- [181] Gómez, S.; Gamazo, C.; San Roman, B.; Ferrer, M.; Sanz, M. L.; Espuelas, S.; Irache, J. M., Allergen immunotherapy with nanoparticles containing lipopolysaccharide from *Brucella ovis*, *Eur. J. Pharm. Biopharm.*, **2008**, 70, 711–717.
- [182] Gómez, S.; Gamazo, C.; San Roman, B.; Grau, A.; Espuelas, S.; Ferrer, M.; Sanz, M. L.; Irache, J. M., A novel nanoparticulate adjuvant for immunotherapy with *Lolium perenne*, *J. Immunol. Methods*, **2009**, 348, 1–8.
- [183] Beilvert, F.; Tissot, A.; Langelot, M.; Mével, M.; Chatin, B.; Lair, D.; Magnan, A.; Pitard, B., DNA/amphiphilic block copolymer nanospheres reduce asthmatic response in a mouse model of allergic asthma, *Hum. Gene Ther.*, **2012**, 23, 597–608.
- [184] Kitaoka, M.; Shin, Y.; Kamiya, N.; Kawabe, Y.; Kamihira, M.; Goto, M., Transcutaneous Peptide Immunotherapy of Japanese Cedar Pollinosis Using Solid-in-Oil Nanodispersion Technology, *AAPS PharmSciTech*, **2015**, 16, 1418–1424.
- [185] Litwin, A.; Flanagan, M.; Entis, G.; Gottschlich, G.; Michael, J. G.; Esch, R.; Gartside, P., Immunologic Effects of Encapsulated Short Ragweed Extract, *Ann. Allergy Asthma Immunol.*, **1996**, 77, 132–138.
- [186] Litwin, A.; Flanagan, M.; Entis, G.; Gottschlich, G.; Esch, R.; Gartside, P.; Michael, J., Oral immunotherapy with short ragweed extract in a novel encapsulated preparation: A double-blind study, *J. Allergy Clin. Immunol.*, **1997**, 100, 30–38.
- [187] TePas, E. C.; Hoyte, E. G.; McIntire, J. J.; Umetsu, D. T., Clinical efficacy of microencapsulated timothy grass pollen extract in grass-allergic individuals, *Ann. Allergy Asthma Immunol.*, **2004**, 92, 25–31.
- [188] Wheeler, A. W.; Henderson, D. C.; Youlten, L.; Al-Janabi, I. I.; Hickman, B. E.; Taylor, I. H.; Moran, D. M., Immunogenicity in Guinea Pigs and Tolerance in Grass Pollen-Sensitive Volunteers of Enteric-Coated Grass Pollen Allergens, *Int. Arch. Allergy Immunol.*, **1987**, 83, 354–358.
- [189] Horak, F.; Wheeler, A. W., Oral hyposensitisation with enteric-coated allergens as extension therapy following a basic subcutaneous course of injections, *Int. Arch. Allergy Appl. Immunol.*, **1987**, 84, 74–78.
- [190] Wheeler, A. W.; Drachenberg, K. J., New routes and formulations for allergen-specific immunotherapy, *Allergy*, **1997**, 52, 602–612.
- [191] Herzberger, J.; Niederer, K.; Pohlit, H.; Seiwert, J.; Worm, M.; Wurm, F. R.; Frey, H., Polymerization of Ethylene Oxide, Propylene Oxide, and Other Alkylene Oxides, *Chem. Rev.*, **2016**, 116, 2170–2243.
- [192] Pohlit, H.; Bellinghausen, I.; Schömer, M.; Heydenreich, B.; Saloga, J.; Frey, H., Biodegradable pH-Sensitive Poly(ethylene glycol) Nanocarriers for Allergen Encapsulation and Controlled Release, *Biomacromolecules*, **2015**, 16, 3103–3111.
- [193] Dumortier, H., When carbon nanotubes encounter the immune system, *Adv. Drug Deliv. Rev.*, **2013**, 65, 2120–2126.

- [194] Laverny, G.; Casset, A.; Purohit, A.; Schaeffer, E.; Spiegelhalter, C.; Blay, F. de; Pons, F., Immunomodulatory properties of multi-walled carbon nanotubes in peripheral blood mononuclear cells from healthy subjects and allergic patients, *Toxicol. Lett.*, **2013**, 217, 91–101.
- [195] Ronzani, C.; Casset, A.; Pons, F., Exposure to multi-walled carbon nanotubes results in aggravation of airway inflammation and remodeling and in increased production of epithelium-derived innate cytokines in a mouse model of asthma, *Arch. Toxicol.*, **2014**, 88, 489–499.
- [196] Pescatori, M.; Bedognetti, D.; Venturelli, E.; Ménard-Moyon, C.; Bernardini, C.; Muresu, E.; Piana, A.; Maida, G.; Manetti, R.; Sgarrella, F.; Bianco, A.; Delogu, L. G., Functionalized carbon nanotubes as immunomodulator systems, *Biomaterials*, **2013**, 34, 4395–4403.
- [197] Ryan, J. J.; Bateman, H. R.; Stover, A.; Gomez, G.; Norton, S. K.; Zhao, W.; Schwartz, L. B.; Lenk, R.; Kepley, C. L., Fullerene nanomaterials inhibit the allergic response, *J. Immunol.*, **2007**, 179, 665–672.
- [198] Norton, S. K.; Dellinger, A.; Zhou, Z.; Lenk, R.; Macfarland, D.; Vonakis, B.; Conrad, D.; Kepley, C. L., A new class of human mast cell and peripheral blood basophil stabilizers that differentially control allergic mediator release, *Clin. Transl. Sci.*, **2010**, 3, 158–169.
- [199] Norton, S. K.; Wijesinghe, D. S.; Dellinger, A.; Sturgill, J.; Zhou, Z.; Barbour, S.; Chalfant, C.; Conrad, D. H.; Kepley, C. L., Epoxyeicosatrienoic acids are involved in the C70 fullerene derivative-induced control of allergic asthma, *J. Allergy Clin. Immunol.*, **2012**, 130, 761–769.
- [200] Kaidashev, I. P.; Mikitiuk, M.; Kutzenko, N.; Bobrova, N.; DuBuske, L. M., Fullerene C60 and Fullerene - Allergen Conjugates Influence Allergic Responses In A Mouse Model Of Asthma, *J. Allergy Clin. Immunol.*, **2010**, 125, AB36.
- [201] Bobrova, N. A.; Mikitiuk, M. V.; Kutsenko, L. A.; Kaïdashev, I. P., [Effect of fullerene C60 on free-radical induced lipid peroxidation processes in bronchial asthma], *Patol. Fiziol. Eksp. Ter.*, **2012**, 109–114.
- [202] Shershakova, N.; Baraboshkina, E.; Andreev, S.; Purgina, D.; Struchkova, I.; Kamyshnikov, O.; Nikonova, A.; Khaitov, M., Anti-inflammatory effect of fullerene C60 in a mice model of atopic dermatitis, *J. Nanobiotechnol.*, **2016**, 14, 8–18.
- [203] Fernández, T. D.; Pearson, J. R.; Leal, M. P.; Torres, M. J.; Blanca, M.; Mayorga, C.; Le Guével, X., Intracellular accumulation and immunological properties of fluorescent gold nanoclusters in human dendritic cells, *Biomaterials*, **2015**, 43, 1–12.
- [204] Popescu, R.; Grumezescu, A., Metal Based Frameworks for Drug Delivery Systems, *Curr. Top. Med. Chem.*, **2015**, 15, 1532–1542.
- [205] Barreto, E.; Serra, M. F.; dos Santos, Rafael Vital; dos Santos, Cássio Eráclito Alves; Hickmann, J.; Cotias, A. C.; Rodrigues Pão, Camila Ribeiro; Trindade, S. G.; Schimidt, V.; Giacomelli, C.; Carvalho, V. F.; Rodrigues e Silva, Patricia Machado; Cordeiro, Renato Sérgio Balão; Martins, M. A., Local Administration of Gold Nanoparticles Prevents Pivotal

- Pathological Changes in Murine Models of Atopic Asthma, *J. Biomed. Nanotechnol.*, **2015**, 11, 1038–1050.
- [206] Veiseh, O.; Gunn, J. W.; Zhang, M., Design and fabrication of magnetic nanoparticles for targeted drug delivery and imaging, *Adv. Drug Deliv. Rev.*, **2010**, 62, 284–304.
- [207] Kumar, C. S.; Mohammad, F., Magnetic nanomaterials for hyperthermia-based therapy and controlled drug delivery, *Adv. Drug Deliv. Rev.*, **2011**, 63, 789–808.
- [208] Marengo, M.; Bonomi, F.; Iametti, S.; Prinz, E.; Hempelmann, R.; Boye, M.; Frokiaer, H., Recognition and uptake of free and nanoparticle-bound betalactoglobulin—a food allergen—by human monocytes, *Mol. Nutr. Food Res.*, **2011**, 55, 1708–1716.
- [209] Umashankar, M. S.; Sachdeva, R. K.; Gulati, M., Aquasomes, *Nanomedicine: NBM*, **2010**, 6, 419–426.
- [210] Pandey, R. S.; Sahu, S.; Sudheesh, M. S.; Madan, J.; Kumar, M.; Dixit, V. K., Carbohydrate modified ultrafine ceramic nanoparticles for allergen immunotherapy, *Int. Immunopharmacol.*, **2011**, 11, 925–931.
- [211] Bettencourt, A.; Almeida, A. J., Poly(methyl methacrylate) particulate carriers in drug delivery, *J. Microencapsul.*, **2012**, 29, 353–367.
- [212] Lv, H.; Zhang, S.; Wang, B.; Cui, S.; Yan, J., Toxicity of cationic lipids and cationic polymers in gene delivery, *J. Control. Release*, **2006**, 114, 100–109.
- [213] Taepaiboon, P.; Rungsardthong, U.; Supaphol, P., Drug-loaded electrospun mats of poly(vinyl alcohol) fibres and their release characteristics of four model drugs, *Nanotechnology*, **2006**, 17, 2317–2329.
- [214] Carr, D. A.; Peppas, N. A., Assessment of poly(methacrylic acid- co - N -vinyl pyrrolidone) as a carrier for the oral delivery of therapeutic proteins using Caco-2 and HT29-MTX cell lines, *J. Biomed. Mater. Res.*, **2010**, 92A, 504–512.
- [215] Park, T. G., Degradation of poly(lactic-co-glycolic acid) microspheres, *Biomaterials*, **1995**, 16, 1123–1130.
- [216] La Rica, R. de; Aili, D.; Stevens, M. M., Enzyme-responsive nanoparticles for drug release and diagnostics, *Adv. Drug Deliv. Rev.*, **2012**, 64, 967–978.
- [217] Felber, A. E.; Dufresne, M.-H.; Leroux, J.-C., pH-sensitive vesicles, polymeric micelles, and nanospheres prepared with polycarboxylates, *Adv. Drug Deliv. Rev.*, **2012**, 64, 979–992.
- [218] Fomina, N.; Sankaranarayanan, J.; Almutairi, A., Photochemical mechanisms of light-triggered release from nanocarriers, *Adv. Drug Deliv. Rev.*, **2012**, 64, 1005–1020.
- [219] Wang, Y.; Byrne, J. D.; Napier, M. E.; DeSimone, J. M., Engineering nanomedicines using stimuli-responsive biomaterials, *Adv. Drug Deliv. Rev.*, **2012**, 64, 1021–1030.
- [220] Shim, M. S.; Kwon, Y. J., Stimuli-responsive polymers and nanomaterials for gene delivery and imaging applications, *Adv. Drug Deliv. Rev.*, **2012**, 64, 1046–1059.
- [221] Hoffman, A. S., Stimuli-responsive polymers, *Adv. Drug Deliv. Rev.*, **2013**, 65, 10–16.

- [222] Fleige, E.; Quadir, M. A.; Haag, R., Stimuli-responsive polymeric nanocarriers for the controlled transport of active compounds, *Adv. Drug Deliv. Rev.*, **2012**, 64, 866–884.
- [223] Bennet, D.; Kim, S., Polymer Nanoparticles for Smart Drug Delivery. In: Sezer, A. D., Application of Nanotechnology in Drug Delivery, InTech, **2014**.
- [224] Mohanan, D.; Gander, B.; Kündig, T. M.; Johansen, P., Encapsulation of antigen in poly(D,L-lactide-co-glycolide) microspheres protects from harmful effects of  $\gamma$ -irradiation as assessed in mice, *Eur. J. Pharm. Biopharm.*, **2012**, 80, 274–281.
- [225] Tahara, Y.; Akiyoshi, K., Current advances in self-assembled nanogel delivery systems for immunotherapy, *Adv. Drug Deliv. Rev.*, **2015**, 95, 65–76.
- [226] Habibi, N.; Kamaly, N.; Memic, A.; Shafiee, H., Self-assembled peptide-based nanostructures, *Nano Today*, **2016**, 11, 41–60.
- [227] Fernandes, R.; Gracias, D. H., Self-folding polymeric containers for encapsulation and delivery of drugs, *Adv. Drug Deliv. Rev.*, **2012**, 64, 1579–1589.
- [228] Somiya, M.; Kuroda, S., Development of a virus-mimicking nanocarrier for drug delivery systems, *Adv. Drug Deliv. Rev.*, **2015**, 95, 77–89.
- [229] Kwon, K.-C.; Verma, D.; Singh, N. D.; Herzog, R.; Daniell, H., Oral delivery of human biopharmaceuticals, autoantigens and vaccine antigens bioencapsulated in plant cells, *Adv. Drug Deliv. Rev.*, **2013**, 65, 782–799.
- [230] Chacko, R. T.; Ventura, J.; Zhuang, J.; Thayumanavan, S., Polymer nanogels, *Adv. Drug Deliv. Rev.*, **2012**, 64, 836–851.
- [231] Ghobril, C.; Rodriguez, E. K.; Nazarian, A.; Grinstaff, M. W., Recent Advances in Dendritic Macromonomers for Hydrogel Formation and Their Medical Applications, *Biomacromolecules*, **2016**, 17, 1235–1252.
- [232] Koker, S. de; Cock, L. J. de; Rivera-Gil, P.; Parak, W. J.; Auzély Velty, R.; Vervaet, C.; Remon, J. P.; Grooten, J.; Geest, B. G. de, Polymeric multilayer capsules delivering biotherapeutics, *Adv. Drug Deliv. Rev.*, **2011**, 63, 748–761.
- [233] Ariga, K.; Lvov, Y. M.; Kawakami, K.; Ji, Q.; Hill, J. P., Layer-by-layer self-assembled shells for drug delivery, *Adv. Drug Deliv. Rev.*, **2011**, 63, 762–771.
- [234] Sato, K.; Yoshida, K.; Takahashi, S.; Anzai, J.-i., pH- and sugar-sensitive layer-by-layer films and microcapsules for drug delivery, *Adv. Drug Deliv. Rev.*, **2011**, 63, 809–821.

### 1.3 Polyethers Bearing Cleavable Moieties

Jana Herzberger,<sup>1,2</sup> Kerstin Niederer,<sup>1</sup> Hannah Pohlit,<sup>1,2,3,4</sup> Jan Seiwert,<sup>1</sup> Matthias Worm,<sup>1,4</sup>

Frederik R. Wurm,<sup>5,4</sup> and Holger Frey<sup>1,2</sup>

<sup>1</sup>Institute of Organic Chemistry, Johannes Gutenberg-University Mainz, Duesbergweg 10-14, 55128 Mainz, Germany

<sup>2</sup>Graduate School Materials Science in Mainz, Staudingerweg 9, 55128 Mainz, Germany

<sup>3</sup>Department of Dermatology, University Medical Center, Langenbeckstraße 1, 55131 Mainz, Germany

<sup>4</sup>Max Planck Graduate Center, Staudingerweg 9, 55128 Mainz, Germany

<sup>5</sup>Max Planck Institute for Polymer Research, Ackermannweg 10, 55128 Mainz, Germany

Published in: *Chemical Reviews*, **2016**, 116 (4), 2170–2243.

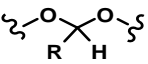
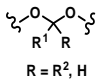
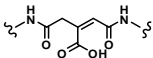
Excerpt from Polymerization of Ethylene Oxide, Propylene Oxide, and Other Alkylene Oxides: Synthesis, Novel Polymer Architectures, and Bioconjugation: Chapter 6.2 Cleavable Polyethers (see Appendix A2).

#### 6.2.1. Polyethers Bearing Cleavable Moieties.

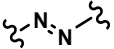
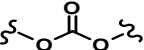
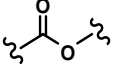
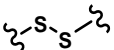
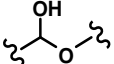

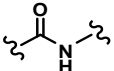
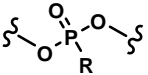
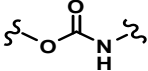
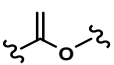
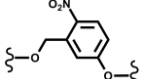
Ethers are characterized by their high stability toward chemical or physical treatment. Consequently, low molecular weight ethers are typical solvents in organic chemistry. Also polyethers are very stable and flexible polymers. Under oxidative stress, however, PEG may be degraded by reactive oxygen species (ROS) due to  $\beta$ -scission, as observed in long-term *in vivo* experiments.<sup>[1]</sup> Degradation of PEG under application of voltage and air,<sup>[2]</sup> UV light,<sup>[3]</sup> ultrasonication,<sup>[4]</sup> and temperature<sup>[3]</sup> is described in literature. The degradation rate depends on whether the experiment is conducted in bulk or in aqueous solution and on pH values.<sup>[5]</sup> If higher oxidative stability is required for certain applications, aromatic polyethers can be applied.<sup>[6]</sup> Aromatic polyethers are known to exhibit higher stability against oxidation compared to PEG,

albeit at the expense of low solubility in water and a lack of biocompatibility. If PEG-derivatives are expected to degrade, which may be beneficial for specific biomedical applications such as reversible PEGylation (see section 6.1), incorporation of cleavable moieties into the polymer backbone is necessary. PEG is regarded as the gold standard for polymer-drug conjugation in order to prevent proteolytic degradation of pharmaceutical agents (see section 6.1), as it is nontoxic, chemically inert, water-soluble and has a low immunogenicity.<sup>[7]</sup> However, PEG is not biodegradable restricting its use to a maximum molecular weight of 40 kDa, as higher molecular weight PEGs can accumulate in human tissue and may lead to storage diseases.<sup>[8]</sup> This molecular weight threshold represents the renal excretion limit of human kidneys exhibiting a natural boundary for the utility of PEG. However, the use of high molecular weight PEG is particularly favorable, as blood circulation times of PEGylated drugs prolong with increasing molecular weights of PEG<sup>[9]</sup> making the design of in-chain cleavable PEG derivatives especially desirable. A variety of different stimuli, such as potential pH-sensitivity, redox-response and enzymatic cleavage, have been employed to trigger the in-chain scission of the PEG backbone or the detachment of PEGs from the drug conjugate within a targeted tissue or cellular compartment.<sup>[10]</sup> More recently, light as a stimulus has likewise been exploited to induce cleavage of PEG derived structures.<sup>[11]</sup> Table 1 compiles different cleavable moieties which have been used as linkers of PEG conjugates or have been incorporated into the polyether backbone as in-chain junctions. Additionally their synthesis strategies and the respective cleaving stimuli are attributed. A comprehensive review article has recently been published focusing on strategies to incorporate cleavable moieties into PEG chains and PEG conjugates.<sup>[10]</sup> It is obvious that PEG-based lipids bearing cleavable moieties have become increasingly attractive for the design of surface modified liposomes (stealth liposomes) as drug delivery systems.<sup>[12]</sup>

**Table 1:** Compilation of cleavable groups, synthesis strategies and respective cleaving stimuli reported for PEGs and derivatives.<sup>[a]</sup>

Cleavable Unit	Structure	Synthetic Approach	Degradation <sup>[b]</sup>	Ref.
Acetals		PEG coupling	pH < 7.4	13-16
Acetals/ ketals		Cleavable AROP initiator	pH < 7.4	17,18
Aconitic acid diamides		PEG coupling	pH < 7.4	19



Azo groups		PEG coupling	enzymatic	20,21
Carbonates		PEG coupling	basic hydrolysis	22,23
Carboxylates		PEG coupling	hydrolytic, enzymatic	24,25
Disulfides		PEG coupling	reductive	26,27
Hemi-acetals		PEG oxidation	acidic or basic	28
Orthoesters		PEG coupling	pH < 7.4	29
Peptides		PEG coupling	enzymatic	30,31
Phospho-esters		PEG coupling	acidic or basic	32,33
Urethane		PEG coupling	(hydrolytic)	34,35
Vinyl ethers		Elimination functionalized PEG, PEG coupling	pH < 7.4 or light/ <sup>1</sup> O <sub>2</sub>	36
o-Nitro benzyl ethers		PEG coupling	light	11

[a] Adapted with permission from Dingels, C.; Frey, H. In *Hierarchical Macromolecular Structures: 60 Years after the Staudinger Nobel Prize II*; Percec, V., Ed.; Springer International Publishing: 2013; Vol. 262, p 167. Copyright 2013 Springer.<sup>[10]</sup> [b] Conditions may vary for the same cleavable unit due to different adjacent moieties.

The presence of stimuli-cleavable linkers in the lipid structures triggers shedding of liposomes within a particular cellular compartment or tissue to improve the efficacy of a liposomal formulation. Numerous reports on acid-labile PEG lipids based on cholesterol with cleavable junctions, such as aconitic acid, hydrazones, or vinyl ethers, have been established.<sup>536</sup> Alternative polymers which combine the properties of PEG, such as high water-solubility, low protein adsorption with degradability may be polypeptides, polypeptoides (i.e., polysarcosin), HES, poly-N-(2-hydroxypropyl) methacrylamide (PHPMA), polyglutamic acid (PGA), polyacetal (“fleximer”), poly(oxazoline)s, poly(phosphoester)s, and polysialic acid.<sup>37,38-44</sup>

---

**References**

- [1] Ulbricht, J.; Jordan, R.; Luxenhofer, R., On the Biodegradability of Polyethylene Glycol, Polypeptoids and Poly(2-oxazoline)s. *Biomaterials* **2014**, 35, 4848–4861.
- [2] Harding, J. R.; Amanchukwu, C. V.; Hammond, P. T.; Shao-Horn, Y., Instability of Poly(ethylene oxide) Upon Oxidation in Lithium–Air Batteries. *J. Phys. Chem. C* **2015**, 119, 6947–6955.
- [3] de Sainte Claire, P., Degradation of PEO in the Solid State: A Theoretical Kinetic Model. *Macromolecules* **2009**, 42, 3469–3482.
- [4] Kawasaki, H.; Takeda, Y.; Arakawa, R., Mass Spectrometric Analysis for High Molecular Weight Synthetic Polymers Using Ultrasonic Degradation and the Mechanism of Degradation. *Anal. Chem.* **2007**, 79, 4182–4187.
- [5] Hassouna, F.; Morlat-Thérias, S.; Mailhot, G.; Gardette, J. L., Influence of Water on the Photodegradation of Poly(ethylene oxide). *Polym. Degrad. Stab.* **2007**, 92, 2042–2050.
- [6] Jayakannan, M.; Ramakrishnan, S., Recent Developments in Polyether Synthesis. *Macromol. Rapid Commun.* **2001**, 22, 1463.
- [7] Alconcel, S. N. S.; Baas, A. S.; Maynard, H. D. FDA-Approved Poly(ethylene glycol)-Protein Conjugate Drugs. *Polym. Chem.* **2011**, 2, 1442–1448.
- [8] Pasut, G.; Veronese, F. M., Polymer–Drug Conjugation, Recent Achievements and General Strategies. *Prog. Polym. Sci.* **2007**, 32, 933–961.
- [9] Yamaoka, T.; Tabata, Y.; Ikada, Y., Distribution and Tissue Uptake of Poly(ethylene glycol) with Different Molecular Weights after Intravenous Administration to Mice. *J. Pharm. Sci.* **1994**, 83, 601–606.
- [10] Dingels, C.; Frey, H., In Hierarchical Macromolecular Structures: 60 Years after the Staudinger Nobel Prize II; 1st ed.; Percec, V., Ed.; Springer International Publishing **2013**, Vol. 262, 167–190.
- [11] Yamahira, S.; Yamaguchi, S.; Kawahara, M.; Nagamune, T., Collagen Surfaces Modified with Photo-Cleavable Polyethylene Glycol-Lipid Support Versatile Single-Cell Arrays of Both Non-Adherent and Adherent Cells. *Macromol. Biosci.* **2014**, 14, 1670–1676.
- [12] Pattni, B. S.; Chupin, V. V.; Torchilin, V. P., New Developments in Liposomal Drug Delivery. *Chem. Rev.* **2015**, 115, 10938–10966.
- [13] Knorr, V.; Allmendinger, L.; Walker, G. F.; Paintner, F. F.; Wagner, E., An Acetal-Based PEGylation Reagent for pH-Sensitive Shielding of DNA Polyplexes. *Bioconjugate Chem.* **2007**, 18, 1218–1225.
- [14] Cui, W.; Qi, M.; Li, X.; Huang, S.; Zhou, S.; Weng, J., Electrospun Fibers of Acid-Labile Biodegradable Polymers with Acetal Groups as Potential Drug Carriers. *Int. J. Pharm.* **2008**, 361, 47–55.
- [15] Pohlitz, H.; Bellinghausen, I.; Schömer, M.; Heydenreich, B.; Saloga, J.; Frey, H., Biodegradable pH-Sensitive Poly(ethylene glycol) Nanocarriers for Allergen Encapsulation and Controlled Release. *Biomacromolecules* **2015**, 16, 3103–3111.

- [16] Schröder, R.; Pohlitz, H.; Schüler, T.; Panthöfer, M.; Unger, R. E.; Frey, H.; Tremel, W., Transformation of Vaterite Nanoparticles to Hydroxycarbonate Apatite in a Hydrogel Scaffold: Relevance to Bone Formation. *J. Mater. Chem. B* **2015**, *3*, 7079–7089.
- [17] Dingels, C.; Wurm, F.; Wagner, M.; Klok, H. A.; Frey, H., Squaric Acid Mediated Chemoselective PEGylation of Proteins: Reactivity of Single-Step-Activated Alpha-Amino Poly(ethylene glycol)s. *Chem. - Eur. J.* **2012**, *18*, 16828–16835.
- [18] Feng, X.; Chaikof, E. L.; Absalon, C.; Drummond, C.; Taton, D.; Gnanou, Y., Dendritic Carrier Based on PEG: Design and Degradation of Acid-Sensitive Dendrimer-Like Poly(ethylene oxide)s. *Macromol. Rapid Commun.* **2011**, *32*, 1722–1728.
- [19] DuBois Clochard, M.-C.; Rankin, S.; Brocchini, S., Synthesis of Soluble Polymers for Medicine that Degrade by Intramolecular Acid Catalysis. *Macromol. Rapid Commun.* **2000**, *21*, 853–859.
- [20] Lai, J.; Wang, L.-Q.; Tu, K.; Zhao, C.; Sun, W., Linear Azo Polymer Containing Conjugated 5,5'-Azodisalicylic Acid Segments in the Main Chain: Synthesis, Characterization, and Degradation. *Macromol. Rapid Commun.* **2005**, *26*, 1572–1577.
- [21] Lai, J.; Tu, K.; Wang, H.; Chen, Z.; Wang, L.-Q., Degradability of the Linear Azo Polymer Conjugated 5,5'-Azodisalicylic Acid Segment in the Main Chain for Colon-Specific Drug Delivery. *J. Appl. Polym. Sci.* **2008**, *108*, 3305–3312.
- [22] Tziampazis, E.; Kohn, J.; Moghe, P. V., PEG-Variant Biomaterials as Selectively Adhesive Protein Templates: Model Surfaces for Controlled Cell Adhesion and Migration. *Biomaterials* **2000**, *21*, 511–520.
- [23] Sharma, R. I.; Kohn, J.; Moghe, P. V., Poly(ethylene glycol) Enhances Cell Motility on Protein-Based Poly(ethylene glycol)-Polycarbonate Substrates: A Mechanism for Cell-Guided Ligand Remodeling. *J. Biomed. Mater. Res.* **2004**, *69A*, 114–123.
- [24] Hawker, C. J.; Chu, F.; Pomery, P. J.; Hill, D. J. T., Hyperbranched Poly(ethylene glycol)s: A New Class of Ion-Conducting Materials. *Macromolecules* **1996**, *29*, 3831–3838.
- [25] d'Acunz, F.; Kohn, J., Alternating Multiblock Amphiphilic Copolymers of PEG and Tyrosine-Derived Diphenols. 1. Synthesis and Characterization. *Macromolecules* **2002**, *35*, 9360–9365.
- [26] Lee, Y.; Koo, H.; Jin, G.-w.; Mo, H.; Cho, M. Y.; Park, J.-Y.; Choi, J. S.; Park, J. S., Poly(ethylene oxide sulfide): New Poly(ethylene glycol) Derivatives Degradable in Reductive Conditions. *Biomacromolecules* **2005**, *6*, 24–26.
- [27] Lee, J.; Joo, M. K.; Kim, J.; Park, J. S.; Yoon, M.-Y.; Jeong, B., Temperature-Sensitive Biodegradable Poly(ethylene glycol). *J. Biomater. Sci., Polym. Ed.* **2009**, *20*, 957–965.
- [28] Reid, B.; Tzeng, S.; Warren, A.; Kozielski, K.; Elisseff, J., Development of a PEG Derivative Containing Hydrolytically Degradable Hemiacetals. *Macromolecules* **2010**, *43*, 9588–9590.
- [29] Qi, M.; Li, X.; Yang, Y.; Zhou, S., Electrospun Fibers of Acid-Labile Biodegradable Polymers Containing Ortho Ester Groups for Controlled Release of Paracetamol. *Eur. J. Pharm. Biopharm.* **2008**, *70*, 445–452.
- [30] Ulbrich, K.; Strohmalm, J.; Kopeček, J., Poly(ethylene glycol)s Containing Enzymatically Degradable Bonds. *Makromol. Chem.* **1986**, *187*, 1131–1144.

- [31] Pechar, M.; Ulbrich, K.; Šubr, V.; Seymour, L. W.; Schacht, E. H., Poly(ethylene glycol) Multiblock Copolymer as a Carrier of Anti-Cancer Drug Doxorubicin. *Bioconjugate Chem.* **2000**, *11*, 131–139.
- [32] Gitsov, I.; Johnson, F. E., Synthesis and Hydrolytic Stability of Poly(oxyethylene-H-phosphonate)s. *J. Polym. Sci., Part A: Polym. Chem.* **2008**, *46*, 4130–4139.
- [33] Wang, D.-A.; Williams, C. G.; Li, Q.; Sharma, B.; Elisseeff, J. H., Synthesis and Characterization of a Novel Degradable Phosphate-Containing Hydrogel. *Biomaterials* **2003**, *24*, 3969–3980.
- [34] Fu, H.; Gao, H.; Wu, G.; Wang, Y.; Fan, Y.; Ma, J., Preparation and Tunable Temperature Sensitivity of Biodegradable Polyurethane Nanoassemblies from Diisocyanate and Poly(ethylene glycol). *Soft Matter* **2011**, *7*, 3546–3552.
- [35] Liu, X.-M.; Quan, L.-d.; Tian, J.; Laquer, F. C.; Ciborowski, P.; Wang, D., Syntheses of Click PEG–Dexamethasone Conjugates for the Treatment of Rheumatoid Arthritis. *Biomacromolecules* **2010**, *11*, 2621–2628.
- [36] Lundberg, P.; Lee, B. F.; van den Berg, S. A.; Pressly, E. D.; Lee, A.; Hawker, C. J.; Lynd, N. A., Poly[(ethylene oxide)-co-(methylene ethylene oxide)]: A Hydrolytically Degradable Poly(ethylene oxide) Platform. *ACS Macro Lett.* **2012**, *1*, 1240–1243.
- [37] Barz, M.; Luxenhofer, R.; Zentel, R.; Vicent, M. J., Overcoming the PEG-Addiction: Well-Defined Alternatives to PEG, from Structure–Property Relationships to Better Defined Therapeutics. *Polym. Chem.* **2011**, *2*, 1900.
- [38] Duncan, R.; Vicent, M. J., Polymer Therapeutics–Prospects for 21st Century: The End of the Beginning. *Adv. Drug Delivery Rev.* **2013**, *65*, 60–70.
- [39] Duncan, R., Polymer Conjugates as Anticancer Nanomedicines. *Nat. Rev. Cancer* **2006**, *6*, 688–701.
- [40] Hardwicke, J.; Moseley, R.; Stephens, P.; Harding, K.; Duncan, R.; Thomas, D. W., Bioresponsive Dextrin-rhEGF Conjugates: In Vitro Evaluation in Models Relevant to its Proposed Use as a Treatment for Chronic Wounds. *Mol. Pharmaceutics* **2010**, *7*, 699–707.
- [41] Tao, L.; Liu, J.; Xu, J.; Davis, T. P., Synthesis and Bioactivity of Poly(HPMA)-Lysozyme Conjugates: The Use of Novel Thiazolidine-2-Thione Coupling Chemistry. *Org. Biomol. Chem.* **2009**, *7*, 3481–3485.
- [42] Besheer, A.; Hertel, T. C.; Kressler, J.; Mäder, K.; Pietzsch, M., Enzymatically Catalyzed HES Conjugation Using Microbial Transglutaminase: Proof of Feasibility. *J. Pharm. Sci.* **2009**, *98*, 4420–4428.
- [43] Mero, A.; Pasut, G.; Dalla Via, L.; Fijten, M. W.; Schubert, U. S.; Hoogenboom, R.; Veronese, F. M., Synthesis and Characterization of Poly(2-ethyl 2-oxazoline)-Conjugates with Proteins and Drugs: Suitable Alternatives to PEG-Conjugates? *J. Controlled Release* **2008**, *125*, 87–95.
- [44] Steinbach, T.; Wurm, F. R., Poly(Phosphoester)s: A New Platform for Degradable Polymers. *Angew. Chem., Int. Ed.* **2015**, *54*, 6098–6108.

## Chapter 2. Biodegradable pH-Sensitive Poly(ethylene glycol) Nanocarriers for Allergen Encapsulation and Controlled Release

Hannah Pohlit,<sup>1,2,3</sup> Iris Bellinghausen,<sup>1</sup> Martina Schömer,<sup>2</sup> Bärbel Heydenreich,<sup>1</sup> Joachim Saloga,<sup>1</sup> and Holger Frey<sup>2</sup>

1 Department of Dermatology, University Medical Center Mainz, Langenbeckstr. 1, 55131 Mainz, Germany.

2 Institute of Organic Chemistry, University of Mainz, Duesbergweg 10-14, 55128 Mainz, Germany.

3 Graduate School Materials Science in Mainz, Staudinger Weg 9, 55128 Mainz, Germany

Published in: *Biomacromolecules*, **2015**, 16, 3103-3111. Reprinted with permission from *Biomacromolecules*, **2015**, 16, 3103-3111. Copyright (2015) American Chemical Society.

**Keywords:** acid-labile, immunotherapy, nanoparticles, PEG, allergens

### Abstract

In the last decades, the number of allergic patients has increased dramatically. Allergen-specific immunotherapy (SIT) is the only available cause-oriented therapy so far. SIT reduces the allergic symptoms, but also exhibits some disadvantages; that is, it is a long-lasting procedure and severe side effects like anaphylactic shock can occur. In this work, we introduce a method to encapsulate allergens into nanoparticles to avoid severe side effects during SIT. Degradable nanocarriers combine the advantage of providing a physical barrier between the encapsulated cargo and the biological environment as well as responding to certain local stimuli (like pH) to release their cargo. This work introduces a facile strategy for the synthesis of acid-labile poly(ethylene glycol) (PEG)-macromonomers that degrade at pH 5 (physiological pH inside the endolysosome) and can be used for nanocarrier synthesis. The difunctional, water-soluble PEG dimethacrylate (PEG-acetal-DMA) macromonomers with cleavable acetal units were analyzed with <sup>1</sup>H NMR, SEC, and MALDI-ToF-MS. Both the allergen and the macromonomers were entrapped inside liposomes as templates, which were produced by dual centrifugation (DAC). Radical polymerization of the

methacrylate units inside the liposomes generated allergen-loaded PEG nanocarriers. *In vitro* studies demonstrated that dendritic cells (DCs) internalize the protein-loaded, nontoxic PEG-nanocarriers. Furthermore, we demonstrate by cellular antigen stimulation tests that the nanocarriers effectively shield the allergen cargo from detection by immunoglobulins on the surface of basophilic leucocytes. Uptake of nanocarriers into DCs does not lead to cell maturation; however, the internalized allergen was capable to induce T cell immune responses.

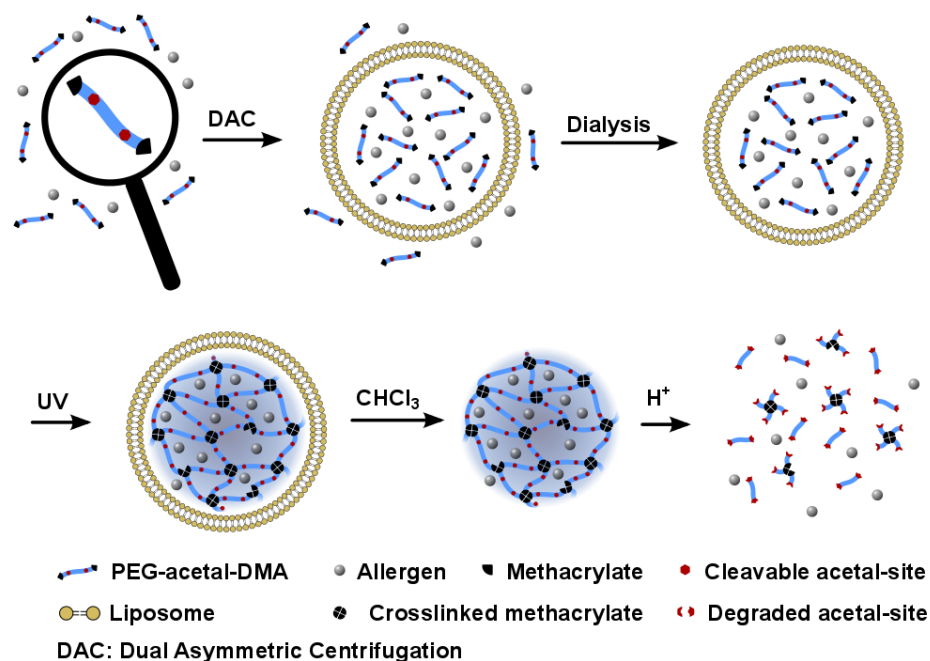
## Introduction

In biomedical applications, micro- and nanocarriers are gaining increasing interest for the transport of active compounds (i.e., drugs, therapeutic proteins as insulin<sup>[1]</sup> or cytokines<sup>[2]</sup> and living cells).<sup>[3,4]</sup> Nanocarriers may serve several important purposes: (i) protection of a sensitive cargo against degradation; (ii) delivery of poorly soluble drugs; (iii) high local concentration and targeting of the desired localization in the body or cell type.<sup>[5]</sup> In summary, nanocarriers may aid to minimize side effects. For actual use in the body, the respective polymers have to be (bio)degradable, in view of both the release of their cargo and safe elimination of polymer remnants. For polymer based nanocarriers, the discharge of their cargo depends on diffusion, degree of swelling, and the rate of their biodegradation (hydrolysis, enzymatic degradation).<sup>[6-8]</sup> Degradable nanocarriers possess the advantage of providing a physical barrier between the encapsulated cargo and its surroundings. It would be desirable to trigger release of the cargo in response to certain local stimuli.<sup>[2]</sup> To achieve degradability in polymeric nanoparticles, several moieties can be introduced into a polymer backbone or the cross-linker, for example, pH-, thermo-, redoxpotential-, enzyme-, and photoresponsive structures.<sup>[9-11]</sup> For instance, Grafahrend *et al.* presented bioactive, degradable extracellular matrix-mimetic scaffolds (PLGA, ester linkages undergo hydrolysis) which enable adhesion of cells for biomedical implants.<sup>[12]</sup> pH-responsive polymers have been widely employed as nanocarriers for drug delivery,<sup>[6,9,13-15]</sup> either with an acid-labile linker (such as acetals, ketals, imines, orthoesters, or hydrazones) between the drug molecule and the polymer<sup>[16-18]</sup> or as block copolymers forming micelles<sup>[19-21]</sup> or polymersomes<sup>[22,23]</sup> that incorporate the drug. Tomlinson *et al.* synthesized an acid-labile polyacetal-doxorubicin (APEGDOX) conjugate, which is less toxic and exhibits prolonged blood half-life and enhanced tumor accumulation compared to free DOX.<sup>[16]</sup>

PEG is a highly established material that has undergone extensive clinical studies as well as several decades of biomedical application in drug delivery, cosmetics, surface modification, and a variety of industrial processes.<sup>[24]</sup> Acid degradable PEG containing an acetal group,<sup>[25,26]</sup> dendrimer-like

PEG,<sup>[27]</sup> polycondensation of PEG and aldehyde,<sup>[28]</sup> polyacetals derived from diphenol monomers and PEG<sup>[29]</sup> or hemiacetal containing PEG<sup>[30]</sup> have been reported.

Polymeric nanoparticles (NP) possess great potential in the treatment of allergic diseases like hay fever or asthma. They are already widely distributed as engineered systems to tune immunity in cancer and autoimmune disease.<sup>[31–33]</sup> We chose the usage of liposome nanoreactors for uniform nanoparticles synthesis as previously described by Kazakov *et al.*<sup>[34]</sup> Through the encapsulation of allergens (proteins and peptides), their delivery to antigen-presenting cells (APC), particularly dendritic cells (DCs), might be realized without activation of other immune cells via recognition by antibodies. The only cause-related therapy against allergy available to date is specific immunotherapy (SIT).<sup>[35,36]</sup> Recent efforts to avoid IgE mediated side effects occurring sometimes during SIT are chemically modified allergoids,<sup>[37]</sup> allergen-polymer aggregates,<sup>[38]</sup> or nanocarrier systems.<sup>[8,39]</sup> Thus, targeted and controlled release of the allergen inside the APC may be a key step in modulating the immune responses against harmless allergens toward tolerance or anergy. A recently published, comprehensive review article from Gamazo *et al.* summarizes the use of NPs for allergen delivery systems.<sup>[40]</sup> Among other, nanoparticles consisting of biodegradable PLGA are popular candidates for transportation of therapeutic proteins. These systems suffer from the disadvantage of slow degradation because of hydrolysis that can take up to several weeks. In addition, a local acidic microenvironment occurs due to release of the degradation product lactic acid.<sup>[41]</sup> Other types of well established nanocarriers are made, for example, of chitosan or PVM-MA, but also show slow degradation and release of cargo over several days to weeks.<sup>[40]</sup> Here, we present a novel type of PEG-derived NPs that only degrade upon certain stimuli (i.e., acidic environment inside the lysosome), which enables fast release of the allergen cargo as well as degradation of the NP. In this work, we introduce a novel type of PEG acetal dimethacrylate (PEG-acetal-DMA) macromonomer with acid labile acetal sites, which is suitable for the generation of PEG nanoparticles (PEG-NP) via radical polymerization. These NP were loaded with proteins, and their transport to the site of action as well as deliberate release of the load in the endolysosome (pH 4.5–5) is shown in Figure 1. Furthermore, a potent immune response is demonstrated.



*Figure 1.* Schematic overview of the encapsulation concept: Entrapment of both allergen and macromonomer in liposomes, photoinitiated radical polymerization, acid-triggered degradation, and release of encapsulated protein cargo.

## Experimental Section

**Materials.** PEG2000, para-toluenesulfonic acid, sodium hydroxide, deuterated water  $D_2O$ , ovalbumin (OVA grade VI, >99%, from chicken egg), 2-hydroxy-2-methylpropiophenone (photoinitiator, PI), and L- $\alpha$ -phosphatidylcholine (>99%, from egg) were purchased from Sigma-Aldrich (St. Louis, MO) and used without further purification. Dichloromethane (p.a., Sigma-Aldrich) was dried according to literature procedures. 2-(Vinylloxy)ethyl methacrylate was synthesized per a modified procedure of Vysotskaya *et al.*<sup>[42]</sup> Dulbecco's phosphate buffered saline (PBS, Invitrogen, Carlsbad, CA), glass beads (1 mm diameter, P. Marienfeld GmbH, Lauda-Königshofen, Germany), ethanol (100% undenatured, Merck, Darmstadt, Germany), grass pollen extract (*Phleum pratense*), dust mite allergen (*Dermatophagoides pteronyssinus*), (both supplied from ALK-Abelló, Hamburg, Germany), Centrisart I tubes (Sartorius, Göttingen, Germany), Alexa Fluor 633 C5 maleimide (A20342), Alexa Fluor 633 protein labeling kit (A20170, Invitrogen), Ficoll Paque 1.077 g/mL (PAA Laboratories GmbH, Cölbe, Germany), IMDM (PAA Laboratories GmbH), LysoTracker Green DND-26 (Molecular Probes, Eugene, OR), Hoechst 33342 (Invitrogen), IL-4, TNF- $\alpha$ , and IL-1 $\beta$  (Miltenyi Biotec, Bergisch Gladbach, Germany), GM-CSF (Leukine; Immunex Corp., Seattle, WA), prostaglandin E2 (Cayman Chemical, Ann Arbor, MI), fluorescein



isothiocyanate (FITC)-conjugated HLA-DR (L243), phycoerythrin (PE)-conjugated CD80 (L307.4), CD83 (HB15e), CD86 (2331[FUN-1]), and mouse IgG isotype controls (all from BD Biosciences, San Jose, CA), antibody-coated paramagnetic MicroBeads (MACS, Miltenyi Biotec), AlexaFluor 647-conjugated CD4 (MT310; Santa Cruz Biotechnology, Santa Cruz, CA), [methyl-<sup>3</sup>H]thymidine ([<sup>3</sup>H]TdR; ICN, Irvine, CA), PE Annexin V and 7-AAD (BD Biosciences), and cellular antigen stimulation test (CAST-2000 ELISA; Bühlmann Laboratories AG, Schönenbuch, Switzerland) were used as purchased. All other chemicals and solvents were purchased by Acros Organics, Geel, Belgium.

**Characterization Methods.** <sup>1</sup>H NMR spectra (300 and 400 MHz) were recorded using a Bruker AC300 or a Bruker AMX400 spectrometer. All spectra were referenced internally to residual proton signals of the deuterated solvent. For SEC measurements in dimethylformamide (DMF, containing 0.25 g/L of lithium bromide as an additive), an Agilent 1100 series was used as an integrated instrument, including a PSS HEMA column (106/105/104 g mol<sup>-1</sup>) and a refractive index (RI) detector. Calibration was carried out using poly(ethylene oxide) standards provided by Polymer Standards Service.

MALDI-ToF mass spectrometry was performed on a Shimadzu Axima CFR MALDI-ToF mass spectrometer equipped with a nitrogen laser delivering 3 ns laser pulses at 337 nm. Dithranol was used as a matrix, and potassium trifluoro acetate was added to facilitate ionization of polymer samples.

For light scattering, a Zetasizer Nano Series Nano ZS (Malvern instruments) was used with a constant scattering angle of 173° and measuring temperature of 25 °C. The samples were diluted (1:1000) and measured three times in a disposable plastic cuvette.

A Philips EM420 transmission electron microscope (TEM) using a LaB6 cathode at an acceleration voltage of 120 kV was used to obtain TEM images. TEM grids (carbon film on copper, 300 mesh) were purchased from Electron Microscopy Sciences, Hatfield, PA. Staining was not necessary. As autoclave a high pressure laboratory autoclave model II from Carl Roth GmbH + Co. KG was used. Circular dichroism (CD) spectra were measured over the range of approximately 190–320 nm by using a J-815 CD spectrometer (Jasco Labor- and Datentechnik, Groß-Umstadt, Germany). All measurements were made by using 10 mm quartz glass Suprasil cells (volume 350 µL) and protein solutions of approximately 1 mg/mL. The instrument was calibrated by measuring PBS as baseline. Each solution was measured five times at 20 ± 1 °C with a scan rate of 50 nm/min. Absorption spectra were measured in the same instrument.

**Flow cytometry analysis and confocal laser scanning microscopy.** For characterization of allergen uptake by immature DCs, allergen was labeled using an Alexa Fluor 633 protein labeling kit according to the manufacturer's protocol (Molecular Probes). For characterization of flow cytometry analysis, labeled NPs or unlabeled allergen were added to DCs on day 6 of culture and internalization was analyzed after at different time points in a FACS Calibur (BD Biosciences) equipped with CELLQUEST software (Becton Dickinson). For confocal laser scanning microscopy, internalization of labeled free allergen or allergen encapsulated in NPs was observed as followed: Labeled free protein or protein-loaded NPs were added to DCs on day 6 of culture and internalization was analyzed after 4 h of incubation using the Zeiss laser scanning system LSM 710 (Zeiss, Göttingen, Germany). DCs were labeled with 60 nM LysoTracker Green DND-26 and 200 ng/mL Hoechst 33342 10 min before analysis.

**Preparation of Macromonomer (PEG-acetal-DMA).** PEG2000 (2 g, 1 mmol), 2-(vinylloxy)ethyl methacrylate (781  $\mu$ L, 5 mmol), and *para*-toluenesulfonic acid (19 mg, 0.1 mmol) were dissolved in 5 mL dichloromethane. Next, 20 mg of hydroquinone were added as radical inhibitor. The reaction mixture was stirred at room temperature for 25 min followed by quenching with triethylamine (27.7  $\mu$ L, 0.2 mmol). As workup, the reaction mixture was extracted with the same volume of sodium hydroxide solution (1 mol/L); thereafter the aqueous phase was again extracted with dichloromethane twice. Organic phases were combined and dried over magnesium sulfate, and then the solvent was removed by rotary evaporation. The crude product was precipitated in cold diethyl ether, and additional hydroquinone (20 mg) was added before final drying at high vacuum to obtain PEG-acetal-DMA as colorless solid in quantitative yield.  $^1\text{H NMR}$  (300 MHz,  $\text{CDCl}_3$ )  $\delta$ [ppm] = 1.33 (d, 7H, CH-CH<sub>3</sub>,  $J$  = 5.37 Hz), 1.92 (t, 6H, CH<sub>3</sub>), 3.59–3.96 (m, 310H, CH<sub>2</sub>), 4.31–4.34 (m, 4H, CH<sub>2</sub>-O-CH), 4.89 (q, 2H, CH-CH<sub>3</sub>), 5.94 (d, 4H, CH<sub>2</sub> = C,  $J$  = 126.14 Hz).

**Preparation of NPs.** Volumes of 148.3  $\mu$ L phosphatidylcholine solution (100 mg/mL in ethanol) and 246.7  $\mu$ L cholesterol solution (25 mg/mL in ethanol) were mixed in a vial. The solvent was removed by vacuum centrifugation and subsequent freeze-drying. Next, 60 mg of glass beads were added together with the liquid phase containing 19.5 mg of PEG-acetal-DMA, 26  $\mu$ L of PBS, 0.5  $\mu$ L of PI, and 150  $\mu$ g of protein (allergen or OVA) dissolved in 10  $\mu$ L of PBS. In the case of empty NPs, the volume of the protein solution was substituted by PBS. The reaction mixture was centrifuged for 2 min in a normal centrifuge to guarantee contact between the dried lipids and the liquid phase and then incubated for 10 min for swelling. After that the reaction vessel was

centrifuged 25 min at 3500 rpm and room temperature in the DAC (dual centrifuge, Rotanta 460, Hettich Zentrifugen, Andreas Hettich GmbH & Co KG, Tuttlingen, Germany). To redisperse the liposomes, 120  $\mu$ L of PBS were added to the reaction mixture and centrifuged twice 2 min at 3500 rpm at room temperature in the DAC. Before the second centrifugation, the reaction container was turned about 180°. Purification of the liposomes was achieved by using ultrafiltration concentrators Centriscart I tubes with a MWCO (molecular weight cutoff) of 100 kDa to remove nonencapsulated macromonomer and protein. The liposomes were diluted with 2 mL of PBS and subsequently centrifuged for 60 min at 3200 rpm and 5 °C. This purification step was repeated once. The macromonomer was photopolymerized by irradiation at 365 nm for 10 s (black light blue lamp F8 T5 BLB, Sylvania, Antwerpen, Belgium). The liposome templates were removed by 2-fold addition of 200  $\mu$ L of chloroform and decantation of the aqueous layer after vortexing and phase separation. NPs were stored at 4 °C. For fluorescent labeling of NPs, Alexa Fluor 633 C5 maleimide (1 mol% referred to PEG-acetal-DMA) was added prior to the centrifugation process and upon radical polymerization statistically incorporated into the NP network.

**Blood Donors.** Buffy coats were obtained from eight allergic donors sensitized to *Phleum pratense* with an ImmunoCAP class  $\geq 2$  (Transfusion Centre, Mainz, Germany). Specific sensitization was verified by detection of allergen-specific IgE in the sera (ImmunoCAP specific IgE blood test; Phadia AB, Uppsala, Sweden). The study was approved by the local ethics committee. Informed consent was obtained from all subjects before the study.

**Generation of Monocyte-Derived DCs.** Peripheral blood mononuclear cells (PBMCs) and autologous plasma were isolated from heparinized blood by Ficoll Paque 1.077 g/mL density centrifugation. CD14<sup>+</sup> cells were enriched by incubation of  $5 \times 10^6$  PBMC in a 12-well-plate (Greiner, Frickenhausen, Germany) with 1 mL/well Iscove's modified Dulbecco's medium containing L-glutamine and 25 mM HEPES (IMDM) and 3% autologous plasma, which was collected from the upper phase after Ficoll density centrifugation and which was heat inactivated for 30 min at 56 °C. Nonadherent cells were washed twice with prewarmed PBS. The remaining monocytes were incubated with 1.5 mL/well IMDM, 1% autologous plasma, 1000 U/mL IL-4, and 200 U/mL granulocyte-macrophage colonystimulating factor (GM-CSF). On day 6, the immature DCs were pulsed with 5  $\mu$ g/mL fluorescent dye-labeled allergen or allergen loaded NPs as indicated (grass pollen extract or dust mite extract) and stimulated with 1000 U/mL tumor necrosis factor  $\alpha$  (TNF  $\alpha$ ), 2000 U/mL IL-1 $\beta$ , and 1  $\mu$ g/mL prostaglandin E2 (maturation cocktail) to reach final

maturation.<sup>[43,44]</sup> After 48 h, the mature DCs were harvested, washed twice with PBS, and used for T cell stimulation assays or for analysis of surface marker expression and nanoparticle uptake by flow cytometry. The following antihuman mAbs for staining of DCs (20 min at 4 °C) were used: FITC-conjugated HLA-DR, phycoerythrin (PE)-conjugated CD80, CD83, and CD86, and mouse IgG isotype controls. To investigate cytotoxicity of NP degradation products, NPs without liposomes were acidified to pH 1 for 30 min, 37 °C and then neutralized to pH 7 prior to cell incubation. Additionally, PBS containing liposomes were tested (data not shown).

**Purification of T Cells.** Autologous CD4<sup>+</sup> T cells were obtained from PBMCs using antibody-coated paramagnetic MicroBeads (MACS) according to the protocol of the manufacturer (Miltenyi Biotec). Separation was controlled by flow cytometry (purity > 98% CD4<sup>+</sup> T cells). AlexaFluor-647-conjugated CD4 was used for staining of T cells.

**Coculture of T Cells and Autologous Allergen (Or Allergen-Loaded NPs)-Pulsed DCs.** For the proliferation assay,  $1 \times 10^5$  CD4<sup>+</sup> T cells were cocultured in triplicate with  $1 \times 10^4$  DCs, pulsed with allergen or allergen loaded NPs, in 200  $\mu$ L IMDM supplemented with 5% heat inactivated autologous plasma. After 5 days, the cells were pulsed with 37 kBq/well of [methyl-<sup>3</sup>H]thymidine ([<sup>3</sup>H]TdR) for 8 h. Incorporation of [<sup>3</sup>H]TdR was measured in a beta counter (1205 Betaplate; LKB Wallac, Turku, Finland). All proliferative responses were scaled to the medium control in order to obtain proliferation indices.

**Annexin V Assay.** The cells were stained with PE annexin V and 7-AAD from BD Biosciences according to the protocol of the manufacturer. DCs were matured with maturation cocktail and incubated with NPs (5  $\mu$ g/mL allergen) or degradation products of empty NPs (equivalent or double amount to nondegraded NPs) for 48 h prior to annexin staining. For the degradation products, NPs were acidified to pH 4 for 48 h and then neutralized to pH 7.5.

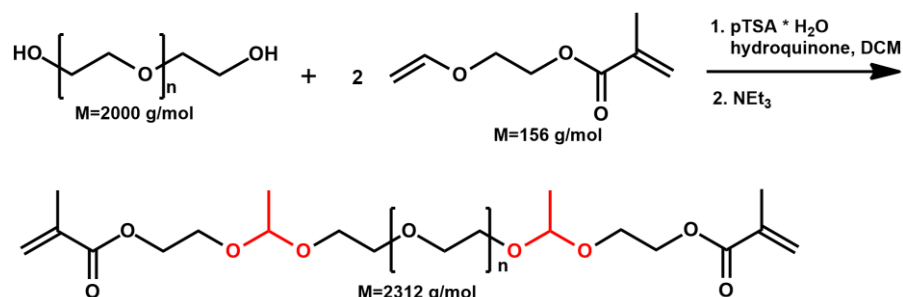
**Determination of Leukotriene Release from Activated Basophils (CAST-ELISA).** Allergenicity was tested via leukotriene release of activated basophils using the cellular antigen stimulation test (CAST-2000 ELISA) according to the protocol of the manufacturer. Briefly, dextran (250  $\mu$ L) was added to 1 mL of EDTA-blood of six atopic donors sensitized to *Phleum pratense* with an ImmunoCAP class  $\geq 2$  and incubated for 90 min at room temperature to allow sedimentation of erythrocytes. Then, peripheral blood leucocytes were centrifuged at 130g for 15 min and resuspended in 1 mL of stimulation buffer containing IL-3. A volume of 200  $\mu$ L of peripheral blood

leukocytes was stimulated with 50  $\mu\text{L}$  of allergen or allergen loaded NPs at different concentrations or mouse anti-human IgE receptor antibody as positive control for 40 min at 37  $^{\circ}\text{C}$ . Finally, the cells were centrifuged and supernatants were stored at  $-20^{\circ}\text{C}$  until analysis of leukotriene concentration.

**Statistics.** ANOVA was used for analysis of variance between different experimental groups. Student's paired t test was used to test the statistical significance of the results;  $P \leq 0.05$  was considered to be significant.

### Results and Discussion

PEG-acetal-DMA was prepared by reacting linear dihydroxyfunctional PEG quantitatively with 2-(vinylloxy)ethyl methacrylate with the hydroxyl end groups of PEG under acidic catalysis, generating two acetal units in the resulting PEGdimethacrylate. Subsequent purification was possible by simple precipitation (Scheme 1). The difunctional product was analyzed by  $^1\text{H}$  NMR, GPC, and MALDI-ToF (Figures S1–S4).



*Scheme 1.* PEG-Acetal-DMA Macromonomer Synthesis.

Two macromonomers were synthesized with different PEG chain lengths (600 and 2300  $\text{g mol}^{-1}$ ). However, for the subsequent preparation of the corresponding NPs, only the higher molecular weight polymers were used, since the aqueous solubility of the macromonomer depends on the PEG chain length. Clearly, solubility in aqueous solutions is indispensable for NP synthesis. As a side reaction, transacetalization leads to a high molecular weight shoulder at ca. 4200  $\text{g mol}^{-1}$  in SEC, but the presence of transacetalized product is not a disadvantage for the planned application (see Figure S4). Lysis of the macromonomer under acidic conditions was studied by GPC (Figure S5) and  $^1\text{H}$  NMR kinetics at pH 5 (Figure 2) and pH 4 (Figure S6). Linear acetal units are known to be cleaved at pH values of approximately 5, and the pH present in the endolysosome is reported to be about pH 4.5–5.<sup>[45]</sup>

To simulate physiological conditions, as present for instance in lysosomes, the macromonomer was acidified to pH 5 and NMR was measured after different periods. In the positive control experiment, the macromonomer was treated with deuterated hydrochloric acid, which resulted in complete degradation (Figure 2).

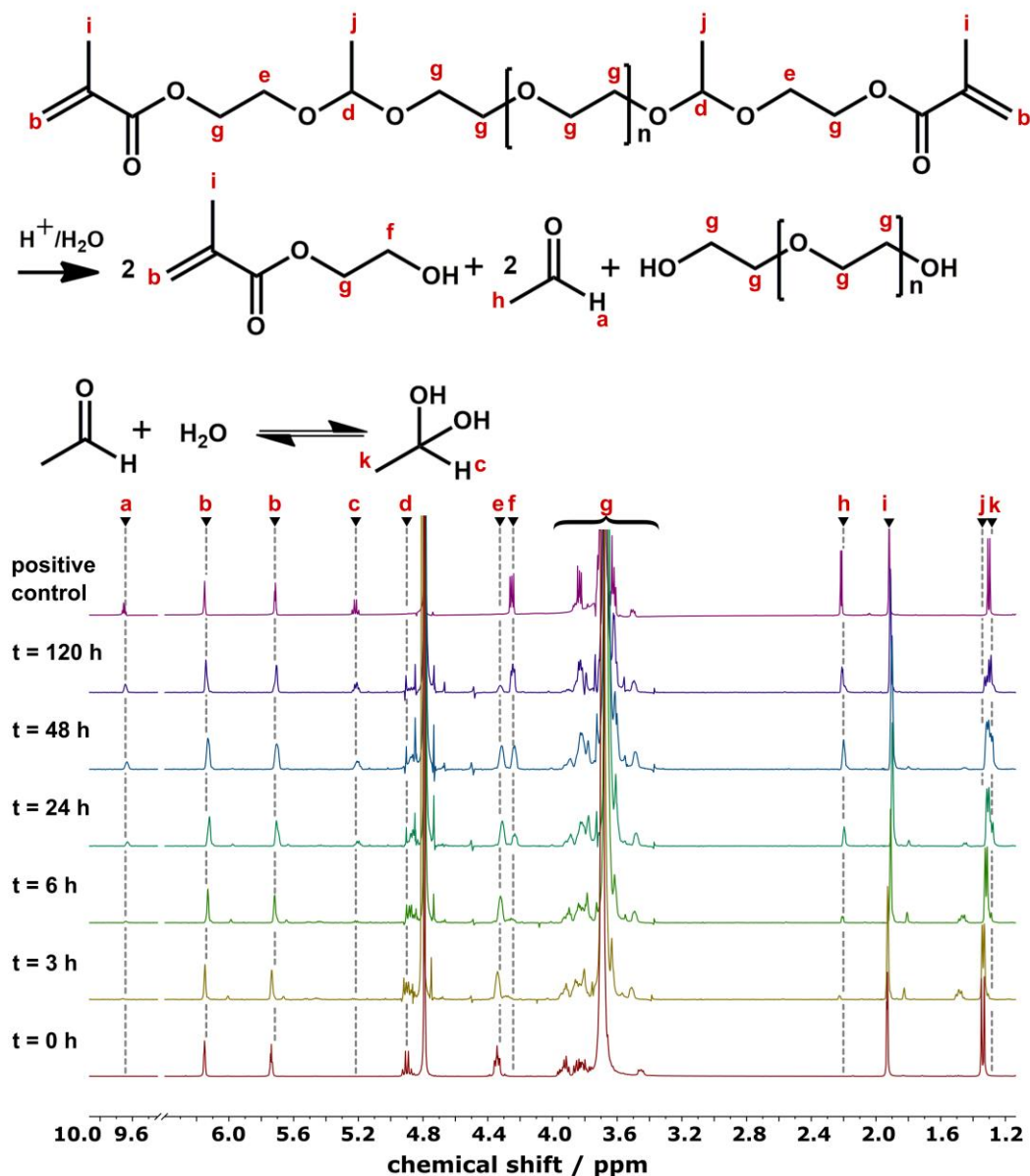


Figure 2. Lysis of macromonomer in aqueous solution at pH 5, monitored via  $^1\text{H}$  NMR kinetics. As a positive control, PEG-acetal-DMA was degraded at pH 3.

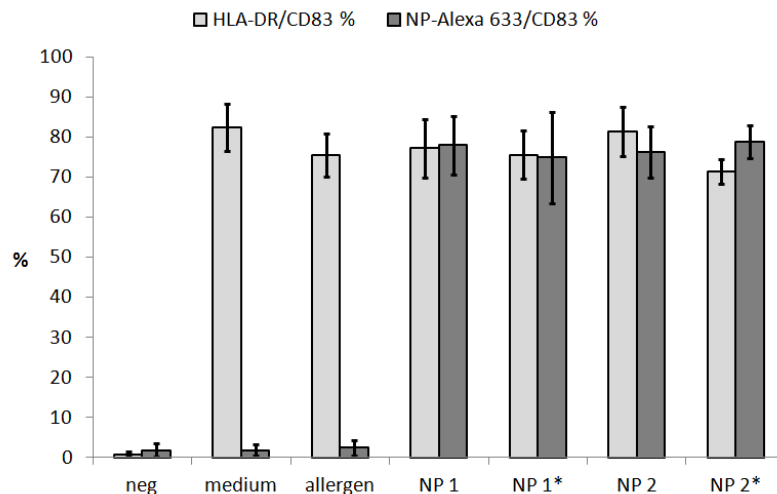
The integrals of the acetal and the methacrylate end group (d,j) decrease significantly with reaction time and disappear completely in case of the positive control. In contrast, the signals of the decomposition product acetaldehyde (a,h) increase compared to the constant signal of the

methylene group (b). Cleavage of the acetal groups furthermore results in a shift of the methylene protons next to it from 4.32 to 4.25 ppm (e,f). At 48 h, half of the acetal groups are cleaved, which is important because 48 h is the time an APC can effectively present an antigen-fragment before it is mortified. That means an encapsulated allergen has to be released before. The formed acetaldehyde forms the hydrate in aqueous solution (c,k). At pH 4, half of the acetal groups are cleaved in 1–2 h and degradation is completed in less than 24 h (see Figure S6). The solvent deuterium isotope effect is likely to slightly lower the reaction rate constant in water,<sup>[46]</sup> which needs to be further investigated.

NPs were generated using liposome templates<sup>[47]</sup> to obtain uniform size and form distributions by DAC, a novel technique introduced by the group of Massing *et al.*<sup>[48–50]</sup> The advantage of DAC compared to other NP preparation methods is its potential to carry out all synthesis steps at room temperature, under sterile conditions and in small volumes, which results in high encapsulation efficiencies for the cargo. After removal of nontrapped macromonomer and cargo by dialysis, the methacrylate groups were cross-linked by photoinitiated radical polymerization, creating a three-dimensional network. Subsequent to polymerization, the liposome templates were removed for some experiments to study the influence of the lipids on NP internalization (Scheme 1). CD spectra indicate that the secondary protein structure is mainly preserved (Figure S7).

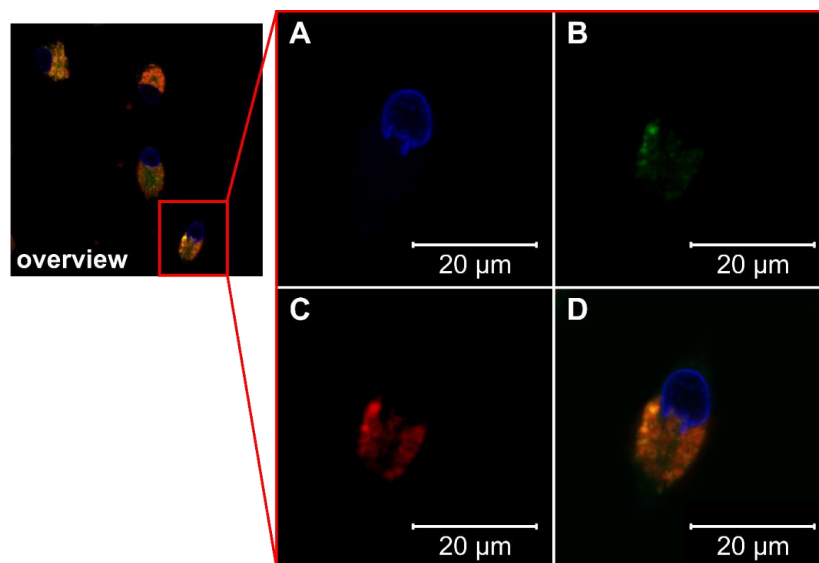
The NPs synthesized showed a size of 150–200 nm with narrow size distribution (hydrodynamic radius analyzed by light scattering in PBS, see Figure S8). By TEM, the estimated projected area diameter (core size) shows a smaller size, as generally expected due to sample preparation under vacuum. The NPs have a circular shape and are monodisperse (see Figure S9).

The amount of encapsulated protein was quantified by protein assay and by fluorescence photometry. Both techniques resulted in an encapsulation efficiency up to 45% for liposome-free NPs and up to 60% for liposome-containing NPs. The difference in encapsulation efficiencies may occur because of protein trapped between the inner liposome shell and the polymerized NP. Fluorescence-labeled NPs were used to determine the uptake of NPs into immature DCs, which was quantified by flow cytometry 48 h after further maturation (Figure 3).



*Figure 3.* Uptake of fluorescence-labeled degradable PEG-NPs into DCs; NP 1 = with allergen and liposome; NP 1\* = with allergen without liposome; NP 2 = empty with liposome; NP 2\* = empty without liposome; neg = untreated/unstained cells; n = 3.

No significant fluorescence, that is, uptake, could be detected in mature DCs (treated with maturation cocktail-containing medium with or without grass pollen or house dust mite allergen). The percentage of fluorescent cells increased in DCs treated with fluorescence-labeled NPs compared to DCs incubated with unlabeled allergen. Expression of the dendritic cell-specific maturation marker CD83 was not affected by allergen and NPs. To ensure endocytosis instead of mere surface adsorption, immature DCs treated with allergen-loaded NPs were investigated by confocal laser scanning microscopy after 4 h of incubation (Figure 4).

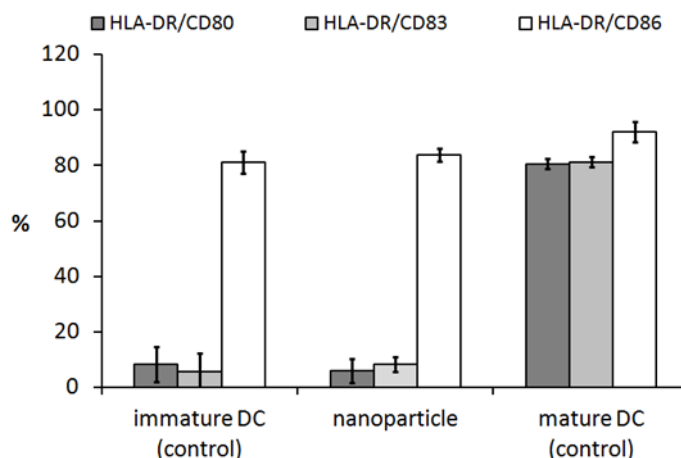


*Figure 4.* Uptake of NPs into DCs investigated by laser scanning confocal microscopy (A, nucleus, blue staining with Hoechst 33342; B, lysosomes, green staining with Lyso Tracker green DND-26; C, NPs loaded with red fluorescent grass pollen allergen (allergen-Alexa 633); D, overlay of A–C).



Colocalization of allergen and lysosomes appears as a yellow fluorescence in overlay (D) in Figure 4. The images give clear evidence of endocytotic uptake of the NPs and entrapped allergen, which leads to the desired localization of NP in lysosomes. This is a prerequisite for acidic degradation of the NPs and concurrent release of their cargo inside the APC. Potential cytotoxicity of the PEG-nanocarriers is a key issue for clinical application. In this context, an apoptosis assay was carried out. Fluorescent staining was performed with annexin V (apoptosis marker) and 7-AAD (DNA marker) to distinguish living cells from dead cells. No nanoparticle or degradation product related cytotoxicity could be detected upon incubation of DCs with nanoparticles compared to medium as negative control (Figure S10).

To investigate whether NPs per se lead to dendritic cell maturation probably due to LPS contamination, immature DCs were incubated with maturation cocktail or NPs (loaded with grass pollen allergen, house dust mite allergen, or empty) or were left untreated and analyzed by flow cytometry 48 h later (Figure 5).



*Figure 5.* Investigation of maturation markers on dendritic cells, measured by flow cytometry;  $n = 3$ .

As expected, immature DCs constitutively express MHC-class II molecules (HLA-DR) and CD86, and show no or only low expression of CD80 and CD83, while mature DCs strongly express these maturation markers. Remarkably, in contrast to other observations<sup>[51,52]</sup> where NPs led to cell maturation, DCs incubated with our NPs remain immature.

To investigate whether the allergen is shielded by the NP, we tested allergen detection by IgE-loaded basophilic leucocytes and subsequent leukotriene release upon stimulation with grass pollen or house dust mite allergen alone, allergen entrapped in NP (NP 1 are liposome containing,

NP 1\* are liposome-free), or empty NP (NP 2 are liposome containing, NP 2\* are liposome-free; see Figure 6).

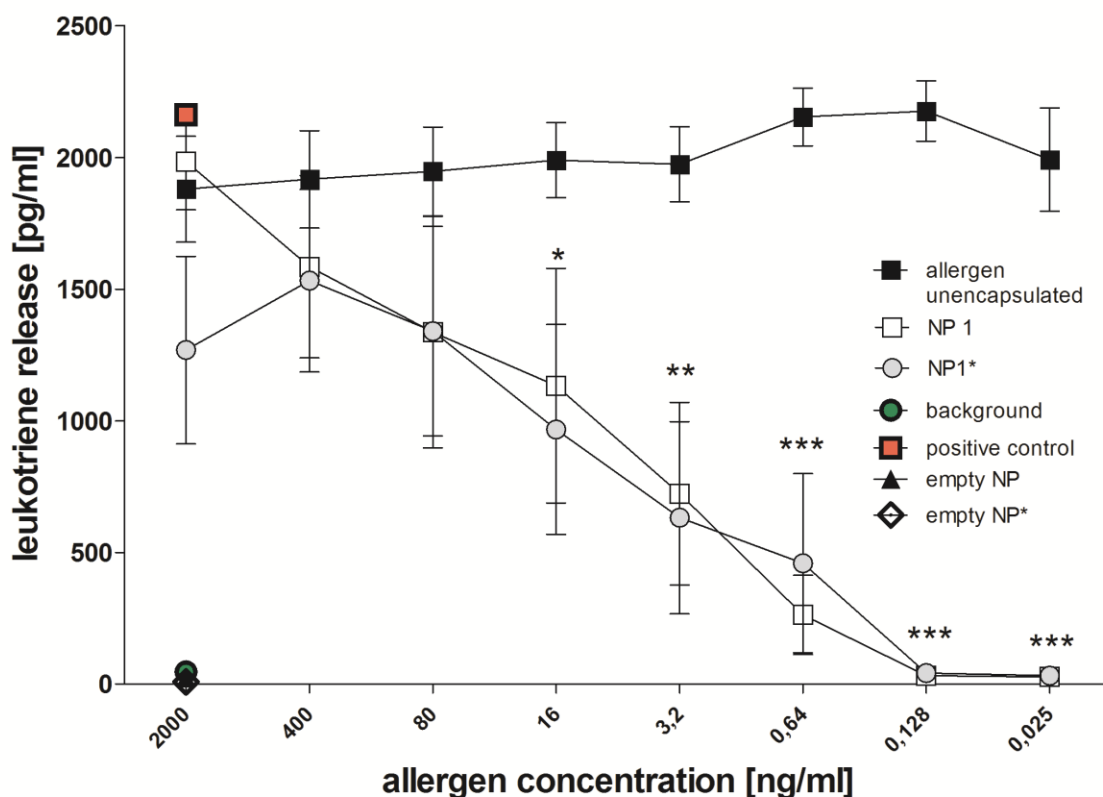
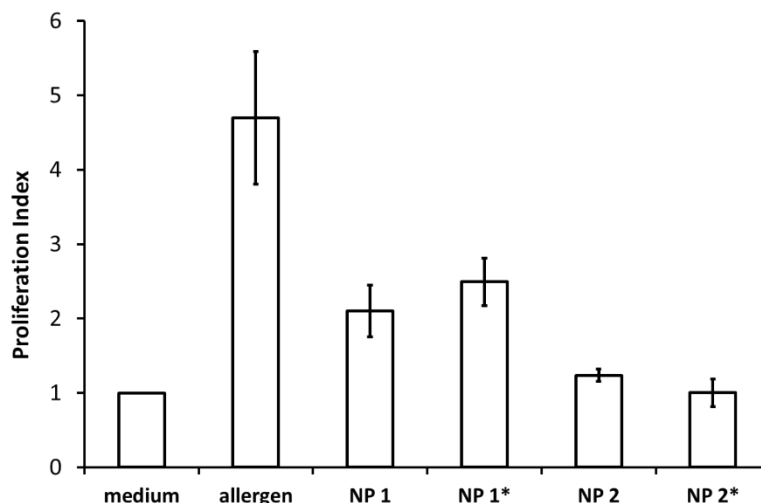


Figure 6. Leukotriene release of basophilic leucocytes from allergic donors incubated with allergen alone, allergen entrapped in NPs (NP 1 and NP 1\*), and empty NPs (NP 2 and NP 2\*). Experiments were carried out with cells of  $n = 4$  allergic donors. \* $p \leq 0.05$  compared to allergen alone.

The leukotriene release stayed at a constant level for cells incubated with allergen alone. Basophilic leukocytes treated with allergen-loaded NPs showed a significantly lower leukotriene release which dropped to zero at a certain concentration. Empty NP and medium did not lead to leukotriene release as expected. In order to demonstrate delivery of allergen into the antigen presenting pathway, DCs from allergic donors were incubated with grass pollen or house dust mite allergen loaded or empty liposome-containing (NP 1 or NP 2) and liposome-free NPs (NP 1\* or NP 2\*) or allergen alone, respectively, matured for 48 h, and subsequently cocultured with autologous CD4<sup>+</sup> T cells (Figure 7).



*Figure 7.* T cell proliferation assay with DCs incubated with medium, allergen, allergen-loaded, or empty NPs. Experiments carried out with cells of  $n = 7$  allergic donors. \* $p \leq 0.05$  compared to empty NPs.

After 5 days of coculture, the strength of T cell proliferation was measured by [ $^3\text{H}$ ]-thymidine incorporation in counts per minute (cpm) as a result of effective T cell activation by DCs. Figure 7 demonstrates strong proliferation of  $\text{CD4}^+$  T cells stimulated with allergen-treated DCs compared to  $\text{CD4}^+$  T cells stimulated with DCs that were left untreated (medium). DCs which had been treated with allergen-loaded NPs with (NP 1) and without liposomes (NP 1\*) induced about 41% and 53%, respectively, of the proliferation intensity observed for T cells stimulated with DCs treated with free allergen. Empty NPs as control (NP 2 and NP 2\*) did not lead to enhanced T cell proliferation. These results provide strong evidence that allergens encapsulated in the degradable PEG-NPs can be liberated and retain their biological activity. In all *in vitro* experiments investigated, no difference in behavior between liposome-containing and liposome-free NP could be observed. We are currently examining the leakage of protein from the NPs, which may be affected by the existence of the liposome shell. The reduced proliferative response to encapsulated allergens compared to free allergens is most likely due to reduced uptake of encapsulated allergens compared to free allergens (see Figure S11). This potential disadvantage could be overcome by increased amounts of allergens encapsulated (not leading to increased side effects due to encapsulation) or by functionalization of nanoparticles with mannose, for example, enhancing uptake into dendritic cells. The group of Fréchet created OVA-loaded pH-sensitive hydrogel NPs made of polyacrylamide<sup>[53]</sup> or dextran<sup>[54]</sup> with a degradable cross-linker that were able to activate  $\text{CD8}^+$  T cells more efficiently than free OVA. Jain *et al.* synthesized PEG nanocarriers loaded with OVA and modified with an adjuvant for antigen delivery into antigen-

presenting cells. The nanocarriers were tested in murine cell lines and led to CD4<sup>+</sup> and CD8<sup>+</sup> T cell activation (measured by IL-2 production), but did not include any degradable sites.<sup>[55]</sup> The NPs presented here, which combine acid-degradability with the desired features of PEG-derived NPs, were tested *in vitro* on human cells and showed immune reactions for CD4<sup>+</sup> T cell proliferation. For the novel NPs introduced here, no cross-linkers are needed, so the whole nanoparticle network can be degraded and excreted via the kidney. The goal for these nanoparticles is to deliver their cargo into the antigen presenting pathway and to avoid undesired effects during SIT.

### **Conclusion**

In summary, we introduce a new type of degradable PEG-based dimethacrylate and have been able to demonstrate the usefulness of acetal-functionalized PEG nanoparticles that were allergen-loaded and degradable inside the lysosome, to induce specific immune responses. The whole chain of events from the design of acid-labile PEG macromonomers, the generation of protein-loaded nanoparticles, their uptake by cells, and controlled release of the cargo, which results in a specific immune response, was demonstrated. These promising results encourage further research. The concept of encapsulation bears promise for application not only in specific immunotherapy with allergens, but also for vaccination in general and different forms of immunotherapy for cancer or AIDS.

### **Acknowledgements**

The authors gratefully acknowledge the support of this research by Thomas Fritz, Markus Hirsch, Steffen Lorenz, Jan Morsbach, and Fabienne Ludwig. A prototype of a dual centrifuge was kindly provided by Ulrich Massing and Andreas Hettich GmbH & Co. This work was supported by the Max Planck Graduate Center with the Johannes Gutenberg-Universität Mainz (MPGC) as well as by NMFZ (Naturwissenschaftlich-medizinisches Forschungszentrum of the University Medical Center Mainz). H.P. is a recipient of a fellowship through funding of the Excellence Initiative (DFG/GSC 266) in the context of the graduate school of excellence "MAINZ" (Materials Science in Mainz).

### **Abbreviations**

PEG, poly(ethylene glycol); PVM-MA, poly(methyl vinyl ether/maleic acid anhydride) copolymers; NP, nanoparticles; APC, antigen-presenting cell; DCs, dendritic cell; SIT, specific immunotherapy; DMA, dimethacrylate; OVA, ovalbumin; PBS, Dulbecco's phosphate buffered saline; FITC,

fluorescein isothiocyanate; DMF, dimethylformamide; RI, refractive index; TEM, transmission electron microscopy; CD, circular dichroism; DAC, dual centrifugation; NP 1, liposome containing allergen loaded nanoparticle; NP 1\*, liposome-free allergen loaded nanoparticle; NP 2, liposome containing empty nanoparticle; NP 2\* liposome-free empty nanoparticle; cpm, counts per minute.

## References

- [1] Chaturvedi, K.; Ganguly, K.; Nadagouda, M. N.; Aminabhavi, T. M., Polymeric hydrogels for oral insulin delivery. *J. Controlled Release* **2013**, 165, 129–138.
- [2] Lin, C.-C.; Metters, A. T.; Anseth, K. S., Functional PEG-peptide hydrogels to modulate local inflammation induced by the proinflammatory cytokine TNF-alpha. *Biomaterials* **2009**, 30, 4907–4914.
- [3] Kloxin, A. M.; Kasko, A. M.; Salinas, C. N.; Anseth, K. S., Photodegradable hydrogels for dynamic tuning of physical and chemical properties. *Science* **2009**, 324, 59–63.
- [4] Steinhilber, D.; Rossow, T.; Wedepohl, S.; Paulus, F.; Seiffert, S.; Haag, R., A microgel construction kit for bioorthogonal encapsulation and pH-controlled release of living cells. *Angew. Chem., Int. Ed.* **2013**, 52, 13538–13543.
- [5] Onaca-Fischer, O.; Liu, J.; Inglin, M.; Palivan, C. G., Polymeric Nanocarriers and Nanoreactors. *Curr. Pharm. Des.* **2012**, 18, 2622–2643.
- [6] Gupta, P.; Vermani, K.; Garg, S., Hydrogels. *Drug Discovery Today* **2002**, 7, 569–579.
- [7] Gómez, S.; Gamazo, C.; San Roman, B.; Grau, A.; Espuelas, S.; Ferrer, M.; Sanz, M. L.; Irache, J. M., A novel nanoparticulate adjuvant for immunotherapy with *Lolium perenne*. *J. Immunol. Methods* **2009**, 348, 1–8.
- [8] Schöll, I.; Weissenbock, A.; Forster-Waldl, E.; Untersmayr, E.; Walter, F.; Willheim, M.; Boltz-Nitulescu, G.; Scheiner, O.; Gabor, F.; Jensen-Jarolim, E., Allergen-loaded biodegradable poly(D,L-lactic-co-glycolic) acid nanoparticles down-regulate an ongoing Th2 response in the BALB/c mouse model. *Clin. Exp. Allergy* **2004**, 34, 315–321.
- [9] Fleige, E.; Quadir, M. A.; Haag, R., Stimuli-responsive polymeric nanocarriers for the controlled transport of active compounds: concepts and applications. *Adv. Drug Delivery Rev.* **2012**, 64, 866–884.
- [10] Mura, S.; Nicolas, J.; Couvreur, P., Stimuli-responsive nanocarriers for drug delivery. *Nat. Mater.* **2013**, 12, 991–1003.
- [11] Steinhilber, D.; Sisson, A. L.; Mangoldt, D.; Welker, P.; Licha, K.; Haag, R., Synthesis, Reductive Cleavage, and Cellular Interaction Studies of Biodegradable, Polyglycerol Nanogels. *Adv. Funct. Mater.* **2010**, 20, 4133–4138.
- [12] Grafahrend, D.; Heffels, K.-H.; Beer, M. V.; Gasteier, P.; Möller, M.; Boehm, G.; Dalton, P. D.; Groll, J., Degradable polyester scaffolds with controlled surface chemistry combining minimal protein adsorption with specific bioactivation. *Nat. Mater.* **2011**, 10, 67–73.
- [13] Lin, C.-C.; Anseth, K. S., PEG hydrogels for the controlled release of biomolecules in regenerative medicine. *Pharm. Res.* **2009**, 26, 631–643.

- [14] Balamurali, V.; Pramodkuma, T. M.; Srujana, N.; Venkatesh, M. P.; Gupta, N. V.; Krishna, K. L.; Gangadhara, H. V., pH Sensitive Drug Delivery Systems. *Am. J. Drug Discovery Dev.* **2011**, *1*, 24–48.
- [15] Li, L.; Xu, Y.; Milligan, I.; Fu, L.; Franckowiak, E. A.; Du, W., Synthesis of highly pH-responsive glucose poly(orthoester). *Angew. Chem., Int. Ed.* **2013**, *52*, 13699–13702.
- [16] Tomlinson, R.; Heller, J.; Brocchini, S.; Duncan, R., Polyacetaldoxorubicin conjugates designed for pH-dependent degradation. *Bioconjugate Chem.* **2003**, *14*, 1096–1106.
- [17] Gu, Y.; Zhong, Y.; Meng, F.; Cheng, R.; Deng, C.; Zhong, Z., Acetal-linked paclitaxel prodrug micellar nanoparticles as a versatile and potent platform for cancer therapy. *Biomacromolecules* **2013**, *14*, 2772–2780.
- [18] Lu, L.; Zou, Y.; Yang, W.; Meng, F.; Deng, C.; Cheng, R.; Zhong, Z., Anisamide-Decorated pH-Sensitive Degradable Chimaeric Polymersomes Mediate Potent and Targeted Protein Delivery to Lung Cancer Cells. *Biomacromolecules* **2015**, *16*, 1726–1735.
- [19] Thambi, T.; Deepagan, V. G.; Yoo, C. K.; Park, J. H., Synthesis and physicochemical characterization of amphiphilic block copolymers bearing acid-sensitive orthoester linkage as the drug carrier. *Polymer* **2011**, *52*, 4753–4759.
- [20] Sawant, R. M.; Hurley, J. P.; Salmaso, S.; Kale, A.; Tolcheva, E.; Levchenko, T. S.; Torchilin, V. P., "SMART" drug delivery systems: double-targeted pH-responsive pharmaceutical nanocarriers. *Bioconjugate Chem.* **2006**, *17*, 943–949.
- [21] Huang, F.; Cheng, R.; Meng, F.; Deng, C.; Zhong, Z., Micelles Based on Acid Degradable Poly(acetal urethane): Preparation, pH Sensitivity, and Triggered Intracellular Drug Release. *Biomacromolecules* **2015**, *16*, 2228–2236.
- [22] Du, Y.; Chen, W.; Zheng, M.; Meng, F.; Zhong, Z., pH-sensitive degradable chimaeric polymersomes for the intracellular release of doxorubicin hydrochloride. *Biomaterials* **2012**, *33*, 7291–7299.
- [23] Chen, W.; Meng, F.; Cheng, R.; Zhong, Z., pH-Sensitive degradable polymersomes for triggered release of anticancer drugs: a comparative study with micelles. *J. Controlled Release* **2010**, *142*, 40–46.
- [24] Zalipsky, S., Harris, J. M., Eds. Introduction to Chemistry and Biological Applications of Poly(ethylene glycol). In *Poly(ethylene glycol) Chemistry and Biological Applications*; ACS Symposium Series; American Chemical Society: Washington, DC, **2009**; Chapter 110.1021/bk-1997-0680.ch001.
- [25] Dingels, C.; Müller, S. S.; Steinbach, T.; Tonhauser, C.; Frey, H., Universal concept for the implementation of a single cleavable unit at tunable position in functional poly(ethylene glycol)s. *Biomacromolecules* **2013**, *14*, 448–459.
- [26] Dingels, C.; Frey, H., From Biocompatible to Biodegradable: Poly(ethylene glycol)s with Predetermined Breaking Points. *Adv. Polym. Sci.* **2013**, *262*, 167–190.
- [27] Feng, X.; Chaikof, E. L.; Absalon, C.; Drummond, C.; Taton, D.; Gnanou, Y., Dendritic carrier based on PEG: design and degradation of acid-sensitive dendrimer-like poly(ethylene oxide)s. *Macromol. Rapid Commun.* **2011**, *32*, 1722–1728.

- [28] Wang, Y.; Morinaga, H.; Sudo, A.; Endo, T., Synthesis of amphiphilic polyacetal by polycondensation of aldehyde and polyethylene glycol as an acid-labile polymer for controlled release of aldehyde. *J. Polym. Sci., Part A: Polym. Chem.* **2011**, *49*, 596–602.
- [29] Rickerby, J.; Prabhakar, R.; Ali, M.; Knowles, J.; Brocchini, S., Water-soluble polyacetals derived from diphenols. *J. Mater. Chem.* **2005**, *15*, 1849.
- [30] Reid, B.; Tzeng, S.; Warren, A.; Kozielski, K.; Elisseeff, J., Development of a PEG Derivative Containing Hydrolytically Degradable Hemiacetals. *Macromolecules* **2010**, *43*, 9588–9590.
- [31] Zhao, L.; Seth, A.; Wibowo, N.; Zhao, C.-X.; Mitter, N.; Yu, C.; Middelberg, A. P. J., Nanoparticle vaccines. *Vaccine* **2014**, *32*, 327–337.
- [32] de Temmerman, M.-L.; Rejman, J.; Demeester, J.; Irvine, D. J.; Gander, B.; de Smedt, S. C., Particulate vaccines: on the quest for optimal delivery and immune response. *Drug Discovery Today* **2011**, *16*, 569–582.
- [33] Dierendonck, M.; de Koker, S.; de Rycke, R.; Bogaert, P.; Grooten, J.; Vervaet, C.; Remon, J. P.; de Geest, B. G., Single-step formation of degradable intracellular biomolecule microreactors. *ACS Nano* **2011**, *5*, 6886–6893.
- [34] Kazakov, S.; Kaholek, M.; Teraoka, I.; Levon, K., UV-Induced Gelation on Nanometer Scale Using Liposome Reactor. *Macromolecules* **2002**, *35*, 1911–1920.
- [35] Srivastava, D.; Arora, N.; Singh, B. P., Current immunological approaches for management of allergic rhinitis and bronchial asthma. *Inflammation Res.* **2009**, *58*, 523–536.
- [36] Akdis, C. A.; Akdis, M., Mechanisms of allergen-specific immunotherapy. *J. Allergy Clin. Immunol.* **2011**, *127*, 18–27.
- [37] Heydenreich, B.; Bellinghausen, I.; Lorenz, S.; Henmar, H.; Strand, D.; Würtzen, P. A.; Saloga, J., Reduced in vitro T-cell responses induced by glutaraldehyde-modified allergen extracts are caused mainly by retarded internalization of dendritic cells. *Immunology* **2012**, *136*, 208–217.
- [38] Licciardi, M.; Montana, G.; Bondì, M. L.; Bonura, A.; Scialabba, C.; Melis, M.; Fiorica, C.; Giammona, G.; Colombo, P., An allergenpolymeric nanoaggregate as a new tool for allergy vaccination. *Int. J. Pharm.* **2014**, *465*, 275–283.
- [39] McGee, J.; Davis, S.; Ohagan, D., The immunogenicity of a model protein entrapped in poly(lactide-co-glycolide) microparticles prepared by a novel phase separation technique. *J. Control. Release* **1994**, *31*, 55–60.
- [40] Gamazo, C.; Gastaminza, G.; Ferrer, M.; Sanz, M. L.; Irache, J. M., Nanoparticle based-immunotherapy against allergy. *Immunotherapy* **2014**, *6*, 885–897.
- [41] Park, T. G., Degradation of poly(lactic-co-glycolic acid) microspheres. *Biomaterials* **1995**, *16*, 1123–1130.
- [42] Vysotskaya, O. V.; Oparina, L. A.; Parshina, L. N.; Gusarova, N. K.; Trofimov, B. A., Functional Acetal Methacrylates: III. Electrophilic Addition of Diols to 2-(Vinylxy)ethyl Methacrylate. *Russ. J. Org. Chem.* **2002**, *38*, 1082–1087.
- [43] Jonuleit, H.; Kühn, U.; Müller, G.; Steinbrink, K.; Paragnik, L.; Schmitt, E.; Knop, J.; Enk, A. H., Pro-inflammatory cytokines and prostaglandins induce maturation of potent

- immunostimulatory dendritic cells under fetal calf serum-free conditions. *Eur. J. Immunol.* **1997**, 27, 3135–3142.
- [44] Kaliński, P.; Hilken, C. M.; Snijders, A.; Snijdewint, F. G.; Kapsenberg, M. L., IL-12-deficient dendritic cells, generated in the presence of prostaglandin E2, promote type 2 cytokine production in maturing human naive T helper cells. *J. Immunol.* **1997**, 159, 28–35.
- [45] Gillies, E. R.; Goodwin, A. P.; Fréchet, J. M. J., Acetals as pH-sensitive linkages for drug delivery. *Bioconjugate Chem.* **2004**, 15, 1254–1263.
- [46] Cordes, E. H.; Bull, H. G., Mechanism and catalysis for hydrolysis of acetals, ketals, and ortho esters. *Chem. Rev.* **1974**, 74, 581–603.
- [47] An, S. Y.; Bui, M.-P. N.; Nam, Y. J.; Han, K. N.; Li, C. A.; Choo, J.; Lee, E. K.; Katoh, S.; Kumada, Y.; Seong, G. H., Preparation of monodisperse and size-controlled poly(ethylene glycol) hydrogel nanoparticles using liposome templates. *J. Colloid Interface Sci.* **2009**, 331, 98–103.
- [48] Massing, U.; Cicko, S.; Ziroli, V., Dual asymmetric centrifugation (DAC)—a new technique for liposome preparation. *J. Control. Release* **2008**, 125, 16–24.
- [49] Hirsch, M.; Ziroli, V.; Helm, M.; Massing, U., Preparation of small amounts of sterile siRNA-liposomes with high entrapping efficiency by dual asymmetric centrifugation (DAC). *J. Control. Release* **2009**, 135, 80–88.
- [50] Fritz, T.; Hirsch, M.; Richter, F. C.; Müller, S. S.; Hofmann, A. M.; Rusitzka, K. A. K.; Markl, J.; Massing, U.; Frey, H.; Helm, M., Click modification of multifunctional liposomes bearing hyperbranched polyether chains. *Biomacromolecules* **2014**, 15, 2440–2448.
- [51] Frick, S. U.; Bacher, N.; Baier, G.; Mailänder, V.; Landfester, K.; Steinbrink, K., Functionalized polystyrene nanoparticles trigger human dendritic cell maturation resulting in enhanced CD4+ T cell activation. *Macromol. Biosci.* **2012**, 12, 1637–1647.
- [52] Yang, D.; Zhao, Y.; Guo, H.; Li, Y.; Tewary, P.; Xing, G.; Hou, W.; Oppenheim, J. J.; Zhang, N., [Gd@C(82)(OH)(22)]<sub>(n)</sub> nanoparticles induce dendritic cell maturation and activate Th1 immune responses. *ACS Nano* **2010**, 4, 1178–1186.
- [53] Cohen, J. A.; Beaudette, T. T.; Tseng, W. W.; Bachelder, E. M.; Mende, I.; Engleman, E. G.; Fréchet, J. M. J., T-cell activation by antigen-loaded pH-sensitive hydrogel particles in vivo: the effect of particle size. *Bioconjugate Chem.* **2009**, 20, 111–119.
- [54] Bachelder, E. M.; Beaudette, T. T.; Broaders, K. E.; Dashe, J.; Fréchet, J. M. J., Acetal-derivatized dextran: an acid-responsive biodegradable material for therapeutic applications. *J. Am. Chem. Soc.* **2008**, 130, 10494–10495.
- [55] Jain, S.; Yap, W. T.; Irvine, D. J., Synthesis of protein-loaded hydrogel particles in an aqueous two-phase system for coincident antigen and CpG oligonucleotide delivery to antigen-presenting cells. *Biomacromolecules* **2005**, 6, 2590–2600.



## Supporting Information

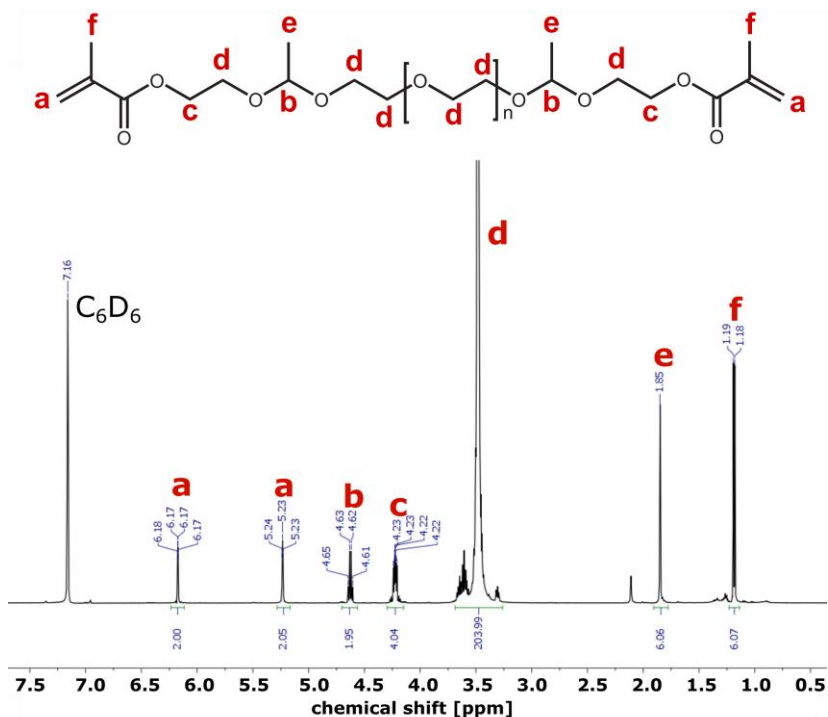


Figure S1. <sup>1</sup>H-NMR-Spectrum (300 MHz, C<sub>6</sub>D<sub>6</sub>) PEG-Acetal-DMA Mn = 2300 g mol<sup>-1</sup>.

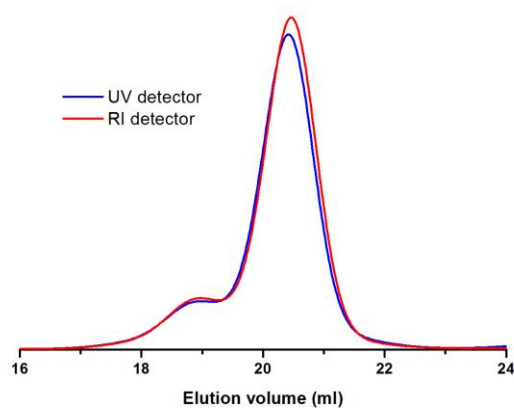


Figure S2. Gel permeation chromatography elugram (eluent: DMF, PEG-calibration) of PEG-acetal-DMA (Mn = 2300 g mol<sup>-1</sup>, red line: RI detector, blue line: UV detector). Besides the distribution at ca. 2000 g mol<sup>-1</sup> both lines show a high molecular weight shoulder at ca. 4200 g mol<sup>-1</sup> due to transacetalization reactions of PEG-acetal-DMA (see Figure S4).

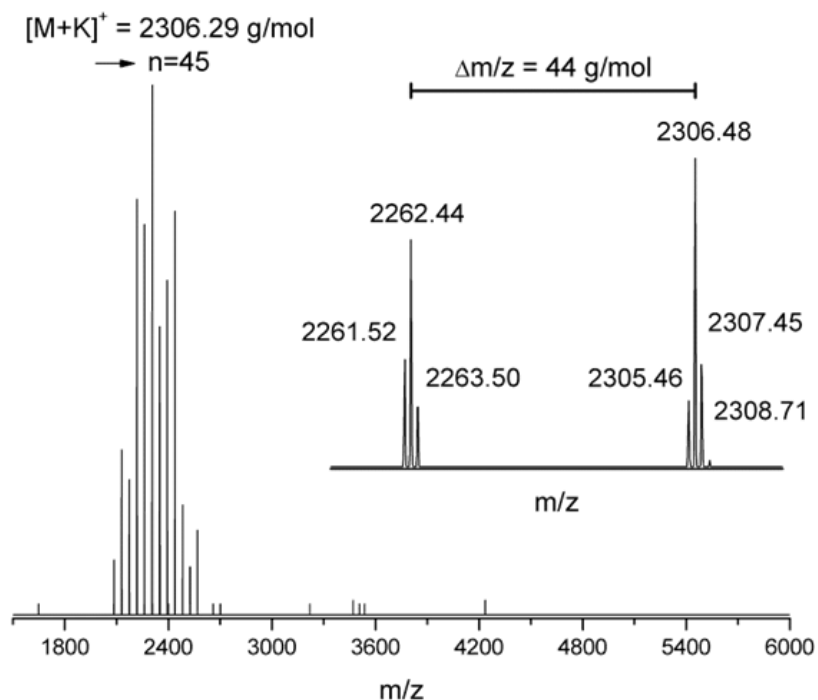


Figure S3. MALDI-ToF analysis (matrix: dithranol, salt: potassium triflate) of PEG-acetal-DMA ( $M_n = 2300 \text{ g mol}^{-1}$ ). Only one distribution can be observed that can be assigned to the difunctional product, the presence of monofunctionalized product can be excluded.

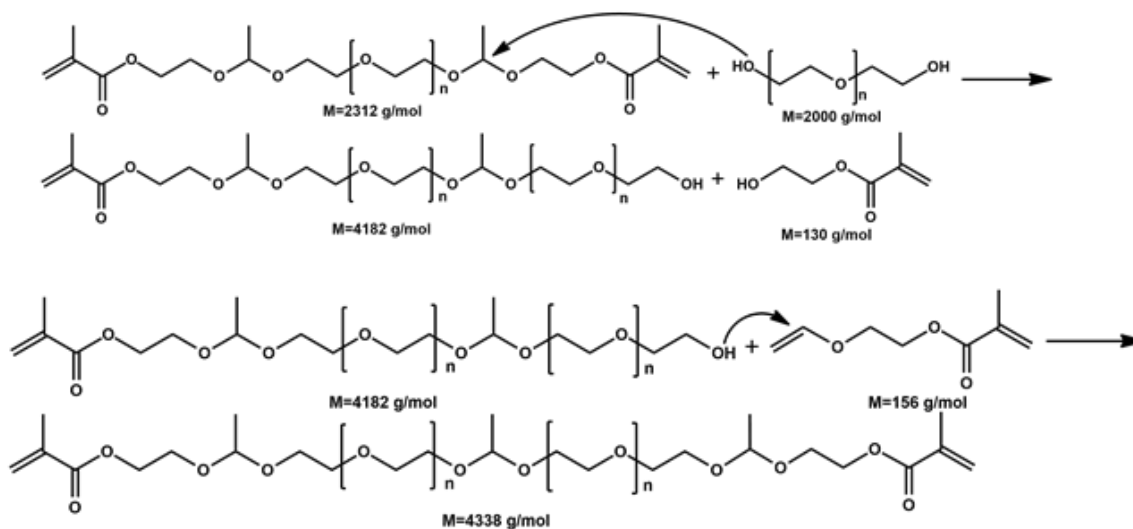
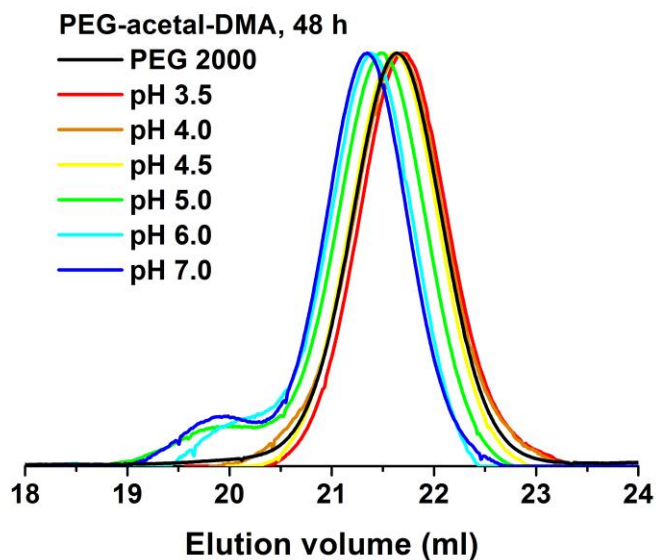


Figure S4. Chemical equation of transacetalization and functionalization reactions of PEG-acetal-DMA ( $M_n = 2300 \text{ g mol}^{-1}$ ) to PEG acetal DMA with  $M_n = 4200 \text{ g mol}^{-1}$ .

To confirm acid-degradability, the macromonomer was dissolved in citrate-phosphate buffer (pH 3.5 – pH 6 at 38 °C for 48 h). As a negative control, the macromonomer was dissolved in PBS at pH 7 to demonstrate stability of the macromonomer under neutral conditions. Clearly, upon acidification, the macromonomer is cleaved in 48 hours until acidification to pH 4.5 and a shift in molecular weight back to the  $M_n$  of PEG is observed in GPC (PEG-2000 as control).



*Figure S5.* Lysis of macromonomer in aqueous solution at pH 3.5–pH 7, monitored via GPC analysis (eluent: DMF, PEG-calibration). Black line: PEG ( $M_n = 2000 \text{ g mol}^{-1}$ ) before functionalization, red line: PEG-acetal-DMA pH 3.5, orange line: PEG-acetal-DMA pH 4, yellow line: PEG-acetal-DMA pH 4.5, green line: PEG-acetal-DMA pH 5.0, cyan line: PEG-acetal-DMA pH 6.0, blue line: negative control, PEG-acetal-DMA at pH 7,  $M_n = 2300 \text{ g mol}^{-1}$ .

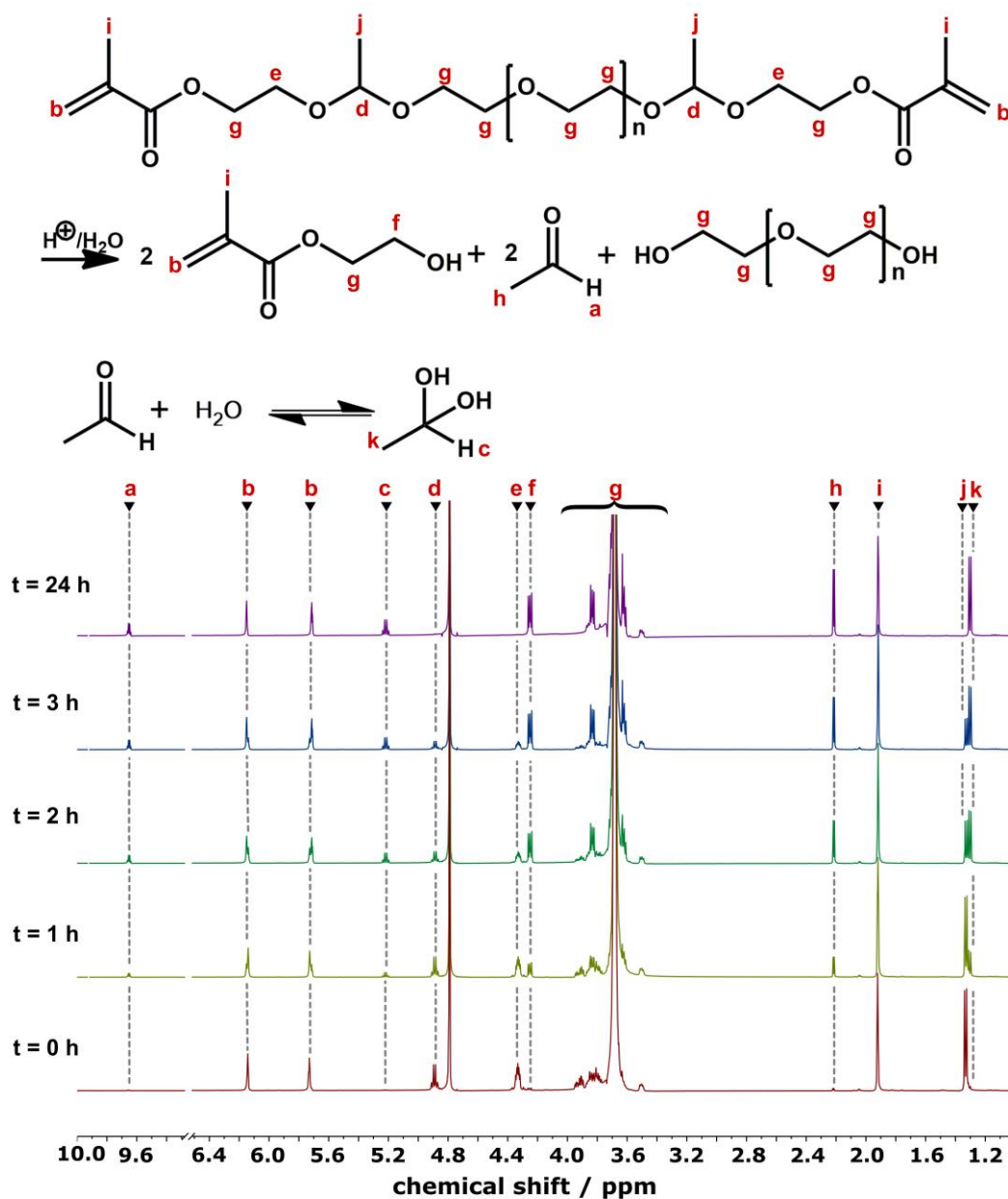
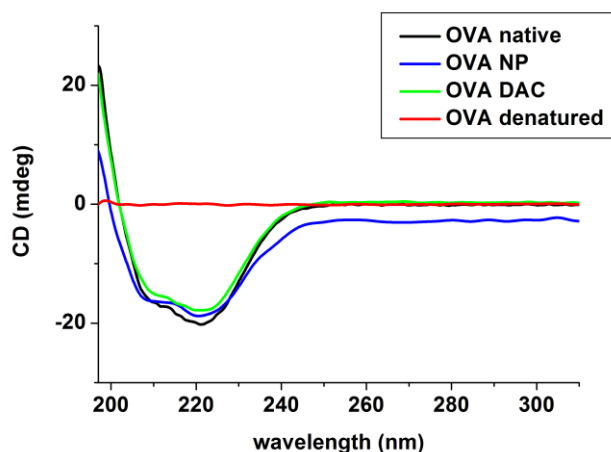
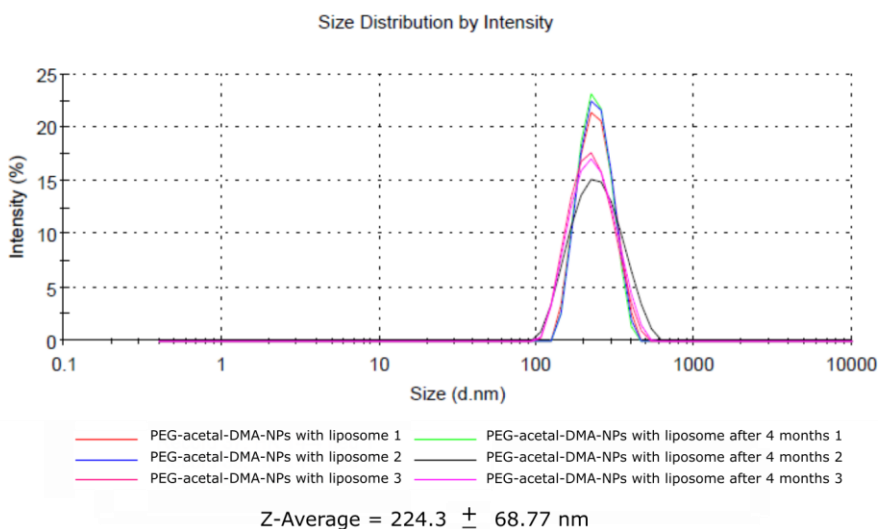


Figure S6. Lysis of macromonomer PEG-acetal-DMA in aqueous solution at pH 4, monitored via  $^1H$ -NMR kinetics. As a positive control, PEG-acetal-DMA was degraded at pH 3. At pH 4, half of the acetal groups are cleaved in 1-2 hours and degradation is completed in less than 24 hours. The formed acetaldehyde forms the hydrate in aqueous solution (c,k).

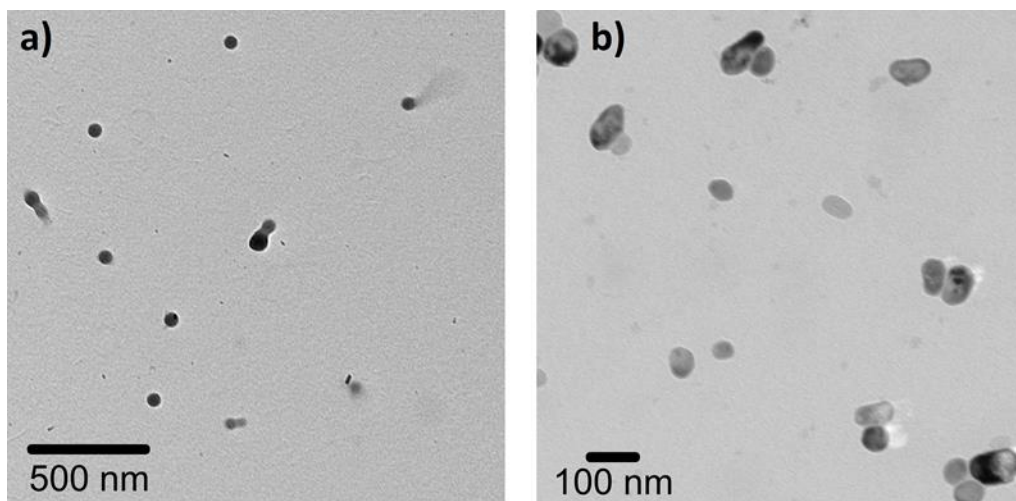


*Figure S7.* CD spectra of model protein ovalbumin (OVA) native (1 mg/ml, before centrifugation), OVA DC (1 mg/ml, after centrifugation with ceramic-beads), OVA NP (0.2 mg/ml, OVA inside the PEG-acetal-DMA NP without liposomes) and OVA denatured (1 mg/ml of OVA native, treated for 48 h at 80 °C). Spectra were measured with a 0.1 cm cell in the far UV region and scaled to the absorption maximum.

The far UV CD spectra of ovalbumin as a model protein gave almost the same curve (Fig S7) for OVA native, OVA DC and OVA NP. These results indicate that the secondary structure of ovalbumin appears to be mainly preserved under the nanoparticle synthesis conditions. OVA that was heat-denatured did not show any secondary structure.

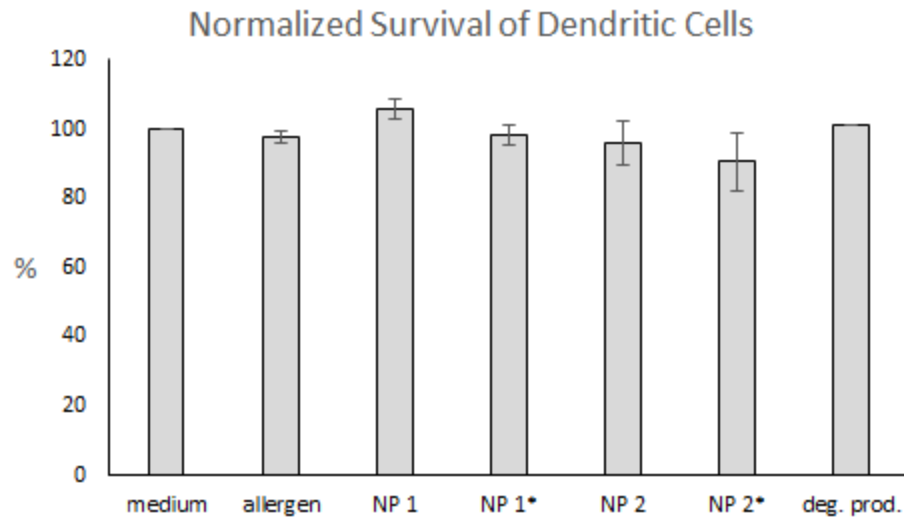


*Figure S8.* Size distribution analysis of PEG-acetal-DMA-nanoparticles with liposomes by zetasizer. The result is expressed as average value ± standard deviation. Comparison of particle size after synthesis and after 4 months of storage at 4° C (both measurements in triplicate). The diameter of the NPs stayed constant at 225 nm over the time-period of 4 months.

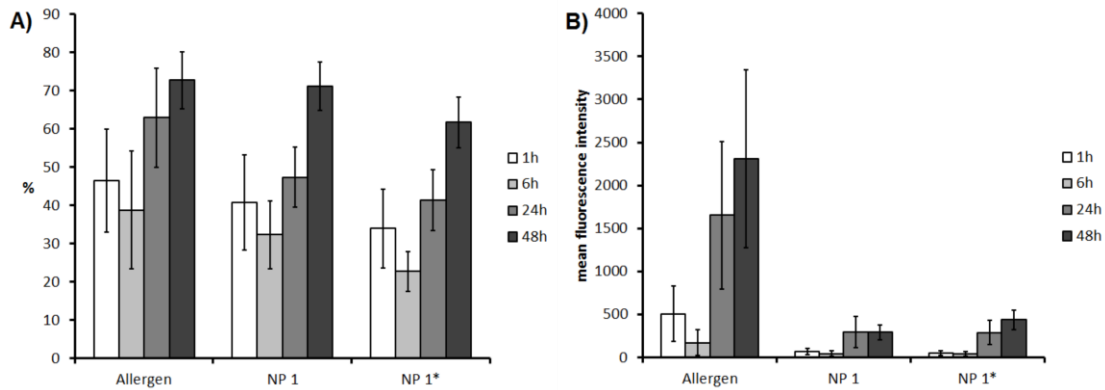


*Figure S9.* TEM images of a) NP with liposomes, loaded with grass pollen allergen and b) NP after removal of liposomes, loaded with grass pollen allergen (solvent: milliQ-water,  $c = 1.0$  g/l).

In order to support the results of the DLS measurements, additional transmission electron microscopy (TEM) measurements were carried out to obtain information on the shape of the structures formed. To perform this experiment the nanoparticles were dissolved in milliQ-water, and one drop of the solution ( $c = 1.0$  mg/ml) was deposited on a carbon-coated copper TEM grid. Subsequently the solvent was evaporated under vacuum. No further sample treatment was necessary. Relating to the size, the difference between the TEM and DLS results are explained by drying effects.



*Figure S10.* Apoptosis assay of mature dendritic cells; flow cytometry measurement of annexin V and 7-AAD positive cells; the graph shows the normalized cell survival compared to the medium control. NP 1 = with allergen and liposome; NP 1\* = with allergen without liposome; NP 2 = empty with liposome; NP 2\* = empty without liposome. Degradation products (deg. prod.) were tested in apoptosis assay after acidification to pH 4 for 48 hours and subsequent neutralization.



*Figure S11.* Uptake of protein labeled with fluorescent dye into dendritic cells (A percentage of fluorescent cells, B mean fluorescence intensity of fluorescent cells) NP 1= with liposome, NP 1\* = without liposome; n=7. \* =  $p \leq 0.05$  compared to medium control.

## Chapter 3. PEG Dimethacrylates with Cleavable Ketal Sites

### A Precursor for Cleavable Hydrogels

Hannah Pohlit<sup>1,2,3</sup>, Daniel Leibig<sup>2,3</sup>, Holger Frey<sup>2,\*</sup>

<sup>1</sup>Department of Dermatology, University Medical Center Mainz, Langenbeckstr. 1, 55131 Mainz, Germany

<sup>2</sup>Institute of Organic Chemistry, Johannes Gutenberg University Mainz, Duesbergweg 10-14, 55128 Mainz, Germany

<sup>3</sup>Graduate School Materials Science in Mainz, Staudinger Weg 9, 55128 Mainz, Germany

\* corresponding author: Holger Frey, hfrey@uni-mainz.de

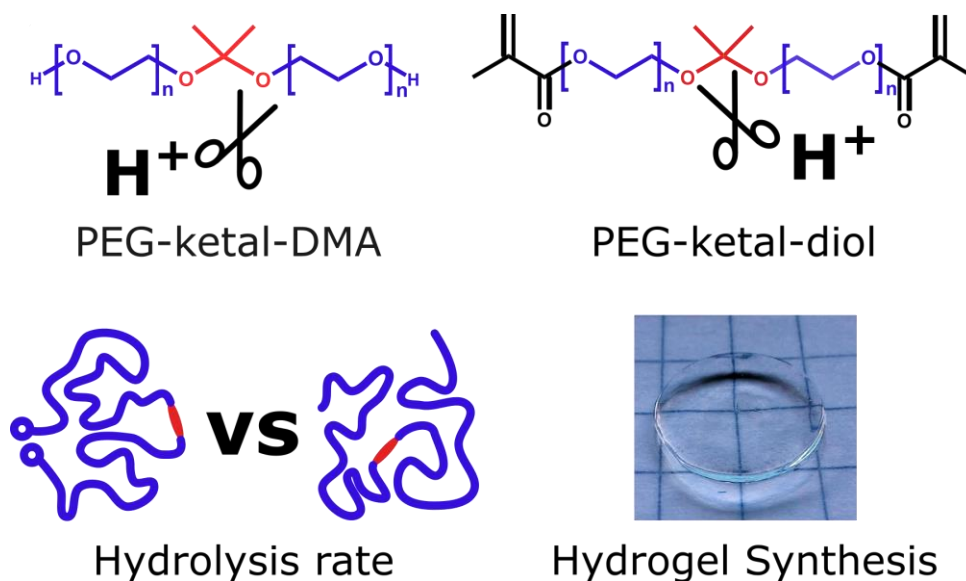
To be submitted.

#### Abstract

Stimuli-responsive drug-delivery systems for the transport and targeted release of therapeutic proteins have gained increasing interest during the last decades. We describe poly(ethylene glycol) (PEG) based macromonomers containing acid-labile ketal moieties as well as terminal methacrylate units that are amenable to radical polymerization. The synthesis of PEGs of different molecular weights (ranging from 2000 to 13,000 g mol<sup>-1</sup> with polydispersities < 1.15) with a central ketal unit (PEG-ketal-diol) and their conversion to PEG-ketal-dimethacrylates (PEG-ketal-DMA) is introduced. Degradation rates of both PEG-ketal-diols and PEG-ketal-dimethacrylates were investigated by *in-situ* <sup>1</sup>H NMR kinetic studies in deuterated phosphate buffer. The hydrolysis half-life times varied from 82.4 min (pH = 5, room temperature, PEG-ketal-diol) to 5.6 min (pH = 5, body temperature, PEG-ketal-DMA). As expected, the degradation rate of the ketal moieties increased with temperature, resulting in hydrolysis half-life times from 82.4 min (296 K) to 10.4 min (310 K) at an increase of temperature about 14 °C. Unexpectedly, all PEG-ketal-dimethacrylates degraded faster than PEG-ketal diols of similar molecular weights under the same conditions. An arrangement of the methacrylate units in the way of flower-like micelles may account for the higher hydrolysis rates in PEG-ketal-DMA. Hydrogels containing of 0, 5, or 10



weight% of PEG-ketal-DMA and 100, 95, or 90 weight% of PEG-DMA, respectively, were synthesized and disintegration of the gels was investigated in buffers at different pH values. Visible disintegration of the gels required 8 hours at pH 5 for hydrogels with 10% of degradable PEG-ketal-DMA and more than 21 days at pH 5 for hydrogels with 5% incorporation of PEG-ketal-DMA. No visible degradation was observed at all at pH 7.6 or for PEG hydrogels without degradable PEG-ketal-DMA units prepared for comparison.



**Keywords:** PEG, acid-labile, ketal, degradation studies, *in-situ* NMR kinetics, drug delivery

## Introduction

Polymeric drug carrier systems offer significant advantages for nanomedical applications.<sup>[1; 2]</sup> They can protect their therapeutic payload from degradation, enable the transport of poorly water-soluble drugs and at the same time they allow for targeted transport to the desired site of action instead of unspecific distribution throughout the body.<sup>[3; 4]</sup> Furthermore, by modifying the nanoparticle (NP) surface, one may generate a target function for a specific cell type or attach polymer molecules (e.g. polyethylene glycol (PEG)) to impede uptake of the NP by phagocytes.<sup>[5; 6]</sup> Stimuli-responsive drug delivery systems, so called “smart” systems, can capitalize on specific chemical triggers to tailor release profiles. These reactions include solubility switches due to specific protonation, hydrolytic or enzymatic cleavage, conformational changes or structural response to physical stimuli, such as temperature, pressure or magnetic/electrical field changes.<sup>[7–10]</sup> Cleavable moieties must be incorporated into the polymer backbone in order to

achieve biodegradability of the polymer carrier system, which is essential for repetitive applications *in vivo* to prevent deposition of polymer nanoparticle remnants leading to the so-called storage disease.<sup>[11–14]</sup>

pH changes *in vivo* can occur intracellularly in the lysosome, in cancer or inflammatory tissue, or in organs like the vaginal or the gastric/intestinal tract. Drug delivery systems with pH-dependent cleavage sites are gaining increasing interest due to their potential for intracellular degradation and release of the cargo. Acid-labile polymers, therefore, even if known and explored for decades, still represent promising molecular building blocks for drug delivery systems. One can distinguish between systems with moieties that are susceptible to (de)protonation, leading to changes in solubility and/or conformation upon pH changes and systems with acid-cleavable moieties that may degrade and release target molecules.<sup>[7; 15–18]</sup> Furthermore, pH-sensitivity can enable lysosomal escape through the “proton sponge” effect and directed transport of cargo molecules into the cytosol of a cell.<sup>[19]</sup> Acid-labile polymers have been employed as materials for drug delivery systems for many years. Examples for acid-labile structures include acetals,<sup>[20; 21]</sup> ketals,<sup>[22; 23]</sup> tertiary esters,<sup>[24]</sup> imines,<sup>[25]</sup> orthoesters,<sup>[26; 27]</sup> cis-aconitates,<sup>[28; 29]</sup> hydrazones,<sup>[30; 31]</sup> or  $\beta$ -thiopropionates.<sup>[32]</sup>

The combination of acid-cleavable moieties with the highly biocompatible polymer poly(ethylene glycol) (PEG) is desirable, since PEG exhibits multiple favorable properties required for polymers used for drug delivery and is therefore often viewed as the “gold standard”. It is FDA approved and has been used for biomedical applications over decades.<sup>[33]</sup> PEG is also employed in industrial applications, in cosmetics, and for surface modification of therapeutic proteins (“PEGylation”) and in anti-fouling coatings.<sup>[34]</sup>

A prominent approach is the combination of hydrophobic and hydrophilic polymers in amphiphilic block structures linked by ketal units forming micelles that disassemble in acidic environment.<sup>[35]</sup> Also, pendant ketals along the polymer backbone can be used to transform the hydrophobic part of the amphiphile into a hydrophilic structure.<sup>[36]</sup> Another strategy builds upon the use of small molecules with ketal units as cross-linker for hydrogel or nanogel synthesis.<sup>[14]</sup> PEG Hydrogels have been extensively investigated as sustained release drug delivery systems, especially as scaffolds for tissue engineering.<sup>[37]</sup> There is a large number of reports on polymeric systems other than PEG that contain ketal units in the backbone.<sup>[38–47]</sup> Most of them show degradation kinetics that is too slow<sup>[44]</sup> or the respective materials are too hydrophobic<sup>[48]</sup> for application as stimuli-responsive drug carrier systems. An interesting approach was described by Olejniczak *et al.*, wherein a ketal

unit and a light-sensitive moiety were incorporated into the same polymer backbone. Upon irradiation a carbonyl function is liberated in-situ that catalyzes hydrolysis of the ketal units in the backbone.<sup>[49]</sup>

To date, there are only a few reports on ketal groups incorporated in PEG. Feng *et al.* synthesized acid-labile PEG-dendrimers, and confirmed uniformity of high generation dendrimers by degradation studies.<sup>[50]</sup> Low molecular weight cross-linkers such as 2,2-di(acryloyloxy-1-ethoxy)propane with one repeating unit of ethylene glycol have been published by Heath *et al.*<sup>[51]</sup> To the best knowledge of the authors, only one report exists on ketals incorporated into linear oligo ethylene glycol chains. Kim *et al.* synthesized cross-linker monomers with a dimethyl ketal unit that degrades under the release of acetone, applicable in self-exfoliating garments.<sup>[22]</sup>

In a previous work, we described the use of PEG nanogels for protein delivery containing acetals as labile units.<sup>[52]</sup> Ketals show faster degradation kinetics compared to acetals. In the present work, we introduce ketal units into the backbone of PEG to obtain acid-labile macromonomers that can be radically cross-linked. In a model study, the degradation of the ketal units incorporated in the PEG macromonomers was monitored via online <sup>1</sup>H NMR kinetic measurements as described by Jain *et al.*<sup>[45]</sup> PEG-ketal-dimethacrylates (PEG-ketal-DMA) are utilized for the synthesis of acid-labile PEG-hydrogels for proof-of-principle studies of degradation. We suggest that the results of these fundamental studies can be transferred to nanogels as well.

## Materials and methods

### Materials

Dimethylformamide (DMF), Potassium triflate, sulfuric acid, toluene, dichloromethane, ethyl acetate, benzene, petroleum ether, potassium hydroxide, tetrahydrofuran (THF), *candida antarctica* lipase B (CALB), ethylene oxide, diethyl ether, 2-hydroxy-4'-(2-hydroxyethoxy)-2-methylpropiophenone, citric acid, and disodium hydrogen phosphate were purchased from Sigma Aldrich. THF used for AROP was dried with sodium prior to use and stored over sodium/benzophenone. LiBr, molecular sieve 4 Å, ethylene glycol, magnesium sulfate, para-toluenesulfonic acid, and hydroquinone were purchased from Acros. Dithranol was purchased from Fluka and acetic acid was obtained from VWR. Sodium bicarbonate, calcium chloride, ethanol, and sterile water were purchased from Fisher Scientific. 2,2-Dimethoxypropane and vinyl-methacrylate were purchased from TCI. Alox and silica gel were purchased from

Macherey/Nagel. PBS buffer was obtained from gibco life technologies. 1-butanol was purchased from Alfa Aesar. Spectra/POR Dialysis membranes CE Tubing MWCO 100-500 Da were purchased from Spectrum labs. Deuterated water was purchased from Deutero GmbH and sodium dihydrogenphosphate and disodium hydrogenphosphate from Merck. All chemicals were used as received without further purification unless stated otherwise. 48 well plates for hydrogel synthesis and disposable petri dishes with lid were purchased from Greiner, Frickenhausen, Germany.

### **Characterization methods**

$^1\text{H}$  NMR spectra (300 and 400 MHz) were recorded using a Bruker AC300 or a Bruker AMX400 spectrometer.  $^1\text{H}$  NMR kinetic spectra were recorded at 400 MHz on a Bruker Advance III HD 400 (5 mm BBFO-SmartProbe with z-gradient and ATM). All spectra are referenced internally to residual proton signals of the deuterated solvent.  $^1\text{H}$  NMR kinetic spectra were analyzed with MestReNova v10.0.1 and the calculations were performed in OriginPro 2016G.

For size exclusion chromatography (SEC) measurements in dimethylformamide (DMF, containing  $0.25\text{ g L}^{-1}$  of lithium bromide as an additive), an Agilent 1100 series was used as an integrated instrument, including a PSS HEMA column (106/104/102 Å porosity) and a refractive index (RI) detector. Calibration was carried out using poly(ethylene oxide) standards and the software used for analysis was PSS WinGPC Unity v7 provided by Polymer Standards Service GmbH.

MALDI-ToF mass spectrometry was performed on a Shimadzu Axima CFR MALDI-ToF mass spectrometer equipped with a nitrogen laser delivering 3 ns laser pulses at 337 nm. Dithranol or  $\alpha$ -cyano-4-hydroxy-cinnamonic acid (CHCA) with glycerol was used as matrix, and potassium trifluoroacetate was added to facilitate ionization of polymer samples. The MS spectra were analyzed with Kompact Version 2.4.1 from Kratos Analytical Ltd.

For pH measurements, a Hanna instruments HI 991001 pH electrode was used.

Illustrations were designed with Adobe Illustrator© CS5 v15.0.2.

## Synthetic procedures

### Synthesis of ethylene glycol monoacetate (1)

The synthetic procedure was modified from a synthesis route by LEK Pharmaceuticals.<sup>[53]</sup> Molecular sieve (0.8 g, 4 Å) was flame dried. Dry ethylene glycol (20.0 mL,  $m = 22.3$  g,  $n = 0.359$  mol, 1 eq.), acetic acid (20.6 mL,  $m = 21.6$  g,  $n = 0.360$  mol, 1 eq.), and sulfuric acid (0.50 mL,  $m = 0.92$  g,  $n = 9.4$  mmol, 0.026 eq.) were added under argon and kept on a shaker plate at room temperature for 72 h. The reaction was neutralized by addition of saturated sodium hydrogen carbonate solution (25 mL). Molecular sieve was filtered off. Aqua dest. (20 mL) was added and the aqueous phase was extracted three times with toluene (50 mL each) and 5 times with dichloromethane (50 mL each). The toluene phase was discarded. The dichloromethane extracts were combined and dried over magnesium sulfate. Dichloromethane was removed under reduced pressure to obtain the crude product (20.0 g). The crude product was purified by silica gel chromatography with pure ethyl acetate as eluent. The pure product was recovered ( $rf = 0.69$ ) as colorless liquid (18.8 g, yield = 56%,  $M = 104.10$  g mol<sup>-1</sup>). <sup>1</sup>H NMR (300 MHz, CDCl<sub>3</sub>)  $\delta$  [ppm] = 2.08 (s, 3H, CO-CH<sub>3</sub>), 2.39 (s, 1H, CH<sub>2</sub>-OH), 3.78-3.81 (m, 2H, CH<sub>2</sub>-OH), 4.16-4.19 (m, 2H, CH<sub>2</sub>-O-CO), see Fig. S1.

### Synthesis of propane-2,2-diylbis(oxyethane-2,1-diyl) diacetate (2)

2,2-dimethoxypropane (6.13 mL,  $m = 5.21$  g,  $n = 50.0$  mmol, 1 eq.), ethylene glycol monoacetate ((1), 10.4 g,  $n = 99.9$  mmol, 2 eq.), a spatula-tip full of para-toluenesulfonic acid and benzene (150 mL) were placed in a round bottom flask equipped with a Soxhlet extractor filled with calcium chloride. The mixture was refluxed for 16 h. Subsequently the solvent was evaporated. The crude product was purified by neutral aluminum oxide column chromatography with petroleum ether : ethyl acetate (5:1). The pure product was recovered ( $rf = 0.83$ ) as a colorless liquid (6.71 g, yield = 54%,  $M = 248.27$  g mol<sup>-1</sup>). <sup>1</sup>H NMR (400 MHz, C<sub>6</sub>D<sub>6</sub>)  $\delta$  [ppm] = 1.18 (s, 6H, C(CH<sub>3</sub>)<sub>2</sub>), 1.70 (s, 6H, CO-CH<sub>3</sub>), 3.41-3.44 (m, 4H, CH<sub>2</sub>-O-C(CH<sub>3</sub>)<sub>2</sub>), 4.09-4.12 (m, 4H, CH<sub>2</sub>-O-CO) see Fig. S2.

### Synthesis of 2,2'-(propane-2,2-diylbis(oxy))diethanol (3)

Propane-2,2-diylbis(oxyethane-2,1-diyl) diacetate ((2), 2.5 g,  $M = 248.27$  g mol<sup>-1</sup>,  $n = 10.0$  mmol, 1 eq.), potassium hydroxide (2.8 g,  $n = 50.0$  mmol, 5 eq.), ethanol (50 mL) and MilliQ water (180  $\mu$ L,  $n = 10.0$  mmol, 1 eq.) were refluxed for 2 h. After removal of the solvent, the solid crude product

was dissolved in PBS buffer and extracted three times with 1-butanol (30 mL each). The pure colorless product was obtained after evaporation of 1-butanol (yield = 84%,  $M = 164.20 \text{ g mol}^{-1}$ ).  $^1\text{H NMR}$  (400 MHz,  $\text{CD}_2\text{Cl}_2$ )  $\delta$  [ppm] = 1.18 (s, 6H,  $\text{C}(\text{CH}_3)_2$ ), 1.70 (s, 6H,  $\text{CO-CH}_3$ ), 3.41-3.44 (m, 4H,  $\text{CH}_2\text{-O-C}(\text{CH}_3)_2$ ), 4.09-4.12 (m, 4H,  $\text{CH}_2\text{-O-CO}$ ) see Fig. S3.

### Synthesis of 2,2'-(propane-2,2-diylbis(oxy))dipoly(ethylene glycol)

The procedure is exemplified for the synthesis of polymer sample PEG(2700)-ketal-diol. It was carried out accordingly for all PEG-ketal-DMA polymers presented in this paper. Cesium hydroxide (37 mg,  $n = 0.22 \text{ mol}$ , 1 eq.) was weighted into a flame dried Schlenk flask under argon in a glove box. 2,2'-(propane-2,2-diylbis(oxy))diethanol (**3**), 36 mg,  $n = 0.22 \text{ mmol}$ , 1 eq.) was dissolved in a mixture of benzene (2 mL) and ethanol (1 mL) and was added via syringe. After stirring the solution for 1 h the moisture was removed by azeotropic distillation and drying under high vacuum overnight. Dry THF was cryo-transferred into the Schlenk flask and dry DMSO (3 mL) was added via syringe. After 30 min of stirring to allow solvation, ethylene oxide (1.0 mL,  $n = 20 \text{ mmol}$ , 92 eq.) was cryo-transferred via a graduated ampule to the macroinitiator solution. The reaction mixture was allowed to warm up to room temperature and then stirred for 2 d at 50 °C. After quenching the reaction with methanol (5 mL) and stirring for 2 h, the polymer was dialyzed in a MWCO = 100-500  $\text{g mol}^{-1}$  dialysis tube twice against methanol for 16 h to remove DMSO. The polymer was precipitated from methanol in cold diethyl ether twice and dried under high vacuum to obtain a colorless powder (yield: 583 mg (50 - 83%, depending on molecular weight)).  $^1\text{H NMR}$  (400 MHz,  $\text{C}_6\text{D}_6$ )  $\delta$  [ppm] = 1.32 (s, 6H,  $\text{C}(\text{CH}_3)_2$ ), 3.40-3.56 (m, 253H,  $(\text{CH}_2\text{-CH}_2\text{-O})_n$ ) see Fig. S4.

### Synthesis of 2,2'-(propane-2,2-diylbis(oxy))dipoly(ethylene glycol)dimethacrylate

The procedure is described exemplary for the synthesis of polymer sample PEG-(2700)-ketal-DMA, however it was carried out accordingly for all PEG-ketal-DMA polymers discussed in this paper. PEG(2700)-ketal-diol (300 mg,  $n = 0.111 \text{ mmol}$ , 1 eq.) were dissolved in THF (8 mL). CALB (30 mg), hydroquinone (30 mg) and vinylmethacrylate (133  $\mu\text{L}$ , 10 eq.,  $n = 1.11 \text{ mmol}$ ,  $m = 124 \text{ mg}$ ) were added and stirred at 50 °C for 48 h. CALB was filtered off and the solvent was constricted under reduced pressure. The crude product was dissolved in methanol and precipitated twice into cold diethyl ether. The polymer was dried under high vacuum to obtain the beige-colored powder (yield: 201 mg (63 - 81%, depending on molecular weight)).  $^1\text{H NMR}$  (400 MHz,  $\text{C}_6\text{D}_6$ )  $\delta$  [ppm] = 1.32

(s, 6H,  $C(CH_3)_2$ ), 1.85 (s, 6H,  $CH_2-C-CH_3$ ), 3.40-3.56 (m, 242H,  $(CH_2-CH_2-O)_n$ ), 4.17-4.20 (t, 4H,  $CH_2-O-CO$ ), 5.22 (m, 2H,  $CH_2=C-CH_3$ ), 6.18 (m, 2H,  $CH_2=C-CH_3$ ) see Fig. S8.

### **$^1H$ NMR degradation kinetics of PEG-ketal-diol or PEG-ketal-DMA in deuterated phosphate buffer pH 6**

Deuterated phosphate buffer solution were produced by mixing of two stock solutions and pH adjustment was controlled with pH electrode. Stock A contained of 100 mM  $Na_2HPO_4$  and stock B contained of 100 mM  $NaH_2PO_4$  in deuterated water. The measured pH was converted to pD as described elsewhere.<sup>[54]</sup>

For in-situ  $^1H$  NMR degradation kinetics, the respective polymer (50 mg) was dissolved in deuterated phosphate buffer (pH 6.1, 0.7 mL) and placed in a NMR tube immediately after dissolution. The NMR tube was placed in a preheated NMR spectrometer (23 °C and 37 °C), and the sample was locked to the solvent and shimmed after the sample temperature was constant ( $\Delta T = 0.1$  K) for 2 min. Spectra were recorded with 16 scans at 2-minute intervals during the first hour, then at 5-minute intervals for 2 hours, at 10-minute intervals within the next 5 hours due to the decreasing of the reaction rate. The kinetic analysis was stopped manually after the complete conversion of the cleavage reaction was verified.

### **Synthesis of PEG-dimethacrylate (13)**

PEG(2000) (1 g,  $n = 0.5$  mmol) was dissolved in benzene (5 mL) in a Schlenk flask and dried under high vacuum after azeotropic distillation of benzene to remove water. PEG was dissolved in toluene (10 mL). *Candida antarctica* lipase B (CALB, 100 mg) beads and vinyl methacrylate (600  $\mu$ L, 10 eq.,  $n = 5$  mmol,  $m = 560$  mg) were added and the reaction was performed at 50 °C for 72 h. After removal of CALB beads by filtration through a filtration paper, the solvent was removed by rotary evaporation. The crude product was purified by twofold precipitation from methanol into ice-cold diethyl ether. Hydroquinone (approx. 10 mg) was added for storage. The pure product was dried under high vacuum for 24 hours. The pure product was recovered as a colorless powder (875 mg, yield = 80%,  $M = 2178$  g mol<sup>-1</sup>).  $^1H$  NMR (400 MHz,  $CDCl_3$ )  $\delta$  [ppm] = 6.11 (s, 2H,  $CH_2-C-CH_3$ ), 5.56 (s, 2H,  $CH_2-C-CH_3$ ), 4.28 (m, 4H,  $CH_2-O-CO$ ), 3.47-3.74 (m, 191H,  $(CH_2-CH_2-O)_n$ ), 1.93 (s, 3H,  $-CH_3$ ), see Figure S12.

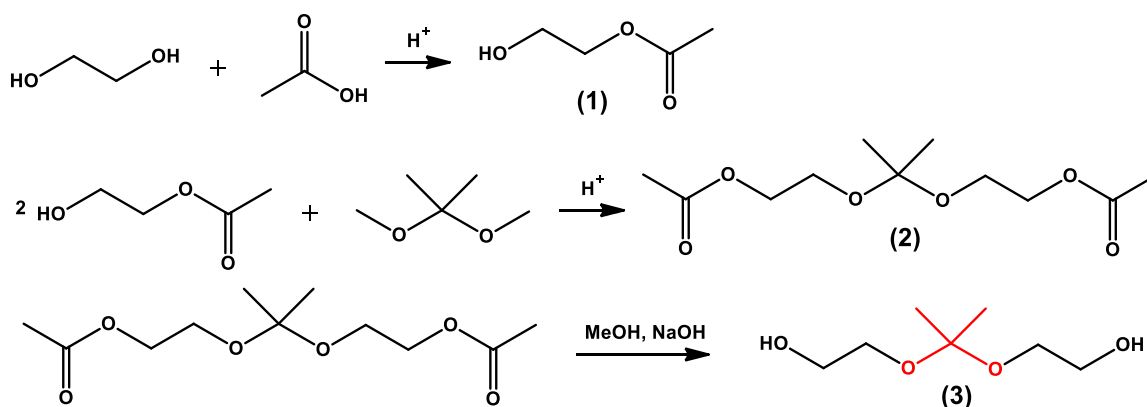
## Hydrogel synthesis and degradation studies

The hydrogel synthesis was adapted from Schroeder *et al.*<sup>[55]</sup> Briefly, 10 weight% polymer solutions of PEG-ketal-DMA and PEG-DMA were prepared and mixed in different compositions to obtain hydrogels with different degradability. 2-hydroxy-4'-(2-hydroxyethoxy)-2-methylpropiophenone (2  $\mu\text{l}$  per 100  $\mu\text{L}$  polymer solution, pre-diluted 1:10 in ethanol) as a photoinitiator was added to the polymer solution, mixed, and 100  $\mu\text{L}$  of this solution were transferred into a well of a 48-well disposable plate. Polymerization was carried out at 365 nm for 15 minutes. The hydrogels were transferred into disposable petri dishes with lid and covered with phosphate buffer solution or phosphate-citrate buffer solution at the desired pH. Phosphate-citrate buffer solution was produced by mixing of two stock solutions and pH adjustment was controlled with a pH electrode. Stock A contained of 10 mM citric acid monohydrate and stock B contained of 200 mM  $\text{Na}_2\text{HPO}_4$  in sterile water. The hydrogels were incubated on a shaking incubator at 150 rpm for several days.

## Results and Discussion

### Initiator synthesis

The initiator for PEG-ketal-DMA was synthesized in a three step synthesis process. The first step includes an esterification reaction of acetic acid with ethylene glycol. The monoester product **1** was purified by column chromatography. The second step is a transketalization reaction performed with a soxhlet apparatus to shift the chemical equilibrium to the benefit of the product **2**. The initiator **3** is obtained after a saponification step to remove the acetate protecting group (see Scheme 1).

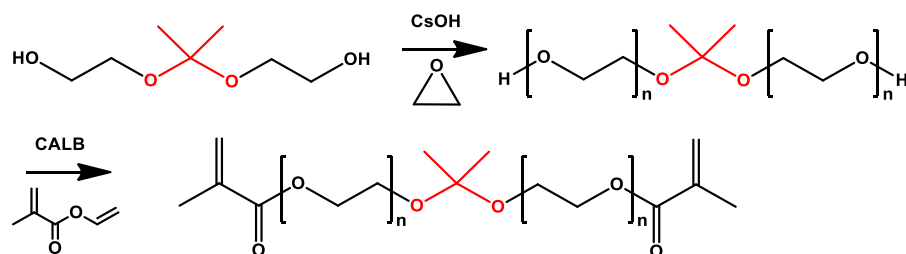


Scheme 1. Synthesis of the ketal-initiator **3**.



**EO polymerization and MA functionalization**

A set of 6 different PEG-ketal polymers with molecular weights ranging from 2000 to 13000  $\text{g mol}^{-1}$  with polydispersities  $< 1.15$  were synthesized by polymerization of ethylene oxide (EO) using the initiator **3** (for SEC traces see Figure S7). In a subsequent functionalization step, two methacrylate functionalities were attached to the chain ends of PEG. *Candida antarctica* lipase B (CALB) was used for mild transesterification between the hydroxyl function of PEG and vinyl methacrylate (see Scheme 2 and Table 1). Three PEG-ketal-diol polymers with varied molecular weights (PEG(2700)-ketal-diol, PEG(8200)-ketal-diol and PEG(12800)-ketal-diol (**5**, **8** and **9**) were functionalized in this manner. PEG-ketal-diols with a molecular weight of 2700, 8200 and 12800  $\text{g mol}^{-1}$  were chosen to represent the entire molecular weight spectrum synthesized.  $^1\text{H}$  NMR, size exclusion chromatography (SEC) and matrix assisted laser desorption ionization - time of flight mass spectrometry (MALDI-ToF-MS) characterization are shown in Figure 1 exemplarily for PEG(2700)-ketal-DMA.



*Scheme 2.* Ketal-diol initiated polymerization of ethylene oxide and subsequent CALB-catalyzed functionalization with methacrylate units (used for samples **5**, **8** and **9**, see Table 1).

*Table 1.* Characteristics of the cleavable PEG-ketal-diols and PEG-ketal-dimethacrylates.

Sample	Sample name	$M_{n,SEC}$ ( $\text{g mol}^{-1}$ )	$M_{n,NMR}$ ( $\text{g mol}^{-1}$ )	$\bar{D}_{SEC}$
<b>4</b>	PEG(2100)-ketal-diol	1600	2100	1.10
<b>5</b>	PEG(2700)-ketal-diol	2400	2700	1.09
<b>6</b>	PEG(4200)-ketal-diol	3200	4200	1.15
<b>7</b>	PEG(5000)-ketal-diol	4500	5000	1.09
<b>8</b>	PEG(8200)-ketal-diol	6600	8200	1.07
<b>9</b>	PEG(12800)-ketal-diol	8000	12800	1.12

<b>10</b>	PEG(2700)-ketal-DMA <sup>a</sup>	2500	2700	1.07
<b>11</b>	PEG(9700)-ketal-DMA <sup>b</sup>	5900	9700	1.10
<b>12</b>	PEG(13200)-ketal-DMA <sup>c</sup>	8000	13200	1.13

<sup>a</sup> derived from **5**. <sup>b</sup> derived from **8**. <sup>c</sup> derived from **9**.

The functionalized polymer PEG(2700)-ketal-DMA was characterized by <sup>1</sup>H NMR, size exclusion chromatography (SEC) and MALDI-ToF mass spectrometry (see Figure 1). In the <sup>1</sup>H NMR spectrum, all peaks could be assigned. In general, the molecular masses determined by <sup>1</sup>H NMR were systematically higher than the values determined by SEC. Depending on the matrix used for MALDI-ToF MS and the time delay between sample preparation and sample measurement, we always observed degradation of a certain fraction of the ketal, independent of the presence or absence of methacrylate units. Even with pencil lead as a matrix, we observed partial degradation. In dithranol with potassium trifluoroacetate as counter ion, least degradation was observed. Half of the ketal was degraded when measured in  $\alpha$ -cyano-4-hydroxycinnamic acid (CHCA) matrix (see Fig. S5), and complete degradation was achieved upon addition of glycerol in CHCA matrix (see Fig. S6). After complete acidic degradation for all three PEG-ketal-DMAs (see Fig. S6, S9, and S10), only PEG-monomethacrylate as the expected degradation product was found in MALDI-ToF-MS. Taking these results into account, the molecular weights determined by <sup>1</sup>H NMR and MALDI-ToF-MS are in good agreement and appear to be more credible than SEC molecular weights. We also attempted measurements with electrospray ionization mass spectrometry (ESI-MS), but also obtained degradation during the measurement (data not shown here). As the degradation is absent in SEC and <sup>1</sup>H NMR measurements, the degradation appears during mass spectrometry sample preparation and not during synthesis or purification of the macromonomer. As lyophilized materials, the macromonomers are stable for several months at 4 °C.

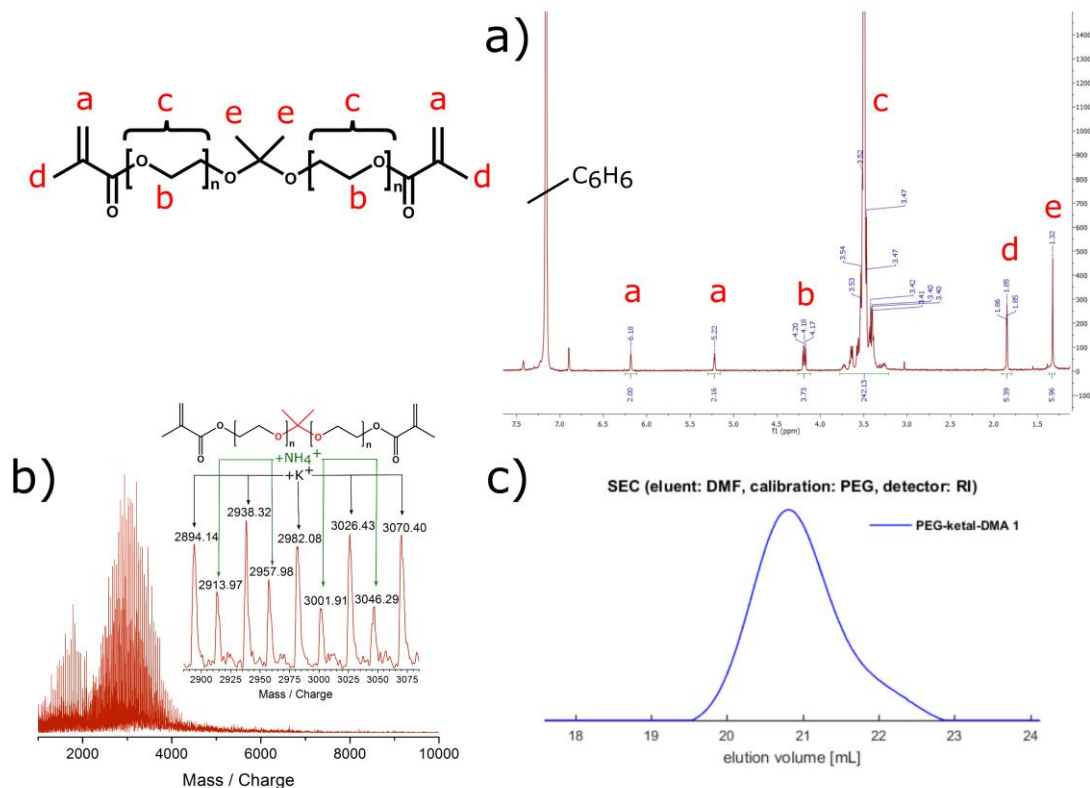


Figure 1. Characterization of PEG(2700)-ketal-DMA. a) <sup>1</sup>H NMR (400 MHz, C<sub>6</sub>D<sub>6</sub>). b) MALDI-ToF-MS measurements using a dithranol matrix and KTFA as salt. c) SEC elugram (eluent: DMF, PEG calibration, RI detector signal).

To the best of our knowledge, this is the first example of a linear PEG ( $> 1000 \text{ g mol}^{-1}$ ) with incorporated ketal unit and methacrylate termini. The incorporation of ketal units in oligo(ethylene glycol)s with one to six repeating units and methacrylate or acrylate functionalization has been described as degradable cross-linkers by Kim *et al.*<sup>[22]</sup> and Heath *et al.*<sup>[51]</sup> Due to the low molecular weight nature of bismethacrylates, they could be purified by flash column chromatography or were used without further purification. The obtained yields after purification were rather low (below 40%) or not determined.

Based on the ring-opening polymerization of ethylene oxide we were able to tailor the molecular weight and furthermore to achieve aqueous solubility of the degradable PEG-macromonomers. Water-solubility is crucial for many hydrogel applications to afford good mixing behavior of the cross-linker and the other polymeric components forming the polymer network. For our targeted application as a macromonomer for the synthesis of degradable PEG-nanogels, water-solubility is mandatory for the nanogel synthesis step, which is carried out in aqueous solution to enable

protein encapsulation. All synthesized macromonomers (PEG-ketal-diols and PEG-ketal-DMA) were highly water soluble.

A crucial feature for the ketal-based macromonomers is their degradation behavior in acidic aqueous solution, particularly in view of their use for nanocarriers. To investigate the degradation kinetics of both PEG-ketal-diols and PEG-ketal-DMA macromonomers, we measured the *in-situ*  $^1\text{H}$  NMR kinetics of the degradation of macromonomers dissolved in deuterated phosphate buffer solutions buffered to different pH values (degradation scheme see Scheme S1). *In-situ*  $^1\text{H}$  NMR measurements have been extensively used to monitor polymerization reactions online.<sup>[59–62]</sup> It is also possible to use this technique to analyze the cleavage of ketal macromonomers by monitoring the changes of typical NMR signals *in situ* during the hydrolysis reaction.

To cover the whole range of molecular weights synthesized, we conducted degradation studies with the PEG-ketal-diols **5**, **8** and **9** as well as various PEG-ketal-DMA **10**, **11** and **12**. In the following section, we focus on degradation rates of PEG(2700)-ketal-DMA **10**, which probably is the most suited candidate for nanogel synthesis due to the crosslinking density achieved. The macromonomer PEG(2700)-ketal-DMA **10** showed complete degradation at pH 7.6 after 2 days (data not shown). This fact requires storage of PEG-ketal-DMA as a powder or at basic pH. We were particularly interested in the degradation in slightly acidic environment, as it is present inside of the endolysosome in a cell (as low as pH 4.5)<sup>[56]</sup> or in inflammatory/cancerous tissue (about pH 6.5)<sup>[57; 58]</sup>.

The degradation at a pH value of 5 was complete within less than 7 minutes and therefore out of the scope of *in-situ*  $^1\text{H}$  NMR measurements. For that reason we decided to study degradation by  $^1\text{H}$  NMR measurements at pH 6.1. Exemplarily, we show the  $^1\text{H}$  NMR spectra of the degradation of PEG(2700)-ketal-diol (**6**) at 23 °C in deuterated buffer at pH 6.1 (see Figure 2). The  $^1\text{H}$  NMR spectra were normalized to the constant peaks of the polymer backbone at 3.6 ppm. We observed a decrease of the signal intensity of the resonance corresponding to the methyl groups at the ketal moieties (at 1.33 ppm), simultaneously to an increase of the signal intensity of the methyl group of the degradation product acetone (at 2.13 ppm) over degradation time.

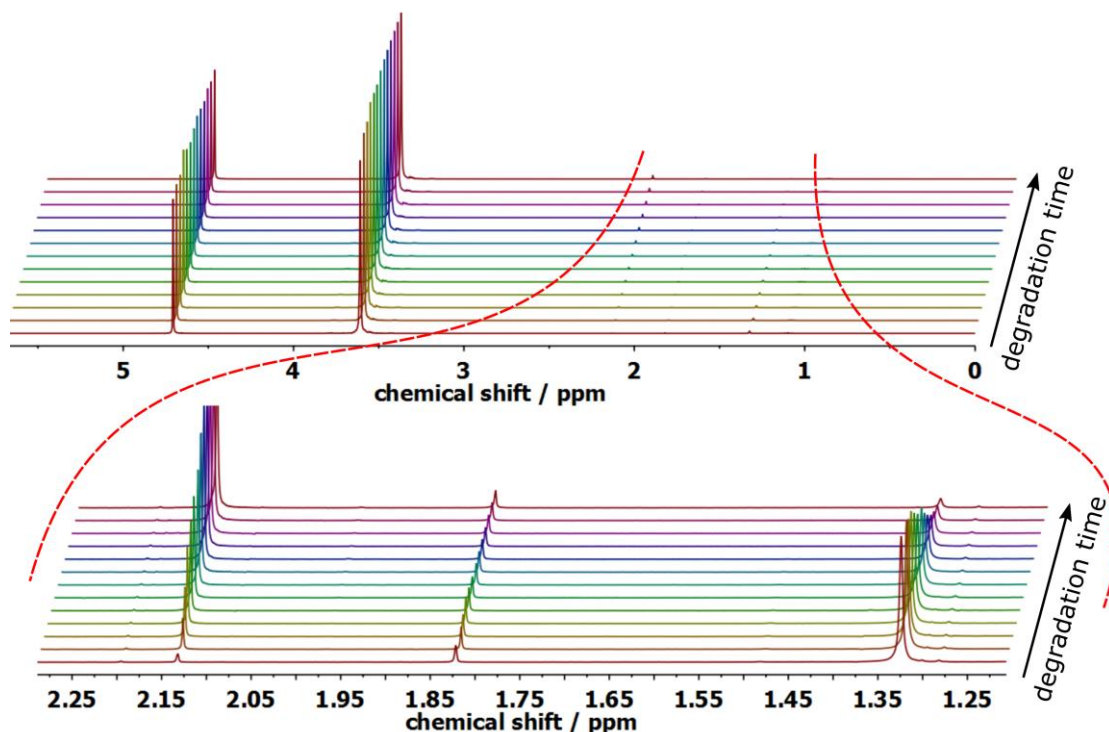


Figure 2. *In-situ*  $^1\text{H}$  NMR spectra of the degradation of PEG(2700)-ketal-diol at 23 °C in deuterated phosphate buffer at pH 6.1, revealing a decrease of the ketal methyl group signal intensity (1.33 ppm) as well as an increase of the acetone methyl group signal intensity (2.13 ppm) over time. In order to aid clarity, an excerpt of 13 spectra is shown over the whole measurement range (top) and a magnification for the measurement range 2.25 to 1.25 ppm (bottom).

The integrals of the ketal methyl group signals at 1.33 ppm were plotted over the reaction time (see Figure 3). From this presentation it is possible to calculate hydrolysis half-life times ( $t_{1/2}$ ) for the different macromonomers studied. The degradation at room temperature (23 °C) was compared to the degradation rate at body temperature (37 °C). As expected, faster degradation at higher temperatures ( $t_{1/2}$  (PEG(2700)-ketal-diol at 23 °C) = 82.4 min versus  $t_{1/2}$  (PEG(2700)-ketal-diol at 37 °C) = 10.4 min) was observed. Surprisingly, in addition we observed a dependency of the presence or absence of methacrylate units with otherwise equal molecular weight on the degradation rate. Esterification with methacrylate groups resulted in significantly increased degradation half-life times ( $t_{1/2}$  (PEG(2700)-ketal-diol at 23 °C) = 82.4 min versus  $t_{1/2}$  (PEG(2700)-ketal-DMA at 23 °C) = 23.2 min and ( $t_{1/2}$  (PEG(2700)-ketal-diol at 37 °C) = 10.4 min versus  $t_{1/2}$  (PEG(2700)-ketal-DMA at 37 °C) = 5.6 min. Sheno *et al.* synthesized polyglycerol using the same ketal initiator as presented here. At pH 6.1, they observed half-life times of  $t_{1/2} = 1$  h for a polymer with  $5200 \text{ g mol}^{-1}$ .<sup>[63]</sup> Under the given circumstances of structural difference, these

reports are on the same order of magnitude and hence consistent with our findings. Kim *et al.* synthesized the polymer structure with the smallest deviation compared to the structures presented in this manuscript. They analyzed the hydrolysis rates of their OEG-ketal-DMA and achieved half-life times of  $t_{1/2} = 18$  min at pH 5 and  $t_{1/2} = 2$  min at pH 4.<sup>[22]</sup> These results prompt the conclusion that the hydrolysis rate increases with higher molecular weight of the PEG chains, i.e. increasing hydrophilicity.

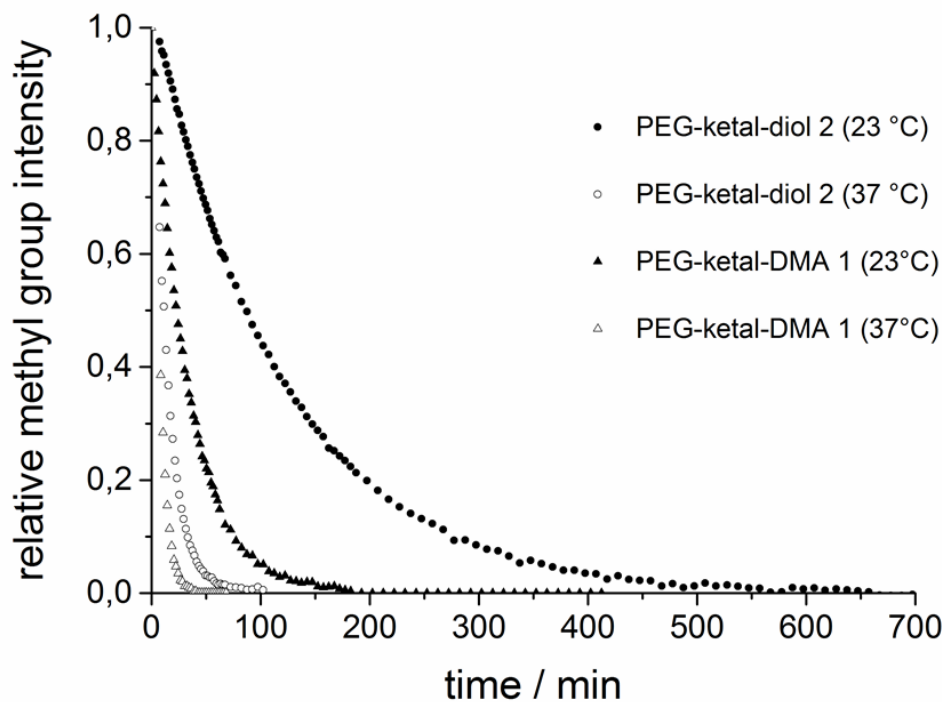
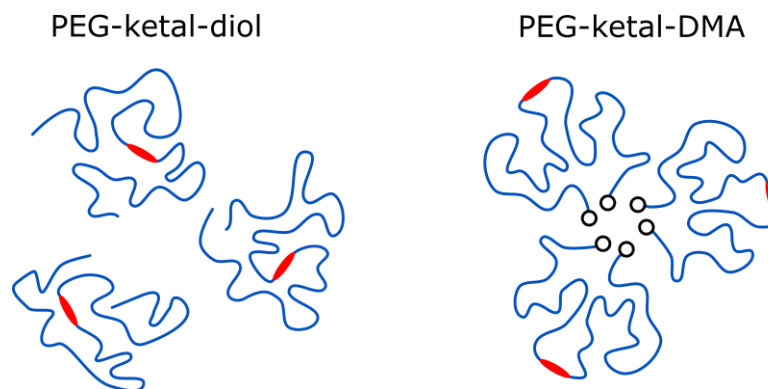


Figure 3. Comparison of *in-situ*  $^1\text{H}$  NMR integrals of the degradation of PEG(2700)-ketal-diol and PEG(2700)-ketal-DMA at 23 °C and 37 °C, respectively, in deuterated phosphate buffer at pH 6.1.

We furthermore investigated the influence of the degree of polymerization of the polyether backbone on the degradation rates. PEG(2700)-ketal-DMA, PEG(9700)-ketal-DMA, and PEG(13200)-ketal-DMA were incubated at 37 °C in deuterated phosphate buffer at pH 6.1 and *in-situ*  $^1\text{H}$  NMR kinetics were measured. No influence of molecular weight on degradation times could be observed (see Figure S15).

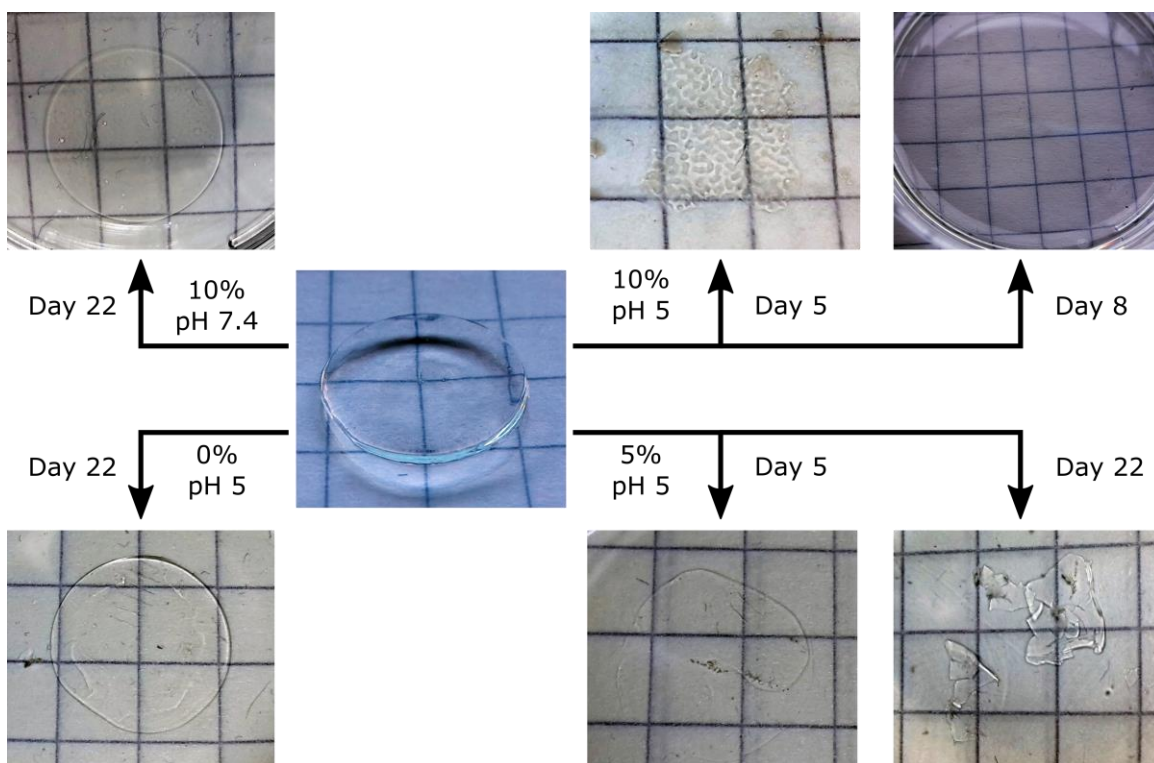
We hypothesize that the different degradation rates for PEG-ketal-diol and PEG-ketal-DMA may result from the polymer conformation in aqueous solution (see Figure 4). PEG-ketal-diol chains with hydroxyl groups at the chain end may form a polymer coil with the ketal group located in the

center, i.e. shielded inside the polymer coil. In the PEG-ketal-DMA molecules instead, the methacrylate units may associate to form a kind of “flower-like micelles”, as known from literature.<sup>[64]</sup> This may result in an improved accessibility of the ketal units and thereby in an increased degradation rate.



*Figure 4.* Possible polymer chain arrangement of PEG-ketal-diol and PEG-ketal-DMA in aqueous solution. The methacrylate units loosely associate to form “flower-like micelle”-structures which results in an improved accessibility of the ketal units.

In a series of experiments, 10 weight% PEG-DMA hydrogels with different amounts of PEG-ketal-DMA (0%, 5% or 10%) were synthesized in a 48-well-plate at pH 7.4. The 10 weight% polymer solution were mixed with a photo-initiator solution and crosslinked for 15 minutes using a 365 nm UV lamp. The obtained hydrogels were incubated in a citrate/phosphate buffer at pH 5, pH 6 or in a phosphate buffer at pH 7.4 as control in plastic petri dishes and shaken on a shaker plate at 150 rpm at room temperature.



*Figure 5.* Incubation of PEG-hydrogels in citrate-phosphate buffers at different pH values. 10% PEG-ketal-DMA hydrogel disintegrated at pH 5 within 8 days (top right), whereas 5% PEG-ketal-DMA hydrogel did not show complete disintegration after 22 days (bottom right). 10% PEG-ketal-DMA hydrogel incubated at pH 7.4 (top left) and the hydrogels without PEG-ketal-DMA incubated at pH 5 (bottom left) did not show visible disintegration within 22 days.

The disintegration of the gels took generally longer than the hydrolysis of the PEG-ketal-DMA macromonomers. Complete disintegration of hydrogels is defined as invisibility of the hydrogels to the unaided eye. The hydrogel containing 10% PEG-ketal-DMA dissolved completely within 8 days. Compared to that, the hydrogel with 5% PEG-ketal-DMA content disintegrated only partially within 22 days. Hydrogels that do not contain PEG-ketal-DMA do not show any signs of disintegration at pH 5 in the same time-frame. On the other hand, hydrogels that contain 10% of PEG-ketal-DMA, but were incubated at pH 7.4, did not show disintegration.

From these exploratory results one can estimate that disintegration times of nanogels will be in between the hydrolysis times of the macromonomer and the disintegration times of the hydrogels, as they feature a considerably higher surface to volume ratio.



## Conclusion and Outlook

In summary, we introduced a new PEG-based acid-labile macromonomer with methacrylate units that enables three-dimensional cross-linking. This type of macromonomer is highly interesting for the formulation of drug delivery systems for transportation of therapeutic proteins, as it combines the excellent properties of poly(ethylene glycol) (biocompatibility, water-solubility, low immunogenicity) with stimuli-responsive units that enable triggered drug release. The synthesis of the macromonomer via anionic ring-opening polymerization allows for the adjustment of molecular weights and aqueous solubility (starting at a molecular weight of 1000 g mol<sup>-1</sup>). PEG-ketal-diols of different molecular weights ranging from 2000 to 13,000 g mol<sup>-1</sup> (polydispersities < 1.15) and their conversion to PEG-ketal-dimethacrylates is described. The synthesized macromonomers degrade readily under slightly acidic conditions (pH 6.1) as present in endolysosomes, cancerous and inflammatory tissue and are stable as lyophilized materials at 4 °C. As the macromonomer also degrades at pH 7 within several days, this leads to a clear caveat working with these ketals requires pH values > 7, which should be kept in mind when handling these compounds. The hydrolysis half-life times investigated by *in-situ* <sup>1</sup>H NMR kinetic studies varied from 82.4 min to 5.6 min. An increase in temperature leads to reduced half-life times as expected. All PEG-ketal-dimethacrylates showed faster degradation compared to their PEG-ketal diol counterpart under the same hydrolysis conditions, which may be by virtue of an arrangement of the methacrylate units in the way of flower-like micelles. No influence of molecular weights on the hydrolysis half-life times could be observed. Acid-labile hydrogels were prepared from PEG-ketal-DMA and PEG-DMA in different compositions. When incubated in buffer at pH 5, complete degradation occurred within 8 days for the 10% PEG-ketal-DMA hydrogel whereas the 5% PEG-ketal-DMA hydrogel showed much slower disintegration. Hydrogels that did not contain PEG-ketal-DMA did not show visible disintegration, just as hydrogels containing 10% of PEG-ketal-DMA incubated at pH 7.4. The investigation of protein release from nanogels prepared from the new acid-labile PEG-ketal-DMA structures seems encouraging.

## Acknowledgements

The authors gratefully acknowledge the support of this research by Dr. Elena Berger-Nicoletti, Steffen Hildebrand, Dr. Johannes Liermann, Nadine Schenk, Monika Schmelzer, and Matthias Worm. This work was supported by the Max Planck Graduate Center with the Johannes Gutenberg

University Mainz (MPGC) as well as by funding of the Excellence Initiative (DFG/GSC 266) in the context of the graduate school of excellence “MAINZ” (Materials Science in Mainz).

### Abbreviations

CALB, *candida antarctica* lipase B; CHCA,  $\alpha$ -cyano-4-hydroxycinnamic acid; DMF, dimethylformamide; ESI-MS, electrospray ionization mass spectrometry; MALDI-ToF-MS, matrix assisted laser desorption ionization - time of flight mass spectrometry; NaH<sub>2</sub>PO<sub>4</sub>, sodium phosphate monobasic; Na<sub>2</sub>HPO<sub>4</sub>, sodium phosphate dibasic; NMR, nuclear magnetic resonance spectroscopy; RI, refractive index; SEC, size exclusion chromatography; THF, tetrahydrofuran.

### References

- [1] Du, A. W.; Stenzel, M. H., Drug carriers for the delivery of therapeutic peptides, *Biomacromolecules*, **2014**, 15, 1097–1114.
- [2] Elsabahy, M.; Wooley, K. L., Design of polymeric nanoparticles for biomedical delivery applications, *Chem. Soc. Rev.*, **2012**, 41, 2545–2561.
- [3] Onaca-Fischer, O.; Liu, J.; Inglin, M.; Palivan, C. G., Polymeric nanocarriers and nanoreactors: a survey of possible therapeutic applications, *Curr. Pharm. Des.*, **2012**, 18, 2622–2643.
- [4] Tang, Z.; He, C.; Tian, H.; Ding, J.; Hsiao, B. S.; Chu, B.; Chen, X., Polymeric nanostructured materials for biomedical applications, *Prog. Polym. Sci.*, **2016**, 60, 86–128.
- [5] Joshi, M. D.; Unger, W. J.; Storm, G.; van Kooyk, Y.; Mastrobattista, E., Targeting tumor antigens to dendritic cells using particulate carriers, *J. Control. Release*, **2012**, 161, 25–37.
- [6] Cruz, L. J.; Tacken, P. J.; Rueda, F.; Domingo, J. C.; Albericio, F.; Figdor, C. G., Targeting nanoparticles to dendritic cells for immunotherapy, *Methods Enzymol.*, **2012**, 509, 143–163.
- [7] Mura, S.; Nicolas, J.; Couvreur, P., Stimuli-responsive nanocarriers for drug delivery, *Nat. Mater.*, **2013**, 12, 991–1003.
- [8] Karimi, M.; Eslami, M.; Sahandi-Zangabad, P.; Mirab, F.; Farajisafilo, N.; Shafaei, Z.; Ghosh, D.; Bozorgomid, M.; Dashkhaneh, F.; Hamblin, pH-Sensitive stimulus-responsive nanocarriers for targeted delivery of therapeutic agents, *Wiley Interdiscip. Rev. Nanomed. Nanobiotechnol.*, **2016**.
- [9] Unsoy, G.; Gunduz, U., Smart Drug Delivery Systems in Cancer Therapy, *CDT*, **2016**, 17, 1.
- [10] Cheng, R.; Meng, F.; Deng, C.; Klok, H.-A.; Zhong, Z., Dual and multi-stimuli responsive polymeric nanoparticles for programmed site-specific drug delivery, *Biomaterials*, **2013**, 34, 3647–3657.

- [11] Goddard, P.; Williamson, I.; Brown, J.; Hutchinson, L. E.; Nicholls, J.; Petrak, K., Soluble Polymeric Carriers for Drug Delivery Part 4, *J. Bioact. Compat. Polym.*, **1991**, 6, 4–24.
- [12] Pasut, G.; Veronese, F. M., Polymer–drug conjugation, recent achievements and general strategies, *Prog. Polym. Sci.*, **2007**, 32, 933–961.
- [13] Hoffman, A. S., Stimuli-responsive polymers: biomedical applications and challenges for clinical translation, *Adv. Drug Deliv. Rev.*, **2013**, 65, 10–16.
- [14] Zhang, X.; Malhotra, S.; Molina, M.; Haag, R., Micro- and nanogels with labile crosslinks – from synthesis to biomedical applications, *Chem. Soc. Rev.*, **2015**, 44, 1948–1973.
- [15] Balamurali, V.; Pramodkuma, T. M.; Srujana, N.; Venkatesh, M. P.; Gupta, N. V.; Krishna, K. L.; Gangadhara, H. V., pH Sensitive Drug Delivery Systems, *Amer. J. Drug Disc. Devel.*, **2011**, 1, 24–48.
- [16] Cuggino, J. C.; Molina, M.; Wedepohl, S.; Igarzabal, C. I. A.; Calderón, M.; Gugliotta, L. M., Responsive nanogels for application as smart carriers in endocytic pH-triggered drug delivery systems, *Eur. Polym. Chem.*, **2016**, 78, 14–24.
- [17] Gao, W.; Chan, J. M.; Farokhzad, O. C., pH-Responsive nanoparticles for drug delivery, *Mol. Pharm.*, **2010**, 7, 1913–1920.
- [18] Nicolas, J.; Mura, S.; Brambilla, D.; Mackiewicz, N.; Couvreur, P., Design, functionalization strategies and biomedical applications of targeted biodegradable/biocompatible polymer-based nanocarriers for drug delivery, *Chem. Soc. Rev.*, **2013**, 42, 1147–12358.
- [19] Amiji, Mansoor M., Polymeric gene delivery. Principles and applications. CRC Press. Boca Raton, Fla., **2005**.
- [20] Tomlinson, R.; Heller, J.; Brocchini, S.; Duncan, R., Polyacetal-doxorubicin conjugates designed for pH-dependent degradation, *Bioconjugate Chem.*, **2003**, 14, 1096–1106.
- [21] Gillies, E. R.; Frechet, J. M., pH-Responsive copolymer assemblies for controlled release of doxorubicin, *Bioconjugate Chem.*, **2005**, 16, 361–368.
- [22] Kim, S.; Linker, O.; Garth, K.; Carter, K. R., Degradation kinetics of acid-sensitive hydrogels, *Polym. Degrad. Stab.*, **2015**, 121, 303–310.
- [23] Ruff, L. E.; Mahmoud, E. A.; Sankaranarayanan, J.; Morachis, J. M.; Katayama, C. D.; Corr, M.; Hedrick, S. M.; Almutairi, A., Antigen-loaded pH-sensitive hydrogel microparticles are taken up by dendritic cells with no requirement for targeting antibodies, *Integr. Biol. (Camb)*, **2013**, 5, 195–203.
- [24] Koylu, D.; Carter, K. R., Stimuli-Responsive Surfaces Utilizing Cleavable Polymer Brush Layers, *Macromolecules*, **2009**, 42, 8655–8660.
- [25] Fleige, E.; Achazi, K.; Schaletzki, K.; Triemer, T.; Haag, R., pH-responsive dendritic core-multishell nanocarriers, *J. Control. Release*, **2014**, 185, 99–108.
- [26] Wang, C.; Ge, Q.; Ting, D.; Nguyen, D.; Shen, H. R.; Chen, J.; Eisen, H. N.; Heller, J.; Langer, R.; Putnam, D., Molecularly engineered poly(ortho ester) microspheres for enhanced delivery of DNA vaccines, *Nat. Mater.*, **2004**, 3, 190–196.

- [27] Heller, J.; Chang, A. C.; Rood, G.; Grodsky, G. M., Release of insulin from pH-sensitive poly(ortho esters), *J. Control. Release*, **1990**, 13, 295–302.
- [28] Liu, J.; Huang, Y.; Kumar, A.; Tan, A.; Jin, S.; Mozhi, A.; Liang, X.-J., pH-Sensitive nano-systems for drug delivery in cancer therapy, *Biotechnol. Adv.*, **2014**, 32, 693–710.
- [29] Hu, F. Q.; Zhang, Y. Y.; You, J.; Yuan, H.; Du YZ, pH triggered doxorubicin delivery of PEGylated glycolipid conjugate micelles for tumor targeting therapy, *Mol. Pharm.*, **2012**, 9, 2469–2478.
- [30] Bae, Y.; Fukushima, S.; Harada, A.; Kataoka, K., Design of environment-sensitive supramolecular assemblies for intracellular drug delivery: polymeric micelles that are responsive to intracellular pH change, *Angew. Chem. Int. Ed. Engl.*, **2003**, 42, 4640–4643.
- [31] Chen, D.; Liu, W.; Shen, Y.; Mu, H.; Zhang, Y.; Liang, R.; Wang, A.; Sun, K.; Fu, F., Effects of a novel pH-sensitive liposome with cleavable esterase-catalyzed and pH-responsive double smart mPEG lipid derivative on ABC phenomenon, *Int. J. Nanomedicine*, **2011**, 6, 2053–2061.
- [32] Molla, M. R.; Marcinko, T.; Prasad, P.; Deming, D.; Garman, S. C.; Thayumanavan, S., Unlocking a Caged Lysosomal Protein from a Polymeric Nanogel with a pH Trigger, *Biomacromolecules*, **2014**, 15, 4046–4053.
- [33] Zalipsky, Samuel; Harris, J. Milton, Poly(ethylene glycol). Chapter 1: Introduction to Chemistry and Biological Applications of Poly(ethylene glycol), *ACS Symposium Series*, **1997**, 1–13.
- [34] Herzberger, J.; Niederer, K.; Pohlit, H.; Seiwert, J.; Worm, M.; Wurm, F. R.; Frey, H., Polymerization of Ethylene Oxide, Propylene Oxide, and Other Alkylene Oxides: Synthesis, Novel Polymer Architectures, and Bioconjugation, *Chem. Rev.*, **2016**, 116, 2170–2243.
- [35] Liu, Y.; Wang, W.; Yang, J.; Zhou, C.; Sun, J., pH-sensitive polymeric micelles triggered drug release for extracellular and intracellular drug targeting delivery, *Asian J. Pharmacol.*, **2013**, 8, 159–167.
- [36] Yang, X.; Cui, C.; Tong, Z.; Sabanayagam, C. R.; Jia, X., Poly( $\epsilon$ -caprolactone)-based copolymers bearing pendant cyclic ketals and reactive acrylates for the fabrication of photocrosslinked elastomers, *Acta Biomater.*, **2013**, 9, 8232–8244.
- [37] Lin, C.-C.; Anseth, K. S., PEG hydrogels for the controlled release of biomolecules in regenerative medicine, *Pharm. Res.*, **2009**, 26, 631–643.
- [38] Binauld, S.; Stenzel, M. H., Acid-degradable polymers for drug delivery, *Chem. Commun.*, **2013**, 49, 2082.
- [39] Chen, D.; Wang, H., Novel pH-Sensitive Biodegradable Polymeric Drug Delivery Systems Based on Ketal Polymers, *J. Nanosci. Nanotech.*, **2014**, 14, 983–989.
- [40] Shenoi, R. A.; Lai, B. F.; Imran ul-haq, M.; Brooks, D. E.; Kizhakkedathu, J. N., Biodegradable polyglycerols with randomly distributed ketal groups as multi-functional drug delivery systems, *Biomaterials*, **2013**, 34, 6068–6081.
- [41] Shim, M. S.; Kwon, Y. J., Dual mode polyspermine with tunable degradability for plasmid DNA and siRNA delivery, *Biomaterials*, **2011**, 32, 4009–4020.

- [42] Morachis, J. M.; Mahmoud, E. A.; Sankaranarayanan, J.; Almutairi, A., Triggered Rapid Degradation of Nanoparticles for Gene Delivery, *Drug Deliv.*, **2012**, 2012, 1–7.
- [43] Lim, H.; Noh, J.; Kim, Y.; Kim, H.; Kim, J.; Khang, G.; Lee, D., Acid-Degradable Cationic Poly(ketal amidoamine) for Enhanced RNA Interference In Vitro and In Vivo, *Biomacromolecules*, **2013**, 14, 240–247.
- [44] Lee, S.; Yang, S. C.; Heffernan, M. J.; Taylor, W. R.; Murthy, N., Polyketal Microparticles, *Bioconjugate Chem.*, **2007**, 18, 4–7.
- [45] Jain, R.; Standley, S. M.; Fréchet, J. M. J., Synthesis and Degradation of pH-Sensitive Linear Poly(amidoamine)s, *Macromolecules*, **2007**, 40, 452–457.
- [46] Heffernan, M. J.; Murthy, N., Polyketal Nanoparticles, *Bioconjugate Chem.*, **2005**, 16, 1340–1342.
- [47] Guo, S.; Nakagawa, Y.; Barhoumi, A.; Wang, W.; Zhan, C.; Tong, R.; Santamaria, C.; Kohane, D. S., Extended Release of Native Drug Conjugated in Polyketal Microparticles, *J. Am. Chem. Soc.*, **2016**, 138, 6127–6130.
- [48] Yang, S. C.; Bhide, M.; Crispe, I. N.; Pierce, R. H.; Murthy, N., Polyketal Copolymers, *Bioconjugate Chem.*, **2008**, 19, 1164–1169.
- [49] Olejniczak, J.; Nguyen Huu, V. A.; Lux, J.; Grossman, M.; He, S.; Almutairi, A., Light-triggered chemical amplification to accelerate degradation and release from polymeric particles, *Chem. Commun.*, **2015**, 51, 16980–16983.
- [50] Feng, X.; Chaikof, E. L.; Absalon, C.; Drummond, C.; Taton, D.; Gnanou, Y., Dendritic Carrier Based on PEG, *Macromol. Rapid Commun.*, **2011**, 32, 1722–1728.
- [51] Heath, W. H.; Palmieri, F.; Adams, J. R.; Long, B. K.; Chute, J.; Holcombe, T. W.; Zieren, S.; Truitt, M. J.; White, J. L.; Willson, C. G., Degradable Cross-Linkers and Strippable Imaging Materials for Step-and-Flash Imprint Lithography, *Macromolecules*, **2008**, 41, 719–726.
- [52] Pohlit, H.; Bellinghausen, I.; Schomer, M.; Heydenreich, B.; Saloga, J.; Frey, H., Biodegradable pH-Sensitive Poly(ethylene glycol) Nanocarriers for Allergen Encapsulation and Controlled Release, *Biomacromolecules*, **2015**, 16, 3103–3111.
- [53] LEK Pharmaceuticals Ljubljana, Synthesis of acetoxyacetaldehyde. EU Patent, EP2327683 A1, **2009**.
- [54] Glasoe, P. K.; Long, F. A., Use of glass electrodes to measure acidities in deuterium oxide, *J. Phys. Chem.*, **1960**, 64, 188–190.
- [55] Schröder, R.; Pohlit, H.; Schüller, T.; Panthöfer, M.; Unger, R. E.; Frey, H.; Tremel, W., Transformation of vaterite nanoparticles to hydroxycarbonate apatite in a hydrogel scaffold, *J. Mater. Chem. B*, **2015**, 3, 7079–7089.
- [56] Asokan, A.; Cho, M. J., Exploitation of Intracellular pH Gradients in the Cellular Delivery of *Macromolecules*, **2002**, 91, 903–913.
- [57] Lee, E. S.; Gao, Z.; Bae, Y. H., Recent progress in tumor pH targeting nanotechnology, *J. Control. Release*, **2008**, 132, 164–170.

- [58] Guragain, S.; Bastakoti, B. P.; Malgras, V.; Nakashima, K.; Yamauchi, Y., Multi-Stimuli-Responsive Polymeric Materials, *Chemistry*, **2015**, 21, 13164–13174.
- [59] Aguilar, M. R.; Gallardo, A.; Fernández, M. d. M.; Román, J. S., In Situ Quantitative <sup>1</sup>H NMR Monitoring of Monomer Consumption, *Macromolecules*, **2002**, 35, 2036–2041.
- [60] Natalello, A.; Werre, M.; Alkan, A.; Frey, H., Monomer Sequence Distribution Monitoring in Living Carbanionic Copolymerization by Real-Time <sup>1</sup>H NMR Spectroscopy, *Macromolecules*, **2013**, 46, 8467–8471.
- [61] Leibig, D.; Müller, A. H. E.; Frey, H., Anionic Polymerization of Vinylcatechol Derivatives, *Macromolecules*, **2016**, 49, 4792–4801.
- [62] Herzberger, J.; Fischer, K.; Leibig, D.; Bros, M.; Thiermann, R.; Frey, H., Oxidation-Responsive and "Clickable" Poly(ethylene glycol) via Copolymerization of 2-(Methylthio)ethyl Glycidyl Ether, *J. Am. Chem. Soc.*, **2016**, 138, 9212–9223.
- [63] Shenoj, R. A.; Lai, B. F. L.; Kizhakkedathu, J. N., Synthesis, Characterization, and Biocompatibility of Biodegradable Hyperbranched Polyglycerols from Acid-Cleavable Ketal Group Functionalized Initiators, *Biomacromolecules*, **2012**, 13, 3018–3030.
- [64] Ishii, S.; Kaneko, J.; Nagasaki, Y., Dual Stimuli-Responsive Redox-Active Injectable Gel by Polyion Complex Based Flower Micelles for Biomedical Applications, *Macromolecules*, **2015**, 48, 3088–3094.

## Supporting Information

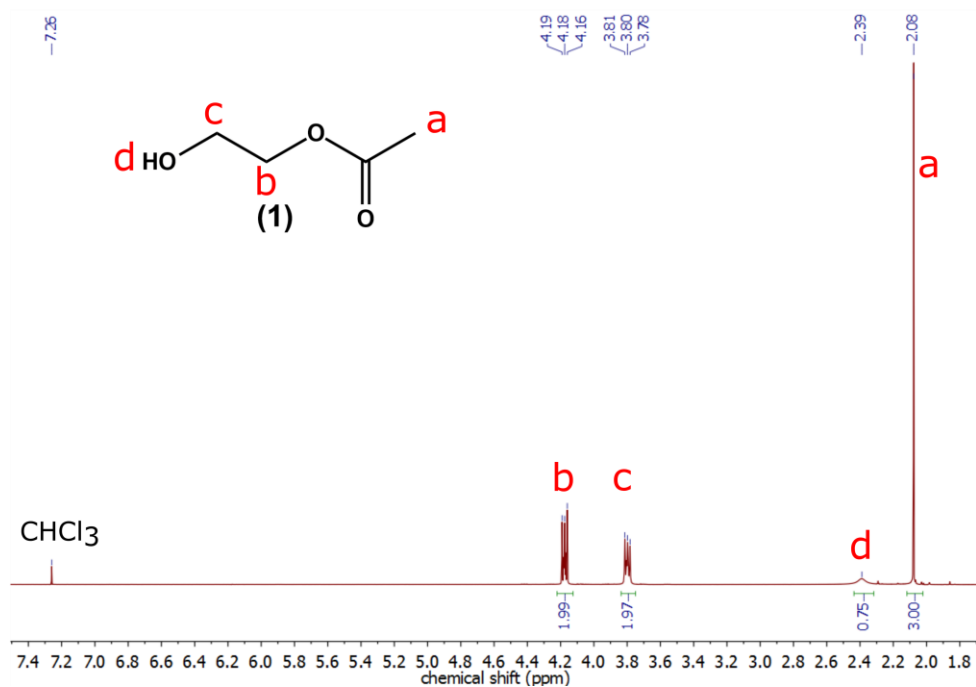


Figure S1. <sup>1</sup>H-NMR spectrum (300 MHz, CDCl<sub>3</sub>) of ethylene glycol monoacetate (1).

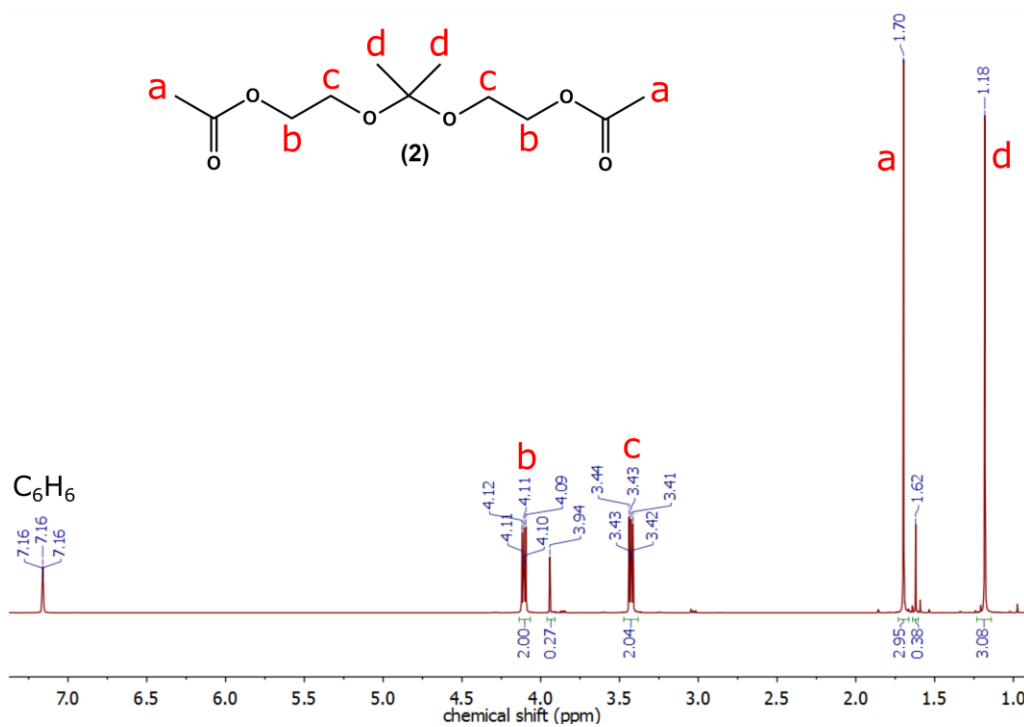


Figure S2. <sup>1</sup>H-NMR spectrum (400 MHz, C<sub>6</sub>D<sub>6</sub>) of propane-2,2-diylbis(oxyethane-2,1-diyl) diacetate (2).

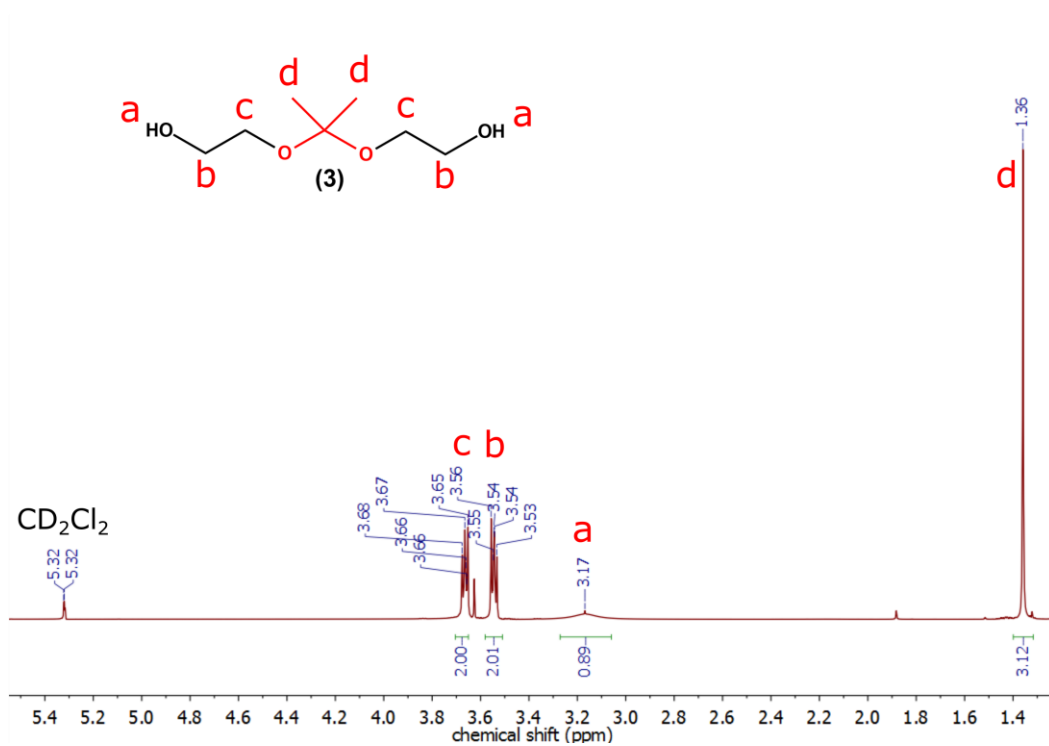


Figure S3.  $^1\text{H-NMR}$  spectrum (400 MHz,  $\text{CD}_2\text{Cl}_2$ ) of 2,2'-(propane-2,2-diylbis(oxy))diethanol (**3**).

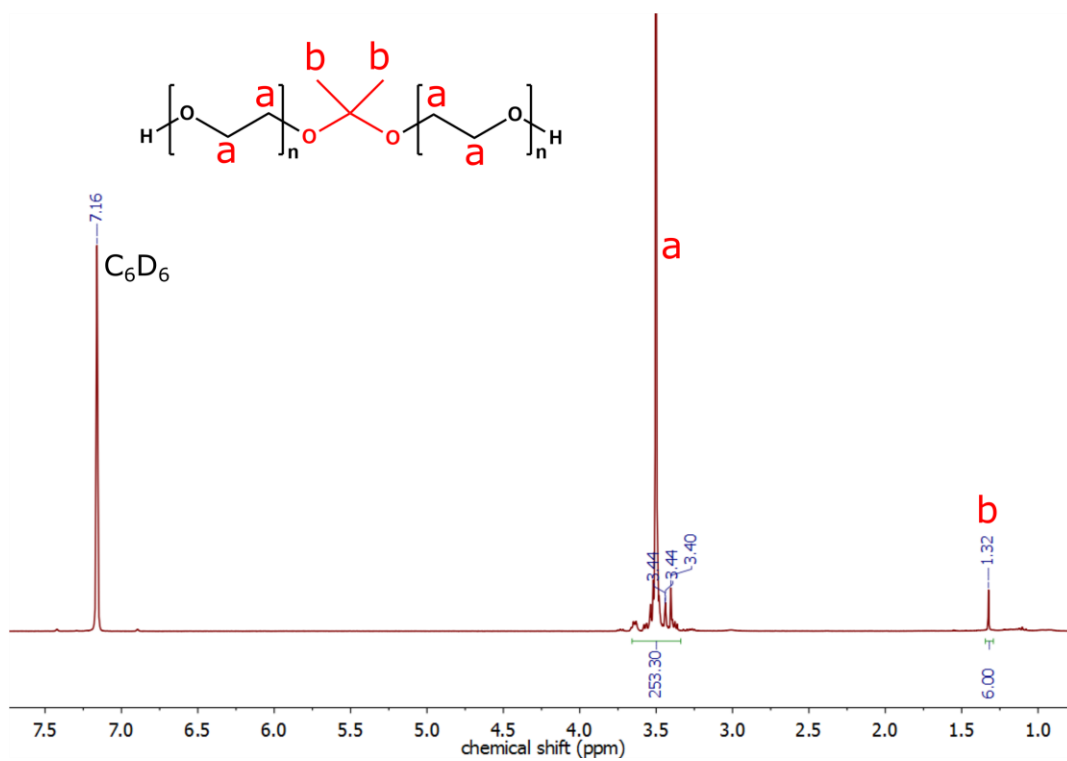


Figure S4.  $^1\text{H-NMR}$  spectrum (400 MHz,  $\text{C}_6\text{D}_6$ ) of 2,2'-(propane-2,2-diylbis(oxy))dipoly(ethylene glycol) (**4**).



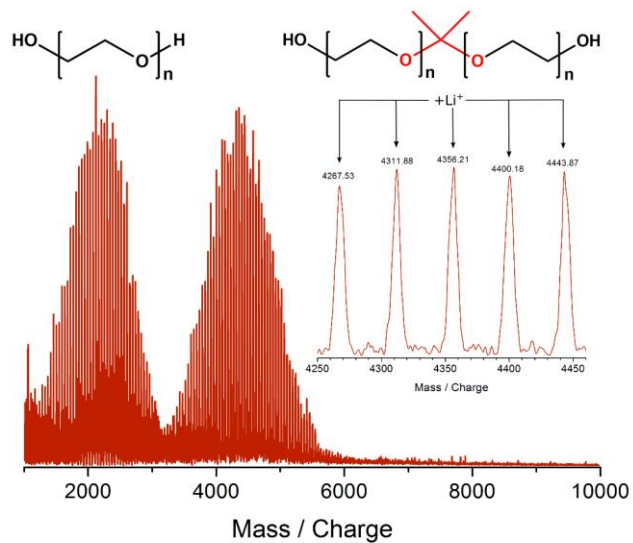


Figure S5. MALDI-ToF-MS of PEG(4200)-ketal-diol (**6**, partially degraded) using a CHCA matrix and KTFA as salt.

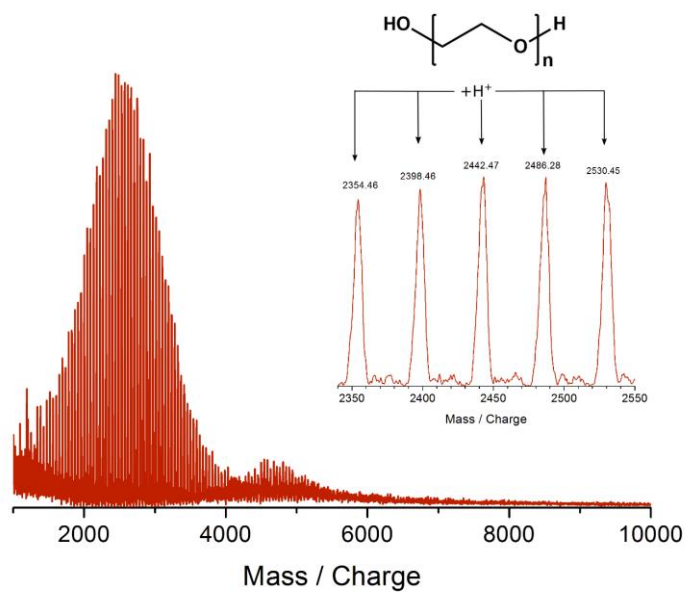


Figure S6. MALDI-ToF-MS of PEG(5000)-ketal-diol (**7**) after complete degradation using a CHCA matrix and KTFA as salt.

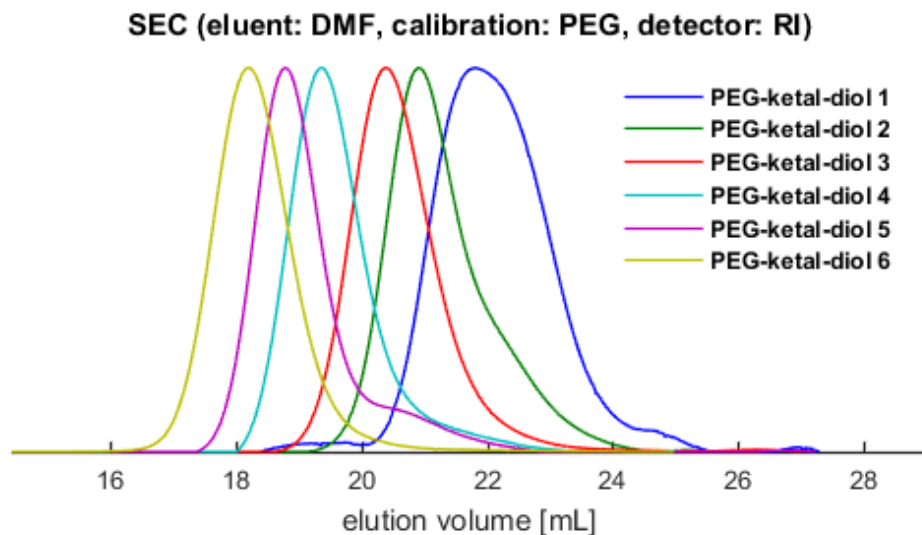


Figure S7. SEC elugrams of all PEG-ketal-diols (eluent: DMF, PEG calibration, RI detector signal). Molecular weights and polydispersities are specified in Table 1.

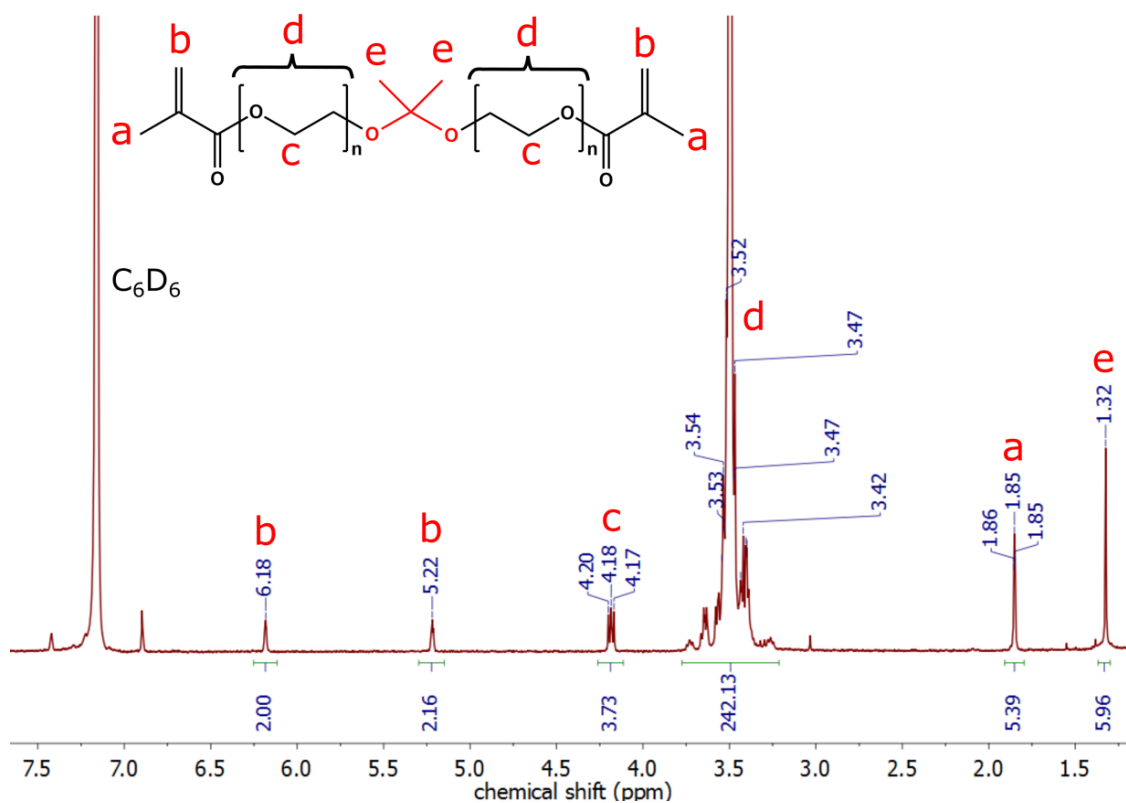


Figure S8.  $^1H$ -NMR spectrum (400 MHz,  $C_6D_6$ ) of 2,2'-(propane-2,2-diylbis(oxy))dipoly(ethylene glycol)dimethacrylate (PEG(2700)-ketal-DMA, (**10**)).

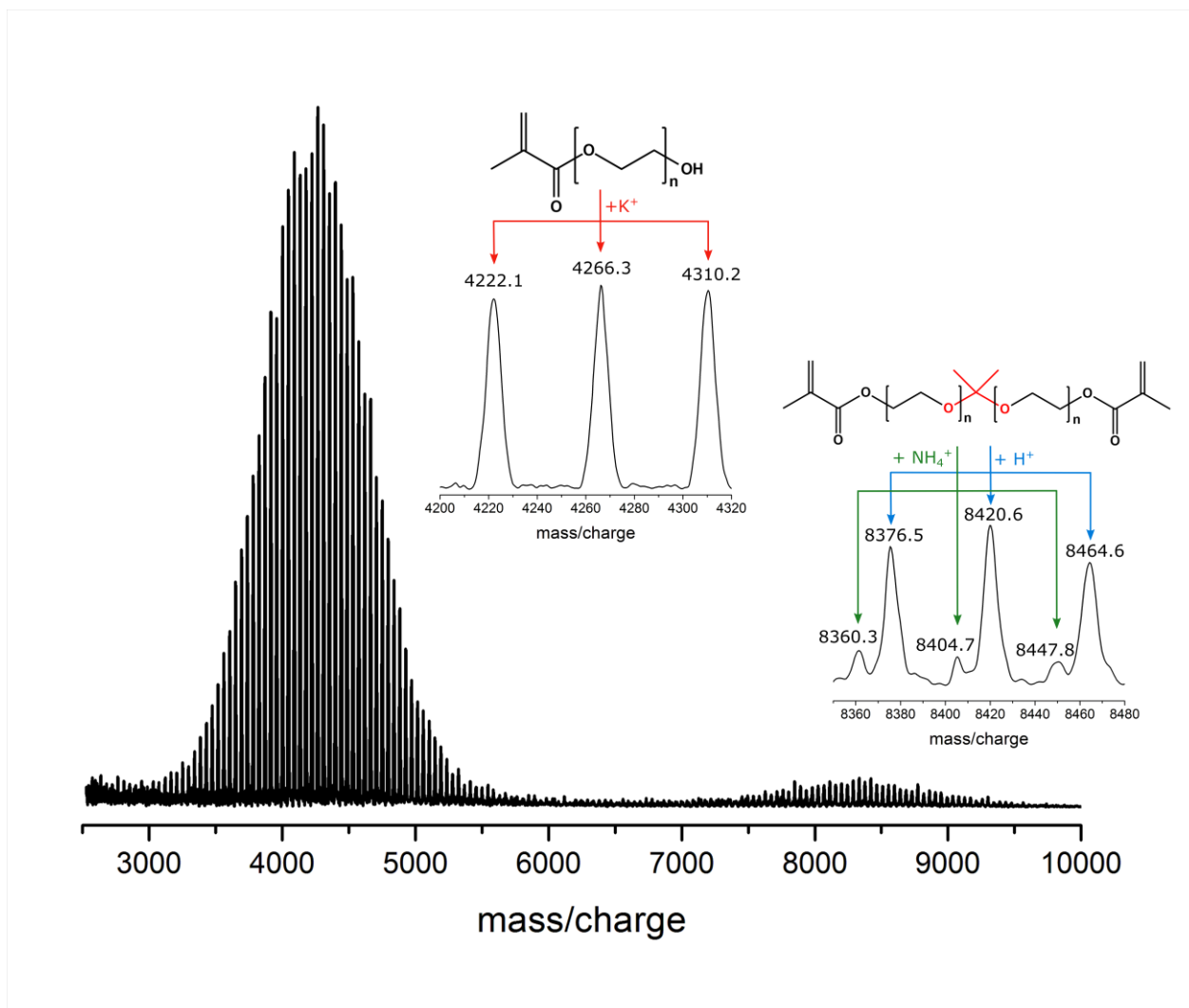


Figure S9. MALDI-ToF-MS of PEG(9700)-ketal-DMA (**11**) after complete degradation using a dithranol matrix and KTFA as a salt.

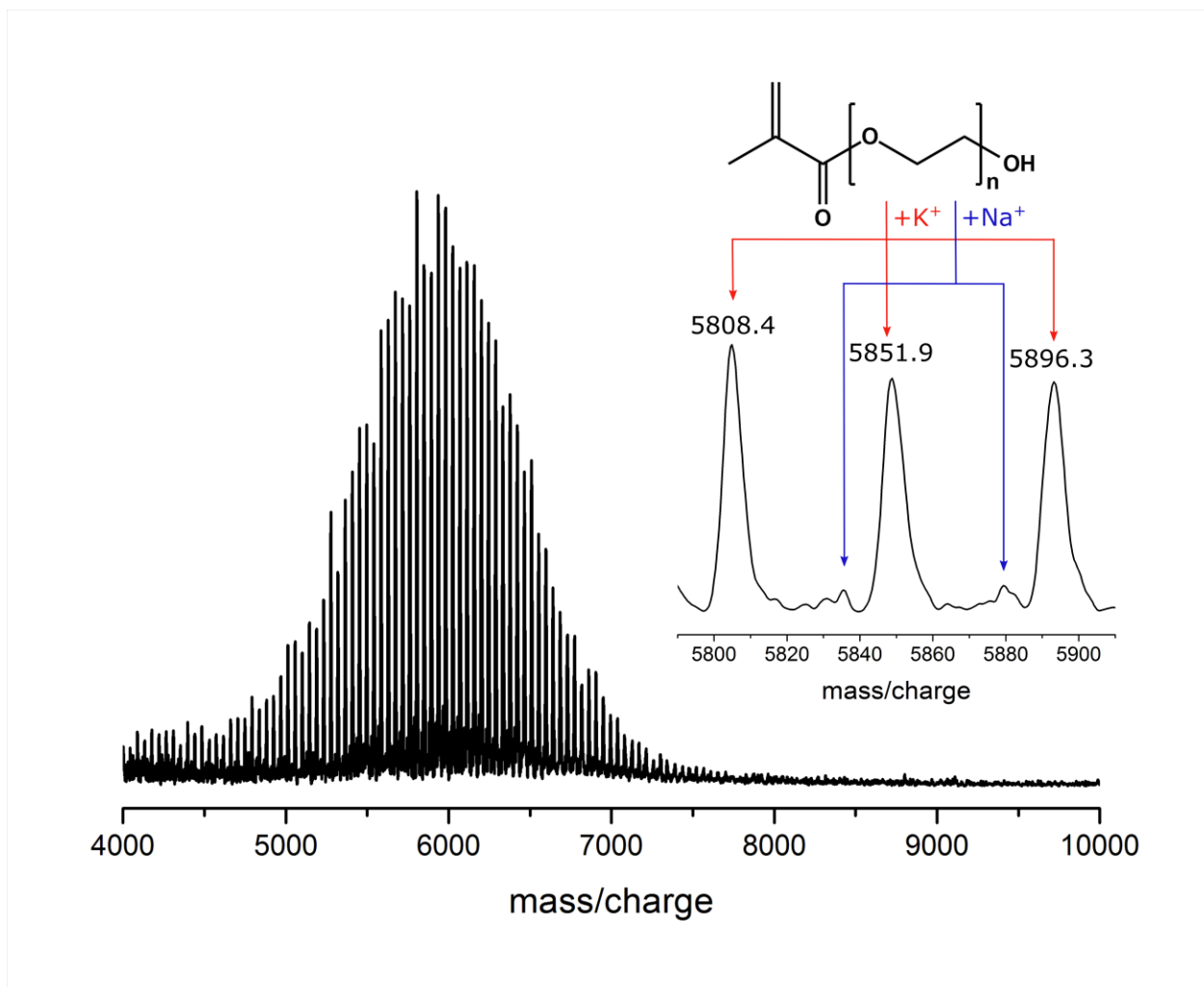


Figure S10. MALDI-ToF-MS of PEG(13200)-ketal-DMA (**12**) after complete degradation using dithranol matrix and KTFA as salt.

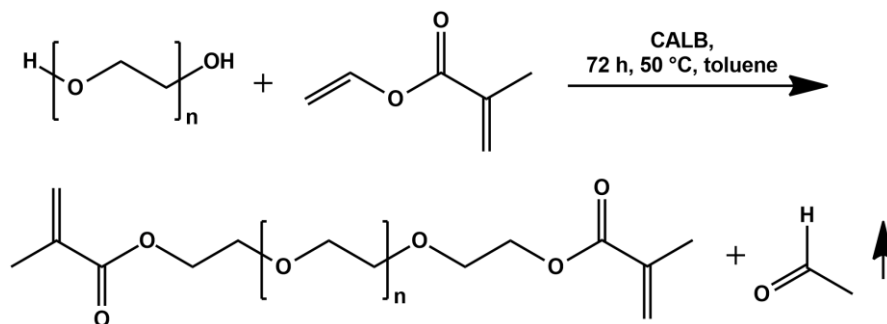


Figure S11. Reaction scheme of PEG-dimethacrylate (**13**) synthesis.

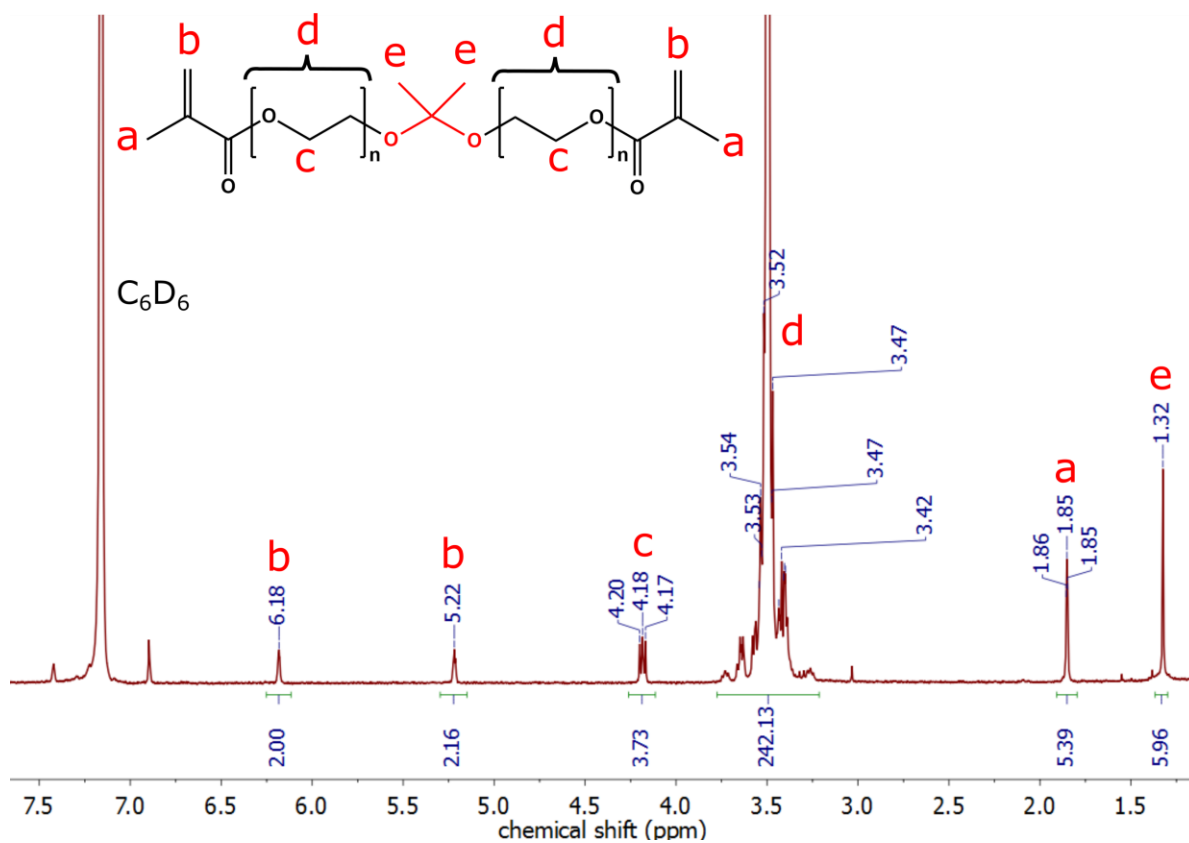


Figure S12.  $^1\text{H-NMR}$  spectrum (400 MHz,  $\text{CDCl}_3$ ) of poly(ethylene glycol)-dimethacrylate (PEG(2000)-DMA, **13**).

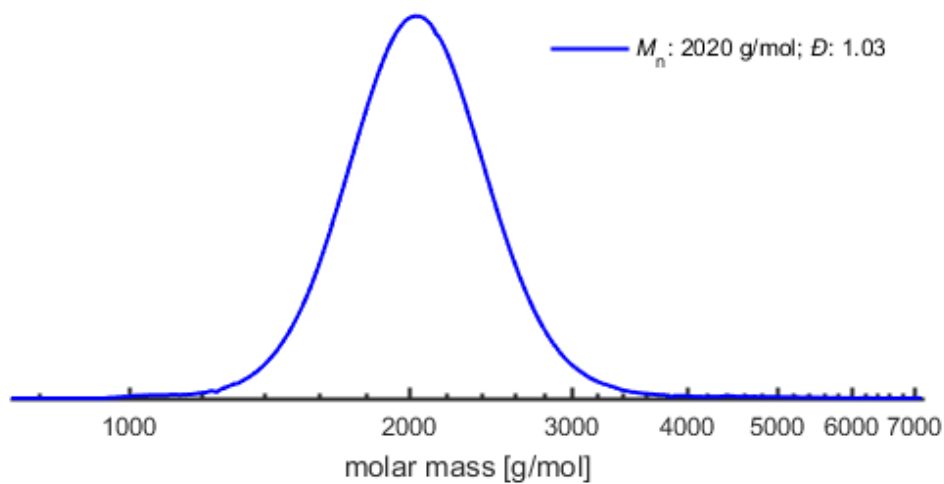


Figure S13. SEC result for PEG-dimethacrylate (eluent: DMF, PEG calibration, RI detector signal).

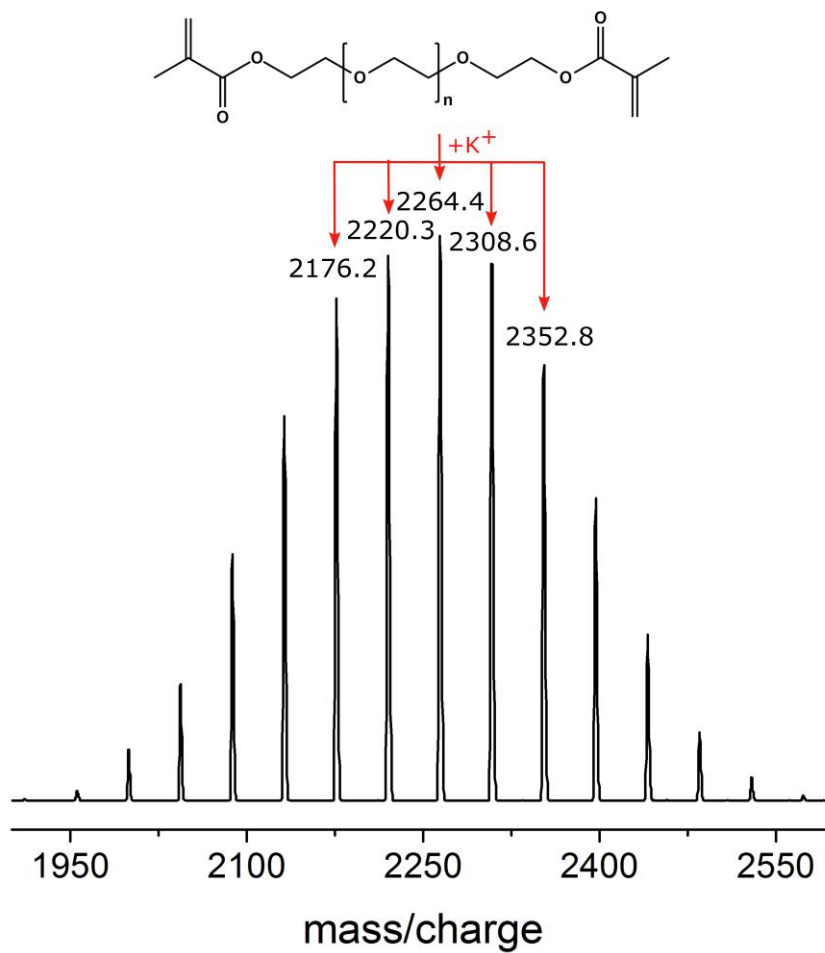
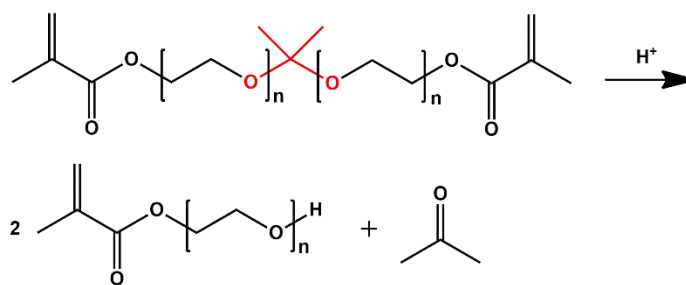


Figure S14. MALDI-ToF-MS of PEG(2000)-DMA (**13**) using a dithranol matrix and KTFA as salt.



Scheme S1. Degradation of the PEG-ketal-DMA.

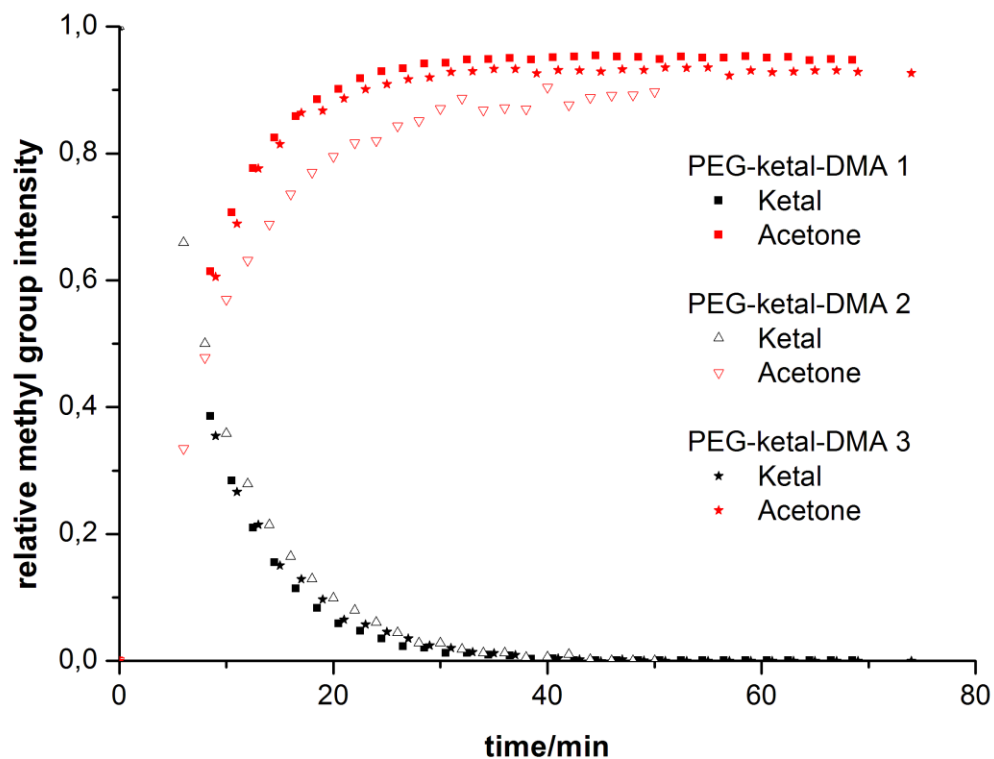


Figure S15. Comparison of *in-situ*  $^1\text{H}$  NMR integrals of the degradation of PEG(2700)-ketal-DMA, PEG(9700)-ketal-DMA, and PEG(13200)-ketal-DMA at 37 °C in deuterated phosphate buffer at pH 6.1. Decreasing relative methyl group intensity of the ketals in black and increasing relative methyl group intensity of acetone in red.

## Chapter 4. A Magic Effect of Silver Oxide on the Monotosylation of PEG? A Facile and General Route to Heterobifunctional PEG via Polymer Desymmetrization

*Hannah Pohlit<sup>1,2,3</sup>, Matthias Worm<sup>2</sup>, Jens Langhanki<sup>2</sup>, Elena Berger-Nicoletti<sup>2</sup>, Till Opatz<sup>2</sup>, Holger Frey<sup>2,\*</sup>*

<sup>1</sup>Department of Dermatology, University Medical Center Mainz, Langenbeckstr. 1, 55131 Mainz, Germany

<sup>2</sup>Institute of Organic Chemistry, Johannes Gutenberg University Mainz, Duesbergweg 10-14, 55128 Mainz, Germany

<sup>3</sup>Graduate School Materials Science in Mainz, Staudinger Weg 9, 55128 Mainz, Germany

\* corresponding author: Holger Frey, hfrey@uni-mainz.de

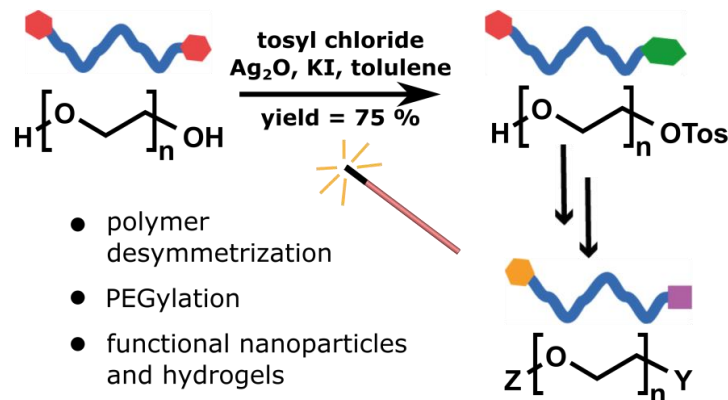
To be submitted.

### **Abstract**

Heterobifunctional polyethylene glycols (PEGs) are key structures for bioconjugation in the context of the “PEGylation” strategy to enhance blood circulation times of e.g., peptide drugs or “stealth” liposomes. The formation of heterobifunctional PEGs from symmetric PEG diols is challenging because of limited yields of the targeted monofunctional product and difficulties associated with separation steps. Based on a detailed comparison of reaction conditions, we have developed a “polymer desymmetrization” strategy to maximize the yields of monofunctional PEG tosylate. The tosylation reaction in presence of the heterogeneous catalyst silver oxide and potassium iodide in a specific stoichiometric ratio proved to be highly efficient, resulting in 71-76% yield of monofunctional PEG depending on molecular weight, exceeding the expected value of 50% in a statistical reaction. For characterization as well as for the preparative separation of monotosylated PEG, we developed a HPLC method, using an evaporative light scattering detector, enabling both analytic and semi-preparative separation of mono-tosylated PEGs up to 8000 g mol<sup>-1</sup>. To demonstrate the efficiency of the procedure, we synthesized an  $\alpha$ -azido- $\omega$ -methacryloyl-PEG, a building block suitable for azide-alkyne click-type reactions that can be incorporated into polymer networks via radical polymerization. We click-functionalized  $\alpha$ -azido-



$\omega$ -methacryloyl-PEG with a mannose-functionalized alkyne to enable functionalization of nanogels for enhanced cell uptake via the mannose receptor. The synthesis strategy is suitable for a broad range of applications in the field of hydrogel and nanogel functionalization.



**Keywords:** heterobifunctional PEG, click reaction, polymer desymmetrization

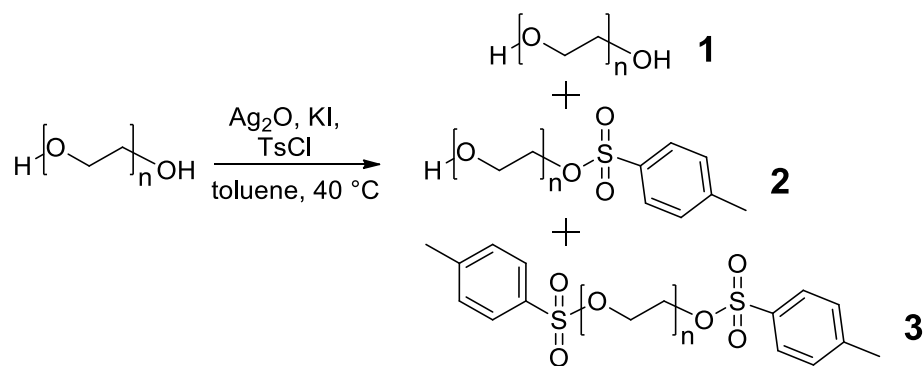
### Introduction and Motivation

Poly(ethylene glycol) (PEG) shows highly desirable characteristics for biomedical applications. It is soluble in water and a variety of organic solvents, as well as non-toxic, chemically inert and mostly non-immunogenic. These advantages render PEG the current gold standard polymer for anti-fouling materials, drug-delivery systems or attachment to therapeutic molecules to enhance water-solubility, blood-circulation times and bioavailability.<sup>[1; 2]</sup> To achieve targeted drug delivery, the attachment of targeting molecules to nanocarrier systems is often required.<sup>[3; 4]</sup> For conjugation of targeting molecules to the nanocarrier surface, heterobifunctional PEGs (PEGs bearing two different end groups) are particularly interesting. Depending on the end groups of the polymer chain, one can choose between different conjugation strategies to attach targeting molecules (i.e. antibodies or sugar-based substrates).<sup>[5]</sup> Popular conjugation chemistries target amino acid residues present in proteins and peptides (e.g., reaction of mPEG-N-hydroxysuccinimide with lysine residues), click chemistry (“alkyne azide click”, AAC) or thioether formation (“thiol-ene click”).

At present, various heterobifunctional PEGs are commercially available. Four different strategies have been described to obtain heterobifunctional oligo(ethylene glycol)s (OEGs) and PEGs: (i) ring-opening polymerization of ethylene oxide (EO) using an initiator and a termination reagent with different functional moieties. This method limits the availability of functional groups, as they need

to survive the strongly basic conditions of the oxyanionic polymerization. Furthermore, the synthesis needs to be carried out under inert atmosphere to exclude polymer chain growth initiated by traces of water and requires handling of the toxic gas EO.<sup>[6–23]</sup> (ii) The second method involves iterative coupling reactions of heterobifunctional oligomers to build up OEGs and PEGs. This method requires considerable synthetic effort and purification in between the individual coupling steps.<sup>[24; 25]</sup> (iii) The third strategy consists of a monofunctionalization of readily available and inexpensive OEG/PEG-diol with a functional group and subsequent (chromatographic) isolation of the desired heterobifunctional PEG molecule. Symmetrical PEG-diols as inexpensive starting materials are available in large quantities and with a broad range of molecular weights. For statistical reasons, this functionalization always results in a mixture of non-, mono-, and disubstituted PEG, resulting in low yields of the desired monofunctional product. Furthermore, difficulties have been reported for the purification of higher molecular weight PEGs (with  $M_n$  exceeding  $1000 \text{ g mol}^{-1}$ ), as the chemical differences (none, one or two end groups) between the reaction products decrease with molecular weight as a result of the decreasing influence of the end group with molecular weight.<sup>[26–36]</sup> For this reason, the third approach has been mostly used for low molecular weight oligomers or heterobifunctional PEGs that possess ionizable end groups that facilitate separation by ion exchange chromatography.<sup>[37]</sup> In this work, the third method based on polymer desymmetrization of PEG was exclusively employed for the synthesis of monotosylated PEG ( $M_n = 1500$  to  $8000 \text{ g mol}^{-1}$ ), which is a valuable intermediate that can be converted into a broad range of heterobifunctional PEGs.

In recent years, several reports have described an enhanced selectivity during tosylation of oligo(ethylene glycol)s to monosubstituted product upon addition of silver oxide and potassium iodide. Bouzide *et al.* were the first to report the beneficial use of silver oxide together with potassium iodide for the tosylation reaction of OEGs.<sup>[38]</sup> This method mediates sulfonation reactions of alcohols in high yields under neutral reaction conditions without the release of chloride as a by-product. Potassium iodide is required because it converts the tosyl chloride to the much more reactive tosyl iodide *in situ* and thereby accelerates the reaction rate.<sup>[38]</sup> In a subsequent publication, Bouzide *et al.* investigated monotosylation reactions, and observed high yields of monotosylated OEGs (yield 61–92% monotosylated product for OEG with molecular weights of  $62 - 282 \text{ g mol}^{-1}$ ). From simple statistical considerations for a 1:1 reaction of PEG with tosyl chloride one would expect a product ratio of 25% PEG-diol **1**, 50% PEG-monotosylate **2** and 25% PEG-ditosylate **3** (see Scheme 1).



*Scheme 1.* Tosylation reaction of OEG or PEG with silver oxide and potassium iodide in toluene at 40 °C with expected product mixture.

The authors tentatively explained the enhanced yields of monotosylated OEG by coordination of the silver cation with the oxygen atoms in the OEG backbone (see Scheme 2).<sup>[39]</sup> The general concept can be transferred to monoacylation, monobenzoylation, or monophosphorylation of e.g. carbohydrates,<sup>[40–42]</sup> and has also been used for other oligo(ethylene glycol)s<sup>[43]</sup> or poly(ethylene glycol)s.<sup>[27; 44–47]</sup> Hsu *et al.* as well as Mahou *et al.* explain the selectivity towards mono-functionalized PEG with intramolecular hydrogen bonding. They propose that intramolecular hydrogen bonding is responsible for deprotonation of one hydroxyl group by silver oxide because the other hydroxyl group becomes less acidic.<sup>[46; 47]</sup> However, it is unlikely that the preferred monosubstitution of poly(ethylene glycol) depends on the coordination of all oxygen atoms to the silver cation, as it was proposed for oligo(ethylene glycol). Furthermore, due to the low solubility of silver oxide in toluene, free silver cations would rather interact with iodide than with the ether oxygens. Obviously, the silver oxide-based strategy bears high promise although it currently lacks a conclusive, mechanistic picture. Unfortunately, none of the existing publications suggests a mechanism for the preferential monotosylation reaction of poly(ethylene glycol), and analytical data are limited or missing. Based on our previous experience, characterization of monosubstitution products by <sup>1</sup>H NMR and GPC is not adequate, as the global information obtained from NMR and GPC cannot conclusively distinguish between a monotosylated PEG and a mixture of non- and ditosylated PEG. MALDI-ToF MS alone is not suitable to quantify the amount of the different PEG structures in a reaction mixture with non-, mono-, and ditosylated PEG. To date, there is no systematic analysis and comparison of monotosylation reactions of dihydroxyfunctional (= unfunctionalized) PEG conducted with the additives silver oxide and potassium iodide versus conventional statistical monotosylation reactions without any catalyst added. In the first part of this work, the effect of silver oxide and potassium iodide on the yield of

monotosylated PEG is investigated. As an example for the synthetic value of monotosylated PEG, modification of PEG chains with an azide functionality as well as a methacryloyl unit in  $\omega$ -position is presented, permitting both azide-alkyne click reactions and covalent incorporation of the heterobifunctional polymers into chemical networks via radical polymerization.

## Results and Discussion

### A. Synthesis and purification of monotosylated PEG

The monotosylation step is crucial as it represents the desymmetrization of the PEG diol. Subsequently, recovery of the pure monofunctionalized product is essential for the subsequent transformations to obtain pure products. For statistical reasons, in a stoichiometric ratio of PEG and tosyl chloride, i.e., using a 1:1 ratio of PEG and tosyl chloride, one would expect a mixture of the possible reaction products PEG-diol **1**, PEG-monotosylate **2** and PEG-ditosylate **3** a ratio of 1:2:1. Improving the yield of monotosylated PEG is highly desirable. An enhanced selectivity towards monotosylation of PEG has been proposed for reactions in the presence of silver oxide and potassium iodide in toluene.<sup>[47; 46]</sup> To the best of our knowledge, the beneficial effects of silver oxide and potassium iodide for the tosylation reaction have not been studied for polymer diols, such as PEG in comparison to statistical tosylation reactions so far. Therefore, we decided to vary and compare different reaction conditions with regard to the amount of monotosylated PEG produced.

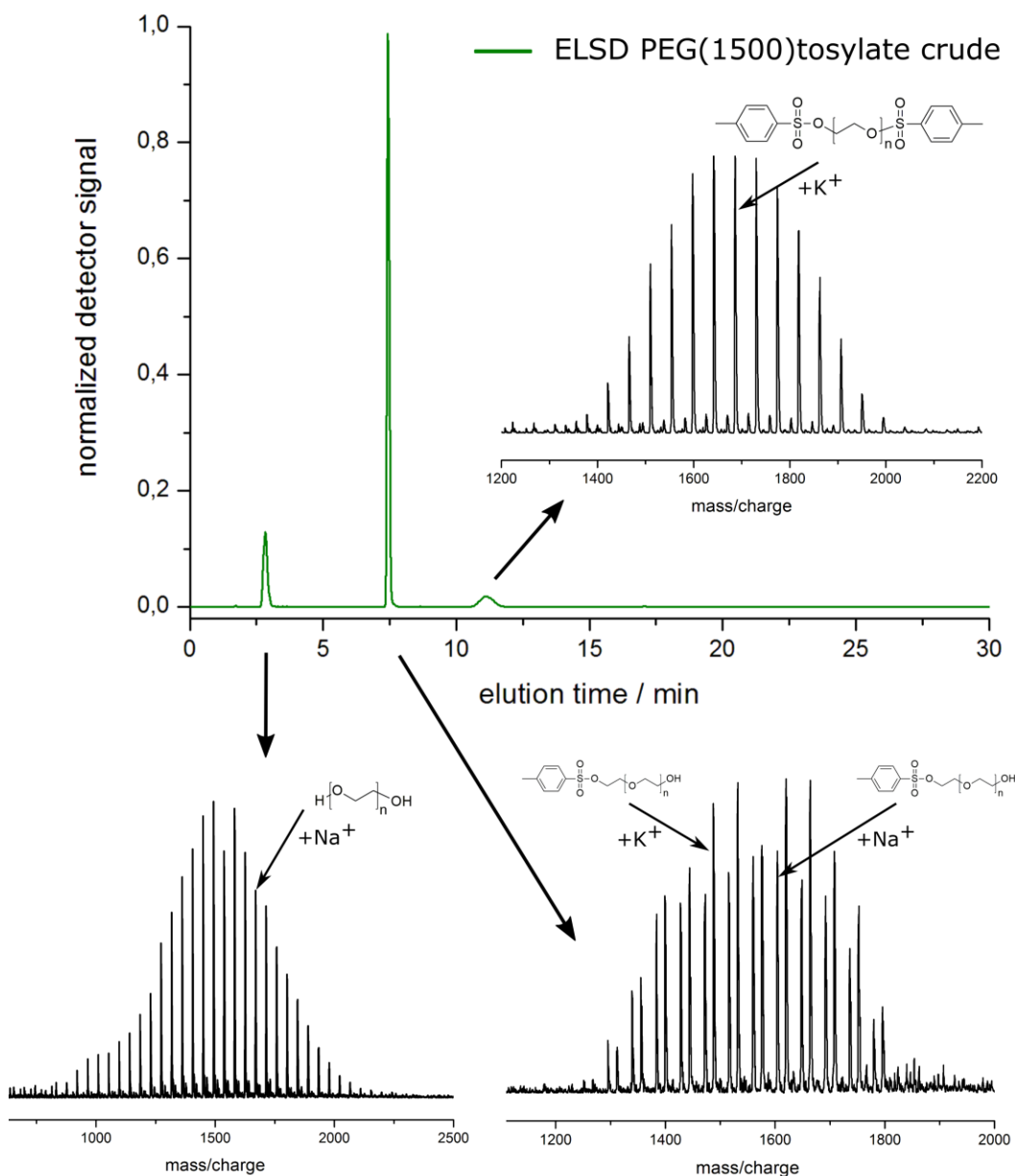
To date, merely  $^1\text{H}$  NMR and MALDI-ToF MS have been employed to confirm formation of the pure monotosylated product. However,  $^1\text{H}$  NMR spectroscopy is inappropriate to exclude the presence of diol-PEG and ditosylated PEG. The integrals of the hydroxyl group and the tosylate group may be in good agreement for monotosylated PEG product in  $^1\text{H}$  NMR (as an example see Figure S1), however detailed investigation of the sample by MALDI-ToF mass spectrometry shows distributions that can be clearly assigned to the monotosylated product **2**, diol-PEG **1** or ditosylated PEG **3** (see Figure S3). On the other hand it is not possible to quantify the amount of non-, mono-, and ditosylated PEG by MALDI-ToF MS, as we were able to confirm by mixing the purified components in different ratios, subsequently analyzing the integrals appearing in the MALDI-ToF MS (see Figure S37 - Figure S40). The signals cannot clearly be assigned to the non-, mono-, and ditosylated compounds **1**, **2** and **3**, since combination with different cations may result in the same  $m/z$  value (see Figure S37). Furthermore, the fraction of polymer coordinating to a

certain type of cation is not predictable and not reproducible. These facts lead to a visible trend upon mixing of different PEG species, but it is not sufficient to obtain a calibration curve (see Figure S40). The observation that quantification of different polymer species possessing different end groups in a polymer mixture is not adequate by MALDI-ToF-MS, for example  $\alpha$ -(2-propenyl)- $\omega$ -(2-propenyloxy)-poly(oxyethylene),  $\alpha$ -(2-propenyl)- $\omega$ -carboxy-methylthio-poly(oxyethylene) and  $\alpha$ -carboxymethylthioethyl- $\omega$ -carboxymethylthio-oligo (ethylene glycol), is described by Völcker *et al.*<sup>[28]</sup>

To investigate how silver oxide and potassium iodide enhance the yield of monotosylated product, statistical tosylation of PEG samples of different molecular weights was performed in a variety of solvents. Both the stoichiometric ratio (PEG/solvent/silver oxide) and the mode of addition of tosyl chloride (in one dose or via slow addition) was varied and analyzed. To exclude adsorption of one component of the reaction mixture to the silver oxide surface, silver oxide was also added subsequent to a tosylation reaction under statistical conditions (see Table 1, sample C14). Silver oxide is insoluble in the solvents employed, which results in a heterogeneous character of the reaction mixture and influences its interplay with PEG and tosyl chloride. Reverse phase HPLC was employed to quantify the amounts of the three possible reaction products and was optimized to separate the monotosylated PEG ( $M_n = 1500$  to  $8000 \text{ g mol}^{-1}$ ) on a semi-preparative scale for further reactions. A range of molecular weights of PEG was chosen (see Table 1) that represents the most commonly used molecular weights for PEGylation and functionalization of nanoparticles or liposomes.<sup>[5]</sup> Using a 20 minutes HPLC gradient (40% to 100% acetonitrile) method it was possible to separate all three possible reaction products. The elution of the reaction products was monitored by means of an evaporative light scattering detector. The purity of the separated PEG products was confirmed by MALDI-ToF-MS.

Figure 1 shows the typical separation and characterization, employing a mixture of PEG-1500-diol **1**, PEG-1500-monotosylate **2** and PEG-1500-ditosylate **3**, obtained in a reaction using silver oxide and potassium iodide (1.5 eq. of  $\text{Ag}_2\text{O}$ , 0.2 eq. of KI, 12.5 mL of toluene) that was analyzed with the HPLC method. For detailed mass spectrometry data of the distinct tosylation products, see Figures S5 - S7. Remarkably, HPLC separation of unreacted diol **1**, targeted monotosylated PEG **2** and ditosylated PEG **3** was applicable even for PEG chains with higher molecular weights (up to  $8000 \text{ g mol}^{-1}$ ) with only little variation of the gradient program (see Figure S12). Integration of

the peak area allows to determine the relative amounts of the reaction products obtained from a crude reaction mixture.

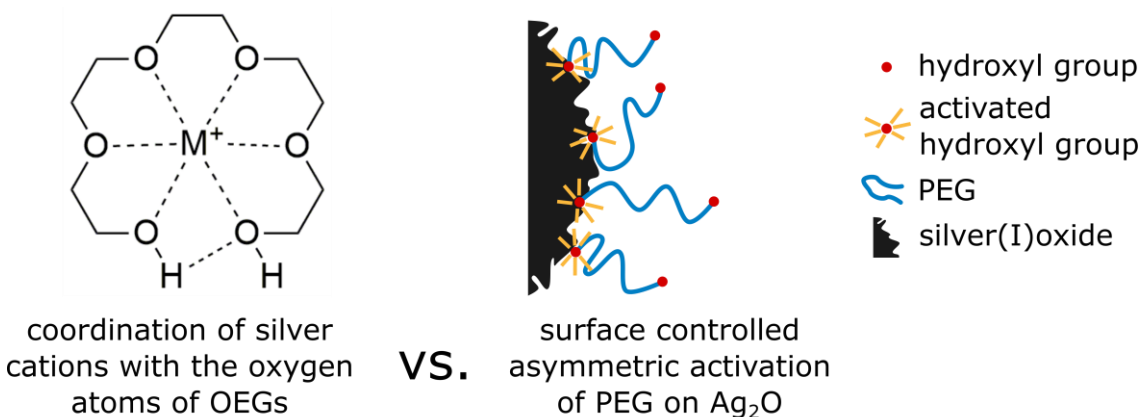


*Figure 1.* Typical separation of crude mixture of PEG-1500-diol **1**, PEG-1500-monotosylate **2** and PEG-1500-ditosylate **3** with reverse phase HPLC. The purity of the separated PEG-derived structures was confirmed by MALDI-ToF-MS after separation.

The tosylation reaction catalyzed with silver oxide and potassium iodide yields between 76.2% and 42.0% of monotosylated PEG **2**. The amount of the targeted monotosylated product **2** is lowered with increasing molecular weight of PEG. The difunctional side product ditosylate-PEG **3**

was produced in surprisingly low yields in the range of 14.4% – 2.7%, and unreacted PEG **1** was recovered with yields in the range of 15.8% – 55.2% (see Table 1). A systematic comparison of the influence of different reaction conditions on the yield of monotosylated product is summarized in Table 1.

To investigate (and eventually to confirm or dispute) the influence of silver oxide and potassium iodide, statistical tosylation (non-catalyzed tosylation reaction) of PEG in dichloromethane with triethylamine and tosyl chloride was performed. Under these conditions, regardless of slow addition of tosyl chloride to the solution or addition in one portion, the tosylation afforded 33.5% and 55.2% of monotosylated PEG-2000 **2**, respectively (see Table 1, samples C12 and C13). These results are in good agreement with literature regarding the tosylation of PEG-2000, giving values of 34% PEG, 49% PEG-monotosylate and 12% PEG-ditosylate.<sup>[26]</sup> The reaction with silver oxide constantly produced higher yields of monotosylated PEG **2** for PEG with Mn between 1500 and 8000 g mol<sup>-1</sup> compared to the statistical reaction conditions (see Table 1, samples C1, C4, C5, C7). Possibly, the underlying key effect for enhanced monotosylation adding silver oxide compared to the statistical reaction is the insolubility of silver oxide in organic solvents and its low solubility in water (solubility product  $K_{sp}(\text{Ag}_2\text{O})$  in water at 20 °C =  $1.69 \times 10^{-6} \text{ mol}^3\text{L}^{-3}$ ).<sup>[48]</sup> Silver(I)oxide shows a rather inhomogeneous particle size distribution in the size range of a few nanometers up to 5  $\mu\text{m}$ , which supports a heterogeneous catalysis process at the surface of the silver oxide particles (see Figure S41 and Figure S42). The hydroxyl end groups of PEG can dynamically interact with free coordination sites at the silver oxide surface, forming weak interactions with the silver(I)oxide particles, thereby promoting polarization and tosylation of hydroxyl groups. Backfolding, i.e., loop formation of polymer chains is entropically disfavored, therefore coordination of both hydroxyl groups of PEG to  $\text{Ag}_2\text{O}$  is unlikely. Based on our results (Table 1) we suggest a surface-controlled activation of PEG at the heterogeneous surface of the silver oxide particles. However, the significantly enhanced amount of monotosylated product must be due to a complex interplay between surface activation and exchange dynamics at the surface.



*Scheme 2.* Coordination of oligo(ethylene glycol) with silver cations, as proposed by Bouzide *et al.* (left) versus surface controlled asymmetric activation of PEG at the heterogeneous silver oxide catalyst particles (right).

To elucidate to which extent this effect depends on the stoichiometric ratio of PEG, silver oxide and solvent, reaction time and reaction temperature, another set of experiments was conducted. 15 equivalents or 30 equivalents of silver oxide instead of 1.5 eq. under otherwise the same reaction conditions resulted incomparable amounts of monotosylation product (see Table 1, sample C7 and C8). In contrast, dilution (only 0.15 eq. of silver oxide or 10-fold the amount of solvent) resulted in drastically decreased yields of monotosylated product **2** (see Table 1, samples C6 and C9). The catalyst-free statistical reaction with triethylamine in toluene or dichloromethane or in pyridine resulted in a lower yield of monotosylated PEG **2** compared to catalyzed reactions, independent of molecular weight (see Table 1, samples C2-C3, C10-16, C19, C22, C25). To exclude an adsorption effect of one subset of products, the reaction was performed under statistical conditions in DCM. After 16 h of reaction time, Ag<sub>2</sub>O was added and removed by filtration after 30 minutes of stirring. The amount of monotosylated product and side products remained constant compared to the reactions in which no silver oxide was added (see Table 1, sample C16). Mahou *et al.* suggested the selectivity towards mono-functionalized PEG depends on coordination of hydroxyl groups to silver cations and activation through intramolecular hydrogen bonding. However, if silver nitrate is used as a catalyst instead of silver oxide, no selectivity towards mono-functionalized PEG was observed (see Table 1, sample C10). It is noteworthy that even silver nitrate is insoluble in toluene and reacts with potassium iodide to precipitated silver iodide.



The role of KI was also investigated by Bouzide *et al.*<sup>[38]</sup> Potassium iodide was reported to enhance tosylation reaction rates, as it converts the tosyl chloride to the much more reactive tosyl iodide *in situ*.<sup>[38]</sup>

In general, with increasing molecular weight of PEG, the conversion and the yields of monotosylated PEG under the same reaction conditions decreased. For this reason, we altered the reaction conditions to three equivalents of silver oxide and 48 hours reaction time for PEG-4000 and PEG-8000, respectively (see Table 1, samples C17-C25). With three eq. of Ag<sub>2</sub>O, PEG-4000 could be converted to PEG-monotosylate with yields of 60.2% (**2**, see Table 1, sample C18) which compares favorably to 25.2% of PEG-monotosylate (**2**, see Table 1, sample C19) obtained under uncatalyzed reaction conditions. For PEG-8000, prolongation of reaction conditions from 16 to 48 hours resulted in 32.8% and 42.0% of the targeted monotosylated product compared to 9.4% and 12.6% from uncatalyzed, but otherwise similar reaction conditions (see Table 1, samples C21, C22, C24, C25).

To conclude this series of experiments, we observed that silver oxide in combination with KI reproducibly provides an enhanced selectivity towards monotosylation reactions of poly(ethylene glycol)s (42 – 76% monotosylated product depending on molecular weight). In contrast, the uncatalyzed tosylation reaction resulted in a yield of monotosylated product ranging from 12 to 55% depending on molecular weight in a range expected for the statistical process. For PEG-2000 or lower molecular weights, 1.5 equivalents of Ag<sub>2</sub>O were sufficient to obtain high yields of monotosylated product (see Table 1, samples C1 and C5). For PEG with a molecular weight above 2000 g mol<sup>-1</sup>, the amount of catalyst had to be increased to 3 equivalents, and the reaction time had to be prolonged to 48 hours to afford high monotosylation yields (see Table 1, samples C18 and C24). Slower reaction kinetics for larger PEGs are not surprising, as larger PEGs are sterically disfavored to react at both hydroxyl groups of the polymer coils.

*Table 1.* Comparison of the influence of different reaction conditions on the amount of monotosylated PEG. Amounts of reaction products were calculated from peak areas in analytical HPLC measurements. Gray-shaded fields: uncatalyzed reaction conditions, non-shaded fields: Ag<sub>2</sub>O-catalyzed reaction conditions.

Condition #	Reaction conditions (1.0 eq. PEG, 1.0 eq. TsCl, 40 °C, 16 h)	PEG (M <sub>n</sub> / g mol <sup>-1</sup> )	Yield 1 / %	Yield 2 / %	Yield 3 / %
C1	1.5 eq. Ag <sub>2</sub> O, 0.2 eq. KI, 12.5 mL toluene	1500	17.9	73.3	8.8
C2	1.5 eq. NEt <sub>3</sub> , 12.5 mL DCM <sup>1</sup>	1500	76.1	23.5	0.4
C3	1.5 eq. NEt <sub>3</sub> , 25 mL DCM <sup>1</sup>	1500	90.1	9.9	0.0
C4	1.5 eq. Ag <sub>2</sub> O, 0.2 eq. KI, 12.5 mL toluene	2000	14.4	71.2	14.4
C5	1.5 eq. Ag <sub>2</sub> O, 0.2 eq. KI, 25 mL toluene	2000	15.8	76.2	7.9
C6	1.5 eq. Ag <sub>2</sub> O, 0.2 eq. KI, 125 mL toluene	2000	99.5	0.5	0.0
C7	15 eq. Ag <sub>2</sub> O, 2 eq. KI, 12.5 mL toluene	2000	22.8	69.7	7.5
C8	30 eq. Ag <sub>2</sub> O, 4 eq. KI, 12.5 mL toluene	2000	29.6	70.4	0.0
C9	0.15 eq. Ag <sub>2</sub> O, 0.02 eq. KI, 12.5 mL toluene	2000	99.4	0.6	0.0
C10	1.5 eq. AgNO <sub>3</sub> , 0.02 eq. KI, 12.5 mL toluene	2000	74.6	23.2	2.1
C11	1.5 eq. NEt <sub>3</sub> , 12.5 mL toluene	2000	77.2	22.5	0.3
C12	1.5 eq. NEt <sub>3</sub> , 12.5 mL DCM <sup>1</sup>	2000	42.9	55.2	1.9
C13	1.5 eq. NEt <sub>3</sub> , 12.5 mL DCM <sup>1</sup> , TsCl dissolved in DCM added dropwise	2000	65.4	33.5	1.1
C14	1.5 eq. NEt <sub>3</sub> , 25 mL DCM <sup>1</sup>	2000	81.2	18.8	0.0
C15	12.5 mL pyridine	2000	96.9	3.1	0.0
C16	1.5 eq. NEt <sub>3</sub> , 12.5 mL DCM, subsequent addition of Ag <sub>2</sub> O	2000	38.7	55.3	6.0
C17	1.5 eq. Ag <sub>2</sub> O, 0.2 eq. KI, 12.5 mL toluene	4000	57.3	41.8	0.9
C18	3 eq. Ag <sub>2</sub> O, 0.4 eq. KI, 12.5 mL toluene	4000	26.6	60.2	13.2
C19	1.5 eq. NEt <sub>3</sub> , 12.5 mL DCM <sup>1</sup>	4000	74.0	25.2	0.8
C20	1.5 eq., Ag <sub>2</sub> O, 0.2 eq. KI, 12.5 mL toluene	8000	88.3	11.4	0.3
C21	3 eq. Ag <sub>2</sub> O, 0.4 eq. KI, 12.5 mL toluene	8000	65.2	32.8	2.0
C22	1.5 eq. NEt <sub>3</sub> , 12.5 mL DCM <sup>1</sup>	8000	90.6	9.4	0.0

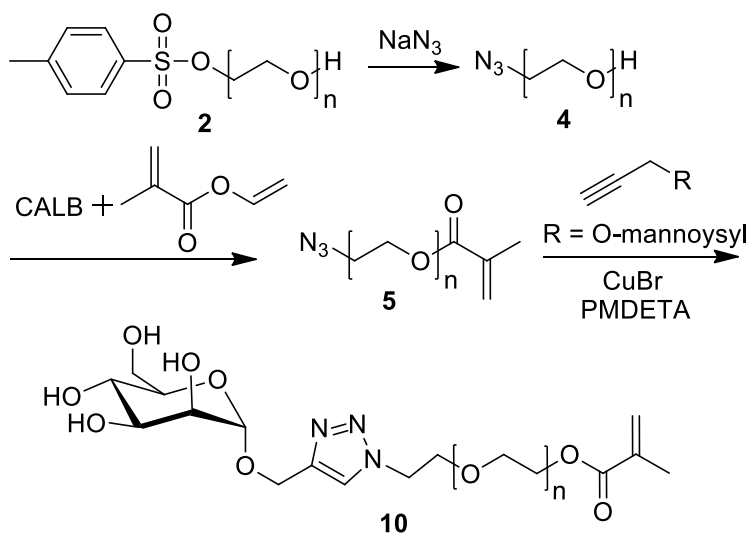
C23	1.5 eq., Ag <sub>2</sub> O, 0.2 eq. KI, 12.5 mL toluene, 48 h	8000	73.4	25.6	1.0
C24	3 eq. Ag <sub>2</sub> O, 0.4 eq. KI, 12.5 mL toluene, 48 h	8000	55.2	42.0	2.7
C25	1.5 eq. NEt <sub>3</sub> , 12.5 mL DCM <sup>1</sup> , 48 h	8000	87.4	12.6	0.0

<sup>1</sup> DCM = dichloromethane

Efficient removal of unsubstituted PEG **1** and disubstituted product **3** is a key requirement for the preparation of pure monotosylated product **2**. For all molecular weights investigated, excellent separation via analytical as well as semipreparative HPLC was achieved. Remarkably, even the reaction products of PEG with 8000 g mol<sup>-1</sup> can be separated with the HPLC method described with baseline resolution, merely on the basis of the different end groups. (See Table 1, samples C20 - C25) The results assessed in the analytical HPLC measurements were reproduced on a semi-preparative scale (up to 200 mg of crude product per injection), again with baseline separation of the three relevant PEG species. Thus, this polymer desymmetrization method permits to obtain pure monotosylated product on a gram scale after several runs of semi-preparative HPLC. The purified monotosylated product could be converted to heterobifunctional PEGs with a variety of functional groups. As an example, the synthesis of  $\alpha$ -4-( $\alpha$ -D-mannopyranosyl-oxymethylene)-1,2,3, triazol-1-yl- $\omega$ -methacryloyl-PEG, a polymer which is suited for hydrogel and nanogel functionalization, is described below.

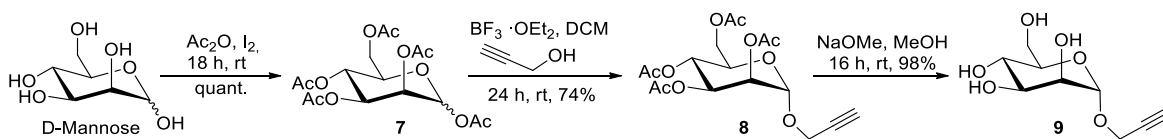
#### **B. Conversion of heterobifunctional PEG to $\alpha$ -4-( $\alpha$ -D-mannopyranosyloxymethylene)-1,2,3, triazol-1-yl- $\omega$ -methacryloyl-PEG**

This section shows an example for the preparative value of the monotosylated PEGs. Targeting of the mannose receptor on CD11c positive cells (e.g. dendritic cells) is important to enhance efficient cell-specific uptake of nanoparticles.<sup>[49–52]</sup> For the conjugation of mannose to the polymer chain, a copper(I)-catalyzed alkyne-azide cycloaddition (CuAAC)<sup>[53; 54]</sup> click reaction was used. In a four step sequence, the commercial PEG-diol was transformed into  $\alpha$ -4-( $\alpha$ -D-mannopyranosyloxymethylene)-1,2,3, triazol-1-yl- $\omega$ -methacryloyl-PEG, a building block that is highly valuable to incorporate a functionality into nanoparticles synthesized by radical polymerization (see Scheme 3). To the best of our knowledge, this is the first report regarding a facile method to attach both methacrylate, enabling a radical polymerization, and mannose to a heterobifunctional PEG chain.



*Scheme 3.* Reaction scheme of subsequent transformation of PEG-monotosylate (**2**) to  $\alpha$ -4-( $\alpha$ -D-mannopyranosyloxymethylene)-1,2,3-triazol-1-yl- $\omega$ -methacryloyl-PEG (**10**) in a three step reaction.

In the first step, we substituted the tosylate moiety by an azide to obtain  $\alpha$ -azide- $\omega$ -hydroxyl-PEG. Already in the two-step reaction of PEG-diol to  $\alpha$ -azide- $\omega$ -hydroxyl-PEG, the preparative value of the synthesized heterobifunctional product increases dramatically. The chemical characterization is shown in Figure S17 - Figure S19 in the Supporting Information. All resonances in the  $^1\text{H}$  NMR can be assigned, and there are no signals indicating unreacted tosylate moieties. SEC and MALDI-ToF-MS measurements also show a monomodal distribution and the absence of residual monotosylate-PEG (confirmed by MALDI-ToF-MS). The free hydroxyl group at the  $\omega$ -position can be further functionalized to enable crosslinking by radical polymerization. This was achieved by a mild transesterification reaction of the hydroxyl group with vinyl methacrylate in the presence of *Candida antarctica* lipase B (CALB). Complete functionalization with methacrylate was confirmed by  $^1\text{H}$  NMR, SEC, and MALDI-ToF-MS analysis (see Figure S20 – Figure S14).



*Scheme 4.* Reaction Scheme of Propargyl  $\alpha$ -D-mannopyranoside (**9**).

Propargyl  $\alpha$ -D-mannopyranoside was synthesized in a three step sequence as shown in Scheme 4. The CuAAC reaction was tested with phenyl acetylene as a model reaction. According to  $^1\text{H}$  NMR

and MALDI-ToF-MS, the click reaction was quantitative, and no residual  $\alpha$ -azido- $\omega$ -methacryloyl-PEG could be detected (see Figure S23 - Figure S25). The whole chain of reactions from PEG-diol to  $\alpha$ -1,2,3-triazole-4-phenyl- $\omega$ -methacrylate-PEG was additionally monitored by FTIR (see Figure S26).

For the application in nanogel synthesis, the covalent attachment of target molecules like mannose to the polymer is a crucial requirement. Therefore we used copper(I)-catalyzed alkyne-azide cycloaddition to attach a mannose-substituted alkyne to the  $\alpha$ -azido- $\omega$ -methacrylate-PEG. All resonances could be assigned in the  $^1\text{H}$  NMR spectrum. The integral of H-5 of the triazole ring at 8.11 ppm and the peaks of the mannose are slightly underestimated (0.72 instead of 1.00 for H-5), which may be due to shielding of the highly polar mannose molecule by the PEG chains in organic solvents (see Figure S34). A similar effect was not detected in the case of phenylacetylene. A shift towards higher molecular weights is visible in SEC measurements compared to  $\alpha$ -azido- $\omega$ -methacryloyl-PEG (see Figure S35). In the SEC elugramm, a higher molecular weight shoulder at approx.  $4000 \text{ g mol}^{-1}$  is visible, which may be due to starting crosslinking of methacrylate units during SEC sample preparation. No higher molecular weight shoulder is visible in MALDI-ToF-MS spectra (see Figure S36). The successful click reaction was confirmed by MALDI-ToF-MS.

## Materials and Methods

### Materials

Dimethylformamide, potassium trifluoroacetate, toluene, dichloromethane, benzene, methanol, acetonitrile, *Candida antarctica* lipase B (CALB), silver(I)oxide, silver nitrate, potassium iodide, Cu(I)Br, and diethyl ether were purchased from Sigma Aldrich. LiBr, magnesium sulfate, phenylacetylene, tosyl chloride, *N,N,N',N'',N'''*-pentamethyldiethylenetriamine (PMDETA), sodium azide, and hydroquinone were purchased from Acros. Dithranol was purchased from Fluka and vinyl-methacrylate were purchased from TCI. Deuterated DMSO and methanol were purchased from Deutero GmbH. PEG standards were obtained from Polymer Standards Service GmbH. Lewatit Mono Plus S100CHC4124 was a gift from Lanxess. Dimethylformamide (DMF, Extra dry, AcroSeal<sup>®</sup>) and pyridine was purchased from Acros. All chemicals were used without further purification, unless otherwise stated. Acetonitrile and dichloromethane was distilled from calcium hydride. The eluents for column chromatography (cyclohexane and ethyl acetate) were distilled prior to use. Deuteriochloroform was stored over alumina (Brockmann activity I).

All reactions involving air or moisture sensitive reagents or intermediates were performed under an inert atmosphere of argon in glassware that was oven dried using standard Schlenk techniques. Reaction temperatures referred to the temperature of the particular cooling/heating bath.

Chromatography:

Thin-layer chromatography (TLC) was carried out on silica gel 60 F254 plates (Merck) or RP silica gel RP-18 F254s plates (Merck). Compounds were visualized using UV light and/or by immersion in a solution of m-methoxyphenol (0.1 mL) in ethanol (95 mL) and sulfuric acid (2 mL) followed by heating. Chromatography was performed using flash chromatography of the indicated solvent system on 35–70  $\mu\text{m}$  silica gel (Acros Organics).

### Characterization Methods

$^1\text{H}$  NMR spectra (400 MHz) were recorded using a Bruker AMX400 spectrometer and referenced internally to residual signals of the deuterated solvent.  $^1\text{H}$  NMR spectra were analyzed with MestReNova v10.0.1.

For size exclusion chromatography (SEC) measurements, an Agilent 1100 series integrated instrument was used, including a PSS HEMA column (106/104/102  $\text{\AA}$  porosity) and a refractive index (RI) and ultraviolet (UV) detector. Samples were measured in dimethylformamide (DMF, containing 0.25 g  $\text{L}^{-1}$  of lithium bromide as an additive) and calibration was carried out using poly(ethylene oxide) standards. The standards and the software used for analysis (PSS WinGPC Unity v7) were provided by Polymer Standards Service GmbH. Data was plotted with MATLAB.

MALDI-ToF mass spectrometry was performed on a Shimadzu Axima CFR MALDI-ToF mass spectrometer equipped with a nitrogen laser delivering 3 ns laser pulses at 337 nm. Dithranol was used as matrix, and potassium trifluoroacetate was added to facilitate ionization of polymer samples. The MS spectra were analyzed with Kompact Version 2.4.1 from Kratos Analytical Ltd.

The freeze-drier used was a Christ Alpha 2-4 LD Plus.

The gradient HPLC system for analytical and semi-preparative setup consisted of an Agilent Technologies 1260 Infinity system with a 1260 Quat Pump, 1260 ALS autosampler, 1260 VWD UV-vis variable-wavelength spectrophotometric detector and a Softa 1300 evaporative light scattering detector. The UV detector was operated at a wavelength of 254 nm. For analysis, a Reprosil 100 (C18, 5  $\mu\text{m}$  particle size, 4.6 x 250 mm i.d.) column from Maisch GmbH was used.

Data was analyzed with PSS WinGPC Unity v7, provided by Polymer Standards Service GmbH. For separation, a Reprosil 100 (C18, 5  $\mu\text{m}$  particle size, 20 x 250 mm i.d. protected with 20 x 30 mm i.d. column guard) column from Maisch GmbH was used. The mobile phases consisted of acetonitrile (Inlet A), and Milli Q water (Inlet B).

Fourier transform infrared spectroscopy (FTIR) was measured using a Nicolet iS10 spectrometer from Thermo Fisher Scientific Inc. The software for spectra analysis was Omnic Software v8.1.210.

## Synthetic procedures

### Synthesis of $\alpha$ -tosyl- $\omega$ -hydroxyl-PEG (**1**, **2** and **3**)

The synthesis of  $\alpha$ -tosyl- $\omega$ -hydroxyl-PEG was modified from Mahou *et al.*<sup>[47]</sup> Exemplarily, the synthesis of  $\alpha$ -tosyl- $\omega$ -hydroxyl-PEG-1500 is described below. PEG (1.00 g,  $M = 1500 \text{ g mol}^{-1}$ ,  $n = 0.667 \text{ mmol}$ ) was dissolved in benzene (5 mL) in a Schlenk flask and dried under high vacuum after azeotropic distillation of benzene to remove water. For the standard experiment, PEG was dissolved in dry toluene (12.5 mL) and the reaction solution was heated to 40 °C. Under vigorous stirring,  $\text{Ag}_2\text{O}$  (261 mg, 1.5 eq,  $n = 1.00 \text{ mmol}$ ) and potassium iodide (25 mg, 0.2 eq.,  $n = 0.15 \text{ mmol}$ ) were added under inert conditions. After 15 minutes of stirring, tosyl chloride (150 mg, 1.05 eq,  $n = 0.788 \text{ mmol}$ ) was added under argon counterflow and the reaction mixture was rigorously stirred overnight at 40 °C. The amount of solvent, silver oxide, reaction temperature and reaction time were modified according to Table 1. The solution was filtered through a filtration paper at 40 °C followed by solvent removal by rotary evaporation. The crude product was purified by twofold precipitation from methanol into ice-cold diethyl ether. The pure product was dried under high vacuum for 24 hours. The product mixture (**1**, **2** and **3**) was recovered as colorless powder (891 mg, yield = 80%,  $M = 1670 \text{ g mol}^{-1}$ ).  $^1\text{H NMR}$  (400 MHz, DMSO)  $\delta$  [ppm] = 7.78 (d, 2H,  $\text{C}_{\text{arom}}\text{H}-\text{C}-\text{SO}_3$ ), 7.48 (d, 2H,  $\text{C}_{\text{arom}}\text{H}-\text{C}-\text{CH}_3$ ), 4.58 (t, 1H,  $-\text{OH}$ ), 4.11 (m, 2H,  $\text{CH}_2-\text{SO}_3$ ), 3.40-3.56 (m, 119H,  $(\text{CH}_2-\text{CH}_2-\text{O})_n$ ), 2.42 (s, 3H,  $-\text{CH}_3$ ), see Figure S1.

For the non-catalyzed tosylation reaction, a procedure reported by Li *et al.* was used and slightly modified.<sup>[26]</sup> In short, PEG (1.0 g,  $M = 2000 \text{ g mol}^{-1}$ ) was dried with azeotropic distillation of benzene. PEG was dissolved in DCM (12.5 mL), followed by the addition of tosyl chloride (95 mg, 1 eq.) and TEA (138  $\mu\text{l}$ , 2 eq.), and stirred under argon atmosphere at 40 °C for 16 h. The solvent was removed by rotary evaporation. The crude product was purified by twofold precipitation from methanol into ice-cold diethyl ether. The pure product was dried under high vacuum for 24 hours.

The pure product mixture (**1**, **2** and **3**) was recovered as colorless powder (873 mg, yield = 78%,  $M = 2170 \text{ g mol}^{-1}$ ).

For the different reaction conditions, reactants and solvent conditions were modified, as stated in Table 1.

#### **Analysis and purification of (1, 2 and 3) via HPLC**

Analytical: The mixture of  $\alpha$ -tosyl- $\omega$ -hydroxyl-PEG (**2**), diol-PEG (**1**) and  $\alpha,\omega$ -ditosyl-PEG (**3**) (1 mg) was dissolved in acetonitrile (ACN) : water (40:60, 1 mL), filtered through a Rotilabo<sup>®</sup> syringe filter (PTFE, pore size 0.45  $\mu\text{m}$ ) and was analyzed by RP-HPLC with an Acetonitrile/water gradient. Gradient conditions: linear gradient from 40% ACN to 70% ACN over 7.5 min, then a linear gradient to 100% ACN over 1.5 min, and then isocratic at 100% ACN for 3 min. Subsequently the starting gradient was restored in one minute and a 8 min reconditioning time of 40% ACN : 60% water was allowed before further gradient analyses. Total run time was 20 min at a flow rate of 1  $\text{mL min}^{-1}$ . For PEG > 2000  $\text{g mol}^{-1}$ , a linear gradient from 40% ACN to 50% ACN over 7.5 min, then a linear gradient to 100% ACN for 1.5 min, and then isocratic at 100% ACN for 3 min was used. Then the starting gradient was restored in one minute and a 8 min reconditioning time of 40% ACN : 60% water was allowed before further gradient analyses.

Semi-Preparative scale: The mixture of  $\alpha$ -tosyl- $\omega$ -hydroxyl-PEG (**2**), diol-PEG (**1**) and  $\alpha$ -tosyl- $\omega$ -tosyl-PEG (**3**) (100 mg) was dissolved in acetonitrile (ACN) : water (40:60), filtered through a Rotilabo<sup>®</sup> syringe filter (PTFE, pore size 0.45  $\mu\text{m}$ ) and were separated by RP-HPLC with an acetonitrile/water gradient. Gradient conditions: linear gradient from 40% ACN to 70% ACN over 7.5 min, then a linear gradient to 100% ACN over 1.5 min, and then isocratic at 100% ACN for 3 min. Subsequently the starting gradient was restored in one minute and an 8 min reconditioning time of 40% ACN : 60% water was allowed before further sample injection. Total run time was 20 min at a flow rate of 10  $\text{mL min}^{-1}$ . The sample fraction of monotosylated PEG (**2**) between 5.5 and 6.5 minutes was collected, dried in a freeze-drier and analyzed by MALDI-ToF-MS. For PEG > 2000  $\text{g mol}^{-1}$ , a linear gradient from 40% ACN to 50% ACN for 7.5 min, then a linear gradient to 100% ACN over 1.5 min, and then isocratic at 100% ACN for 3 min was used. Subsequently the starting gradient was restored in one minute and a 8 min reconditioning time of 40% ACN : 60% water was allowed before further sample injection.



#### Synthesis of $\alpha$ -azide- $\omega$ -hydroxyl-PEG (4)

The synthesis of  $\alpha$ -azide- $\omega$ -hydroxyl-PEG was developed based on Mahou *et al.*<sup>[47]</sup> Exemplarily, the synthesis of  $\alpha$ -azide- $\omega$ -hydroxyl-PEG-1500 is described below.  $\alpha$ -tosyl- $\omega$ -hydroxyl-PEG ((2), 500 mg,  $M = 1670 \text{ g mol}^{-1}$ ,  $n = 0.299 \text{ mmol}$ ) and sodium azide (97 mg, 5 eq.,  $n = 1.5 \text{ mmol}$ ) were dissolved in dry dimethylformamide (DMF, 10 mL) and stirred overnight at 90 °C und argon atmosphere. After cooling to room temperature, DMF was removed under reduced pressure. The crude product was dissolved in dichloromethane (DCM, 5 mL) and extracted twice with brine (5 mL) each and twice with deionized water (5 mL) each. The organic phase was dried with magnesium sulfate. After removal of DCM the crude product was precipitated twice from DCM into ice-cold diethyl ether. The pure product was dried under high vacuum for 24 hours. The pure product was recovered as colorless powder (266 mg, yield = 58%,  $M = 1541 \text{ g mol}^{-1}$ ).  $^1\text{H NMR}$  (400 MHz, DMSO)  $\delta$  [ppm] = 4.58 (t, 1H, -OH), 3.46-3.56 (m, 132H,  $(\text{CH}_2\text{-CH}_2\text{-O})_n$ ), 3.41 (m, 4H,  $-(\text{CH}_2)_2\text{-N}_3$ ), see Figure S17.

#### Synthesis of $\alpha$ -azido- $\omega$ -methacryloyl-PEG (5)

Exemplarily, the synthesis of  $\alpha$ -azide- $\omega$ -methacrylate-PEG-1500 is described below.  $\alpha$ -tosyl- $\omega$ -azide PEG ((4), 266 mg,  $M = 1541 \text{ g mol}^{-1}$ ,  $n = 0.173 \text{ mmol}$ ) was dissolved in toluene (2 mL). *Candida antarctica* lipase B (CALB, 58 mg) beads and vinyl methacrylate (104  $\mu\text{L}$ , 5 eq.,  $n = 0.865 \text{ mmol}$ ,  $m = 97.0 \text{ mg}$ ) were added and the reaction were allowed to proceed for 48 h at 50 °C. After filtration through a filtration paper the solvent was removed by rotary evaporation. The crude product was purified by twofold precipitation from methanol into ice-cold diethyl ether. Hydroquinone (approx. 2 mg) was added for storage. The pure product was dried under high vacuum for 24 hours. The pure product was recovered as colorless powder (202 mg, yield = 73%,  $M = 1609 \text{ g mol}^{-1}$ ).  $^1\text{H NMR}$  (400 MHz, DMSO)  $\delta$  [ppm] = 6.03 (m, 1H,  $\text{CH}_2\text{-C-CH}_3$ ), 5.69 (m, 1H,  $\text{CH}_2\text{-C-CH}_3$ ), 4.20 (m, 2H,  $\text{CH}_2\text{-O-CO}$ ), 3.65 (m, 2H,  $\text{CH}_2\text{-CH}_2\text{-O-CO}$ ), 3.43-3.56 (m, 119H,  $(\text{CH}_2\text{-CH}_2\text{-O})_n$ ), 3,39 (m, 2H,  $\text{CH}_2\text{-N}_3$ ), 1.88 (s, 3H,  $-\text{CH}_3$ ), see Figure S20.

**Synthesis of  $\alpha$ -4-phenyl-1,2,3,4-triazol-1-yl- $\omega$ -methacryloyl-PEG (6)**

Exemplarily, the synthesis of  $\alpha$ -4-phenyl-1,2,3,4-triazol-1-yl- $\omega$ -methacryloyl-PEG-1500 is described below.  $\alpha$ -azido- $\omega$ -methacryloyl-PEG ((5), 150 mg,  $M = 1609 \text{ g mol}^{-1}$ ,  $n = 0.0932 \text{ mmol}$ ), phenylacetylene (15  $\mu\text{L}$ , 1.5 eq.,  $n = 0.14 \text{ mmol}$ ,  $m = 14 \text{ mg}$ ),  $N,N,N',N'',N'''$ -pentamethyldiethylenetriamine (PMDETA, 5.9  $\mu\text{L}$ , 0.3 eq.,  $n = 0.028 \text{ mmol}$ ,  $m = 4.9 \text{ mg}$ ), and methanol (2 mL) were mixed in a Schlenk flask. Three cycles of freeze pump-thaw were performed for degassing the solvent. Addition of CuBr (4 mg, 0.3 eq.,  $n = 0.03 \text{ mmol}$ ) under argon counterflow. Stirring at room temperature overnight, protected from light by tin foil. Addition of three tips of a spatula acidic ion exchange resin Lewatit Mono Plus, stirring for approx. 1 h until discoloration of the solution. The solution was filtered through a filtration paper followed by solvent removal by rotary evaporation. The crude product was purified by twofold precipitation from methanol into ice-cold diethyl ether. The pure product was dried under high vacuum for 24 hours. The pure product was recovered as colorless powder (139 mg, yield = 87%,  $M = 1711 \text{ g mol}^{-1}$ ).  $^1\text{H NMR}$  (400 MHz, DMSO)  $\delta$  [ppm] = 8.53 (s, 1H, CH-N), 7.84 (m, 2H,  $C_{\text{arom}}H(\text{ortho})$ ), 7.44 (m, 2H,  $C_{\text{arom}}H(\text{meta})$ ), 7.34 (m, 2H,  $C_{\text{arom}}H(\text{para})$ ), 6.03 (m, 1H,  $\text{CH}_2\text{-C-CH}_3$ ), 5.69 (m, 1H,  $\text{CH}_2\text{-C-CH}_3$ ), 4.57 (m, 2H,  $\text{CH}_2\text{-N}$ ), 4.20 (m, 2H,  $\text{CH}_2\text{-O-CO}$ ), 3.87 (m, 2H,  $\text{CH}_2\text{-CH}_2\text{-N}$ ), 3.65 (m, 2H,  $\text{CH}_2\text{-CH}_2\text{-O-CO}$ ), 3.43-3.56 (m, 158H,  $(\text{CH}_2\text{-CH}_2\text{-O})_n$ ), 1.88 (s, 3H,  $-\text{CH}_3$ ), see Figure S23.

**Synthesis of 1,2,3,4,6-Penta-O-acetyl- $\alpha,\beta$ -D-mannopyranose (7)**

The synthesis of peracetylated mannose was modified from Kartha *et al.*<sup>[55]</sup> Iodine (560 mg, 2.2 mmol, 0.04 eq.) and acetic anhydride (50 mL) were mixed under Ar atmosphere. D-Mannose (10.0 g, 55.5 mmol, 1 eq.) was added portion by portion at 0 °C. After stirring for 30 min at 0 °C and additionally for 18 hours at room temperature TLC (cyclohexane/toluene/ethylacetate 3:3:1) showed complete consumption of the starting material. The reaction mixture was diluted with dichloromethane (50 mL) and was washed twice with cold saturated aqueous  $\text{Na}_2\text{SO}_3$  solution (2  $\times$  80 mL), then with a saturated aqueous solution of  $\text{NaHCO}_3$  (4  $\times$  50 mL). The separated organic layer was dried over anhydrous  $\text{MgSO}_4$ . The solvent was removed in vacuo to afford the desired peracetylated D-mannose (21.5 g, 55.1 mmol, 99%, mixture of both anomers  $\alpha/\beta$  1: 4.75) as a yellowish high viscous oil.

Rf = 0.30 (silica gel, cyclohexane/toluene/ethyl acetate, 3:3:1);

Signals assignable to  $\beta$ -anomer:  $^1\text{H}$  NMR, COSY (400 MHz,  $\text{CDCl}_3$ )  $\delta$  (ppm) = 6.09 (d,  $^3J = 1.9$  Hz, 1H, H 1), 5.34–5.36 (m, 2H, H 3, H 4), 5.25–5.27 (m, 1H, H-2), 4.28 (dd,  $^2J = 12.4$  Hz,  $^3J = 4.9$  Hz, 1H, H 6a), 4.10 (dd,  $^2J = 12.4$  Hz,  $^3J = 2.5$  Hz, 1H, H 6b), 4.03–4.07 (m, 1H, H 5), 2.18, 2.17, 2.10, 2.05, 2.01 (5  $\times$  s, 15H,  $\text{COCH}_3$ );  $^{13}\text{C}$  NMR, HSQC, HMBC (100.6 MHz,  $\text{CDCl}_3$ )  $\delta$  (ppm) = 170.8, 170.2, 169.9, 169.7, 168.2 (5  $\times$   $\text{COCH}_3$ ), 90.7 (C-1), 70.7 (C-5), 68.8 (C-3), 68.4 (C-2), 65.6 (C-4), 62.2 (C-6), 21.0, 20.9, 20.9, 20.8, 20.8 (5  $\times$   $\text{COCH}_3$ ).

The spectral data are in accordance with literature.<sup>[56]</sup>

### Synthesis of Propargyl 2,3,4,6-Tetra-*O*-acetyl- $\alpha$ -D-mannopyranoside (8)

The synthesis of propargyl 2,3,4,6-tetra-*O*-acetyl- $\alpha$ -D-mannopyranoside was modified from Daly *et al.*<sup>[57]</sup> 1,2,3,4,6-Penta-*O*-acetyl- $\alpha,\beta$ -D-mannopyranose (**7**, 10.0 g, 25.6 mmol, 1 eq.) and propargyl alcohol (7.18 g, 7.48 mL, 128 mmol, 5 eq.) was dissolved in dichloromethane (100 mL). After stirring for 20 minutes at room temperature, the reaction mixture was cooled to 0 °C and  $\text{BF}_3 \cdot \text{OEt}_2$  (16.22 mL, 128 mmol, 5 eq.) was added dropwise. The mixture was stirred for 15 min at this temperature, then at room temperature for 24 h. The solution was treated with saturated  $\text{NaHCO}_3$  solution (25 mL). Subsequently the aqueous layer was extracted with dichloromethane (2  $\times$  50 mL), and the combined organic layers were dried over anhydrous  $\text{MgSO}_4$ . The solvent was removed in vacuo and the residue was purified by flash column chromatography (cyclohexane/ethyl acetate, 1:1) to give the title compound (7.23 g, 18.7 mmol, 73%) as a colorless viscous oil.

R<sub>f</sub> = 0.43 (silica gel, cyclohexane/ethyl acetate, 1:1);

$^1\text{H}$  NMR, COSY (400 MHz,  $\text{CDCl}_3$ )  $\delta$  (ppm) = 5.36 (m, 3H, H 2, H-3, H 4), 5.02 (d, 1H,  $^3J = 1.7$  Hz, H 1), 4.31–4.25 (m, 3H, H-6a,  $\text{CH}_2\text{-C}\equiv\text{C}$ ), 4.10 (dd,  $^2J = 12.2$  Hz,  $^3J = 2.5$  Hz, 1H, H 6b), 4.01 (ddd,  $^3J = 9.3$  Hz,  $^3J = 5.2$  Hz,  $^3J = 2.5$  Hz, 1H, H 5), 2.47 (t,  $^4J = 2.4$  Hz, 1H, CH), 2.15, 2.09, 2.03, 1.98 (4  $\times$  s, 12H,  $\text{COCH}_3$ );  $^{13}\text{C}$  NMR, HSQC, HMBC (100.6 MHz,  $\text{CDCl}_3$ )  $\delta$  (ppm) = 170.8, 170.1, 170.0, 169.8 (4  $\times$   $\text{COCH}_3$ ), 96.4 (C-1), 86.0 (C $\equiv$ CH), 75.7 (C $\equiv$ CH), 69.5 (C-2), 69.1 (C-5), 69.1 (C-3), 66.1 (C-4), 62.4 (C-6), 55.1 (CH<sub>2</sub>), 21.0, 20.9, 20.8, 20.8 (4  $\times$   $\text{COCH}_3$ ),

IR (ATR)  $\lambda_{\text{max}}/\text{cm}^{-1}$  1756, 1738, 1431, 1256, 1232, 1186, 1056, 1013, 979, 795, 691;

$[\alpha]_D^{22} + 53.4^\circ$  (c = 1.00,  $\text{CHCl}_3$ );

HRMS (ESI): calculated for  $[\text{C}_{17}\text{H}_{22}\text{O}_{10} + \text{Na}]^+$ : 409.1111, found: 409.1116.

**Synthesis of Propargyl - $\alpha$ -D-mannopyranoside (9)**

The synthesis of propargyl- $\alpha$ -D-mannopyranoside was modified from Daly *et al.*<sup>[57]</sup> Propargyl 2,3,4,6-tetra-*O*-acetyl- $\alpha$ -D-mannopyranoside (**8**, 7.00 g, 17.9 mmol) was dissolved in methanol (70 mL) and sodium methoxide was added until pH 9–10 (approx. 60 mg). The reaction mixture was stirred at room temperature for 16 h. Subsequently, the solution was neutralized with Amberlite 120 H<sup>+</sup> resin until pH 7. The mixture was filtered over Celite, which was washed thoroughly with methanol. The solvent was removed in vacuo to afford the desired 1-propargyl- $\alpha$ -D-mannopyranoside (3.83 g, 17.6 mmol, 98%) as a highly viscous syrup which solidified soon to an amorphous solid.

R<sub>f</sub> = 0.85 (RP-silica gel, acetonitrile/water, 1:9);

<sup>1</sup>H NMR, COSY (400 MHz, CD<sub>3</sub>OD)  $\delta$  (ppm) = 4.96 (d, <sup>3</sup>J = 1.7 Hz, 1H, H 1), 4.27 (d, 1H, <sup>4</sup>J = 2.4 Hz, CH<sub>2</sub>), 3.84 (dd, <sup>2</sup>J = 11.8 Hz, <sup>3</sup>J = 2.3 Hz, 1H, H 6a), 3.79 (dd, 1H, <sup>3</sup>J = 3.1 Hz, <sup>3</sup>J = 1.7 Hz, H 2), 3.74–3.58 (m, 3H, H 3, H-4, H-6b), 3.54–3.47 (m, 1H, H-5), 2.86 (t, 4J = 2.4 Hz, CH); <sup>13</sup>C NMR, HSQC, HMBC (100.6 MHz, CD<sub>3</sub>OD)  $\delta$  (ppm) = 99.8 (C 1), 80.0 (C $\equiv$ CH), 76.0 (C $\equiv$ CH), 75.1 (C 5), 72.5 (C 3), 72.0 (C 2), 68.5 (C-4), 62.8 (C-6), 54.8 (CH<sub>2</sub>-C $\equiv$ CH),

IR (ATR)  $\lambda_{\text{max}}$ /cm<sup>-1</sup> 3403, 3276, 2934, 2909, 1586, 1343, 1252, 1134, 1061, 963, 916, 814, 663;

$[\alpha]_D^{22} + 116.7^\circ$  (c = 1.00, MeOH);

HRMS (ESI): calculated for [C<sub>9</sub>H<sub>14</sub>O<sub>6</sub> + Na]<sup>+</sup>: 241.0688, found: 214.0692.

**Synthesis of  $\alpha$ -4-( $\alpha$ -D-mannopyranosyloxymethylene)-1,2,3, triazol-1-yl- $\omega$ -methacryloyl-PEG (10)**

Exemplarily, the synthesis of  $\alpha$ -4-( $\alpha$ -D-mannopyranosyloxymethylene)-1,2,3, triazol-1-yl- $\omega$ -methacryloyl-PEG-2000 is described below.  $\alpha$ -azido- $\omega$ -methacryloyl-PEG (**6**), 96 mg, M = 2106 g mol<sup>-1</sup>, n = 0.046 mmol), mannose alkyne (**9**), 12.5 mg, 1.24 eq., n = 0.057 mmol), PMDETA (2.9  $\mu$ L, 0.3 eq., n = 0.014 mmol, m = 2.4 mg), and methanol (1 mL) were mixed in a Schlenk flask. Three cycles of freeze pump-thaw were performed for degassing the solvent. Addition of CuBr (2 mg, 0.3 eq., n = 0.01 mmol) under argon counterflow. Stirring at room temperature overnight, protected from light by tin foil. Addition of two tips of a spatula acidic ion exchange resin Lewatit Mono Plus, stirring for approx. 1 h until discoloration of the solution. The solution was filtered through a filtration paper followed by solvent removal by rotary evaporation. The crude product

was purified by twofold precipitation from methanol into ice-cold diethyl ether. The pure product was dried under high vacuum for 24 hours and thereafter recovered as colorless powder (103 mg, yield = 96%,  $M = 2324.2 \text{ g mol}^{-1}$ ).  $^1\text{H NMR}$  (400 MHz, MeOH)  $\delta$  [ppm] = 8.11 (s, 1H, CH-N), 6.14 (m, 1H, CH<sub>2</sub>-C-CH<sub>3</sub>), 5.66 (m, 1H, CH<sub>2</sub>-C-CH<sub>3</sub>), 4.61 (m, 2H, CH<sub>2</sub>-Mannose), 4.31 (m, 2H, CH<sub>2</sub>-O-CO), 3.93 (m, 2H, CH<sub>2</sub>-N), 3.53-3.86 (m, 261H, (CH<sub>2</sub>-CH<sub>2</sub>-O)<sub>n</sub>), 1.96 (s, 3H, -CH<sub>3</sub>), see Figure S34.

### Conclusions and Outlook

Heterobifunctional PEGs are highly valuable reaction products as they are widely used for bioconjugation (“PEGylation”) of e.g. proteins, nanoparticles, hydrogels, nanogels and liposomes. The preparation of heterobifunctional PEGs from symmetrical PEG diols is desirable, but the polymer desymmetrization step is challenging due to low yields and demanding separation of the reaction products, especially for PEG exceeding  $1000 \text{ g mol}^{-1}$ . Monotosylation of PEG via an Ag<sub>2</sub>O/KI catalyzed strategy was compared to the non-catalyzed tosylation reaction with respect to enhancing the amount of monotosylated reaction product. The addition of silver oxide and potassium iodide resulted in higher yields of monofunctionalized PEG (71 - 76%,  $M_n 2000 \text{ g mol}^{-1}$ ) compared to the uncatalyzed, statistical tosylation reaction (below 56%) with one equivalent of tosyl chloride. The yield for monotosylated product decreased under the same reaction conditions with increasing molecular weight of the polymer due to inferior accessibility of the chain ends of the coiled polymer chains (11.4% for Ag<sub>2</sub>O-catalyzed compared to 9.4% uncatalyzed). For this reason, reaction time and silver(I)oxide equivalents were adjusted to yield 42.0% of monotosylated PEG-8000 compared to 12.6% for the uncatalyzed reaction under comparable reaction conditions.

An analytical HPLC method was developed to analyze the crude reaction mixture. Monotosylated PEG was separated from the crude product by an adapted semi-preparative HPLC method with baseline resolution. As an example of the further use of the monotosylated PEG-synthon, using a three step route, the  $\alpha$ -tosyl- $\omega$ -hydroxyl-PEG could be converted into the complex, heterobifunctional  $\alpha$ -4-( $\alpha$ -D-mannopyranosyloxymethylene)-1,2,3, triazol-1-yl- $\omega$ -methacryloyl-PEG, which can be applied for functionalization of hydrogels and nanogels. To the best of our knowledge, this is the first report on the combination of a PEG spacer, mannose and methacrylate to obtain  $\alpha$ -4-( $\alpha$ -D-mannopyranosyl-oxymethylene)-1,2,3, triazol-1-yl- $\omega$ -methacryloyl-PEG. Since click reactions are highly selective even in the presence of numerous other functional groups, this synthesis strategy is suitable for broad application in the field of hydrogel and nanogel

functionalization. In brief, the desymmetrization strategy for PEG has been proven to represent a versatile method to provide pure  $\alpha$ -tosyl- $\omega$ -hydroxyl-PEG in a molecular weight range of 1500 to 8000 g mol<sup>-1</sup>. This compound is a key intermediate for heterobifunctional PEGs, rendering this approach highly valuable for a broad range of new PEGylation reagents.

### Acknowledgements

The authors gratefully acknowledge the support of this research by Tobias Bauer, Jan Blankenburg, Steffen Hildebrand, Monika Schmelzer, Patrick Verkoyen, and Matthias Worm. The authors thank Mirko Montigny and Romina Schröder for TEM measurements. This work was supported by the Max Planck Graduate Center with the Johannes Gutenberg University Mainz (MPGC) as well as by funding of the Excellence Initiative (DFG/GSC 266) in the context of the graduate school of excellence "MAINZ" (Materials Science in Mainz).

### Abbreviations

ACN, acetonitrile; CALB, *Candida antarctica* lipase B; CD11c, cluster of differentiation 11c; CuAAC, copper(I)-catalyzed alkyne-azide cycloaddition; DCM, dichloromethane; DMF, dimethylformamide; DMSO, dimethylsulfoxide; ELSD, evaporative light-scattering detector; EO, ethylene oxide; FTIR, Fourier transform infrared spectroscopy; HPLC, High-performance liquid chromatography; MALDI-ToF-MS, matrix assisted laser desorption ionization - time of flight mass spectrometry; NMR, nuclear magnetic resonance spectroscopy; OEG, oligo(ethylene glycol); PEG, poly(ethylene glycol); PMDETA, *N,N,N',N'',N'''*-Pentamethyldiethylentriamine; RI, refractive index; SEC, size exclusion chromatography; TFA, trifluoroacetic acid; THF, tetrahydrofuran; TsCl, tosyl chloride; UV, ultraviolet.

### Literature

- [1] Knop, K.; Hoogenboom, R.; Fischer, D.; Schubert, U. S., Poly(ethylene glycol) in drug delivery: pros and cons as well as potential alternatives, *Angew. Chem. Int. Ed. Engl.*, **2010**, 49, 6288–6308.
- [2] Lin, C.-C.; Anseth, K. S., PEG hydrogels for the controlled release of biomolecules in regenerative medicine, *Pharm. Res.*, **2009**, 26, 631–643.
- [3] Perez-Herrero, E.; Fernandez-Medarde, A., Advanced targeted therapies in cancer: Drug nanocarriers, the future of chemotherapy, *Eur. J. Pharm. Biopharm.*, **2015**, 93, 52–79.
- [4] Biju, V., Chemical modifications and bioconjugate reactions of nanomaterials for sensing, imaging, drug delivery and therapy, *Chem. Soc. Rev.*, **2014**, 43, 744–764.

- [5] Herzberger, J.; Niederer, K.; Pohlit, H.; Seiwert, J.; Worm, M.; Wurm, F. R.; Frey, H., Polymerization of Ethylene Oxide, Propylene Oxide, and Other Alkylene Oxides: Synthesis, Novel Polymer Architectures, and Bioconjugation, *Chem. Rev.*, **2016**, 116, 2170–2243.
- [6] Akiyama, Y.; Otsuka, H.; Nagasaki, Y.; Kato, M.; Kataoka, K., Selective Synthesis of Heterobifunctional Poly(ethylene glycol) Derivatives Containing Both Mercapto and Acetal Terminals, *Bioconjug. Chem.*, **2000**, 11, 947–950.
- [7] Cammas, S.; Nagasaki, Y.; Kataoka, K., Heterobifunctional Poly(ethylene oxide), *Bioconjug. Chem.*, **1995**, 6, 226–230.
- [8] Hayashi, H.; Iijima, M.; Kataoka, K.; Nagasaki, Y., pH-Sensitive Nanogel Possessing Reactive PEG Tethered Chains on the Surface, *Macromolecules*, **2004**, 37, 5389–5396.
- [9] Nagasaki, Y.; Kutsuna, T.; Iijima, M.; Kato, M.; Kataoka, K.; Kitano, S.; Kadoma, Y., Formyl-Ended Heterobifunctional Poly(ethylene oxide), *Bioconjug. Chem.*, **1995**, 6, 231–233.
- [10] Nakamura, T.; Nagasaki, Y.; Kataoka, K., Synthesis of heterobifunctional poly(ethylene glycol) with a reducing monosaccharide residue at one end, *Bioconjug. Chem.*, **1998**, 9, 300–303.
- [11] Yagci, Y.; Ito, K., Macromolecular Architecture Based on Anionically Prepared Poly(ethylene oxide) Macromonomers, *Macromol. Symp.*, **2005**, 226, 87–96.
- [12] Yokoyama, M.; Okano, T.; Sakurai, Y.; Kikuchi, A.; Ohsako, N.; Nagasaki, Y.; Kataoka, K., Synthesis of poly(ethylene oxide) with heterobifunctional reactive groups at its terminals by an anionic initiator, *Bioconjug. Chem.*, **1992**, 3, 275–276.
- [13] Zhang, S.; Du, J.; Sun, R.; Li, X.; Yang, D.; Zhang, S.; Xiong, C.; Peng, Y., Synthesis of heterobifunctional poly(ethylene glycol) with a primary amino group at one end and a carboxylate group at the other end, *React. Funct. Polym.*, **2003**, 56, 17–25.
- [14] Nagasaki, Y.; Ogawa, R.; Yamamoto, S.; Kato, M.; Kataoka, K., Synthesis of Heterotelechelic Poly(ethylene glycol) Macromonomers. Preparation of Poly(ethylene glycol) Possessing a Methacryloyl Group at One End and a Formyl Group at the Other End, *Macromolecules*, **1997**, 30, 6489–6493.
- [15] Wagener, K. B.; Thompson, C.; Wanigatunga, S., Chain propagation/step propagation polymerization. 4. A DSC study of phase separation in regular poly(oxyethylene)-block-poly(pivalolactone) telechelomers, *Macromolecules*, **1988**, 21, 2668–2672.
- [16] Wang, Y.; Chen, S.; Huang, J., Synthesis and Characterization of a Novel Macroinitiator of Poly(ethylene oxide) with a 4-Hydroxy-2,2,6,6-tetramethylpiperidinyloxy End Group, *Macromolecules*, **1999**, 32, 2480–2483.
- [17] Hua, F.; Yang, Y., Synthesis of block copolymer by “living” radical polymerization of styrene with nitroxyl-functionalized poly(ethylene oxide), *Polymer*, **2001**, 42, 1361–1368.
- [18] Cianga, I.; Senyo, T.; Ito, K.; Yagci, Y., Electron Transfer Reactions of Radical Anions with TEMPO, *Macromol. Rapid Commun.*, **2004**, 25, 1697–1702.
- [19] Zhang, J.; Su, Z.-G.; Ma, G.-H., Synthesis and characterization of heterotelechelic poly(ethylene glycol)s with amino acid at one end and hydroxyl group at another end, *J. Appl. Polym. Sci.*, **2008**, 110, 2432–2439.

- [20] Akiyama, Y.; Nagasaki, Y.; Kataoka, K., Synthesis of heterotelechelic poly(ethylene glycol) derivatives having alpha-benzaldehyde and omega-pyridyl disulfide groups by ring opening polymerization of ethylene oxide using 4-(diethoxymethyl)benzyl alkoxide as a novel initiator, *Bioconjug. Chem.*, **2004**, 15, 424–427.
- [21] Yang, S.; Kim, Y.; Kim, H. C.; Siddique, A. B.; Youn, G.; Kim, H. J.; Park, H. J.; Lee, J. Y.; Kim, S.; Kim, J., Azide-based heterobifunctional poly(ethylene oxide)s, *Polym. Chem.*, **2016**, 7, 394–401.
- [22] Hiki, S.; Kataoka, K., A Facile Synthesis of Azido-Terminated Heterobifunctional Poly(ethylene glycol)s for “Click” Conjugation, *Bioconjug. Chem.*, **2007**, 18, 2191–2196.
- [23] Li, Z.; Chau, Y., Synthesis of X(Y)-(EO)(n)-OCH(3) type heterobifunctional and X(Y)-(EO)(n)-Z type heterotrifunctional poly(ethylene glycol)s, *Bioconjug. Chem.*, **2011**, 22, 518–522.
- [24] Székely, G.; Schaepertoens, M.; Gaffney, P. R. J.; Livingston, A. G., Beyond PEG2000: Synthesis and Functionalisation of Monodisperse PEGylated Homostars and Clickable Bivalent Polyethyleneglycols, *Chem. Eur. J.*, **2014**, 20, 10038–10051.
- [25] Wawro, A. M.; Muraoka, T.; Kinbara, K., Chromatography-free synthesis of monodisperse oligo(ethylene glycol) mono-p-toluenesulfonates and quantitative analysis of oligomer purity, *Polym. Chem.*, **2016**, 7, 2389–2394.
- [26] Li, J.; Kao, W. J., Synthesis of polyethylene glycol (PEG) derivatives and PEGylated-peptide biopolymer conjugates, *Biomacromolecules*, **2003**, 4, 1055–1067.
- [27] Li, J.; Crasto, C. F.; Weinberg, J. S.; Amiji, M.; Shenoy, D.; Sridhar, S.; Buble, G. J.; Jones, G. B., An approach to heterobifunctional poly(ethyleneglycol) bioconjugates, *Bioorg. Med. Chem. Lett.*, **2005**, 15, 5558–5561.
- [28] Völcker, N. H.; Klee, D.; Hanna, M.; Höcker, H.; Bou, J. J.; Ilarduya, A. M. de; Muñoz-Guerra, S., Synthesis of heterotelechelic poly(ethylene glycol)s and their characterization by MALDI-TOF-MS, *Macromol. Chem. Phys.*, **1999**, 200, 1363–1373.
- [29] Huang, J., Syntheses of polyethylene glycol (PEG) with different functional groups at each end. I. Preparation of monotrityl PEG using polyvinyl alcohol (PVA) matrix, *J. Appl. Polym. Sci.*, **1992**, 46, 1663–1671.
- [30] Furukawa, S.; Katayama, N.; Iizuka, T.; Urabe, I.; Okada, H., Preparation of polyethylene glycol-bound NAD and its application in a model enzyme reactor, *FEBS Lett.*, **1980**, 121, 239–242.
- [31] Dicus, C.; Nantz, M., Synthesis of a Heterobifunctional PEG Spacer Terminated with Aminooxy and Bromide Functionality, *Synlett*, **2006**, 2006, 2821–2823.
- [32] Aronov, O.; Horowitz, A. T.; Gabizon, A.; Gibson, D., Folate-targeted PEG as a potential carrier for carboplatin analogs. Synthesis and in vitro studies, *Bioconjug. Chem.*, **2003**, 14, 563–574.
- [33] Pale-Grosdemange, C.; Simon, E. S.; Prime, K. L.; Whitesides, G. M., Formation of self-assembled monolayers by chemisorption of derivatives of oligo(ethylene glycol) of structure HS(CH<sub>2</sub>)<sub>11</sub>(OCH<sub>2</sub>CH<sub>2</sub>)<sub>m</sub>OH on gold, *J. Am. Chem. Soc.*, **1991**, 113, 12–20.



- [34] Haselgruebler, T.; Amerstorfer, A.; Schindler, H.; Gruber, H. J., Synthesis and Applications of a New Poly(ethylene glycol) Derivative for the Crosslinking of Amines with Thiols, *Bioconjug. Chem.*, **1995**, 6, 242–248.
- [35] Passemard, S.; Staedler, D.; Ucnova, L.; Schneiter, G. S.; Kong, P.; Bonacina, L.; Juillerat-Jeanneret, L.; Gerber-Lemaire, S., Convenient synthesis of heterobifunctional poly(ethylene glycol) suitable for the functionalization of iron oxide nanoparticles for biomedical applications, *Bioorg. Med. Chem. Lett.*, **2013**, 23, 5006–5010.
- [36] Liu, X.-h.; Wang, H.-k.; Herron, J. N.; Prestwich, G. D., Photopatterning of Antibodies on Biosensors, *Bioconjug. Chem.*, **2000**, 11, 755–761.
- [37] Thompson, M. S.; Vadala, T. P.; Vadala, M. L.; Lin, Y.; Riffle, J. S., Synthesis and applications of heterobifunctional poly(ethylene oxide) oligomers, *Polymer*, **2008**, 49, 345–373.
- [38] Bouzide, A.; LeBerre, N.; Sauvé, G., Silver(I) oxide-mediated facile and practical sulfonylation of alcohols, *Tetrahedron Lett.*, **2001**, 42, 8781–8783.
- [39] Bouzide, A.; Sauvé, G., Silver(I) Oxide Mediated Highly Selective Monotosylation of Symmetrical Diols. Application to the Synthesis of Polysubstituted Cyclic Ethers, *Org. Lett.*, **2002**, 4, 2329–2332.
- [40] Yang, Q.; Lei, M.; Yin, Q.-J.; Yang, J.-S., Silver(I) oxide-mediated regioselective 2-monoacylation in 3-O-benzyl- $\alpha$ -L-rhamnopyranosides and application in synthesis of a protected tetrasaccharide fragment of potent cytotoxic saponins gleditsiosides C and D, *Carbohydr. Res.*, **2007**, 342, 1175–1181.
- [41] Wang, H.; She, J.; Zhang, L.-H.; Ye, X.-S., Silver(I) oxide mediated selective monoprotection of diols in pyranosides, *J. Org. Chem.*, **2004**, 69, 5774–5777.
- [42] Takeda, S.; Chino, M.; Kiuchi, M.; Adachi, K., Direct mono-phosphorylation of 1,3-diols. A synthesis of FTY720-phosphate, *Tetrahedron Lett.*, **2005**, 46, 5169–5172.
- [43] Dreaden, E. C.; Mwakwari, S. C.; Sodji, Q. H.; Oyelere, A. K.; El-Sayed, M. A., Tamoxifen-poly(ethylene glycol)-thiol gold nanoparticle conjugates: enhanced potency and selective delivery for breast cancer treatment, *Bioconjug. Chem.*, **2009**, 20, 2247–2253.
- [44] Shenoy, D.; Fu, W.; Li, J.; Crasto, C.; Jones, G.; DiMarzio, C.; Sridhar, S.; Amiji, M., Surface functionalization of gold nanoparticles using hetero-bifunctional poly(ethylene glycol) spacer for intracellular tracking and delivery, *Int. J. Nanomed.*, **2006**, 1, 51–57.
- [45] Bae, J. W.; Lee, E.; Park, K. M.; Park, K. D., Vinyl Sulfone-Terminated PEG–PLLA Diblock Copolymer for Thiol-Reactive Polymeric Micelle, *Macromolecules*, **2009**, 42, 3437–3442.
- [46] Hsu, C.-W.; Olabisi, R. M.; Olmsted-Davis, E. A.; Davis, A. R.; West, J. L., Cathepsin K-sensitive poly(ethylene glycol) hydrogels for degradation in response to bone resorption, *J. Biomed. Mater. Res. A*, **2011**, 98, 53–62.
- [47] Mahou, R.; Wandrey, C., Versatile Route to Synthesize Heterobifunctional Poly(ethylene glycol) of Variable Functionality for Subsequent Pegylation, *Polymers*, **2012**, 4, 561–589.
- [48] Weast, Robert C., CRC handbook of chemistry and physics, A ready-reference book of chemical and physical data. CRC Press, Boca Raton, **1982**, 63rd ed.

- [49] Coen, R. de; Vanparijs, N.; Risseeuw, M. D. P.; Lybaert, L.; Louage, B.; Koker, S. de; Kumar, V.; Grooten, J.; Taylor, L.; Ayres, N.; van Calenbergh, S.; Nuhn, L.; Geest, B. G. de, pH-Degradable Mannosylated Nanogels for Dendritic Cell Targeting, *Biomacromolecules*, **2016**, 17, 2479–2488.
- [50] Kang, B.; Okwieka, P.; Schöttler, S.; Winzen, S.; Langhanki, J.; Mohr, K.; Opatz, T.; Mailänder, V.; Landfester, K.; Wurm, F. R., Carbohydrate-Based Nanocarriers Exhibiting Specific Cell Targeting with Minimum Influence from the Protein Corona, *Angew. Chem. Int. Ed. Engl.*, **2015**, 54, 7436–7440.
- [51] Raviv, L.; Jaron-Mendelson, M.; David, A., Mannosylated Polyion Complexes for In Vivo Gene Delivery into CD11c+ Dendritic Cells, *Mol. Pharmaceutics*, **2014**, 12, 453–462.
- [52] Yin, L.; Chen, Y.; Zhang, Z.; Yin, Q.; Zheng, N.; Cheng, J., Biodegradable Micelles Capable of Mannose-Mediated Targeted Drug Delivery to Cancer Cells, *Macromol. Rapid Commun.*, **2015**, 36, 483–489.
- [53] Anseth, K. S.; Klok, H.-A., Click Chemistry in Biomaterials, Nanomedicine, and Drug Delivery, *Biomacromolecules*, **2016**, 17, 1–3.
- [54] Moses, J. E.; Moorhouse, A. D., The growing applications of click chemistry, *Chem. Soc. Rev.*, **2007**, 36, 1249–1262.
- [55] Kartha, K.; Field, R. A., Iodine, *Tetrahedron*, **1997**, 53, 11753–11766.
- [56] Tomasic, T.; Hajsek, D.; Svajger, U.; Luzar, J.; Obermajer, N.; Petit-Haertlein, I.; Fieschi, F.; Anderluh, M., Monovalent mannose-based DC-SIGN antagonists: targeting the hydrophobic groove of the receptor, *Eur. J. Med. Chem.*, **2014**, 75, 308–326.
- [57] Daly, R.; Vaz, G.; Davies, A. M.; Senge, M. O.; Scanlan, E. M., Synthesis and biological evaluation of a library of glycoporphyrin compounds, *Chem. Eur. J.*, **2012**, 18, 14671–14679.

## Supporting Information

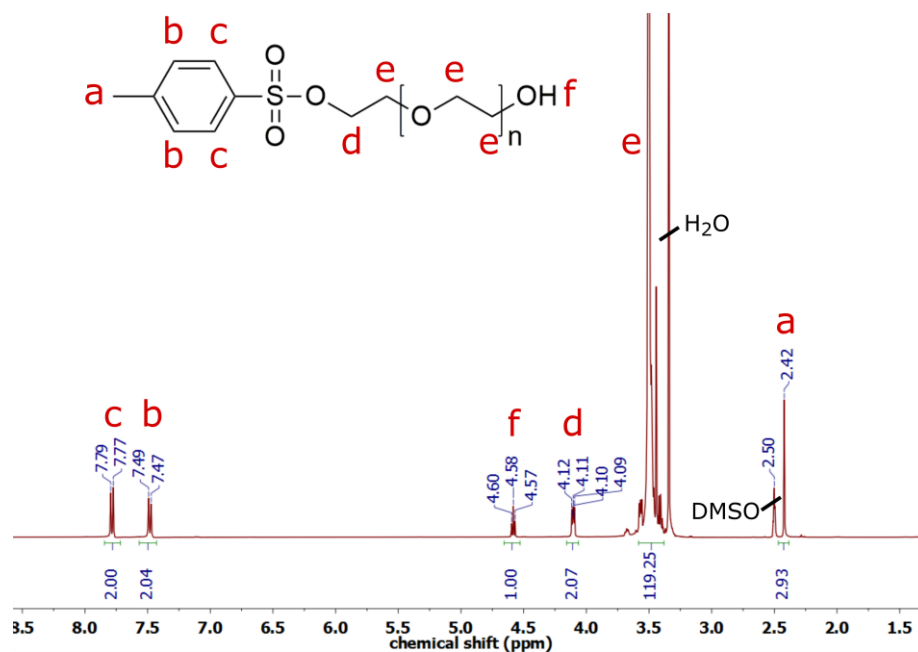
 $\alpha$ -tosyl- $\omega$ -hydroxyl-PEG (1, 2, and 3)

Figure S1.  $^1\text{H-NMR}$  spectrum (400 MHz, DMSO) of  $\alpha$ -tosyl- $\omega$ -hydroxyl-PEG-1500 (C12), before purification by semi-preparative HPLC.

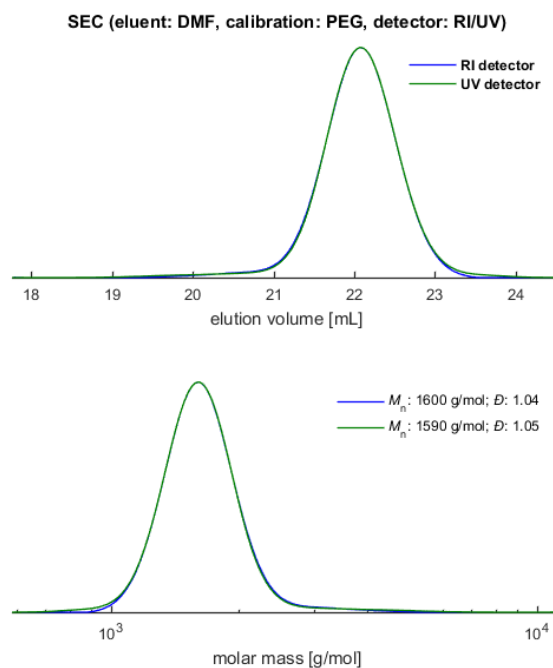


Figure S2. SEC elugram and mass distribution of  $\alpha$ -tosyl- $\omega$ -hydroxyl-PEG-1500 (C12), (eluent: DMF, PEG calibration, RI and UV detector signals), after purification by semi-preparative HPLC.

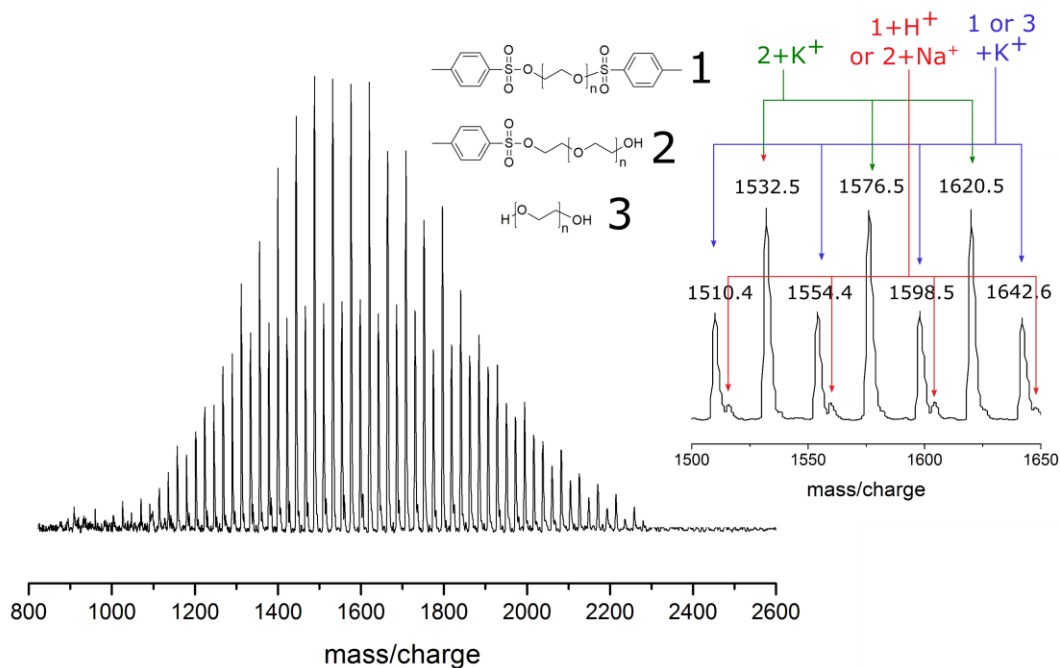


Figure S3. MALDI-ToF-MS of the crude tosylation product mixture of PEG-1500-tosylate (C12) using a dithranol matrix and KTFA as salt.

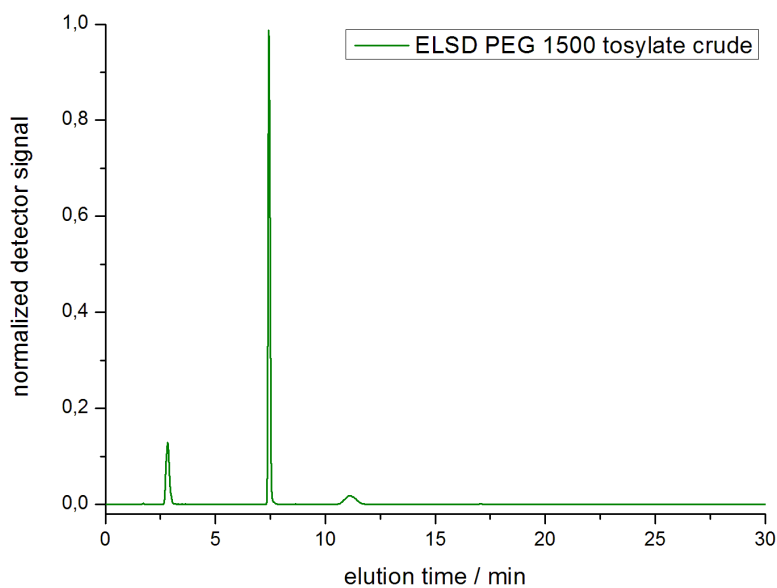


Figure S4. Reverse phase HPLC measurement of the crude tosylation products using a gradient method from 40 – 100% acetonitrile in 30 min. The three products are baseline-separated with elution times of PEG-1500-diol (**1**) at 2.6 min, PEG-1500-monotosylate (**2**) at 7.5 min and PEG-1500-ditosylate (**3**) at 11.5 min (Sample C12).

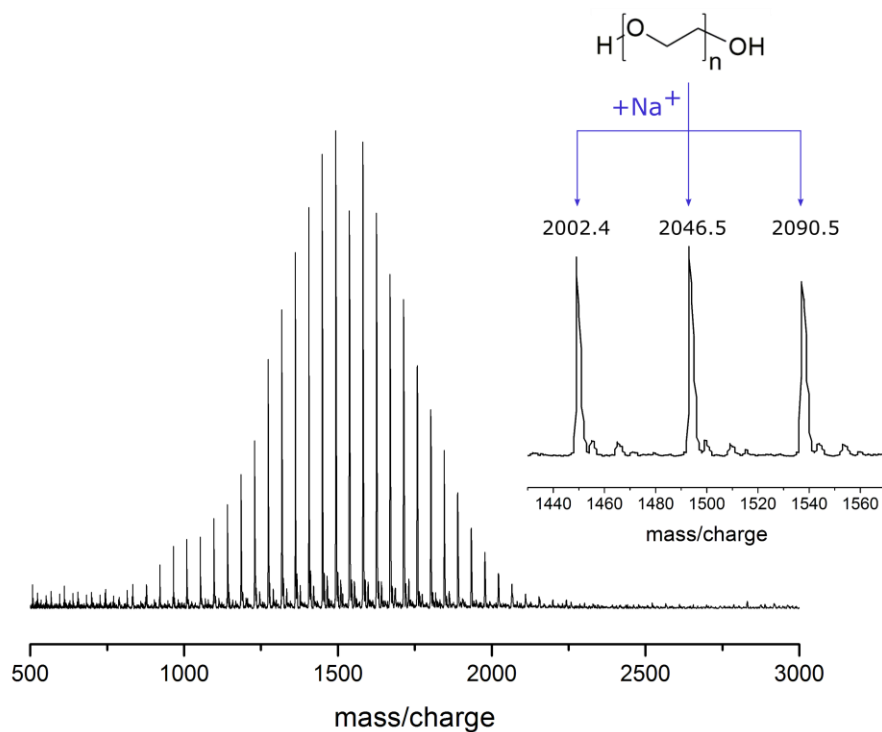


Figure S5. MALDI-ToF-MS of  $\alpha,\omega$ -dihydroxyl-PEG-1500 (C12, **1**) using a dithranol matrix and KTFA as salt, purified with semi-preparative HPLC, product eluted at 2.6 min.

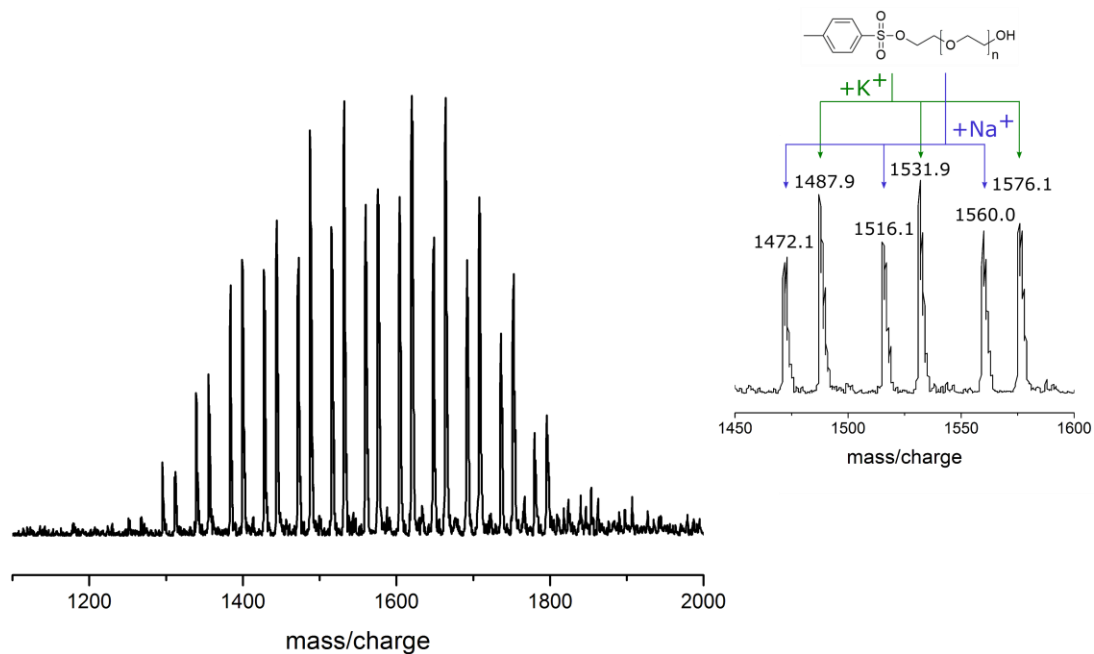


Figure S6. MALDI-ToF-MS of  $\alpha$ -tosyl- $\omega$ -hydroxyl-PEG-1500 (C12, **2**) using a dithranol matrix and KTFA as salt, purified with semi-preparative HPLC, product eluted at 7.5 min.

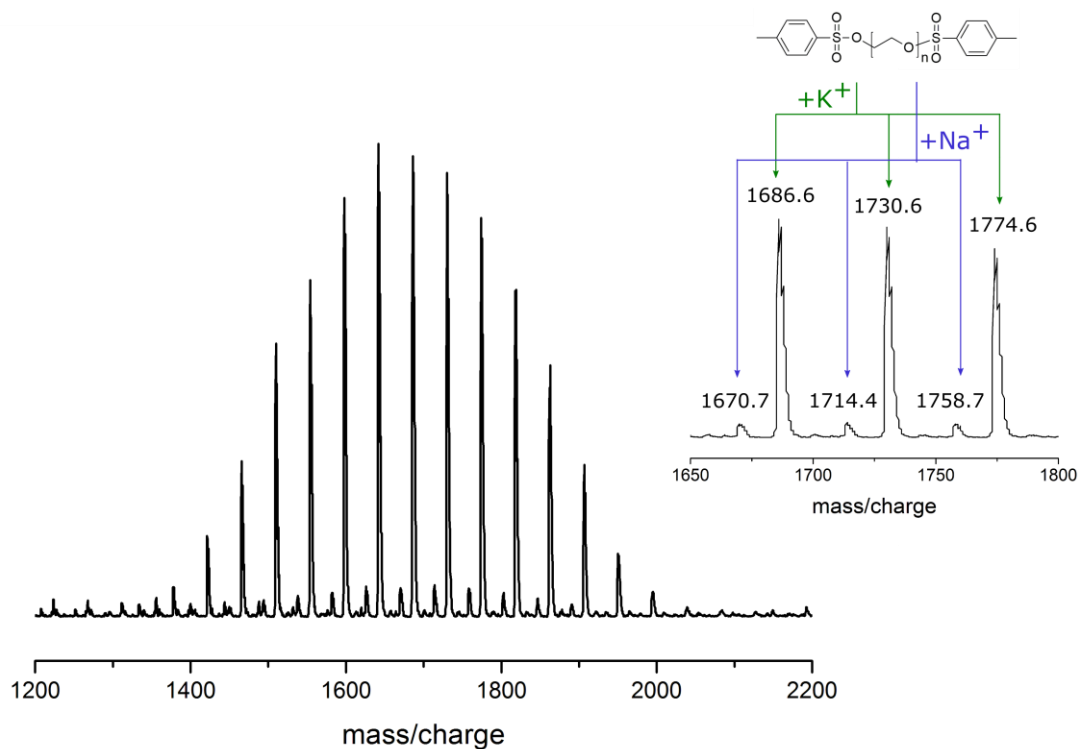


Figure S7. MALDI-ToF-MS of  $\alpha,\omega$ -ditosyl-PEG-1500 (C12, **3**) using a dithranol matrix and KTFA as salt, purified with semi-preparative HPLC, product eluted at 11.5 min.

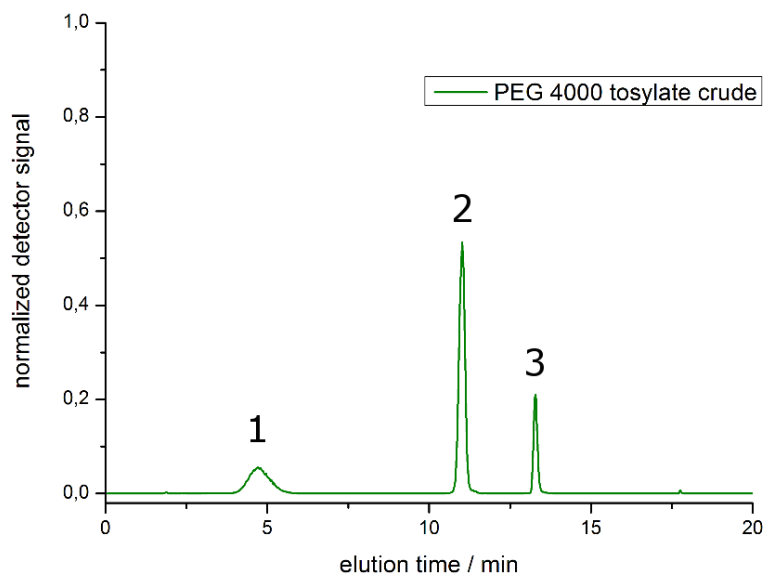


Figure S8. Reverse phase HPLC measurement of the crude tosylation products using a gradient method from 40 – 100% acetonitrile in 30 min. The three products are baseline-separated with elution times of PEG-4000-diol (**1**) at 4.5 min, PEG-4000-monotosylate (**2**) at 10.5 min and PEG-4000-ditosylate (**3**) at 13.0 min (Sample C18).

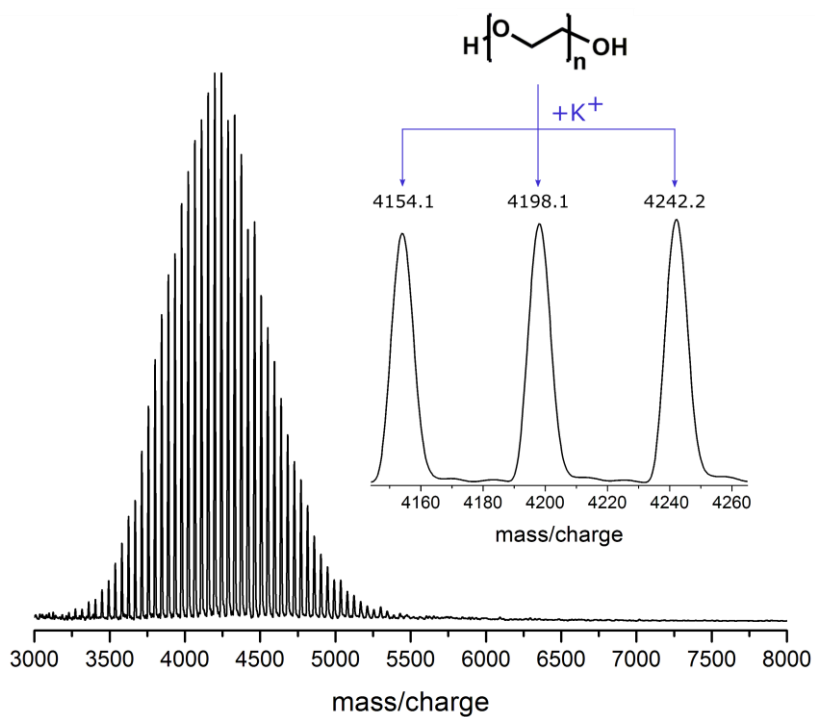


Figure S9. MALDI-ToF-MS of  $\alpha,\omega$ -dihydroxyl-PEG-4000 (**1**, C18) using a dithranol matrix and KTFA as salt, purified with semi-preparative HPLC, product eluted at 4.5 min.

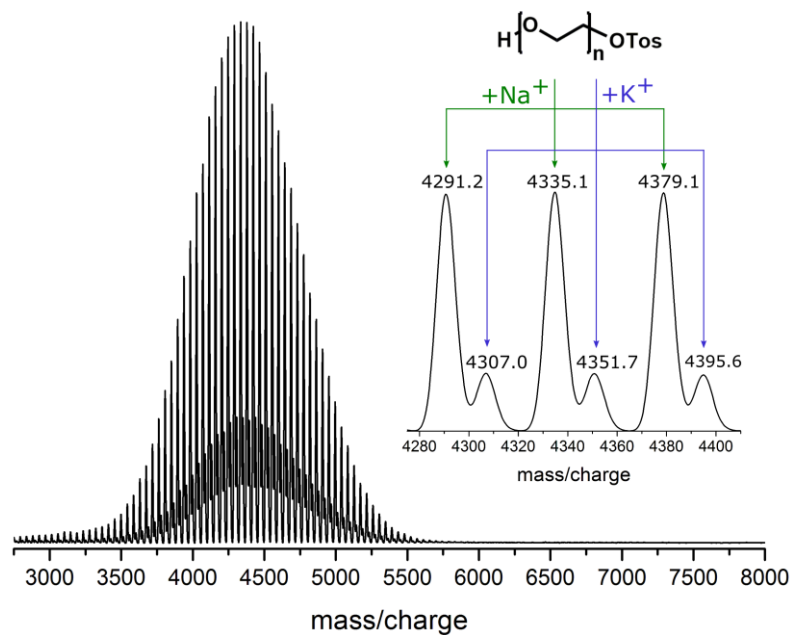


Figure S10. MALDI-ToF-MS of  $\alpha$ -tosyl- $\omega$ -hydroxyl-PEG-4000 (**2**, C18) using a dithranol matrix and KTFA as salt, purified with semi-preparative HPLC, product eluted at 10.5 min.

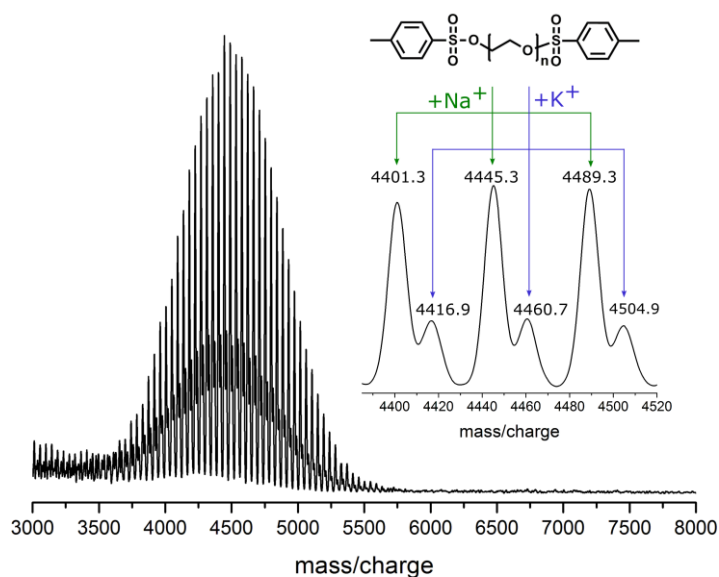


Figure S11. MALDI-ToF-MS of  $\alpha,\omega$ -ditosyl-PEG-4000 (**3**, C18) using a dithranol matrix and KTFA as salt, purified with semi-preparative HPLC, product eluted at 13.0 min.

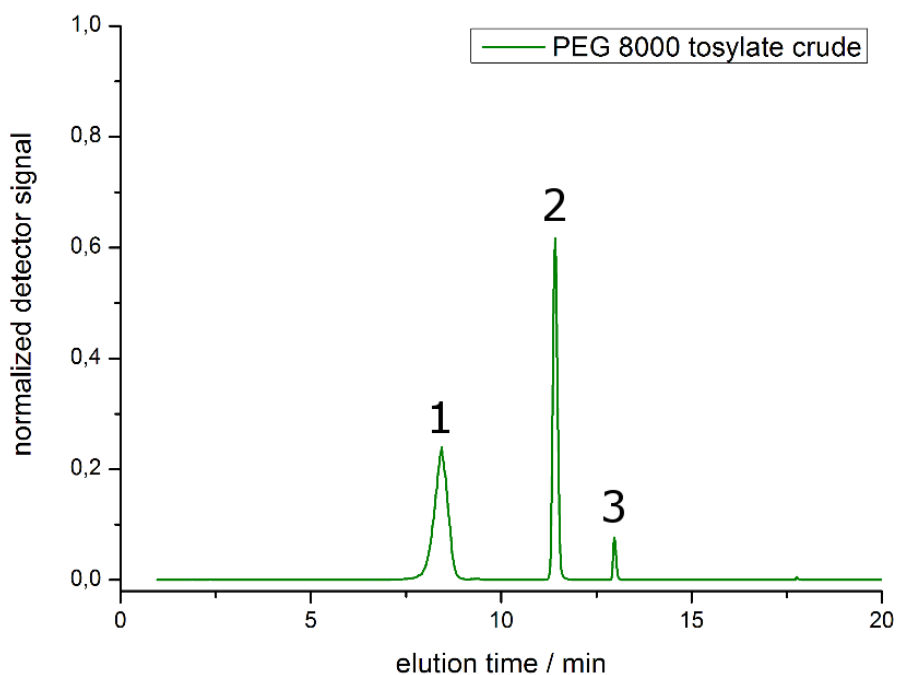


Figure S12. Reverse phase HPLC measurement of the crude tosylation products using a gradient method from 40 – 100% acetonitrile in 30 min. The three products are baseline-separated with elution times of PEG-8000-diol (**1**) at 8.5 min, PEG-8000-monotosylate (**2**) at 11.5 min and PEG-8000-ditosylate (**3**) at 13.0 min (Sample C24).



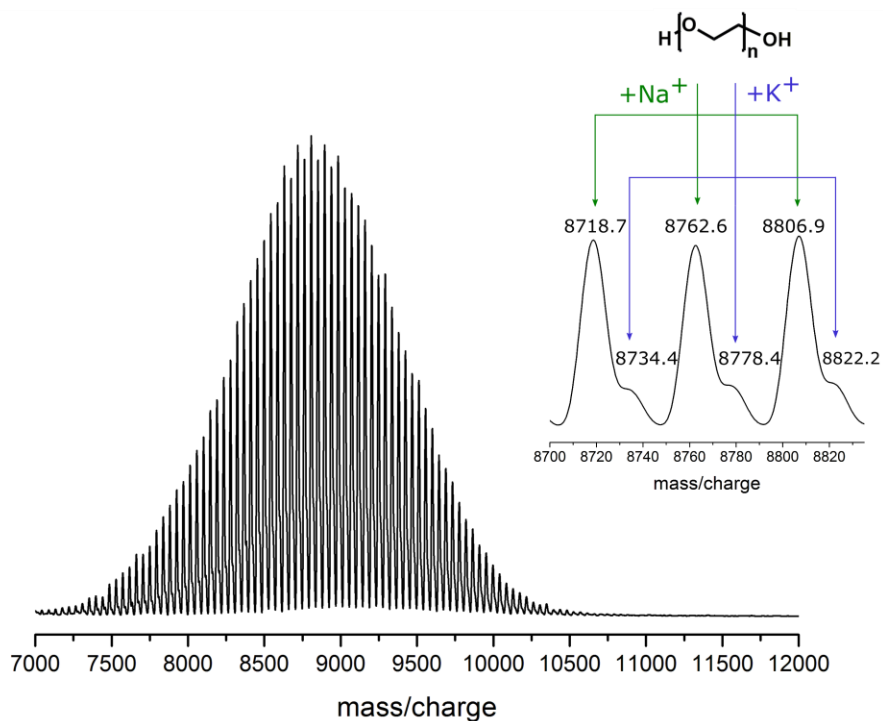


Figure S13. MALDI-ToF-MS of  $\alpha,\omega$ -dihydroxyl-PEG-8000 (**1**, C<sub>24</sub>) using a dithranol matrix and KTFA as salt, purified with semi-preparative HPLC, product eluted at 8.5 min.

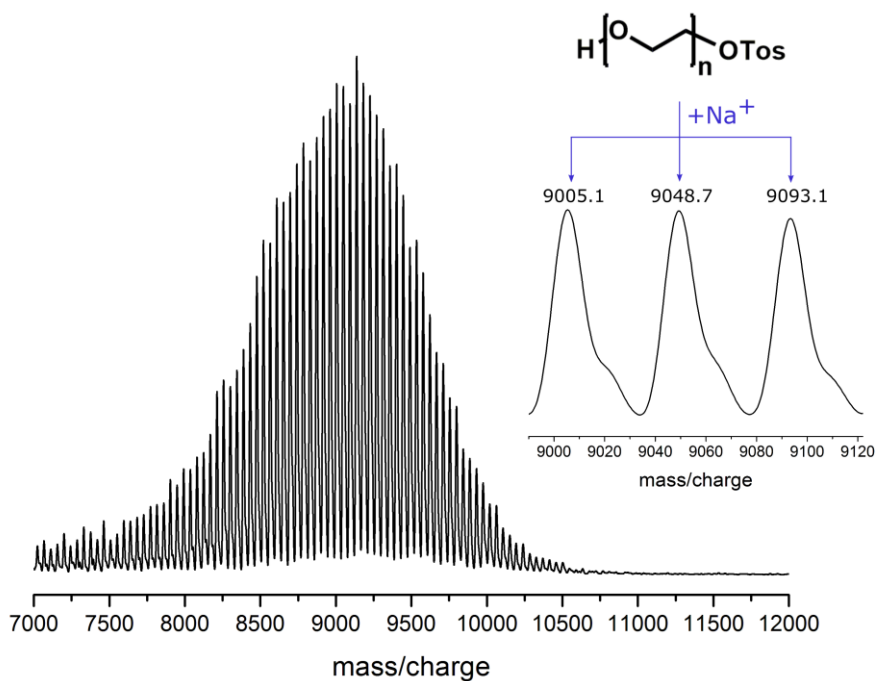


Figure S14. MALDI-ToF-MS of  $\alpha$ -tosyl- $\omega$ -hydroxyl-PEG-8000 (**2**, C<sub>24</sub>) using a dithranol matrix and KTFA as salt, purified with semi-preparative HPLC, product eluted at 11.5 min.

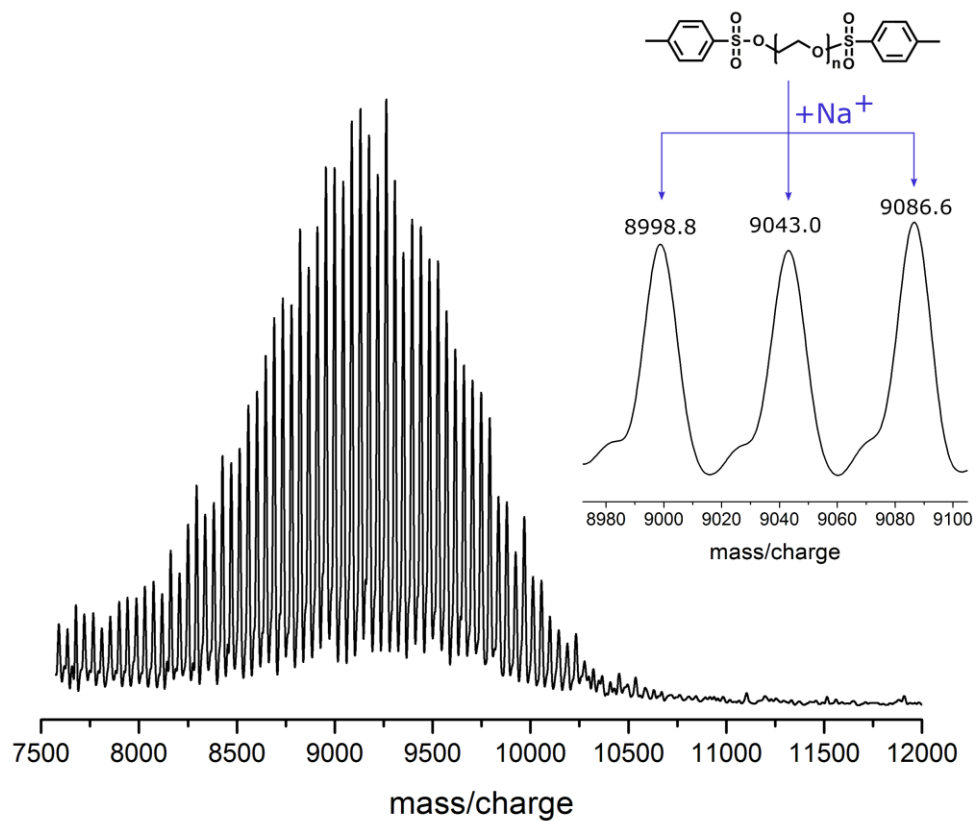


Figure S15. MALDI-ToF-MS of  $\alpha,\omega$ -ditosyl-PEG-8000 (**3**, C<sub>24</sub>) using a dithranol matrix and KTFA as salt, purified with semi-preparative HPLC, product eluted at 13.0 min.

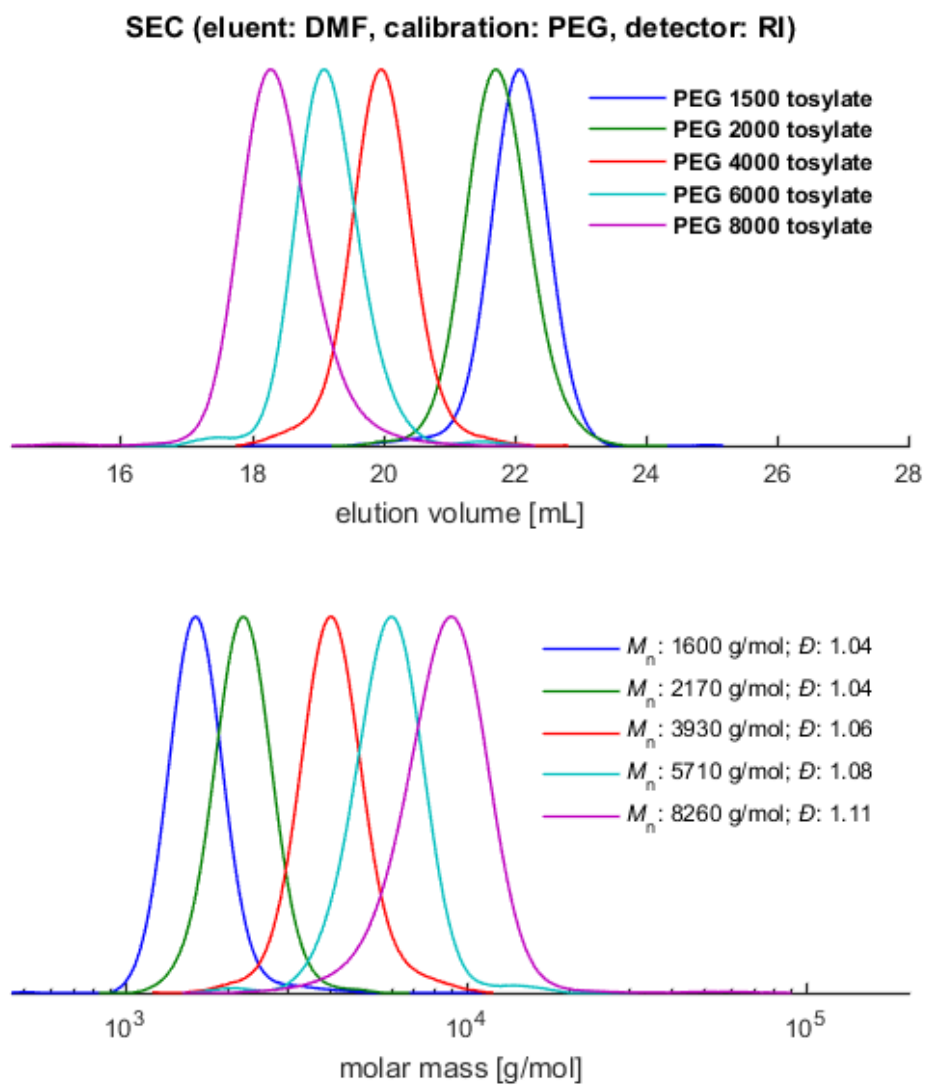


Figure S16. SEC traces of  $\alpha$ -tosyl- $\omega$ -hydroxyl-PEG prepared (eluent: DMF, PEG calibration, RI detector signal) of samples purified with semi-preparative HPLC. PEG-6000 sample is not discussed in the manuscript.

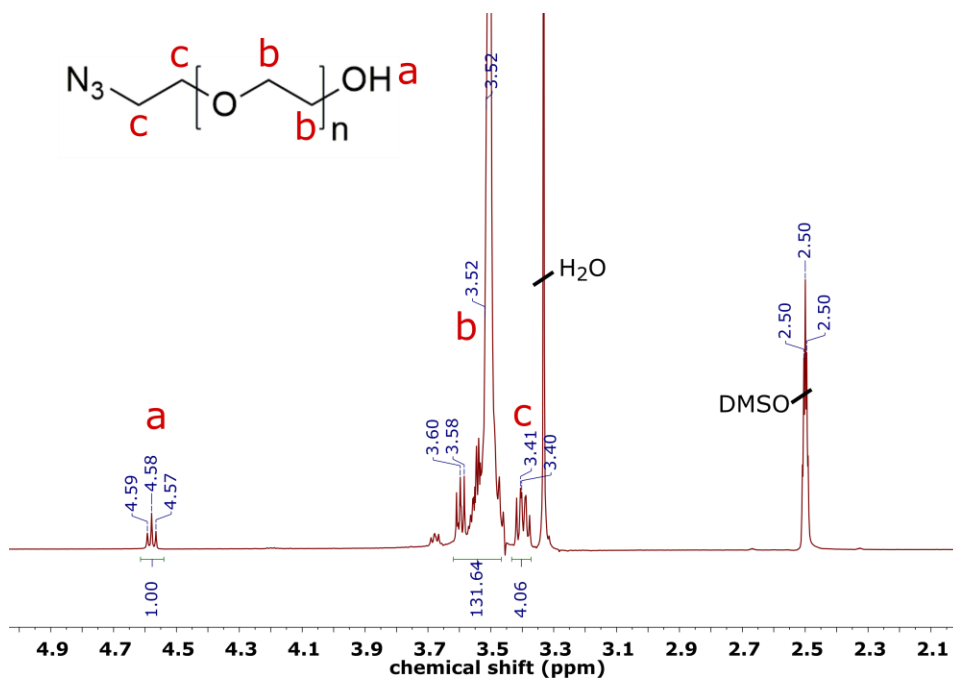
$\alpha$ -azido- $\omega$ -hydroxyl-PEG (4)

Figure S17.  $^1\text{H-NMR}$  spectrum (400 MHz, DMSO) of  $\alpha$ -azido- $\omega$ -hydroxyl-PEG-1500 (4).

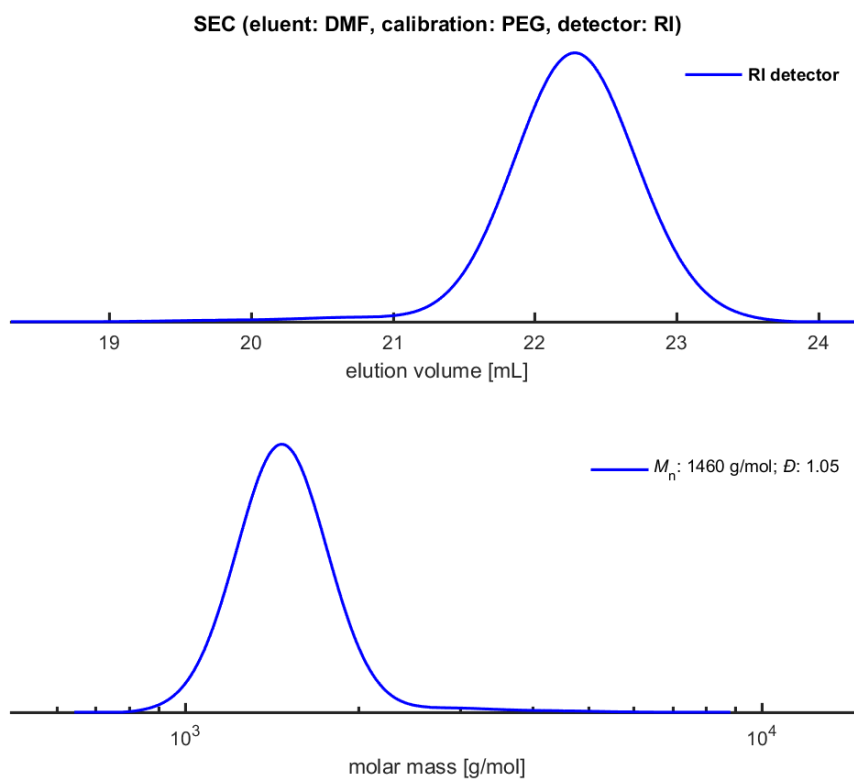


Figure S18. SEC elugram and mass distribution of  $\alpha$ -azido- $\omega$ -hydroxyl-PEG-1500 (4), (eluent: DMF, PEG calibration, RI and UV detector signals).

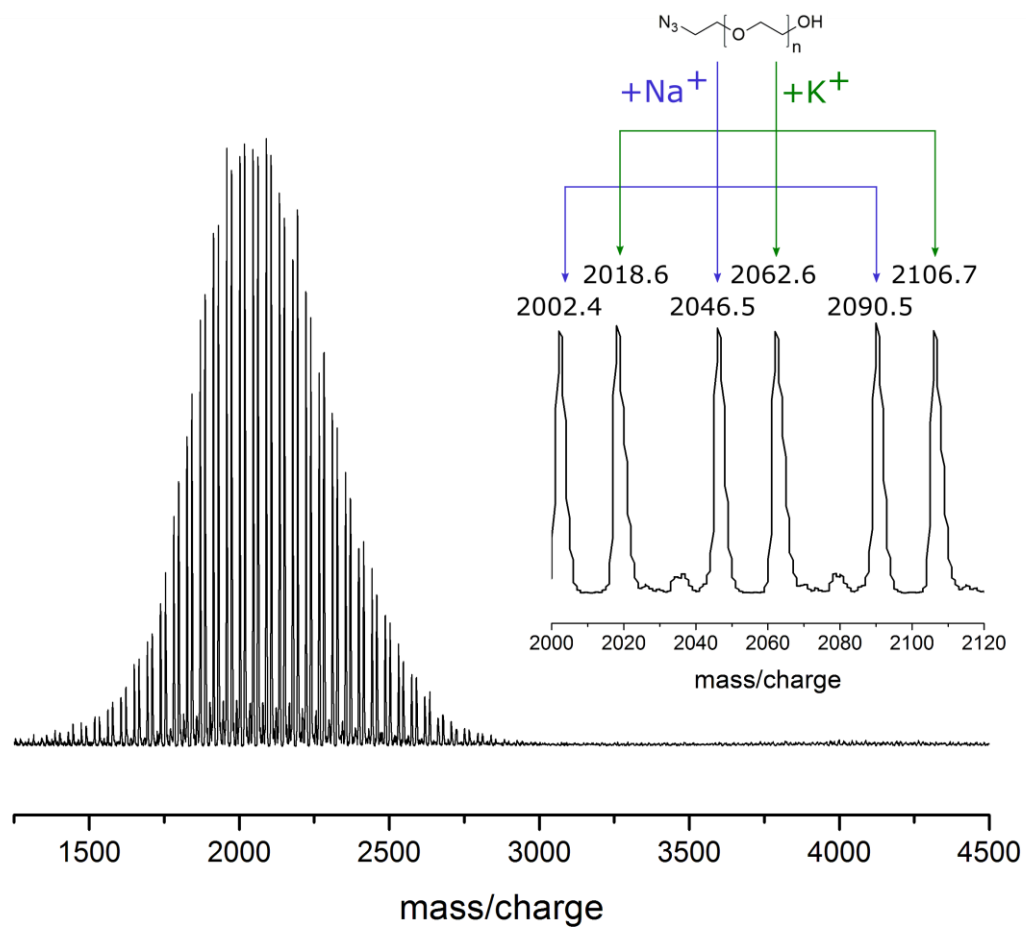
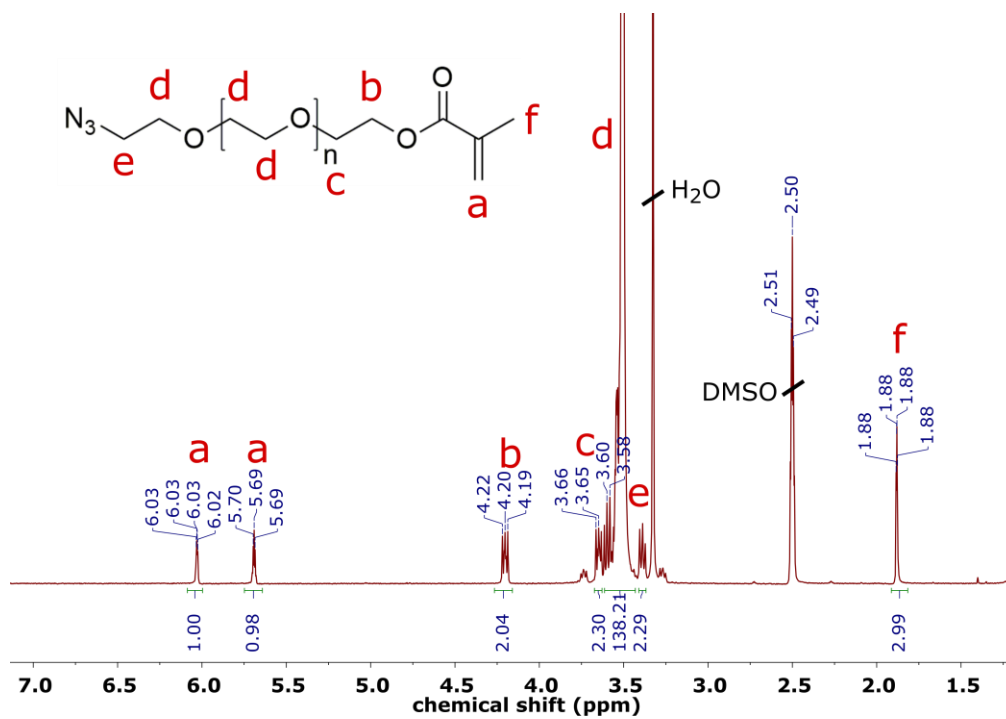
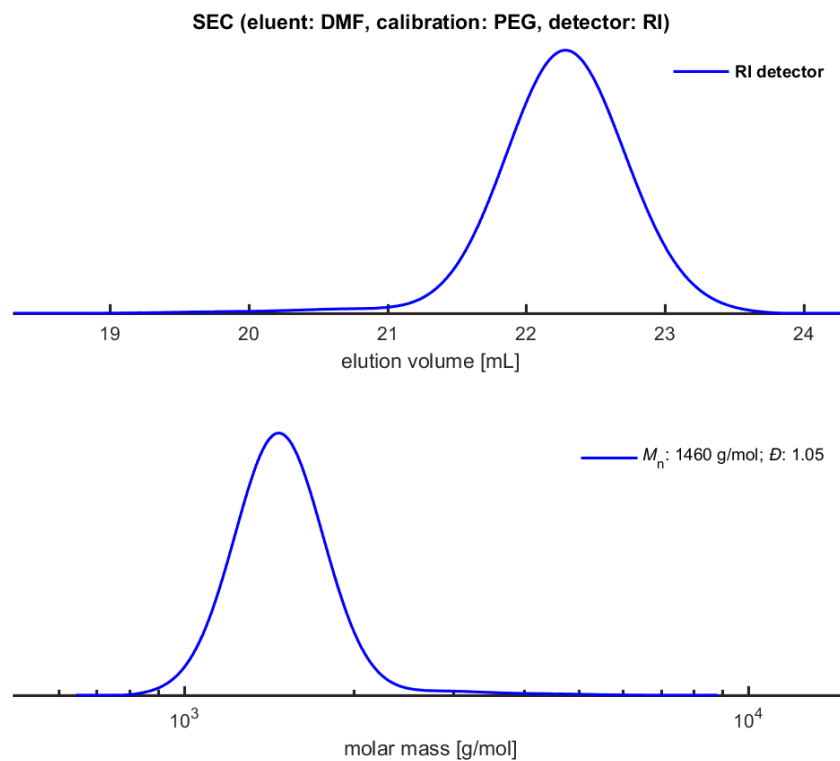


Figure S19. MALDI-ToF-MS of  $\alpha$ -azido- $\omega$ -hydroxyl-PEG-2000 (**4**), using a dithranol matrix and KTFA as salt.

**$\alpha$ -methacryloyl- $\omega$ -azido-PEG (5)**Figure S20.  $^1\text{H-NMR}$  spectrum (400 MHz, DMSO) of  $\alpha$ -methacryloyl- $\omega$ -azido-PEG-1500 (5).Figure S21. SEC elugram and mass distribution of  $\alpha$ -methacryloyl- $\omega$ -azido-PEG-2000 (5), (eluent: DMF, PEG calibration, RI and UV detector signals).

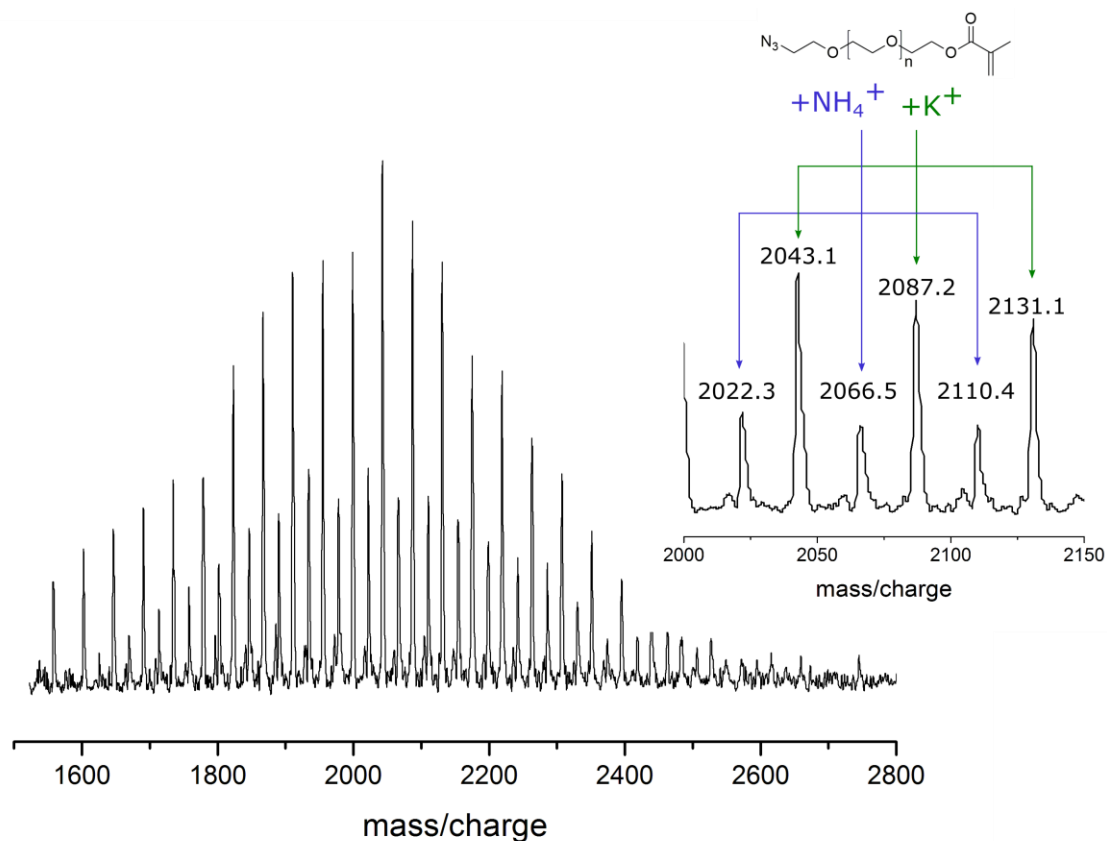
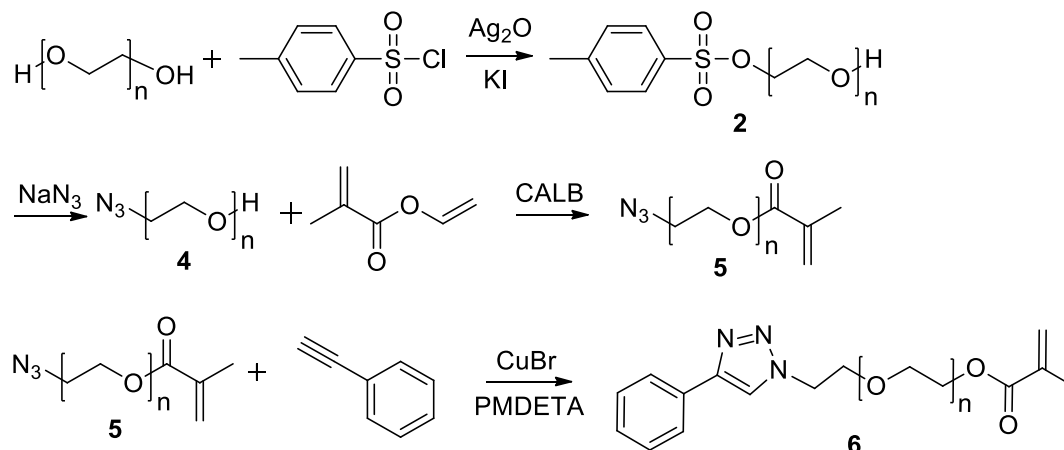


Figure S22. MALDI-ToF-MS of  $\alpha$ -methacryloyl- $\omega$ -azido-PEG-2000 (**5**) using a dithranol matrix and KTFA as salt.

#### $\alpha$ -4-phenyl-1,2,3-triazol-1-yl- $\omega$ -methacryloyl-PEG (**6**)



Scheme 1. Reaction scheme of heterobifunctional functionalization of poly(ethylene glycol) in a four step reaction with phenyl acetylene as test reaction.

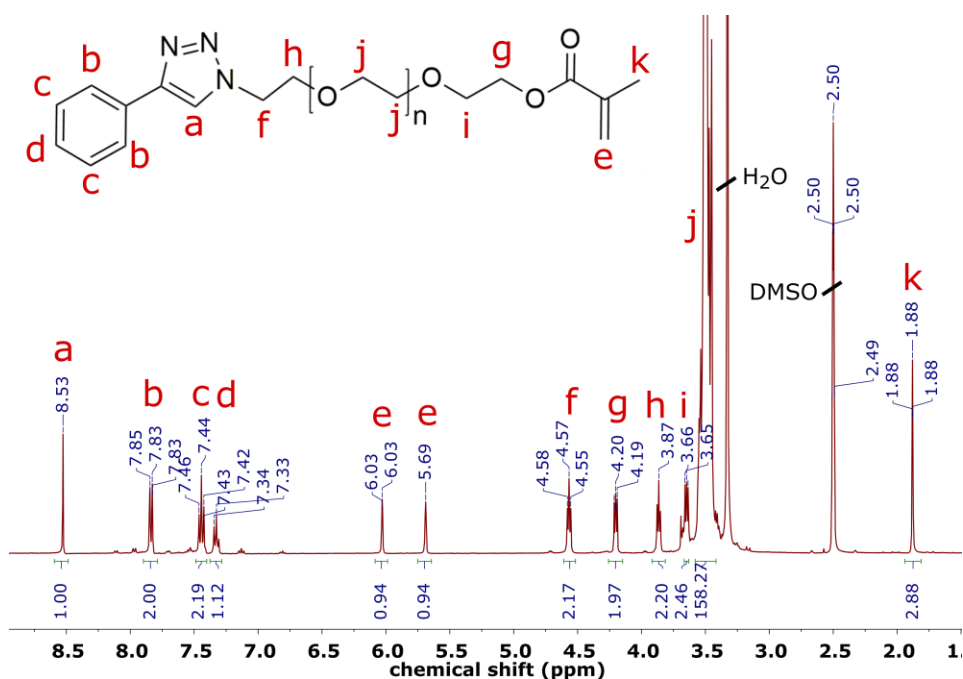


Figure S23.  $^1\text{H-NMR}$  spectrum (400 MHz, DMSO) of  $\alpha$ -4-phenyl-1,2,3-triazol-1-yl- $\omega$ -methacryloyl-PEG-1500 (6).

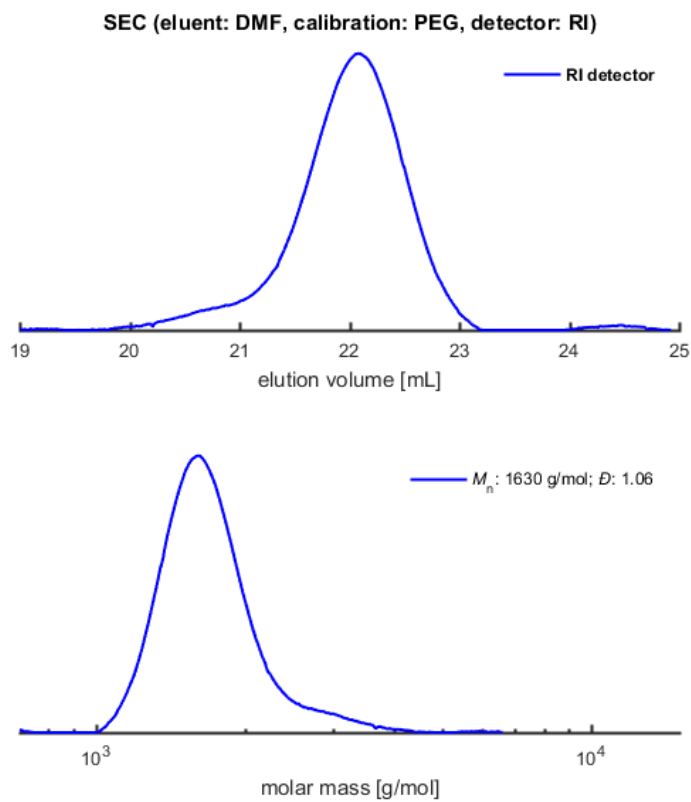


Figure S24. SEC elugram and mass distribution of  $\alpha$ -4-phenyl-1,2,3-triazol-1-yl- $\omega$ -methacryloyl-PEG-1500 (6), (eluent: DMF, PEG calibration, RI and UV detector signals).



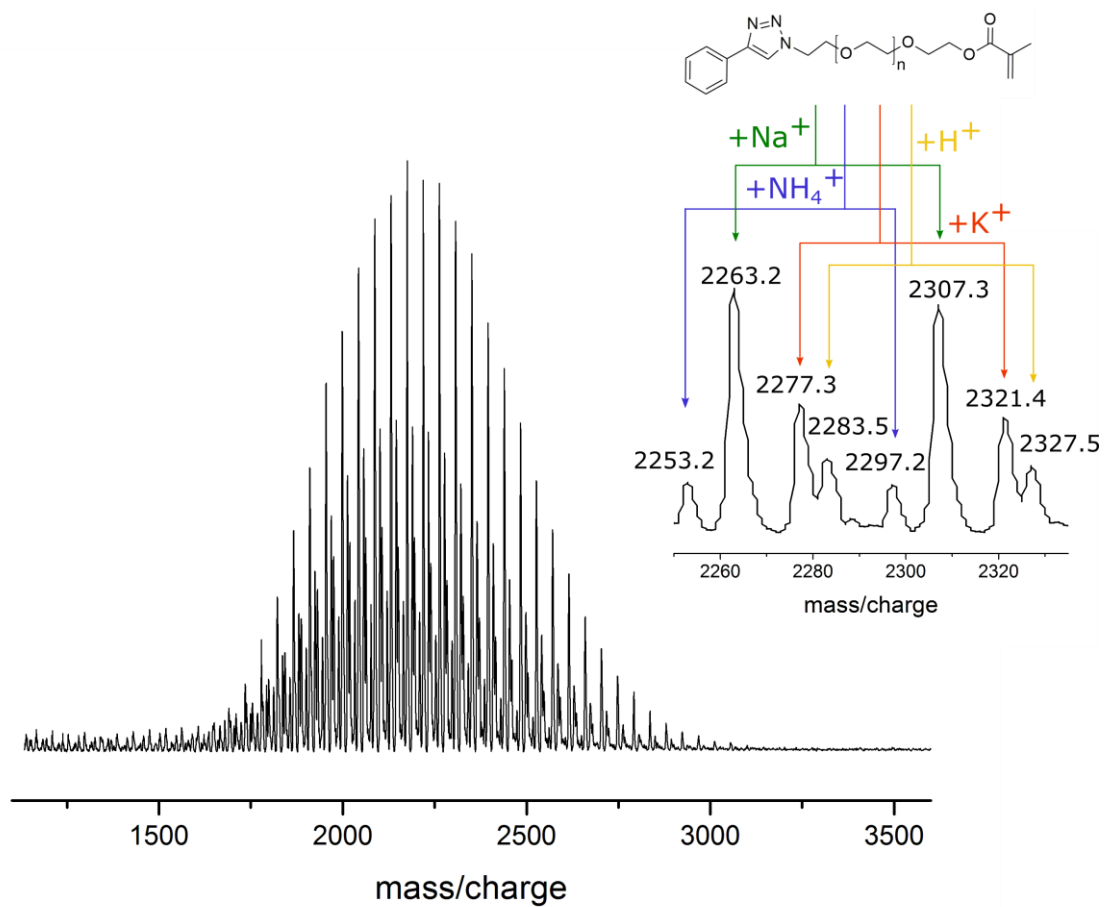


Figure S25. MALDI-ToF-MS of  $\alpha$ -4-phenyl-1,2,3-triazol-1-yl- $\omega$ -methacryloyl-PEG-2000 (**6**), using a dithranol matrix and KTFA as salt.

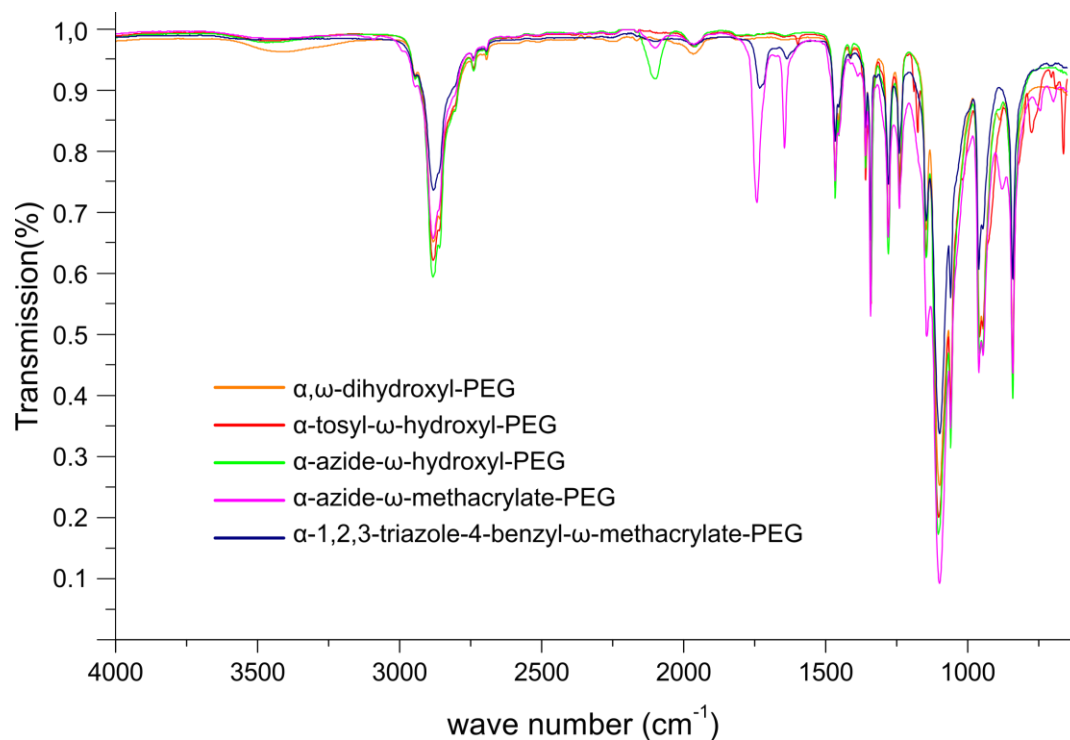
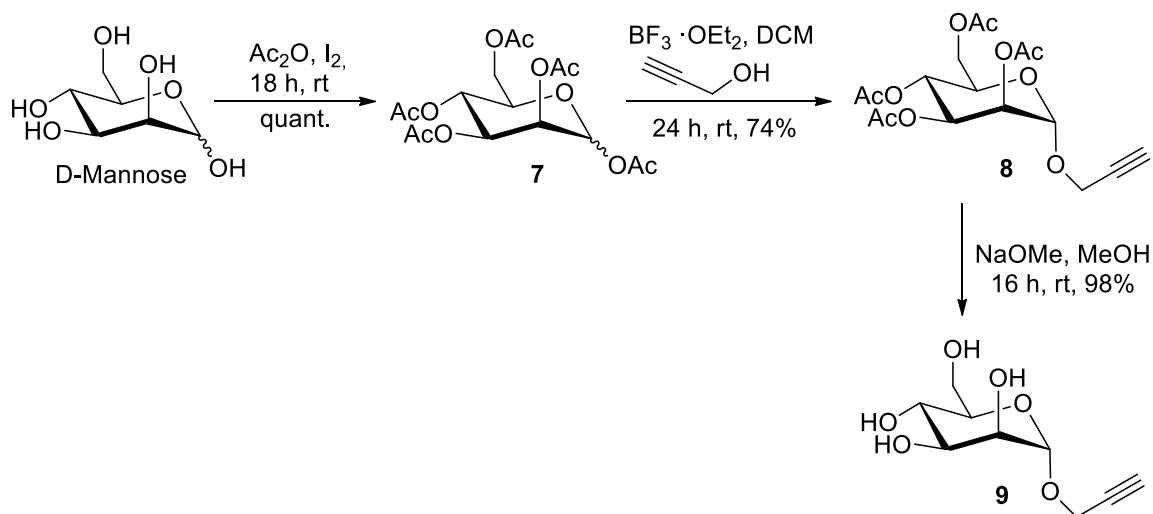
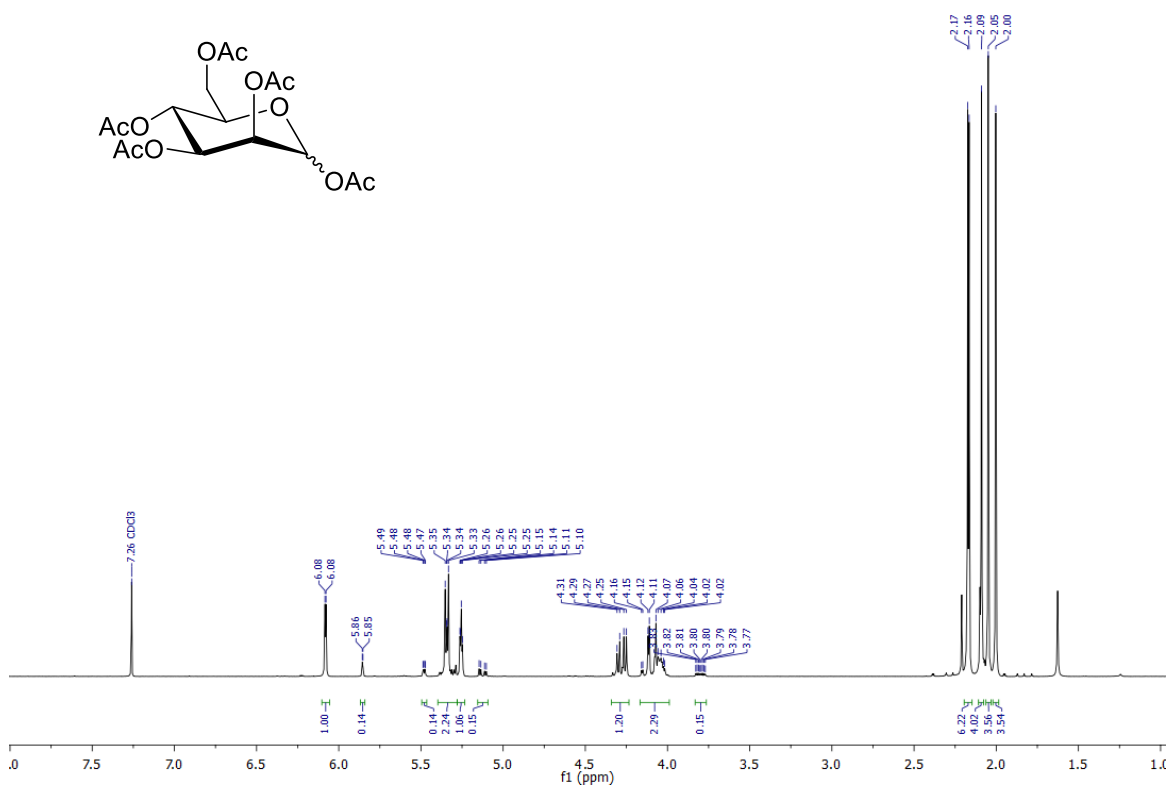


Figure S26. FTIR spectra of the different reactions steps from  $\alpha,\omega$ -dihydroxyl-PEG to the clicked  $\alpha$ -4-phenyl-1,2,3, triazol-1-yl- $\omega$ -methacryloyl-PEG.  $\alpha,\omega$ -dihydroxyl-PEG (orange line),  $\alpha$ -tosyl- $\omega$ -hydroxyl-PEG (red line),  $\alpha$ -azido- $\omega$ -hydroxyl-PEG (green line),  $\alpha$ -azido- $\omega$ -methacryloyl-PEG (pink line),  $\alpha$ -4-phenyl-1,2,3, triazol-1-yl- $\omega$ -methacryloyl-PEG (blue line).

The broad band at  $3600\text{-}3200\text{ cm}^{-1}$  of the hydroxyl group is visible for PEG-diol (orange line) disappears during the first reaction step and a new signal at  $650\text{ cm}^{-1}$  (red line) appears for the deformation vibration. During the second reaction step, the aromatic deformation vibration vanishes and an azide stretch vibration at  $2160\text{-}2120\text{ cm}^{-1}$  can be observed (green line). This peak remains and two additional peaks at  $1650\text{-}1600\text{ cm}^{-1}$  (conjugated alkene) and  $1685\text{-}1666\text{ cm}^{-1}$  (conjugated ketone) are visible after attachment of the methacrylate units (pink line). The peaks for the methacrylate unit remain, but the azide peak disappears after the last reaction step (blue line).

Propargyl- $\alpha$ -D-mannopyranoside (**9**)Figure S27. Reaction Scheme for the synthesis of propargyl- $\alpha$ -D-mannopyranoside (**9**).Figure S28.  $^1\text{H}$  NMR spectrum (400 MHz,  $\text{CDCl}_3$ ) of 1,2,3,4,6-Penta-O-acetyl- $\alpha,\beta$ -D-mannopyranose (**7**).

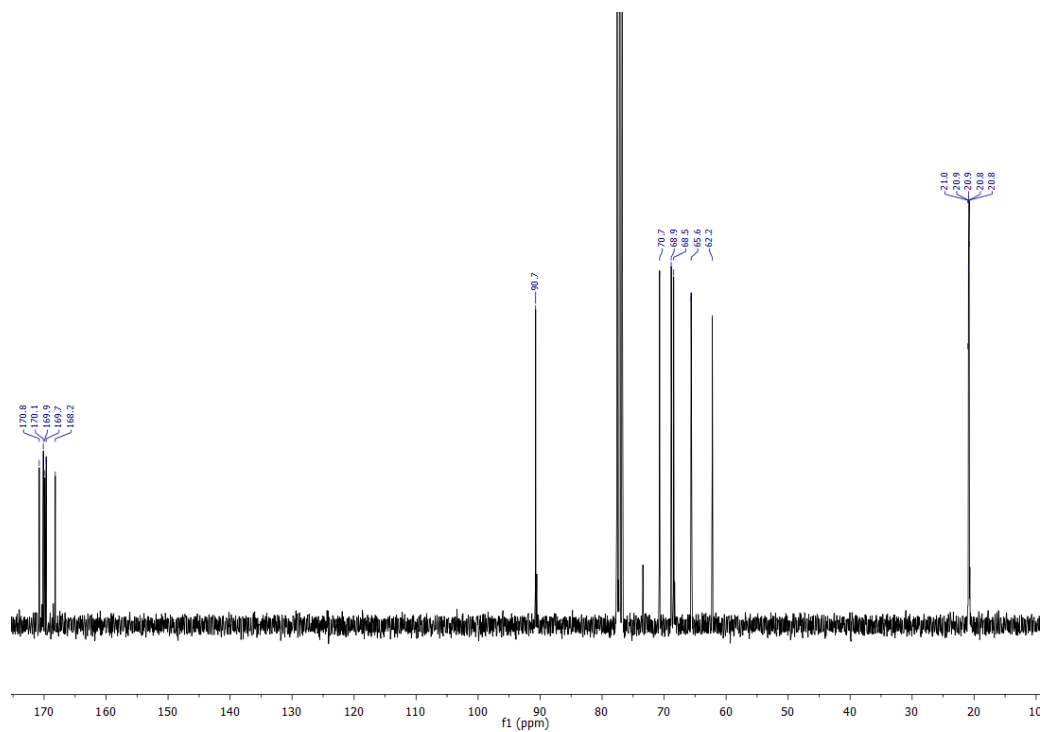


Figure S29.  $^{13}\text{C}$  NMR Spectrum (100.6 MHz,  $\text{CDCl}_3$ ) of 1,2,3,4,6-Penta-*O*-acetyl- $\alpha,\beta$ -D-mannopyranose (**7**).

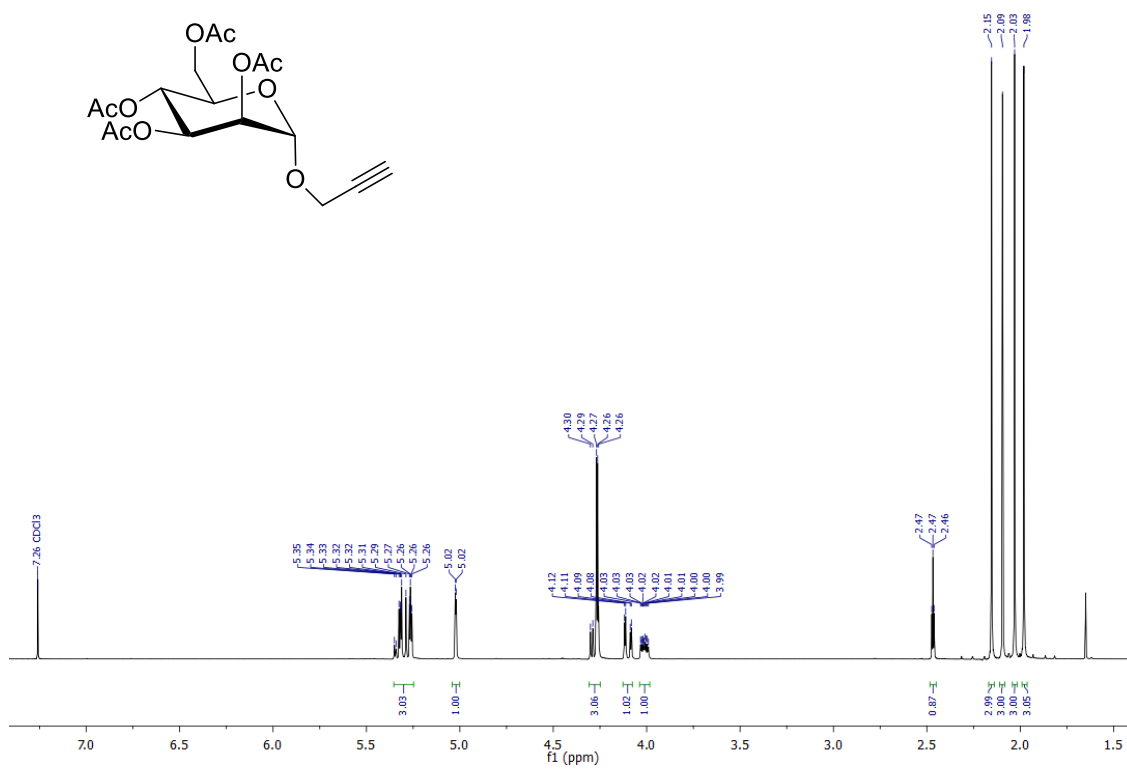


Figure S30.  $^1\text{H}$  NMR spectrum (400 MHz,  $\text{CDCl}_3$ ) of Propargyl-2,3,4,6-Tetra-*O*-acetyl- $\alpha$ -D-mannopyranoside (**8**).

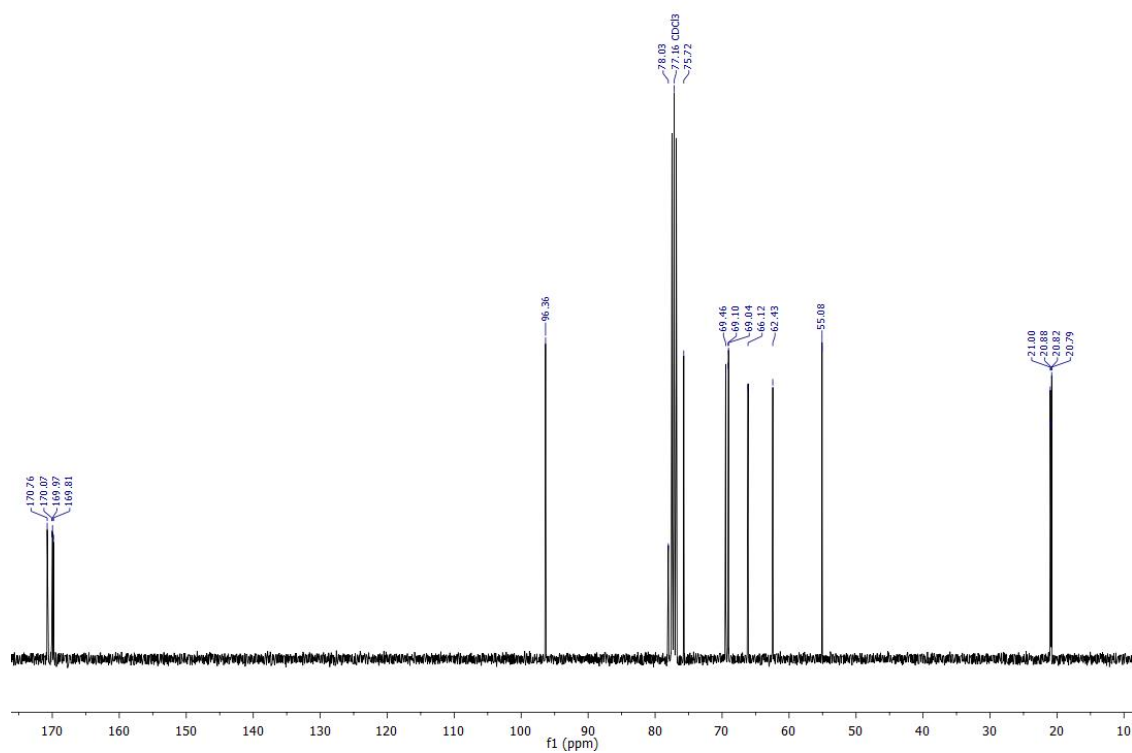


Figure S31.  $^{13}\text{C}$  NMR Spectrum (100.6 MHz,  $\text{CDCl}_3$ ) of Propargyl-2,3,4,6-Tetra-*O*-acetyl- $\alpha$ -D-mannopyranoside (**8**).

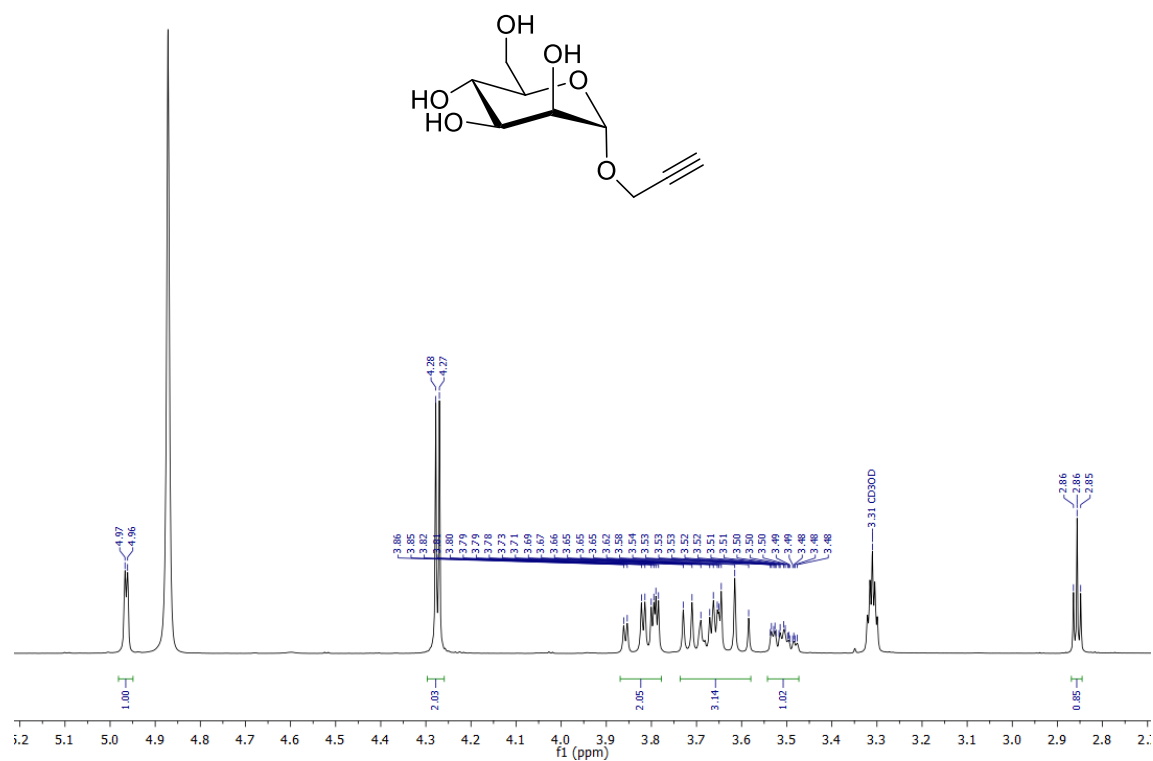


Figure S32.  $^1\text{H}$  NMR spectrum (400 MHz,  $\text{CDCl}_3$ ) of Propargyl- $\alpha$ -D-mannopyranoside (**9**).

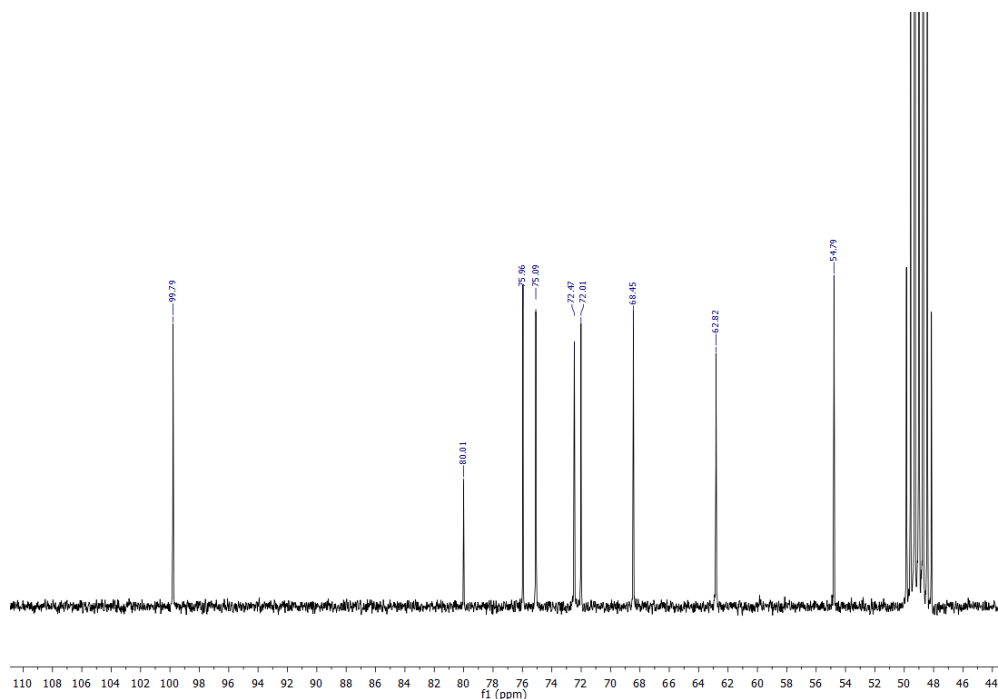


Figure S33.  $^{13}\text{C}$  NMR Spectrum (100.6 MHz,  $\text{CDCl}_3$ ) of Propargyl-2,3,4,6-Tetra-*O*-acetyl- $\alpha$ -D-mannopyranoside (**9**).

$\alpha$ -4-( $\alpha$ -D-mannopyranosyloxymethylene)-1,2,3, triazol-1-yl- $\omega$ -methacryloyl-PEG

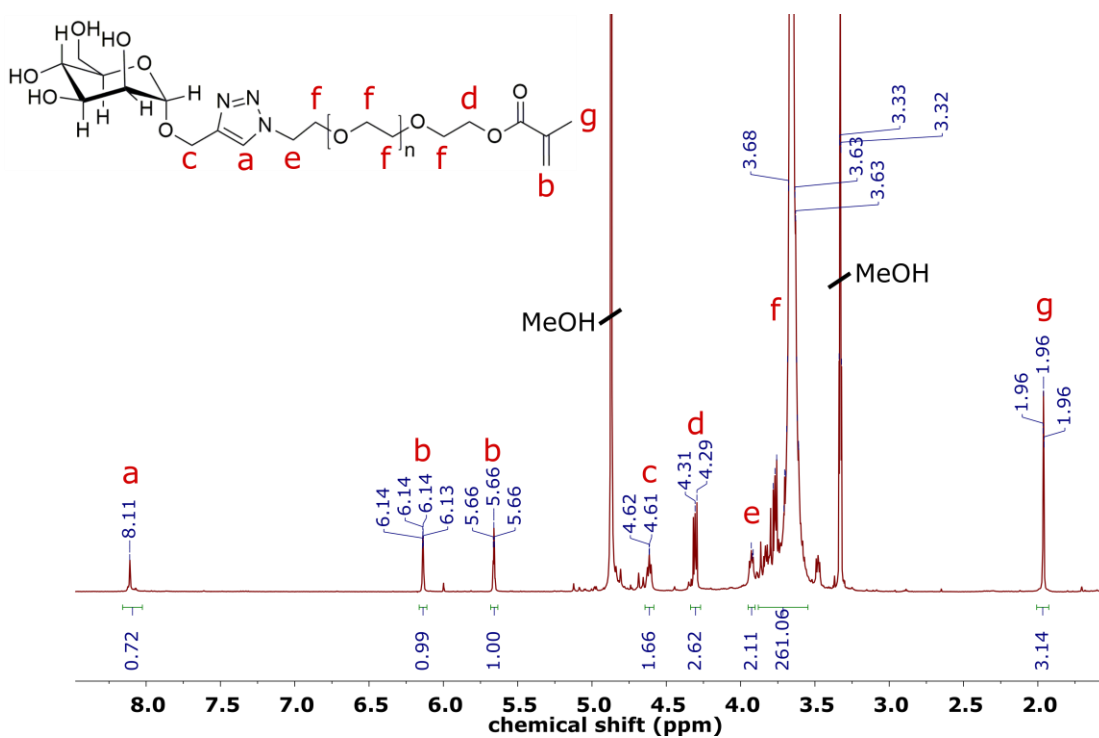


Figure S34.  $^1\text{H}$ -NMR spectrum (400 MHz, MeOH) of  $\alpha$ -4-( $\alpha$ -D-mannopyranosyloxymethylene)-1,2,3, triazol-1-yl- $\omega$ -methacryloyl-PEG-2000 (**10**).

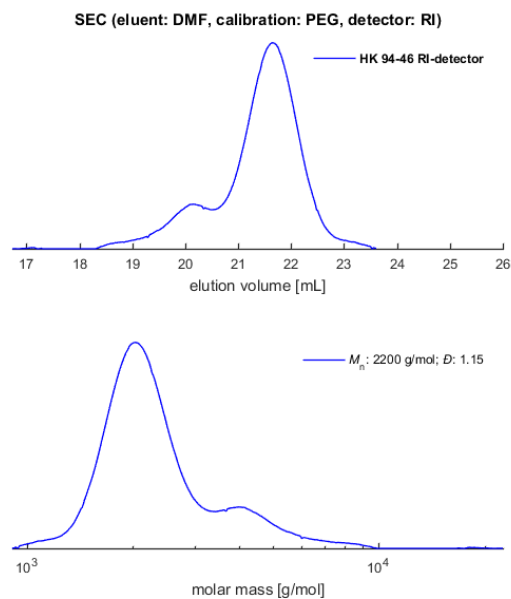


Figure S35. SEC elugram of  $\alpha$ -4-( $\alpha$ -D-mannopyranosyloxymethylene)-1,2,3, triazol-1-yl- $\omega$ -methacryloyl-PEG-2000 (**10**), (eluent: DMF, PEG calibration, RI detector signal). A higher molecular weight shoulder at approx. 4000 g mol<sup>-1</sup> is visible, which may be due to starting crosslinking of methacrylate units during SEC sample preparation.

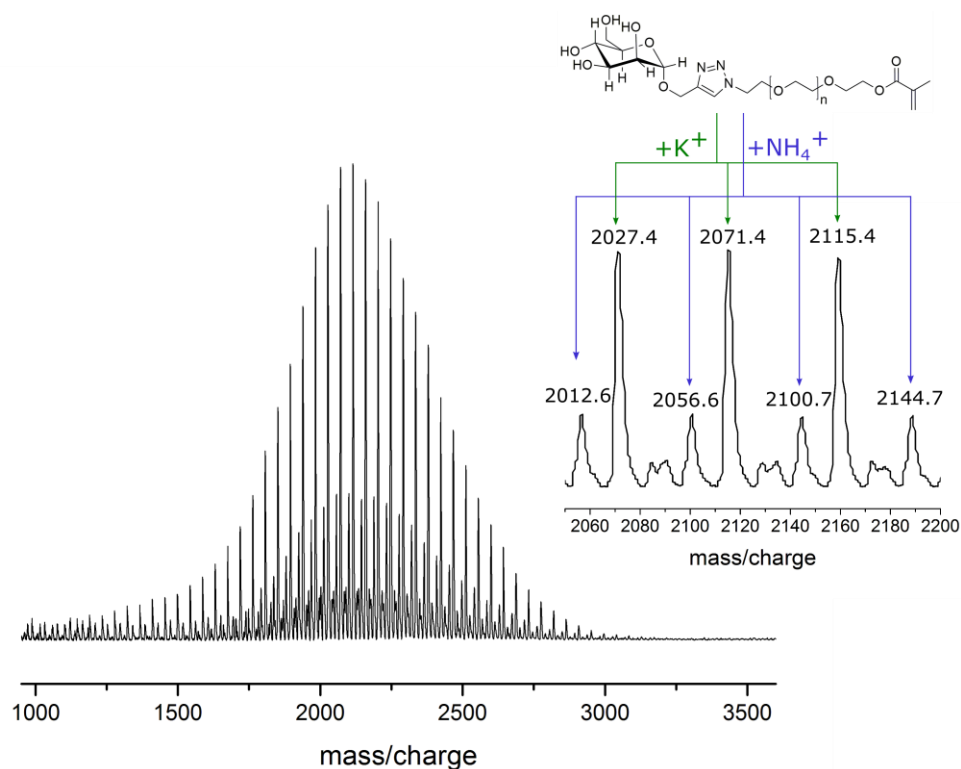


Figure S36. MALDI-ToF-MS of  $\alpha$ -4-( $\alpha$ -D-mannopyranosyloxymethylene)-1,2,3, triazol-1-yl- $\omega$ -methacryloyl-PEG-2000 (**10**), using a dithranol matrix and KTFA as salt.

	$\text{HO}(\text{CH}_2\text{CH}_2\text{O})_n\text{H}$ with $n = 39$ or $40$	$\text{C}_7\text{H}_7\text{SO}_3(\text{CH}_2\text{CH}_2\text{O})_n\text{H}$ with $n = 36$ or $37$	$\text{C}_7\text{H}_7\text{SO}_3(\text{CH}_2\text{CH}_2\text{O})_n$ $\text{C}_7\text{H}_7\text{O}_2\text{S}$ With $n = 36$ or $37$
$\text{H}^+$	1781 Da	1803 Da	1781 Da
$\text{Li}^+$	1787 Da	1809 Da	1787 Da
$\text{Na}^+$	1803 Da	1781 Da	1803 Da
$\text{K}^+$	1775 Da	1797 Da	1819 Da
None	1780 Da	1802 Da	1780 Da

Figure S37. Calculated average masses of PEG-1500-diol (1), PEG-1500-monotosylate (2), and PEG-1500-ditosylate (3) with different cations.

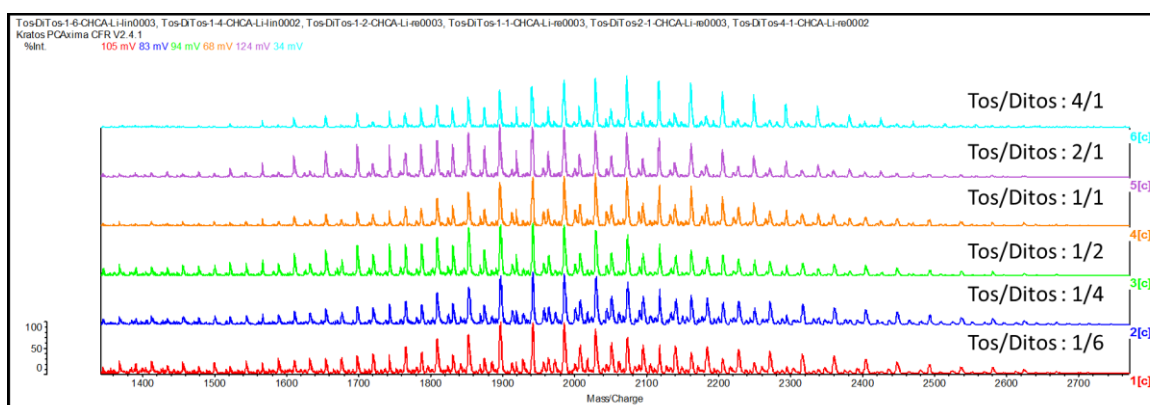


Figure S38. MALDI-ToF-MS spectra obtained by mixing PEG-1500-monotosylate 2 and PEG-1500-ditosylate 3 in different ratios.

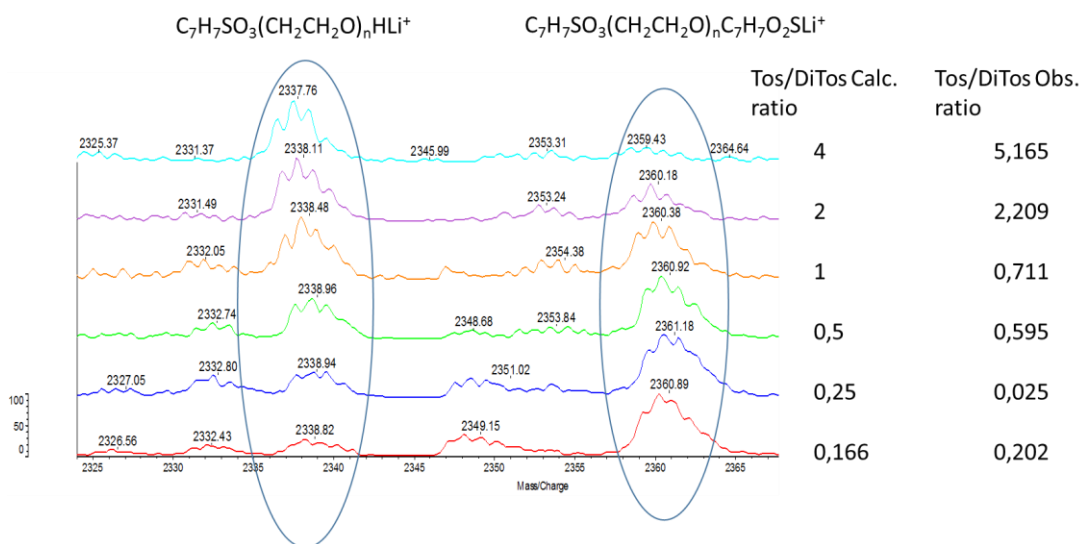


Figure S39. Magnification of MALDI-ToF-MS spectra obtained by mixing PEG-1500-monotosylate 2 and PEG-1500-ditosylate 3 in different ratios.



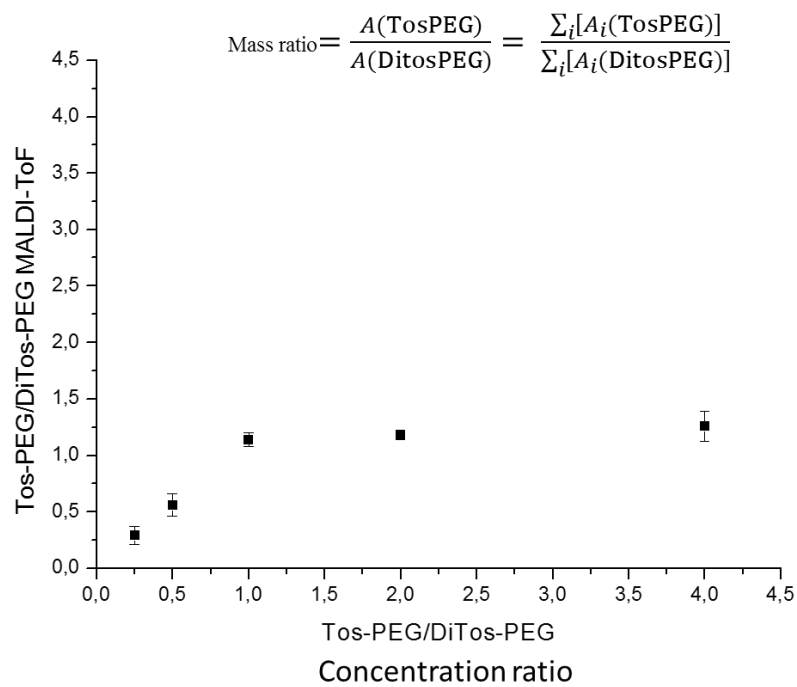


Figure S40. Calibration curve for PEG-1500-ditosylate **3** with PEG-1500-monotosylate **2** as internal standard.

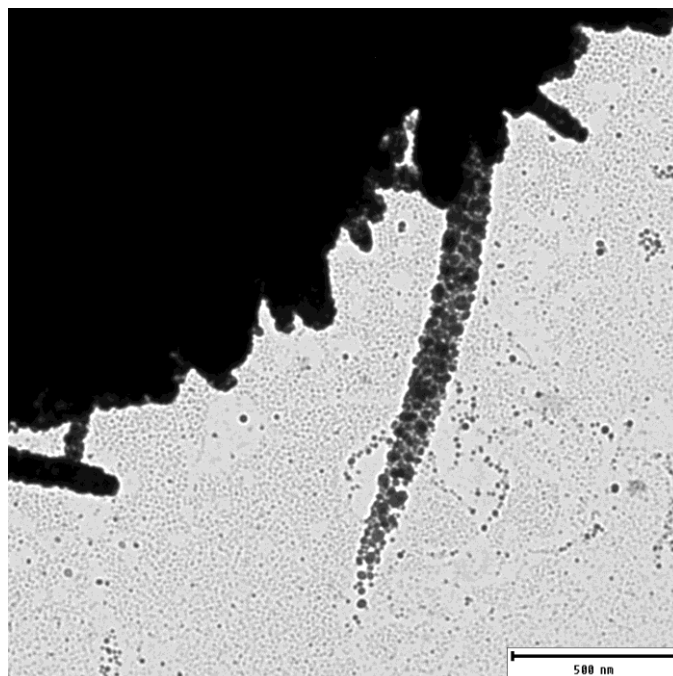
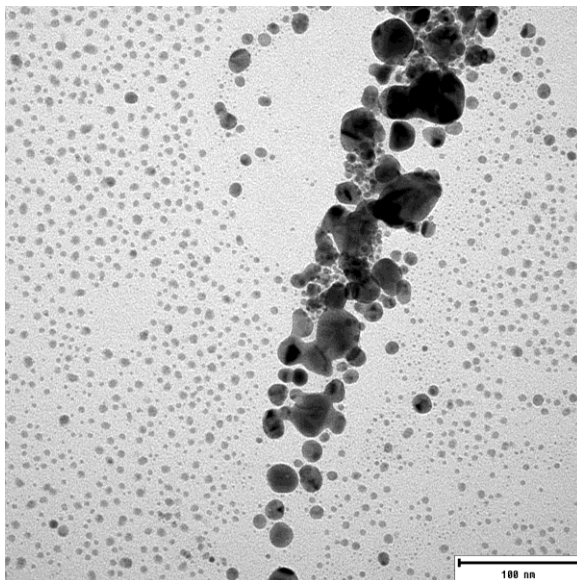


Figure S41. TEM image of silver(I)oxide (solvent: ethanol,  $c \approx 1 \text{ mg mL}^{-1}$ ).



*Figure S42.* Magnification of TEM image of silver(I)oxide (solvent: ethanol,  $c \approx 1 \text{ mg mL}^{-1}$ ).

### **Methods**

Illustrations were designed with Adobe Illustrator<sup>®</sup> CS5 v15.0.2.

## Chapter 5. Transformation of vaterite nanoparticles to hydroxylcarbonate apatite in a hydrogel scaffold: Relevance to bone formation

Romina Schröder,<sup>1,4</sup> Hannah Pohlitz,<sup>2,3</sup> Timo Schüler,<sup>1</sup> Martin Panthöfer,<sup>1</sup> Ronald E. Unger,<sup>4</sup> Holger Frey,<sup>2</sup> Wolfgang Tremel<sup>1</sup>

<sup>1</sup>Institute of Inorganic Chemistry and Analytical Chemistry, Johannes Gutenberg-University of Mainz, Duesbergweg 10-14, 55128 Mainz, Germany

<sup>2</sup>Institute of Organic Chemistry, Johannes Gutenberg-University of Mainz, Duesbergweg 10-14, 55128 Mainz, Germany

<sup>3</sup>Graduate School Materials Science in Mainz, Staudinger Weg 9, 55128 Mainz, Germany

<sup>4</sup>Institute of Pathology, REPAIR Lab, Johannes Gutenberg-University of Mainz, Langenbeckstraße 1, 55131 Mainz, Germany

Published in: *J. Mater. Chem. B*, **2015**, 3, 7079-7089. Reproduced by permission of The Royal Society of Chemistry.

### Abstract

Biomimetic materials have been gaining increasing importance for use as bone biomaterials, because they may provide regenerative alternatives for the use of autologous tissues for bone regeneration. We demonstrate a promising alternative for the use of biomimetic materials based on a biodegradable PEG hydrogel loaded with vaterite nanoparticles as mineral storage. Vaterite, the least stable CaCO<sub>3</sub> polymorph, is stable enough to ensure the presence of a potential ion buffer for bone regeneration, but still has sufficient reactivity for the transformation from CaCO<sub>3</sub> to hydroxyapatite (HA). A combination of powder X-ray diffraction (PXRD), electron microscopy, and fourier-transform infrared (FT-IR) and Raman spectroscopy showed the transformation of vaterite nanoparticles incorporated in a PEG-acetal-DMA hydrogel to hydroxycarbonate apatite (HCA) crystals upon incubation in simulated body fluid at human body temperature within several hours. The transformation in the PEG-acetal-DMA hydrogel scaffold in simulated body fluid or phosphate saline buffer proceeded significantly faster than for free vaterite. The vaterite-loaded hydrogels were free of endotoxin and did not exhibit an inflammatory effect on endothelial cells.

These compounds may have prospects for future applications in the treatment of bone defects and bone degenerative diseases.

## Introduction

Driven by the need for synthetic bone and tissue substitutes that promote bone healing *in vivo* there has been much interest in understanding the structure of bone and bone formation mechanisms.<sup>[1]</sup> Bone is a nanocomposite composed of organic (mainly collagen) and inorganic (nanocrystalline hydroxycarbonate apatite (HCA)) components, with a complex hierarchical structure ranging from the nano- to the macroscale.<sup>[2,3]</sup> Bone tissue engineering pursues different strategies to recapitulate those biomaterials which are present in native bone (e.g. HCA and collagen)<sup>[4,5]</sup> and by providing designed scaffolds that mimic essential features of the natural extracellular matrix in order to induce the proliferation and differentiation of stem or progenitor cells for bone regeneration and vascularization.

Inorganic materials like hydroxyapatite (HA), calcium phosphate, calcium sulfate or calcium carbonate have been used for bone grafting, but their resorption is very slow, which increases the risk of infection. A low degradation rate may lead to the accumulation of foreign mineral. For optimal bone regeneration the rate of resorption should match the rate of bone formation,<sup>[6]</sup> and the mineral supply should be sufficiently stable to ensure the presence of an ion buffer for bone regeneration at the position of the implantation. Amorphous precursor phases may serve as mineral buffer to build mature crystalline mineral phases via a series of intermediates under kinetic control.<sup>[7]</sup> The resulting crystalline phases exhibit high strength and fracture toughness.<sup>[7,8]</sup> Amorphous calcium phosphate (ACP) has been reported to transform into crystalline calcium phosphate (mainly apatite).<sup>[9-11]</sup> Recent studies on bone and teeth formation revealed the transient of amorphous mineral precursors to be a general strategy for calcium carbonate- and orthophosphate-based biomineralization in both vertebrates and invertebrates.<sup>[12-16]</sup> ACP has been postulated to play a key role as bone mineral precursor in vertebrates.<sup>[16]</sup> Mahamid *et al.*<sup>[15]</sup> described ACP to be a major component of the initial mineral phase of bone. Complexing agents like citrate were suggested to affect early ACP formation<sup>[16,17]</sup> through the stabilization of ACP clusters whose subsequent aggregation can be promoted by the presence of non-collagenous proteins. This was supported by the preparation of citrate-functionalized carbonate-apatite nanoparticles that lead to a gradual and homogeneous release of  $\text{Ca}^{2+}$  ions for the precipitation of nanocrystalline apatite.<sup>[18]</sup>

Amorphous  $\text{CaCO}_3$  (ACC) has been considered a potential inorganic precursor to induce the formation of bone minerals.<sup>[19]</sup> Recently we demonstrated that non-agglomerated and non-functionalized nanoparticles of vaterite, the least stable crystalline polymorph of  $\text{CaCO}_3$ , can be synthesized.<sup>[20,21]</sup> Because of their positively charged surface, they can be functionalized with carboxylate or phosphonate bearing ligands, and they have a moderate solubility that allows their dissolution and transformation to HCA.<sup>[22]</sup> Therefore it was tempting to combine the bioactivity and osteoconductivity of vaterite nanoparticles with the flexibility and degradability of a hydrogel in order to develop a new bone grafting material.

A common class of hydrogels in (bio)mineralization systems are physical gels based on polysaccharides such as agarose, pectin, alginate, and cellulose, or proteins such as collagen, gelatin and silk fibroin.<sup>[23-29]</sup> From a chemical perspective, poly(ethylene glycol) (PEG) or hydrogels from phosphorylated block copolymers are well-known for its use in pharmaceutical and biomedical applications.<sup>[30-38]</sup> Desirable characteristics like excellent solubility in aqueous and organic media, biocompatibility and flexibility of the backbone chain have made PEG the “gold standard” in recent years.

In this contribution we demonstrate a promising alternative for the use of biodegradable nanoparticles, which have inherent potential bone targeting abilities. A difunctional degradable PEG-acetal-dimethacrylate (DMA) hydrogel with cleavable acetal units was loaded with vaterite nanoparticles and incubated with Dulbecco’s phosphate buffered saline (DPBS) or simulated body fluid (SBF). Complete degradation of conventional PEG-diacrylate hydrogels by hydrolysis of the ester bond has been reported to take approximately 28-30 weeks.<sup>[39]</sup> A major advantage of PEG-acetal-DMA compared to conventional PEG without additional cleavable units is the faster degradation of the implanted hydrogels due to facile hydrolysis of the acetal moieties. Fragments of the hydrogel detached by hydrolysis can be internalized by phagocytes, e.g., macrophages. After phagocytosis, the hydrogel fragment undergoes fast further degradation due to the acidic conditions inside the endolysosome at the introduced acetal units. The degradation products can be excreted from the body via renal clearance.<sup>[40]</sup> The vaterite nanoparticles and the PEG-acetal-DMA precursor were prepared by using recently developed synthetic protocols. Powder X-ray diffraction (PXRD), electron microscopy, and Fourier-transform (FT-IR) infrared and Raman spectroscopy showed the transformation of the hydrogel incorporated vaterite nanoparticles to hydroxycarbonate apatite (HCA) crystals after incubation in simulated body fluid at human body temperature. The transformation in the hydrogel scaffold in simulated body fluid or phosphate saline buffer is faster than for free vaterite. The surface of the vaterite nanoparticles shows strong

interaction with the PEG-acetal-DMA hydrogel. Furthermore we were able to show that the materials were free of endotoxin and did not induce an inflammatory response by *in vitro* tests with human endothelial cells.

### Experimental Section

**Materials.** NaHCO<sub>3</sub>, ethylene glycol, 2-hydroxy-4'-(2-hydroxyethoxy)-2-methylpropiophenone, PEG8000, *para*-toluensulfonic acid, sodium hydroxide and dichloromethane were purchased from Sigma Aldrich. Dulbecco's phosphate buffered saline (DPBS) and CaCl<sub>2</sub>·4H<sub>2</sub>O were purchased from Life Technologies and Merck. Hydroquinone, trimethylamine, magnesium sulfate and diethylether were purchased by Acros Organics. All reagents and solvents were of analytical grade and used as received. 2-(vinylloxy)ethyl methacrylate was synthesized after a modified procedure of Vysotskaya *et al.*<sup>[41]</sup> We prepared a simulated body fluid (SBF) following the recipe proposed by Kokubo and Takadama.<sup>[42]</sup> The ion concentrations of SBF are as follows: 142.0 mM Na<sup>+</sup>, 5.0 mM K<sup>+</sup>, 1.5 mM Mg<sup>2+</sup>, 2.5 mM Ca<sup>2+</sup>, 147.8 mM Cl<sup>-</sup>, 4.2 mM HCO<sub>3</sub><sup>-</sup>, 1.0 mM HPO<sub>4</sub><sup>2-</sup>, 0.5 mM SO<sub>4</sub><sup>2-</sup>. The pH of the SBF solution was finally adjust to 7.37 at 37 °C by using 1M HCl. All syntheses were carried out with MilliQ-water (18.2 MΩ·cm, 25 °C).

### Synthesis.

**Synthesis of vaterite nanoparticles and their transformation to HCA.** Vaterite nanoparticles were synthesized as reported in reference<sup>[21]</sup>. 5 mmol calcium chloride tetrahydrate were dissolved in 50 mL of ethylene glycol by sonication at 40 °C (Emmi 40HC by EMAG-Technologies, max. power 250 W, frequency 45 kHz, 100% ultrasonic power). 10 mmol of sodium bicarbonate were dispersed in 50 mL of ethylene glycol by mechanical stirring and added to the calcium chloride solution. The resulting dispersion was heated and sonicated for 30 minutes by 40 °C. CaCO<sub>3</sub> nanoparticles were separated from the turbid sol product by centrifugation (9000 rpm, 30 minutes), washed several times with water and ethanol and dried at high vacuum. The yields (60%) were determined gravimetrically.

The obtained vaterite nanoparticles were soaked in SBF (1 mg/mL) and incubated at 37 °C in a shaking incubator (150 rpm) for 24 h, 48 h and 72 h for their transformation into HCA. Before characterization the precipitate was washed several times with water and ethanol and dried at high vacuum.

**Synthesis of PEG-acetal-DMA hydrogel and vaterite incorporated PEG-acetal-DMA hydrogel and SBF incubation. Synthesis of PEG-acetal-DMA precursor.**

PEG-acetal-DMA was synthesized using a recently reported method.<sup>[43]</sup> 1 mmol PEG8000, 5 mmol 2-(vinylloxy)ethyl methacrylate and 0.1 mmol *p*-toluene-sulfonic acid were dissolved in 5 mL of dichloromethane. 20 mg of hydroquinone were added as radical inhibitor. The reaction mixture was stirred at room temperature for 25 minutes followed by quenching with 0.2 mmol of triethylamine. As work-up, the reaction mixture was extracted with the same volume of 1 mol/L of sodium hydroxide solution. Subsequently, the aqueous phase was again extracted with dichloromethane twice. Organic phases were combined and dried over magnesium sulfate, and then the solvent was removed by rotary evaporation. The crude product was precipitated twice in cold diethylether and additional 20 mg hydroquinone was added before final drying at high vacuum to obtain PEG-acetal-DMA as colorless solid in quantitative yield.

**Photopolymerization and vaterite nanoparticle incorporation.** For preparation of nanoparticle-free PEG-acetal-DMA hydrogel, a 10% (w/v) solution of PEG-acetal-DMA in DPBS was mixed with 0.2% (w/v) photoinitiator 2-hydroxy-4'-(2-hydroxyethoxy)-2-methyl-propiophenone used as 10% (w/v) solution in 70% ethanol. For preparation of vaterite nanoparticle incorporated PEG-acetal-DMA hydrogel, freshly prepared vaterite nanoparticles were dispersed in DPBS under ultrasonication for 10 minutes to give a 1% dispersion. PEG-acetal-DMA and the photoinitiator were added as described above. 1 mL of the polymer- or polymer/vaterite-solution was transferred to a 24-well plate and the same volume of isopropanol was added to remove emerging air bubbles and to suppress capillary effects. The polymerization was initiated by 365 nm UV irradiation for 15 minutes.

**SBF incubation.** The obtained hydrogels were soaked in SBF (5 mL) and incubated at 37 °C in a shaking incubator (at 150 rpm) for 24 h to observe HCA-forming ability of vaterite-loaded hydrogels. Before further characterization the hydrogels were washed several times with water, frozen in liquid nitrogen, immediately fractured and lyophilized. Thus, the natural morphology of the swollen hydrogels was maintained.

**Sample characterization.**

The vaterite nanoparticles, HCA and the hydrogels were characterized by scanning and transmission electron microscopy (SEM, TEM), X-ray powder diffraction (XRD), fourier transform

infrared spectroscopy (FT-IR) and micro-Raman spectroscopy. The elemental compositions of the samples after SBF incubation were analyzed by using energy dispersive spectroscopy (EDS).

**Electron microscopy.** The surface morphology and internal structure of the samples before and after soaking in SBF were visualized by scanning electron microscopy (SEM) using a Nova NanoSEM 630 (FEI) at an acceleration voltage of 6 kV and a working distance from 4 to 5 nm. A low voltage high contrast detector (vCD) was used as secondary electron detector. All samples were prepared on a silicon-wafer (Si) and sputter-coated with 7.5 nm of gold (Au) to reduced charging of the sample. EDS was performed using an EDAX detector, an acceleration voltage of 30 kV. The samples were sputter-coated with 7.5 nm of silver (Ag) using a Bal-Tec, MED020 coater.

Transmission electron micrographs of vaterite nanoparticle powder and their converted HCA-powder were prepared by dispersing the powders in ethanol, placing a droplet onto a carbon-coated copper grid and drying at ambient temperature. The measurements were carried out by a Philips EM 420 electron microscope at an accelerating voltage of 120 kV.

**X-ray Diffraction (XRD).** Powder XRD patterns of the samples were obtained on a Bruker AXS D8 Discover diffractometer using Cu-K $\alpha$  ( $\lambda = 1.5405 \text{ \AA}$ ) radiation. XRD patterns were recorded in a  $2\theta$  range from  $5^\circ$  to  $80^\circ$  at ambient temperature. The powder samples of vaterite nanoparticles and the final HCA powders were prepared on a glass substrate by gentle pressing. The freeze-dried hydrogels were prepared as pellets at 5 bar for 30 minutes to obtain a smooth surface. The measurement proceeded across the entire surface of the pellet to ensure a random particle distribution. The XRD phase identification was performed using JCPDS standard XRD cards. Quantitative phase analysis was performed by full pattern profile fits according to establishes structure models ("Rietveld Refinement"). Reflection profiles were generated applying the fundamental parameter approach as implemented in TOPAS Academic V5.<sup>[44,45]</sup> The results are compiled in Table 1. Besides strain the crystallite size was the only sample (phase) dependent, refineable parameter for the profiles.

**Fourier-Transform Infrared (FT-IR) and Raman spectroscopy.** In order to identify the existence of functional groups (e.g. phosphate or carbonate) in the samples, Raman and FT-IR spectra were recorded. A Nicolet iS10 FT-IR spectrometer (Thermo Scientific) was used in the range from  $550$  to  $4000 \text{ cm}^{-1}$  with a resolution of  $4 \text{ cm}^{-1}$ . All Raman spectra were recorded using a Horiba Jobin Yvon LabRAM HR 800 spectrometer equipped with a CCD detector and an integrated Olympus



BX41 optical microscope using a 50 x magnification with a slit width of 100  $\mu\text{m}$ . Nd-YAG-Laser ( $\lambda = 632,817 \text{ nm}$ ). A spot size of 2 x 2  $\mu\text{m}$  was used for excitation. The Raman spectra were recorded in the range of 150-1600  $\text{cm}^{-1}$ .

**Table 1.** Results of the quantitative phase analysis based on the XRD data after soaking vaterite nanoparticles in SBF at 37 °C for 24 h, 48 h, and 72 h.

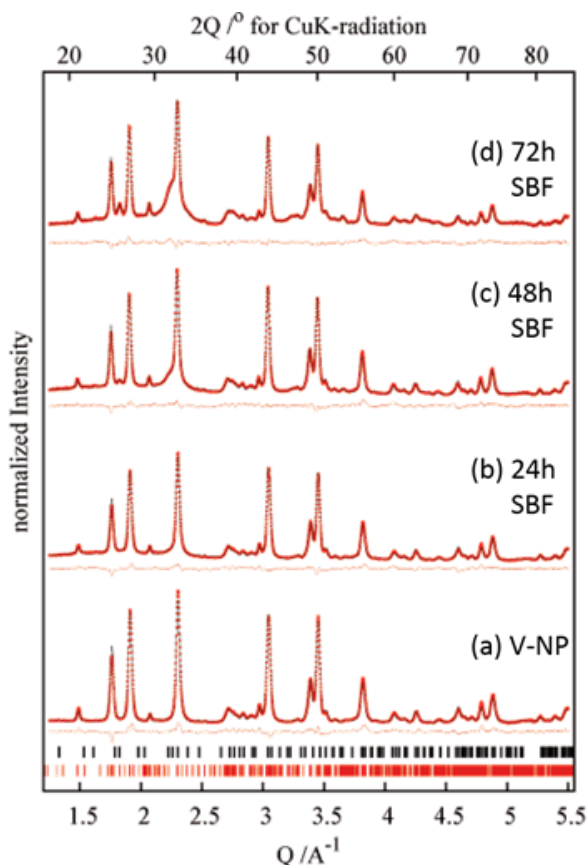
	Vaterite in SBF after 24 h	Vaterite in SBF after 48 h	Vaterite in SBF after 72 h
<b>Table 1</b> Results of the quantitative phase analysis based on the XRD data after soaking vaterite nanoparticles in SBF at 37 °C for 24 h 48 h and 72 h			
Diffractometer	Bruker AXS D8 Discover with HiStar		
Sample preparation	On a glass substrate by gently pressing		
Measuring mode	Reflection		
Wavelength	CuK $\alpha$ (graphite monochromatized)		
Measuring range	$5.7 \leq 2\theta^\circ \leq 86.6$ ; $0.48 \leq Q/\text{\AA}^{-1} \leq 5.59$		
Temperature/K	298		
Profile fit	Rietveld refinement according to reported crystal structure models		
Background	Chebyshev		
Profile function	Fundamental parameters approach, crystallite size anisotropy modeled in quadratic correction		
Program	TOPAS Academic V5		
Total no. of parameters/background	30/12	30/12	30/12
$R_{\text{wp}}$	5.36	6.05	4.56
GoF	0.68	0.77	0.59
DW	0.07	0.05	0.08
Biso (overall)	1.20(6)	1.35(8)	
<b>CaCO<sub>3</sub> Calcite</b>			
Space group	$R\bar{3}c$		
Cell parameters/\AA	$a = 4.996(2)$ $c = 17.042(8)$	$a = 4.996(2)$ $c = 17.047(9)$	$a = 4.995(2)$ $c = 17.051(8)$
Crystallite size/nm	55(4)	51(3)	44(2)
Mass fraction/%wt	1.9(1)	2.2(3)	2.9(1)
<b>CaCO<sub>3</sub> vaterite</b>			
Space group	$C\bar{1}$		
Cell parameters/\AA	$a = 12.359(1)$ $b = 7.1684(6)$ $c = 25.722(1)$ $\beta = 98.98(9)^\circ$	$a = 12.370(2)$ $b = 7.1678(9)$ $c = 25.763(1)$ $\beta = 99.47(1)^\circ$	$a = 12.359(2)$ $b = 7.164(1)$ $c = 25.704(2)$ $\beta = 98.95(2)^\circ$
Crystallite size/nm	37(1)	39(1)	39(3)
Mass fraction/wt%	93.4(3)	81.6(5)	60.8(8)
<b>Ca<sub>5</sub>(PO<sub>4</sub>)<sub>3</sub>OH hydroxy-apatite</b>			
Space group	$P6_3/m$		
Cell parameters/\AA	$a = 9.46(1)$ $c = 6.935(5)$	$a = 9.477(5)$ $c = 6.892(2)$	$a = 9.458(3)$ $c = 6.884(1)$
Crystallite size/nm	17(2) by 32(3)	15(1) by 30(1)	13(1) by 26(1)
Mass fraction/wt%	4.7(3)	16.2(5)	36.2(8)

**Swelling ratio (SR).** SRs at equilibrium of the obtained hydrogels were determined by gravimetry. The hydrogels were washed several times and swelled in DPBS or SBF, then dried by lyophilisation until constant weight was obtained. The dried gels were reimmersed in DPBS or SBF at 37 °C in a shaking incubator (150 rpm), and the weight of swollen hydrogels was measured in an equilibrium-swollen state. The swelling ratio was calculated according to

$$\text{SR} = \frac{m_w}{m_d} = \frac{m_s - m_d}{m_d} \quad (1),$$

where  $m_w$  is the amount of water absorbed by the gel,  $m_d$  is the mass of dried hydrogel and  $m_s$  is the mass of swollen hydrogel.<sup>[44]</sup>

**Adhesion molecule – enzyme immunoassay (CAM-EIA).** A CAM-EIA was used to analyze the amounts of E-selectin induced by the vaterite nanoparticles, PEG-acetal-DMA precursor and PEG-acetal-DMA hydrogels. The CAM-EIA was carried out as reported earlier.<sup>[47]</sup> This assay has a dual function in that an induction of E-selectin on the cells is an indicator of the presence of endotoxin, also known as lipopolysaccharid (LPS), or that the compounds administered have an inflammatory potential.

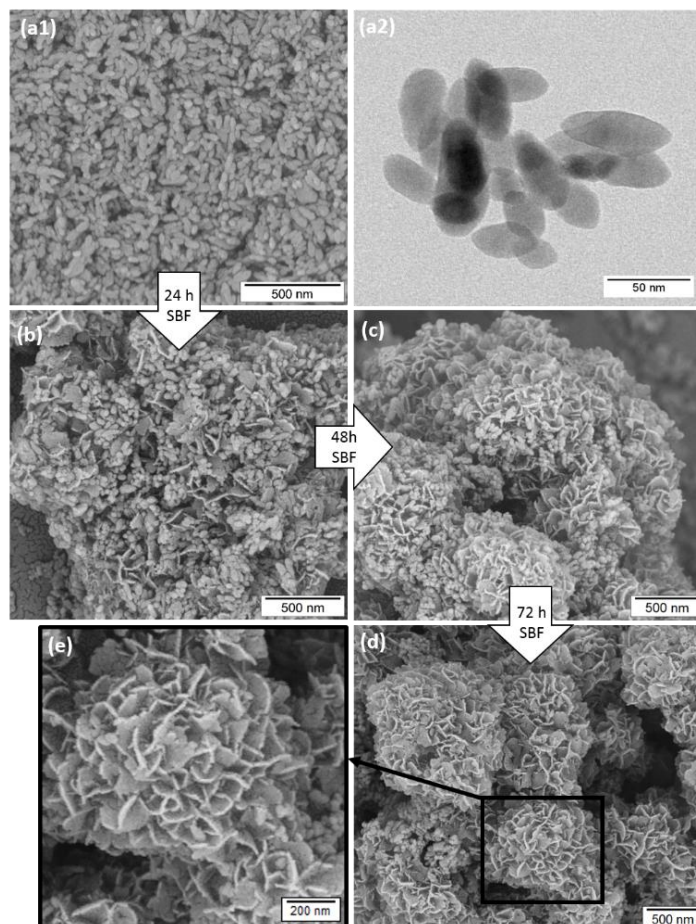


*Figure 1.* Quantitative phase analysis of the XRD data by profile analysis after soaking vaterite nanoparticles (V-NP) in SBF. Red dots are measured data, black lines correspond to the adjustment, the red lines show the difference. The red marks indicate vaterite (JCPDF 33-0268). the black marks indicate hydroxyapatite (JCPDF 1-084-1998).

## Results and Discussion

**Transformation of vaterite-nanoparticles to HCA.** Vaterite nanoparticles (V-NP) were obtained by ultrasonication of a solution of  $\text{CaCl}_2 \cdot 4\text{H}_2\text{O}$  and  $\text{NaHCO}_3$  in ethylene glycol. The precipitate remains nanocrystalline because the dispersant is only weakly coordinating. Fig. 1 shows XRD patterns, SEM (Fig. 2a1) and TEM images (Fig. 2a2) of the vaterite nanoparticles. XRD analysis shows that

vaterite is the predominant  $\text{CaCO}_3$  phase with traces of calcite. SEM and TEM images show vaterite nanoparticles with a typical ellipsoidal shape and dimensions of approximately  $25 \times 50 \text{ nm}$ .<sup>[20]</sup>



*Figure 2.* SEM and TEM images (a1, a2) before and after soaking vaterite nanoparticles in SBF at  $37^\circ\text{C}$  for (b) 24 h, (c) 48 h and (d) 72 h. (e) Magnified SEM image of the corresponding surface, showing plate-shaped agglomerates consisted of plate-like HCA nanocrystals.

The vaterite nanoparticles were immersed in SBF to assess their *in vitro* bone-like HCA forming ability. Fig. 1 shows the results after 24 h, 48 h and 72 h of immersion in SBF. The XRD patterns show additional reflections at  $2\theta \sim 26^\circ$  and  $2\theta \sim 32^\circ$  due to formation of HCA.<sup>[48,49]</sup> With longer immersion time these intensities increase. The mass fraction (%wt) of vaterite, HA and calcite were determined by quantitative phase analysis of XRD data. The results are compiled in Table 1 and 2. Fig. 3 shows the mass fractions of vaterite, HA and calcite as a function of incubation time in SBF. SEM images show significant morphological changes after time passages of 24 h, 48 h and 72 h (Fig. 2b-e). Vaterite remains stable at ambient temperature as long as water is completely eliminated from the environment, for ex-ample, in a desiccator or in ethanol.

Table 2. Results of the quantitative phase analysis of the XRD data after 24 h, 48 h and 72 h incubation of vaterite in SBF.

Incubation time / h	vaterite / %wt	HA / %wt	calcite / %wt
24	93,4(3)	4,7(3)	1,9(1)
48	81,6(5)	16,2(5)	2,2(3)
72	60,8(8)	36,2(8)	2,9(1)

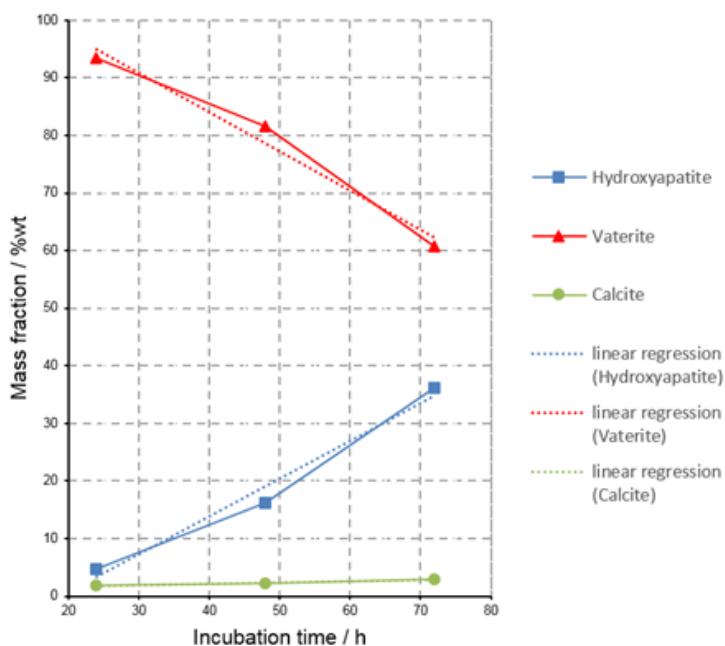


Figure 3. Phase composition from XRD data as a function of incubation time in SBF.

Plate-like nanocrystals were formed in increasing amounts in SBF and self-assembled to plate-shaped agglomerates with typical HCA morphology.<sup>[50,51]</sup> The basic building blocks of these aggregates are nano-plates with sizes of 26-32 nm in length and 13-17 nm in width as determined by profile analysis of the X-ray diffractograms and image analysis (see Fig. 4 and Table 3). The decreasing particle size with incubation time may be explained as follows. The density of a highly crystalline sample is higher than that of a sample with low crystallinity. During incubation there is no additional crystal growth any more, only the crystallinity of the crystallites increases. As the crystallite size is confined, the reorganization of the crystallites leads to a compactization, i.e. an increasing density through a transport of material/ions from the rim to the core of the particles. Therefore, the crystallite size decreases as confirmed by the Rievelde refinement.

*Table 3.* Results of the crystallite size determination of HA by profile analysis of XRD data after 24 h, 48 h and 72 h incubation of vaterite in SBF.

Incubation time / h	length of HA / nm	width of HA / nm
24	32(3)	17(2)
48	30(1)	15(1)
72	26(1)	13(1)

EDS analysis of the agglomerates shows the presence of C, O, Ca and P (Fig. 4). The relative stability and large size of the HCA aggregates enabled us to observe details of the transformation mechanism, which resulted in flower-like aggregates of HCA.

The topography of the resulting particles was found to consist of aggregated nanoplates, the individual plates having a similar size as the original vaterite nanoparticles (Fig. 2b-e). This change in morphology indicates a change in the dissolution-crystallization process as crystal growth proceeds. In the second phase of crystal growth, the ion reservoir from the vaterite precursor migrates and crystallizes as discrete entities on the growing HCA crystal, i.e. the plate-like HCA forms by secondary nucleation on top of the vaterite nanoparticles (Fig. 2b-e). After about 72 h the transformation was complete approx. 40% of the vaterite was consumed by the growing HCA crystals. The crystallinity increases with time. The crystal surfaces were composed of irregularly pitted (001) faces. This surface texture implies that the growth of the HCA crystals occurs through particle aggregation. We assume that  $\text{Ca}^{2+}$  and  $\text{CO}_3^{2-}$  ions are released by dissolution of the vaterite nanoparticles upon immersion in SBF. Consequently a high local  $\text{Ca}^{2+}$  concentration is observed above the supersaturation point, which includes HCA nucleation on the vaterite surface in SBF. The transformation of vaterite to HCA with time was analyzed by TEM “snap-shots”. Fig. 5 shows vaterite nanoparticles after soaking in SFB for 24 h (b) and 72 h (c).

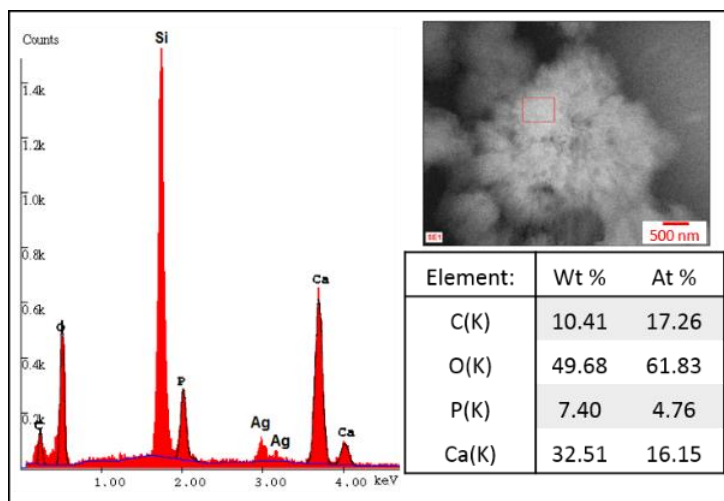


Figure 4. EDS spectrum of the HCA agglomerates showing the presence of C, O, P and Ca after incubating vaterite nanoparticles for 72 h in SBF. The Si and Ag signals were obtained due to the sample preparation.

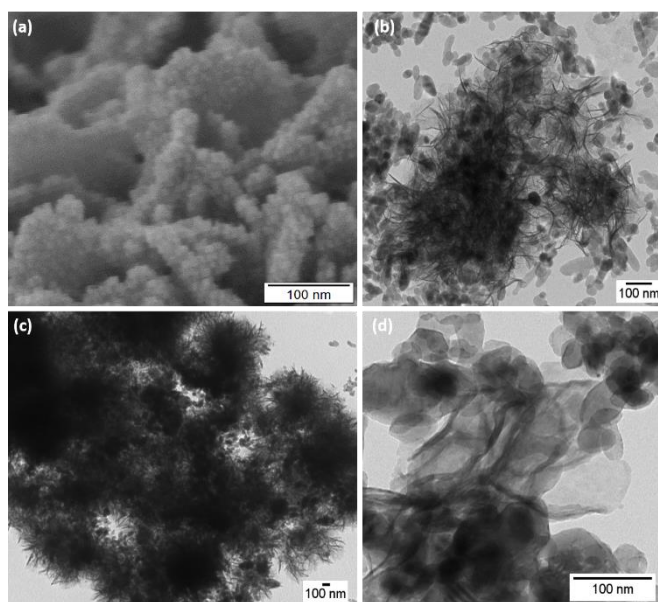
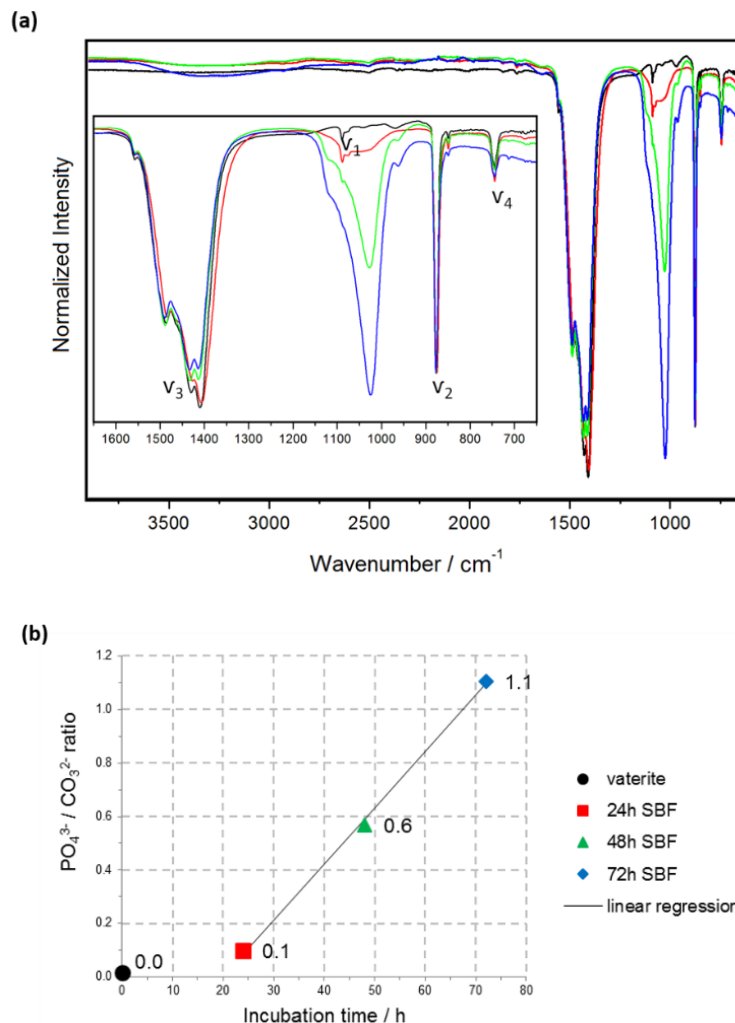


Figure 5. (a) Magnified SEM image, showing plate-shaped agglomerates consisted of plate-like nanocrystals after 72 h of incubation in SBF. (b) TEM image HCA agglomerates after 24 h and (c) 72 h of incubation in SBF. (d) Magnified TEM image of a plate-like HCA layer on top of the vaterite nanoparticles.

The presence of phosphate groups in the converted plate-shaped HCA was confirmed using FT-IR and Raman spectroscopy (Fig. 5a and Fig. 6). All FT-IR spectra of vaterite before and after soaking in SBF show the typical vibrational frequencies of the  $\text{CO}_3^{2-}$  ion. All bands in the range from  $1487\text{ cm}^{-1}$  to  $1411\text{ cm}^{-1}$  are assigned to the antisymmetric  $\nu_3$  stretching mode, the band at  $877\text{ cm}^{-1}$  corresponds to  $\nu_2$  mode (out-of-plane bending motion). The band at  $744\text{ cm}^{-1}$  corresponds to the

v4 mode (in-plane bending motion), and the band at  $1089\text{ cm}^{-1}$  corresponds to v1 symmetric stretching mode.<sup>[51]</sup>



*Figure 6.* (a) FT-IR spectra before (black) and after soaking vaterite nanoparticles in SBF at  $37\text{ }^\circ\text{C}$  for 24 h (red), 48 h (green) and 72 h (blue) including the four vibrational frequencies of  $\text{CO}_3^{2-}$  ion ( $\nu_1$ ,  $\nu_2$ ,  $\nu_3$  and  $\nu_4$ ) and normalized to  $\nu_2$ . (b)  $\text{PO}_4^{3-} / \text{CO}_3^{2-}$  ratio as a function of SBF incubation period calculated from the intensity of the FT-IR bands of the antisymmetric stretching mode of  $\text{PO}_4^{3-}$  group and the  $\nu_3$  vibration of the  $\text{CO}_3^{2-}$  group.

The  $\nu_1$  frequency of vaterite is the most intense signal of the Raman spectrum (Fig. 7, black) and shows a typical triplet in the region between  $1075\text{ cm}^{-1}$  and  $1089\text{ cm}^{-1}$ .<sup>[52]</sup> In addition to the vibrations of the  $\text{CO}_3^{2-}$  group bands with increasing intensities at  $963\text{ cm}^{-1}$  and at  $1024\text{ cm}^{-1}$  were observed during incubation in SBF, which were as-signed to the non-degenerate symmetric ( $963\text{ cm}^{-1}$ ) and the triply de-generate antisymmetric P-O stretching modes ( $1024\text{ cm}^{-1}$ ) of the phosphate group.<sup>[53,54]</sup> The simultaneous presence of the characteristic  $\text{CO}_3^{2-}$  and  $\text{PO}_4^{3-}$  bands indicates that the vaterite nanoparticles transformed to spherical HCA agglomerates. Fig. 7b

shows the ratio of the  $\text{PO}_4^{3-}$  to the  $\text{CO}_3^{2-}$  groups as a function of incubation time in SBF based on the intensity of FT-IR bands of the antisymmetric stretching mode of  $\text{PO}_4^{3-}$  group and the  $\nu_3$  vibration of the  $\text{CO}_3^{2-}$  group. As a result the  $\text{PO}_4^{3-}/\text{CO}_3^{2-}$  ratio increases linearly with incubation time in SBF, up to a 1:1 ratio after 72 h. The absorption bands at  $1487\text{ cm}^{-1}$ ,  $1411\text{ cm}^{-1}$  and especially at  $877\text{ cm}^{-1}$  correlate to type B HCA as found in bone mineral, where the carbonate ions substitute for phosphate ions.<sup>[55,56]</sup> After 72 h of incubation in SBF the Raman spectrum (Fig. 7, blue) shows also a characteristic signal at  $962\text{ cm}^{-1}$  for the nondegenerated symmetric stretch of the P-O bond of the phosphate group. In addition, weak signals of the phosphate group are detected at  $447\text{ cm}^{-1}$  (doubly degenerate O-P-O bending mode),  $594\text{ cm}^{-1}$  (triply degenerate O-P-O bending mode) and  $1040\text{ cm}^{-1}$  (triply degenerate asymmetric P-O stretching mode).<sup>[51]</sup> The band position at  $962\text{ cm}^{-1}$  indicates the presence of highly crystalline phosphate apatite, but the full width at half maximum (FWHM) indicates smaller and unordered crystallites due to carbonate substitution of phosphate.<sup>[57]</sup>

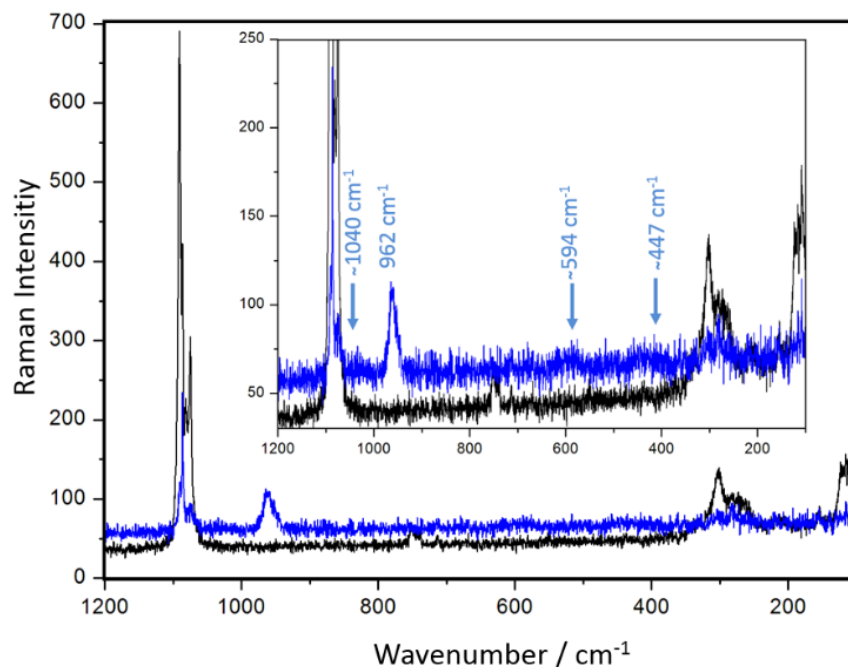


Figure 7. Raman spectra before (black) and after (blue) 72 h of incubation in SBF.

#### Transformation of vaterite nanoparticles to HCA in PEG-acetal-DMA hydrogel

For using vaterite nanoparticles as bone grafting biomaterial a three-dimensional scaffold is necessary, including a high water content and a physicochemical similarity to natural extracellular matrices (ECM). We used a biodegradable PEG-acetal-DMA hydrogel as support for three-dimensional scaffolding. 10% PEG-acetal-DMA hydrogels containing vaterite nanoparticles were



obtained via polymerization initiated by UV-radiation at 365 nm for 15 minutes. The analytical results concerning the structural properties of the hydrogels at the equilibrium swelling ratio are compiled in Table 4. The equilibrium swelling state was achieved after 24 h of immersion of the hydrogels in DPBS as well as in SBF. The vaterite incorporated hydrogels showed almost the same swelling behavior in DPBS as vaterite-free hydrogels, but the immersion in SBF showed clear differences. The swelling ratio in SBF decreased from vaterite-free to vaterite-loaded hydrogels. This may be caused by the limited flexibility of the PEG-acetal-DMA polymer chains, which are partly coordinated to the vaterite nanoparticles, and especially by ion-dipole interactions to the salts of SBF. The salt content in SBF is much higher than in DPBS. Through these interactions the water absorption capacity is reduced, and therefore the swelling behavior is limited. A decreased swelling ratio of the vaterite-loaded hydrogel in SBF leads to a smaller increase in size of the hydrogel, which renders them suitable for biomedical applications in which the implant should not increase significantly in size.

*Table 4.* Swelling ratio (SR) after 24 h of immersion in DPBS and SBF determined for 10% PEG-acetal-DMA hydrogels (HG), without vaterite or containing 1% of vaterite nanoparticles (+V).

Sample	SR (DPBS)	SR (SBF)
PEG-acetal-DMA HG	10.2 ± 0.5	11.2 ± 0.6
PEG-acetal-DMA HG + V	10.2 ± 0.2	9.2 ± 0.7

Fig. 8 shows digital photographs of the swollen (A) vaterite-free and (B) vaterite-loaded PEG-acetal-DMA hydrogels after 24 h of incubation in DPBS and SBF. The milky clouding of the vaterite-loaded hydrogels result from the incorporation of vaterite nanoparticles in the three dimensional network of PEG-acetal-DMA precursors. The distribution of the vaterite nanoparticles in PEG-acetal-DMA hydrogels is not homogeneous, due to the sedimentation of the vaterite nanoparticles during photopolymerization of the hydrogel, which may be an advantage for applications as hard tissue regenerating material. Our hydrogels show two different sides with different physiological properties. The top side contains vaterite nanoparticles with high transformation ability to HCA, which is osteoconductive and similar to the apatite in living bone. The bottom side contains vaterite-free hydrogel, which may act as an extracellular matrix that stimulates cell proliferation and natural bone regeneration.

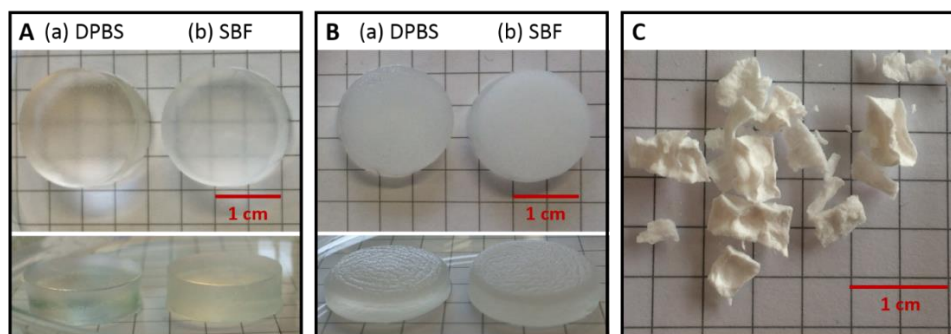
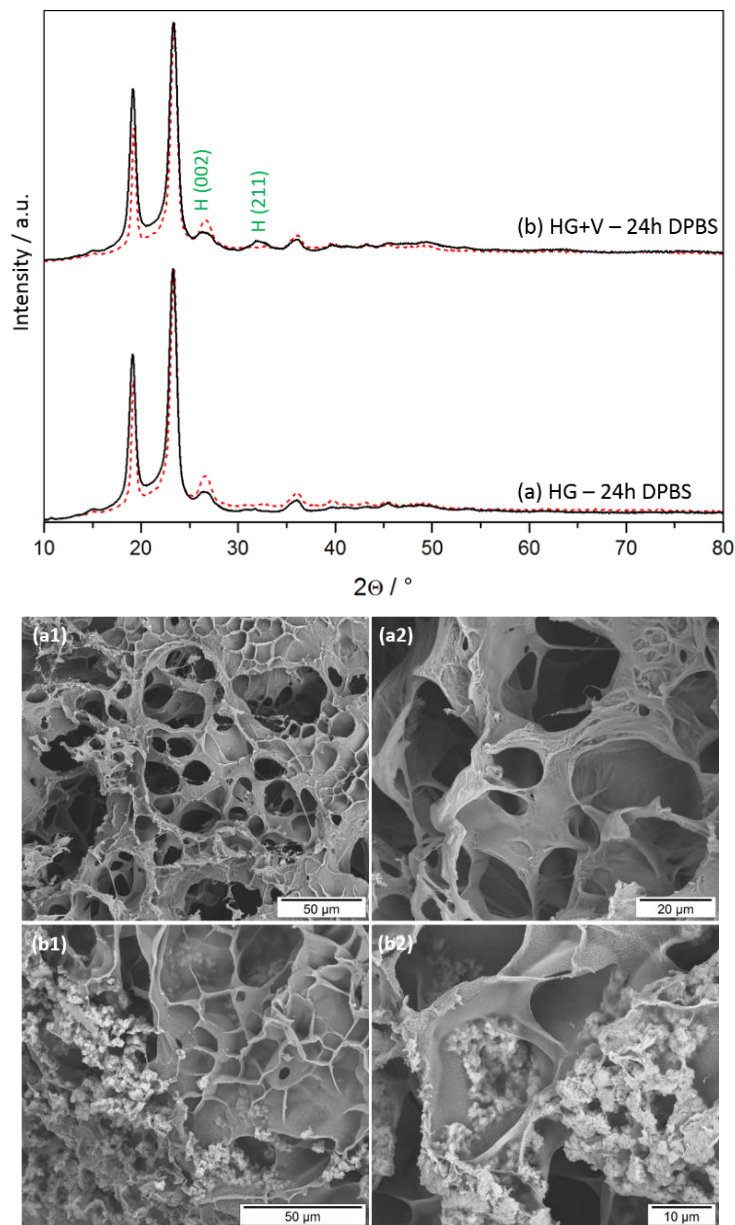


Figure 8. Digital images of swollen PEG-acetal-DMA hydrogels (A) with-out vaterite nanoparticles and (B) with vaterite-nanoparticles in (a) DPBS and (b) SBF and (C) pieces of lyophilized PEG-acetal-DMA hy-drogel without vaterite-nanoparticles.

### Morphology and characterization of the prepared PEG-acetal-DMA hydrogels

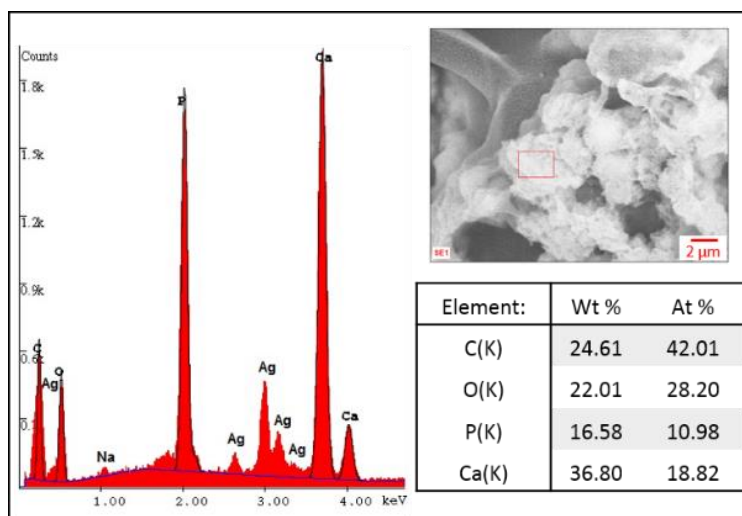
The morphology and mineralization ability of vaterite-free and vaterite-loaded PEG-acetal-DMA hydrogels were analyzed on lyophilized samples (see Fig. 8C) of the corresponding hydrogel. We analyzed the *in vitro* (bone-like) HCA generating ability of vaterite-loaded hydrogels after soaking in DPBS and SBF by XRD (Fig. 9 and 11) and SEM. In both cases, after 24 h of incubation in DPBS and SBF, we found chemically inert vaterite-free hydrogels showing the characteristic reflections of the PEG-acetal-DMA precursor. In comparison, the XRD patterns of vaterite-loaded hydrogels showed additional broad signals at  $2\theta \sim 26^\circ$  and  $2\theta \sim 32^\circ$  after soaking for 24 h in DBPS and SBF, which were assigned to HCA (similar as for the vaterite-nanoparticles). The characteristic reflections of vaterite could no longer be detected. This indicates a complete transformation of the vaterite nanoparticles into HCA within the PEG-acetal-DMA hydrogels after 24 h incubation in DPBS as well as in SBF. This can be rationalized from the well-known reactivity of vaterite even in the presence of water traces.<sup>[19,20,22]</sup>



*Figure 9.* (Top) XRD patterns of PEG-acetal-DMA precursor, vaterite-free (HG) and vaterite-loaded PEG-acetal-DMA hydrogel (HG+V) after immersion in DPBS for 24 h. H indicates hydroxyapatite (JCPDF 1-084-1998). The diffraction pattern of the polymer is indicated by the dashed line. (Bottom) the corresponding SEM images of lyophilized (a1-a2) vaterite-free and (b1-b2) vaterite-loaded PEG-acetal-DMA hydrogels after immersion in DPBS for 24 h.

SEM images in Fig. 9 and 11 show (a1-a2) characteristic meshes of a three-dimensional polymer network. After soaking vaterite-loaded hydrogels in DPBS (Fig. 8b1-b2) and in SBF (Fig. 11b1-b2) for 24 h we observed plate-like agglomerates on the polymer surface (similar as before for the reaction of vaterite nanoparticles). EDS analysis of these agglomerates indicated the presence of C, O, Ca and P (Fig. 10 and 12). After soaking vaterite-loaded hydrogels in DPBS for 24 h a Ca:P ratio of 1.7 was obtained, whereas soaking of the hydrogels in SBF resulted to a Ca:P ratio of 1.4.

Calcium-deficient hydroxyapatite (a precursor of HCA) is known to have Ca:P ratios between 1.5 and 1.65.<sup>58</sup> In addition, we detected small amounts of Na as well as Mg after incubation in SBF (similar as in natural inorganic bone material).<sup>[58]</sup>

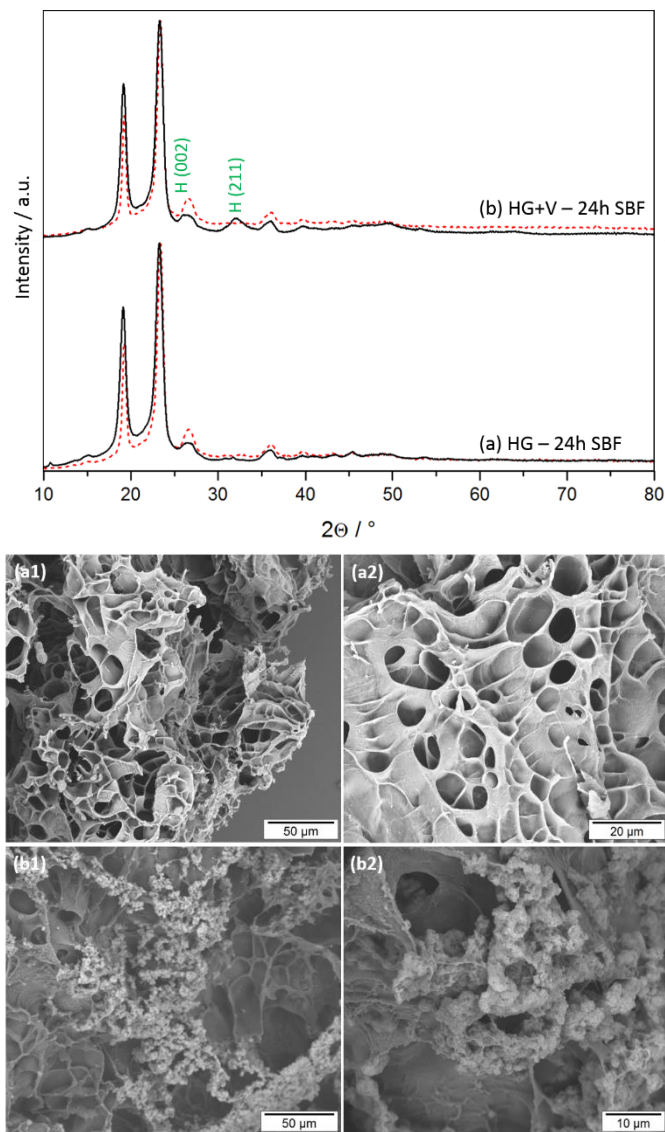


*Figure 10.* EDS spectra of the incorporated plate-like agglomerates after 24 h of incubating vaterite-loaded hydrogels in PBS, showing the presence of C, O, P and Ca. The Si and Ag signals were obtained due to the sample preparation.

The presence of phosphate groups of the resulting plate-like HCA was confirmed by FT-IR and Raman spectroscopy (Fig. 13 and 14). After 24 h of incubation in DPBS or SBF the FT-IR spectra of vaterite-loaded hydrogels showed the characteristic bands of the PEG-acetal-DMA precursor and a new band at  $1033\text{ cm}^{-1}$ , which corresponds to the triply degenerate antisymmetric stretching mode of the phosphate group (marked with a red arrow).

Additional bands in the Raman spectra were observed after 24 h of incubation in DPBS as well as SBF. The strong band at  $962\text{ cm}^{-1}$  corresponds to non-degenerate symmetric P-O stretching mode, while the weak band at  $440\text{ cm}^{-1}$  corresponds to a doubly degenerate O-P-O bending mode of the phosphate group (marked with a red arrow). The transformation of vaterite nanoparticles to HCA within the hydrogel scaffold proceeds significantly faster than for free vaterite. After soaking vaterite-loaded hydrogels in both, DPBS and SBF, media for 24 h no characteristic XRD reflections or IR and Raman bands could be detected, which indicates a complete transformation of vaterite to HCA within this period. The rapid transformation in the PEG-acetal-DMA hydrogel may be attributed to the larger surface due to the compartmentalization in the gel and presence of functional carbonyl groups. Functional groups have been reported to interact with the dissolved calcium ions of vaterite and thus the nucleation of HCA is induced or rather accelerated.<sup>[59,60]</sup> The incorporation of smaller amounts (1%, w/v) vaterite nanoparticles in PEG-acetal-DMA hydrogels

changed mineralization behavior dramatically. In the absence of vaterite particles there is no mineralizing activity after 24 h, and the hydrogels remain chemically inert.



*Figure 11.* (Top) XRD patterns of PEG-acetal-DMA precursor, vaterite-free (HG) and vaterite-loaded PEG-acetal-DMA hydrogel (HG+V) after immersion in SBF for 24 h. H indicates hydroxyapatite (JCPDF 1-084-1998). The diffraction pattern of the polymer is indicated by the dashed line. (Bottom) the corresponding SEM images of lyophilized (a1-a2) vaterite-free and (b1-b2) vaterite-loaded PEG-acetal-DMA hydrogels after immersion in SBF for 24 h.

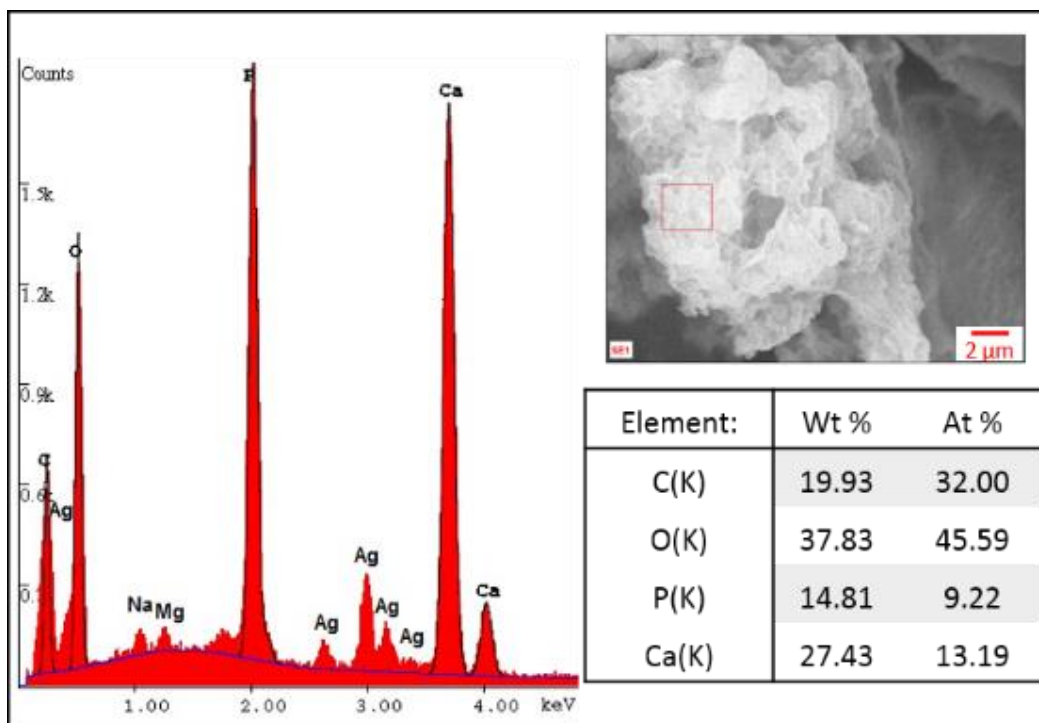


Figure 12. EDS spectra of the incorporated plate-like agglomerates after 24 h of incubating vaterite-loaded hydrogels in SBF, showing the presence of C, O, P and Ca. The Si and Ag signals are due to the sample preparation.

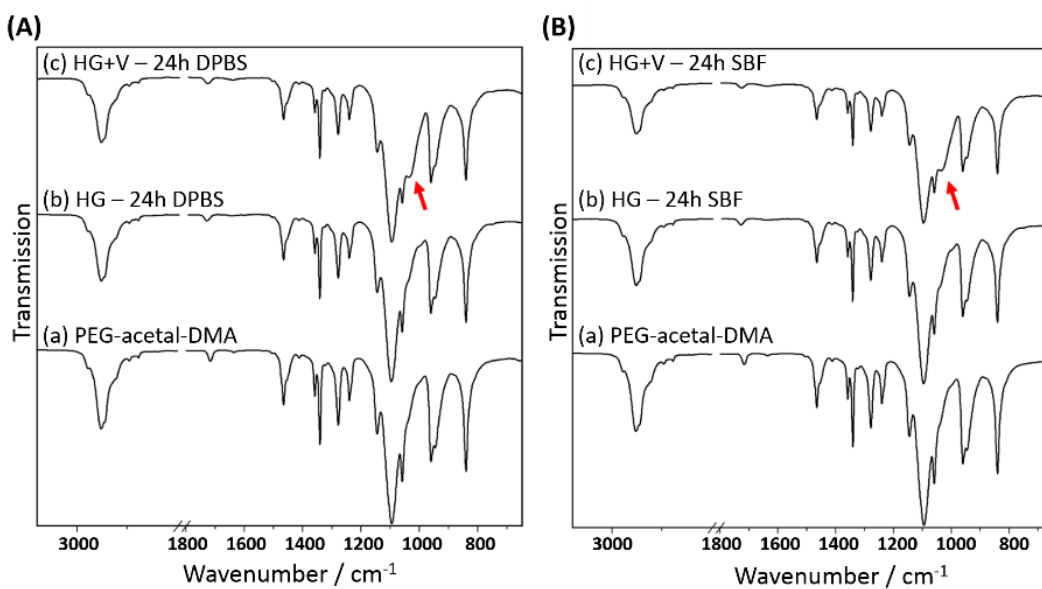


Figure 13. FT-IR spectra of (a) PEG-acetal-DMA precursor, (b) vaterite-free and (c) vaterite-loaded PEG-acetal-DMA hydrogels after soaking in (A) DPBS and (B) SBF for 24 h.

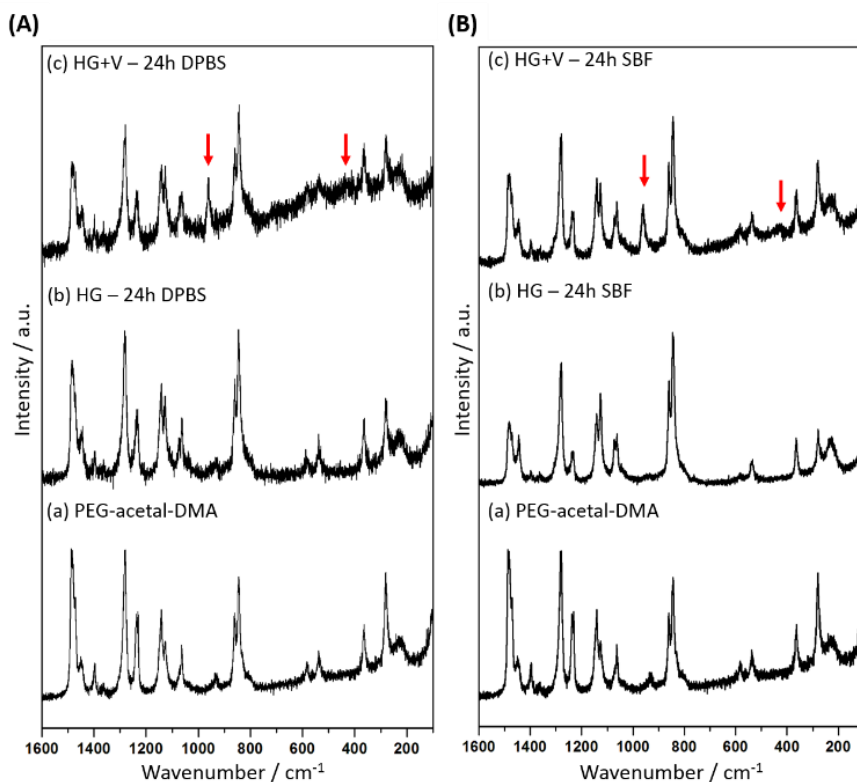


Figure 14. Raman spectra of PEG-acetal-DMA precursor (a), vaterite-free (b) and vaterite-loaded (c) PEG-acetal-DMA hydrogels after soaking in (A) DPBS and (B) SBF for 24 h.

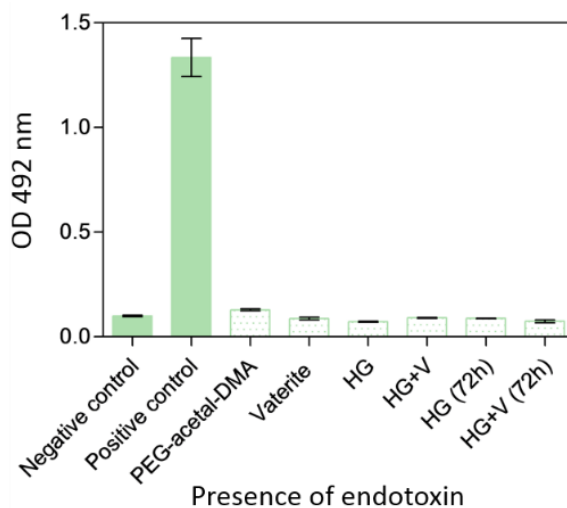


Figure 15. Results of the CAM-EIA method, containing unstimulated HUVEC (negative control), 1  $\mu\text{g}/\text{mL}$  LPS stimulated HUVEC (positive control) and HUVEC which were stimulated with vaterite nanoparticles, PEG-acetal-DMA precursor and PEG-acetal-DMA hydrogels (HG) containing or not vaterite nanoparticles (V) directly after photopolymerization and also after 72 h incubation in medium M199 (Sigma-Aldrich, Steinbach, Germany) + 20% FCS (Life Technologies, Karlsruhe, Germany) + 2 mM Glutamax I (Life Technologies) + 100 U/100  $\mu\text{g}/\text{mL}$  Pen/Strep + 25  $\mu\text{g}/\text{mL}$  sodium heparin (Sigma Aldrich) + 25  $\mu\text{g}/\text{mL}$  endothelial growth factor supplement (ECGS, Becton Dickinson, Bradford, MA).

## Conclusions

We have demonstrated a promising alternative for the use of biodegradable nanoparticles with potential bone targeting capability based on a multi-functional PEG hydrogel loaded with vaterite nanoparticles as (Ca<sup>2+</sup> cation) mineral. Vaterite, the least stable CaCO<sub>3</sub> polymorph, is inherently labile to ensure the presence of a potential ion buffer for bone regeneration, but still has sufficient reactivity for the required transformation of CaCO<sub>3</sub> to hydroxycarbonate apatite. A combination of powder X-ray diffraction (PXRD), electron microscopy, and FT-IR and Raman spectroscopy showed the transformation of vaterite nanoparticles incorporated in a PEG-acetal-DMA hydrogel to hydroxycarbonate apatite crystals with low crystallinity upon incubation in simulated body fluid at human body temperature. XRD and FTIR/Raman data also showed that the hydrogel plays an important role in the transformation process. The transformation of the vaterite nanoparticles to HCA in the PEG-acetal-DMA hydrogel scaffold proceeded significantly faster than for free vaterite, which clearly shows that the hydrogel actively controlled the transformation process within the gel. This might be explained by the larger surface area (i) due to the compartmentalization in the gel, (ii) the smaller diffusion distances in the gel compartments and (iii) presence of functional carbonyl groups. FTIR data revealed chemical interactions between the hydrogel and the mineral phase, which may be assigned to complexation of exposed the Ca<sup>2+</sup> surface ions through the carbonyl groups in the hydrogel, which have been postulated to interact with Ca<sup>2+</sup> ions of the CaCO<sub>3</sub> particle surface that aid or accelerate the nucleation of HCA.<sup>[59,60]</sup>

Using the combination of vaterite nanoparticles with a hydrogel simulate the inorganic and the organic components of natural bone, including the two main characteristics – hardness (of HCA after transformation of vaterite nanoparticles in SBF) and elasticity (of the polymer strands). An interesting aspect of the used PEG-acetal-DMA hydrogel is their biodegradability by cleavage of the acetal units to excretable PEG segments. Thus, the hydrogel would not remain permanently in the body, but rather serves as a porous three dimensional scaffold offering the ingrowth of blood vessels and bone-forming cells for regeneration of new bone tissue. The vaterite-containing hydrogels were evaluated and shown to be free of endotoxin and to exhibit no inflammatory potential. This may have prospects for future applications in the treatment of bone defects and bone degenerative diseases. The results presented in this work demonstrate important aspects of hydrogel-controlled crystallization, which contributes to the understanding of composite material design.



## Acknowledgements

This research was partially supported by the Deutsche Forschungsgemeinschaft (DFG) within the priority program 1415 “Crystalline Non-Equilibrium Phases”. The facilities of the Electron Microscopy Center in Mainz (EZMZ) were supported by the State Cluster of Excellence COMATT and the SFB 625.

## References

- [1] Boskey, A. L.; Coleman, R., Aging and Bone. *J. Dent. Res.* **2010**, *89*, 1333-1348.
- [2] Weiner, S.; Traub, W.; Wagner, H. D., Lamellar Bone: Structure–Function Relations. *J. Struct. Biol.* **1999**, *126*, 241-255.
- [3] Fratzl, P.; Weinkamer, R., Nature’s hierarchical materials. *Prog. Mater. Sci.* **2007**, *52*, 1263-1334.
- [4] Amini, A. R.; Laurencin, C. T.; Nukavarapu, S. P., Bone tissue engineering: recent advances and challenges. *Crit. Rev. Biomed. Eng.* **2012**, *40*, 363-408.
- [5] Zhu, J.; Marchant, R. E., Design properties of hydrogel tissue-engineering scaffolds. *Exp. Rev. Med. Dev.* **2011**, *8*, 607-626.
- [6] Wensch, S.; Stahl, J. P.; Horas, U.; Heiss, C.; Kilian, O.; Trinkaus, K., In vivo mechanisms of hydroxyapatite ceramic degradation by osteoclasts: fine structural microscopy. *J. Biomed. Mater. Res. A* **2003**, *67*, 713–718.
- [7] Fratzl, P.; Fischer, F. D.; Svoboda, J.; Aizenberg, J., A kinetic model of the transformation of a micropatterned amorphous precursor into a porous single crystal. *Acta Bio-mater.* **2010**, *6*, 1001-1005.
- [8] Natalio, F.; Coralles, T.; Panthöfer, M.; Lieberwirth, I.; Schollmeyer, D.; Müller, W.E.G.; Kappl, M.; Butt, H.-J.; Tremel, W., Flexible minerals: self-assembled calcite spicules with extreme bending strength. *Science* **2013**, *339*, 1298-1302.
- [9] Posner, S.; Betts, F.; Blumenthal, N. C., Formation and structure of synthetic and bone hydroxyapatites. *Progr. Cryst. Growth Char.* **1980**, *3*, 49-64.
- [10] Eanes, D.; Termine, J. D.; Nysten, M. U., An electron microscopic study of the formation of amorphous calcium phosphate and its transformation to crystalline apatite. *Calcif. Tissue Res.* **1973**, *12*, 143-158.
- [11] Wang L.; Nancollas, G. H., Calcium orthophosphates: crystallization and dissolution. *Chem. Rev.* **2008**, *108*, 4628–4669.
- [12] Weiner, S., Transient precursor strategy in mineral formation of bone. *Bone* **2006**, *39*, 431-433.
- [13] Olszta, M. J.; Odom, D. J.; Douglas, E. P.; Gower, L. B., A new paradigm for biomineral formation: mineralization via an amorphous liquid-phase precursor. *Connect. Tiss. Res.* **2003**, *44*, 326-334.

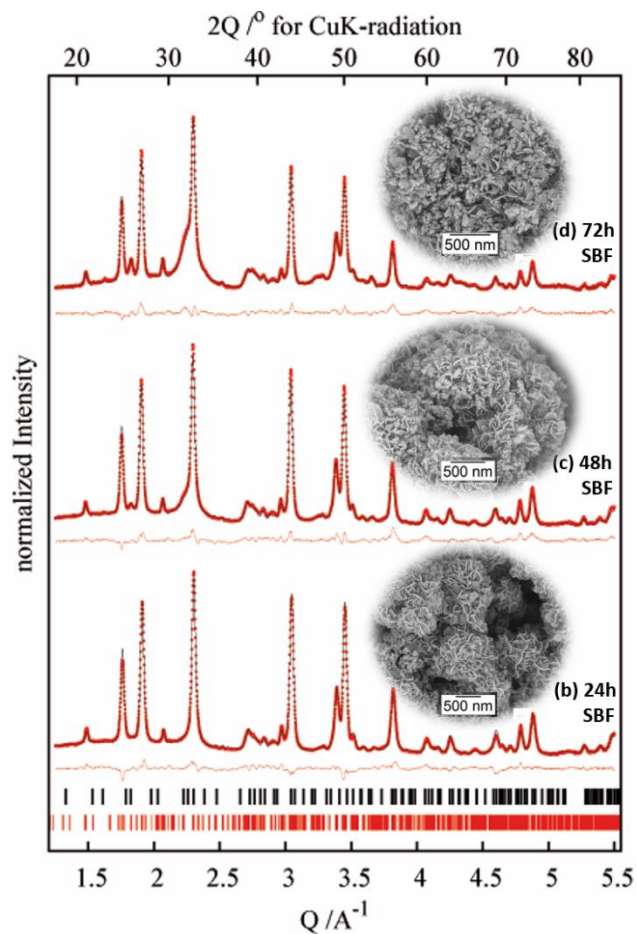
- [14] Tsuji, T.; Onuma, K.; Yamamoto, A.; Iijima, M.; Shiba, K., ect transformation from amorphous to crystalline calcium phosphate facilitated by motif-programmed artificial proteins. *Proc. Natl. Acad. Sci. U. S. A.* **2008**, 105, 16866-16870.
- [15] Mahamid, J.; Aichmayer, B.; Shimoni, E.; Ziblat, R.; Li, C.; Siegel, S.; Paris, O.; Fratzl, P.; Weiner, S.; Addadi, L., Mapping amorphous calcium phosphate transformation into crystalline mineral from the cell to the bone in zebrafish fin rays. *Proc. Natl. Acad. Sci. U. S. A.* **2010**, 107, 6316-6321.
- [16] Hu, Y.-Y.; Rawal, A.; Schmidt-Rohr, K., Strongly bound citrate stabilizes the apatite nanocrystals in bone. *Proc. Natl. Acad. Sci. U. S. A.* **2010**, 107, 22425–22429.
- [17] Xie B.; Nancollas, G.H., How to control the size and morphology of apatite nanocrystals in bone. *Proc. Natl. Acad. Sci. U. S. A.* **2010**, 107, 22369-22370.
- [18] Delgado-López, J. M.; Iafisco, M.; Rodríguez, I.; Tampieri, A.; Prat, M.; Gómez-Morales, J., Crystallization of bioinspired citrate-functionalized nanoapatite with tailored carbonate content. *Acta Biomater.* **2012**, 8, 3491–3499.
- [19] Gower, L. B., Biomimetic model systems for investigating the amorphous precursor pathway and its role in biomineralization. *Chem. Rev.* **2008**, 108, 4551-4627.
- [20] Schüller T.; Tremel, W., Versatile wet-chemical synthesis of non-agglomerated CaCO<sub>3</sub> vaterite nanoparticles. *Chem. Commun.* **2011**, 47, 5208-5210.
- [21] Mugnaioli, E.; Andrusenko, I.; Schüller, T.; Loges, N.; Panthöfer, M.; Tremel, W.; Kolb, U., Ab initio structure determination of vaterite by automated electron diffraction. *Angew. Chem. Int. Ed.* **2012**, 51, 7041-7045.
- [22] Schüller, T.; Renkel, J.; Hobe, S.; Susewind, M.; Panthöfer, M.; Jakob, D.; Hoffmann-Röder, A.; Paulsen, H.; Tremel, W., Designed peptides for biomineral polymorph recognition: a case study for calcium carbonate. *J. Mater. Chem. B* **2014**, 2, 3511-3518.
- [23] Wallace D. G.; Rosenblatt, J., Collagen gel systems for sustained delivery and tissue engineering. *Adv. Drug Deliv. Rev.* **2003**, 55, 1631–1649.
- [24] Tlatlik, H.; Simon, P.; Kawska, A.; Zahn, D.; Kniep, R., Biomimetic Fluorapatite–Gelatin Nanocomposites: Pre-Structuring of Gelatin Matrices by Ion Impregnation and Its Effect on Form Development. *Angew. Chem. Int. Ed.* **2006**, 45, 1905-1910.
- [25] Xie, M.; Olderøy, M. Ø.; Andreassen, J.-P.; Selbach, S. M.; Strand, B. L.; Sikorski, P., Alginate-controlled formation of nanoscale calcium carbonate and hydroxyapatite mineral phase within hydrogel networks. *Acta Biomaterialia* **2010**, 6, 3665–3675.
- [26] Kniep R.; Simon, P., “Hidden” Hierarchy of Microfibrils within 3D-Periodic Fluorapatite–Gelatin Nanocomposites: Development of Complexity and Form in a Biomimetic System. *Angew. Chem. Int. Ed.* **2008**, 47, 1405-1409.
- [27] Liu, X.; Ma, L.; Mao, Z.; Gao, C., Chitosan-based biomaterials for tissue repair and regeneration. *Adv. Polym. Sci.* **2011**, 244, 81–128.
- [28] Sun J.; Tan, H., Alginate-based biomaterials for regenerative medicine applications. *Materials* **2013**, 6, 1285-1309.

- [29] Kim, U. J.; Park, J.; Li, C.; Jin, H. J.; Valluzzi, R.; Kaplan, D. L., Structure and properties of silk hydrogels. *Biomacromolecules* **2004**, 5, 786–792.
- [30] Seal, B. L.; Otero, T.C.; Panitch, A., Polymeric biomaterials for tissue and organ regeneration. *Mater. Sci. Eng.* **2001**, R 34 , 147-230.
- [31] Nicodemus D. D.; Bryant, S. J., Cell encapsulation in biodegradable hydrogels for tissue engineering applications. *Cell Tissue Eng. Part B Rev.* **2008**, 14, 149–165.
- [32] Stevens, M. M., Biomaterials for bone tissue engineering. *Materials Today* **2008**, 11, 18-25.
- [33] Geckil, H.; Xu, F.; Zhang, X.; Moon, S.; Demirci, U., Engineering hydrogels as extracellular matrix mimics. *Nanomedicine (Lond)* **2010**, 5, 469–484.
- [34] Tan H.; Marra, K. G., Injectable, biodegradable hydrogels for tissue engineering applications. *Materials* **2010**, 3, 1746-1767.
- [35] Bae, K. H.; Wang, L.-S.; Kurisawa, M., Injectable biodegradable hydrogels: progress and challenges. *J. Mater. Chem. B*, **2013**, 1, 5371–5388.
- [36] Murphy S.V.; Atala, A., 3D bioprinting of tissues and organs. *Nat. Biotechnol.* **2014**, 32, 773-785.
- [37] Browning, M. B.; Cereceres, S. N.; Luong P.T.; Cosgriff-Hernandez, E. M., Determination of the in vivo degradation mechanism of PEGDA hydrogels. *J. Biomed. Mater. Res. A*, **2014**, 12, 4244-4251.
- [38] Lin, Z.; Cao, S.; Chen, X.; Wu, W.; Li, J., sponsive hydrogels from phosphorylated ABA triblock copolymers: a potential scaffold for bone tissue engineering. *Biomacromolecules* **2013**, 14, 2206–2214.
- [39] Xin, J.; Chen, T.; Lin, Z.; Dong, P.; Tan, H.; Li, J., Phosphorylated dendronized poly (amido amine) s as protein analogues for directing hydroxylapatite biomineralization. *Chem. Commun.* **2014**, 50, 6491-6493.
- [40] Dingels, C.; Schömer M.; Frey, H., Die vielen Gesichter des Poly (ethylenglykol)s. *Chem. unserer Zeit*, **2011**, 45, 338 – 349.
- [41] Vysotskaya, O. V.; Oparina, L. A.; Parshina, L. N.; Gusarova N. K.; Trofimov, B. A., Functional acetal methacrylates: III. Electrophilic addition of diols to 2-(vinylloxy) ethyl methacrylate. *Russ. J. Org. Chem.* **2002**, 38, 1082–1087.
- [42] Kokubo T.; Takadama, H., How useful is SBF in predicting in vivo bone bioactivity? *Biomaterials* **2006**, 27, 2907–2915.
- [43] Pohlit, H.; Bellinghausen, I.; Schömer, M.; Heydenreich, B.; Saloga, J.; Frey, H., Biodegradable pH-sensitive poly (ethylene glycol) nanocarriers for allergen encapsulation and controlled release. *Biomacromolecules* **2015**, 16, 3103-3111.
- [44] Bueno, V. B.; Bentini, R.; Catalani, L. H.; Barbosa, L. R.; Petri, D. F. S., Synthesis and characterization of xanthan–hydroxyapatite nanocomposites for cellular uptake. *Mater. Sci. and Eng. C* **2014**, 37, 195–203.

- [45] Unger, R. E.; Peters, K.; Sartoris, A.; Freese, C.; Kirkpatrick, C. J., Human endothelial cell-based assay for endotoxin as sensitive as the conventional Limulus Amebocyte Lysate assay. *Biomaterials* **2014**, 35, 3180–3187.
- [46] Maeda, H.; Maquet, V.; Chen, Q.; Kasuga, T.; Jawad, H.; Boccaccini, A., Bioactive coatings by vaterite deposition on polymer substrates of different composition and morphology. *Mater. Sci. and Eng. C* **2007**, 27, 741–745.
- [47] Kim S.; Park, C. B., Mussel-inspired transformation of CaCO<sub>3</sub> to bone minerals. *Biomaterials* **2010**, 31, 6628–6634.
- [48] Palmer, L. C.; Newcomb, C. J.; Kaltz, S. R.; Spoerke, E. D.; Stupp, S. I., Biomimetic systems for hydroxyapatite mineralization inspired by bone and enamel. *Chem. Rev.* **2008**, 108, 4754–4783.
- [49] Andersen F. A.; Brecevic, L., Infrared spectra of amorphous and crystalline calcium carbonate. *Acta Chem. Scand.* **1991**, 45, 1018–1024.
- [50] Wehrmeister, U.; Soldati, A. L.; Jacob, D. E.; Häger, T.; Hofmeister, W., Raman spectroscopy of synthetic, geological and biological vaterite: a Raman spectroscopic study. *J. Raman Spectrosc.* **2010**, 41, 193–201.
- [51] Koutsopoulos, S., Synthesis and characterization of hydroxyapatite crystals: a review study on the analytical methods. *J. Biomed. Mater. Res.* **2002**, 62, 600–612.
- [52] Chavan, P. N.; Bahir, M. M.; Mene, R. U.; Mahabole, M. P.; Khairnar, R. S., Study of nanobiomaterial hydroxyapatite in simulated body fluid: Formation and growth of apatite. *Mater. Sci. Eng. B* **2010**, 168, 224–230.
- [53] Fleet, M. E.; Liu, X.; King, P. L., Accommodation of the carbonate ion in apatite: An FTIR and X-ray structure study of crystals synthesized at 2–4 GPa. *Am. Mineral.* **2004**, 89, 1422–1432.
- [54] Constanz, B. R.; Ison, I. C.; Fulmer, M. T.; Poser, R. D.; Smith, S. T.; VanWagoner, M.; Ross, J.; Goldstein, S. A.; Jupiter, J. B.; Rosenthal, D. I., Skeletal repair by in situ formation of the mineral phase of bone. *Science* **1995**, 267, 1796–1799.
- [55] Soares, L. G. P.; Marques, A. M. C.; Guarda, M. G.; Aciole, J. M. S.; Andrade, A. S.; Pinheiro, A. L. B.; Silveira, L., *Lasers Med. Sci.* **2014**, 29, 1927–1936.
- [56] Dorozhkin S. V.; Epple, M., Biological and medical significance of calcium phosphates. *Angew. Chem. Int. Ed.* **2002**, 41, 3130–3146.
- [57] Dorvee, J. R.; Boskey, A. L.; Estroff, L. A., Rediscovering hydrogel-based double-diffusion systems for studying biomineralization. *CrystEngComm*, **2012**, 14, 5681–5700.
- [58] Asenath-Smith, E.; Li, H.; Keene, E. C.; Wei Seh Z.; Estroff, L. A., Crystal growth of calcium carbonate in hydrogels as a model of biomineralization. *Adv. Funct. Mater.* **2012**, 22, 2891–2914.
- [59] Maeda, H.; Kasuga, T.; Nogami, M.; Ueda, M., Preparation of bonelike apatite composite for tissue engineering scaffold. *Sci. Technol. Adv. Mater.* **2005**, 6, 48–53.

- [60] Kasuga, T.; Maeda, H.; Kato, K.; Nogami, M.; Hata, K.-I.; Ueda, M., Preparation of poly (lactic acid) composites containing calcium carbonate (vaterite). *Biomaterials* **2003**, 24, 3247–3253.

## Supporting Information



*Figure S1.* Quantitative phase analysis and determination of the crystallite size based on the XRD data after soaking vaterite nanoparticles in SBF at 37 °C for (a) 24 h (b) 48 h and (c) 72 h. Red dots are measured data, black lines correspond to the adjustment and the red lines show the difference. The red marks indicate vaterite and the black marks indicate HA.

## Appendix





## A1. Polyethylenglykol-(PEG)-Nanopartikel zur Verkapselung und pH-abhängigen intrazellulären Freisetzung von Allergenen

Hannah Pohlit<sup>1,2,3</sup>

<sup>1</sup>Hautklinik, Universitätsmedizin Mainz, Langenbeckstraße 1, 55131 Mainz, Deutschland

<sup>2</sup>Institut für Organische Chemie, Universität Mainz, Duesbergweg 10-14, 55099 Mainz, Deutschland

<sup>3</sup>Graduiertenschule Materials Science in Mainz, Staudingerweg 9, 55128 Mainz, Deutschland

Veröffentlicht in: *Spitzenforschung in der Allergologie – Auszeichnungen und innovative Fortschritte 2015/2016*, Lebendige Wissenschaft Medizin, **2015**, 54-57, ISSN: 1861-4620.

Der vorliegende Beitrag stellt eine Zusammenfassung der folgenden Publikation dar: Biodegradable pH-Sensitive Poly(ethylene glycol) Nanocarriers for Allergen Encapsulation and Controlled Release, Pohlit, H., Bellinghausen, I., Schömer, M., Heydenreich, B., Saloga, J., Frey, H., *Biomacromolecules*, 2015, 16, 3103-3111. Aus dieser Publikation können weitere Angaben zu Methoden und Ergebnissen entnommen werden.

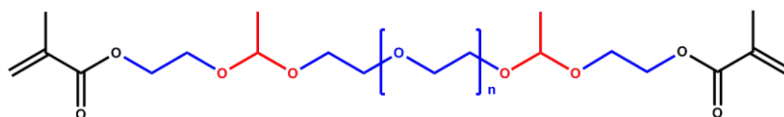
### Einleitung

Weltweit ist die Zahl von Allergikern in den letzten Jahrzehnten alarmierend gestiegen und ein weiterer Anstieg ist zu befürchten. Die bisher einzige kausal orientierte Therapie ist die Allergen-spezifische Immuntherapie, welche jedoch eine lange Behandlungsdauer und mögliche unerwünschte Wirkungen, wie z. B. einen anaphylaktischen Schock, mit sich bringt.<sup>[1, 2]</sup> Um die unerwünschten Wirkungen zu vermindern oder sogar ganz zu verhindern, wurden in den letzten Jahren verschiedene Ansätze verfolgt.<sup>[3]</sup> Durch chemische Modifikation der applizierten Allergene werden sogenannte Allergoide erzeugt, bei denen idealerweise B-Zell-Epitope zerstört, T-Zell-Epitope jedoch erhalten bleiben sollen, was jedoch nach einigen Untersuchungen nicht vollständig gelingt.<sup>[4]</sup> Weitere Ansätze zielen darauf ab, das Allergen durch Einschluss in Transportvehikel vor der Erkennung durch Antikörper und Zellen mit IgE-Rezeptor abzuschirmen. Diese Konzepte haben jedoch bisher meist den Nachteil, dass kein spezifischer Abbaumechanismus »on demand« vorhanden ist, welcher die schnelle und zielgerichtete Freisetzung des Allergens sicherstellt.<sup>[5 - 7]</sup>

Das Konzept unserer biokompatiblen und abbaubaren PEG-Nanopartikel besteht darin, ein weit verbreitetes und seit Jahrzehnten erprobtes Polymer wie PEG mit einer spezifischen Spaltstelle auszustatten. Wird aus diesem neuartigen PEG ein mit Allergenen beladener Nanopartikel hergestellt, erlaubt ein Stimulus im Endolysosom (fallender pH-Wert) den Abbau der Nanopartikel und somit die Allergenfreisetzung innerhalb der antigenpräsentierenden Zelle.<sup>[8]</sup>

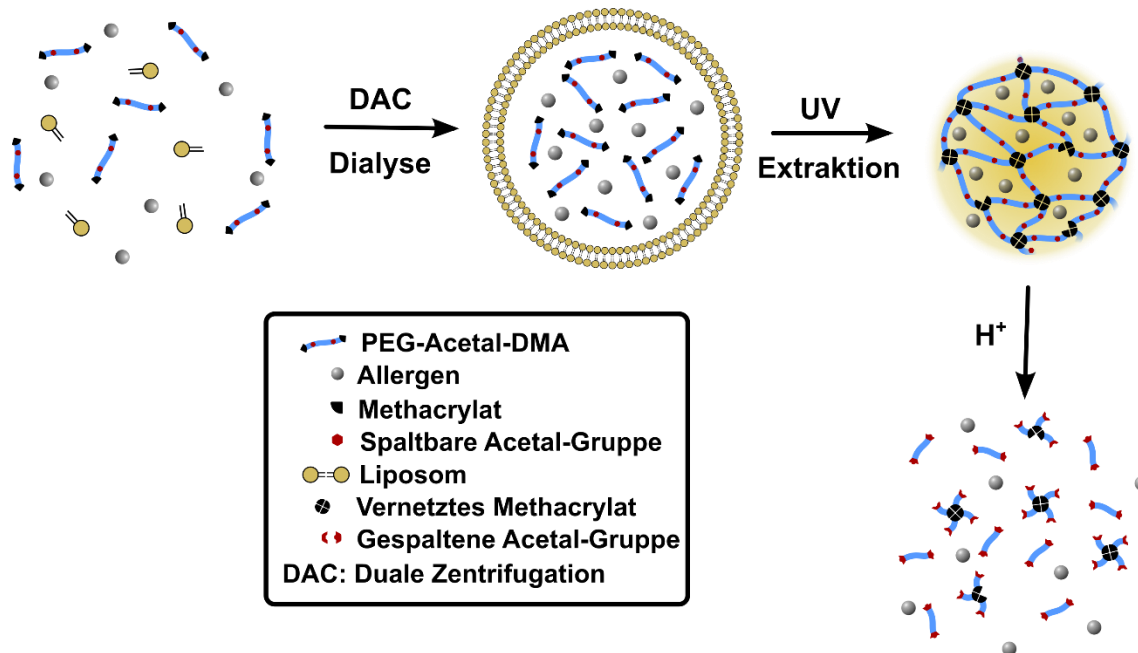
### Eigene Ergebnisse

Um säurespaltbare Nanopartikel zu erhalten, wurde in einem ersten Schritt ein molekularer Baustein hergestellt, der sowohl eine spezifische Spaltstelle aufweist, als auch die reidimensionale Vernetzung zu einem Nanopartikel-Netzwerk durch radikalische Polymerisation erlaubt. Mit der Wahl von Polyethylenglykol (PEG, blau, siehe Abbildung 1) wurde darauf geachtet, ein gut was serlösliches und nicht-toxisches Polymer zu verwenden, welches schon mehrere Jahrzehnte in Arznei- und Lebensmitteln eingesetzt wird. Durch den Einbau von Acetal-Gruppen (rot, siehe Abbildung 1) kann das Polymer bei einem physiologischen pH-Wert von 5 gespalten werden, wie er im Endolysosom vorkommt. Die eingebrachten Methacrylatgruppen (schwarz, siehe Abbildung 1) ermöglichen eine einfache Vernetzung der einzelnen Polymerketten zu einem Polymernetzwerk durch UV-Bestrahlung.



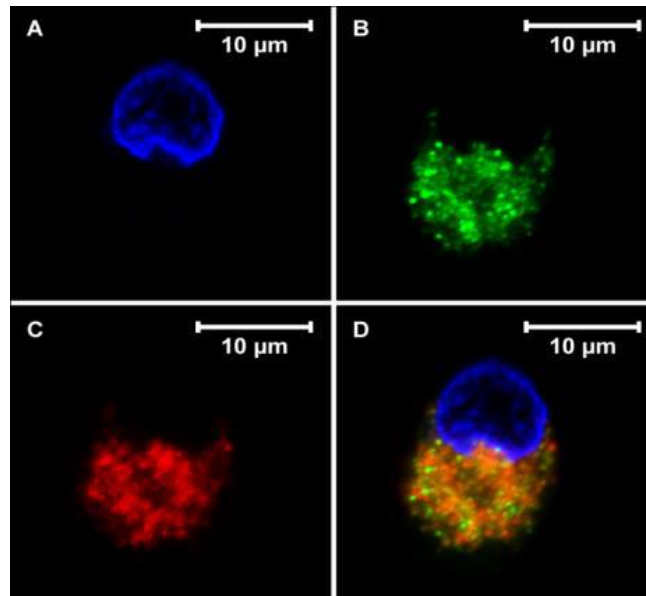
*Abbildung 1.* Struktur des neuartigen Polytehylen glykol-Acetal-Dimethacrylates (PEG-Acetal-DMA).

Die Herstellung der Nanopartikel erfolgte mittels Liposomen als Template. Durch das Mischen von Allergenen mit Polymer, Lipiden und Phosphatpuffer bilden sich durch Selbstaggregation Liposomen, welche durch duale Zentrifugation homogenisiert werden können. Das Allergen welches nicht physikalisch in die Liposomen eingeschlossen wurde, kann durch Dialyse entfernt werden. Nach Bestrahlung der Liposomen mit UV-Strahlung, um die Polymerketten zu vernetzen, kann das Templat, die Liposomenhülle, entfernt werden. Der pure PEG-Partikel kann durch Ansäuern wieder abgebaut werden und das Allergen freisetzen (siehe Abbildung 2).



**Abbildung 2.** Syntheschema der Nanopartikelherstellung: Durch Mischen der Allergene mit dem PEG-Acetal-DMA und Lipiden in Phosphatpuffer entstehen Liposomen, welche mittels DAC homogenisiert werden. Ein Dialyseschritt entfernt nicht-eingeschlossenes Allergen, anschließend werden durch UV-Strahlung die Polymerketten vernetzt. Herabsetzen des pH-Wertes führt zum Abbau des Nanopartikels.

Die Effektivität der hergestellten und mit Gräser oder Hausstaubmilben-Allergenen beladenen Nanopartikel wurde *in vitro* an Blutzellen von allergischen Donoren untersucht. Es konnte gezeigt werden, dass die hergestellten Nanopartikel keinen maturierenden Einfluss auf dendritische Zellen ausüben. Durch einen Apoptose-Assay konnte die toxische Wirkung auf dendritische Zellen ausgeschlossen werden. Mit Hilfe von FACS-Messungen und durch Konfokale Laser Scanning Mikroskopie (CLSM) konnte die Aufnahme der Nanopartikel in dendritische Zellen gezeigt werden (siehe Abbildung 3).



*Abbildung 3.* Konfokale Laser Scanning Mikroskopie einer dendritischen Zelle. In Bild A ist der Zellkern, in Bild B die Lysosomen und in Bild C die Nanopartikel gefärbt. In der Überlagerung von A, B und C in Bild D erscheint gelb-orangene Fluoreszenz, welche ein Hinweis auf Co-Lokalisation von Allergen und Lysosomen ist.

Für die CLSM Aufnahmen wurden dendritische Zellen vier Stunden mit rot-fluoreszierenden Nanopartikeln inkubiert, bevor die Zellen mit Hoechst 33342 (blau) und LysoTracker green gefärbt und mit dem Mikroskop untersucht wurden. Die Aufnahmen zeigen eine Überlagerung von grüner und roter Fluoreszenzintensität, was auf die Co-Lokalisation der Nanopartikel und der Lysosomen schließen lässt. Um zu überprüfen, dass das in die Nanopartikel eingeschlossene Allergen vor der Erkennung durch Immunglobuline auf der Oberfläche von basophilen Leukozyten geschützt ist, wurde ein Cellular Antigen Stimulation Test (CAST) mit anschließendem ELISA durchgeführt. Basophile Leukozyten von allergischen Spendern, die mit nichtverkapseltem Allergen inkubiert wurden, zeigten eine konstant hohe Leukotrienausschüttung. Zellen, die mit den allergen-beladenen Nanopartikeln (A – NP) inkubiert wurden, zeigten dahingegen eine stark verringerte Leukotrienausschüttung. Leere Nanopartikel führten zu keiner messbaren Leukotrienausschüttung (siehe Abbildung 4).

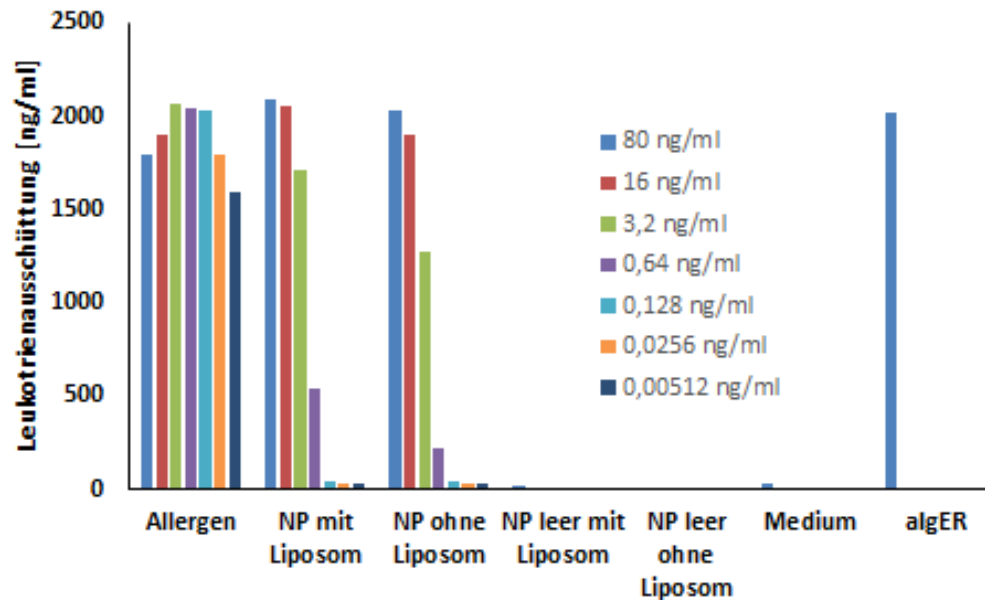


Abbildung 4. CAST-ELISA. Basophile Leukozyten von allergischen Donoren wurden mit unverkapseltem Allergen, allergen-beladenen Nanopartikeln oder leeren Nanopartikeln inkubiert und die Leukotrienausschüttung wurde vermessen. Als Negativkontrolle wurden die Zellen mit Medium inkubiert, als Positivkontrolle wurden sie mit anti-IgE-Rezeptor stimuliert. Gezeigt ist ein repräsentatives Einzelbeispiel.

Ein T-Zell-Proliferationsassay von mit Allergen bzw. A-NP-beladenen dendritischen Zellen und autologen T-Zellen wurde herangezogen um die Freisetzung sowie die Funktionalität des Allergens nach der Verkapselung in unsere PEG-Nanopartikel zu untersuchen. T-Zellen, die mit nichtverkapseltem Allergen-beladenen DCs co-kultiviert wurden, zeigten eine im Vergleich zur Mediumkontrolle erhöhte allergen-spezifische Proliferation (Positivkontrolle). T-Zellen, deren dendritischen Zellen mit A-NP beladen wurden, zeigten ebenfalls eine signifikant erhöhte allergen-spezifische Proliferation, wenn auch weniger stark ausgeprägt als die der Positivkontrolle. Wurden die T-Zellen mit DCs inkubiert, die mit leeren Nanopartikeln beladen wurden, so kommt es zu keiner signifikant erhöhten Proliferation (siehe Abbildung 5). Diese Ergebnisse zeigen, dass das Allergen aus den Nanopartikeln freigesetzt wird und die T-Zell-Epitope während der Nanopartikelherstellung erhalten bleiben.

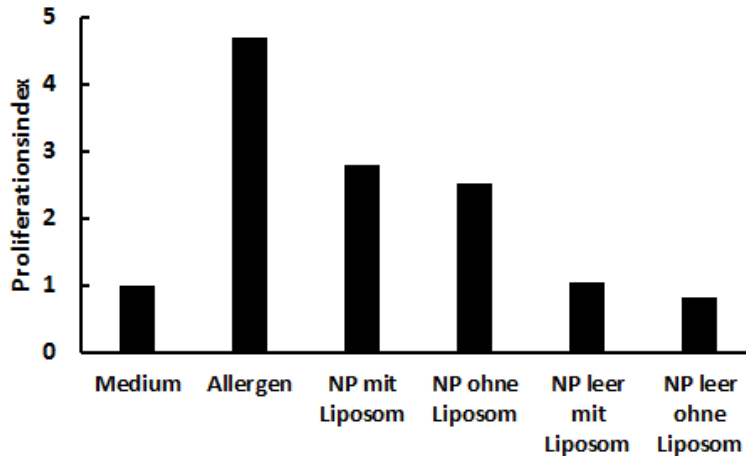


Abbildung 5. T-Zell-Proliferationsassay mit dendritischen Zellen, welche vor der Co-Kultur mit autologen T-Zellen mit nicht-verkapseltem Allergen, allergen-beladenen Nanopartikeln oder leeren Nanopartikeln inkubiert wurden. Gezeigt ist ein repräsentatives Einzelbeispiel.

### Zusammenfassung und Ausblick

Es konnte ein neuartiges Polymer hergestellt werden, das als Baustein für die spaltbaren PEG-Nanopartikel verwendet werden kann. Die homogenen, mit Allergen beladenen Nanopartikel wurden mit Hilfe von Liposomen als Template hergestellt. Die so erhaltenen abbaubaren PEG Nanopartikel zeigten keine Toxizität und führten nicht zur Ausreifung von dendritischen Zellen, wurden von diesen jedoch in das Endolysosom aufgenommen. Das Allergen war innerhalb der Nanopartikel vor der Erkennung durch Immunglobulinen auf basophilen Leukozyten geschützt. Die Co-Kultivierung von mit Nanopartikeln beladenen dendritischen Zellen und T-Zellen führte zu einer signifikant gesteigerten allergenspezifischen Proliferationsrate. Diese vielversprechenden ersten Ergebnisse ermutigen die weitere Analyse und die Verbesserung der beschriebenen Nanopartikel. Die nächsten Schritte werden die Funktionalisierung der Nanopartikel sowie die Herstellung und Untersuchung von anderen spaltbaren Gruppen im Polymer zum schnelleren Abbau der Nanopartikel beinhalten. Da das Allergen für den Einschluss in die Nanopartikel nicht modifiziert wird und das Konzept nicht auf einer kovalenten Bindung zwischen dem Allergen und dem Nanopartikel beruht, ist es universell einsetzbar (z. B. für die Verkapselung von Allergen/Antigen-Gemischen oder einem Gemisch aus Allergenen/Antigenen und einem biological response modifier).

## Danksagung

Für die finanzielle Unterstützung möchte ich mich bei der Graduiertenschule Materials Science in Mainz (MAINZ, (DFG/GSC 266), dem Max Planck Graduate Center (MPGC) und dem Naturwissenschaftlich-medizinischen Forschungszentrum der Universitätsmedizin Mainz (NMFZ) bedanken. Ganz herzlich möchte ich mich auch bei meinen Co-Autoren I. Bellinghausen, M. Schömer, B. Heydenreich, H. Frey und J. Saloga bedanken, sowie für die Unterstützung bei Diskussionen und im Labor bei T. Fritz, M. Schmelzer, E. Berger-Nicoletti, E. Sellenies-Huber und F. Ludwig.

## Literatur

- [1] Srivastava D.; Arora N.; Singh B. P., Current immunological approaches for management of allergic rhinitis and bronchial asthma, *Inflamm. Res.* **2009**, 58, 523 – 536.
- [2] Akdis C. A.; Akdis M., Mechanisms of allergen-specific immunotherapy, *J. Allergy Clin. Immunol.* **2011**, 127, 18 – 27.
- [3] Gamazo C.; Gastaminza G.; Ferrer M.; Sanz M. L.; Irache J. M., Nanoparticle based-immunotherapy against allergy, *Immunotherapy* **2014**, 6, 885 – 897.
- [4] Heydenreich B.; Bellinghausen I.; Lorenz, S.; Henmar, H.; Strand, D.; Würtzen, P. A.; Saloga, J., Reduced in vitro T-cell responses induced by glutaraldehyde-modified allergen extracts are caused mainly by retarded internalization of dendritic cells, *Immunology* **2012**, 136, 208 – 217.
- [5] Schöll I.; Weissenböck A.; Forster-Waldl E.; Untersmayr, E.; Walter, F.; Willheim, M.; Boltz-Nitulescu, G.; Scheiner, O.; Gabor, F.; Jensen-Jarolim, E., Allergen-loaded biodegradable poly(d,l-lactic-co-glycolic) acid nanoparticles down-regulate an ongoing Th2 response in the BALB/c mouse model, *Clin. Exp. Allergy* **2004**, 34, 315 – 321.
- [6] McGee J., Davis S.; Ohagan D., The immunogenicity of a model protein entrapped in poly(lactide-co-glycolide) microparticles prepared by a novel phase separation technique, *J. Control. Release* **1994**, 31, 55 – 60.
- [7] Licciardi M.; Montana G.; Bondi M. L.; Bonura, A.; Scialabba, C.; Melis, M.; Fiorica, C.; Giammona, G.; Colombo, P., An allergen-polymeric nanoaggregate as a new tool for allergy vaccination, *Int. J. Pharm.* **2014**, 465, 275 – 283.
- [8] Pohlitz, H.; Bellinghausen, I.; Schömer, M.; Heydenreich, B.; Saloga, J.; Frey, H., Biodegradable pH-sensitive poly (ethylene glycol) nanocarriers for allergen encapsulation and controlled release. *Biomacromolecules* **2015**, 16, 3103-3111.

**Dipl. Chem. Hannah Pohlit**

Hautklinik  
Gebäude 401, Labor 153  
Universitätsmedizin Mainz  
Langenbeckstraße 1  
55131 Mainz  
Telefon: 06131 172238  
E-Mail: h.pohlit@uni-mainz.de



Dipl. Chem. Hannah Pohlit (geb. Köhring) ist Doktorandin der Hautklinik der Universitätsmedizin Mainz in der Arbeitsgruppe von Prof. Joachim Saloga sowie im Institut für Organische Chemie an der Universität Mainz in der Arbeitsgruppe von Prof. Holger Frey. Sie studierte von 2006 bis 2012 Biomedizinische Chemie als Diplomstudiengang an der Johannes Gutenberg-Universität Mainz. Während ihres Studiums forschte sie für ein halbes Jahr im »Marine Biodiscovery Centre« an der Universität Aberdeen, UK, an Tiefseebakterien. Ihre Abschlussarbeit fertigte sie bereits in den Laboren von Prof. Saloga und Prof. Frey an und konnte erste Ergebnisse bei der Verkapselung von Allergenen erzielen. Nach ihrem Abschluss erhielt sie die Möglichkeit, ein Forschungspraktikum bei BASF in Tarrytown, NY, USA, zu absolvieren währenddessen sie antibakterielle Polymere untersuchte. Seit Ende 2012 arbeitet Hannah Pohlit an ihrer interdisziplinären Doktorarbeit und erhält dafür Unterstützung von 2 Graduiertenschulen. Hannah Pohlit ist Junior-Mitglied in der EAACI, der DGAKI sowie der Gesellschaft Deutscher Chemiker (GDCh). Frau Pohlit erhielt mehrere Förderungen und Auszeichnungen, unter anderem: 2008 – 2012 Studienstipendium des »Evangelischen Studienwerks Villigst«; 2009 – 2011 Teilnehmerin der Lebenswissenschaftlichen Kollegs »Immunologie und Infektologie« der Studienstiftung des Deutschen Volkes; 2011 Förderungsstipendium der Studienstiftung Rheinland-Pfalz; ab 2013 Doktorandenstipendium der Graduiertenschule »Materials Science in Mainz« (MAINZ). Außerdem ist Sie seit 2013 Mitglied des Max Planck Graduate Centers (MPGC) und seit 2014 Juniormitglied der Gutenberg Akademie. Im Jahr 2014 erhielt Hannah Pohlit den Junior members poster award der DGAKI und 2015 ein Reisestipendium für die 13th EAACI Winter School in Les Arcs, Frankreich.



---

## A2. Polymerization of Ethylene Oxide, Propylene Oxide, and Other Alkylene Oxides: Synthesis, Novel Polymer Architectures, and Bioconjugation

*Jana Herzberger,<sup>1,2</sup> Kerstin Niederer,<sup>1</sup> Hannah Pohlit,<sup>1,2,3,4</sup> Jan Seiwert,<sup>1</sup> Matthias Worm,<sup>1,3</sup>*

*Frederik R. Wurm,<sup>5,3</sup> and Holger Frey<sup>1,2</sup>*

<sup>1</sup>Institute of Organic Chemistry, Johannes Gutenberg-University Mainz, Duesbergweg 10-14, 55128 Mainz, Germany

<sup>2</sup>Graduate School Materials Science in Mainz, Staudingerweg 9, 55128 Mainz, Germany

<sup>3</sup>Max Planck Graduate Center, Staudingerweg 6, 55128 Mainz, Germany

<sup>4</sup>Department of Dermatology, University Medical Center, Langenbeckstraße 1, 55131 Mainz, Germany

<sup>5</sup>Max Planck Institute for Polymer Research, Ackermannweg 10, 55128 Mainz, Germany

Published in: *Chemical Reviews*, **2016**, 116 (4), 2170–2243. Reprinted with permission from *Chemical Reviews*, **2016**, 116 (4), 2170–2243. Copyright (2016) American Chemical Society.



# CHEMICAL REVIEWS

## Polymerization of Ethylene Oxide, Propylene Oxide, and Other Alkylene Oxides: Synthesis, Novel Polymer Architectures, and Bioconjugation

Jana Herzberger,<sup>†,‡</sup> Kerstin Niederer,<sup>†</sup> Hannah Pohlitz,<sup>||,†,‡,§</sup> Jan Seiwert,<sup>†</sup> Matthias Worm,<sup>†,§</sup> Frederik R. Wurm,<sup>⊥,§</sup> and Holger Frey<sup>\*,†,‡</sup>

<sup>†</sup>Institute of Organic Chemistry, Johannes Gutenberg-University Mainz, Duesbergweg 10-14, D-55128 Mainz, Germany

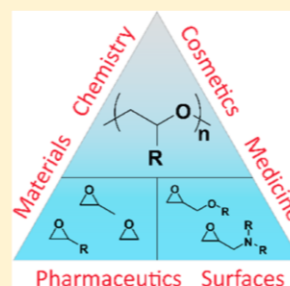
<sup>‡</sup>Graduate School Materials Science in Mainz, Staudingerweg 9, D-55128 Mainz, Germany

<sup>§</sup>Max Planck Graduate Center, Staudingerweg 6, D-55128 Mainz, Germany

<sup>||</sup>Department of Dermatology, University Medical Center, Langenbeckstraße 1, D-55131 Mainz, Germany

<sup>⊥</sup>Max Planck Institute for Polymer Research, Ackermannweg 10, D-55128 Mainz, Germany

**ABSTRACT:** The review summarizes current trends and developments in the polymerization of alkylene oxides in the last two decades since 1995, with a particular focus on the most important epoxide monomers ethylene oxide (EO), propylene oxide (PO), and butylene oxide (BO). Classical synthetic pathways, i.e., anionic polymerization, coordination polymerization, and cationic polymerization of epoxides (oxiranes), are briefly reviewed. The main focus of the review lies on more recent and in some cases metal-free methods for epoxide polymerization, i.e., the activated monomer strategy, the use of organocatalysts, such as *N*-heterocyclic carbenes (NHCs) and *N*-heterocyclic olefins (NHOs) as well as phosphazene bases. In addition, the commercially relevant double-metal cyanide (DMC) catalyst systems are discussed. Besides the synthetic progress, new types of multifunctional linear PEG (*mf*-PEG) and PPO structures accessible by copolymerization of EO or PO with functional epoxide comonomers are presented as well as complex branched, hyperbranched, and dendrimer like polyethers. Amphiphilic block copolymers based on PEO and PPO (Poloxamers and Pluronics) and advances in the area of PEGylation as the most important bioconjugation strategy are also summarized. With the ever growing toolbox for epoxide polymerization, a “polyether universe” may be envisaged that in its structural diversity parallels the immense variety of structural options available for polymers based on vinyl monomers with a purely carbon-based backbone.



### CONTENTS

1. Introduction	2171	3.1. Multifunctional PEGs	2188
Historical Remarks	2171	3.2. Glycidyl Amine Comonomers and Polyethers with Pendant Amino Groups	2192
1.1. PEG (PEO)	2171	3.2.1. Introduction of Primary Amino Groups	2193
1.2. PPO	2172	3.2.2. Secondary Amino Groups	2194
1.3. Other Poly(alkylene oxides)	2172	3.2.3. Tertiary Amino Groups	2194
2. Polymerization of Alkylene Oxides: Methods	2172	3.2.4. Other Polyether Derivatives Bearing Nitrogen Moieties	2194
2.1. Oxyanionic Polymerization	2172	3.3. In Situ Monomer Sequence Characterization	2195
2.1.1. Ethylene Oxide	2172	3.4. Polymerization of Longer Alkylene Oxides	2196
2.1.2. Anionic Polymerization of Propylene Oxide and Higher Alkylene Oxides	2174	3.4.1. Poly(propylene oxide), Poly(1,2-butylene oxide) and Higher 1,2-Alkylene Oxide Polymers	2196
2.2. Coordination Polymerization	2174	4. Block Copolymers of PEG and PPO	2200
2.3. Activated Monomer Strategy	2175	4.1. Poloxamers and Poloxamines	2200
2.4. <i>N</i> -Heterocyclic Carbenes (NHCs) and <i>N</i> -Heterocyclic Olefins (NHOs) as Organocatalysts for Metal-Free Polyether Synthesis	2178	4.1.1. Poloxamines	2202
2.5. Phosphazene Bases: Metal-Free Initiators	2180	4.1.2. PEO–PPO Diblock Copolymers	2203
2.6. Heterogeneous Catalysis—Double Metal Cyanide Catalysts for Epoxide Polymerization	2183		
2.7. Cationic Polymerization	2185		
3. Poly(alkylene oxide) Structures: Innovative Polyether Structures	2188		

**Special Issue:** Frontiers in Macromolecular and Supramolecular Science

**Received:** July 29, 2015

**Published:** December 29, 2015

## Chemical Reviews

Review

5. Star-Shaped and Hyperbranched Poly(alkylene oxides)	2204
5.1.1. Star Polymers	2204
5.1.2. Branched and Hyperbranched PEG, PPO, and PBO Derivatives	2206
6. Biomedical Applications	2208
6.1. Bioconjugation and PEGylation	2208
6.2. Cleavable Polyethers	2220
6.2.1. Polyethers Bearing Cleavable Moieties	2220
7. Conclusions	2221
Author Information	2221
Corresponding Author	2221
Notes	2221
Biographies	2221
Acknowledgments	2222
Abbreviations	2222
References	2224

## 1. INTRODUCTION

Aliphatic polyethers generated by the ring-opening polymerization (ROP) of the epoxide monomers ethylene oxide (EO), propylene oxide (PO), and, to a lesser extent, butylene oxide (BO) are a highly established and important class of polymers that are commercially used for an immense variety of applications. The characteristic properties of polyether-based materials are due to their unique backbone, in particular its high flexibility leading to low glass transitions below  $-60\text{ }^{\circ}\text{C}$ , and its hydrophilicity due to the C–O–C bond. These properties can not be matched by a carbon-based backbone, as it is present in polyolefins or other vinyl polymers.

Although generally three- to five-membered cyclic ethers can be polymerized to generate polyethers by ROP, epoxides clearly represent the most versatile class of monomers for polyether synthesis,<sup>1,2</sup> since they can be polymerized by different mechanisms, and EO and PO are readily available in industry in large quantities directly from the oxidation of the respective alkenes. The driving force for the ROP is the high ring strain of epoxides, which is on the order of 110–115 kJ/mol for ethylene oxide.<sup>3</sup> This enables polymerization of epoxide (IUPAC: oxirane) monomers in three ways: (i) base-initiated, (ii) acid-initiated, and (iii) by coordination polymerization.

Other classes of epoxide monomers, such as epichlorohydrin, longer alkylene epoxides, a large variety of glycidyl ethers, and glycidyl amines, play an increasing role in academia and are highly promising as comonomers for specialty applications in the future. However, they currently lack the commercial importance of the structurally simple key monomers shown in Scheme 1 that are produced on a scale of more than 33 million tons per year. This review summarizes the enormous progress in the

polymerization of the alkylene oxides EO, PO, and BO in the last two decades, focusing both on novel polymerization techniques and innovative polyether architectures that are often obtained in combination with a small fraction of other epoxide comonomers. Important applications of the respective polyethers have seen a tremendous development in the last two decades, which will also be reviewed. A particular emphasis is placed on amphiphilic polyether copolymers and on advances in the PEGylation of biomolecules.

## Historical Remarks

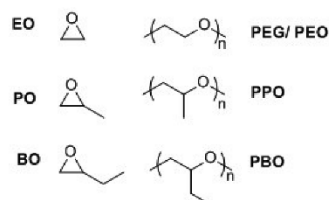
As early as 1863, Wurtz reported the polymerization of EO with alkali metal hydroxide or zinc chloride.<sup>4</sup> In several key works, Staudinger and Schweitzer prepared a series of poly(ethylene glycol) samples from EO as model polymers and separated the polymers according to their molecular weights for detailed viscosimetry studies in 1929.<sup>5</sup> Already in the 1930s, poly(ethylene glycol) was commercialized, based on the addition of EO to ethylene glycol under basic conditions. Within one decade, a variety of applications was developed in areas ranging from pharmaceuticals to lubricants, cosmetics and detergents. In 1940, in a famous work Flory established the mechanism of the base-initiated polymerization of EO, predicting a Poisson-type distribution for a living chain-growth process for the first time.<sup>6</sup> The anionic polymerization of propylene oxide was rapidly developed in the 1940s to generate liquid polyols that were established for hydraulic fluids and lubricants. The introduction of PEO as polar, water-soluble block for nonionic surfactants represents another key development in the 1950s. The respective “fatty alcohol ethoxylates” and “alkyl phenol ethoxylates” are prepared on a million ton scale today and represent the most important class of nonionic surfactants.<sup>7,8</sup>

## 1.1. PEG (PEO)

Poly(ethylene glycol) is the gold standard biocompatible polymer for pharmaceutical, cosmetic, and medical applications and is used for an extremely wide range of products ranging from skin care products to tablet formulations, laxatives, and food additives.<sup>9,10</sup> Higher molecular weight polymers of EO are commonly called poly(ethylene) oxide (PEO) or sometimes poly(oxyethylene) (POE), whereas polymers with molecular weights below 30 000 g/mol are referred to as poly(ethylene glycol) (PEG). However, for medical applications in general the abbreviation “PEG” is common and exclusively used. The abbreviation mPEG designates a monomethyl-ether terminated PEG with a single terminal hydroxyl group that can be further functionalized for block copolymer synthesis or bioconjugation with PEG, commonly called “PEGylation”. PEG is a crystalline thermoplastic polyether that is highly water-soluble in practically all concentrations and exhibits very low immunogenicity, antigenicity and toxicity.<sup>11</sup> The high aqueous solubility of PEG is unique among aliphatic polyethers that are commonly not water-soluble.<sup>12</sup> This feature is ascribed to the distance of the oxygens in the polymer structure that is compatible with the distance of the hydrogens in the water molecule.<sup>13</sup>

PEG and PEO are liquids or low melting solids, depending on molecular weight. The melting point of PEG depends on the chain length ( $65\text{ }^{\circ}\text{C}$  for high molecular weight PEO) and can be tailored in the physiological temperature range by blending and cocrystallizing different molecular weights of PEG, which is important for skin creams, ointments, and suppositories. PEG is available under several trade names that are established for medical, cosmetic, and pharmaceutical purposes, e.g., Carbowax, Macrogol, Fortrans, Pegoxol, Polyox. Besides the use of PEG as a

Scheme 1. Monomers EO, PO, and BO and respective polyethers formed after polymerization



material on the macroscopic scale, it is widely employed on a molecular basis for the modification of therapeutic peptides or proteins and liposomes to greatly enhance blood circulation times. This so-called “PEGylation” strategy relies on the “stealth properties” introduced by the attachment of PEG chains.<sup>14,15</sup>

In recent years, several excellent reviews have been published on specific topics related to PEG, for instance pharmaceutical applications of PEG, particularly PEGylation<sup>16,17</sup> synthesis of high molecular weight PEO,<sup>18</sup> and regarding the introduction of degradation sites into PEG.<sup>19</sup> These topics will therefore not be discussed specifically in this review. The current review focuses on recent advances in the polymerization of epoxides as well as novel, often complex polymer architectures available via this route. Recent developments for nonionic, amphiphilic block copolymers of PEG with the rather apolar poly(propylene oxide) will also be recapitulated as well as advances in the field of “PEGylation” as the key bioconjugation technique at present.

### 1.2. PPO

Poly(propylene oxide) (PPO), often designated poly(propylene glycol) (PPG) for lower molecular weights, is commonly produced by the ROP of PO. The flexible polymer (glass transition  $-70\text{ }^{\circ}\text{C}$ ) is noncrystalline due to the use of the racemic PO monomer, which leads to a nonstereoregular (atactic) structure. In contrast to PEG or PEO, PPO is not water-soluble at room temperature due to the additional methyl group in each repeating unit that sterically shields the backbone. However, rather low molecular weight PPGs are soluble in aqueous solution at low temperature and exhibit a lower critical solution temperature at around  $15\text{ }^{\circ}\text{C}$  that depends on molecular weight.<sup>20</sup> The base-initiated polymerization of PO in industry mostly relies on potassium hydroxide and alcohols as initiators.<sup>21</sup> Since a major fraction of PO is used for the preparation of star polymers, so-called polyether-polyols, multifunctional initiators, such as glycerol, pentaerythritol, or sorbitol are often used. PPO-based star polyether polyols play a key role in the synthesis of polyurethane flexible foams due to their chain flexibility, i.e., low glass transition and their amorphous nature.<sup>22</sup> Generally, PPG is used for lubricants, antifoaming agents, softeners, rheology modifiers, flexible poly(urethane) foams, and nonionic surfactants, often in combination with PEG. The synthesis of PPO, differences compared to the polymerization of EO and recent developments in this area will be discussed in section 2.1.2 of this review.

### 1.3. Other Poly(alkylene oxides)

In contrast to EO and PO the 1,2-butylene oxide monomer, designated butylene oxide (BO) throughout this article, has to be produced in a two-step industrial process and cannot be obtained by direct oxidation of the respective alkene.<sup>23</sup> The synthesis relies on the oxidation of butadiene to vinylloxirane and subsequent hydrogenation. 1-Butylene oxide is the longest alkylene oxide available on industrial scale. The properties of poly(butylene oxide) (PBO) resemble PPO, however, as expected, it is more hydrophobic. The high hydrophobicity of PBO is advantageous for several applications, for instance for polyurethanes that have to be stable toward water or hot water vapor. Small amounts of PBO added to lubricants can serve to improve their properties. In several cases, BO is used as a comonomer to modify the properties of other polyethers, i.e., to increase their apolar and amorphous structure. The increased hydrophobicity of PBO is an advantage for surfactants combining PEO and PBO blocks.<sup>24</sup>

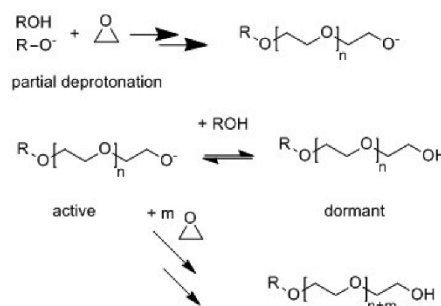
## 2. POLYMERIZATION OF ALKYLENE OXIDES: METHODS

### 2.1. Oxyanionic Polymerization

**2.1.1. Ethylene Oxide.** The oxyanionic polymerization of epoxides represents the “classical” technique for the synthesis of the respective polyethers. It has been the key technique for the polymerization of EO since the 1930s and is still employed for the major fraction of PEO and PPO produced, despite the fundamental disadvantages and molecular weight limitations of the technique for the polymerization of PO and other alkylene oxides (vide infra). The anionic polymerization of EO is based on nucleophiles as initiators. The widely applied standard method for the technical synthesis of low molecular weight PEG is the controlled addition of EO to water or alcohols as initiators in the presence of alkaline catalysts. In most cases alkali metal compounds with high nucleophilicity are employed for this purpose. For higher molecular weights, alkali metal hydrides, alkyls, aryls, hydroxides, alkoxides, and amides can be employed for the living anionic polymerization of EO in an inert solvent. As in all ionic polymerizations, the counterion plays a key role and should exhibit low Lewis acidity and preferentially little or no interaction with the chain end. Solvents employed for the anionic polymerization of epoxides must be polar and aprotic; therefore, tetrahydrofuran (THF), dioxane, dimethyl sulfoxide (DMSO), and hexamethylphosphoramide (HMPA) are often used.<sup>25</sup> Furthermore, polymerization in the bulk monomer is possible, if low molecular weights are targeted, albeit at the expense of a higher polydispersity. The fundamentals of this established technique are well understood since the late 1980s, which is mainly due to fundamental kinetic studies by Sigwalt and Boileau,<sup>26</sup> Kazanskii et al., and Tsvetanov and co-workers.

Alkoxides with sodium, potassium, or cesium counterions in ethers (most often THF) or other polar, aprotic solvents represent the most popular initiator systems. The addition of complexing agents, such as crown ethers suitable for the respective cation can strongly accelerate epoxide polymerization.<sup>27,28</sup> Since the polymerization of epoxides is a living process, a Poisson-distribution is obtained<sup>6</sup> and facile and quantitative end-functionalization of the resulting PEG can be achieved.<sup>29</sup> The active alkoxide chain end of the growing PEG is rather stable with respect to termination, and the mechanism of the polymerization is therefore simple (Scheme 2). One has to emphasize that partial deprotonation of the alkoxide initiator (often only 10–20%) is sufficient for polymerization due to the

**Scheme 2.** Oxyanionic Polymerization of EO with Rapid Degenerative Proton Transfer Leading to an Equilibrium between Active Alkoxides and Dormant PEG–OH Species



## Chemical Reviews

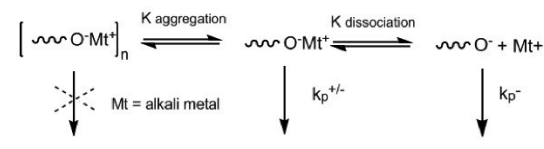
## Review

rapid proton exchange equilibrium in the system. In such systems, chain growth can be viewed as a polymerization with degenerative chain transfer, i.e., reversible termination, the hydroxyl terminated chains being the dormant species and the alkoxide termini the active chain end. Proton exchange is extremely rapid, and therefore the combination of alkoxide with the respective alcohol is employed as initiator system in most instances, particularly in the synthesis of polyether polyols (i.e., PPO or PPO/PEG star polymers) to retain solubility of the respective multihydroxyfunctional initiator.

Besides alkoxides, also highly nucleophilic hydrides, amides and alkyl- or aryl compounds of sodium, potassium, and cesium can be employed to initiate the polymerization of EO.<sup>30</sup>

The oxyanionic polymerization of EO in solution relies on the oxygen atom at the charged end of the growing chains as the active center, where the negative charge is localized. Depending on the counterion, solvated contact ion pairs may be present. In addition, the active chain ends can be highly associated even in dilute solution. The presence and reactivity of aggregated species and ion pairs versus free ions and their respective contributions to the oxyanionic polymerization of EO (cf. Scheme 3) has been

**Scheme 3. Aggregated Chains (Left), Solvated Ion Pairs and Free Ions in Epoxide Polymerization and Their Respective Propagation Rate Constants**



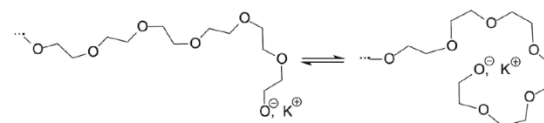
subject of numerous studies, mainly in the 1970s. In solvents of low or medium polarity, alkali metal alkoxides of sodium show a strong tendency to aggregate, which leads to complex polymerization kinetics. The polymerization of EO within alkoxide aggregates is slow or negligible in most cases.<sup>25</sup> EO polymerization kinetics has been investigated in various media, i.e., in HMPA, DMSO, and various ethers, mainly THF.<sup>26</sup> In the case of K or Cs counterions, the alkoxide-initiated polymerization in solution proceeded almost exclusively by free ions due to the high dissociation constant of these ions ( $k_d = 9.4 \times 10^{-2} \text{ mol L}^{-1}$  at 50 °C). In THF the propagation rate constant  $k_p^-$  of the free alkoxide anions was found to be  $1.7 \text{ L mol}^{-1} \text{ s}^{-1}$  at 20 °C by Solovyanov and Kazanskii,<sup>31</sup> using Cs as a counterion.

In the case of lithium alkoxides, typically no polymerization occurs, but merely a single ring-opening step that results in a bond of rather covalent character between the alkoxide chain end and the Li counterion. The failure of a polymerization in this case may also be explained on the basis of the hard and soft acid and base (HSAB) concept,<sup>32</sup> taking into account the strong interaction between the “hard” oxygen anion and the “hard” lithium cation. However, capitalizing on the absence of further epoxide polymerization, EO and other epoxides have frequently been employed for the functional termination of BuLi-initiated carbanionic polymerization to generate hydroxyl-functional vinyl polymers, since in most cases attachment of only one hydroxyethyl unit at the chain end is achieved.<sup>33–35</sup> However, for some epoxides very slow oligomerization over a period of several weeks was observed with Li-based initiators.<sup>36</sup> Also the strong aggregation in the case of Li-counterions additionally impedes polymerization.<sup>37</sup>

In the case of a sodium-methoxide initiated polymerization of EO a contact ion pair is observed. Commonly the reaction rate of the alkoxide-initiated polymerization is slow but can be accelerated to a certain extent by raising temperature and also by a small excess of the respective alcohol.<sup>38</sup> In this case the presence of an initiator complex between alcohol and alkoxide has been suggested that leads to some degree of separation of the ion pair at the chain end. The rather low rate of the EO polymerization in various solvents permits direct in situ observation by NMR spectroscopy, as will be detailed in section 3.3 of this review, enabling direct observation of the monomer sequence along the chains formed.<sup>39</sup> Since the late 1990s studies regarding the terminal functionalization of PEG have profited greatly from the advent of MALDI-TOF spectroscopy, since PEG shows excellent desorption characteristics for a number of typical matrices employed for this method, permitting precise evaluation of the extent of terminal functionalization.<sup>40,41</sup>

Pioneering works by Panayotov et al.,<sup>42</sup> Kazanskii and co-workers,<sup>43–45</sup> Sigwalt and Boileau,<sup>46,47</sup> as well as Berlinova et al.<sup>48,49</sup> have created a detailed understanding of the mechanism of the oxyanionic EO polymerization. An excellent review of the kinetic characteristics of the oxyanionic polymerization in comparison with other living ionic polymerization strategies was published by Penczek et al.<sup>30</sup> A peculiar feature of the synthesis of PEG by anionic polymerization is the capability of the oxygen atoms in the polyether backbone to aid in the solvation of the cation of the ion pair. The mobility of the PEG-segments in combination with its solvating properties lead to the formation of ion-triplets and self-solvation.<sup>48–51</sup> Thus, a “penultimate effect” can be observed, i.e., the activity of the chain ends depends on the number of EO units already added (Scheme 4). The activation energy for the EO addition to the

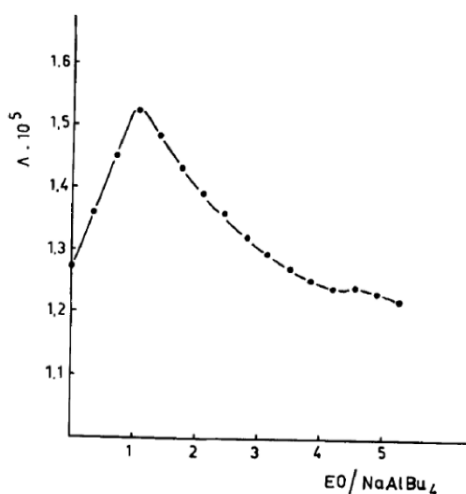
**Scheme 4. Interaction and Complexation of Potassium Counterion at the Chain End of PEG with Crown Ether like Structure, Resulting in a Penultimate Effect on EO Polymerization<sup>30</sup>**



growing end is  $74.5 \text{ kJ mol}^{-1}$ . This, as well as the insensitivity of the rate of propagation to the nature of the solvent is explained by the self-association “shielding” effect of monomer units located near the alkoxide chain end. In addition, interaction between the cation employed and the EO monomer may also play a role.<sup>46,47,52</sup>

Another important feature of the EO polymerization process is its strong temperature dependence. Interestingly, at very low temperature the monomer EO can even be employed as an inert ether solvent for the anionic polymerization of MMA and 2-vinylpyridine, demonstrating its stable character for the carbanionic low temperature polymerization.<sup>53</sup>

Conductivity measurements were employed to study the presence of free ions as well as associated species in the polymerization (for a typical result see Figure 1). The conductivity of short-chain living polymers  $R-(\text{CH}_2\text{CH}_2\text{O})_{n-1}\text{CH}_2\text{CH}_2\text{O}^- \text{M}^+$  in THF is a function of chain length and tends to reach a steady-state value for  $n$  between 3 and 7.<sup>43,48,49</sup> Interestingly, the rate of propagation in the EO polymerization



**Figure 1.** Result of conductivity measurements at different EO/NaAlBu<sub>4</sub> ratios in toluene,<sup>42</sup> demonstrating the presence of different types of complexes at different initiator concentrations. Reproduced with permission from Tsvetanov, C. B.; Petrova, E. B.; Panayotov, I. M. *J. Macromol. Sci. Chem.* **1985**, *22*, 1309; Publishers Taylor & Francis.

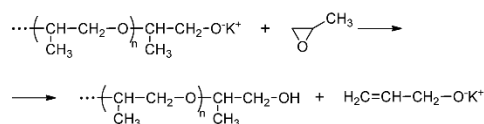
was observed to be almost independent of the solvent employed.<sup>42</sup>

In summary, the oxanionic polymerization of EO is characterized by (i) tight ion pairs with low dissociation constants ( $10^{-8}$ – $10^{-12}$  mol L<sup>-1</sup>) in THF; (ii) the presence of ion triplets and higher associates; (iii) competitive interaction of the growing chains with monomer unit sequences and most likely also with the EO monomer. This complex nature of the active center presents a fundamental problem in the anionic polymerization of EO, but also for PO and other oxiranes in solution. An upper limit of 50 000 g/mol for the attainable molecular weights has been reported for this common approach.<sup>37</sup>

In order to achieve an effective polymerization, primary hydroxyl groups are preferable, since they exhibit higher reactivity than secondary alkoxides. The polymerization rate of EO is consequently considerably faster than that of PO, which plays an important role in the frequently used anionic copolymerization of EO and PO. Generally, the reactivity of alkylene oxides decreases with increasing length and bulkiness of the alkyl substituent at the epoxide moiety. High temperature and high pressure polymerization aid to overcome the problems mentioned to some extent. In addition, the use of potassium or cesium as counterions in ether solution leads to a considerably lower degree of association, and consequently polymerization by the free ions, which also improves molecular weight control.

**2.1.2. Anionic Polymerization of Propylene Oxide and Higher Alkylene Oxides.** The oxanionic polymerization of propylene oxide is hampered by proton abstraction from the methyl group by the highly basic initiator system and consequently extensive chain transfer to the PO monomer. Subsequent elimination reaction creates an allyl alkoxide that can initiate polymerization of a new chain (Scheme 5). This results in low molecular weight PPO with an unsaturated allyl end group. Due to this reaction, the molecular weight of PPO and also longer alkylene oxides prepared by oxanionic polymerization is limited to 6000 g/mol, which correlates with the ratio of the

#### Scheme 5. Molecular Weight-Limiting Chain Transfer to Monomer and Subsequent Elimination Reaction in the Oxanionic Polymerization of PO



polymerization rate constant and the rate constant of chain transfer to the PO monomer ( $k_p/k_{tm}$ ).<sup>54</sup> The counterion influences the chain transfer to the monomer and the resulting isomerization of PO to allyl alcohol. This decreases in the order  $\text{Na}^+ > \text{K}^+ > \text{Cs}^+$ , which is related to the interactions between the metal cation and the alkoxide.<sup>55</sup> Therefore, improved conditions to maintain the living character and to achieve higher molecular weights have been a major objective of research on PO polymerization, ever since PPO has been employed for important applications as telechelic oligomers and high molecular weight elastomers.

The above side reactions may be overcome to a great extent when employing cesium-initiating systems, which are often used in academic research, but not for large scale industrial synthesis.<sup>56</sup> In addition, the transfer side reaction can be suppressed to some extent by counterion complexation with crown ethers that also leads to an acceleration of the polymerization. Nevertheless, even in such systems the molecular weight ( $M_n$ ) of poly(1,2-propylene oxide) (PPO) does not exceed 15 000 g/mol. Price et al. showed that molecular weights of 13 000 are the result of carrying out the polymerization in neat propylene oxide at 40 °C with potassium and 18-crown-6 ether as an additive.<sup>57</sup> Alternative strategies and recent progress enabling to overcome these limitations for PO and other substituted epoxide monomers, such as glycidyl ethers, are presented in sections 2.3 and 3.1 of this review.

#### 2.2. Coordination Polymerization

Since high molecular weight polymers of EO with molecular weights exceeding 30 000 g/mol are commonly called PEO, this term will also be used in the ensuing paragraph. PEO with molecular weights exceeding 100 000 g/mol is of great interest for hydrogels, PEO fibers, mechanically strong films and for surface modification, albeit preparation by oxanionic polymerization is not possible. Sloop et al.<sup>58</sup> and Doytcheva et al.<sup>59</sup> showed for instance that PEO with molecular weights exceeding 200 000 g/mol (up to 7 000 000 g/mol) can be cross-linked by irradiation with UV light, when a hydrogen-abstrating benzophenone (BP) as a photoinitiator is present. Mechanically stable hybrid films of high molecular weight PEO combined with another water-soluble polymer (e.g., polysaccharide) can be prepared from a common solvent.<sup>60</sup> UV-cross-linking can be successfully performed not only with PEO films, but also with PEO in aqueous solution.<sup>61</sup>

An excellent overview of the coordination polymerization (sometimes also called “anionic coordination polymerization”) leading to high molecular weight PEO with molecular weights up to several millions was recently given by Dimitrov and Tsvetanov.<sup>18</sup> Therefore, this technique will be described only briefly in this review. Due to the limitations of the oxanionic polymerization, the coordination polymerization has been studied for a long time, particularly aiming at the preparation of high molecular weights for PEO as well as for other epoxide monomers. A large number of initiators has been investigated

with respect to kinetics and molecular weight control. Alkaline-earth carbonates and aluminum isopropoxide-zinc chloride, alkyl aluminum-water-acetylacetonate, diethyl zinc-aluminum oxide, bimetallic oxido-alkoxide catalysts have been employed by Hill et al.,<sup>62</sup> Miller and Price,<sup>63</sup> Vandenberg,<sup>64</sup> Osgan and Teyssie,<sup>65</sup> Hsieh,<sup>66</sup> and more recently Zhang and Shen.<sup>67</sup> Commonly, the catalysts consist of an organometallic compound and a protic compound that lead to multinuclear structures with an active metal-heteroatom (Mt-X) bond. The metal may be Al, Zn, and Cd, and X = O, S, and N. Also nonassociated mononuclear species with the Mt-X active bond (Mt = Al and Zn, X = Cl, O, and S) can be used.

The coordination of the epoxide results in two main effects: (i) activation of the monomer for the polymerization, and (ii) generation of a specific orientation of the reacting molecules that may lead to stereospecific polymerization of PO or longer alkylene oxides. The currently established most effective initiators are derivatives of divalent and trivalent metals, e.g., Ca, Zn, and Al. It is obvious that metals used for this purpose should exhibit Lewis acidity. In industry, mostly calcium and zinc/aluminum-based catalysts are used. Zhang and Shen<sup>67</sup> used alkaline-earth carbonate,  $[(RO)_2Al-O-Zn-Al(OR)_2]$ , trialkylaluminum-water-zinc acetylacetonate, trialkylaluminum-water, and rare earth metal acetylacetonate as catalysts to obtain high-MW PEO.

The polymerization of heterocyclic monomers with coordination catalysts represents a peculiar group of coordination polymerization processes that differs essentially from the highly relevant coordination polymerization of vinyl monomers. Both the mode of monomer coordination and chain formation mechanism of the coordinating monomer are different. With the exception of Ca-based catalysts, oxirane polymerizations rely on monomer coordination at the active site of the catalyst via  $\sigma$ -bond formation between the monomer heteroatom and the catalyst metal atom. This is followed by a nucleophilic attack of the initiating group or polymer-chain active site on the coordinating monomer in the initiation or propagation step, respectively.

Calcium initiators generally exhibit weaker coordination with epoxides than aluminum or zinc complexes. Consequently, they are particularly effective for the polymerization of EO, which forms complexes more readily compared to other epoxides. Calcium initiators form weaker complexes with the substituted oxiranes, PO in particular, and therefore slow polymerization is observed.

Alkaline-earth amides and amide-alkoxides are applied for the commercial production of high molecular weight PEO and are considered to be the most active catalysts for EO polymerization. They are active in the temperature range 0 °C – 50 °C. This is unusual, considering that alkaline earth carbonates and oxides require much higher temperatures, commonly exceeding 70 °C. As Tsvetanov et al. pointed out,<sup>18</sup> the fact that calcium amide catalysts are very active at temperatures below the melting point of PEO (65 °C), possesses considerable industrial significance. It would be technologically impractical or even impossible to carry out the polymerization of EO in bulk or in solution because of the high viscosity and heat-transfer problems. In addition, rapid degradation of PEO occurs in strong shear fields. The synthesis of PEO resins in the form of free-flowing white powders is therefore commonly realized in a precipitant medium, where the polymer is directly generated in the form of fine particles. This polymerization represents a precipitation (dispersion) polymerization, since the hydrocarbon reaction medium dissolves only

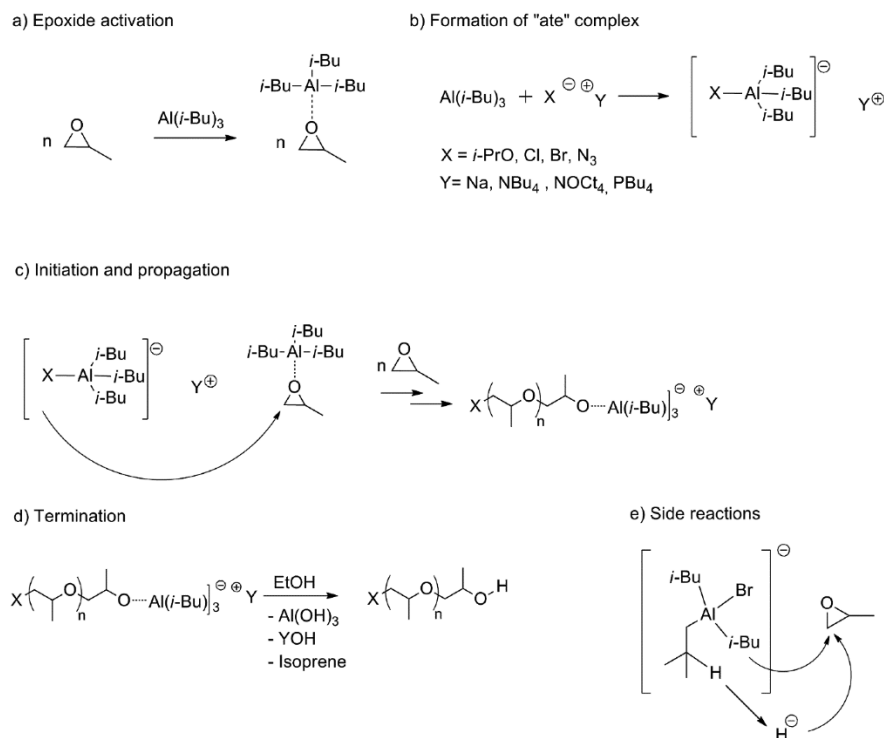
the monomer, not the PEO formed. While PEO is insoluble in hydrocarbons, the apolar PPO, poly(1,2-epoxybutane) (PBO), and PEEGE form highly swollen gels under these conditions.<sup>68</sup> Therefore, hydrocarbons are considered to act as organic reaction diluents. Below the melting point, the polymer formed remains in granular form. The temperature is easily controlled by the rate of monomer feed. The main prerequisite for the successful dispersion polymerization is the addition of a nonionic surfactant or amphiphilic block copolymer to stabilize the interface of the polymer particles formed. The most efficient type of dispersant is based on block or graft copolymers. Suitable polymer dispersants commonly consist of two polymer segments, one segment being soluble in the liquid medium, which is interspersed by short segments of the other that are strongly adsorbed at the particle surface, anchoring the dispersant there. Calcium-based catalysts are often highly active. For instance, the Union Carbide Ca-amide catalyst reported by Goeke and Karol produces 1800 g of PEO per g of Ca.<sup>69</sup> Thus, the resulting PEO particles contain only a small amount of catalyst impurity and thus no further purification of the polymer is required. The polymer powder can be directly recovered by filtration and is used without further processing.

Although a variety of calcium-based catalysts is known, systematic studies on catalyst activity and the polymerization mechanism are scarce and synthetic details are mostly not disclosed by the manufacturers. Most of the catalyst systems known are published in the patent literature. Elucidation of the structure of catalyst active site is extremely difficult. There are hardly any publications describing the synthesis of Ca catalysts in more detail.<sup>70,71</sup> In addition, the catalyst systems are little defined heterogeneous aggregates. Like in other heterogeneous catalysis strategies, the catalyst is formed on silica carriers or on modified hydrophobic silica carriers. The activity of the catalysts can be enhanced by the use of a scavenging agent with no activity in the polymerization process, such as  $R_3Al$ ,  $LiAlH_4$ ,  $n-BuLi$ , and  $ZnEt_2$ . The scavenger removes traces of oxygen and moisture from the polymerization mixture. The rather low catalyst activity greatly differs from the heterogeneous Ziegler–Natta type olefin polymerization, where extremely high catalyst efficiencies are achieved.

The synthesis of high molecular weight copolymers of ethylene oxide and other epoxides with polar functional groups via the coordination methods remains an interesting challenge. Polar epoxide monomers may undergo various side reactions involving either cationic or anionic polymerization, making the propagation process complex. In summary, in view of the highly interesting properties and application potential of high molecular weight PEG and its copolymers, it is a pity that at present hardly any academic research efforts and recent developments can be noted in the area of the coordination polymerization of epoxides and practically all published works date back in the 1980s and 1990s.

### 2.3. Activated Monomer Strategy

In this section we give an overview of the “activated monomer mechanism” for the polymerization of epoxide monomers, developed by Carlotti and Deffieux, which represents a major breakthrough for many functional epoxides.<sup>72,25</sup> In 2013, Carlotti et al. published a detailed review regarding polyether syntheses based on such activated or metal-free anionic ring-opening polymerizations of epoxides.<sup>73</sup> The “controlled” high speed anionic polymerization of PO by the monomer-activation technique was introduced in 2004.<sup>72</sup> Remarkably, this represents

**Scheme 6.** Reaction Mechanism of the “Activated Monomer” Technique, Exemplified for the Polymerization of Propylene Oxide (PO)<sup>72,84</sup>

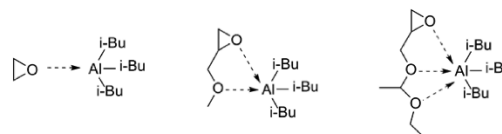
the first method that permits to obtain high molecular weight PPO ( $M_n$  up to 170 000 g/mol).<sup>72</sup> Inspired by the work of Inoue and co-workers<sup>74–78</sup> and Braune and Okuda,<sup>79</sup> monomer activation results from the interaction of a Lewis acid with the epoxide ring, reducing the electron density in the epoxide ring, thereby facilitating subsequent ring-opening. The initiation proceeds through formation of an “ate complex” between the Lewis acid (catalyst) and a weak nucleophile (initiating species), as illustrated in Scheme 6. Chain growth results exclusively in head-to-tail (H-T) linkages with no appearance of H–H or T-T junctions, and for racemic epoxides an atactic microstructure is obtained, indicating a coordination type mechanism.<sup>72,80</sup>

The first initiating systems of this type were based on alkali metal alkoxides with trialkyl-aluminum species, resulting in an enhanced polymerization rate and little occurrence of transfer reactions compared to conventional AROP.<sup>72</sup> Improved initiator systems are based on organic salts, containing noncoordinating cations such as tetraalkyl ammonium halides or phosphonium salts combined with triisobutylaluminum as a catalyst, which fully suppress transfer reactions.<sup>72,80–84</sup> However, besides the desired initiation via the respective halide anion, concurrent ring opening via hydride or *iso*-butyl groups is reported, which may lower molecular weights and lead to a fraction of ill-defined chain ends (Scheme 6e).<sup>84,85</sup>

Suitable solvents for the activated monomer approach are aprotic and should preferably possess no complexing oxygen atoms. For example, THF complexes the aluminum compound and thereby impedes activation of the epoxides. A suitable alternative solvent for THF is 2-methyltetrahydrofuran (MeTHF).<sup>86</sup> Further, the use of cyclohexane, toluene, dichloro-

methane, chlorobenzene,<sup>87</sup> and fluorinated benzene was reported in literature.<sup>72,80,84,85,88,89</sup>

Note that the ratio of Lewis acid (catalyst) to the actual initiator has to exceed unity to ensure the formation of the “ate”-complex and simultaneously implement an activation of the epoxide ring, resulting in successful polymerization. Monomers with strong coordination capability require higher amounts of the catalyst to overcome strong interactions with the Lewis acid (Scheme 7). However, low ratios are preferred, to ensure narrow molecular weight distributions.<sup>72</sup>

**Scheme 7.** Complexation of Triisobutylaluminum by Oxygen Atoms<sup>84</sup>

<sup>84</sup>Interaction of triisobutylaluminum with EO, GME, and EEGE (from left to right).

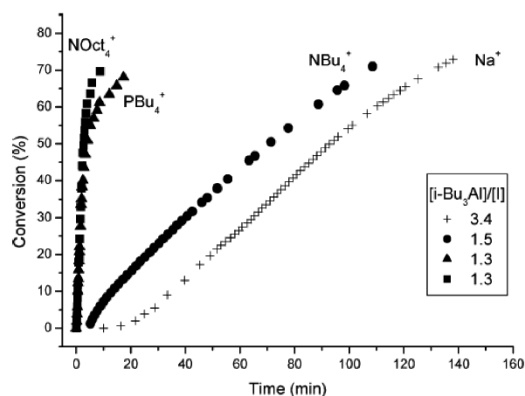
Strong activation of the epoxide ring brings about several advantages: (i) polymerizations can be carried out under mild reaction conditions (low temperatures,  $-30$  °C to room temperature) and (ii) with weak nucleophilic “ate” complexes as initiator and propagating species. Consequently, molecular weight limiting transfer-to-monomer reactions are suppressed, and high molecular weight polyethers are accessible, while the



## Chemical Reviews

Review

molecular weight distribution remains narrow. Additionally, polymerization rates are dramatically increased, and the reactions can be carried out in hydrocarbon solvents (Figure 2).<sup>72,88,90</sup>



**Figure 2.** Conversion plotted versus time for PO polymerization initiated by *i*-PrONa, NBu<sub>4</sub>Cl, NOct<sub>4</sub>Br, and PBu<sub>4</sub>Cl in cyclohexane with the respective Lewis acid to initiator ratio and degrees of polymerization around 170–192. Adapted with permission from Labbé, A.; Carloti, S.; Billouard, C.; Desbois, P.; Deffieux, A. *Macromolecules* 2007, 40, 7842–7847.<sup>80</sup> Copyright 2007 American Chemical Society.

Within less than 2 h, PPO samples with remarkably high molecular weights of 170 000 g·mol<sup>-1</sup> and rather low PDI = 1.34 were accessible.<sup>72,80</sup> Note that the use of conventional alkali metal initiators restricts the molecular weight of PPO to about 6000 g·mol<sup>-1</sup>,<sup>91</sup> and even the use of soft counterions such as cesium or the addition of crown ethers still limits the molecular weight to about 15 000 g·mol<sup>-1</sup>.<sup>92,93</sup> Further, the authors demonstrated the applicability of this method by preparing a number of high molecular weight polyethers such as high molecular weight PEEGE (up to 85 000 g·mol<sup>-1</sup>),<sup>89</sup> PEG (up to 36 000 g·mol<sup>-1</sup>) and PPO–PEG copolymers.<sup>88</sup> The fascinating synthetic options created by this method permitted to study the molecular weight dependence of the viscoelastic properties of linear polyglycerol (*lin*PG) in the entire molecular weight range of 1 kg·mol<sup>-1</sup> to 100 kg·mol<sup>-1</sup>. Detailed rheological features of *lin*PG and its permethylated analogue (*lin*PG-OMe) were reported, demonstrating the effect of a hydrogen bonding network from nonentangled to well-entangled chains.<sup>94</sup>

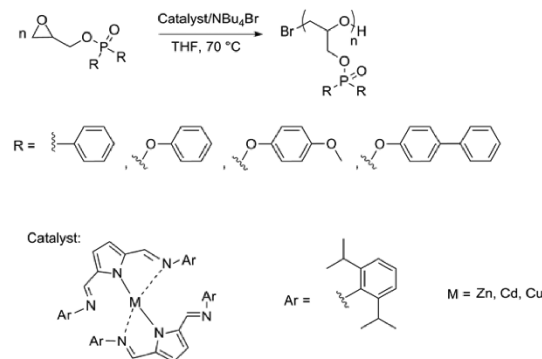
In general, the strong activation of the epoxide ring enables to polymerize a broad family of less reactive and sterically hindered epoxides, such as epoxides bearing hydrophobic alkyl chains (1,2-butene oxide, 1,2-hexene oxide, 1,2-octadecene oxide) and glycidyl methyl ether.<sup>95–99</sup> In addition, with the controlled polymerization of epichlorohydrin (ECH), Carloti and co-workers demonstrated the high tolerance of this method toward functional groups. Interaction of the active species with the chloromethyl function was not observed, and homopolymers of PECH with molecular weights up to 80 000 g·mol<sup>-1</sup> and PDIs below 1.25 were realized.<sup>100</sup> This strategy gives access to a library of novel polymers, based on postpolymerization modification of the chloride groups of PECH. Lynd and co-workers presented hydrolytically degradable PEG by copolymerizing ECH with EO. The copolymers were treated with potassium *tert*-butoxide to obtain poly(methylene ethylene oxide) units, leading to degradation at slightly acidic pH.<sup>101</sup> Also starting from PECH, Meyer et al. prepared poly(glycidyl amine).<sup>102</sup> Recently, Baker et

al. reported the synthesis of a polyether-based poly(ionic liquid) by derivatizing the chlorides of PECH with 1-butylimidazol, followed by anion exchange with lithium bis-(trifluoromethanesulfonyl)imide.<sup>103</sup> The modified polymers showed conductivities of 10<sup>-5</sup> S cm<sup>-1</sup> at 30 °C and 10<sup>-3</sup> S cm<sup>-1</sup> at 90 °C. Other challenging epoxides such as glycidyl methacrylate, fluorinated epoxides, allyl glycidyl ether and epicyclohexane<sup>87</sup> were also successfully polymerized.<sup>84,85,97,98,104</sup>

In 2010, Carloti and co-workers demonstrated that the activation of ethylene oxide even enables lithium salts to polymerize epoxides. In particular, this strategy permits the synthesis of PS-*b*-PEO and PI-*b*-PEO block copolymers in a one-pot reaction.<sup>105</sup> Further, the monomer activation with a Lewis acid can be combined with initiation via phosphazene alkoxides. Molecular weights of PPO up to 80 000 g·mol<sup>-1</sup> were obtained in this case. However, a certain extent of transfer reactions yielding unsaturated chain ends was still observed.<sup>90</sup>

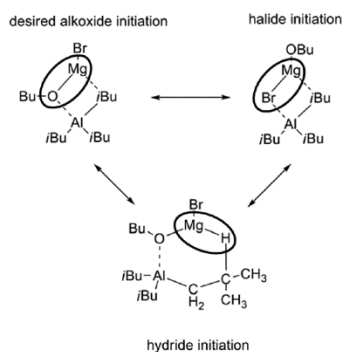
Recently, Babu and Muralidharan expanded the “activated monomer approach” towards the activation of the epoxide ring via Zn(II), Cd(II), or Cu(II) complexes of 2,5-bis(*N*-(2,6-diisopropylphenyl) iminomethyl)pyrrole.<sup>106</sup> The authors demonstrated successful polymerization of various phosphate based epoxides in THF at 70 °C by using tetrabutylammonium bromide as the actual initiator (Scheme 8).

#### Scheme 8. Synthesis of Phosphate-Containing Linear Polyethers Based on Monomer Activation<sup>106</sup>



Very recently, Roos and Carloti demonstrated the use of Grignard reagents as deprotonating agents for PO polymerization.<sup>86</sup> The authors deprotonated 1-butanol with various Grignard reagents and observed successful polymerization of PO in the presence of triisobutylaluminum as an activator. Molecular weights ranged from 2,500 to 10,000 g·mol<sup>-1</sup>, while PDIs remained moderate (1.20–1.37). The formation of allylic end groups was completely suppressed; however initiation via various species was detected. MALDI-ToF measurements revealed initiation by (i) 30% desired alkoxide magnesium halide (RO<sup>-</sup>MgX), (ii) 20% hydride initiation from triisobutylaluminum (H<sup>-</sup>MgX) and (iii) 50% halide initiation from the alkoxide magnesium halide (X<sup>-</sup>MgOR), as illustrated in Scheme 9.

Despite its fundamental advantages, the “activated monomer technique” also bears some challenges. To obtain low PDIs, the catalyst to initiator ratio has to be kept at a minimum and needs to be adjusted for each monomer system with respect to the targeted molecular weight. Further, removal of the residual initiator counterions, i.e., the tetraalkyl ammonium salts, is often

**Scheme 9. Proposed Initiation Species for Grignard/Alcohol/Triisobutylaluminum System**<sup>86</sup>

difficult and time-consuming. Simple precipitation of the polymer often leads to unsatisfactory results. Column chromatography or long-term dialysis can be performed, albeit with reduction of the polymer yield.<sup>97</sup> More hydrophobic polyethers, such as PEEGE, can also be purified by consecutive washing with saturated  $\text{NaHCO}_3$  solution,  $\text{NaCl}$  solution (10%), and water.<sup>94</sup>

Direct calculation of the absolute  $M_n$  via  $^1\text{H}$  NMR spectroscopy using  $^1\text{H}$  NMR signals of the initiator is generally not possible for the activated monomer approach, given the nature of the initiator species (bromide, chloride, and azide). In the literature, molecular weights are determined by SEC measurements (refractive index signal or UV signal). However, molecular weights analyzed by a general SEC setup are not absolute values. Alternatively, end-group functionalization or absolute methods, such as static light scattering, have to be performed. Even though the formation of unsaturated end-groups can be mainly suppressed, undesired initiation by hydride or *iso*-butyl groups was also reported (Scheme 6e).<sup>80,84</sup>

In summary, the “activated monomer mechanism” has become a well-established alternative to the conventional AROP within the past decade and is a crucial method, both to prepare high molecular weight polyethers and to polymerize a broad family of epoxides bearing functional groups to generate novel functional polyethers.

#### 2.4. *N*-Heterocyclic Carbenes (NHCs) and *N*-Heterocyclic Olefins (NHOs) as Organocatalysts for Metal-Free Polyether Synthesis

*N*-Heterocyclic carbenes (NHCs) have seen a tremendous development since the turn of the millennium and are known as efficient ligands of transition metal complexes<sup>107,108</sup> or as organocatalysts for reactions, such as the benzoin condensation or the Stetter-reaction.<sup>109–111</sup> Recently, Taton et al. reviewed the

use of *N*-heterocyclic carbenes (NHCs) in organocatalysis, mainly focusing on general macromolecular chemistry.<sup>112,113</sup> In 2015, Naumann and Dove further highlighted a current trend regarding NHCs as organocatalysts for various polymerizations.<sup>114,115</sup> Here we summarize current reports devoted to NHCs as initiators and/or as organocatalysts for the metal-free ROP of epoxides.

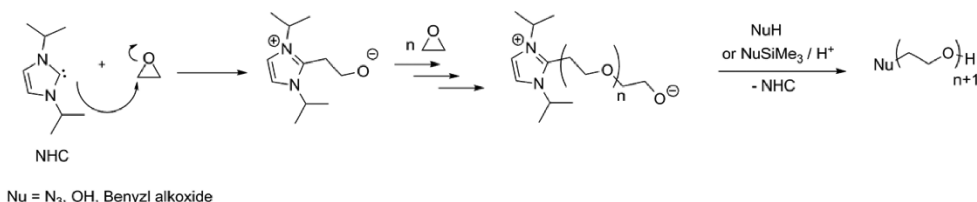
In 1991, Arduengo et al. presented the first crystalline diaminocarbene and introduced the class of *N*-heterocyclic carbenes (NHC).<sup>116</sup> While the first step-growth polymerization via NHC catalysis followed in the late 1990s,<sup>117,118</sup> the use for EO polymerization was not established until 2009, when it was introduced in a seminal work by Taton and Gnanou et al.<sup>119</sup> The authors showed that the strong nucleophilicity of 1,3-bis-(diisopropyl)imidazol-2-ylidene enabled the direct attack at the methylene group of EO, generating an imidazolium alkoxide for further polymerization of EO. The proposed polymerization mechanism is based on the formation of a zwitterionic species (imidazolium alkoxide), as displayed in Scheme 10. Termination with suitable nucleophiles releases the NHC and affords well-defined  $\alpha,\omega$ -bifunctional PEG.

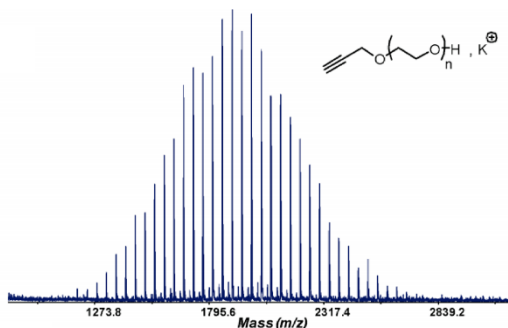
This technique enabled the controlled synthesis of heterotelechelic PEG up to  $13\,000\text{ g}\cdot\text{mol}^{-1}$ , with narrow molecular weight distributions without the need to remove metallic initiators. Most important, no cyclic species were detected. In general, the NHC method allows for facile synthesis of azide-functional PEG, which is suitable for subsequent azide–alkyne click-chemistry. Furthermore, the authors demonstrated the versatility of the NHC method by combining the ring-opening polymerization of epoxides with cyclic esters. In particular, PEG-*b*-PCL block copolymers were synthesized by simple addition of  $\epsilon$ -caprolactone (CL) to the NHC-initiated PEG-chain.

In addition, Taton et al. demonstrated the successful polymerization of EO by using NHC as a true organocatalyst. A typical procedure relies on a ratio of  $[\text{NHC}]/[\text{NuE}]/[\text{EO}] = 0.1:1:100$ , whereas NuE (Nu = nucleophilic and E = electrophilic part, e.g.,  $\text{PhCH}_2\text{OH}$ ,  $\text{HC}\equiv\text{CH}_2\text{OH}$ ,  $\text{N}_3\text{SiMe}_3$ , and  $\text{PhCH}_2\text{OSiMe}_3$ ) represents the chain regulator.<sup>120</sup> Well-defined, heterotelechelic PEGs up to  $12\,000\text{ g}\cdot\text{mol}^{-1}$  were synthesized with narrow molecular weight distributions (PDI = 1.07–1.15). As an example, Figure 3 shows the MALDI TOF MS spectrum of  $\alpha$ -propargyl, $\omega$ -hydroxyl heterodifunctional PEG, confirming the absence of any side products and the preservation of the alkyne functionality during polymerization.<sup>120</sup>

The authors considered two possible mechanisms, based on either monomer activation (path a) or chain-end activation (path b) by the NHC, as illustrated in Scheme 11.

Motivated by the successful metal-free synthesis of PEG, Taton et al. also implemented the NHC method for the polymerization of PO.<sup>121</sup> Yet, low monomer conversion ( $\leq 40\%$ )

**Scheme 10. Proposed Reaction Scheme of the Zwitterionic ROP of EO**<sup>119</sup>

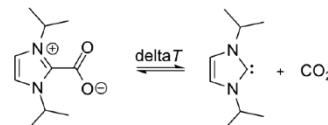


**Figure 3.** MALDI TOF MS of  $\alpha$ -propargyl, $\omega$ -hydroxyl heterodifunctional PEO. Adapted with permission from Raynaud, J.; Absalon, C.; Gnanou, Y.; Taton, D. *Macromolecules* **2010**, *43*, 2814–2823.<sup>120</sup> Copyright 2010 American Chemical Society.

was observed and the absence of unsaturated impurities was only ensured for low molecular weight PPOs ( $4500 \text{ g}\cdot\text{mol}^{-1}$ ).

Recently, Lindner et al. reported several NHC–CO<sub>2</sub> adducts as feasible precatalysts for the homopolymerization of PO and the block copolymerization with  $\epsilon$ -caprolactone (CL) or block and random copolymerization with (*S,S*)-lactide (LA), respectively.<sup>122</sup> NHC–CO<sub>2</sub> adducts are thermally labile progenitors that allow the in situ generation of NHCs (Scheme 12), as recently reviewed by Naumann and Buchmeiser.<sup>123</sup> The homopolymerization of PO was performed by release of the

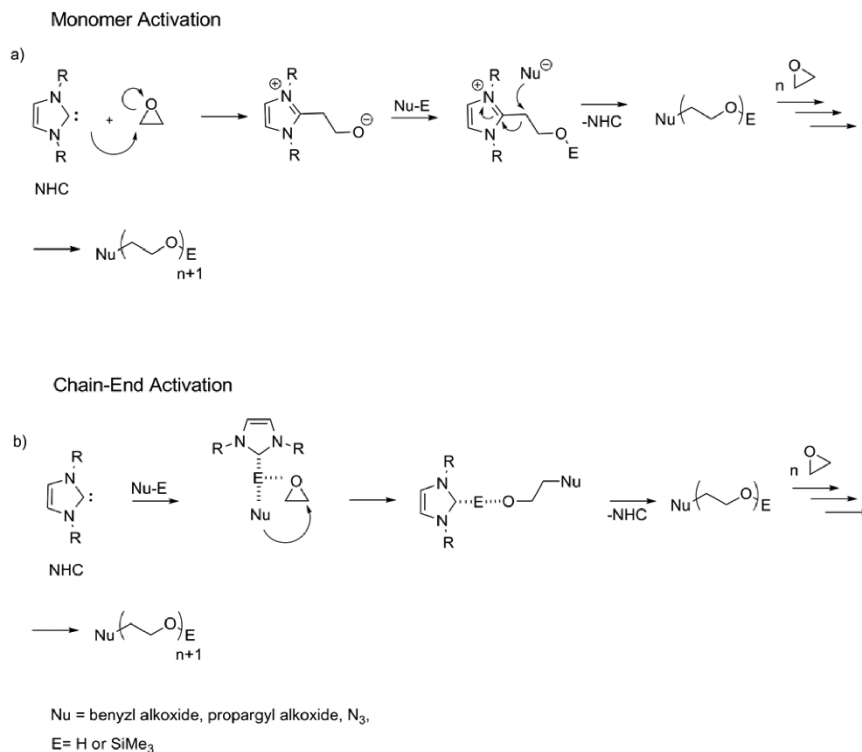
**Scheme 12.** Example of a CO<sub>2</sub>-Protected NHC<sup>122</sup>



NHC at  $120^\circ\text{C}$  and initiation with diethylene glycol. Oligomeric PPO with narrow MWD (1.08–1.23) was obtained. Moreover, the authors presented block copolymers of PO and CL, and block and random copolymers of PO and LA, respectively. In contrast to pure PPO, the copolymers showed rather poor monomer conversion and broad MWD ( $\text{PDI} = 1.38\text{--}1.77$ ), assumingly a result of transesterification or backbiting reactions.

In summary, NHCs are suitable initiators and/or catalysts to synthesize  $\alpha,\omega$ -bifunctional PEGs. To date, the successful polymerization of EO and the synthesis of low molecular weight PPO as well as several block copolymers have been presented. It is obvious that this method could also show promising results for other epoxide-based monomers, for instance to generate multifunctional PEG. Further, the random copolymerization of epoxides with cyclic esters is feasible and warrants further study that may lead to unprecedented copolymer structures.<sup>119,122</sup> Nevertheless, NHCs are highly reactive and sensitive compounds and careful handling is necessary. Moisture should be avoided and storage at low temperatures is suggested. However, recently developed imidazolium-2-carboxylates and (benz)imidazolium hydrogen carbonates that can be viewed as masked N-

**Scheme 11.** Proposed mechanisms for the ring-opening polymerization of EO catalyzed by NHC. (a) via monomer activation; (b) via chain-end activation.<sup>120</sup>



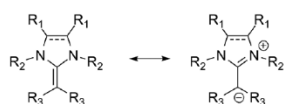
## Chemical Reviews

Review

heterocyclic carbenes permit use for polymerization of various monomers (lactide, MMA) at room temperature and possess greatly improved storage stability.<sup>124</sup> Therefore, intriguing potential for the polymerization of epoxide monomers can be envisaged.

A further step to metal-free polymer synthesis was reported by Naumann and Dove et al., who applied *N*-heterocyclic olefins (NHOs) as organic catalyst for the controlled polymerization of PO.<sup>125</sup> NHOs are highly polarized alkenes with considerable electron density on their exocyclic carbon atom, as illustrated in Scheme 13.<sup>126</sup> To some extent, they combine NHC-like adaptability and carbanionic reactivity. NHOs are air sensitive and should be preferably stored at cold temperatures.<sup>126–128</sup>

**Scheme 13. Mesomeric Structure of NHOs, Showing the Strong Charge Delocalization**<sup>125</sup>



Naumann and Dove et al. prepared a library of NHOs and studied their structural influence on PO polymerization. Similarly as for the NHCs, the authors proposed two possible mechanisms for the polymerization of PO with NHO, which are in agreement with the “monomer activation” and “chain end activation” shown exemplarily in Scheme 11 for NHCs. For NHOs, the zwitterionic “monomer activation” leads to the occurrence of high molecular weight impurities but is mainly disfavored for NHOs. The authors demonstrate that the zwitterionic mechanism can be suppressed completely by increasing steric hindrance and basicity of the catalytically active site. Consequently, the most suitable NHO for ROP of epoxides is shown in Scheme 14, bearing two methyl moieties at the exocyclic carbon atom.

**Scheme 14. Suitable NHO Catalyst to Obtain Well-Defined PPO**<sup>125</sup>



Overall, PPO with molecular weights in the range of 2000–12 000 g·mol<sup>-1</sup> and narrow PDIs below 1.06 were prepared. Despite the high turnover number (TON) of about 2200, the polymerization of PO with organic catalysts is rather slow, e.g., 88% conversion of PO with ratios of 1:10:1000 ([NHO]/[BnOH]/[PO]) was reached in 68 h. Nevertheless, NHOs represent a promising class of catalysts for novel polymer structures.

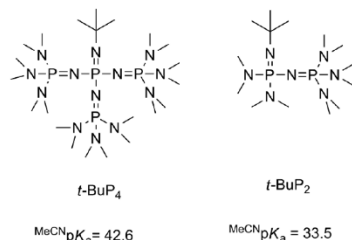
### 2.5. Phosphazene Bases: Metal-Free Initiators

Another metal-free polymerization technique relies on the use of phosphazene bases as deprotonation or complexation agents. While various reviews and books have covered the use of phosphazene bases for living anionic polymerizations,<sup>25,73,129–132</sup> herein an overview of their general use for epoxide polymerization and focus on recent achievements will be presented.

Phosphazene bases, also known as “Schwesinger Bases”, belong to the family of neutral Brønsted “super” bases, which are

highly basic but only weakly nucleophilic (selected phosphazene bases in Scheme 15).<sup>133–135</sup> Despite their exceptional structure,

**Scheme 15. Chemical Structure and Respective p*K*<sub>a</sub> Value of Relevant Phosphazene Bases for Epoxide Polymerization**<sup>14</sup>



<sup>14</sup> 1-*tert*-Butyl-4,4,4-tris(dimethylamino)-2,2-bis[tris(dimethyl-amino)-phosphoranylideneamino]-2λ<sup>5</sup>, 4λ<sup>5</sup>-catenadi(phosphazene) (*t*-BuP<sub>4</sub>) and 1-*tert*-butyl-2,2,4,4,4-pentakis(dimethylamino)-2λ<sup>5</sup>, 4λ<sup>5</sup>-catenadi(phosphazene) (*t*-BuP<sub>2</sub>).

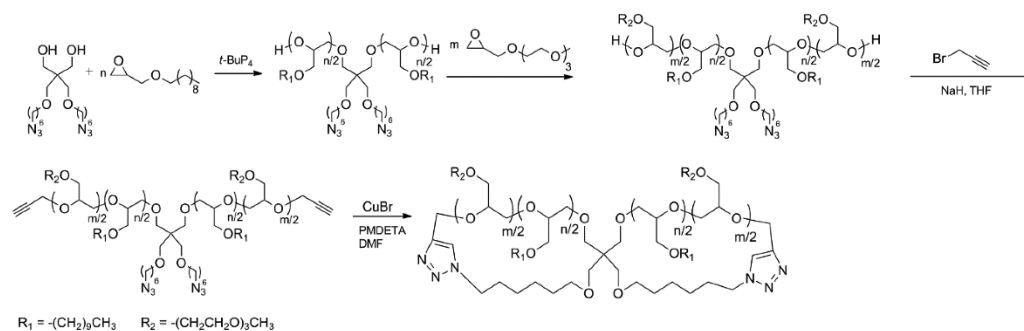
phosphazene bases are commercially available, chemically and thermally stable, and soluble in nonpolar and moderately polar organic solvents (e.g., hexane, toluene, and THF).<sup>133</sup> Nevertheless, the commercially available phosphazene bases may contain their respective isomers as impurities, which could have an influence on their reactivity.<sup>136</sup> In 1996, Möller and co-workers introduced the first polymerization of EO with *t*-BuP<sub>4</sub> as a deprotonation agent.<sup>137</sup> In the family of phosphazene bases, *t*-BuP<sub>4</sub> is one of the strongest phosphazene bases with a p*K*<sub>a</sub> of 42.6 (in acetonitrile)<sup>134</sup> and is typically used for the ROP of epoxides (Scheme 15). As an alternative to phosphazene bases, Rexin and Müllhaupt investigated several bulky phosphonium salts as deprotonation agents for PO polymerization.<sup>138,139</sup> At polymerization temperatures of 100 °C, the total degree of unsaturations was lowered, compared to known phosphazene bases, albeit lower polymerization rates were observed.<sup>138</sup> Recently, Hadjichristidis and Gnanou et al. reported the first successful use of the less conjugated and consequently milder *t*-BuP<sub>2</sub> (MeCN p*K*<sub>a</sub> = 33.5)<sup>134</sup> for the polymerization of EO (Scheme 15).<sup>140</sup> This approach enabled an elegant one-pot synthesis of polyether-polyester block terpolymers (PEO-*b*-PCL-*b*-PLA) with no occurrence of chain transfer reactions (PDI = 1.10).<sup>140</sup> However, prolonged reaction times have been reported for the EO polymerization with *t*-BuP<sub>2</sub>, and no successful polymerizations of other epoxides have been demonstrated to date. For example, only *t*-BuP<sub>4</sub> enabled successful polymerization of 1,2-butene oxide (BO), but neither *t*-BuP<sub>1</sub>, *t*-BuP<sub>2</sub>, nor TiBP, which is due to insufficient basicity.<sup>141</sup> Consequently, *t*-BuP<sub>4</sub> remains the standard phosphazene base for epoxide polymerization, e.g., EEGE,<sup>142</sup> AGE,<sup>143</sup> glycidyl methyl ether (GME),<sup>144</sup> ethyl glycidyl ether (EGE),<sup>144</sup> PO,<sup>141</sup> *tert*-butyl glycidyl ether (*t*BuGE),<sup>141</sup> and benzyl glycidyl ether (BnGE).<sup>141</sup>

The salient feature of phosphazene bases and especially *t*-BuP<sub>4</sub> for epoxide ROP is that they are metal-free and thus alternative deprotonation agents to common alkali hydroxides. After deprotonation, the bulky phosphazanium cation [*t*-BuP<sub>4</sub>]<sup>+</sup>H<sup>+</sup> represents a soft counterion with low tendency for ion-pair association. Consequently, high polymerization rates also in nonpolar solvents under mild reaction temperatures can be observed, as the chain end is highly reactive. Usually, the ratio of phosphazene base: initiator is close to 1, but also lower ratios (as low as 0.01 equiv) have been reported but are accompanied by

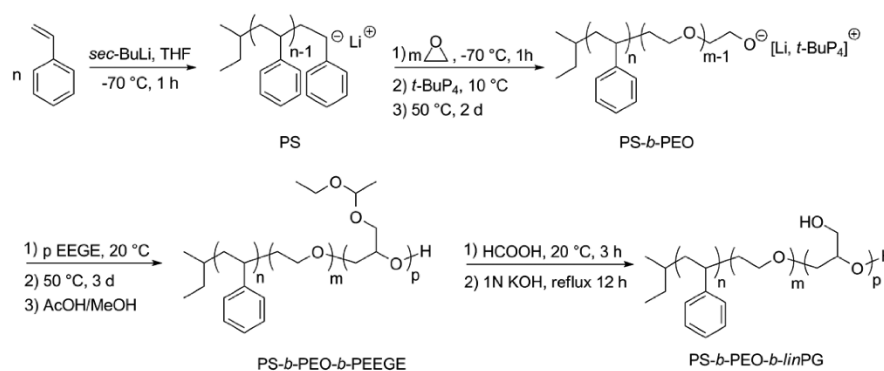
## Chemical Reviews

## Review

**Scheme 16. Synthesis of Figure-Eight Shaped Amphiphilic Block Copolyethers Based on Decyl Glycidyl Ether and 2-(2-(2-Methoxyethoxy)ethoxy)ethyl Glycidyl Ether**<sup>155</sup>



**Scheme 17. One-Pot Synthesis of Poly(styrene)-*block*-poly(ethylene oxide)-*block*-poly(ethoxyethyl glycidyl ether) (PS-*b*-PEO-*b*-PEEGE) Triblock Terpolymers and Subsequent Deprotection to Poly(styrene)-*block*-poly(ethylene oxide)-*block*-*lin*poly(glycerol)**<sup>157</sup>



longer reaction times.<sup>130,145–147</sup> Suitable initiators range from common alcohols<sup>148–151</sup> to secondary amides<sup>152,153</sup> and carboxylic acids.<sup>147</sup> Kakuchi and Satoh et al. demonstrated the power of the phosphazene base approach by polymerizing less reactive monomers, such as styrene oxide,<sup>150</sup> BO,<sup>141,153,154</sup> decyl glycidyl ether and 2-(2-(2-methoxyethoxy)ethoxy)ethyl glycidyl ether<sup>155</sup> as well as several glycidyl amine derivatives (see also section 3.2).<sup>151</sup> Based on a selection of these monomers, the authors synthesized linear, cyclic, figure-eight-shaped, and tadpole-shaped amphiphilic block copolyethers starting from  $\alpha,\omega$ -bifunctional initiators, bearing an alcohol and an azide functionality (Scheme 16).<sup>155</sup>

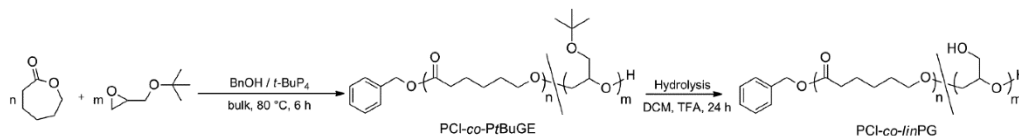
Alternatively, phosphazene bases can be used as complexation agent and enable ROP of epoxides starting from anions bearing lithium as a counterion.<sup>142,148,156</sup> In general, lithium alkoxides are not applicable for epoxide polymerization due to the strong interaction of the lithium cation with the alkoxide. Addition of phosphazene bases breaks down the ion association of lithium cations with the alkoxides, and polymerization can proceed. Thus, switching from carbanionic polymerization to oxanionic polymerization is possible, permitting the one-pot synthesis of a variety of promising block copolymers. For example, Müller and Schmalz et al. presented poly(styrene)-*block*-poly(ethylene oxide)-*block*-poly(ethoxyethyl glycidyl ether) (PS-*b*-PEO-*b*-PEEGE) triblock terpolymers in a one-pot procedure (Scheme 17) that were deprotected to afford PS-*b*-PEO-*b*-*lin*PG with a

linear polyglycerol block (*lin*PG).<sup>157</sup> Narrow PDIs of 1.02 confirm the living character of the polymerization.

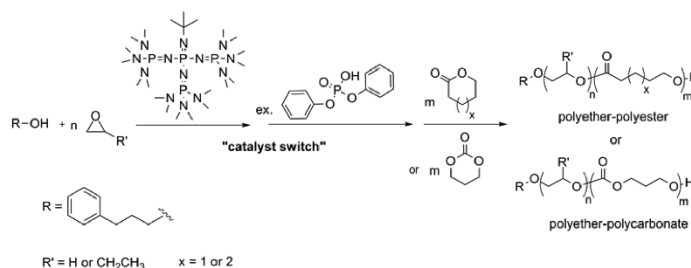
Other examples are PS-*b*-PEO,<sup>148</sup> PB-*b*-PEO,<sup>158–160</sup> PI-*b*-PEO,<sup>158,161</sup> PB-*b*-PI-*b*-PEO,<sup>162</sup> PS-*b*-*lin*PG,<sup>163</sup> P2VP-*b*-PEO-*b*-P(GME-*co*-EGE),<sup>144</sup> and polystyrene-*block*-poly(*p*-hydroxystyrene-*graft*-ethylene oxide)<sup>164</sup> block copolymers. Further, the switch from oxanionic to carbanionic polymerization was demonstrated for EO and dimethylaminoethyl methacrylate (DMAEMA), but only PEO-*b*-PDMAEMA block copolymers with moderate PDIs (1.40–1.70) were obtained.<sup>165</sup>

In 2012, Carlotti and co-workers combined *t*-BuP<sub>4</sub> with the “activated monomer technique” for the rapid polymerization of PO at room temperature (see section 2.3).<sup>90</sup> PPO with molecular weights up to 80 000 g·mol<sup>-1</sup> was obtained. However, the authors reported the occurrence of unsaturated chain ends indicating the occurrence of transfer reactions despite the high molecular weight; consequently the combination of both methods did not lead to a significant improvement of the common “activated monomer technique”.

Phosphazene bases can also function as organocatalyst for the polymerization of cyclic esters e.g., lactide (LA)<sup>166</sup> and  $\epsilon$ -caprolactone (CL).<sup>140</sup> In general, ideal catalysts are weaker phosphazene bases such as BEMP, *t*-BuP<sub>1</sub> or *t*-BuP<sub>2</sub> to suppress undesired transesterification reactions.<sup>140,166,167</sup> The use of the strong *t*-BuP<sub>4</sub> base affords polyesters with rather broad PDIs.<sup>168</sup> Yet, this approach permits the synthesis of random polyester-polyether copolymers, as it was demonstrated for the

Scheme 18. Copolymerization Scheme of Reaction of  $\epsilon$ -CL with *t*BuGE<sup>44</sup>

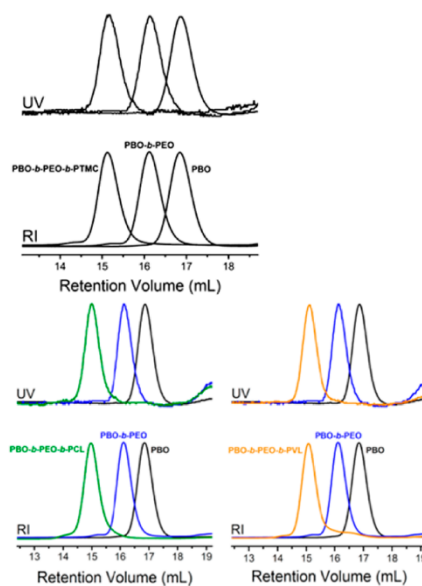
<sup>44</sup>Release of the hydroxyl groups renders PCL-*co*-linPG copolymers.<sup>169</sup>

Scheme 19. Reaction Scheme of the “Catalyst Switch” Approach for the Block Copolymerization of EO/BO with  $\epsilon$ -Caprolactone/ $\delta$ -Valerolactone or Trimethylene Carbonate<sup>145</sup>

copolymerization of  $\epsilon$ -caprolactone (CL) with *tert*-butyl glycidyl ether (*t*BuGE) (Scheme 18).<sup>169</sup> CL ratios were varied from 0 to 100 mol %, resulting in (co)polymers with molecular weights ranging from  $1.38 \times 10^{-4}$  to  $4.92 \times 10^{-4}$  g·mol<sup>-1</sup> and moderate PDIs 1.28–1.43. After cleavage of the *tert*-butyl protecting group, the PCL-*co*-linPG copolymers with PCL < 72 mol % showed faster enzymatic degradation than pure PCL. The authors attribute the accelerated biodegradation to the lower degree of crystallization and higher hydrophilicity of PCL-*co*-linPG than PCL, induced by the incorporated glycerol units.

Recently, Hadjichristidis and Gnanou et al. utilized a “catalyst switch” for the sequential one-pot polymerization of polyether-polyester/polycarbonate block copolymers by applying a combination of phosphazene bases and diphenyl phosphate (DPP).<sup>145</sup> As mentioned before, the strong basicity of *t*-Bu<sub>4</sub>P promotes chain transfer reactions during the ROP of cyclic esters or cyclic carbonates leading to relatively broad PDIs.<sup>145,168,169</sup> By the addition of DPP, the phosphazene base was neutralized and subsequently DPP acted as acidic catalyst for the polymerization of cyclic esters: a basic to acidic catalyst switch. Various epoxides (EO, BO) were polymerized by using an alcohol/*t*-Bu<sub>4</sub>P system, followed by excess addition of DPP and the respective cyclic ester (CL,  $\delta$ -valerolactone) and/or cyclic carbonate (trimethylene carbonate, TMC) (Scheme 19). Block copolymers and triblock terpolymers with molecular weights up to 19 000 g·mol<sup>-1</sup> and narrow PDIs in the range of 1.04–1.17 were obtained (Figure 4).<sup>145</sup> The authors report a retardation effect of the phosphazene diphenyl phosphate on the polymerization rates of the cyclic esters. Thus, the ratio of *t*-Bu<sub>4</sub>P should be kept at a minimum (0.2 equiv).

In 2015, the same group expanded the scope of the “catalyst switch” strategy by synthesizing linear- and three- arm star-terblock quarterpolymers based on the same monomers.<sup>146</sup> To expand the toolbox of suitable monomers, Hadjichristidis and Zhao demonstrated the successful preparation of block copolymers based on BO or 2-ethylhexyl glycidyl ether (EHGE) with various substituted lactones, namely  $\delta$ -hexalactone (HL),  $\delta$ -nonalactone (NL), and  $\delta$ -decalactone (DL).<sup>170</sup>



**Figure 4.** SEC traces of isolated products of PBO, PBO-*b*-PEO, PBO-*b*-PEO-*b*-PCL, PBO-*b*-PEO-*b*-PVL, and PBO-*b*-PEO-*b*-PTMC respectively, synthesized via “catalyst switch” strategy.<sup>145</sup> Adapted with permission from Zhao, J.; Pahovnik, D.; Gnanou, Y.; Hadjichristidis, N. *Macromolecules* 2014, 47, 3814–3822. Copyright 2014 American Chemical Society.

In summary, phosphazene bases permit the synthesis of unprecedented and “challenging” block copolymer pairs with polyether block, such as vinyl polymer-based block copolymers (PS, PI, PB, PVP) with-polyether and polyether-polyester/-carbonate, and also random polyester/polyether copolymers, in a one-pot reaction with no need for isolation or purification after individual synthetic steps. In spite of these advantages, it should be kept in mind that removal of phosphazene bases can be time-consuming and challenging and is not always considered in the

## Chemical Reviews

Review

respective works. A suitable procedure for this purpose is the purification via filtration over alumina.<sup>151,155</sup> However, often-times polymers are purified merely by simple precipitation, and the phosphazene base may remain in the polymer. Especially with a focus on future biomedical applications, complete removal of the charged phosphazene bases is mandatory, since phosphazene base cations are critically discussed with respect to their toxicity. More specifically, preliminary in vitro studies on several human cell lines suggest that *t*-BuP<sub>4</sub> exhibits high cytotoxicity, the toxic species being most probably the corresponding phosphazene ion.<sup>171</sup> Consequently, one might even consider avoiding the use of phosphazene bases for biological or biomedical purposes completely. To date, phosphazene bases have attracted minor attention for industrial polyether synthesis, which might be due to their rather high cost in comparison to established alkoxides.

### 2.6. Heterogeneous Catalysis—Double Metal Cyanide Catalysts for Epoxide Polymerization

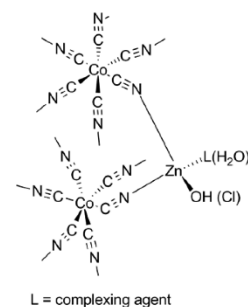
An increasingly important method, yet currently only employed for specialty polyols in industry, particularly for high molecular weight polyalkylene ether polyols is based on the so-called “double metal cyanide catalysts” (DMC).<sup>172</sup> This catalytic system was first developed by General Tire and Rubber in 1966<sup>173</sup> and has its primary use in the preparation of high-quality polyols for the polyurethane (PU) production.<sup>174–178</sup> A detailed overview was given by Ionescu in “Chemistry and Technology of Polyols for Polyurethanes”.<sup>179</sup> Clearly, major progress has been made in this area in the last 15 years. Here, we will give a brief overview of the DMC method and will focus on novel polyether structures obtained with the DMC catalyst.

While this method is well-established for industrial purposes, it has attracted minor attention in the scientific community. High polymerization temperatures, elevated pressures, and a complex catalyst preparation procedure, followed by difficult characterization of the actual catalyst structure render this approach less attractive for scientific purposes. However, the DMC method is applicable to large scale processes. The formation of unsaturated impurities is suppressed, and high molecular weight polyalkylene ether polyols can be achieved. Especially in the industrial production of polyols based on PPO, where mainly potassium hydroxide (KOH) is applied as a deprotonating agent and metal salts have to be removed after polymerization, the DMC catalyst can be a suitable alternative, enabling a continuous process with no need for further purification steps. Nevertheless, the DMC method includes various challenges and limitations, which are discussed in the following.

DMC is a heterogeneous catalyst with the general structure of  $M^1_u[M^2(CN)_6]_v \cdot xM^1X_w \cdot yL \cdot zH_2O$ , where  $M^1 = Zn, M^2 = Co, Fe$ . *L* is an organic complexing agent, such as *tert*-butyl alcohol, diglyme, or other.<sup>180,181</sup> A proposed structure of the DMC catalyst is shown in Scheme 20.<sup>182</sup>

Detailed analysis of the DMC structure is difficult, which is due to its insoluble character and the strong dependence of the crystal structure on the preparation procedure.<sup>180,183,184</sup> Since 1966, intense research efforts were performed to increase the catalytic efficiency of the DMC catalyst with the focus on cost-efficient and eco-friendly<sup>185</sup> systems for industrial applications.<sup>174,181,186–189</sup> In particular, novel complexing agents/cocomplexing agents,<sup>174,188,190,191</sup> numerous additives,<sup>181,186,187,189</sup> and various metal centers<sup>172,184,192–195</sup> were investigated to increase the performance of the DMC. To date, catalyst concentrations of as little as 15–50 ppm are sufficient to

Scheme 20. Proposed Structure of the Active Site of Zn–Co(III) DMC Catalyst<sup>a</sup>

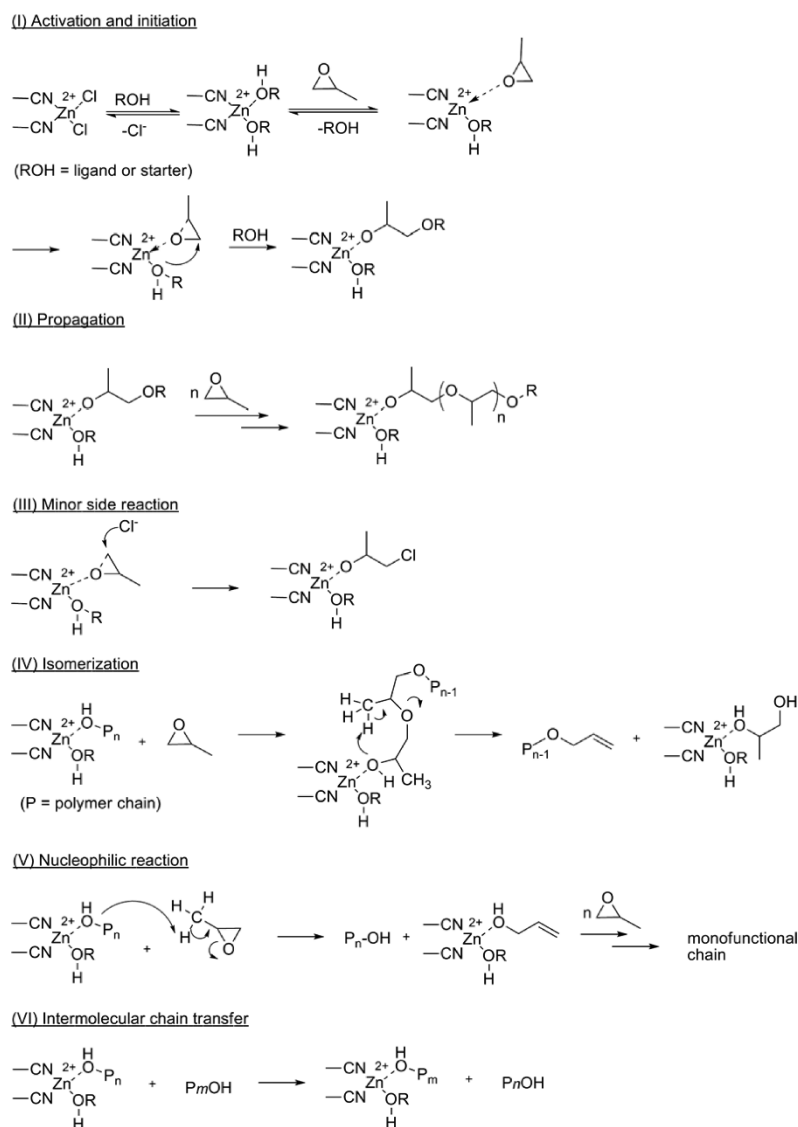


<sup>a</sup>Here, the Zn–OH structure acts as the initiating group. *L* represents a complexing agent, used during the preparation of the catalyst, e.g., *tert*-butanol.<sup>182</sup>

obtain suitable polyols within short reaction times, and the catalyst can remain in the polymers.<sup>179,190</sup> Consequently, no additional purification (filtration of salts) is necessary and the overall production steps are reduced.

Scheme 21 shows the mechanism proposed by Huang et al. and Kim et al. for the DMC-catalyzed PO polymerization<sup>174,181</sup> The active sites of the DMC are believed to be cationic coordinative, however fully conclusive evidence of the proposed mechanism is still lacking, given by the heterogeneous character of the DMC. It is supposed that the polymerization center forms in two stages: (I) The inactive  $(CN)_2ZnCl_2$  species interacts with the added initiator or a present ligand to form a dormant site at the catalyst surface. (II) Coordination of PO and subsequent replacement of a ligand (ROH) take place, followed by the attack of PO and the formation of the active center. Eventually, propagation occurs by nucleophilic attack of the growing PPO chain on activated PO molecules and proceeds until the monomer is consumed completely. The DMC method generates a strict head-to-tail regiosequence and a random configurational sequence of the resulting PPO.<sup>196</sup> The active polymer chain cannot be terminated by protic species; consequently no functional end groups can be introduced via a terminating agent.<sup>196</sup> However, after complete polymerization, the active polymer-DMC adduct is dormant, and the polymer chains can be reactivated by monomer addition at any time. Note that a fast intermolecular chain transfer (VI) between the active polymer chain and dormant hydroxyl-terminated polymer chains ensures narrow molecular weight distributions (e.g.,  $M_w/M_n < 1.1$  for  $M_n < 6000 \text{ g}\cdot\text{mol}^{-1}$ ).<sup>174</sup> Further, the occurrence of unsaturated PPO chains (IV–V) is reduced to around 0.003 mequiv/g, compared to conventional KOH catalyzed PPO with 0.04–0.10 mequiv/g, which represents a significant advantage of the DMC-method for the preparation of specialty polyols.<sup>174</sup> In general, molecular weight distributions and amounts of unsaturated species are strongly influenced by the chosen DMC catalyst system and can vary significantly in literature.

Although unsaturated structures are suppressed, the DMC method possesses some characteristic challenges and limitations. The main characteristic of the DMC is the occurrence of an induction time, before actual chain growth can be observed. The substitution of the soft organic ligands by PO molecules leads to a general induction period of 20–30 min up to several hours. Consequently, in a common reaction procedure, the DMC has to be activated first, before the actual polymerization takes

Scheme 21. Proposed Mechanism of DMC-Catalyzed PO ROP,<sup>181</sup> Including Proposed Side Reactions and the Intermolecular Chain Transfer<sup>174</sup>

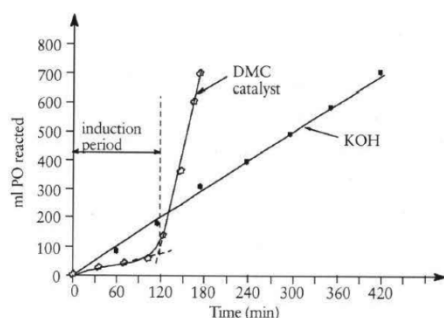
place.<sup>196,197</sup> However, after the induction period, the reaction rate exceeds that of the conventional AROP (Figure 5). Several approaches to avoid an induction period are described in patent literature but will not be discussed in detail here.<sup>198,199</sup>

A major drawback of the DMC catalysis for the polyol industry is the target to produce reactive (EO)-capped polyols with primary hydroxyl termini. These compounds represent an important class of polyols for flexible PU foams. However, if EO is added to a PPO-based polyol, the DMC catalyst leads to a heterogeneous mixture of unreacted PPO-polyol and highly ethoxylated PPO or PEO homopolymer.<sup>200</sup> Consequently, KOH catalysis still remains the method of choice to prepare EO-capped polyols. Additionally, the DMC catalyst shows limitations toward common initiator systems. In particular,

initiators having good coordination capability such as ethylene glycol, glycerol, low-carbon amines, low-carbon acids and urea act as inhibitors and preclude the coordination of PO at the catalyst.<sup>174,181</sup> Therefore, industrially relevant polyols based on sorbitol or sugars are not accessible via DMC catalysis. Suitable initiators are low molecular weight PPOs (400–700 g·mol<sup>-1</sup>) or noncomplexing alcohols.<sup>196</sup> In addition alkaline species deactivate the catalyst surface and impede polymerization. In contrast, long-chain carboxylic acids do not interfere with the catalyst and can be present throughout the polymerization, allowing for novel polyol derivatives.<sup>196</sup>

Another challenging characteristic of the DMC is the occurrence of high molecular weight polymer impurities (100 000–400 000 Da) in very small quantities (60–400





**Figure 5.** PO consumption versus time in PO polymerization with DMC catalysts and conventional KOH. (Reaction conditions:  $T = 110\text{ }^{\circ}\text{C}$ ;  $p = 300\text{ MPa}$ ; catalyst concentration:  $c(\text{KOH}) = 0.25\%$  and  $c(\text{DMC}) = 200\text{ ppm}$  (0.02%).<sup>179</sup> Adapted with permission from M. Ionescu, Rapra Technology, 2005. Copyright 2005 Smithers RAPRA Technology.

ppm).<sup>177,179</sup> To date, intense research has been performed to understand and suppress the formation of high molecular weight tails. Several approaches are described in the patent literature, which, however, are beyond the scope of this article.<sup>201–203</sup>

Considering the tolerance of the DMC catalyst toward epoxide monomers, unexpected observations were reported. As opposed to conventional AROP, ethylene oxide exhibits lower reactivity toward the DMC catalysts than PO. Complexation and activation of PO is considered to be favored, based on the high electron density on the oxygen atom, given by the positive inductive effect of the methylene group. In comparison, EO is less basic than PO, leading to a lower complexation constant.<sup>204</sup> In general, literature mostly reports the homopolymerization of PO or focuses on the copolymerization with carbon dioxide.<sup>205–213</sup> Only little has been reported on other epoxide based copolymers. However, Huang et al. reported the random copolymerization of PO with EO using a DMC system.<sup>214</sup> Narrow molecular weight distributions (PDI = 1.2–1.3) were obtained with low molecular weight fractions of EO (<30%). At higher EO fractions (>78%), turbid solutions were observed, caused by the crystallization of long PEO homopolymer fractions. In 2012, Sun et al. reported the homopolymerization of epichlorohydrin (ECH) with tri-(2-hydroxyethyl) isocyanurate as an initiator, followed by the use of PECH as chain extender for PU elastomers.<sup>215</sup> Recently, the homopolymerization of racemic ECH, S-ECH, and R-ECH was reinvestigated by Zhang et al.<sup>182</sup> Regioregular PECH was obtained with a head-to-tail content exceeding 99%, molecular weights ranging from 900 to 2700 g/mol and PDIs of 1.42 to 1.72. Cyclic or oligomeric byproducts were completely suppressed. Given by the special nature of the DMC catalyst, extraordinary copolymers are accessible, which cannot be obtained by conventional AROP. For example, Langanke et al. reported PPO-*b*-pFA-*b*-PPO and PEO-*b*-pFA-*b*-PEO triblock copolymers initiated from paraformaldehyde (pFA) as a macroinitiator ( $M_w/M_n = 1.11–1.48$ ).<sup>216</sup> Further, the tolerance of the DMC catalyst to ester groups has been exploited to create a new class of biobased polyols for the PU industry, starting from vegetable oils such as castor oil.<sup>217–219</sup>

Chen and co-workers reported the copolymerization of PO with maleic anhydride (MA) to obtain polyether-ester structures (Scheme 22).<sup>220</sup> Copolymers of molecular weights up to 3000 g·mol<sup>-1</sup> and moderate PDIs of 1.35 to 1.54 were reported, with a catalyst efficiency of 10 kg polymer/g catalyst. The reactivity

**Scheme 22.** Reaction Scheme for the Copolymerization of PO with Maleic Anhydride<sup>220</sup>



ratios of MA and PO were calculated by the extended Kelen-Tüdös equation with values of  $r_1(\text{MA}) = 0$  and  $r_2(\text{PO}) = 0.286$ . Copolymers with the monomer ratio MA/PO  $\geq 1$  were almost alternating, whereas homopolymers of MA are not accessible by DMC.

In 2010, Kim and co-workers extended the library of alternating copolymers of PO and cyclic acid anhydrides.<sup>221</sup>

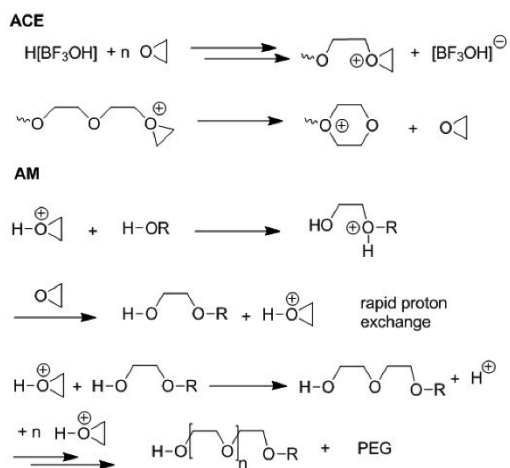
The authors reported the copolymerization of PO with succinic anhydride (SA), maleic anhydride (MA), phthalic anhydride (PA), and glutaric anhydride (GA), respectively. Comonomer ratios were varied from 0 to 50 mol % with molecular weights up to 7000 g·mol<sup>-1</sup> and narrow PDIs below 1.5. However, with increasing molar ratio of cyclic anhydride the polymer yields decreased to less than 30%. The reactivity ratios were calculated by the extended Kelen-Tüdös equation under the assumption that  $r_{AA}$  for any cyclic acid anhydride is zero. The reported reactivity ratios for PO are 0.34, 0.28, and 0.26 for PO/SA, PO/MA, and PO/PA copolymerization, respectively.

In addition to the intriguing copolymers of PO and cyclic anhydrides, the DMC technique enables the copolymerization of CO<sub>2</sub> with various epoxides such as propylene oxide, cyclohexene oxide, epichlorohydrin, and styrene oxide, which are discussed elsewhere.<sup>205–213</sup> In summary, DMC catalysis is a powerful method for novel high molecular weight polyether structures; however, this research field is by no means mature yet and offers promise for the future. It is also worth noting that to date many of the new materials obtained by this technique were characterized only to a very limited extent with respect to their properties.

## 2.7. Cationic Polymerization

The cationic ROP (CROP) of oxygen-containing heterocycles plays an important role for the preparation of the commercial products poly(oxymethylene) (POM, polyacetal), a highly crystalline engineering plastic prepared by ROP of trioxane as well as for the synthesis of poly(tetrahydrofuran) (polyTHF),<sup>222</sup> which is used for soft-elastic segments in thermoplastic elastomers, such as polyurethanes (Lycra) and polyesters (Hytrel). Generally, four-membered and higher cyclic ethers polymerize by cationic mechanism only (with a few rather unusual exceptions that have been mentioned in literature). The basic mechanistic principles of the CROP of heterocycles are well understood, based on work carried out by various groups from the 1960ies to the 1980ies, summarized in excellent reviews by Kubisa and Penczek et al.<sup>223–225</sup> The CROP is rarely used for the polymerization of EO or PO, since the formation of considerable amounts of cyclic polyether byproducts cannot be avoided, which is due to “backbiting” processes, i.e., intramolecular chain transfer.<sup>30,226</sup> For this reason and due to the low number of recent works on the CROP of epoxides this section of the current review is rather brief, and merely the basic principles will be outlined.

The active species in CROP are typically secondary or tertiary oxonium ions, and two fundamentally different mechanisms have to be considered that are illustrated in Figure 6: The activated chain-end mechanism (ACE) that is based on a tertiary oxonium ion located at the chain and as an active center. A nucleophilic attack of the oxygen atom in the cyclic monomer at a carbon

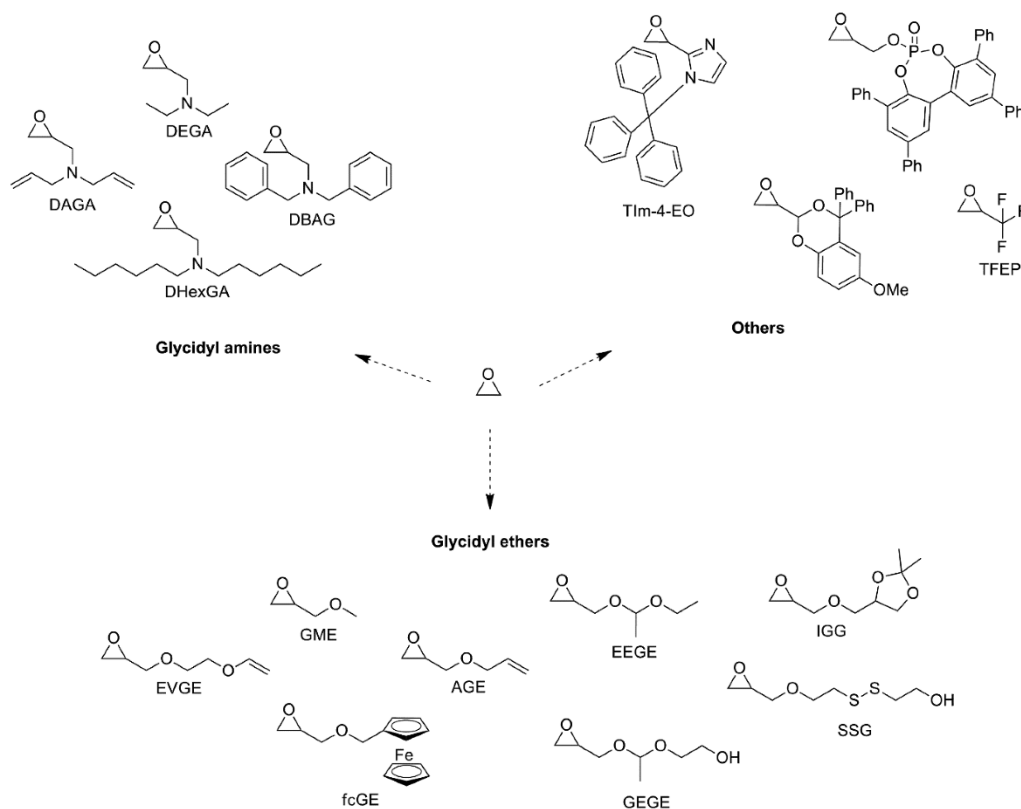


**Figure 6.** Fundamentally different mechanisms that govern the CROP of epoxide monomers: ACE-mechanism (top), leading to the formation of cyclic products together with linear polymer and AM-mechanism (bottom), usually based on added alcohols, which permits to suppress cyclization.

atom in  $\alpha$ -position to the oxygen bearing formally the positive charge leads to propagation. However, since nucleophilic oxygen atoms are also present in the polymer chains formed, both inter- as well as intramolecular chain transfer can occur. In the intramolecular case cyclic byproducts are formed, e.g., 1,4-dioxane or crown ether structures in the case of EO polymerization. The chain transfer to polymer is a typical and unavoidable feature of the CROP, if it is dominated by the ACE mechanism. In the polymerization of EO, the basicity of the polymer unit is higher than that of EO, thus macrocyclization proceeds concurrently with propagation.<sup>225</sup> Cationic polymerization of EO was found to lead to a mixture of rather low molecular weight linear polymer and cyclic oligomers, mainly 1,4-dioxane by Saegusa et al.<sup>227</sup> Similar behavior is known for the polymerization of PO and other substituted epoxides.<sup>228</sup> Generally, the presence of cyclic products is undesired in polyethers, since in this case end group functionality cannot be controlled, pure telechelic products are not accessible, and the cyclic products usually exhibit toxicity for biomedical applications.

In contrast to the ACE mechanism, the “activated monomer mechanism” (AM) permits considerably better control over molecular weights and permits to circumvent the issues related to cyclization.<sup>229,230</sup> Since the late 1980ies it is known that the presence of alcohols as initiators can be exploited to reduce the amount of cyclic oligomers drastically.<sup>231</sup> In this case, the AM

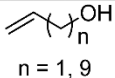
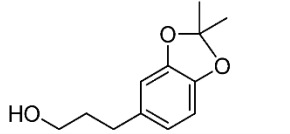
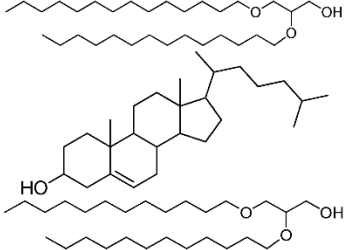
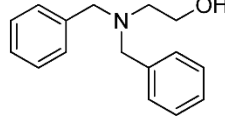
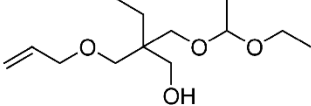
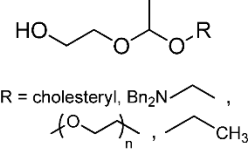
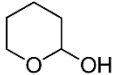
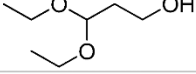
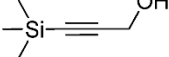
**Scheme 23.** Selected Epoxide Derivatives that Have Been Used to Prepare Multifunctional PEGs via Copolymerization with EO (See also Table 2)



## Chemical Reviews

## Review

Table 1. Selected (Alcohol Based) Functional Initiators

Functionality	Structure of initiator	Counterion, conditions	Features	Ref.
double bond	 n = 1, 9	K <sup>+</sup> , DPMK, potassium naphthalide; low temperatures (≤ 60 °C)	Isomerization of the double bond at high temperatures, “click-chemistry”	245-248
catechol		Cs <sup>+</sup> ; I <sup>+</sup> to cleave the protection group	Adheres on a variety of surfaces, nanoparticle coating	249,250
fatty acid, cholesteryl		Cs <sup>+</sup>	Lipid anchor, applicable for liposome preparation, self assembly	251-253,255
amine		Cs <sup>+</sup> ; H <sub>2</sub> /Pd to cleave the protection group	Possible bioconjugation	257,258
hydroxyl double bond		K <sup>+</sup> , DPMK; formic acid to cleave the acetal protection group	Heterotrifunctional initiator, two functionalities available after polymerization	259
cleavable unit hydroxyl		K <sup>+</sup> , Cs <sup>+</sup> ; acidic cleavage	Several functionalities attached through the acetal can be easily cleaved	260,261
Hydroxyl		K <sup>+</sup> , potassium naphthalide; acidic cleavage		262
Formyl		K <sup>+</sup> , potassium naphthalide; acidic cleavage	Protein conjugation via imine formation	263
Alkyne		K <sup>+</sup> , potassium naphthalide; TBAF to cleave the protection group	Click-chemistry	264

mechanism<sup>229,232</sup> becomes favored over the conventional ACE mechanism. In the presence of hydroxyl-group containing compounds the protonated epoxide monomer may react either with another monomer or with the hydroxyl groups.<sup>232</sup> In case of the AM mechanism, the active centers, i.e., the cationic charges are located on the monomer (Figure 6), and the polymer chain is neutral, which strongly reduces the occurrence of backbiting.<sup>233</sup> Suitable conditions for a controlled AM-type polymerization of EO in the presence of an alcohol-initiator ROH can be created, if rather high ratios [EO]/[ROH] are chosen, however, keeping the instantaneous monomer concentration low. These conditions can be implemented by slow addition of the epoxide monomer to the reaction mixture. Unfortunately, this on the other hand may lead to prolonged reaction times. The CROP of

epoxides under AM conditions has been used for the synthesis of well-defined telechelic oligodiols of PO and epichlorohydrine<sup>234</sup> as well as for amphiphilic block copolymers of PEG and poly(glycidyl methacrylate) by Yan et al.<sup>235</sup> The cationic copolymerization of EO and THF in the presence of diols was found to proceed with simultaneous participation of secondary and tertiary oxonium ions, comprising features of AM and ACE mechanisms.<sup>236</sup> In an unusual strategy, Maghnite-H has been employed as a clay catalyst for the homopolymerization of EO in the presence of ethylene glycol, demonstrating an AM mechanism and the absence of cyclic products.<sup>237</sup>

The propagation rate constants for the CROP are generally significantly higher ( $10^4$  to  $10^6$  mol<sup>-1</sup> L s<sup>-1</sup>) than for the oxanionic polymerization ( $1$  to  $10^4$  mol<sup>-1</sup> L s<sup>-1</sup>). Thus,

sufficient heat dissipation is necessary in the extremely rapid reactions to control molecular weights to a certain extent.<sup>238</sup>

In summary, the CROP under AM conditions offers interesting options for the synthesis of telechelic polymers, macromonomers and several copolymers.<sup>225</sup> However, EO, PO, and BO are mostly polymerized with other techniques described above that offer better control over molecular weights as well as end group fidelity and permit to avoid cyclic side products.

### 3. POLY(ALKYLENE OXIDE) STRUCTURES: INNOVATIVE POLYETHER STRUCTURES

Mainly based on the advances in the “classic” oxyanionic polymerization of EO, numerous specialty companies have been founded since the 1980ies that offer tailor-made PEG homopolymers with specifically designed or activated end groups. Most of these structures are based on *m*PEG (methoxy-PEG), but also several heterobifunctional PEGs are now commercially available on small scale for biomedical purposes and bioconjugation. However, innovative PEG-structures for explorative research can also be created by copolymerization of EO, PO, or longer alkylene oxides with small amounts of (protected) functional comonomers. This leads to functional polyethers with additional “in-chain” functional groups that may possess stimuli-responsive properties, peculiar surface, and interface properties or other biomedically relevant features. In addition, all of these polymers retain the excellent aqueous solubility of PEG and are thus useful for further transformation and (bio)conjugation in water, i.e., for the field of “aqua chemistry” in general.

#### 3.1. Multifunctional PEGs

To broaden the scope of applications for PEG, a broad range of functional groups can be introduced at the chain termini. However, for certain applications additional “in-chain” functional groups at the polyether backbone are desirable. In this context both heterobifunctional as well as heteromultifunctional PEGs have been further developed in the past decade, as detailed below. The state of the art for heterobifunctional structures was summarized in a focused review article by Riffle in 2009.<sup>239</sup> In general, there are three strategies to introduce functional groups at PEG: (i) introduction via a functional initiator ( $\alpha$ -functionalization); (ii) use of a terminating agent containing a functional group ( $\omega$ -functionalization); and (iii) copolymerization with a functional epoxide (see Scheme 23). Postpolymerization modification of the hydroxyl end groups of PEG is also long established but is difficult, if heterobifunctional PEGs are targeted. The ensuing section focuses on direct functionalization methods during the polymerization process without workup.

In the case of AROP, it is a key issue that the functional groups have to endure the harsh reaction conditions (high temperature, strong bases), which is a severe limitation of this approach. Further, if protecting groups are used, they should be easily removable to release the functionality subsequent to the polymerization.<sup>39,73,239–242</sup>

$\alpha$ -Functionalization: strong bases like hydroxides, alkoxides, metal-alkyls, azides<sup>243</sup> and -aryls are employed for oxyanionic polymerization (vide supra).<sup>244</sup> These initiators may contain an orthogonal, sometimes latent functionality that can be introduced via the initiation step (see Table 1). In some cases, it is necessary to protect the additional functionality in order to avoid undesired initiation or termination reactions. To generate a double bond-functionality at one terminus of PEG, allylic alcohol can be used as an initiator. Kataoka and co-workers pioneered

this method in the early 1990s, using potassium naphthalide.<sup>245</sup>

Allyl alcohol is a very useful bifunctional initiator to obtain polymers with orthogonal functionalities.<sup>246,247</sup> Via thiol–ene-click reaction it is subsequently possible to introduce a large variety of other functionalities or functional molecules, e.g., using mercaptopropionic acid or mercaptoethylamine. Recently, Schubert, Lutz et al. demonstrated the use of undecenyl alcohol as an initiator.<sup>248</sup> The authors synthesized  $\alpha$ -undecenyl- $\omega$ -methacryl-PEO. In this case, the methacrylic double bond can be selectively addressed via thiol–ene-click reaction or be polymerized via ATRP, while the undecenyl double bond shows no reactivity. Consequently, orthogonal postfunctionalization of the polymer is possible.

In 2013 our group introduced an acetonide-protected catechol initiator, which was used in the AROP of EO as well as in copolymerizations with other functional epoxides, such as ethoxyethyl glycidyl ether (EEGE) and diallyl glycidyl amine (DAGA). After rapid acidic cleavage of the acetonide group, the catechol-functionalized PEG-copolymers can be used as ligands for metal nanoparticles, rendering them water-soluble.<sup>249,250</sup> Most important, the stealth effect of PEG may allow applying manganese oxide (MnO) nanoparticles as contrast agents for magnetic resonance imaging (MRI).

Polyether based lipid analogs were synthesized by our group using cholesterol and 1,2-bis-*n*-alkyl glyceryl ethers as membrane-interacting initiators.<sup>251–253</sup> These lipid analogs are used for the preparation of liposomes with anchored multifunctional polyether chains. The polymer-coated liposomes show a stealth effect<sup>254</sup> and are promising candidates for drug delivery systems. Garamus and co-workers synthesized polyglycidol-derivatized lipids using a 1,3-didodecyl/tetradecyloxy-propane-2-ol (DDP) initiator. They studied the self-assembly behavior and determined CMC values.<sup>255</sup>

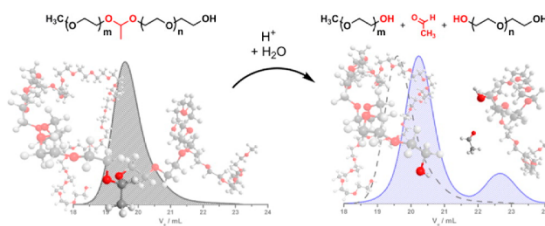
If single amine functionalities at the  $\alpha$ -terminus of PEG are desired, a synthetic detour is indispensable. The use of initiators bearing unprotected amines is not possible, given the nucleophilicity of amines and would result in a mixture of polymers initiated by alcohol and amine.<sup>256</sup> Alternatively, the use of *N,N*-dibenzyl-2-ethanolamine enables conventional polymerization of epoxides. The amine functionality can be released via catalytic hydrogenation.<sup>257,258</sup> Chau and co-workers investigated a heterotrifunctional initiator bearing an allyl functionality and a potential hydroxyl group, protected by an acetal moiety.<sup>259</sup> With this initiator, it is possible to introduce two orthogonal functionalities into the polymer in one step.

A related initiator with an acid cleavable acetal group was used to prepare polyethers with a predefined, cleavable functionality.<sup>260,261</sup> When preparing PEG with this initiator, PEGs with adjustable degree of polymerization with labile acetal unit in the chain are accessible. In particular, this initiator enables the synthesis of cleavable PEG, as shown in Figure 7.

If a special functionality can only be obtained via a postmodification process at the  $\omega$ -end of the polyether, but also a hydroxyl functionality is desired, it is possible to use a pyrane-type of alcohol initiator (Table 1).<sup>262</sup> After modification of the  $\omega$ -side, the hydroxyl functionality can be generated by acidic cleavage of the protecting group. To introduce a carbonyl group, an acetal protected alcohol was employed by Kataoka and co-workers. After AROP, the acetal groups can be cleaved by acidic treatment, releasing a carbonyl functionality. These formyl groups were used for further protein conjugation by Schiff-base formation.<sup>263</sup>

## Chemical Reviews

Review

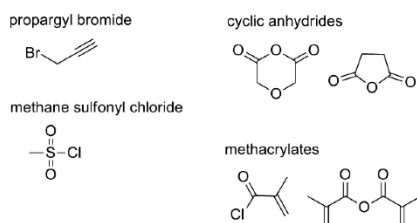


**Figure 7.** Acidic cleavage of an acetal group introduced into the PEG chain by a macroinitiator and GPC traces before and after the cleavage.<sup>260</sup> Adapted with permission from Dingels, C.; Müller, S. S.; Steinbach, T.; Tonhauser, C.; Frey, H. *Biomacromolecules* **2013**, *14*, 448. Copyright 2013 American Chemical Society.

The strong alkaline reaction conditions of the AROP also impede the direct introduction of alkyne functionalities due to its acidic character. Protection with a silyl group was shown to be viable, and removal of the silyl protecting group can be achieved by tetrabutylammonium fluoride subsequent to polymerization.<sup>264</sup>

The living character of the AROP enables the introduction of specific functionalities by the choice of the terminating agent ( $\omega$ -functionalization), which may also bear a functional group that can be attached to the polyether in this manner (see Scheme 24).

**Scheme 24. Selective Terminating Agents for AROP (Propargyl Bromide, Mesylate Group, Cyclic Anhydrides, and Methacrylate Structures)**



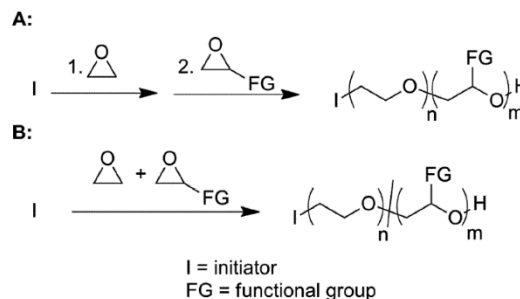
Fundamental requirements for a good terminating agent are its compatibility with the active alkoxide chain-end and stability of its functional group. Ensuing transformation or cross-linking reactions are mostly carried out at these functionalities.

One of the most frequently used terminating agents is propargyl bromide, due to its suitability for click-chemistry.<sup>262,265</sup> Additionally, cyclic anhydrides are suitable terminating agents that lead to terminal carboxylic acids and thus also esters or amides.<sup>264,266,267</sup> In 2010, Hiki and co-workers showed the possibility to either attach azide or amine groups at the PEG  $\omega$ -chain-end starting from mesylate groups<sup>262</sup> and reaction of the active chain end with methane sulfonyl chloride. Tosyl- and trityl sulfonyl chlorides react in the same manner. If methacrylate-type of structures are attached to the chain-end via anhydride or acyl chloride reactions, subsequent radical cross-linking of the polymers is possible.<sup>248,268</sup>

Copolymerization of functional epoxides is required, if multifunctional PEGs (*mf*-PEG) with “in-chain” functional groups are desired (Table 2). Some of the monomers presented here are not polymerizable via the common oxyanionic method. For these cases other techniques, particularly the active monomer strategy, are employed. In addition to random copolymers, functional epoxides can be used to obtain block-

structures via sequential homopolymerization of the respective monomer (see Scheme 25). This section focuses on the

**Scheme 25. Possible Types of Copolymerization<sup>a</sup>**

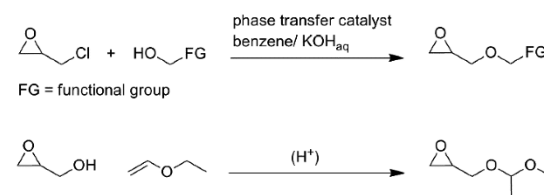


<sup>a</sup>A: Sequential addition of the monomers resulting in block copolymers; B: One pot reaction of two epoxide monomers leading to a random (or gradient) copolymer structure.

preparation of random copolymers as well as block copolymers. With respect to the functional group distribution, it is of crucial importance to study whether truly random copolymers are obtained or gradient-type structures. Based on in situ NMR techniques introduced by our group in 2010,<sup>269</sup> the consumption of both comonomers can be measured directly in the NMR-tube, which can be translated to incorporation of the comonomers in the polyether chain formed. This leads to a precise perception of the functional group distribution in the polymer chains formed from the initiator to the chain terminus, leading a clear perception of a random or gradient structure (see also chapter 3.3).

Most of the comonomers employed can be conveniently obtained in one- or two-step procedures from common reactants. In particular, the inexpensive epichlorohydrin (ECH) serves as one of the starting materials for functional glycidyl ether monomers via  $S_N2$  reaction (see Scheme 26). Some of the functional (co)monomers shown in Table 2 are no glycidyl ethers; however, their synthesis will not be discussed here.

**Scheme 26. Synthesis of Functional Glycidyl Ether Monomers Based on Epichlorohydrin and Nucleophilic Substitution (Top) or Vinyl Ether Addition to Glycidol (Bottom), Leading to Ethoxy Ethyl Glycidyl Ether (EEGE)**



PO is the most explored comonomer for ethylene oxide, as described in sections 2.1.2 and 4 of this review. Epichlorohydrin (ECH) can also be copolymerized with EO. For example, Lundberg and co-workers copolymerized EO and ECH to obtain random copolymers.<sup>101</sup> Elimination of the chlorides resulted in acid degradable PEG.

Allyl glycidyl ether (AGE) as well as ethoxy vinyl glycidyl ether (EVGE) can be used to prepare polyethers with alkenyl

Table 2. Suitable Monomers with Special Functionalities for Copolymerization with EO to Generate Multifunctional PEGs (*mf* PEG)

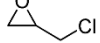
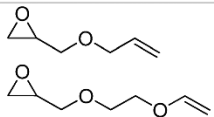
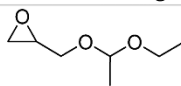
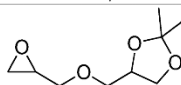
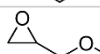
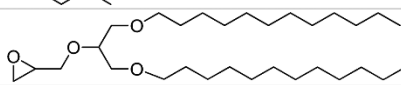
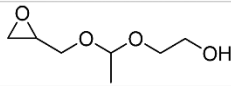
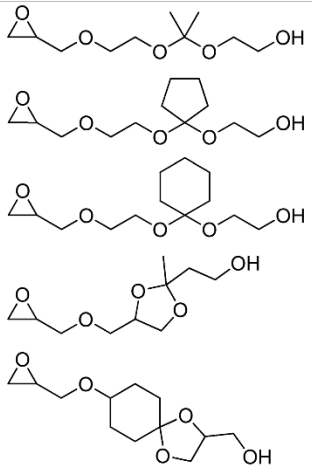
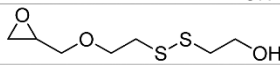
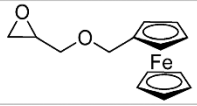
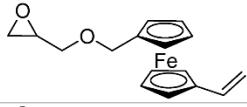
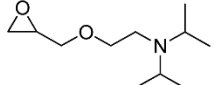
Monomer structure	Specialty	Ref.
	Elimination of chloride, possibility to create cleavage points in the chains.	101
	Thiol-ene click possible. Attachment of various molecules. Block structures form micelles. Thermo-responsive (LCST)	270,271,273-279
	Acidic cleavage of the protection group, release of hydroxyl groups	257,258,265,280,281
	Acidic cleavage of the protection group, resulting in two hydroxyl groups per monomer unit	265,275,282,283
	Thermo-responsive (LCST)	97,99,144
	Lipid mimetic, block structures form micelles	284-286
	Acidic cleavable polymers, hyperbranched structures	287
	Acid degradable polymers, hyperbranched structures, degradation at different pH due to alkyl groups at acetal/ketal unit.	288,289
	Redox degradable cleavage points, hyperbranched structures	290
	Redox active, thermo-responsive (LCST)	292,293
	Orthogonal monomer for radical and anionic polymerization	294
	pH responsive	295

Table 2. continued

Monomer structure	Specialty	Ref.
	Diels-Alder reaction, hydrogel synthesis	296-299
	Supramolecular building block, thermo-responsive (LCST)	300,301
	Acidic cleavage of the protection group and release of a catechol-functionality, adhesion on various surfaces, crosslinking abilities	302
	Side chain liquid crystalline polyether	303
	UV active E/Z isomerization, nematic phase above 200 °C	304
	pH responsive	305
	Photocleavable protecting group	309
	Solid polymer electrolytes, surface interaction by phosphate groups.	106
	Polyethers with low surface energy for specialty coatings.	84,85,310,311

functionality. Both random and block copolymers of EO with AGE and EVGE were reported,<sup>270–272</sup> and thiol–ene click chemistry was used for further derivatization and bioconjugation.<sup>273–276</sup> EVGE shows a crucial advantage over AGE when attaching thiols, due to the absence of additional cross-linking reactions, like in the AGE case.<sup>273</sup> Block and terpolymer structures show micellar and core–shell–corona architectures.<sup>277–279</sup> Multiple hydroxyl groups at the polyether backbone, i.e., multihydroxyfunctional PEGs were obtained by copolymerizing ethoxy ethyl glycidyl ether (EEGE)<sup>257,258,265,280,281</sup> or isopropylidene glyceryl glycidyl ether (IGG) with EO.<sup>265,275,282,283</sup> Both monomers can be used for to create ideally random copolymers with EO as well as

for the formation of block copolymers. After acidic cleavage of the acetal protecting groups, the hydroxyl moieties are addressable for further reactions, e.g., bioconjugation or grafting of other polymers.

Glycidyl methyl ether (GME) possesses the simplest possible glycidyl ether structure. It is surprising that GME cannot be copolymerized with EO to high  $M_n$  via the conventional oxanionic method. Additional activation of the epoxide monomer is required. Both the PGME homopolymer and copolymers of GME with EO show thermoresponsive behavior in water, albeit with cloud points at elevated temperature.<sup>97,99</sup> Copolymers based on GME and ethyl glycidyl ether (EGE) were employed as one block segment of triblock terpolymers, which

aggregate in aqueous solution, triggered by pH as well as by temperature.<sup>144</sup>

Tsvetanov et al. describe a lipid mimetic epoxide monomer namely 1,3-didodecyloxy-2-glycidyl-glycerol (DDGG). It was polymerized on PEG macroinitiators to obtain different diblock copolymers. The self-assembly of the copolymers was studied using DLS and SLS. The micelles were investigated and depending on the composition of the copolymers oil-in-water or water-in-oil emulsion behavior was found.<sup>284–286</sup>

Because PEG is known as a biocompatible but not biodegradable polymer, recently also copolymers with predefined cleavage site were developed. In recent years, some cleavable monomers have been introduced, for instance 1-(glycidyl)oxy ethyl ethylene glycol ether (GEGE), an acidic cleavable epoxide inimer.<sup>287</sup> This inimer leads to branched polyethers when copolymerized with EO or glycidol. The resulting copolymers possess a degradable polyether backbone. Kizhakkedathu et al. studied the degradation behavior of different  $\alpha$ -ethoxy- $\omega$ -hydroxyl-functionalized ketal monomers incorporated into branched polyether structures.<sup>288,289</sup> Recently, Kim and co-workers developed a redox-degradable disulfide bond containing glycidyl monomer (SSG). The branched homo- and copolymers were analyzed with regard to their biocompatibility, copolymerization kinetics and degradability upon treatment with the reducing agent dithiothreitol (DTT).<sup>290</sup> Other examples of cleavable polyethers are given in section 6.2 of this review.

Ferrocene containing materials are gaining broad attention because of their redox-responsive features.<sup>291</sup> The novel monomer ferrocenyl glycidyl ether (FcGE) can transfer these special characteristics to polyether structures. Copolymerization with EO was observed to proceed in a fully random manner and leads to water-soluble ferrocene containing PEGs with up to 10 mol % FcGE.<sup>292</sup> The amount of incorporated FcGE determines the properties of the copolymers. Ferrocene-bearing copolymers with low content of FcGE ( $\leq 5\%$ ) show biocompatibility and exhibit thermoresponsive behavior. Allylglycidyl ether was also combined with FcGE to obtain random copolymers that can be further modified by click-chemistry.<sup>293</sup> Recently, Wurm et al. introduced the vinyl ferrocenyl glycidyl ether (VfcGE).<sup>294</sup> This monomer bears two orthogonal groups which can be polymerized either in an anionic or radical manner. The anionic copolymerization of VfcGE and EO leads to temperature-, redox-, and pH-responsive behavior of the copolymers in water. Polyalkylenes with pendant epoxide side chains were obtained via free radical polymerization of VfcGE. The epoxide chains were reacted with bovine serum albumin to obtain redox-responsive protein nanoparticles.

An interesting amine functional glycidyl ether, namely *N,N*-diisopropyl ethanol amine glycidyl ether (DEGE), was reported by Lynd et al. in 2013.<sup>295</sup> The authors investigated the pH-responsive behavior of block and random copolymers synthesized from DEGE, AGE, and EO. Simultaneously the authors described the formation of macroscopic hydrogels, sol–gel transitions and cross-linking of P(DEGE-*co*-AGE) copolymers to nanogels. Monomers based on glycidyl amines and their respective polymers, are described in section 3.2 of this review.

The significant characteristic of a furfuryl unit is its capability to perform Diels–Alder (DA) reactions. Via polymerization of furfuryl glycidyl ether, homo- and diblock copolymers were synthesized by Schubert and co-workers,<sup>296–299</sup> demonstrating reversible DA-cross-linking of furfuryl groups and bismaleimide-structures. Core-cross-linked micelles and nanoparticles were

examined, showing preservation of the self-assembled structures during DA reaction and also promising self-healing properties.

Adamantyl glycidyl ether (AdaGE) is a promising epoxide monomer to create polyethers that can be used for the formation of supramolecular polymer architectures. Frey et al. described the copolymerization of AdaGE with EEGE.<sup>300</sup> Furthermore, the authors investigated thermal properties and inclusion complex formation with  $\beta$ -cyclodextrin, resulting in supramolecular grafting.<sup>301</sup>

Catechol functionalities are prominent for their outstanding complexation and adhesion on a large variety of surfaces. Recently, a new epoxide monomer, catechol acetone glycidyl ether (CAGE) was developed to prepare multicatechol functional PEGs and hyperbranched polyglycerols with catechol units. Coating of different surfaces with catechol functional polyethers was possible as well as cross-linking by addition of Fe(III) ions, leading to the generation of supramolecular hydrogels.<sup>302</sup>

Side chain liquid crystalline copolyethers with different spacer length were synthesized capitalizing on mesogen-bearing epoxide monomers.<sup>303</sup> The materials exhibited different smectic phases. Polyethers containing azobenzene or cyanoazobenzene functionalities were synthesized via phosphazene base initiation by Peris et al.<sup>304</sup> These polymers exhibit a nematic phase, albeit above 200 °C.

To obtain imidazole functional PEG, Long and co-workers used a trityl-protected imidazole epoxide monomer for the AROP.<sup>305</sup> After removal of the trityl groups, these polyethers possessed imidazole units as a biofunctionality, the key functionality of histidine distributed along the polyether backbone. Imidazole functional polymers are known for their ability for proton transfer,<sup>306</sup> catalytic activity,<sup>307</sup> and metal coordination.<sup>308</sup> In 2014, Lahann et al. described the on-demand fabrication of hydrogels using multifunctional hydrazide and carbonyl functional PEGs as components.<sup>309</sup> To obtain the aldehyde functionality along the backbone the authors synthesized a new latent aldehyde-bearing epoxide monomer. The corresponding polyether releases multiple carbonyl moieties after exposure to UV light.

Motivated by the increased demand for new materials for batteries, Babu and Muralidhakan in a recent work synthesized various polyethers with pendant phosphate groups via monomer activated ring-opening polymerization of oxirane monomers.<sup>106</sup> These materials offer potential for application as solid polymer electrolytes and showed promising Li-ion conductivity. In the early 1990s, Japanese scientists investigated the properties of fluorinated polyethers.<sup>310,311</sup> The authors found that high molecular weights and yields could be easily achieved when employing organozinc compounds as catalysts for (anionic) coordination polymerization. Nozaki et al. recently revisited the polymerization behavior of fluorinated epoxide monomers and studied regularity and tacticity in case of enantiopure epoxides.<sup>84,85</sup>

Many of the recently reported PEG-copolymers show temperature dependent aqueous solubility and a cloud point.<sup>97,99,144,275,277,292,300</sup> This thermoresponsive behavior can be investigated by turbidity measurements.

### 3.2. Glycidyl Amine Comonomers and Polyethers with Pendant Amino Groups

Only very recently, multi amino-functional polyethers are increasingly studied, since they are promising candidates for a variety of applications ranging from surface modification to



## Chemical Reviews

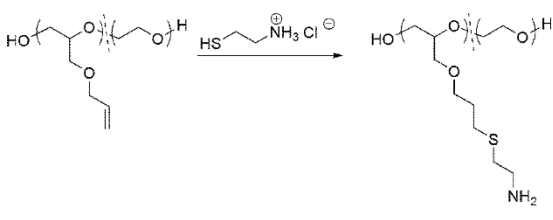
Review

biomedicine.<sup>312</sup> While primary amino groups permit conjugation of biomolecules or low molecular weight compounds,<sup>102,239,272,273</sup> the value of tertiary amino groups should not be underestimated. Ordinary tertiary amine moieties permit triggering the polyethers' properties via the pH-value.<sup>313–315</sup> Further, their substituents can be modified, leading to tailor-made polyethers.<sup>151,295,315</sup> In addition, if a positively charged polyelectrolyte is desired, the tertiary amino groups can be simply quaternized. These cationic PEG-based polyethers may be promising polymer vectors for gene delivery.<sup>316</sup>

Different strategies can be pursued to introduce multiple amino functionalities at the polyether backbone. In general, different synthetic methods have to be applied for primary or tertiary amino groups. In this section, we focus on synthetic approaches based on postpolymerization reactions and direct copolymerization of EO/PO with glycidyl amine derivatives. A detailed overview of multiple amino-functional polyethers, including poly(meth)acrylate derivatives and their potential applications, was given by Wilms et al.<sup>312</sup>

**3.2.1. Introduction of Primary Amino Groups.** Obviously, the direct polymerization of epoxide monomers bearing primary amino groups is not feasible, since the nucleophilic nitrogen atom attacks the epoxide ring. Hence, postpolymerization strategies or the introduction of suitable protecting groups for amine-functional epoxide monomers are necessary. Koyama et al. were the first to obtain PEG with multiple primary amino moieties via copolymerization of ethylene oxide (EO) with allyl glycidyl ether (AGE) followed by thiol–ene coupling of 2-aminoethanethiol to the allylic groups of AGE (Scheme 27).<sup>272</sup> The authors further demonstrated the suitability of these amino-functional PEGs for DNA complexation.<sup>317</sup>

**Scheme 27. Modification of PEG-co-PAGE Copolymers with 2-Aminoethanethiol**<sup>272</sup>

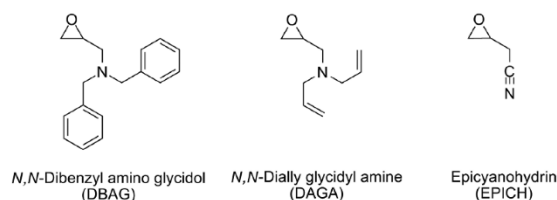


Another postpolymerization approach was reported by Li and Chau, who synthesized a library of multifunctional PEGs by modifying the hydroxyl groups of *lin*PG-co-PEO.<sup>318</sup> The glycerol units were reacted with phthalimide potassium, followed by conversion into primary amines. However, this route shows a limited overall conversion for amino functions of only 34%. Alternatively, Möller and co-workers applied the “activated monomer mechanism” to homo- and copolymerize epichlorohydrin (ECH) with ethoxyethyl glycidyl ether (EEGE), followed by the conversion of the chloride atoms of ECH to azide groups. Eventually, the glycidyl azide segments were

reduced, using triphenylphosphine to obtain primary amines at the polyether backbone (Scheme 28).<sup>102</sup>

In general, postpolymerization modifications are often time-consuming and can suffer from a limited overall conversion. To overcome this problem, glycidyl amine derivatives bearing suitable protecting groups can be used as monomeric building blocks for the direct copolymerization with EO or PO. Our group introduced a protected glycidyl amine, dibenzyl amino glycidol (DBAG) (Scheme 29, left), accessible by a simple two-step

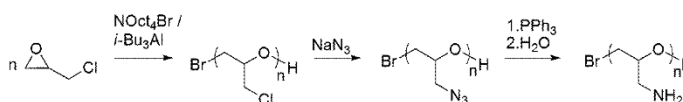
**Scheme 29. Suitable Monomers to Obtain PEG with Primary Amino Functionalities**<sup>4</sup>



<sup>a</sup>*N,N*-Dibenzyl amino glycidol (DBAG),<sup>269</sup> *N,N*-diallyl glycidyl amine (DAGA),<sup>319</sup> and epicyanohydrin (EPICH).<sup>87</sup>

transformation of epichlorohydrin with dibenzyl amine.<sup>269</sup> Copolymerization of 2–15 mol % of DBAG with EO yielded copolymers with a tapered microstructure containing EO rich segments near the initiator and DBAG rich segments near the chain terminus. Liberation of the primary amino groups was performed by catalytic hydrogenation, albeit requiring prolonged reaction times (1–8 days, Pearlman's catalyst). Only limited copolymer yields of 30–50% were achieved due to interaction of the primary amino groups with the carbon-supported catalyst. In particular, this strong adhesion precluded the recovery of block copolymers. This strategy was improved by introduction of *N,N*-diallyl glycidyl amine (DAGA) (Scheme 29, middle).<sup>319</sup> This approach enabled the polymerization of well-defined gradient copolymers as well as block copolymers with DAGA ratios of 2.5–24 mol %. Furthermore, the time for cleavage of the protecting group was reduced from 1 to 8 days to several hours and yields were increased from 30 to 50% to 85% copolymer. In a following publication, the suitability of this comonomer as anchor for dye functionalization or for drug conjugation was demonstrated.<sup>249</sup> In 2015, Satoh and Kakuchi et al. reinvestigated the homopolymerization of DBAG to obtain poly(glycidyl amine) after release of the benzyl groups.<sup>151</sup> While the degree of polymerization of PDBAG was limited in the common AROP,<sup>269</sup> well-defined homopolymers with molecular weights ranging from 6200 to 50 400 g·mol<sup>-1</sup> and PDIs of 1.09–1.22 were obtained with the strong phosphazene base *t*-BuP<sub>4</sub> as a deprotonation agent. The authors attribute the high molecular weights to the mild reaction conditions (room temperature), which suppress weight limiting transfer reactions.<sup>320</sup> Cleavage of the benzyl protecting groups was performed under hydrogen atmosphere in a tetrahydrofuran/methanol mixture with palladium on carbon (Pd/C) as catalyst. This hydrogenation

**Scheme 28. Synthetic Scheme for Poly(glycidyl amine) (PGA) Starting from Epichlorohydrin (ECH)**<sup>102</sup>



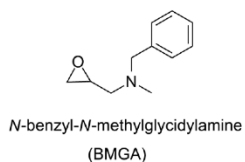
method allowed reducing the reaction time from 8 to 4 days. In contrast to the previous method described by Frey and co-workers,<sup>269</sup> no yield limiting interaction of the released amino groups with the catalyst surface was observed. Successful release of the amino groups was also reflected by the thermal properties of the homopolymers, whereas PDBAG reveals a  $T_g$  of 4.6 °C, the primary amino groups of PGA cause an extremely high  $T_g$  of 68.2 °C.

Further, polyethers with combined amino- and hydroxyl functionalities were obtained by copolymerization of DBAG with benzylglycidylether (BnGE) in a sequential and statistical manner and subsequent deprotection to PGA-*lin*PG copolymers. This strategy is superior to previous results by Möller et al.,<sup>102</sup> since only two reaction steps were required. Monomer reactivity ratios were determined to  $r_{\text{DBAG}} = 0.8$  and  $r_{\text{BGE}} = 3.24$ , indicating a strong compositional drift, with DBAG rich segments near the terminus. From these results and other reported reactivity ratios of glycidyl amine derivatives, an overall lower reactivity of glycidyl amine compared to glycidyl ethers can be concluded.<sup>269,313,315,319,321</sup> Additionally, the authors described the homopolymerization of the optically pure (*S*)-DBAG, yielding amino-functional polyethers with an exclusive isotactic stereosequence.<sup>151</sup>

Epicyanohydrin (EPICH) (Scheme 29, right) is a suitable alternative to the introduced protected glycidyl amine derivatives. This monomer allows the synthesis of amino-functional PEG by simple hydrogenation of the nitrile-group. In contrast to the glycidyl amine derivatives, EPICH cannot be polymerized by conventional AROP.<sup>322,323</sup> Recently, our group demonstrated the successful incorporation of 4–16 mol % EPICH into PEG by the “activated monomer” method. However, the nitrile group is a strong electron withdrawing functional group and supports the transfer to monomer reaction described in section 2.3, resulting in unsaturated chain ends.<sup>87</sup>

**3.2.2. Secondary Amino Groups.** Inspired by DBAG, Satoh and Kakuchi et al. very recently introduced a glycidyl amine derivative bearing only one cleavable substituent: *N*-benzyl-*N*-methylglycidylamine (BMGA) (Scheme 30).<sup>151</sup> Sec-

**Scheme 30. Suitable Glycidyl Amine Derivative for Secondary Amino Groups along the Polyether Backbone: *N*-Benzyl-*N*-methylglycidylamine (BMGA).<sup>151</sup>**



ondary amino-groups are obtained, after polymerization and subsequent cleavage of the benzyl-protecting group. The authors described homo-, block-, as well as statistical (co)polymers of BMGA and DBAG, utilizing the phosphazene base *t*-BuP<sub>4</sub> as deprotonation agent and BuOH as initiator. Investigations on the monomer incorporation revealed similar reactivity ratios for DBAG ( $r_{\text{DBAG}} = 0.91$ ) and BMGA ( $r_{\text{BMGA}} = 0.98$ ), resulting in a random monomer distribution.

**3.2.3. Tertiary Amino Groups.** In contrast to primary amino groups, tertiary amino moieties do not interfere in the polymerization of epoxides as long as the nitrogen atom is shielded by its substituents. Considering alkyl glycidyl amine derivatives, the most simple one, *N,N*-dimethyl glycidyl amine,

cannot be polymerized in a controlled manner, since the methyl groups do not sufficiently shield the nucleophilic nitrogen atom, which results in polycondensation reactions caused by the nucleophilic attack of the nitrogen at the epoxide ring.<sup>324</sup> In an interesting work Dhal and co-workers presented an indirect route to poly(*N,N*-dimethyl glycidyl amine) by nucleophilic substitution of poly(epichlorohydrin) (PECH) with dimethylamine.<sup>325</sup> The authors proposed that these polymers may show high potential as bile acid sequestrant after quaternization of the amino moieties with hydrophobic alkyl halides.

Expanding the alkyl chain of glycidyl amines from methyl to ethyl already permits successful controlled polymerization due to effective shielding of the nitrogen atom by the ethyl substituents. In this context, Ponomarenko et al. long ago already described the copolymerization of PO and *N,N*-diethyl glycidyl amine (DEGA) (see Scheme 31) and calculated the copolymerization parameters using the Fineman–Ross equation, resulting in  $r_{\text{PO}} = 1.90$  and  $r_{\text{DEGA}} = 0.30$ .<sup>321</sup> However, no further characterization of the resulting polymers was reported.

Reuss et al. introduced the copolymerization of DEGA with EO. Well-defined tapered and block copolymer structures were obtained with DEGA ratios up to 29 mol %.<sup>313</sup> The block copolymers were shown to be suitable as dual reducing and capping agent for gold nanoparticle formation. Furthermore, these structures act as a precursor for cationic polyelectrolytes, simply obtained by quaternization of the amino moieties with methyl iodide. Most interesting, PEG-*co*-PDEGA copolymers showed temperature and pH-responsive behavior in aqueous solution, similar to the structurally related poly(*N,N*-dialkylaminoethyl methacrylates).<sup>326</sup> To elucidate the temperature-induced inverse phase transition, the authors measured the occurrence of nanoaggregates by continuous wave electron paramagnetic resonance (CW-EPR) spectroscopy and compared it to the macroscopic cloud points. Interestingly, stable nanoaggregates were formed long before macroscopic changes were detectable.<sup>314,327</sup> Following this strategy, Frey and co-workers expanded the library of alkyl glycidyl amines and synthesized derivatives with longer alkyl chains, *N,N*-di(*n*-butyl) glycidyl amine (DButGA), *N,N*-di(*n*-hexyl) glycidyl amine (DHexGA), *N,N*-di(*n*-octyl) glycidyl amine (DOctGA) (Scheme 31).<sup>315</sup> The authors investigated the influence of the alkyl chain length on the relative reactivity in the copolymerization with EO and the copolymers' thermal behavior in aqueous solution. Interestingly, real-time <sup>1</sup>H NMR kinetic studies showed no dependence of the relative reactivity on the alkyl chain length. All copolymers showed lower relative reactivity than EO, resulting in *r*-parameters of  $r_{\text{EO}} = 1.84$ ,  $r_{\text{DButGA}} = 0.49$ ;  $r_{\text{EO}} = 1.78$ ,  $r_{\text{DHexGA}} = 0.42$ .<sup>315</sup> These results document the formation of gradient structures with increasing glycidyl amine segments toward the chain end.

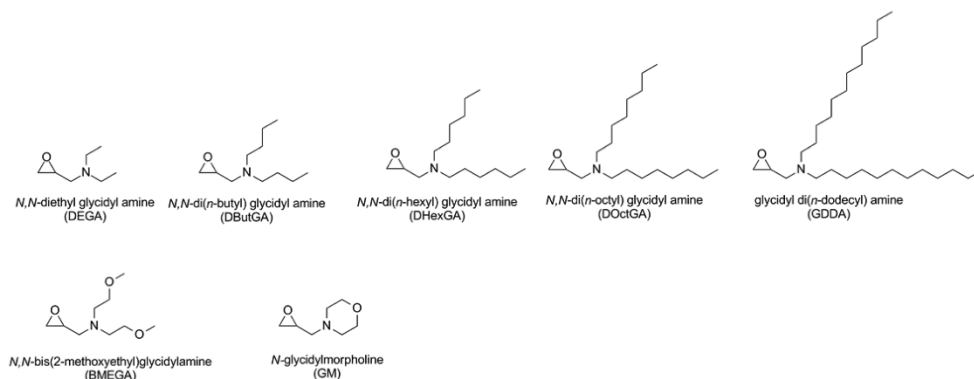
A highly hydrophobic glycidyl amine derivative, glycidyl-didodecylamine (GDDA), was introduced by Rangelov and Tsvetanov (Scheme 31).<sup>328</sup> However, to date, successful polymerization of GDDA has not been achieved.

As mentioned before, 2015, Satoh and co-workers presented more hydrophilic tertiary glycidyl amine derivatives, *N,N*-bis(2-methoxyethyl)glycidylamine (BMEGA) and *N*-glycidylmorpholine (GM) (Scheme 31, bottom).<sup>151</sup> Unlike their hydrophobic counterparts, BMEGA and GM can be successfully homopolymerized. The authors report water-soluble polymers with degrees of polymerizations up to 200 and narrow PDI (<1.18).

**3.2.4. Other Polyether Derivatives Bearing Nitrogen Moieties.** In 2009, Long and co-workers presented two

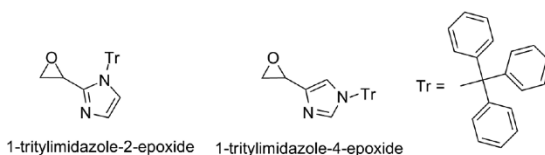
## Chemical Reviews

## Review

Scheme 31. Glycidyl Amine Derivatives Based on Tertiary Amines<sup>a</sup>

<sup>a</sup>*N,N*-Diethyl glycidyl amine (DEGA),<sup>313</sup> *N,N*-di(*n*-butyl) glycidyl amine (DButGA),<sup>315</sup> *N,N*-di(*n*-hexyl) glycidyl amine (DHexGA),<sup>315</sup> *N,N*-di(*n*-octyl) glycidyl amine (DOctGA),<sup>315</sup> glycidyl di(*n*-dodecyl) amine (GDDA),<sup>328</sup> *N,N*-bis(2-methoxyethyl)glycidylamine (BMEGA)<sup>151</sup> and *N*-glycidylmorpholine (GM).<sup>151</sup>

imidazole-substituted epoxides, 1-tritylimidazole-2-epoxide and 1-tritylimidazole-4-epoxide (Scheme 32).<sup>305</sup> The trityl-protect-

Scheme 32. Imidazole-Substituted Epoxides: 1-Tritylimidazole-2-epoxide and 1-Tritylimidazole-4-epoxide<sup>305</sup>

ing group allowed for polymerization by conventional AROP with *tert*-butoxide as an initiator and facile removal by treatment with trifluoroacetic acid, yielding water-soluble homopolymers with degrees of polymerization up to 90. The polymers showed a buffering range within the pH ranges of 3 and 6.5 and are candidates for electroactive devices or biological complexation for nucleic acid binding. The strategy also offers access to polyether-based polymeric ionic liquids (PIL) with polar polyether backbone.

Recently, Baker and co-workers reported poly(ionic liquids) (PILs) based on imidazolium ionic liquids grafted onto PEG.<sup>103</sup> The authors modified poly(epichlorohydrin) with 1-butylimidazole, followed by an anion exchange with lithium bis(trifluoromethanesulfonyl)imide (LiTFSI) to obtain a polyether based PIL (Scheme 33). The described homopolymers showed a conductivity of around  $10^{-3}$  S·cm<sup>-1</sup> at 90 °C, which dropped to around  $10^{-5}$  to  $10^{-6}$  S·cm<sup>-1</sup> at 30 °C, which is not sufficient for practical use.<sup>329</sup> This approach was improved by cationic copolymerization of 2-((2-(2-(2-methoxyethoxy)ethoxy)-

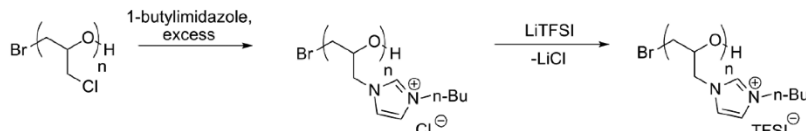
ethoxy)methyl)oxirane with epichlorohydrin, followed by modification of the ECH units. Copolymers with a 1:1 ratio of the mentioned monomers showed an improved conductivity of  $10^{-4}$  S·cm<sup>-1</sup> compared to the described homopolymers.<sup>330</sup>

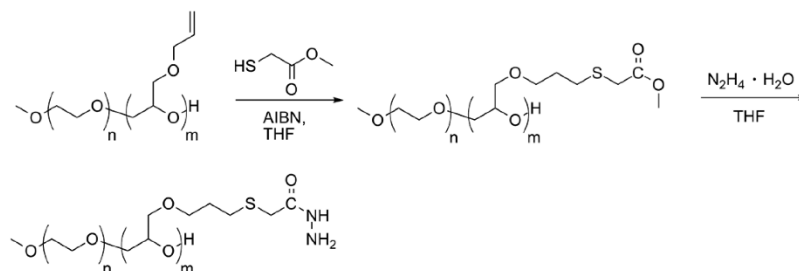
Hawker and co-workers demonstrated the use of another imidazole derivative, histamine, for pH-responsive hydrogels. PAGE-*b*-PEO-*b*-PAGE triblock copolymers were modified with thiol-functional histamine units by thiol-ene-click chemistry.<sup>331</sup> A clear gel to sol transition was reported upon lowering the pH from 7 to 6.6, rendering this material suitable for drug delivery applications with pH as an active trigger.

Starting from PEG-*b*-PAGE copolymers, in 2005 Ulbrich and co-workers showed the introduction of multiple hydrazide functionalities at PEG. The allyl group of the AGE units were reacted with methyl sulfanyl acetate via click chemistry, followed by transformation of the methyl ester to the hydrazide with hydrazine hydrate (Scheme 34).<sup>332</sup> The hydrazide functionality reacts specifically with aldehydes, forming reversible hydrazone linkages under ambient conditions. This concept is particularly interesting for drug delivery based on aldehyde-containing drugs, such as doxorubicin or for glyco-targeting.<sup>276,333</sup> Further, Sokolovskaya et al. applied the high reactivity of the hydrazide group to form acid-labile PEG-based hydrogels, suitable for controlled release applications.<sup>309</sup>

### 3.3. In Situ Monomer Sequence Characterization

Since copolymers of EO and PO with minority fraction of functional comonomers attain increasing significance, understanding of the comonomer sequence, i.e., the random or gradient nature of the polyether chains is crucial. Because different glycidyl ether monomers show varying electronic and steric properties it can be assumed that their reactivity in the ring opening copolymerization differs. Several analytical techniques such as differential scanning calorimetry (DSC), <sup>1</sup>H and <sup>13</sup>C

Scheme 33. Postpolymerization Modification of PECH to Obtain a Polyether Based PIL<sup>103</sup>

Scheme 34. Introduction of Hydrazone Functions into the Polyether Backbone<sup>332</sup>

NMR spectroscopy provide a first hint at the copolymers' microstructure,<sup>102</sup> as demonstrated in a work by the Möller group. The authors copolymerized ethoxyethyl glycidyl ether (EEGE) and epichlorohydrine (ECH) in a random and block type manner and compared the measured glass transition temperatures ( $T_g$ ) with the respective homopolymers, using the Fox equation.<sup>334</sup>

According to <sup>13</sup>C NMR-based microstructure characterization the oxyanionic ring opening copolymerization of EO and glycidyl ethers such as ethoxyethyl glycidyl ether (EEGE),<sup>257,282</sup> 1,2-diisopropyl glycidyl ether (IGG),<sup>282</sup> ethoxy vinyl glycidyl ether (EVGE),<sup>274</sup> glycidyl methyl ether (GME),<sup>97</sup> and ferrocenyl glycidyl ether (FcGE)<sup>292</sup> resulted in random comonomer sequences.

Hawker and Lynd et al. presented an alternative method to investigate the sequence of copolymers via <sup>1</sup>H NMR spectroscopy.<sup>271</sup> The authors copolymerized EO with either allyl glycidyl ether (AGE) or EVGE and detected the proton signals of the benzyl alkoxide initiator in accordance with the added comonomer unit. The authors concluded that both glycidyl ether monomers showed a greater tendency to be incorporated than EO. Transition-state density functional calculations (DFT calculations) were taken as a confirmation of these results.<sup>271</sup> The same authors expanded this work to the copolymerization of EO with an amino-functional glycidyl ether, *N,N*-diisopropyl ethanolamine glycidyl ether (DEGE). Similar to the common glycidyl ethers, DEGE showed higher reactivity than EO. Therefore, a gradient structure was assumed, which is in contrast to the random nature of the copolymerization observed in the above-mentioned studies in DMSO.<sup>295</sup> While this method monitors the addition of the first two monomers in a precise manner, further studies appear necessary to confirm, whether it reflects the actual reactivity of each monomer unit in the course of the formation of the polyether chains.

In recent years, a facile experimental in situ procedure was developed by our group to study the copolymerization at any stage of the reaction. Real-time <sup>1</sup>H NMR measurements can monitor the consumption of the monomers during the copolymerization.<sup>269</sup> Via integration of the unreacted epoxide signals it is possible to calculate the absolute composition of the copolymers at any time. In an exemplary procedure, EO and IGG were copolymerized and the copolymerization kinetics was studied. For this experimental setup the comonomers and the initiator were dissolved in a deuterated solvent. At  $-80$  °C, the initiator solution was transferred to the comonomer solution and vacuum was applied. Subsequently, the tube was flame-sealed and the polymerizations were carried out in vacuo at the desired temperatures directly in the NMR-spectrometer. Figure 8 shows a typical result, demonstrating the decrease of the epoxide signals

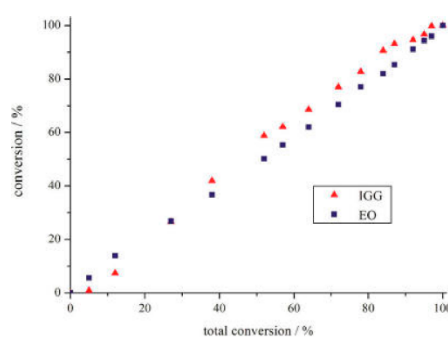


Figure 8. Monomer incorporation versus total conversion obtained from in situ NMR kinetics. Linear progression demonstrates the random polymerization behavior of IGG and EO.<sup>282</sup> Adapted with permission from Mangold, C.; Wurm, F.; Obermeier, B.; Frey, H. *Macromolecules* 2010, 43, 8511. Copyright 2010 American Chemical Society.

of glycidyl ether and EO as well as the increasing signal of the polymer backbone. The rate of polymerization is influenced by the reaction temperature, but the incorporation of the both monomers was equal in all cases. An ideally random distribution of the monomers was obtained.<sup>282</sup>

Allgaier et al. determined the <sup>1</sup>H NMR kinetics of an EO/BO copolymer system. They calculated copolymerization rates and determined the time required to obtain random copolymers without accumulation of one of the comonomers, when added to the reaction vessel over an estimated time.<sup>335</sup>

Recently, this kinetic method was expanded to in situ inverse gated (IG) <sup>13</sup>C NMR spectroscopy to monitor copolymerization in bulk. Wurm et al. successfully analyzed the bulk copolymerization behavior of AGE and FcGE.<sup>293</sup> Both monomers showed an equal consumption, resulting in a random microstructure. The kinetic study was carried out in bulk, and the natural abundance of <sup>13</sup>C isotopes was sufficient to obtain well-resolved <sup>13</sup>C NMR spectra. It was also found that epoxide copolymerizations can be performed in bulk and measured in situ, because the viscosity stayed sufficiently low to obtain quantitative spectra during the whole process. Kim and co-workers recently applied this method to the hyperbranching copolymerization of glycidol and 2-((2-(oxiran-2-ylmethoxy)ethyl)disulfanyl)ethane-1-ol, demonstrating a slight gradient in the hyperbranched structure formed.<sup>290</sup>

### 3.4. Polymerization of Longer Alkylene Oxides

**3.4.1. Poly(propylene oxide), Poly(1,2-butylene oxide) and Higher 1,2-Alkylene Oxide Polymers.** While PEO has unique biomedical applications due to its remarkable water-solubility, substituted poly(alkylene oxide)s, particularly poly-

## Chemical Reviews

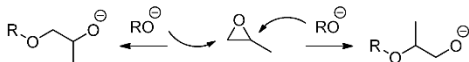
Review

(propylene oxide), play an important role as hydrophobic, chemically inert, amorphous and flexible polyether compounds in the industrial fabrication of polyurethane foams, for nonionic surfactants or lubricants. This chapter summarizes recent innovations in the area of alkylene oxide polymerization. Polymerization techniques established before 1990 are summarized in comprehensive book volumes.<sup>21,57,336</sup>

Among the alkylene oxides, ethylene oxide, propylene oxide, and butylene oxide are available on large industrial scale. Twenty-five million tons of ethylene oxide and 8 million tons of propylene oxide were produced in 2014 (Source: BASF SE), whereas the world annual production of butylene oxide is on the kiloton scale.<sup>336</sup> The epoxides are synthesized from the readily available steam cracking products ethene, propene, and 1-butene. Hexene oxide and higher  $\alpha$ -olefin oxide homologues, however, are solely commercialized as fine chemicals. Therefore, poly(alkylene oxide)s beyond poly(butylene oxide) are of little industrial interest, and the majority of studies are performed in academia, mainly to explore modern polymerization strategies, while only limited attention has been devoted to the examination of their materials properties so far.<sup>337–340</sup>

In general, with increasing alkyl chain length epoxide monomers exhibit lowered reactivity compared to ethylene oxide and glycidyl ethers.<sup>341–343</sup> In contrast to the ROP of EO, the asymmetric substitution pattern of the other 1,2-alkylene oxides results in two different modes of ring-opening and three kinds of monomer unit connections in the corresponding polymer chain (see Scheme 35).

#### Scheme 35. Anionic Ring-Opening Reaction of a Substituted Epoxide by Methylene (Left) or Methine Attack (Right)



Anionic alkylene oxide polymerization largely results in regioregular head-to-tail connections (mainly due to steric reasons), whereas irregular combinations of head-to-tail, head-to-head and tail-to-tail linkages are present in polyalkylene glycols obtained by cationic polymerization due to the stability of the respective carbocations. The microstructure can be characterized by <sup>13</sup>C NMR spectroscopy (Figure 9).<sup>344–346</sup>

Besides this isomerism in the microstructure of the polymer backbone, also different stereoisomers can occur due to the asymmetric substituted methine carbon of the ring. Recently, an excellent and comprehensive review by Coates et al. summarized the state of the art in stereoselective epoxide polymerization and its potential for unusual polyether structures.<sup>347</sup> Therefore, this aspect is not covered in detail herein. In order to achieve stereoselectivity, a large range of metal catalysts have been synthesized and investigated, with focus on aluminum, zinc, iron and cobalt based systems, using porphyrin, calixarene or salen complexes (Scheme 36). All catalysts shown in Scheme 36 and the majority of other stereoselective catalysts produce poly(propylene oxide) with semi-isotactic microstructure. These optically active polymers are semicrystalline, in contrast to stereoirregular PPO, which exhibits an amorphous structure.

Anionic polymerization of substituted alkylene oxides using alkali metal alkoxide or hydroxide initiators comes with the drawback of competing chain transfer reactions, as shown in section 2.1 (Scheme 37). The strongly alkaline alkoxide can, besides acting as a nucleophile that opens the ring, act as a base

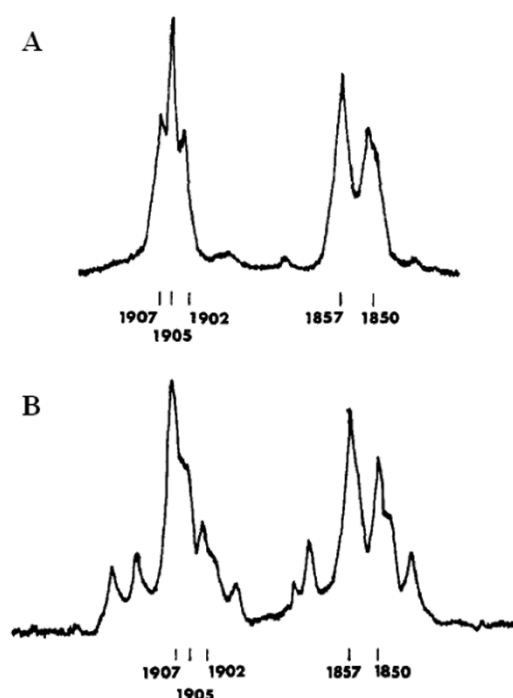
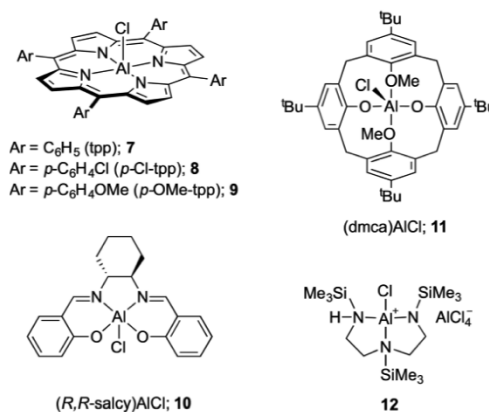


Figure 9. <sup>13</sup>C NMR spectrum with methine and methylene carbon signal pattern of atactic, head-to-tail-linked PPO (A) and PPO with irregular microstructure (B). (Adapted with permission from Oguni, N.; Lee, K.; Tani, H. *Macromolecules* 1972, 5, 819.<sup>344</sup> Copyright 1972 American Chemical Society.)

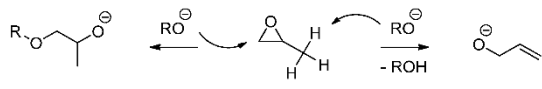
#### Scheme 36. Aluminum Complexes with Porphyrin (7,8,9), Salen (10), Calixarene (11), and Silylamine (12) Ligands for Stereoselective Polymerization of Propylene Oxide (PO)<sup>44</sup>



<sup>44</sup>Adapted with permission from Childers, M.; Longo, J.; Van Zee, N.; LaPointe, A.; Coates, G. *Chem. Rev.* 2014, 114, 8129.<sup>347</sup> Copyright 2014 American Chemical Society.

and abstract a proton from the alkyl substituent at the epoxide ring, generating an unstable carbanion. The ensuing rearrangement results in an allyl alkoxide that is capable of initiating a new polymer chain with an unsaturated chain end (vide supra). This

### Scheme 37. Propagation and Chain Transfer Reaction in the Anionic Polymerization of Propylene Oxide, Limiting Achievable Molecular Weights



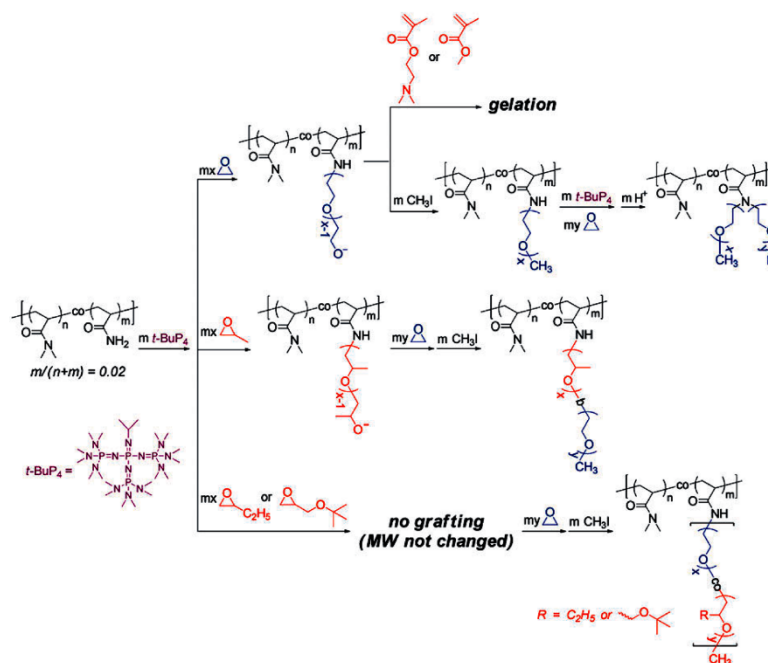
side-reaction limits the achievable molecular weights of PPOs by conventional anionic polymerization ( $T > 90\text{ }^{\circ}\text{C}$ ) to approximately  $6\,000\text{ g mol}^{-1}$ .<sup>21</sup> Sterically hindered epoxides such as 2,3-dimethyl-2,3-butylene oxide undergo almost quantitative elimination to allyl alcohols when treated with catalytic amounts of base. To avoid this issue, cationic ring-opening polymerization is often employed for polymerizing disubstituted epoxide monomers like cyclohexene oxide, despite the well-known disadvantages of this method, such as the lack of control over molecular weights and polydispersity.

Aiming at an improvement of the low monomer reactivity and reducing chain transfer reactions in the anionic polymerization of 1,2-alkylene oxides, tremendous progress has been made in the last two decades. Allgaier et al. employed crown ethers to complex potassium counterions to increase the nucleophilicity of the chain ends. The accompanying increase of basicity did not affect the polymerization negatively, because reaction conditions below room temperature were chosen. With side reactions minimized, PBO, poly(hexene oxide) (PHO), poly(octene oxide), and poly(dodecene oxide) with high molecular weights up to  $65\,000\text{ g mol}^{-1}$  and narrow MWDs became accessible.<sup>340,348</sup> Deuterated analogues were synthesized in order to examine the effect of the side-chain length on the unperturbed chain dimensions and hydrogen dynamics via neutron

scattering.<sup>349,350</sup> Also copolymerization of different alkylene oxides has been performed for some comonomer pairs. Anionic copolymerization of EO and BO was conducted using in situ NMR spectroscopy to determine the copolymerization kinetics,<sup>335</sup> strongly tapered compositional profiles were found. Xiong et al. employed Allgaier's polymerization strategy in order to prepare gradient and block side-chain liquid crystalline copolymers from butylene oxide.<sup>351</sup>

As discussed in detail in section 2.5 “phosphazene bases: metal-free initiators”, increased propagation rates for anionic PO and BO polymerization can be achieved using phosphazene bases as catalysts. *t*-Bu-P<sub>4</sub> was found to both accelerate the reaction and to enable polymerization in a living manner without chain transfer.<sup>138,139,141</sup> Capitalizing on this method, Hadjichristidis and co-workers developed a catalyst switch strategy by which PBO block copolymers with polyesters or polycarbonates could be obtained.<sup>145,146,170</sup> For the preparation of the polyester/polycarbonate block, an excess of diphenyl phosphate was introduced to the reaction mixture before adding the cyclic carbonate or lactone monomer. Phosphazene base-promoted anionic polymerization also gave access to brush copolymers consisting of a polyacrylamide main chain and poly(alkylene oxide) side chains via a “grafting from” approach (Figure 10).<sup>152</sup>

Kappe and co-workers studied the polymerization of alkylene oxides (up to hexane oxide) in the microwave, resulting in low molecular weight polymers, however with fast reaction kinetics. Both oligomers and side products from transfer reactions were studied in detail by SEC.<sup>352–354</sup> Employing PEG monomethyl ether as an initiator, they obtained amphiphilic block copolymers. Short, hydrophobic PBO or PHO segments sufficed to form micelles in aqueous solution.<sup>355</sup>

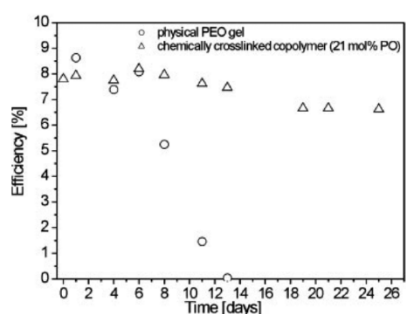


**Figure 10.** Phosphazene base-mediated synthesis of brush polymers with polyacrylamide backbone and polyether side chains (Adapted with permission from Zhao, J.; Alamri, H.; Hadjichristidis, N. *Chem. Commun.* 2013, 49, 7079.<sup>152</sup> Copyright 2013 Royal Society of Chemistry.)

## Chemical Reviews

## Review

By suspension polymerization using a calcium amide/alkoxide initiator system, Petrov and co-workers synthesized amorphous PO and BO homopolymers and PEO-co-PPO copolymers exhibiting low degrees of crystallinity. Without control over the degree of polymerization, high molecular weights in the range of several hundred kDa and MWDs between 2.3 and 3.2 were obtained.<sup>356</sup> The materials were cross-linked photochemically with *N,N'*-methylenebis(acrylamide) and tested as polymer gel electrolytes in dye-sensitized solar cells. A solar cell containing a chemically cross-linked PEO-co-PPO copolymer with 21% PPO content maintained high power conversion efficiency for at least twice the lifetime of a conventional physical PEO gel electrolyte (Figure 11).



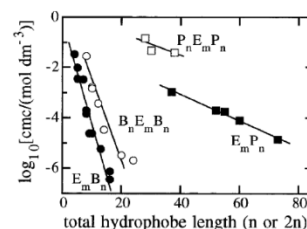
**Figure 11.** Power conversion efficiency over time of dye-sensitized solar cells containing physical PEO gel and chemically cross-linked PEO-co-PPO, respectively (Adapted with permission from Petrov, P.; Berlinova, I. V.; Tsvetanov, C.; Rosselli, S.; Schmid, A.; Zilaei, A.; Miteva, T.; Durr, M.; Yasuda, A.; Nelles, G. *Macromol. Mater. Eng.* **2008**, *293*, 598.<sup>356</sup> Copyright 2008 Wiley.)

As mentioned above, the activated monomer technique allows for minimizing chain transfer reactions during the polymerization of alkylene oxides. PO, BO, 1,2-hexene oxide, and 1,2-octadecene oxide were polymerized rapidly and in a controlled manner, resulting in well-defined polymers with molecular weights up to several ten thousand g/mol.<sup>80,88,96</sup> This strategy gave direct access to  $\alpha$ -azido, $\omega$ -hydroxy-PPO.<sup>83</sup> By combining protonated phosphazene-base alkoxide initiators with triisobutylaluminum, the same group synthesized telechelic PPO polyols.<sup>90</sup>

Via the *N*-heterocyclic carbene-catalyzed polymerization, Taton et al. were able to prepare  $\alpha,\omega$ -difunctionalized PPO with MWs up to 7000 g mol<sup>-1</sup> without the use of additional solvents.<sup>121</sup> Recently, Limbach et al. introduced imidazol(in)ium carbonates as more stable precatalysts which released the *N*-heterocyclic carbene upon heating,<sup>122</sup> demonstrating controlled synthesis of telechelic PPOs. In contrast, copolymerization of PO with  $\epsilon$ -caprolactone and (S,S)-lactide, respectively, resulted in decreased conversion and broadened MWD. Carbene-mediated polymerization of higher alkylene oxide monomers has not been explored yet.

The most prominent polyalkylene glycol surfactants are block copolymers consisting of hydrophilic PEG and hydrophobic PPO segments that are discussed in a separate section (see section 4.1). In search of an alternative for poloxamers and similar EO-PO block copolymers, Booth and co-workers synthesized a great variety of linear and cyclic diblock and triblock, as well as gradient polymers from EO and BO. Polymerizations were performed in bulk, using alcohol-

potassium alkoxide mixtures as initiators, resulting in narrow molecular weight distributions. In general, rather short PBO blocks were synthesized.<sup>357–360</sup> Several groups extensively explored the materials properties of the copolymers, focusing on the dependence of micellization and gelation behavior on the block architecture.<sup>361–368</sup> Following the trend in hydrophobicity, copolymers of EO and BO exhibit lower critical micelle concentrations than copolymers of EO with PO, even if the hydrophobic block is shorter (Figure 12). In this context one may emphasize that low molecular weight PPO homopolymers are water-soluble below a critical solution temperature.<sup>369,370</sup>



**Figure 12.** Critical micelle concentration of amphiphilic diblock and triblock copolymers in aqueous solution at 30 °C, versus PBO (B) and PPO (P) block length, respectively. (PEO (E) block length constant.) (Adapted with permission from Booth, C.; Attwood, D. *Macromol. Rapid Commun.* **2000**, *21*, 501.<sup>361</sup> Copyright 2000 Wiley.)

Bates and co-workers modified the reaction protocol of Booth et al. by using THF as a solvent and completely deprotonated potassium alkoxides as initiators. This strategy enabled the synthesis of narrowly distributed PBO-*b*-PEO and low molecular weight PHO-*b*-PEO block copolymers with low monomer conversion.<sup>338,371</sup> The resulting materials were successfully tested for potential application as tougheners in cured epoxy resins.<sup>372</sup> Higher molecular weight PBO-*b*-PEO and PHO-*b*-PEO block copolymers were obtained by Carlotti et al. via the activated monomer method, and their self-organization in aqueous solution was investigated.<sup>95</sup> As expected from the high hydrophobicity of PHO, they observed very low critical micelle concentrations. Depending on the block lengths and molar ratio of hydrophilic and hydrophobic segments, spherical micelles or vesicles (polymersomes) or both in coexistence were observed.

Multihydroxyfunctional polyalkylene glycol amphiphiles can be accessed by replacing the PEG segments with linear or hyperbranched polyglycerol (PG), retaining the hydrophobic PPO blocks. Following the first report on linear-dendritic PPO-PG block copolymers,<sup>373</sup> linear diblock, triblock, and gradient copolymers were synthesized via polymerization and subsequent deprotection of EEGE.<sup>374–377</sup> Incorporation of small amounts G already lead to water-soluble materials. Carlotti et al. were able to synthesize gradient copolymers of EEGE and <sup>t</sup>BuGE with PO and BO, respectively, with elevated molecular weights up to 85 000 g mol<sup>-1</sup> by the activated monomer strategy.<sup>89</sup> Kakuchi and co-workers combined the protected PG derivatives PBnGE and P<sup>t</sup>BuGE with PBO segments, using phosphazene base-catalyzed polymerization.<sup>141</sup>

More than 60 years ago, random copolymers of EO and PO were commercialized as water-soluble polyalkylene glycol (PAG) lubricants by Union Carbide.<sup>378</sup> EO/PO random copolymers do not show such low surface tensions as the corresponding PEO-*b*-PPO block copolymers, avoiding undesired foaming when in use.

Their properties in aqueous solution have been investigated by François and co-workers.<sup>379</sup>

Similar to the solubilization of hydrophobic compounds in water via PEGylation, oil-soluble gasoline additives were synthesized by butoxylation of hydrophilic amides.<sup>380</sup> Recently, Dow Chemical released oil-soluble PAGs, based on PBO and PPO-*co*-PBO copolymers as performance additives in hydrocarbon lubricants.<sup>381</sup>

As part of their work on epoxide-termination of living carbanionic polystyrene polymerization and subsequent AROP of epoxides, Quirk et al. prepared block copolymers which contained PPO as a semipolar segment.<sup>92</sup> Inspired by this, Bates and co-workers combined PBO with polyolefins and investigated the phase behavior of the completely hydrophobic, but phase-separated block copolymers.<sup>382</sup>

Noh and co-workers employed cationic ring-opening polymerization to copolymerize BO with epichlorohydrin.<sup>383</sup> In a postpolymerization modification step, they etherified the chloride groups to obtain stimuli-responsive poly(ferrocenylglycidylether)-PBO copolymers.

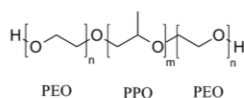
Apart from its use in polyether chemistry, PO features prominently in the preparation of “green” polycarbonate. Driven by the global trend toward green chemistry and biodegradable materials, the copolymerization of PO (and other epoxides) with carbon dioxide has become a focus of major attention. Numerous reviews on the research in this area have been published in recent years.<sup>347,384–393</sup>

## 4. BLOCK COPOLYMERS OF PEG AND PPO

### 4.1. Poloxamers and Poloxamines

Block copolymers composed of PPO and PEO are an important class of biocompatible polymers in both industry as well as academia. Namely, ABA-triblock copolymers with the structure PEO-*b*-PPO-*b*-PEO, known as poloxamers (see Scheme 38) or

**Scheme 38. Structure of Poloxamers Composed of Two PEO Blocks and a Central PPO Block**



Pluronic (trade mark BASF), are among the most relevant nonionic surfactants (= surface active agents) and have been extensively investigated over the last decades.<sup>394,395</sup> Due to the high water-solubility of PEO in a wide temperature range (0–100 °C) and the low solubility of PPO in water at temperatures exceeding  $T_c$  (>15 °C; cloud point), these block copolymers exhibit amphiphilic character accompanied by surface-active properties.<sup>396</sup>

Consequently, the conveniently prepared PEO-*b*-PPO-*b*-PEO copolymers are widely utilized as lubricants, detergents, defoamers, and emulsifying agents in industrial and agricultural processes, as well as in cosmetic products, paints, and food additives.<sup>395</sup> Pluronic are prepared via sequential anionic ring-opening polymerization of PO and EO using potassium and sodium hydroxide as the activator.<sup>397</sup> First, the central PPO segment is synthesized as a precursor, and subsequently chain extended by the polymerization of EO. In order to obtain highly purified block copolymers and to reduce the content of admixtures, such as PPO homopolymers and low molecular weight block copolymers, chromatographic fractionation is often employed after the polymerization.<sup>398</sup>

Due to the vast variety of Pluronic with different molecular composition, a categorization system has been established to allow for an easy description of structure and properties of a given copolymer. For the nonproprietary name poloxamer, the abbreviated expression starts with the capital letter ‘P’ followed by one or two digits corresponding to the approximate molecular weight of the PPO block, when multiplied by a factor of 100. The last digit multiplied by 10 refers to the weight percentage of PEO within the block copolymer. For example, “Poloxamer P407” conforms to a copolymer with a PPO block of about 4000 g/mol and 70% weight content of PEO (see Table 3).

In case of trade names like Pluronic (BASF), Lutrol (BASF), or Synperonic (Croda) prefix letters “L”, “P”, and “F” classify the physical appearance of the pure copolymer as liquid (L), paste (P), and flakes (F). The first one or two digits multiplied by 300 represent the approximate molecular weight of PPO, whereas the last digit multiplied by 10 indicates the total weight percentage of PEO within the polymer. For the previous example of a PEO-*b*-PPO-*b*-PEO copolymer ( $M_n = 4000$  g/mol, 70% PEO), this leads to the term F127. Accordingly, the nomenclature for Pluronic can be converted to the generic term for poloxamers by multiplying the first one or two digits by a factor of 3.<sup>399</sup>

**Table 3. Table of Pluronic Compositions and Properties**

Pluronic	poloxamer	$M_n^a$	$N_{EO}^b$	$N_{PO}^c$	$cmc^d$	HLB <sup>e</sup>	cloud point <sup>f</sup>
L35	101	1900	21.6	16.4	$5.3 \times 10^{-3}$	19	73
L43	123	1850	12.6	22.3	$2.2 \times 10^{-3}$	12	42
L44	124	2200	20.0	22.8	$3.6 \times 10^{-3}$	16	65
L61	181	2000	4.5	31.0	$1.1 \times 10^{-4}$	3	24
L64	184	2900	26.4	30.0	$4.8 \times 10^{-4}$	15	58
P84	234	4200	38.3	43.4	$7.1 \times 10^{-5}$	14	74
P85	235	4600	52.3	39.7	$6.5 \times 10^{-5}$	16	85
L88	238	11400	207.8	39.3	$2.5 \times 10^{-4}$	28	> 100
P103	333	4950	33.8	59.7	$6.1 \times 10^{-6}$	9	86
F108	335	14600	265.4	50.3	$2.2 \times 10^{-5}$	27	> 100
P123	403	5750	39.2	69.4	$4.4 \times 10^{-6}$	8	90
F127	407	12600	200.4	65.2	$2.8 \times 10^{-6}$	22	> 100

<sup>a</sup>Average molecular weights in g/mol. <sup>b/c</sup>Average number of EO/PO units per polymer taken from ref 407. <sup>d</sup>critical micelle concentration in mol/L as determined by pyrene probe measurements and taken from ref 407. <sup>e</sup>Hydrophilic–lipophilic-balance values were taken from ref 407. <sup>f</sup>Cloud points in °C taken from ref 408.



In particular, self-aggregation of PEO-*b*-PPO-*b*-PEO copolymers into micellar structures plays a decisive role regarding a majority of applications especially in nanoscience and nanomedicine.<sup>399,400</sup> Poloxamer micelles composed of PPO-core and PEO-corona permit encapsulation of a wide range of hydrophobic compounds. This behavior motivates their use as drug and gene delivery systems,<sup>398</sup> as well as for nanotechnological applications, for example as surfactants in emulsion polymerization.<sup>401</sup> These self-assembled aggregates vary in size and shape from spherical to rod-like or lamellar structures.<sup>402</sup> In this case, the molecular weights of the PEO/PPO segments dictate the properties of the block copolymers, such as aqueous solubility, critical micelle concentration (CMC), critical micelle temperature (CMT), structure of micelles and aggregation numbers.<sup>403–406</sup> Namely, CMC values are of fundamental significance to evaluate emulsifying properties of poloxamers.

In general, CMC values tend to decrease with increasing hydrophobic PPO chain length due to an increase of the net hydrophobicity favoring the formation of micelles. On the contrary, CMCs increase with growing chain length of the PEO blocks, which has been ascribed to a reduced core hydrophobicity that leads to a destabilization of micelles.<sup>404</sup> Systematic studies on aggregation behavior of Pluronics in aqueous solution have been reported in numerous articles.<sup>403,404</sup>

The remarkable self-assembly and emulsifying properties of Pluronics in conjunction with their excellent biocompatibility has proven particularly advantageous for biomedical and pharmaceutical applications and the development of drug delivery systems.<sup>394,398</sup> Namely, Pluronic formulations have been shown to exhibit great potential in anticancer research, especially regarding the treatment of multidrug resistant (MDR) tumor cell types. Studies in this field report an enhancement in cytotoxic activity of the chemotherapeutic drug doxorubicin toward MDR tumor cell lines by 2 or 3 orders of magnitude.<sup>407,409,410</sup> Besides operating as drug carriers to improve pharmacokinetic performance, Pluronics appeal as biological response modifiers capable of sensitizing multidrug resistant (MDR) cancer cells and increasing drug transport across the cell membrane. Currently, micelles of Pluronic L61 and F127 loaded with doxorubicin are investigated for the treatment of cancer cells resistant to doxorubicin in clinical trials.<sup>411</sup> Credit has to be granted to Kabanov et al. as the pioneers within this research area. Highly promising findings regarding Pluronic-based micelles loaded with paclitaxel as anticancer agent have also been reported by Tsvetanov et al. A comparison of these micellar drug formulations with Taxol revealed improved pharmacokinetic properties and enhanced blood circulation times.<sup>412</sup> Recent developments regarding the effect of Pluronics on MDR tumor cells and their promising perspective in this particular field have been comprehensively reviewed lately.<sup>409</sup>

In addition, drug carrier systems based on Pluronic block copolymer technology represent promising candidates to penetrate the blood brain barrier in order to transport therapeutics to the brain.<sup>413</sup> Another specialized application of Pluronic-based formulations has emerged within the field of gene therapy. When injected into skeletal muscle, plasmid DNA induces gene expression which can be exploited for vaccination strategies or the generation of therapeutic proteins. In several studies, Pluronics have been employed to increase the efficiency of gene transfer technologies.<sup>398</sup>

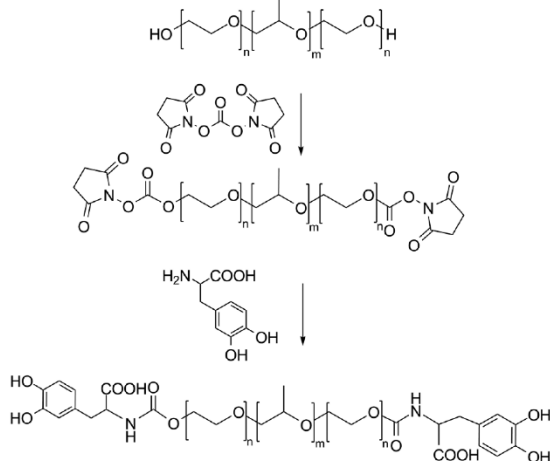
However, a major challenge for drug-loaded micelles as nanocarrier systems arises from the thermodynamic instability of micelles upon dilution, which is also valid for Pluronic-based

micellar formulations. In particular, very hydrophilic block copolymers with high cmc/cmt values suffer from low micelle stability and are crucially subjected to disassembly of micelles. To overcome this drawback, several strategies have been proposed to increase stability of Pluronic micelles. For example, polymerization of suitable monomers (e.g.: *N*-isopropylacrylamides, *N,N*-diethylacrylamide) forming thermoresponsive hydrogels (LCST behavior) inside the micellar core can afford micelles with improved stability profiles and good drug loading capacities. However, the stability gained from this approach was found to be impermanent and depletes within a time frame of days or weeks.<sup>395</sup> Other strategies focused on the cross-linking of the micellar shell to lower the CMC by converting the hydroxyl groups into aldehydes and introducing imine linkages via the addition of diamines.<sup>414</sup> Another noteworthy approach reported by Petrov et al to effectively stabilize Pluronic-based micelles implied the formation of an interpenetrating network via light-initiated cross-linking of a tetrafunctional acrylate monomer.<sup>415</sup> Nevertheless, stabilization of Pluronic micelles without affecting drug release profiles and drug loading capacities remains a fundamental challenge for all these modifications.

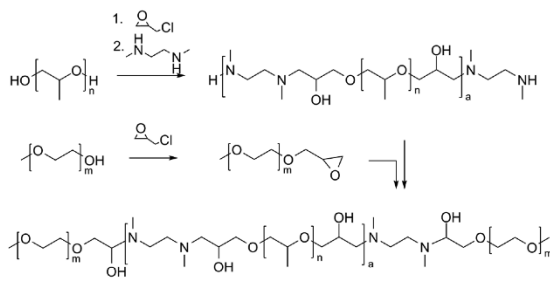
Moreover, Pluronics are utilized for surface-coating of drug-loaded, hydrophobic nanoparticles in order to prolong blood circulation times of the drug carriers. Depending on the size of particles and properties of the coated surface, a certain selectivity in the site of deposition within the body is observed. By controlling the balance between adsorption and desorption of specific blood components referred to as opsonization and dysopsonization, site specific deposition can be influenced using Pluronics as surface-coatings. Effective enhancement of serum life times have been achieved for polymeric particles in a size range from 70 to 200 nm.<sup>400</sup>

Another remarkable property of PEO-*b*-PPO-*b*-PEO copolymers in aqueous solution results from their ability to undergo thermo-reversible gelation at concentrations above the CMC. In particular, gelation of poloxamer 407 (Pluronic F127) has proven beneficial for biomedical purposes, as concentrated solutions appear as viscous liquids at room temperature forming a semisolid transparent gel at body temperature (37 °C).<sup>416</sup> This behavior has motivated use of poloxamer gels for prolonged drug release strategies<sup>416</sup> and for tissue engineering.<sup>394,417–419</sup> Although poloxamers are generally regarded as nontoxic, higher doses (up to 137.5 mg/kg in rabbits) of Poloxamer 407 have been reported to affect serum concentrations of triglycerides and cholesterol.<sup>416</sup> Due to the comparatively weak mechanical strength and rapid erosion of poloxamer gels, for instance, covalent cleavable linkages such as carbonates have been introduced to improve mechanical properties, simultaneously ensuring renal excretion of the degradation fragments.<sup>416</sup> Moreover, pH-responsive poloxamer-based gels have been formed from graft copolymers of poly acrylic acid (PAA) and poloxamers (poloxamer-*g*-PAA). This reduces the amount of material needed to form stable gels at body temperature and represent a promising tool for pH-triggered release strategies.<sup>420</sup> Messersmith and co-workers reported the attachment of DOPA (3,4-dihydroxyphenyl-L-alanine) moieties at both termini of Pluronics to attach catechol groups, creating bioadhesive hydrogels (see Scheme 39).<sup>421</sup> There are several other reports on chemically modified PEO-*b*-PPO-*b*-PEO copolymers and the corresponding hydrogels, these are, however, beyond the scope of this review.

Another interesting approach mimicking the structure of poloxamers has been demonstrated by Park et al. by

**Scheme 39. Synthesis of Catechol-Functional Poloxamers According to Messersmith et al.**<sup>421</sup>

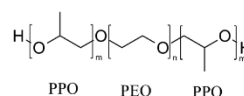
incorporating multiple hydroxyl groups into the backbone to enable the covalent attachment of pharmaceutical drugs.<sup>422</sup> These structures were accessed by first generating a PPO precursor polymer via step-growth polymerization of *N,N'*-dimethylethylenediamine and diepoxy-functional PPO, subsequently end-capping with epoxy-functional mPEG (see Scheme 40).

**Scheme 40. Synthesis of Poloxamer Mimicking Block Structures According to Park et al.**<sup>422</sup>

A promising approach to access novel types of poloxamer analogs bearing multiple hydroxyl functionalities was developed by Tsvetanov and co-workers.<sup>375,376,423</sup> Using PPO as a macroinitiator for the AROP of the acetal-protected glycerol derivative EEGB, linPG-*b*-PPO-*b*-linPG triblock copolymers were obtained after subsequent hydrolysis of the acetal moieties. In several studies, the physicochemical properties of materials were investigated.<sup>318,363</sup>

Given the vast spectrum of applications of poloxamers or poloxamer-based formulations and the strong emphasis on postmodification strategies to improve their performance, to the best of our knowledge, no synthetic routes have been explored to develop novel block copolymer architectures compared to the commercially available standards, e.g., by using multifunctional PEG or PPO blocks to incorporate specific functional groups already during the synthesis.

Besides poloxamers, related triblock copolymers with an inverted substructure composed of a central PEO block flanked by two PPO segments are known as reverse poloxamers (Pluronic R) and are likewise commercially available. Although these structures exhibit interesting properties and are diversely used, for example, as wetting and defoaming agents in industrial processes,<sup>424</sup> these systems have been less investigated compared to the materials mentioned above.<sup>425</sup> However, more recently, increasing attention was drawn to studies of phase behavior and aggregation of reverse poloxamers in aqueous solution.<sup>426–428</sup> In contrast to poloxamers, reverse poloxamers (see Scheme 41)

**Scheme 41. Structure of Reverse Poloxamers Composed of Two PPO and a Central PEO Block**

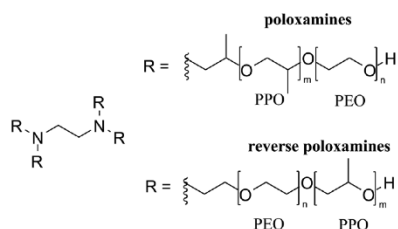
show a reduced capability to form regular micelles in aqueous medium, which is ascribed to a loss of entropy attributed to the looping of the PEO middle block in micellar structures.<sup>425</sup> Instead, PPO-*b*-PEO-*b*-PPO triblock copolymers have been reported to either form random network structures or micellar associations, depending on the concentration, with the two terminal blocks located in different PPO domains.<sup>429</sup>

In addition, micellization and gelation of poloxamer/reverse poloxamer mixtures have been investigated suggesting a critical composition ratio above which the appearance of bridged poloxamer micelles strongly impedes the gelation process.<sup>430,431</sup>

The spectrum of applications for reverse poloxamers, however, appears to be limited in comparison to “normal” poloxamers. This is probably attributed to their unfavorable self-assembly. However, lately, a new perspective for the application of reverse poloxamers has been proposed within the field of gene therapy. Herein, PPO-*b*-PEO-*b*-PPO copolymers were evaluated in terms of their ability to increase muscle transfection compared to naked DNA. It was found that reverse Pluronic promote muscle gene transfer in mice as effectively as regular Pluronic, which might encourage further research activities.<sup>432</sup> However, in order to compete with the steadily growing significance of regular poloxamers, applications benefiting from the use of reverse poloxamers opposed to regular poloxamers need to be developed.

**4.1.1. Poloxamines.** Another group of amphiphilic block copolymers based on PEO and PPO are poloxamines with a distinct tetrabranched block structure bearing a central ethylene diamine bridge. Four symmetric blocks, composed of PEO and PPO, are attached to the amine units and can either contain the PEO block as the outer segment (poloxamines, trade name Tetronics) or as the inner segment (reverse poloxamines, trade name TetronicsR) (see Scheme 42). Poloxamines and reverse poloxamines are synthesized using ethylene diamine as an initiator for the sequential anionic polymerization of PO and EO, resulting in X-shaped polymer architectures.

The presence of the tertiary amine groups adds a dual responsive behavior to these polymeric amphiphiles. Poloxamines exhibit thermo- and pH-responsiveness, which distinguishes their properties from poloxamers. Moreover, the additional amine functionalities enable further modification reactions, such as quaternization to promote cell adhesion for tissue engineering purposes.<sup>433</sup>

**Scheme 42. Structures of Poloxamines (Tetronics) and Reverse Poloxamines (TetronicsR)**

Compared to poloxamers, studies on the phase behavior of poloxamines have been neglected for a long time. However, within the past decade, favorable physicochemical properties of poloxamines regarding drug delivery strategies and tissue engineering have been elucidated<sup>434</sup> and have motivated increasing research efforts in this area.<sup>435</sup> In analogy to their linear counterparts, poloxamines show self-assembly into micellar aggregates in aqueous medium. In contrast, however, aggregation behavior of poloxamines is strongly pH-dependent. The  $pK_a$  values of the amine groups of 3.8–4.0 and 8.0, respectively, do not vary substantially with different PEO/PPO block lengths.<sup>436</sup> A decrease in pH leads to a reduced tendency to aggregate and a more narrow temperature range, in which aggregation occurs. This behavior can be attributed to the Coulombic repulsion between the positively charged polymers. At physiological conditions (pH 7.4), poloxamines are present as single protonated species.<sup>395</sup> A noteworthy approach deploying the pH-dependent aggregation of poloxamines to stabilize DNA complexes was proposed by Pitard et al. Therein, negatively charged DNA-poloxamine supramolecular assemblies were introduced as potential gene delivery systems for the therapy of skeletal or heart muscle-related diseases.<sup>437</sup>

In accordance with poloxamers, surface-coating of hydrophobic nanoparticles using poloxamines has become increasingly attractive in order to prolong the particles' blood circulation times and render them potential drug delivery systems for medical and pharmaceutical purposes.<sup>438</sup> The efficiency of the respective coatings to prevent recognition of the hydrophobic nanoparticles by macrophages strongly depends on the molecular weight and composition of the PEO–PPO copolymers. With increasing hydrophilicity and molecular weight, this shielding effect has been reported to become more effective. In particular, surface-coating strategies of nanoparticles based on biodegradable polymers such as polylactides or polyglycolides have attracted increasing attention lately.<sup>400</sup> A major challenge in this field, however, remains the establishment of a correlation between the structure of particles and their specific interaction with blood components in order to allow for the design of targetable nanocarriers.

Mathet et al. investigated the effect of poloxamines with different molecular architectures on the inhibition of efflux transporters in multidrug-resistant (MDR) tumor cell lines. They proposed poloxamine T304 as both a promising drug carrier system and efflux transport inhibitor for the treatment of MDR tumors.<sup>439</sup> Aside from that, these studies report cytotoxic behavior for the majority of poloxamines investigated, raising the demand for further studies to evaluate their biocompatibility regarding future applications in a pharmaceutical context.

Although reverse poloxamines are commercially available PEO–PPO copolymers and exhibit potential usefulness for some

specialized applications,<sup>371,440</sup> to date their physicochemical properties have only been scarcely investigated<sup>429,435</sup> and will not be discussed within this review.

**4.1.2. PEO–PPO Diblock Copolymers.** Diblock copolymers composed of PEO and PPO represent another class of nonionic amphiphiles based on polyethers. Although diblock structures might be regarded as the most obvious block copolymer structure, these surfactants turn out to be rarely investigated in terms of bulk properties<sup>441</sup> and phase behavior in aqueous solution<sup>442,443</sup> compared to their triblock relatives (PEO-*b*-PPO-*b*-PEO). In contrast to the aforementioned bi- and multifunctional block structures, PEO–PPO diblock copolymers are monofunctional macromolecular alcohols. This characteristic results from the use of monofunctional low-molecular weight alcohols as initiators for the sequential anionic ring-opening polymerization of EO and PO in their synthesis.

Notably, PEO–PPO diblock copolymers have been introduced as valuable structural templates for the preparation of two-dimensional mesoporous silica films<sup>444</sup> and have been shown to act as size-specific solubilizing agents for carbon nanotubes, offering perspectives for improved fractionation strategies.<sup>445</sup>

Lately, increasing attention is dedicated to the behavior of PEO–PPO diblock copolymers at the air–water interface and properties of their polymeric monolayers. These studies, however, exclusively aim at a fundamental understanding of interfacial dynamics.<sup>446,447</sup>

A promising perspective for diblock copolymers based on PEO and PPO has been demonstrated by Firestone et al. for the stabilization of lipid bilayer vesicles (e.g., liposomes) for drug delivery purposes as an inexpensive alternative to PEG-lipid conjugates. In this case the hydrophobic PPO segments function as anchor units within the lipid bilayer, whereas the PEO chain projects into the aqueous surrounding, leading to an enhanced robustness of the vesicular structure. Interestingly, PEO-*b*-PPO copolymers exhibit superior performance compared to poloxamers in terms of their ability to sterically stabilize lipid-based nanocarriers.<sup>448</sup>

Although these diblock copolymers are also commercially available as their triblock analogs, so far a significantly smaller range of applications has been proposed and less effort has been put into elucidating their physicochemical properties. Moreover, to the best of our knowledge and in contrast to the other members of the PEO/PPO-based amphiphiles, no end-functionalized derivatives have been reported, which might be due to their monofunctional nature, limiting chemical modification.

The immense versatility and broad spectrum of applications of PEO/PPO block copolymers in various research areas have been illustrated in this section, focusing on trends and developments within the last 15 years. This class of polyethers undoubtedly represents one of the most widely used amphiphilic materials with paramount significance for both industry and academia. Especially their low cost and commercial availability in a wide range of molecular weights and compositions as well as different architectures (diblock, triblock, tetrabranched) combined with interesting physical and chemical properties warrants the development of further applications. Most of the research carried out in this area to date has been dedicated to PEO-*b*-PPO-*b*-PEO copolymers (poloxamers), while the other members have been neglected for a long time. Only lately increasing interest can be noticed for the properties of the less explored candidates.<sup>400,434,439</sup> In a pharmaceutical context, PEO/PPO copolymers exhibit particular usefulness concerning drug- and gene delivery strategies,<sup>409</sup> which will encourage future research

Table 4. List of Star-Shaped PEG Polymers Reported Since 2010

no. of arms	core molecule	arm attachment method	ref
3	1,3,5-tri(azobenzeneethynyl)-benzene	AF, sonogashira coupling	498
3/6/12	polyester dendrimer	AF, azide-alkyne click	456
4	dityrosine	AF, esterification	499
4	phthalocyanine	AF, cyclotetramerization of phthalonitrile	500
8	octakis(hydridodimethylsiloxy)-octasilsesquioxane	AF, hydrosilylation	501
9	nonaazido-dendrimer	AF, azide-alkyne click	457
14/21	beta-cyclodextrin	CF, AROP	451
Multi	hyperbranched PG	CF, AROP	450
Multi	PS-co-PDVB	AF, azide-alkyne click	493
Multi	hyperbranched polyacetal	AF, hydrazone formation	496
Multi	hyperbranched conjugated polymer	AF, hydrazone formation	494
Multi	hyperbranched conjugated polymer	AF, esterification	495
Multi	hyperbranched P( $\gamma$ -benzyl L-glutamate)	AF, amidation	497
Multi	PDVB	AF, cross-linking ATRP/FRP	474
Multi	P(EGDMA-co-DMAEMA)/P(EGDMA-co-disulfideDMA)	AF, cross-linking ATRP	475
Multi	P(dimethylammonium DEMA)	AF, cross-linking ATRP	476
Multi	P(EGDMA-co-DMAEMA-co-(perfluoroalkyl methacrylate))	AF, cross-linking ATRP	477
Multi	P(EGDMA)/P(PEGDMA), arms attached via acetal linker	AF, cross-linking ATRP	478
Multi	P(EGDMA)	AF, cross-linking eARTP	479
Multi	P(N,N'-methylene bis(acrylamide))	AF, cross-linking RDRP	480
Multi	P(EGDMA)/P(disulfideDMA)/P(ketalDMA)	AF, cross-linking RAFT	481
Multi	acid-labile bis-norbornene cross-linker	AF, cross-linking ROMP	482

Table 5. List of Novel Star-Shaped PEG Block Copolymers (Reported Since 2010)

no. of arms	core molecule	arm A	arm B	method	ref
3	TMP	PCL	PEG	CF, CROP	455
3	phenyl	PIB	PEG	AF, esterification	502
3/4	glycerol triacrylate/bisTMP tetraacrylate	P( $\omega$ -undecen-yl acrylate)	PEG	AF, Heck coupling	503
4	<sup>a</sup>	PCL	PEG	AF, azide-alkyne click	462
4	cystamine	poly( $\epsilon$ -benzyl-oxy-carbonyl-L-lysine)	PEG	AF, thiol-yne click	458
4	PETH	PCL	PEG-glycyrhethinic acid	AF, amidation	504
4	PETH	PLA	PEG	AF, esterification	505
4	porphyrine	PLA	PEG	AF, esterification	491
4	porphyrine	PCL	PEG	AF, esterification	483
4/6	PETH/diPETH	PCL	PEG	AF, esterification	484
7	beta cyclodextrin	PCL-co-DBTC	PEG	AF, esterification	485
A <sub>4</sub> B <sub>8</sub>	PETH	PCL-diol	PEG	AF, esterification	486
8	polyhedral oligomeric silsesquioxanes (POSS)	poly(L-lysine)	PEG	AF, amidation	487
16/32	PAMAM dendrimer	poly(L-lysine)	PEG	AF, esterification	488
Multi	PDVB	PS	PEG	AF, azide-alkyne click	459
Multi	PS-co-PDVB	PMMA	PEG	AF, Diels-Alder click	460
Multi	hbPEI	poly(L-lysine)	PEG	AF, urethane formation	489
Multi	hyperbranched Boltorn H40	<sup>b</sup>	PEG	AF, esterification	490
Multi	poly([4,4'-bioxepane]-7,7'-dione)	PCL	PEG	AF, cross-linking ROP	492

<sup>a</sup>2-(Benzyloxycarbonyl)-2-methylpropane-1,3-diyl bis[3-hydroxy-2-(hydroxymethyl)-2-methylpropanoate]. <sup>b</sup>Biodegradable photoluminescent polymer.

activities in this field. However, aside from numerous reports on chemical modification<sup>421,433</sup> of the commercially available standards, so far, no emphasis has been placed on exploring novel polymeric architectures based on PEO and PPO block-type structures by, for example, using other multifunctional initiators for the polymerization.

## 5. STAR-SHAPED AND HYPERBRANCHED POLY(ALKYLENE OXIDES)

In addition to the linear random and block copolymers discussed in the previous sections, star-shaped, hyperbranched and dendritic polyethers exhibit unique properties that distinguish

them from linear polymers, such as multiple functional end groups, a compact structure, low viscosities both in bulk and solution and a strongly reduced degree of crystallization in comparison to their linear counterparts. These properties are key to numerous advanced applications.

### 5.1.1. Star Polymers

Star-shaped polymers can be obtained by two fundamentally different synthetic strategies: the "core-first" (CF) and the "arm-first" (AF) approach. The "core-first" procedure utilizes a multifunctional initiating core-molecule to start the chain growth of the arms. Defined molecules or polymers with a predetermined number of initiating sites or multifunctional

Table 6. List of PEG Containing Miktoarm Star Copolymers (Reported Since 2010)

no. of arms	core	arm A	arm B	arm C	method	ref
AB <sub>2</sub>		PVFc	PEG		CF, AROP	452
AB <sub>2</sub>		PEG	PS/PtBA		AF, azide–alkyne click	461
AB <sub>2</sub>		PEG	PCL		AF, Diels–Alder click	462
AB <sub>2</sub>		PS/PtBA	PEG		AF, nitroxide radical coupling	461
AB <sub>3</sub>	cholic acid	PEG	PCL		AF, azide–alkyne click	463
AB <sub>3</sub>	PETH triazide	<sup>a</sup>	PEG		AF, azide–alkyne click	464
AB <sub>3</sub> /AB <sub>4</sub>	PETH triazide/PETH tetrazide	PE	PEG		AF, azide–alkyne click	465
A <sub>2</sub> B <sub>2</sub>	coupled propargyl (propyl glycol)	PS/PI	PEG		CF, AROP	453
A <sub>2</sub> B <sub>2</sub>	calixarene	PCL	PEG		AF, azide–alkyne click	466
A <sub>2</sub> B <sub>3</sub>	(HO) <sub>4</sub> / (Allyl) <sub>4</sub>	PEG	PCL/PS/PtBA		CF, AROP	454
A <sub>1</sub> <sub>4</sub> B <sub>7</sub>	beta cyclodextrin	PCL	PEG		AF, azide–alkyne click	467
A <sub>2</sub> B <sub>4</sub>	resorcinarene	PEG	PCL		AF, azide–alkyne click	468
ABC		PEG	PS	PCI	AF, azide–alkyne click	469
ABC	<sup>b</sup>	PS	PCL	PEG	AF, Diels–Alder click	470
ABC	beta cyclodextrin/adamantane (supramolecular)	PEG	PDMAE-MA	PMMA	AF, azide–alkyne click	471
ABC		PEG	PS	<sup>c</sup>	AF, azide–alkyne click	472
ABC		PS-pyrene	PEG	PMMA	AF, esterification	506
ABCDE		PEG	PCL	PS <sup>d</sup>	AF, azide–alkyne click	473
Multi	P(N,N'-Methylenebis(acrylamide))	PEG	PNIPAM		AF, cross-linking RDRP	480
Multi	hyperbranched Boltorn H30	PEG	PCI		AF, esterification	507

<sup>a</sup>Azobenzene-substituted methacrylate. <sup>b</sup>1-(Allyloxy)-3-azidopropan-2-yl (anthracen-9-ylmethyl) succinate. <sup>c</sup>Poly[6-(4-methoxy-azobenzene-4'-oxy)hexyl methacrylate]. <sup>d</sup>Arm D: PLA, Arm E: PAA.

Table 7. List of Star-Shaped PPO/PBO Polymers and Block Copolymers

no. of arms	core molecule	arm A	arm B	method	ref
6	p-tert-butyl-calix[6]arene	PPO	P(2,2-dimethyltri-methylene carbonate)	CF, AROP	508
Multi	hyperbranched polyglycerol	PPO		CF, AROP	509
Multi	hyperbranched polyglycerol	PPO	PEG	CF, AROP	510
3	TMP	PBO	PEG- <i>b</i> -PTMC- <i>b</i> -PVL	CF, AROP	146
4	1,2,4,5-benzenetetramethanol	PBO		CF, AROP	154

cross-linked or dendritic polymers are commonly employed for the core. In the “arm-first” process, end groups of living or functionalized, prefabricated polymer chains are either attached to a multifunctional core or connected via a (cross)linking procedure.

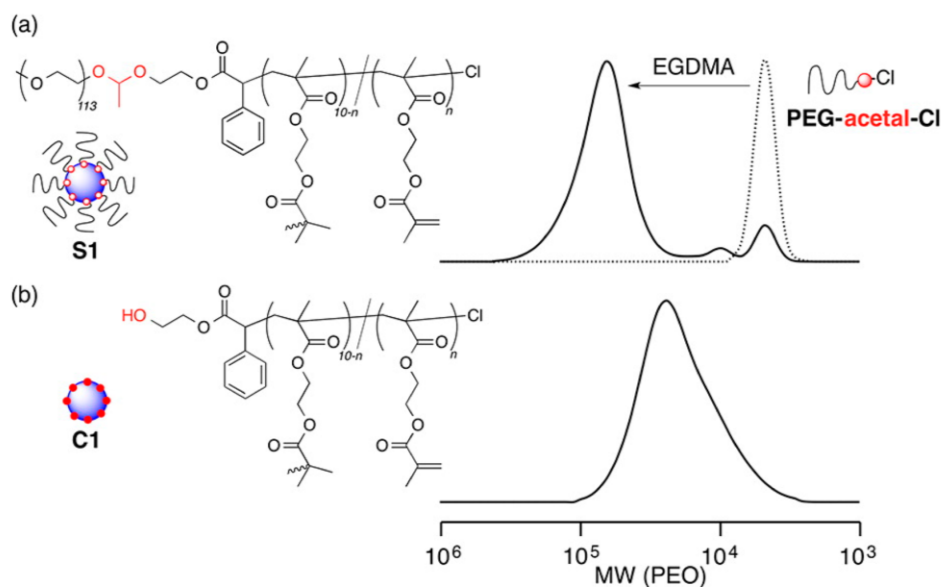
A very detailed and comprehensive review on star-shaped polymers with PEG arms was given by Lapienis in 2009.<sup>449</sup> Therefore, in the current review, mainly recent developments in the synthesis of PEG-based star polymers (Table 4), star-shaped block copolymers (Table 5), and miktoarm star copolymers (Table 6) since 2009 will be covered. Furthermore, star-shaped polymers containing PPO or PBO are summarized in Table 7. Star polymers based on commercially available, four- and eight-armed PEG stars are not considered.

In recent years only few core-first syntheses of PEG star polymers have been reported. Most of them rely on the anionic ring-opening polymerization (AROP) of ethylene oxide (EO). The harsh, strongly alkaline reaction conditions, however, limit the synthetic scope with respect to suitable core molecules and copolymers. Multiarm stars were obtained from hyperbranched polyglycerol and characterized in detail by MALDI-ToF MS.<sup>450</sup> Use of beta-cyclodextrin as an initiator gave access to 14-arm and 21-arm starPEG.<sup>451</sup> Tonhauser et al. introduced iron-containing, water-soluble AB<sub>2</sub> miktoarm stars via living anionic polymerization of vinylferrocene, followed by benzyl glycidyl ether termination, hydrogenerative deprotection and subsequent AROP of EO.<sup>452</sup> By Glaser coupling, Huang et al. obtained polystyrene and polyisoprene (PIP) macroinitiators with two hydroxyl

initiation sites at the center for the ensuing EO polymerization, resulting in amphiphilic A<sub>2</sub>B<sub>2</sub> miktoarm star structures.<sup>453</sup> Wang et al. used an orthofunctional core, having four hydroxyl and four allyl moieties, for the preparation of A<sub>4</sub>B<sub>4</sub> miktoarm star copolymers. In the first step, PEG arms were synthesized and end-capped. Subsequent thiol–ene click reaction converted the allyl groups into initiating sites for the polymerization of poly( $\epsilon$ -caprolactone), polystyrene, and poly(*tert*-butyl acrylate).<sup>454</sup> The only report on cationic polymerization of EO in this area deals with the synthesis of a three-arm star(PCL-*b*-PEG).<sup>455</sup>

Due to the demanding handling of ethylene oxide and the restrictions regarding functional group tolerance, the “arm-first” method and prefabricated PEG polymers are more commonly employed than the “core-first” approach.

Click couplings, especially the copper-catalyzed azide–alkyne cycloaddition, but also thiol–ene and Diels–Alder reactions, have been identified as a convenient method to attach prefabricated PEG chains.<sup>456–460</sup> Since click reactions take place under mild conditions and tolerate a great amount of functional groups, they have found to be particularly useful for the preparation of miktoarm stars.<sup>461–473</sup> Controlled radical polymerization techniques, such as ARTP and RAFT, have also been explored extensively as a synthetic tool for arm-first star polymer synthesis.<sup>474–481</sup> After end functionalizing PEG with a suitable initiator group, cross-linking polymerization of divinyl monomers leads to star architectures. In analogy, ring-opening metathesis polymerization was applied using bis-norbornene monomers.<sup>482</sup> Functional cross-linkers gave access to PEG stars



**Figure 13.** Cleavage of an acetal-linked multiarm star polymer with P(EGDMA) core and PEG arms. (Adapted with permission from Terashima, T.; Nishioka, S.; Koda, Y.; Takenaka, M.; Sawamoto, M. *J. Am. Chem. Soc.* **2014**, *136*, 10254.<sup>478</sup> Copyright 2014 American Chemical Society.)

**Table 8.** List of dendritic PEG and poly(alkylene glycol) derivatives

polymerization method	initiator	linear (macro)monomer unit	branching agent	ref
AB <sub>2</sub> polycondensation	-	-	methyl 3,5-bis[oligo(ethylene glycol)]benzoate	518
A <sub>2</sub> + B <sub>3</sub> polycondensation	-	PEG	1,3,5-benzenetricarbonyl trichloride	519
A <sub>2</sub> + B <sub>3</sub> polycondensation	castor oil	PEG + diisocyanate	tris(bisphenol A) monophosphate	520
A <sub>2</sub> + B <sub>3</sub> polycondensation	-	PPO	3-armed star-penta(4-N-methylbenzamide)	521
multistep anionic polymerization	TME/DPMK	EO	allyl chloride + OsO <sub>4</sub>	522
multistep anionic block copolymerization	PETH	EO	EEGE + deprotection	523
multistep azide-alkyne "click" coupling	-	PEG	Zn(II) tetraphenylporphyrin	524
anionic block copolymerization	PEG + CsOH	EO	glycidol	525
anionic block copolymerization	TME + DPMK	EO + PO	glycidol	526
random anionic copolymerization	calcium amide-alkoxide	EO	glycidol	68
random anionic copolymerization	TMP + K naphthalide	EO	glycidol	527,528
random anionic copolymerization	TMP + KO <sup>t</sup> Bu	PO	glycidol	529
random anionic copolymerization	TMP + KO <sup>t</sup> Bu	BO	glycidol	530
random cationic copolymerization	BF <sub>3</sub> ·OEt <sub>2</sub>	PO/BO	glycidol	531
proton-transfer polymerization	KH	PEG	glycidyl methacrylate	532

with acid-labile, redox-cleavable, cationic, and fluorinated core, respectively (see Figure 13).

A particular research focus is currently on the development of biodegradable materials. Numerous star-shaped poly( $\epsilon$ -caprolactone)s, polylactides and polyamides have been modified with PEG chains as a hydrophilic outer block to impart aqueous solubility. Mostly, the connection was established simply via esterification. These core-shell architectures are mostly designed for encapsulation and release of hydrophobic guest molecules with potential applications as drug carriers in mind.<sup>483–492</sup>

Several works capitalize on the combination of hyperbranched polymer cores and prefabricated PEG blocks to gain facile access to multiarm star polymers and star block polymers.<sup>459,460,489,490,493–497</sup> Cross-linked PS, polyethylenimine, polyesters, and specially designed conjugated polymers have been employed as core molecules.

PPO-containing star polymers are commercially used as building blocks for polyurethane soft foams. Reports on novel star-shaped architectures consisting of propylene oxide and higher alkylene oxides, however, are rare. In core first approaches, six-arm star[PPO-*b*-P(2,2-dimethyltrimethylene carbonate)] with *p*-*tert*-butyl-calix[6]arene core,<sup>508</sup> multiarm starPPO and star(PPO-*b*-PEG) with hyperbranched polyglycerol core have been introduced.<sup>509,510</sup> Using phosphonium catalysts, three-arm starPBO copolymers with polycarbonate and polyester blocks, and four-arm starPBO with 1,2,4,5-benzenetetramethanol core were synthesized by anionic ring-opening polymerization.<sup>146,154</sup>

### 5.1.2. Branched and Hyperbranched PEG, PPO, and PBO Derivatives

Since 1990, hyperbranched polymers have attracted steadily growing attention. They belong to the class of dendritic polymers, i.e., they are characterized by a tree-like branch-on-branch topology. They resemble dendrimers, which are well-

## Chemical Reviews

Review

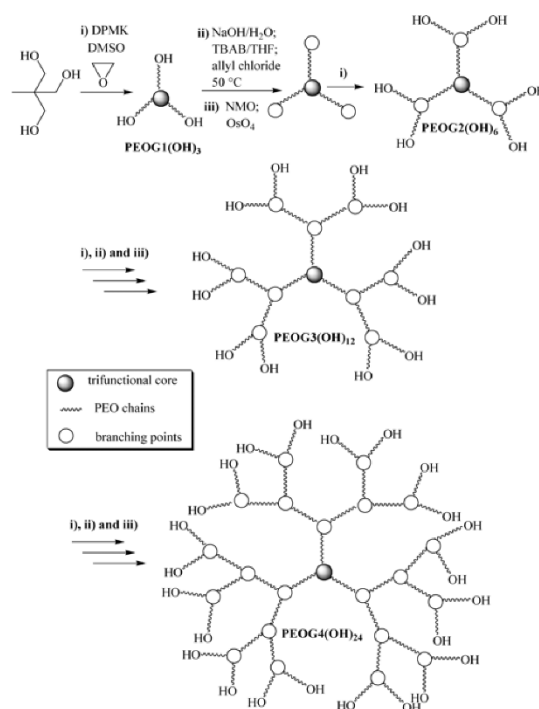
defined, perfectly branched macromolecules that have attracted vast attention because of their compact, globular structure in bulk and solution, and a very large number of end groups available for further modification. Since dendrimer preparation requires generation-wise construction in demanding multistep syntheses, hyperbranched polymers have been explored as less defined, but easily accessible materials. The perfectly branched, but tediously prepared dendrimer structure is traded off for a convenient polymerization that goes along with an irregular, statistical branching and a polydisperse molecular weight distribution.<sup>511</sup> In order to characterize the structure of a hyperbranched polymer, the degree of branching is a decisive variable which can assume values between zero (linear) and one (perfectly branched).<sup>512,513</sup>

Table 8 lists (hyper)branched polymers containing in-chain linear poly(alkylene glycol) segments. Reviews on hyperbranched polyethers in general have been provided by our group.<sup>514,515</sup> In addition to the advances in polyether chemistry, numerous branched poly(PEG acrylates) and poly(PEG methacrylates) have been synthesized in recent years using radical polymerization techniques, such as the so-called “Strathclyde methodology” and the controlled radical homopolymerization of PEG diacrylate.<sup>516,517</sup>

Hawker and co-workers reported the first oligo(ethylene glycol)-based hyperbranched polymers. They synthesized poly(ether esters), consisting of oligo(ethylene glycol) segments and aromatic branching points, via polycondensation of AB<sub>2</sub>-type methyl 3,5-bis[oligo(ethylene glycol)]benzoate macromonomers.<sup>518</sup> The authors observed an elevated Lithium ion conductivity compared to linear PEG. The amorphous structure due to the branched topology leads to an increased chain and Lithium ion mobility. Similar poly(ether esters) were prepared by Long et al. via polycondensation of telechelic PEG oligomers as an A<sub>2</sub>-type macromonomer with 1,3,5-benzenetricarbonyl trichloride as a B<sub>3</sub>-type comonomer.<sup>519</sup> Furthermore, the A<sub>2</sub> + B<sub>3</sub> polycondensation route was used by Patel to synthesize flame retardant, highly branched polyurethanes from PEG, diisocyanate, castor oil and tris(bisphenol A) mono phosphate.<sup>520</sup> Shibasaki et al. obtained poly(propylene oxide)-based A<sub>2</sub>B<sub>3</sub>-type hyperbranched copolymers using 3-armed 4-N-methylbenzamide pentamers as branching agents.<sup>521</sup>

Several dendrimer-like iterative approaches toward branch-on-branch PEG architectures have been reported, all of them pursuing divergent synthesis strategies. In an elegant work, Taton et al. introduced dendrimer-like PEG structures by sequential anionic EO polymerization, allyl chloride termination and subsequent bishydroxylation of the chain ends.<sup>522</sup> This leads to extremely well-defined, demanding PEG-dendrimer structures with very low polydispersity in the range of 1.08–1.15. The synthetic strategy is shown in Figure 14.

Inspired by this approach, Deffieux and coauthors obtained second and third generation dendritic PEG structures by iterative azide-alkyne click coupling of  $\alpha$ -azido-functional PEG with propargylated tetrakis(4-hydroxyphenyl) porphyrin zinc(II) and subsequent attachment of further porphyrin branching points via etherification.<sup>524</sup> Singlet oxygen production and photo stability were tested to investigate the first, second and third generation polymers' suitability for use as photo sensitizers and to establish differences between the generations. Dworak and Walach performed repeated anionic block copolymerization of EO and EEGE, an acetal-protected glycidol derivative, followed by acidic deprotection to generate multiple hydroxyl initiation sites.<sup>523</sup> Short PEG segments (DP = 10) resulted in amorphous materials

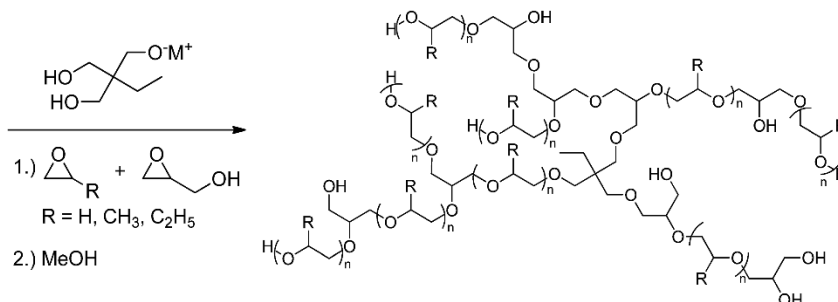


**Figure 14.** Synthetic strategy toward dendrimer-like PEG by Taton et al. (Adapted with permission from Feng, X.-S.; Taton, D.; Chaikof, E. L.; Gnanou, Y. *J. Am. Chem. Soc.* **2005**, *127*, 10956.<sup>522</sup> Copyright 2005 American Chemical Society.)

while longer linear chains led to crystallization. Branched polymers with long PEG segments (DP = 50) exhibited enhanced uptake and transport of a hydrophilic dye into a methylene chloride solution, compared to linear and star-shaped PEG.

Several promising synthetic works rely on the copolymerization of ethylene oxide with unprotected glycidol as a branching agent, resulting in hyperbranched structures with mere polyether scaffold. The glycidol molecule possesses both a polymerizable epoxide ring and an alcohol moiety that is capable of initiating the growth of another chain in an anionic or cationic polymerization. Therefore, glycidol is often described as a latent AB<sub>2</sub> monomer and represents a cyclic “inimer”.

Dworak and co-workers reported the repeated anionic block copolymerization of EO and G.<sup>525</sup> The hyperbranching polymerization of glycidol on a PEG macroinitiator, however, was found to produce significant amounts of hyperbranched polyglycerol homopolymer. In a multistep, one-pot reaction, Taton et al. also synthesized multiblock copolymers, consisting of linear PEG chains interrupted by oligomeric poly(propylene oxide)-*co*-polyglycerol or poly(allyl glycidyl ether)-*co*-polyglycerol branching segments.<sup>526</sup> In 2001, Tsvetanov and co-workers obtained high molecular weight random copolymers of EO and G by simultaneously bubbling EO through and adding G to a calcium amide-alkoxide initiator suspension.<sup>68</sup> This procedure only permitted limited glycidol incorporation up to 3% and resulted in very broad molecular weight distributions (PDIs ranging from 3 to 13). Under different reaction conditions, the controlled copolymerization of this comonomer combination

Scheme 43. Hyperbranched Poly(alkylene glycol)s by Copolymerization of Alkylene Oxides with Glycidol<sup>527,529,530</sup>

was realized by our group. We synthesized hyperbranched PEG with narrow molecular weight distributions, adjustable composition and tunable degree of branching by random anionic copolymerization in a batch process (see Scheme 43).<sup>527</sup> Contrary to the linear anionic polymerization, the resulting molar masses do not depend on the ratio of monomer to initiator. Limited control over the degree of polymerization was achieved by varying the polarity of the reaction media. The access to well-defined hyperbranched PEG copolymers of a wide range of molecular weights enabled a combined investigation by analytical ultracentrifugation, viscometry, translational diffusion measurements and size exclusion chromatography to establish the hydrodynamic properties of these structures. The obtained scaling relations imply an approximately globular, dendrimer-like structure. For the first time, sedimentation and diffusion analysis was employed to tackle the challenge of absolute molar mass characterization of hyperbranched polymers, revealing up to 25 times higher values compared to SEC data using linear standards. The characterization data demonstrate that the copolymerization of EO and glycidol can lead to molecular weights in the range of  $10^6$  g/mol.<sup>528</sup>

Hyperbranched poly(propylene oxide)-*co*-polyglycerol and poly(1,2-butylene oxide)-*co*-polyglycerol were synthesized in a similar manner, but without solvent, leading to moderately distributed, albeit low molecular weight polymers with thermoresponsive properties in aqueous solution.<sup>529,530</sup> By variation of the comonomer ratio, lower critical solution temperatures (LCST) and glass transition temperatures were tailored in a systematic manner. Monitoring the batch copolymerization of BO with G by in situ NMR spectroscopy, our group found a tapered structure with a hyperbranched PG-rich core and PBO arms. Hyperbranched poly(1,2-butylene oxide)-*co*-polyglycerol copolymers with elevated molecular weights up to  $M_w = 35\,000$  g mol<sup>-1</sup> could be prepared under slow monomer addition conditions.

Among other polyglycerol copolymers, Royappa et al. reported various cationic copolymerizations of glycidol with propylene oxide and 1,2-butylene oxide, respectively, using boron trifluoride etherate. However, no information regarding degree of branching and amount of comonomer incorporated was given.<sup>531</sup>

Using glycidyl methacrylate as a branching agent and Potassium hydride as a catalyst, Zhu et al. prepared long-chain hyperbranched PEG by proton-transfer copolymerization with telechelic PEG, albeit with broad molecular weight distribution. Polymer cytotoxicity and hydrolysis of the ester bonds under physiological conditions were studied.<sup>532</sup>

## 6. BIOMEDICAL APPLICATIONS

Recent advances in the functionalization of PEG open manifold perspectives for different biomedical applications. Particularly the area of bioconjugation has profited enormously from the availability of well-defined PEGs with tailored end groups. It is a safe bet that also the advanced structures presented in the preceding sections of this review will be increasingly explored in this field in the future and will permit to improve targeting of bioconjugated therapeutics considerably.

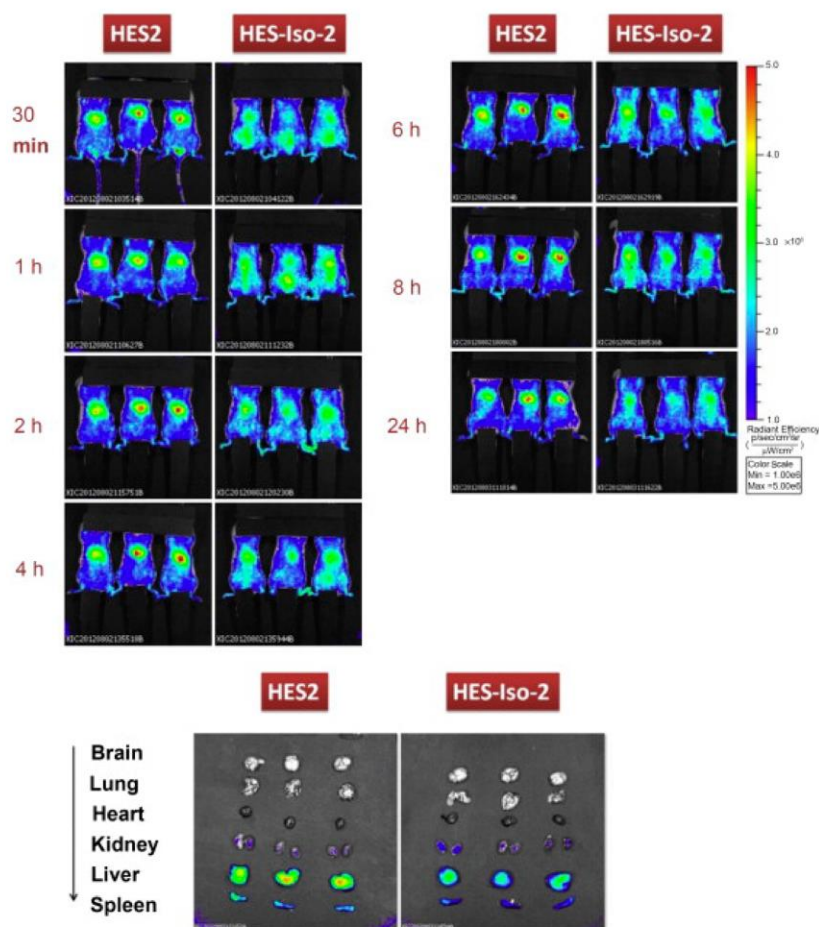
### 6.1. Bioconjugation and PEGylation

The covalent attachment of PEG to surfaces, drugs, or biomolecules is known as “PEGylation”. PEGylation is an extensively used strategy, designed to improve the biochemical and pharmacological properties of therapeutics, particularly their half-life in the bloodstream, but is also employed to improve other key properties, as described in the following.

PEGylation is very often associated with modification of proteins and peptides,<sup>533</sup> but a large variety of molecules and surfaces have been PEGylated. This includes lipids (for the preparation of stealth liposomes,<sup>534–536</sup> i.e., mPEG–1,2-distearoyl-*sn*-glycero-3-phosphoethanolamine (DSPE), folate–PEG–DSPE, the disulfide-linked cleavable lipopolymer, mPEG–dithiodipropionate (DTP)–DSPE,<sup>537</sup> and Gal-PEG-DSPA<sup>538</sup>), DNA, and oligonucleotides (PEGylated nucleotides show improved solubility, inferior degradation through nucleases, as well as cell membrane permeability<sup>539–541</sup>), nanoparticles,<sup>542,543</sup> affinity ligands (PEGylated affinity ligands are often used for purification of biopharmaceuticals<sup>544,545</sup>), cofactors (used in biotechnological processes<sup>546,547</sup>), and drugs. The PEGylation of drugs disparate to proteins and peptides provides enhanced water-solubility, higher stability to pH and temperature changes, which translates to better shelf half-life. PEGylation also preserves their activity, reduces antigenic activity and improves blood-circulation time.<sup>548,549</sup> Also saccharides have been PEGylated.<sup>550</sup>

Abuchowski and Davis et al. introduced the concept of protein conjugation via covalent bonding of PEG, the so-called PEGylation, performed usually by attaching methoxy-PEG (mPEG) containing one protein-reactive end group (Table 10, entry 1) in the late 1970s.<sup>551,552</sup> These PEGylated biohybrids show increased protein half-life times in vivo due to the hydrated polymer shell, exhibit reduced kidney clearance and increased blood circulation times due to steric shielding. Thereby the therapeutic effects are greatly improved, and in addition the respective proteins are protected against undesired proteolytic degradation.<sup>16,553–555</sup>





**Figure 15.** Biodistribution of unmodified (HES2) and PEGylated (HES-Iso-2) hydroxyethyl starch nanocapsules. A total of 1 mg of the capsules was injected intravenously, and the fluorescent intensity was recorded after 30 min, 1, 2, 4, 8, and 24 h. The mice were sacrificed after 24 h and different organs were tested for their fluorescence intensity. The accumulation in liver and spleen is much lower for the PEGylated nanocarriers compared to non-PEGylated nanocarriers.<sup>555</sup> Adapted with permission from Kang, B.; Okwieka, P.; Schottler, S.; Seifert, O.; Kontermann, R. E.; Pfizenmaier, K.; Musyanovych, A.; Meyer, R.; Diken, M.; Sahin, U.; Mailänder, V.; Wurm, F. R.; Landfester, K. *Biomaterials* **2015**, *49*, 125. Copyright 2015 American Chemical Society.

Moreover, such proteins are known to possess a “stealth” effect, preventing phagocytosis and fast elimination from the blood. Additionally, PEGylation reduces immune reactions because of lower opsonization rates and antibody binding. PEGylation also impedes degradation of the biomolecules by enzymes.<sup>556</sup> In addition, PEGylated proteins and nanocarriers (see Figure 15) impart pharmacological advantages such as improved solubility and passive targeting (enhanced permeability and retention (EPR) effect).<sup>557,558</sup>

These benefits of PEGylation are also used in liposome preparations to form so-called “stealth liposomes”.<sup>534,559</sup> PEGylation of liposomes leads to a more comfortable treatment of patients because of fewer injections are necessary due to increased plasma half-life.

From the chemistry side, various possibilities are published to target amino acid residues unselectively or rather selectively (see below).<sup>553,560–563</sup> Some specialized chemistry, however, allows the specific attachment of PEGs to a single amino acid residue. Additionally, physical properties can be tuned, such as photo-

temperature-, or pH-sensitivity. An excellent review by Gauthier and Klok gives an excellent overview on the state of the art in this field.<sup>564</sup>

Currently, 13 FDA-approved PEG-protein-conjugates and one PEG-aptamer conjugate are available on the market for the treatment of different diseases (Table 9).<sup>565,566</sup>

PEGylation has been extensively reviewed during the last decades with focus on: PEGylation in a general sense,<sup>14,555,561,567,568</sup> the influence of the molecular weight of PEG,<sup>569</sup> coupling chemistry,<sup>553,560–562,570,571</sup> site-specific PEGylation,<sup>572–574</sup> purification of PEGylated proteins,<sup>565,575</sup> in bioprocesses,<sup>576</sup> the cost-effectiveness,<sup>577</sup> drawbacks,<sup>535,578,579</sup> and pharmacokinetics.<sup>549,557,580</sup>

First generation PEGylation (see Scheme 44) refers to polymer conjugation toward the pendant  $\epsilon$ -amino groups in lysine residues. This method is feasible due to the high presence of lysines in proteins and their accessibility on their surface. However, several problems are accompanied: due to the possibility of multiple lysine residues per protein, several PEG

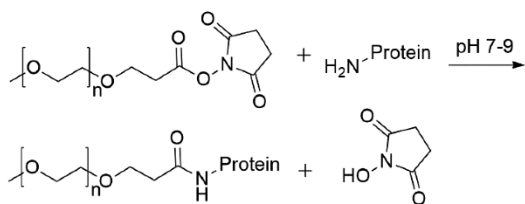
## Chemical Reviews

Table 9. Marketed PEGylated Drugs<sup>a</sup>

brand	active substance	approval	disease
Adagen	Adenosine deaminase	1990	severe combined immunodeficiency
Oncaspar	Asparaginase	1994	acute lymphoblastic leukemia
PEG-Intron	Interferon $\alpha$ -2b	2000	hepatitis C
Doxil/Caelyx	Doxorubicin	2001	cancer
Pegasys	Interferon $\alpha$ -2a	2001	hepatitis C
Neulasta	G-CSF	2002	chemotherapy-induced neutropenia
Somavert	GHA	2003	acromegaly
Macugen	Anti-VEGF aptamer	2004	wet age-related macular degeneration
Mircera	EPO	2007	renal anemia after chronic kidney disease
Cimzia	Antitumor necrosis factor Fab'	2009	Crohn's disease
Krystexxa	Uricase	2010	chronic gout refractory
Omontys	Erythropoiesis-stimulating agent	2012	renal anemia after chronic kidney disease
Movantik	Naloxol	2014	opioid-induced constipation in patients with chronic noncancer pain

<sup>a</sup>Modified from Klein, R.; Wurm, F. R. *Macromol. Rapid Commun.* 2015, 36, 1147. Copyright 2015 John Wiley and Sons.<sup>16,556,565</sup>

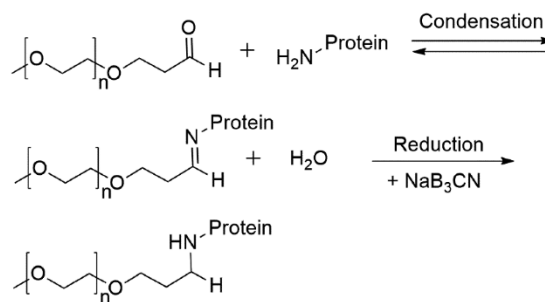
Scheme 44. General Reaction Scheme of a Typical First Generation PEGylation Reaction with mPEG-N-hydroxy-succinimide and the Amine Group of a Lysine Residue of the Protein



chains are attached in a statistical mixture, resulting in positional isomers and difficult reproducibility. If mPEG is contaminated with PEG diol,<sup>581</sup> proteins are partially cross-linked. Another undesired property regarding first generation PEGylation may be unstable bonds. Examples for first generation PEGylated products today in use are Adagen,<sup>582</sup> PEGIntron,<sup>583</sup> and Oncaspar pegaspargase.<sup>584</sup>

Second generation PEGylation (see Scheme 45) refers to the site-specific attachment of the polymer, often in combination with the use of PEGs with higher molecular weight (MW > 5000 g/mol)<sup>585</sup> or multifunctional and branched structures.<sup>586</sup> These conjugates have a higher uniformity and show improved pharmacodynamics and kinetics. Pegfilgrastim (Neulasta) is the best example on the market for N-terminal PEGylation (via mPEG-aldehyde conjugation at N-terminus, Table 10, entry 7) but also Pegasys, Doxil, and Somavert are in use today. A more detailed overview of PEGylated drugs is given in the recent review of Pfister et al.<sup>565</sup>

To enhance the selectivity of the bioconjugation site, several variations in the linking chemistry can be used and they have been reviewed elsewhere.<sup>562</sup> One example is blocking of the active site of the enzyme: this preserves enzymatic activity after

Scheme 45. General Reaction of a Typical Second Generation PEGylation Reaction with mPEG-propionaldehyde and the N-Terminal Amine Group of a Protein<sup>a</sup>

<sup>a</sup>The formed Schiff's base is subsequently reduced to form a stable amine linkage.

polymer conjugation. Caliceti et al. bound the enzyme to an active site inhibitor, immobilized on a resin during the PEGylation process. The authors PEGylated trypsin in the presence of benzamidine and thereby protected the active site of the enzyme.<sup>587</sup> In the same fashion, Salmaso et al. PEGylated avidin without conformational changes of the protein when biotin is present simultaneously. Full enzyme activity was kept when PEG chains >10 000 g/mol were attached.<sup>588</sup> Veronese and co-workers PEGylated uricase in the presence of uric acid as protecting agent, which resulted in retained enzymatic activity.<sup>589</sup> An interesting approach is to modify a free thiol group with a diselenide PEG reagent via thiol/diselenide exchange reaction (see Table 10, entry 25).<sup>590</sup> Undesired PEGylation sites of the protein can also be reversibly protected, i.e., with BOC, Fmoc, or maleic anhydride.<sup>591–593</sup>

The introduction of (non-natural) amino acids incorporated into proteins by specifically engineered bacterial strains is a commonly used strategy to afford site-specific and mono-PEGylation.<sup>563</sup> Cho et al. incorporated *p*-acetylphenylalanine in human growth hormone modifying the genetic code. The mono-PEGylated mutant was tested in clinical studies in rats and was shown to increase potency and reduce injection frequency.<sup>595</sup>

Another strategy is to use genetically modified proteins with all reactive amino acids replaced against nonreactive ones to limit the amount of reactive sites. The key challenge herein is to retain biological activity despite of changing the amino acid sequence of the protein. TNF- $\alpha$  was modified using this strategy and subsequently mono-PEGylated at the N-terminus (Table 10, entry 42).<sup>594</sup>

End-capping after peptide synthesis in solid phase peptide synthesis is another method to obtain mono-PEGylated products through ordinary amine-reactive groups at the PEG.<sup>562,596</sup> A summary of strategies for coupling of synthetic macromolecules to drugs, which are often based on proteins, are listed in Table 10, together with peculiarities, advantages and drawbacks of the respective methods.

The vast majority of papers published in the area of PEGylation rely on commercially available protein-reactive PEGs or mPEGs, which are modified at the terminus to generate a protein-reactive end group. Only few examples can be found, with the same research team (or a collaboration partner) synthesizing the protein-reactive PEG derivatives by AROP of EO and combining it with subsequent bioconjugation. In most reported cases, innovative polymer structures are synthesized

Table 10. Strategies for the PEGylation of Peptides/Proteins

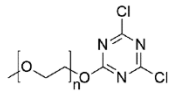
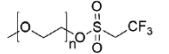
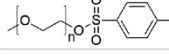
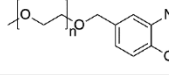
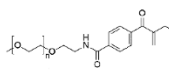
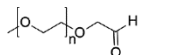
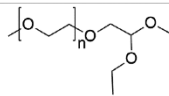
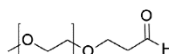
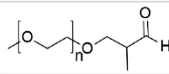
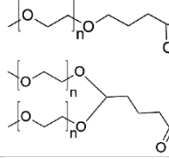
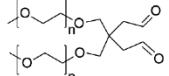
No.	PEG derivative	Amino acid target	Protein(s)	Polymer (Mn in g/mol)	Comments (analysis, activity data, degradable linkers, side reactions, requirements, limitations, reversibility)	Ref.
Alkylation						
		Amine groups <sup>a</sup>				
1		NH <sub>2</sub>	a) Bovine liver catalase b) Rabbit anti-human erythrocyte-IgG	mPEG-dichlorotriazine (200 (b), 1900 (a,b), 5000 (a,b))	Because of toxicity and low specificity no longer used. a) post-PEGylation activity kept up to 95%, low specificity, also reaction with Cys and Tyr. b) protein-activity correlated with PEG content (by <sup>14</sup> C labelling).	a) <sup>551</sup> b) <sup>597</sup>
2		NH <sub>2</sub>	Histones	mPEG-tresylate (5000)	Higher specificity towards amines, however, it leads to mixture of products (reaction with thiols)	<sup>598</sup>
3		NH <sub>2</sub>	Trypsin	mPEG-tosylate (1100, 2000, 5000)	Loss of activity (to 68%)	<sup>599</sup>
4		N-terminus (especially N-terminal Pro)	Lysozyme, RNase A, myoglobin, chymotrypsinogen, green fluorescent protein	PEG-o-aminophenol (5000)	Reacts also with thiols, active species generated <i>in situ</i> using potassium ferricyanide, fast reaction kinetics, low concentrations of the reagent possible	<sup>600</sup>
5		His <sub>6</sub> -tag	Domain antibody, IFN- $\alpha$ -2a	mPEG-monosulfone with conjugated double bond (20000)	Site-specific mono-PEGylation. One mPEG molecule reacts with two histidine residues. When using PEGylating agent in excess, di-PEGylation can be obtained at His <sub>6</sub> -tag, biological activity maintained	<sup>601</sup>
Reductive Alkylation						
6		NH <sub>2</sub>	a) CD4-IgG b) Horseradish peroxidase c) lysozyme	mPEG-acetaldehyde (2000 (c), 5000 (a,b))	a) neutral pH, binding ability to HIV-1 rgp-120 was reduced to 50%. b) modified protein soluble and active in organic solvents (in toluene 0.15 mg/ml) Intermediate Schiff base is reduced with NaBH <sub>4</sub> CN, disadvantage: water-sensitive, reduces disulfide bonds in proteins. c) Reduction step with iridium catalyst, advantage: reaction in aqueous medium, Drawback: no specificity to N-terminus, moderate yield	a) <sup>602</sup> b) <sup>603</sup> c) <sup>604</sup>
7		NH <sub>2</sub>	Lysozyme	mPEG-acetaldehyde diethylacetal (2000)	Aldehydes are susceptible to oxidation, PEG acetaldehyde diethylacetal generates aldehyde <i>in situ</i> , reaction at pH 6, reduction with NaBH <sub>4</sub> CN	<sup>605</sup>
8		N-terminus	a) Recombinant human G-CSF b) Epidermal growth factor	mPEG-propionaldehyde (2000 (b), 5000 (b), 6000 (a))	Slightly acidic pH a) 5 times less aggregation compared to acylation (amid-bond) due to preservation of charge at N-terminus (secondary amine) b) retained biologic activity in vitro (cell proliferation and signal transduction), prolonged circulation time in vivo	a) <sup>606</sup> b) <sup>607</sup>
9		N-terminus	IFN- $\beta$ -1a	mPEG-methylpropionaldehyde (20000)	Specific for N-terminal NH <sub>2</sub> , protein retained 50% of its activity, pharmacokinetic tests in vivo	<sup>608</sup>
10		N-terminus	a) IFN- $\beta$ -1b b) rhGF (recombinant human acid fibroblast growth factor) c) Recombinant human G-CSF	mPEG-butyraldehyde (6000 (c) 20000 (a,b), 30000 (a))	a) irreversible due to NaBH <sub>4</sub> CN reduction b) mono-PEGylation, in vitro less stimulation effect than native protein, better therapeutic efficacy due to enhanced stability	a) <sup>609</sup> b) <sup>610</sup> c) <sup>606</sup>
11		NH <sub>2</sub>	Lysozyme	mPEG-glutaldehyde (10000)	Mild reaction conditions, purification with cation exchange chromatography, 20 times increased biological activity	<sup>611</sup>

Table 10. continued

No.	PEG derivative	Amino acid target	Protein(s)	Polymer (Mn in g/mol)	Comments (analysis, activity data, degradable linkers, side reactions, requirements, limitations, reversibility)	Ref.
	Acylation	Amine groups				
12		NH <sub>2</sub>	Lysozyme	mPEG-succinimidyl carbonate (2000, 5000)	Coupling via carbonate group. Advantage over NHS (ester bond formed) is no hydrolysis because the formed carbamate bond formed is very stable against hydrolytic cleavage. No activity data is shown.	612
13		NH <sub>2</sub>	Lysozyme	mPEG-phenyl NHS carbonate (5000)	"rPEGylation" PEGylation reduces activity, stable at pH 7, but hydrolyses in plasma or at pH 8. Restores enzyme activity.	613
14		NH <sub>2</sub>	Bovine hemoglobin	mPEG-thiazolidine-2-thione (5000)	Stable in aqueous solutions at room temperature (long half-life (240 h) compared to succinimidyl linkers), no change in pI occurs which enables conjugation of pH sensitive proteins	614
15		NH <sub>2</sub>	Ribonuclease A Superoxide dismutase	mPEG-nitrophenylcarbonate (1900, 5000)	Stable at physiological pH, nitrophenyl moiety hinders easy and rapid reaction evaluation (measure unreacted amine groups) due to absorbance, slow reaction	615
16		NH <sub>2</sub>	$\alpha$ -7-Lysine Ribonuclease A	mPEG-2,4,5-trichlorophenylcarbonate (1900, 5000)	Unstable at pH $\geq$ 7	615
17		NH <sub>2</sub>	BSA, trypsin, superoxide dismutase, macroglobulins, lactoferrin	mPEG-carbonylimidazol (1M, 2000, 5000) PEG-diM (4000) PEG-tetraM (20000)	Plasma half-life time significantly increased	616
18		NH <sub>2</sub>	Interferon- $\alpha$ 2b	mPEG-carbonylimidazolium iodide (12000)	Much faster bioconjugation reaction (30 - 150 min) compared to mPEG-carbonylimidazol (10 h)	617
19		N-terminus	Various Peptides When residing at resin	mPEG-COOH (5000)	Coupling reaction via Steglich esterification, completion of reaction confirmed by ninhydrin test, mono-PEGylation (side chain amine groups are protected); work up: SEC (HPLC), no activity data shown Side-chain protecting groups are unaffected	618
20		NH <sub>2</sub>	Lysozyme	mPEG-benzotriazolyl carbonate (5000)	Synthesis of mPEG-benzotriazolyl carbonate without the use of toxic phosgene; PEG is reacted with di(1-benzotriazolyl) carbonate	619
21		NH <sub>2</sub>	Lysozyme	mPEG-dithiobenzyl- <i>p</i> -nitrophenyl carbonate (DTB-NPC, 2000, 5000, 12000)	"rPEGylation" 7 step synthesis. Upon bioconjugation, enzyme activity is completely lost. After reductive cleavage of the disulfide, almost fully restored activity. Partially decomposition in plasma (from SDS PAGE)	620
22		NH <sub>2</sub>	BSA	mPEG-squaric acid ester amide (2100, 5100)	High stability against hydrolysis (several days), allowing longer reaction times compared to PEG-NHS. Reaction tolerates hydroxyl groups, no activity data shown	621
	Disulfide formation	SH			Reversible, cleaved under reductive conditions	
23		SH	a) CWK <sub>18</sub> peptide b) Pseudomonas endotoxin A mutant c) $\alpha$ -hemolysin	mPEG-orthopyridyldisulfide (OPSS, 3000 (c), 5000 (a,b,c), 20000 (b))	Reaction under both acidic and basic conditions (pH 3-10) a) PEG-peptide DNA complex b) Cys residues introduced by genetic engineering as conjugation, protein folding not affected, half-life time is prolonged and toxin activity maintained c) transmembrane protein with single PEG chain attached within the channel lumen	a) <sup>622</sup> b) <sup>623</sup> c) <sup>624</sup>

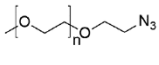
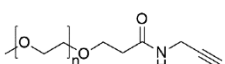
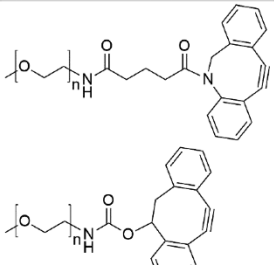
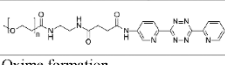
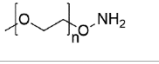
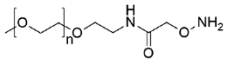
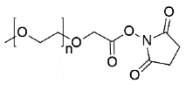
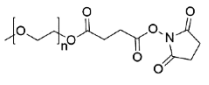
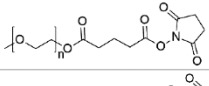
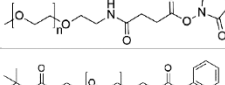
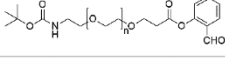
## Chemical Reviews

Review

Table 10. continued

No.	PEG derivative	Amino acid target	Protein(s)	Polymer (Mn in g/mol)	Comments (analysis, activity data, degradable linkers, side reactions, requirements, limitations, reversibility)	Ref.
24		SH	Papain	mPEG-parapyridyl disulfide (OPPS, 5000)	Characterization with MALDI MS, SDS-PAGE and HPLC, no activity data shown	625
25		SH	Recombinant human granulocyte colony-stimulating factor (rhG-CSF)	(mPEG-Se) <sub>2</sub> (20000)	Reactive diselenide which reacts with thiols under S-Se formation, lower PEGylation yield than PEG maleimide. Good <i>in vitro</i> performance, but <i>in vivo</i> less effective than OPSS-PEG	590
Thioether formation (Michael addition)/Thiol-ene-click						
26		SH	Salmon calcitonin	mPEG-(meth)acrylate (500)	Reaction after disulfide cleavage with water soluble organic phosphines, azamichael addition to Lys does not occur, activity retained	626
27		SH	a) Reduced RNase b) CWK <sub>18</sub> peptide	mPEG-vinyl sulfone (5000)	Thiol-selective. a) kinetics dependent on pH: at pH 7-9 fast reaction to SH (30-60 min), at pH 7 no reaction to NH <sub>2</sub> , at pH 9.3 slow reaction to NH <sub>2</sub> (100 h) b) conjugate to bind plasmid DNA	a) 627 b) 622
28		SH	Recombinant interleukin 2 (rIL-2)	mPEG-maleimide (6000)	Single-PEGylation at recombinant cysteine, full bioactivity kept. Faster reaction than with PEG-vinyl sulfone, but not stable in water, undergoes ring-opening. Conjugation under pH 5.5 possible	628
29		SH	IISA: anti-Iler2-Affibody, Laminin-beta-peptide	PEG-monosulfone (5000, 40000)	Exclusive formation of cysteine-conjugate at pH 6-10; treatment with hydride reduces ketone to prevent undesired deconjugation or exchange reactions	629
30		Cys-S-S-Cys	IFN- $\alpha$ -2b CD4-antibody fragment leptin	PEG-monosulfone with conjugated double bond (20000)	Site specific bisalkylation; tertiary structure kept despite of disulfide bridge cleavage due to efficient rebridging, high yield of PEGylated protein	630 568
31		SH	Glutathione	PEG-glycidyl ether (4500)	Protein/peptide coupling via radical thiol-ene addition, multiple peptides per polymer conjugated.	273
32		SH	Salmon calcitonin	mPEG-dibromomaleimide (5000)	Reaction at pH 6.2 in 15 minutes, disulfide rebridging and thereby maintaining tertiary structure, activity not investigated, increased serum half life time, increased resistance to enzymes	631
33		SH	Somatostatin	mPEG-dithiophenolmaleimide (5000)	<i>In situ</i> reduction of natural disulfides to obtain reactive thiols, fast reaction with PEG reagent (completed in 20 minutes), rebridging disulfides, fast reaction needed to avoid protein unfolding and aggregation, retention of biological activity	632
34		SH	Human serum albumin, maltose binding protein	mPEG-N-MSOPEEE-amide (5000)	Chemoselective to cysteine, disulfides are not modified, much more stable than NHS PEG under basic or acidic conditions, or in neutral pH and presence of glutathione	633
35		Allylated cysteine	Serine protease subtilisin	mPEG-allyl (200)	Aqueous cross metathesis. First step: Introducing allyl-sulfide at thiol group (4 °C, 20 min, >95% conversion), second step cross metathesis with Grubbs-Hoveyda 2nd generation catalyst in water/t-butanol mixture, 50% conversion	634

Table 10. continued

No.	PEG derivative	Amino acid target	Protein(s)	Polymer (Mn in g/mol)	Comments (analysis, activity data, degradable linkers, side reactions, requirements, limitations, reversibility)	Ref.
	Alkyne-azide click				Advantage: biorthogonal coupling easily possible; Disadvantage: toxicity of Cu-ions, Cu-mediated denaturation of proteins	
36		$\gamma$ -propargyl-L-glutamate	poly( $\gamma$ -propargyl-L-glutamate)	PEG-azide (750, 1000, 2000, 5000)	Incorporation of unnatural alkynated amino acid, grafting efficiencies up to 100%, CD spectroscopy data, no protein functionality tested, CuBr/PMDETA catalyst necessary	635
37		a) para-azido-Phe b) azido-homoalanine	a) Superoxide dismutase b) CalB	PEG-alkin (5000 (a,b), 20000 (a))	Incorporation of <i>p</i> -azido-phenylalanine in proteins with yeast, homogeneous PEGylation, bioactivity unchanged after PEGylation, copper catalyst needed	a) <sup>636</sup> b) <sup>637</sup>
38		N <sub>3</sub> -homoalanine	AHA-CalB, horseradish peroxidase	DIBAC-PEG or DIBAC-PEG (2000)	Copper-free ring strain promoted cycloaddition, 9 step synthesis of mPEG derivative, fast modification (3h at room temperature and pH 8.5), some PEG derivatives commercially available	638
Norbornene tetrazine ligation						
39		Pyrolysine norbornene	Human carbonic anhydrase II (HCA)	mPEG-tetrazine (1500)	Quantitative reaction (confirmed by SDS-PAGE), analysis with ESI-MS, no activity data shown	639
Oxime formation						
40		formylglycine	Chemokine (C-C motif) ligand 5 (CCL5)	mPEG-aminoxy (2000, 5000, 10000, 20000)	Introducing genetically encoded aldehyde via protein engineering on recombinant protein, no activity data shown	640
41		Thr-OH or Ser-OH at N-Terminus	IL-8, G-CSF, IL-1ra	mPEG-NH <sub>2</sub> (5000, 10000, 20000)	Introduction of N-terminal reactive carbonyl group next to Thr or Ser with sodium periodate. Reaction under acidic conditions (pH 4), attachment of single PEG chain, <i>in vitro</i> biological activity retained	641
Amide formation						
42		NH <sub>2</sub>	a) Bovine lactoferrin b) Peptides	mPEG-N-hydroxysuccinimide (NHS, 20000, 40000)	Most common PEG derivative for PEGylation, reaction and hydrolysis kinetics at different pH (pH 7 and pH 9), Drawback: hydrolysis of ester bond ( $t_{1/2} \geq 2$ h, reaction duration 2 h at pH 7.4, $t_{1/2} = 9$ min, reaction duration 10 min at pH 9)	642
43		NH <sub>2</sub> , His-NH	a) Uricase b) Recombinant human (rh) IL-10, rh IFN- $\alpha$ -2a	mPEG-succinimidyl succinate (5000 (a), 12000 (b))	Reversible PEGylation due to hydrolysis of ester a) at pH 9, less reactive than mPEG-succinimidyl carbonate b) at basic pH mixture of PEGylation at Lys or His; slightly acidic pH leads to modification just at His-NH.	a) <sup>643</sup> b) <sup>644</sup>
44		NH <sub>2</sub>	Recombinant human IL-2	mPEG-succinimidyl glutarate (5000)	Enhanced solubility, partial loss of <i>in vitro</i> bioactivity, decreased plasma clearance and increased antitumor potency in mice.	645
45		NH <sub>2</sub>	Bovine serum albumin (BSA), superoxide dismutase	mPEG succinimidyl succinamide (1900, 5000)	Specific binding properties were decreased for BSA and about constant for superoxide dismutase; plasma clearance time enhanced	646
46		NH <sub>2</sub> of N-Terminal Ser	RNase S, polypeptide PTH	<i>t</i> -Boc-N-amido-PEG-salicylaldehyde (850)	Site-specific PEGylation, via N,O-benzylidene acetal intermediate, no biological data shown	647

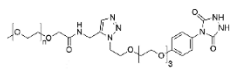
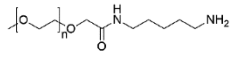
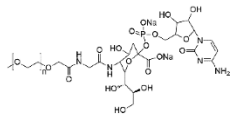
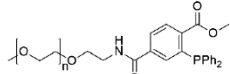
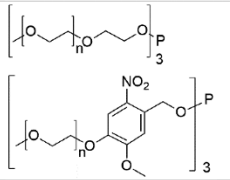
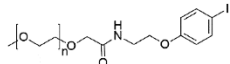
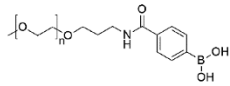
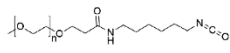
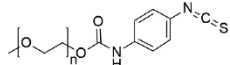
## Chemical Reviews

Review

Table 10. continued

No.	PEG derivative	Amino acid target	Protein(s)	Polymer (Mn in g/mol)	Comments (analysis, activity data, degradable linkers, side reactions, requirements, limitations, reversibility)	Ref.
47		C-terminal thioacid group	Ubiquitin	mPEG-sulfonazide (5000)	C-terminus of protein must be modified with thioacetic group via protein splicing, then site-selective amidation is possible	648
48		NH <sub>2</sub>	Urokinase, tissue-type plasminogen activator	mPEG-methylmalic anhydride (5000)	Reversible PEGylation, under physiological conditions the native protein is regenerated by hydrolysis, but slower blood clearance rate than the native protein	649
Noncovalent coupling						
49		His-tag	TRAIL (tumor necrosis factor-related apoptosis inducing ligand)	mPEG-Ni-nitrilotriacetic acid (NTA), mPEG-Ni-bisNTA (5000)	Reversible PEGylation without loss of bioactivity; for high-throughput testing of protein drugs in vivo	650
50		VEGF	Heparin binding growth factor (VEGF)	PEG-low molecular weight heparin (LMWH) (22000)	4-armPEG stars with low-molecular weight heparin bind reversibly to heparin-binding growth factor (VEGF) in hydrogel	651 652
51		streptavidin	CD133 Antibody	Ni <sub>12</sub> -PEG-biotin (10000)	Site-specific PEGylation due to PEG-biotin and CD133-AB-biotin interaction with streptavidin for recovery and purification of neural stem cells	653
52		$\beta$ -cyclodextrin	Concanavalin A (ConA)	mPEG-adamantyl (5100)	Use of linker molecule $\beta$ -cyclodextrin- $\alpha$ -mannopyranoside, the latter recognizes ConA and combines PEG-adamantyl with ConA for hydrogel preparation	654
Hydrazone formation						
53		N-terminal Ser or Thr	IFN- $\beta$ -1b	mPEG-hydrazide (550 (a), 2000 (a), 5000 (a,b), 12000 (a), 20000 (b))	a) synthesis of mPEG-hydrazide b) periodation of the N-terminus, specific monoPEGylated at N-terminus, higher PEGylation yield compared to PEG-aldehyde, detailed biological studies hydrazone linkage is stable at neutral pH but degradable at pH 2-4, suitable for reversible PEGylation. Reduction with NaCNBH <sub>3</sub> leads to stable conjugates.	a) 655 b) 656
54		SH	hTNF40 Fab	PEG-iodoacetamide (5000)	High selectivity of iodoacetamide towards $\alpha$ -thiol, slow reaction to thioether bond, reaction in the dark to avoid generation of I <sub>2</sub>	655 657
Diazo coupling						
55		a) Tyr b) His, Tyr	a) salmon calcitonin (sCT) b) IFN- $\alpha$ -2b, EPO $\beta$	mPEG-diazonium (2000 (a), 20000 (b), 30000 (b))	Advantage: can be introduced without change of charge or redox sensitivity (compared to Lys or Cys) Generation of diazonium from mPEG-4-aminobenzoic acid ester with <i>in situ</i> -generated HNO <sub>2</sub> by treatment with trifluoroacetic acid and NaNO <sub>2</sub> and a) reaction at pH 4.5, site-specific in the presence of His, Lys and N-terminal amines; sCT function not affected in vitro and in vivo b) reaction at pH 8-9, PEGylation ratio of His or Tyr residues can be varied with pH, fast reaction (3h, 70% conversion) with low excess of PEGylating agents needed, azo group is a chromophore, can be used for reaction control	a) 658 b) 659

Table 10. continued

No.	PEG derivative	Amino acid target	Protein(s)	Polymer (Mn in g/mol)	Comments (analysis, activity data, degradable linkers, side reactions, requirements, limitations, reversibility)	Ref.
Tyrosine click						
56		Tyr	Chymotrypsinogen, antibody trastuzumab	mPEG-4-phenyl-3H-1,2,4-triazoline-3,5(4H)-dione (PTAD, 5000)	Selective PEGylation via tyrosine click reaction, reaction in PBS or TRIS buffer possible, stable conjugates (more robust than conjugates with malcicide-PEG) to extremes of pI (24h at room temperature), temperature (1h at 120 °C) and plasma (1 week at 37°C)	660
Enzyme ligation						
57		Gln	Human II.-2 Salmon calcitonin Human growth factor	mPEG-alkylamine (550 (b), 3000 (a), 10000 (a,b), 12000 (a))	Site-specific PEGylation by enzyme transglutaminase at amino acid glutamine, without decreasing bioactivity b) addition of co-solvents leads to structural changes of protein and enzyme, and results in change of enzyme activity and thus in mono-PEGylation	a) <sup>661</sup> b) <sup>662</sup>
58		Ser/Thr	a) G-CSF, IFN-α2b b) Factor VIII	PEG-Sia-CMP (2000 (b), 5000 (b), 10000 (b), 20000 (a,b), 40000 (b))	Glyco-PEGylation; a) two step procedure, first attachment of Gal-NAc to Ser/Thr with GalNAc transferase, then coupling to PEGylated sialic acid with sialyl transferase, activity kept, homogeneous bioconjugate b) use of natural N-glycans; mono- or diPEGylated product obtained, decreased binding to tissue factor but other functions retained	a) <sup>663</sup> b) <sup>664</sup>
Staudinger Ligation						
59		Azido-homoalanine	Thrombomodulin	mPEG-triarylphosphine (5000)	Enzymatic activity unchanged, site-specific mono-PEGylation at C-terminus, reaction in PBS at neutral pH for 36 h	665
60		Azido-phenylalanine	Protein export protein SecB	mPEG-phosphite (2300, 6000)	Reaction possible in aqueous media as well as in cell lysate, mild reaction conditions, analysis of conjugation with SDS-PAGE. Conjugation with the bottom structure results in light cleavable "rPEGylation". After irradiation for 1-2 h, protein function is regained.	666
Palladium catalyzed ligation						
61		Homopropargyl-glycine	Ubiquitin	mPEG-iodoaryl (5000)	Reaction at 37 °C in water in 30 minutes (80% conversion). Usage of palladium catalyst in Sonogashira cross coupling, copper-free	667
62		p-iodo-phenylalanine	All-β-helix protein, subtilisin	mPEG-phenyl boronic acid (PBA, 2000)	1000 equivalents of PEG component necessary, 70% conversion in 2 h at 37 °C. Addition of external ligands is not required (K <sub>2</sub> PdCl <sub>4</sub> is used as catalyst, mPEG-PBA acts as ligand)	668
Urea/thiourea bond formation						
63		NH <sub>2</sub>	Sarcosine oxidase	mPEG-isocyanate (NCO, 5000)	PEGylation leads to complete activity loss, except if competitive inhibitor is added during reaction. NCO reacts with nucleophiles, which makes it rather unselective	669
64		NH <sub>2</sub>	HSA	mPEG-isothiocyanate (PIT, 3000, 5000)	Formation of stable thiourea bonds, secondary structure influenced slightly during PEGylation (from circular dichroism measurements).	670

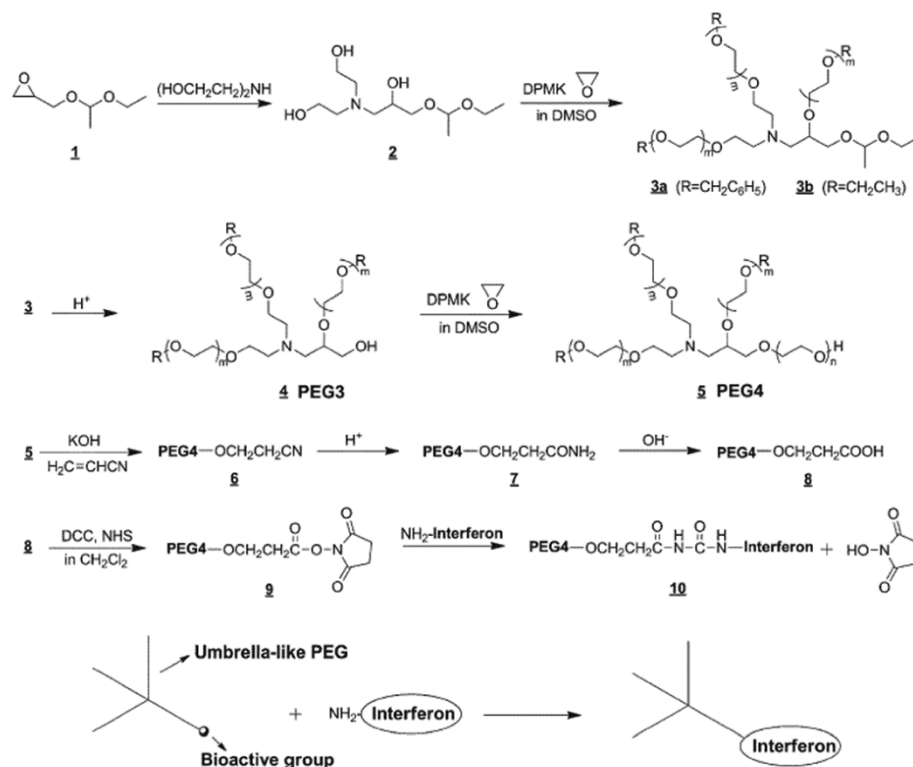
<sup>66</sup>The difference in reactivity of the ε-amine group and the N-terminal amine group ( $pK_a \approx 10$  and  $pK_a \approx 7.8$ , respectively) is reported to be responsible for selective bioconjugation to the N-terminus.<sup>671</sup>

and characterized by innovative synthetic strategies, albeit no actual application is presented.<sup>83,259,318,526,672</sup> Based on this critical remark, this section will only focus on PEG derivatives that are tailor-made by ROP of EO and actually used for bioconjugation. For PEGylation with commercially available, end-group functionalized PEGs please refer to reviews [see refs

14, 535, 549, 553, 555, 557, 560–562, 565, 567, 569–573, and 575–580] and textbooks.<sup>673</sup>

One of the first efforts to combine PEG synthesis with peptides was conducted by Joppich et al. in the 1970s.<sup>674</sup> The group functionalized ethoxy-PEG with an active ester and attached two PEG chains to each side of a tripeptide (Table 10, entry 43). More recently, a 4-arm PEG ("umbrella-like PEG") was





**Figure 16.** Synthesis of NHS-functionalized “umbrella-like” PEG and conjugation of PEG to IFN- $\alpha$ -2b.<sup>675</sup> Adapted with permission from Zhang, Y.; Wang, G.; Huang, J. *J. Polym. Sci. Part A: Polym. Chem.* **2010**, *48*, 5974. Copyright 2010 John Wiley and Sons.

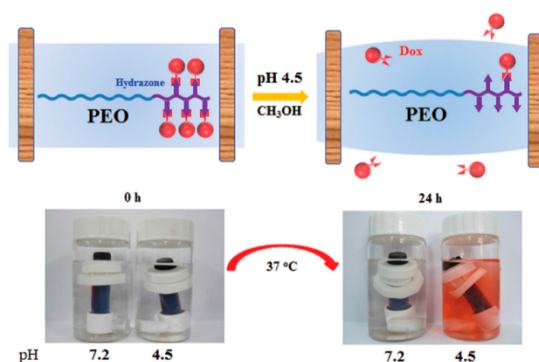
synthesized by the ROP of EO to obtain PEG with a single protein reactive group for conjugation with interferon  $\alpha$ -2b (see Figure 16 and Table 10, entry 42).<sup>675</sup>

Copolymerization of EO with AGE and subsequent transformation of allyl moieties into hydrazide groups was used for the conjugation of multiple molecules of doxorubicin (Dox) under formation of hydrazone bonds (Table 10, entry 53). The cytostatic Dox can be released at physiological pH, and *in vivo* pharmacokinetics revealed prolonged circulation time and higher accumulation in tumor tissue.<sup>333</sup>

Ikeda et al. introduced a new bioconjugation method for attaching PEG to primary amines which can be conducted under mild reaction conditions (Table 10, entry 11). Lysozyme, which was PEGylated with their method showed 20 times increased biological activity compared to conventional PEGylation with PEG-NHS (Table 10, entry 41).<sup>611</sup>

Smart polymeric prodrugs consisting of PEG with some few units of *N*-phenylmaleimide (*N*-PMI) was synthesized by AROP by Siddique et al. Doxorubicin and Methotrexate, two anticancer drugs were conjugated to the hydrazide units and released under acidic conditions (Figure 17).<sup>676</sup>

Kataoka and co-workers developed an oligodeoxynucleotide conjugated PEG which is pH-responsive due to an acetal moiety. The conjugate and linear poly(ethylenimine) formed polyion complexes which degrade at endosomal pH but are stable against deoxyribonuclease.<sup>677</sup> In another publication, the group describes pH-responsive micelles as siRNA delivery systems composed of lactosylated-PEG-siRNA and polyplex that can significantly silence the gene for firefly luciferase expression.<sup>678</sup>



**Figure 17.** Schematic diagram for Dox-release through a dialysis membrane and the photographic images for the release state in methanol of PEO-Dox at pH 7.2 and 4.5 at the incipient point and after 24 h, respectively.<sup>676</sup> Adapted with permission from Siddique, A.; Cho, Y.; Kim, Y.; Bahng, S. H.; Kim, S. W.; Lee, J. Y.; Kang, H. J.; Kim, S.; Bae, Y. H.; Kim, J. *Macromol. Chem. Phys.* **2015**, *216*, 265. Copyright 2015 John Wiley and Sons.

In many recent works, p(OEGMA)s are used for the chemical modifications of (bio)drugs. The advantage of using OEGMA derivatives instead of EO is evident (e.g., facile radical polymerization, nontoxic reagents, avoidance of handling EO); however, those materials will not be reviewed herein. Methacrylic polymers synthesized with controlled radical polymerization

having a mPEG-brush shape can be conjugated, i.e., to the N-terminus of a protein via reductive amination with an aldehyde functionality incorporated into the polymer.<sup>679–681</sup> The recent popularity of OEGMA-type monomers illustrates the strong motivation to introduce PEG segments or blocks into complex polymer architectures in general. Contemporary reviews summarize the use of controlled radical polymerization techniques for protein–polymer conjugation.<sup>562,682–685</sup>

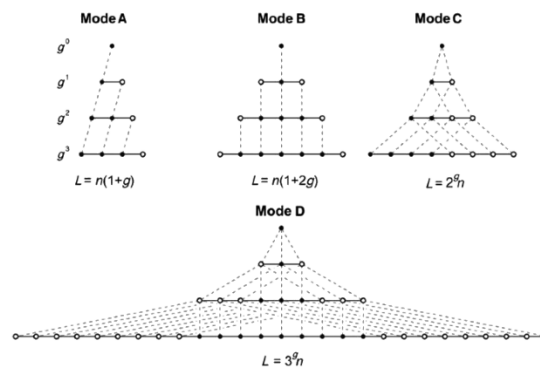
Although PEGylation is a highly valuable concept, the strategy, however, possesses several limitations, which are addressed in recent research: (i) linear PEG possesses only two end groups, of which one is used for conjugation and the second one is mostly a methoxy group; this restricts possibilities for further functionalization and the preparation of multiprotein conjugates; (ii) PEGylation often leads to a reduction or even loss of protein activity.<sup>555</sup> The development of strategies to overcome these limitations and allow access to protein–polymer conjugates with superior properties is a very topical and active field of research.

In this context, site-specific PEGylation approaches have to be mentioned as well as variations of the polymer's architecture, i.e., "branched" PEGs,<sup>554</sup> which influence the pharmacokinetics of the conjugate.<sup>555</sup> In contrast to linear PEGs, branched PEG or branched PEG-like polymers offer additional end groups, which provide enhanced opportunities for further functionalization, e.g., in order to introduce labels or targeting groups (see Figure 19). However, it has to be considered, that additional attachment of labels, etc. may alter the *in vivo* performance of the system.

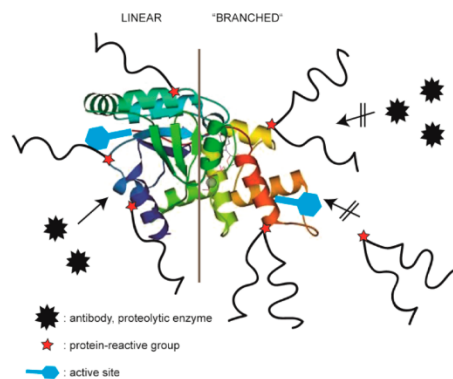
Another fact that affects the reproducibility and homogeneity of a PEGylation is the molecular weight dispersity of PEG. If obtained by established polymerization techniques, all polymers possess a molecular weight distribution based on the statistics of the respective method, even if typically rather narrow distributions with Poisson statistics are obtained by anionic ROP (see above). However, to circumvent the distribution statistics, one alternative is purification of one homologue of PEG (monodisperse PEG with  $\bar{D} = 1.0$ ) by chromatography.<sup>686–690</sup> Another approach is the synthesis of discrete PEGs via multistep reactions in an iterative manner similar to a dendrimer synthesis (Figure 18).<sup>686–690</sup> Usually, the commercially available products are restricted to molecular weights below 2000 g/mol, most often to oligomers (molecular weight up to 300 g/mol). There are different chemical approaches to obtain such discrete PEGs by iterative coupling of protected building blocks for elongation of the chain.<sup>686,691–695</sup>

The same method can be applied for the creation of monodisperse PEG-dendrons<sup>696</sup> or monodisperse cyclic PEG.<sup>697,698</sup>

In recent work, it has been demonstrated that midfunctional PEG with a lysine group located in the middle of the chain lead to improved circulation times compared to linear PEG chains (Table 10, entry 42 and Figure 19).<sup>569</sup> The polymers are attached via the lysine linker to the protein, by which a branching directly at the protein occurs. These midfunctional protein-reactive PEGs are typically called "branched PEGs". A commercial therapeutic for the treatment of hepatitis C ("PEGASYS, Roche", Table 9) is available that relies on this type of branched PEG coupled to interferon  $\alpha$ -2a.<sup>699</sup> A very recent, promising publication of Podobnik et al. shows the attachment of a comb-shaped poly(PEG) polymer (50 000 and 70 000 g/mol), which results in lower viscosity compared to attachment of linear PEGs and thereby enables administration of high doses of PEGylated drug.<sup>700</sup> The respective strategy for branched PEGylation is based on the controlled radical polymerization of appropriate



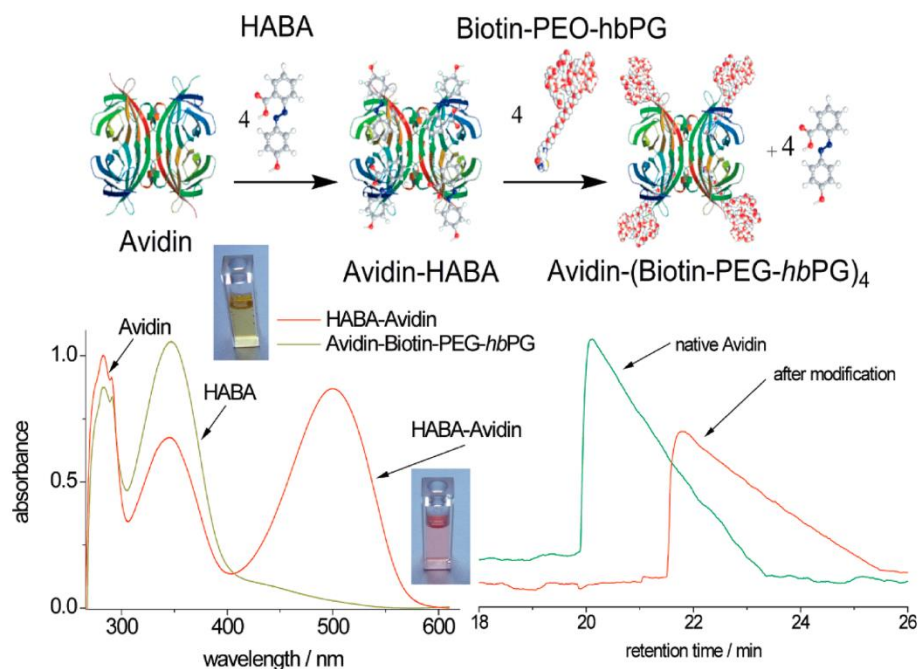
**Figure 18.** Discrete PEG (d-PEG) oligomer synthesis strategies: Each circle represents an EG unit.  $L$  is the oligomer length after  $g$  generations of coupling given a starting material of length  $n$ . Mode A: unidirectional iterative coupling; Mode B: bidirectional iterative coupling; Mode C: chain doubling; Mode D: chain tripling. Adapted with permission from French, A. C.; Thompson, A. L.; Davis, B. *Angew. Chem. Int. Ed.* **2009**, *48*, 1248–1252. Copyright 2009 John Wiley and Sons.<sup>686</sup>



**Figure 19.** Schematic representation of the benefits of PEGylation with linear or branched PEGylation reagents.

side-chain functionalized (meth)acrylate monomers. The most prominent example is poly(ethylene glycol)methacrylate, which can be polymerized, using a variety of controlled radical polymerization techniques and grafted to the protein of interest following both grafting onto and grafting from strategies.<sup>562,701,702</sup> Furthermore, a more recent report describes the synthesis of linear–hyperbranched  $\alpha,\omega_n$ -telechelic block copolymers, based on a linear PEG block and a biocompatible *hb*PG block, in which the polyfunctionality  $\omega_n$  can be adjusted by the degree of polymerization ( $DP_n$ ) of glycidol (OH-groups) and their noncovalent conjugation to the model protein avidin via biotinylated PEG-*b*-*hb*PGs (see Figure 20).<sup>258</sup>

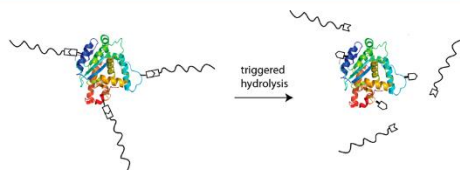
The synthetic pathway that was used in the last example for the preparation of the *hb*PGs offers unprecedented opportunities to tailor the architecture and functionality of nonlinear PEG alternatives. Another alternative to *hb*PGs is the use of linear polyether polyol derivatives with several pendant hydroxyl groups along the polyether backbone. The OH groups can be anchoring points for the inclusion of different functional groups to obtain mono- and heterobifunctional PEG derivatives for bioconjugation.<sup>318</sup>



**Figure 20.** Top: Noncovalent conjugation of avidin with 2-(4-hydroxyphenylazo)benzoic acid (HABA) and subsequent displacement by the biotinylated polymer. Bottom, left: UV/vis spectra of the HABA-avidin complex (red) and after addition of the biotinylated polymer (yellow, characteristic absorption of HABA). Bottom, right: HPLC diagram of native avidin and the noncovalently modified protein.<sup>258</sup> Adapted with permission from Wurm, F.; Klos, J.; Rader, H. J.; Frey, H. J. *Am. Chem. Soc.* **2009**, *131*, 7954. Copyright 2009 American Chemical Society.

Second generation PEGylation leads to site-specific modified proteins, which proved higher bioactivity compared to unselective methods.<sup>555</sup> However, this requires the accessibility of special amino acid residues such as lysine or, more specifically, free cysteine-residues which are natural abundant and require denaturation or genetic engineering to selectively introduce these residues.<sup>562,703,704</sup>

Another strategy to overcome the reduced activity but to retain the positive effects of PEGylation was presented more recently and is based on reversible, i.e., releasable polymer-protein conjugation (rPEGylation, Figure 21). PEGylation often leads to

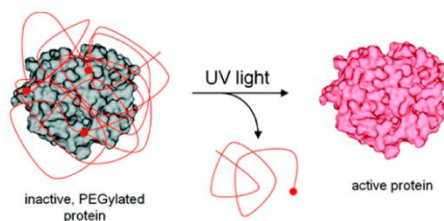


**Figure 21.** Schematic representation of reversible protein modification (rPEGylation).

decreased *in vitro* activity, but this disadvantage is counterbalanced by the increased half-life *in vivo*. To combine optimal activity with the other advantages of PEGylation, reversible PEGylation is of great interest.<sup>705</sup>

The conjugates gradually lose the surrounding polymer shield after administration, because the linkers are susceptible to hydrolysis in biological environment (usually pH-sensitive). Recently, several synthetic pathways to biodegradable functional PEGs have been developed and used for protein conjugation (see

Figure 22).<sup>706,707</sup> The synthesis of the releasable protein-reactive PEGs involves multistep organic syntheses with several



**Figure 22.** Multiple PEGylation results in inactive protein. The ortho-nitrobenzyl functionality is cleaved upon stimulation with UV light and the unPEGylated protein regains full activity.<sup>707</sup> Adapted with permission from Georgianna, W. E.; Lusic, H.; McIver, A. L.; Deiters, A. *Bioconjugate Chem.* **2010**, *21*, 1404. Copyright 2010 American Chemical Society.

purification steps, and especially end-group modifications that are rarely quantitative, making this strategy unattractive at present, but represent a worth-while challenge for the future (see section 6.2).

Current challenges of PEGylation have been discussed in the past decade in the literature.<sup>578,579</sup> At the end of this section it should be mentioned that other biocompatible polymers are currently discussed as alternatives to PEG.<sup>17,708,709</sup> For instance, PG-based protein-conjugates were investigated, and a pronounced influence of the polymer architecture on the activity of the conjugates was proven in this case.<sup>710</sup> In addition, controlled radical polymerization has been applied increasingly for the

synthesis of biocompatible polymers (poly(meth)acrylates and -acrylamides, such as poly(oligoethylene glycol)methacrylate or poly(*N*-isopropylacrylamide) (PNIPAM)) due to the synthetic advantages, such as a straightforward synthesis, controllable molecular weights and architectures as well as rather low polydispersities.<sup>711</sup> Other polymer structures under investigation as possible alternatives for PEGylation are dextran, HES, poly-*N*-(2-hydroxypropyl) methacrylamide (PHPMA), polyglutamic acid (PGAc), polyacetal (“fleximer”), poly(oxazoline)s, poly-(phosphoester)s, and polysialic acid.<sup>712–718</sup>

There is still room for creative design of PEG-derived structures or alternatives for bioconjugation. However, the dominance of PEG in already marketed pharmaceuticals and its well-understood *in vivo* performance (toxicity, clearance, etc.) makes it difficult to replace it for existing pharmaceutical applications. It is also evident that synthetic groups are able to synthesize and tailor various novel “PEG-like” polymers, but only very few are actually investigated for drug conjugation. Thus, especially on the short-term, no replacement for PEG will be available. Biodegradable or partly degradable polymers are currently discussed; however, also their biodegradation profile and the degradation products need to be investigated in detail. Another synthetically versatile class of polymers are poly(oxazolines)s, which convince in their straightforward and versatile synthesis by living cationic polymerization, but for these side-chain polyamides also long-term studies are required. On the other hand, also PEG has been shown to undergo unwanted degradation, oxidation and possibly even the induction of anti-PEG-antibodies. These disadvantages motivate research aiming at an improvement of PEG-based structures, but also motivate the search for alternatives in the future.<sup>719,720</sup>

## 6.2. Cleavable Polyethers

**6.2.1. Polyethers Bearing Cleavable Moieties.** Ethers are characterized by their high stability toward chemical or physical treatment. Consequently, low molecular weight ethers are typical solvents in organic chemistry. Also polyethers are very stable and flexible polymers. Under oxidative stress, however, PEG may be degraded by reactive oxygen species (ROS) due to  $\beta$ -scission, as observed in long-term *in vivo* experiments.<sup>719</sup> Degradation of PEG under application of voltage and air,<sup>721</sup> UV light,<sup>722</sup> ultrasonication,<sup>723</sup> and temperature<sup>722</sup> is described in literature. The degradation rate depends on whether the experiment is conducted in bulk or in aqueous solution and on pH values.<sup>724</sup>

If higher oxidative stability is required for certain applications, aromatic polyethers can be applied.<sup>725</sup> Aromatic polyethers are known to exhibit higher stability against oxidation compared to PEG, albeit at the expense of low solubility in water and a lack of biocompatibility.

If PEG-derivatives are expected to degrade, which may be beneficial for specific biomedical applications such as reversible PEGylation (see section 6.1), incorporation of cleavable moieties into the polymer backbone is necessary. PEG is regarded as the gold standard for polymer-drug conjugation in order to prevent proteolytic degradation of pharmaceutical agents (see section 6.1), as it is nontoxic, chemically inert, water-soluble and has a low immunogenicity.<sup>556</sup> However, PEG is not biodegradable restricting its use to a maximum molecular weight of 40 kDa, as higher molecular weight PEGs can accumulate in human tissue and may lead to storage diseases.<sup>560</sup> This molecular weight threshold represents the renal excretion limit of human kidneys exhibiting a natural boundary for the utility of PEG. However, the use of high molecular weight PEG is particularly favorable, as

blood circulation times of PEGylated drugs prolong with increasing molecular weights of PEG<sup>726</sup> making the design of in-chain cleavable PEG derivatives especially desirable.

A variety of different stimuli, such as potential pH-sensitivity, redox-response and enzymatic cleavage, have been employed to trigger the in-chain scission of the PEG backbone or the detachment of PEGs from the drug conjugate within a targeted tissue or cellular compartment.<sup>19</sup> More recently, light as a stimulus has likewise been exploited to induce cleavage of PEG-derived structures.<sup>727</sup> Table 11 compiles different cleavable

**Table 11. Compilation of Cleavable Groups, Synthesis Strategies and Respective Cleaving Stimuli Reported for PEGs and Derivatives<sup>b</sup>**

Cleavable Unit	Structure	Synthetic Approach	Degradation [a]	Ref.
Acetals		PEG coupling	pH < 7.4	728-731
Acetals/ ketals		Cleavable AROP initiator	pH < 7.4	621,732
Aconitic acid diamides		PEG coupling	pH < 7.4	733
Azo groups		PEG coupling	enzymatic	734,735
Carbonates		PEG coupling	basic hydrolysis	736,737
Carboxylates		PEG coupling	hydrolytic, enzymatic	518,738
Disulfides		PEG coupling	reductive	739,740
Hemiacetals		PEG oxidation	acidic or basic	741
Orthoesters		PEG coupling	pH < 7.4	742
Peptides		PEG coupling	enzymatic	743,744
Phosphoesters		PEG coupling	acidic or basic	745,746
Urethane		PEG coupling	(hydrolytic)	747,748
Vinyl ethers		Elimination functionalized PEG, PEG coupling	pH < 7.4 or light/ <sup>l</sup> O <sub>2</sub>	101
o-Nitro benzyl ethers		PEG coupling	light	727

<sup>a</sup>Conditions may vary for the same cleavable unit due to different adjacent moieties. <sup>b</sup>Adapted with permission from Dingels, C.; Frey, H. In *Hierarchical Macromolecular Structures: 60 Years after the Staudinger Nobel Prize II*; Percec, V., Ed.; Springer International Publishing: 2013; Vol. 262, p 167. Copyright 2013 Springer.<sup>19</sup>

moieties which have been used as linkers of PEG conjugates or have been incorporated into the polyether backbone as in-chain junctions. Additionally their synthesis strategies and the respective cleaving stimuli are attributed.

A comprehensive review article has recently been published focusing on strategies to incorporate cleavable moieties into PEG chains and PEG conjugates.<sup>19</sup>

It is obvious that PEG-based lipids bearing cleavable moieties have become increasingly attractive for the design of surface-modified liposomes (stealth liposomes) as drug delivery systems.<sup>749</sup> The presence of stimuli-cleavable linkers in the

## Chemical Reviews

## Review

lipid structures triggers shedding of liposomes within a particular cellular compartment or tissue to improve the efficacy of a liposomal formulation. Numerous reports on acid-labile PEG lipids based on cholesterol with cleavable junctions, such as aconitic acid, hydrazones, or vinyl ethers, have been established.<sup>536</sup>

Alternative polymers which combine the properties of PEG, such as high water-solubility, low protein adsorption with degradability may be polypeptides, polypeptoides (i.e., poly-sarcosin), HES, poly-*N*-(2-hydroxypropyl) methacrylamide (PHPMA), polyglutamic acid (PGA), polyacetal ("fleximer"), poly(oxazoline)s, poly(phosphoester)s, and polysialic acid.<sup>708,712–718</sup>

## 7. CONCLUSIONS

From this article summarizing the developments in the polymerization of alkylene oxides since 1995, with a particular focus on the most important and simple epoxide monomers EO, PO, and BO, some important trends emerge. On one hand, besides the long established anionic, coordination, and cationic polymerization techniques, with the anionic mechanism being the most widely used approach, several other alternative pathways to polyethers have been introduced in the last two decades. Phosphazenes, organocatalysts, *N*-heterocyclic carbenes, and monomer activation strategies using various catalysts, such as aluminum alkylates, permit homo- and copolymerization of alkylene oxides in a controlled or "living" manner to high molecular weights. Since highly basic initiators are avoided, these novel techniques have opened routes for the (co)polymerization of functional epoxide monomers or the use of initiators that are not applicable in the classic ionic polymerization (due to termination or chain transfer reactions or insufficient reactivity). In addition the direct combination of the ROP of epoxides with other ring-opening strategies has become possible, e.g., to generate poly(ether-*block*-ester) block copolymers.

For pharmaceutical and biomedical applications poly(ethylene glycol) and copolymers of EO and PO are key materials that are generally still prepared by classic alkali alkoxide initiated (living) anionic polymerization. Besides the excellent control over molecular weights and polydispersities this permits also the direct use in medical, cosmetic or pharmaceutical products since only nontoxic metal ions (Na and K) are used in the polymerization. For all new strategies, convenient removal of activating groups prior to use, regardless if metal or organo-catalyst, remains a challenge to date, and in some cases it is mandatory because of the toxicity of the respective structures. Thus, although the related technique dates back in the 1930s, classical oxanionic polymerization is still superior to all other controlled or living polymerization techniques for key biomedical applications.

PEG as a water-soluble and highly biocompatible material is the current gold standard for a vast variety of water-based applications, e.g. dispersion stabilization, food additives, and biomedical uses. As a linear polymer, however, only terminal functional groups are present. Several rather recent publications thus describe the incorporation of a large variety of additional functional groups into such polyethers, especially PEG, to generate multifunctional PEG (*mf*-PEG). Based on these approaches, new heterobifunctional and heteromultifunctional PEGs have become available, i.e., in-chain multifunctional PEGs. The approach of choice is the linear or branching copolymerization of EO with a minor fraction of functional comonomers to preserve the advantageous properties of PEG while adding

functional groups. The polymers have been characterized in detail with respect to their monomer sequence by newly developed in situ NMR techniques. Besides concurrent copolymerization, enormous progress in the efficient synthesis of graft, star, (hyper)branched, and dendritic polyethers can also be noted.

Particularly the field of PEGylation, i.e., the covalent attachment of PEG of different architecture to biomolecules, nanocarriers, surfaces, and drugs, is a growing field of research with great promise for the future. Due to the extraordinarily low protein-affinity of PEGylated materials, they are invisible to the immune system ("stealth effect") and allow for prolonged body-circulation times and low immunogenicity. In this area, also alternatives to the highly established PEG are currently discussed,<sup>645</sup> albeit other materials will have to undergo broad screening and testing for eventual approval.

With the high extent of control, choice of mechanisms, and the plethora of monomers available today, the ever growing toolbox of epoxide chemistry has broadened the options for the simple monomer structures EO, PO and BO enormously during the last two decades. Eventually, a "polyether universe" may be envisaged that in its vast structural variety parallels the immense structural options available for polymers based on vinyl monomers with a purely carbon-based backbone. With the new methods and reagents in hand, exploration of the materials properties of functional polyethers is at its height, and one can be excited about the developments still to come.

## AUTHOR INFORMATION

## Corresponding Author

\*E-mail: hfrey@uni-mainz.de.

## Notes

The authors declare no competing financial interest.

## Biographies



Jana Herzberger (first from the left) studied Chemistry at the Johannes Gutenberg-University Mainz (JGU), spending an exchange semester at the Polymer Science and Engineering Department, UMass-Amherst. She is currently working on her Ph.D. thesis, funded by the Fonds der Chemischen Industrie and the Excellence Initiative, "Materials Science in Mainz" (DFG/GSC 266). Her research focuses on the synthesis of multi-functional polyethylene glycols from novel epoxide building blocks.

Kerstin Niederer (second from the left) studied Biomedical Chemistry at the JGU Mainz, where she received her diploma degree in 2013. Currently, she is working on her Ph.D. thesis at the University of Mainz and the Seoul National University (South Korea) as a fellow of the

## Chemical Reviews

“International Research Training Group 1404”. Her research interests focus on multifunctional linear and hyperbranched polyethers.

Hannah Pohlitz (third from the left) studied Biomedical Chemistry at the JGU Mainz. Since 2012, she has been a Ph.D. student both in the research laboratories of Prof. Dr. Holger Frey at the Institute of Organic Chemistry and in the lab of Prof. Dr. Joachim Saloga at the Department of Dermatology in Mainz, focusing on encapsulation of allergens into degradable PEG-nanoparticles. Her research is supported by the Graduate School MAINZ, the Max Planck Graduate Center (MPGC), and the Gutenberg-Akademie.

Jan Seiwert (middle) studied chemistry at the JGU Mainz and is a Ph.D. student in the group of Prof. Holger Frey. His research interests are focused on the synthesis, characterization and application of novel hyperbranched poly(alkylene oxide)s obtained from the copolymerization of glycidol with EO, PO, and BO.

Matthias Worm (third from the right) studied Chemistry at the JGU Mainz and at the Seoul National University in South Korea. Since 2013 he is a Ph.D. student in the research group of Prof. Holger Frey focusing on the synthesis of cleavable polyether-based structures. His research is funded by the Max Planck Graduate Center and the Sonderforschungsbereich SFB 1066.

Dr. Frederik R. Wurm (born 1981; second from the right) studied Chemistry at the JGU Mainz (D) and received his PhD in 2009 under guidance of Holger Frey. After two year stay at EPFL (CH) as a Humboldt fellow, he joined the department of Katharina Landfester at MPIP and was selected as Junior Faculty Member of the Max Planck Graduate Center. In his interdisciplinary research poly(ether)s and poly(phosphoester)s are the major synthetic platforms to prepare novel materials for adhesives, tissue engineering, sensing, nanocarriers, and polymer therapeutics.

Prof. Holger Frey (born 1965; first from the right) became chaired professor for Organic and Macromolecular Chemistry at the JGU Mainz in 2003 after his studies at the University of Freiburg, Carnegie-Mellon University Pittsburgh (U.S.A.), and Ph.D. thesis at the University of Twente (NL). His research interests are centered in the areas of oxyanionic and carbanionic polymerization, polyester synthesis and hyperbranched polymers. The work of his group at JGU generally aims at the development of convenient routes for the preparation of polymers with special architecture, functionality, and materials properties. He has authored more than 300 peer-reviewed original works and reviews in this area.

## ACKNOWLEDGMENTS

The authors thank Dr. Zarbakhsh from BASF for valuable advice with respect to technical polyether synthesis, particularly in the area of DMC-catalysis.

## ABBREVIATIONS

AB	antibody
AdaGE	adamantyl glycidyl ether
AF	arm-first
AGE	allyl glycidyl ether
AHA	activator of 90 kDa heat shock protein
	ATPase homologue
AROP	anionic ring opening polymerization
ATRP	atom-transfer radical-polymerization
BMEGA	<i>N,N</i> -bis(2-methoxyethyl)glycidylamine
BMGA	<i>N</i> -benzyl- <i>N</i> -methylglycidylamine
BnGE	benzylglycidylether
BO	1,2-butylene oxide

BOC	<i>tert</i> -butyloxycarbonyl
BSA	bovine serum albumin
BuOH	<i>n</i> -butanol
CaLB	<i>Candida antarctica</i> lipase B
CCL5	chemokine (C–C motif) ligand 5
CD	cluster of differentiation
CF	core-first
CL	caprolactone
CMC	critical micelle concentration
CMT	critical micelle temperature
ConA	concanavalin A
CuAAC	azide–alkyne cycloaddition
CW-EPR	continuous wave electron paramagnetic resonance (CW-EPR) spectroscopy
	polycationic peptide
CWK	cystein
Cys	diels–Alder reaction
DA	diallyl glycidyl amine
DAGA	dibenzyl amino glycidol
DBAG	5,5-dibromomethyl-trimethylene carbonate
DBTC	<i>N,N</i> -di( <i>n</i> -butyl) glycidyl amine
DButGA	<i>N,N</i> -diethyl glycidyl amine
DEGA	<i>N,N</i> -diisopropyl ethanolamine glycidyl ether
DEGE	diethylaminoethyl methacrylate
DEMA	density functional theory
DFT	<i>N,N</i> -di( <i>n</i> -hexyl) glycidyl amine
DHexG	dibenzoazacyclooctyne
DIBAC	dibenzocyclooctyne
DIBC	decalactone
DL	dimethacrylate
DMA	2-(dimethylamino)ethyl methacrylate
DMAEMA	double metal cyanide
DMC	deoxyribonucleic acid
DNA	<i>N,N</i> -di( <i>n</i> -octyl) glycidyl amine
DOctGA	3,4-dihydroxyphenyl- <i>L</i> -alanin
DOPA	doxorubicin
DOX	degree of polymerization
DP	diphenylmethylpotassium
DPMK	degree of polymerization
DPn	diphenyl phosphate
DPP	differential scanning calorimetric
DSC	1,2-distearoyl- <i>sn</i> -glycero-3-phosphoethanol-amine
DSPE	dithiobenzyl
DTB	dithiodipropionate
DTP	dithiothreitol
DTT	electrochemical atom-transfer radical-polymerization
eATRP	epichlorohydrine
	ethoxy ethyl glycidyl ether
ECH	ethylene glycol dimethacrylat
EEGE	ethyl glycidyl ether
EGDMA	epidermal growth factor
EGE	ethylhexyl glycidyl ether
EGF	ethylene oxide
EHGE	epicyanohydrin
EO	erythropoietin
EPICH	enhanced permeability and retention
EPO	equivalents
EPR	electrospray ionization mass spectrometry
eq	ethoxy vinyl glycidyl ether
ESI-MS	fragment antigen-binding
EVGE	ferrocenyl glycidyl ether
Fab	
FcGE	

## Chemical Reviews

Review

FMOC	fluorenylmethoxycarbonyl	PAG	poly(alkylene glycol)
FRP	free radical polymerization	PAGE	polyacrylamide gel electrophoresis
G	glycidol	PB	poly butadiene
GA	glutaric anhydrid	PBO	poly(butylene oxide)
Gal	galactose	PBS	phosphate buffered saline
G-CSF	granulocyte-colony stimulating factor	PCL	polycaprolactone
GDDA	glycidyl-didodecylamine	Pd/C	palladium on carbon
Gln	glutamine	PDI	poly dispersity index
GM	<i>N</i> -glycidylmorpholine	PDVB	polydivinylbenzene
GME	glycidyl methyl ether	PECH	poly epichlorohydrin
HABA	2-(4-hydroxyphenylazo)benzoic acid	PEEGE	poly ethoxy ethyl glycidyl ether
hb	hyperbranched	PEG	poly(ethylene glycol)
hbPG	hyperbranched polyglycerol	PEGDMA	poly(ethylene glycol) dimethacrylate
HCA	human carbonic anhydrase	PEI	polyethylenimine
Her2	human epidermal growth factor receptor 2	PEO	poly(ethylene oxide)
HES	hydroxy ethyl starch	PETH	pentaerythritol
H–H	head to head	pFA	paraformaldehyd
HL	hexalactone	PG	polyglycerol
HLB	hydrophilic–lipophilic-balance	PGAc	polyglutamic acid
HPLC	high-performance liquid chromatography	PGA	poly glycidyl amine
HSA	human serum albumin	PHO	poly(hexene oxide)
H-T	head to tail	PHPMA	poly- <i>N</i> -(2-hydroxypropyl) methacrylamid
hTNF	human tumor necrosis factors	PI	polyimide
IFN	interferon	PIP	poly isoprene
IG	inverse gated	PIB	polyisobutylene
IGG	1,2-diisopropyl glycidyl ether	PIL	poly(ionic liquid)
IgG	immunoglobulin G	PIT	isothiocyanate
IL	interleukin	pK <sub>a</sub>	acid dissociation constant
IM	carbonylimidazol	PLA	polylactic acid
KOH	potassium hydroxide	PMI	phenylmaleimide
LA	lactide acid	PMMA	poly(methyl methacrylate)
LCST	lower critical solution temperature	PNIPAM	poly( <i>N</i> -isopropylacrylamide)
linPG	linear polyglycerol	PO	propylene oxide
LITFSI	bis(trifluoromethanesulfonyl)imide	POS	polyhedral oligomeric silsesquioxanes
LMWH	low molecular weight heparin	ppm	parts per million
Lys	lysine	PPO	poly(propylene oxide)
MA	maleic anhydrid	PPSS	parapyridyldisulfide
MALDI-ToF MS	matrix assisted laser desorption/ionization	PS	polystyrene
MDR	multidrug resistant	PTAD	4-phenyl-3H-1,2,4-triazoline-3,5(4H)-dione
<i>mf</i> -PEG	multifunctional polyethyleneglycol	PtBA	poly( <i>tert</i> -butyl acrylate)
Mn	number-average molecular weight	PTH	parathyroid hormone
MPa	megapascal	PTMC	poly(trimethylene carbonate)
mPEG	methoxy-PEG	PU	polyurethane
MSOPEEE	<i>N</i> -(2-(2-(2-(4-(5-(methylsulfonyl)-1,3,4-oxadiazolyl)phenoxy)ethoxy)ethoxy)-ethoxy)ethyl)	PVFc	polyvinylferrocene
MW	molecular weight	PVL	poly( $\delta$ -valerolactone)
MWD	molecular weight distribution	r	reactivity ratio
NAC	<i>N</i> -acetylcysteine	RAFT	reversible addition–fragmentation chain transfer
NCO	isocyanate	RDRP	reversible-deactivation radical polymerization
NHC	<i>N</i> -heterocyclic carbenes	rhaFGF	recombinant human acid fibroblast growth factor
NHO	<i>N</i> -heterocyclic olefins	rhG-CSF	recombinant human granulocyte colony-stimulating factor
NHS	<i>N</i> -hydroxysuccinimide	rIL-2	recombinant interleukin 2
NL	nonalactone	RNase	ribonuclease
NMR	nuclear magnetic resonance	ROMP	ring opening metathesis polymerization
NPC	<i>p</i> -nitrophenyl carbonate	ROP	ring opening polymerization
NTA	nitrilotriacetic acid	SA	succinic anhydrid
OEGMA	oligoethylene glycol methacrylate	sCT	salmon calcitonin
OPSS	ortopyridyldisulfide	SDS	sodium dodecyl sulfate
P2VP	poly 2 vinyl pyridene	SEC	size-exclusion chromatography
PA	phthalic anhydrid	SecB	cystosolic export factor
PAA	poly acrylic acid	Ser	serine

Sia	sialyl
siRNA	small interfering ribonucleic acid
tBuGE	tert-butylglycidylether
t-Bu-P4	1-tert-butyl-4,4,4-tris(dimethylamino)-2,2-bis[tris(dimethylamino)-phosphoranylidenamino]-2 $\Lambda$ 5,4 $\Lambda$ 5-catenadi(phosphazene)
Tc	cloud point
Tg	glass transition temperature
THF	tetrahydrofuran
Thr	threonine
TMC	trimethylene carbonate
TME	trimethylolethane
TMP	trimethylolpropane
TNF- $\alpha$	tumor necrosis factor alpha
TON	turn over number
TRAIL	tumor necrosis factor-related apoptosis inducing ligand
T-T	tail to tail
Tyr	tyrosin
UV/vis	ultraviolet–visible spectroscopy
VEGF	heparin binding growth factor
VfcGE	vinyl ferrocenyl glycidyl ether

## REFERENCES

- (1) Polymer Science: A Comprehensive Reference. *Ring-Opening Polymerization and Special Polymerization Processes*; Penczek, S.; Grubbs, R. H., Eds.; Elsevier: Amsterdam, 2012; Vol. 4.
- (2) Carlotti, S. and Peruch, F. *Cyclic Monomers: Epoxides, Lactide, Lactones, Lactams, Cyclic Silicon-Containing Monomers, Cyclic Carbonates, and Others. Anionic Polymerization: Principles, Practice, Strength, Consequences and Applications*; Hadjichristidis, N., Hiraio, A., Eds.; Springer, 2015; pp 191–306.
- (3) Dudev, T.; Lim, C. Ring Strain Energies from Ab Initio Calculations. *J. Am. Chem. Soc.* **1998**, *120*, 4450–4458.
- (4) Wurtz, C. A. Mémoire Sur L'oxyde D'éthylène Et Les Alcools Polyéthyléniques. *Ann. Chim. Phys.* **1863**, *69*, 317–354.
- (5) Staudinger, H.; Schweitzer, O. Über Hochpolymere Verbindungen, 20. Mitteil.: Über Die Poly-Äthylenoxyde. *Ber. Dtsch. Chem. Ges. B* **1929**, *62*, 2395–2405.
- (6) Flory, P. J. Molecular Size Distribution in Ethylene Oxide Polymers. *J. Am. Chem. Soc.* **1940**, *62*, 1561–1565.
- (7) Kosswig, K. *Ullmann's Encyclopedia of Industrial Chemistry*; Wiley-VCH Verlag GmbH & Co. KGaA: Berlin, 2000.
- (8) Robson, R. J.; Dennis, E. A. The Size, Shape, and Hydration of Nonionic Surfactant Micelles. Triton X-100. *J. Phys. Chem.* **1977**, *81*, 1075–1078.
- (9) Hargreaves, A. E.; Hargreaves, T. *Chemical Formulation: An Overview of Surfactant-Based Preparations Used in Everyday Life*; Royal Society of Chemistry: London, 2003; Vol. 32.
- (10) Dingels, C.; Schömer, M.; Frey, H. Die vielen Gesichter des Poly(ethylenglykols). *Chem. Unserer Zeit* **2011**, *45*, 338–349.
- (11) Fruijtjer-Pöllöth, C. Safety Assessment on Polyethylene Glycols (PEGs) and Their Derivatives as Used in Cosmetic Products. *Toxicology* **2005**, *214*, 1–38.
- (12) Klein, R.; Wurm, F. R. Aliphatic Polyethers: Classical Polymers for the 21st Century. *Macromol. Rapid Commun.* **2015**, *36*, 1147–1165.
- (13) Kjellander, R.; Florin, E. Water Structure and Changes in Thermal Stability of the System Poly(ethylene oxide)–Water. *J. Chem. Soc., Faraday Trans. 1* **1981**, *77*, 2053–2077.
- (14) Veronese, F. M.; Pasut, G. PEGylation, Successful Approach to Drug Delivery. *Drug Discovery Today* **2005**, *10*, 1451–1458.
- (15) Lasic, D. D.; Needham, D. The "Stealth" Liposome: A Prototypical Biomaterial. *Chem. Rev.* **1995**, *95*, 2601–2628.
- (16) Knop, K.; Hoogenboom, R.; Fischer, D.; Schubert, U. S. Poly(ethylene glycol) in Drug Delivery: Pros and Cons as Well as Potential Alternatives. *Angew. Chem., Int. Ed.* **2010**, *49*, 6288–6308.
- (17) Pelegri-O'Day, E. M.; Lin, E. W.; Maynard, H. D. Therapeutic Protein-Polymer Conjugates: Advancing Beyond PEGylation. *J. Am. Chem. Soc.* **2014**, *136*, 14323–14332.
- (18) Dimitrov, I.; Tsvetanov, C. B. in *Polymer Science: A Comprehensive Reference*; Vol. 4, pp 551–569; Penczek, S.; Grubbs, R. H., Eds.; Matyjaszewski, K., Möller, M. Series Eds.; Elsevier: Amsterdam, 2012.
- (19) Dingels, C.; Frey, H. In *Hierarchical Macromolecular Structures: 60 Years after the Staudinger Nobel Prize II*; 1st ed.; Percec, V., Ed.; Springer International Publishing: 2013; Vol. 262, 167–190.
- (20) Dai, S.; Tam, K. C. Isothermal Titration Calorimetric Studies on the Temperature Dependence of Binding Interactions between Poly(propylene glycol)s and Sodium Dodecyl Sulfate. *Langmuir* **2004**, *20*, 2177–2183.
- (21) Gagnon, S. D. In *Encyclopedia of Polymer Science and Technology*; John Wiley & Sons, Inc.: 2002.
- (22) Chattopadhyay, D.; Raju, K. Structural Engineering of Polyurethane Coatings for High Performance Applications. *Prog. Polym. Sci.* **2007**, *32*, 352–418.
- (23) Arnold, C. *CHEmanager* **2013**, 19–20.
- (24) Schillén, K.; Claesson, P. M.; Malmsten, M.; Linse, P.; Booth, C. Properties of Poly(ethylene oxide)–Poly(butylene oxide) Diblock Copolymers at the Interface between Hydrophobic Surfaces and Water. *J. Phys. Chem. B* **1997**, *101*, 4238–4252.
- (25) Deffieux, A.; Carlotti, S.; Barrère, A. in *Polymer Science: A Comprehensive Reference*; Vol. 4, pp 117–140; Penczek, S.; Grubbs, R. H., Eds.; Matyjaszewski, K., Möller, M. Series Eds.; Elsevier: Amsterdam, 2012.
- (26) Deffieux, A.; Boileau, S. Anionic Polymerization of Ethylene Oxide with Cryptates as Counterions: I. *Polymer* **1977**, *18*, 1047–1050.
- (27) Stolarzewicz, A.; Neugebauer, D.; Grobelny, Z. Influence of the Crown Ether Concentration and the Addition of Tert-Butyl Alcohol on Anionic Polymerization of (Butoxymethyl)Oxirane Initiated by Potassium Tert-Butoxide. *Macromol. Chem. Phys.* **1995**, *196*, 1295–1300.
- (28) Stolarzewicz, A.; Neugebauer, D.; Grobelny, J. Potassium Hydride — the New Initiator for Anionic Polymerization of Oxiranes. *Macromol. Rapid Commun.* **1996**, *17*, 787–793.
- (29) Tsvetanov, C.; Dimitrov, I.; Doytcheva, M.; Petrova, E.; Dotcheva, D.; Stamenova, R. In *Applications of Anionic Polymerization Research*; Quirk, R., Ed.; American Chemical Society: Washington DC, 1997, 236.
- (30) Penczek, S.; Cypriak, M.; Duda, A.; Kubisa, P.; Slomkowski, S. Living Ring-Opening Polymerizations of Heterocyclic Monomers. *Prog. Polym. Sci.* **2007**, *32*, 247–282.
- (31) Solovyanov, A. A.; Kazanski, K. S. Kinetics and Mechanism of Anionic Polymerization of Ethylene-Oxide in Ether Solutions. *Vysokomol. Soedin. A* **1972**, *14*, 1063–1070.
- (32) Pearson, R. G. Hard and Soft Acids and Bases. *J. Am. Chem. Soc.* **1963**, *85*, 3533–3539.
- (33) Hsieh, H.; Quirk, R. P. *Anionic Polymerization: Principles and Practical Applications*; CRC Press, 1996.
- (34) Quirk, R. P.; You, F.; Wesdemiotis, C.; Arnould, M. A. Anionic Synthesis and Characterization of  $\omega$ -Hydroxyl-Functionalized Poly (1,3-cyclohexadiene). *Macromolecules* **2004**, *37*, 1234–1242.
- (35) Tonhauser, C.; Frey, H. A Road Less Traveled to Functional Polymers: Epoxide Termination in Living Carbanionic Polymer Synthesis. *Macromol. Rapid Commun.* **2010**, *31*, 1938–1947.
- (36) Quirk, R. P.; Guo, Y.; Wesdemiotis, C.; Arnould, M. A. Investigation of Ethylene Oxide Oligomerization During Functionalization of Poly(butadienyl)lithium Using MALDI-ToF MS and  $^1\text{H}$  NMR Analyses. *Polymer* **2004**, *45*, 3423–3428.
- (37) Encyclopedia of Polymer Science and Engineering, Vol. 2, *Anionic Polymerization to Cationic Polymerization*, Mark, H. F., Kroschwitz, J. I., Eds. 1985, 17, 377–377, DOI: [10.1002/pi.4980170412](https://doi.org/10.1002/pi.4980170412).
- (38) Wojtech, V. B. Zur Darstellung Hochmolekularer Polyäthylenoxyde. *Makromol. Chem.* **1963**, *66*, 180–195.



## Chemical Reviews

## Review

- (39) Mangold, C.; Wurm, F.; Frey, H. Functional PEG-Based Polymers with Reactive Groups Via Anionic ROP of Tailor-Made Epoxides. *Polym. Chem.* **2012**, *3*, 1714.
- (40) Enjalbal, C.; Ribière, P.; Lamaty, F.; Yadav-Bhatnagar, N.; Martinez, J.; Aubagnac, J.-L. MALDI-ToF MS Analysis of Soluble PEG Based Multi-Step Synthetic Reaction Mixtures with Automated Detection of Reaction Failure. *J. Am. Soc. Mass Spectrom.* **2005**, *16*, 670–678.
- (41) Kempfner, J.; Marchetti-Deschmann, M.; Siekmann, J.; Turecek, P. L.; Schwarz, H. P.; Allmaier, G. Gemma and MALDI-ToF MS of Reactive PEGs for Pharmaceutical Applications. *J. Pharm. Biomed. Anal.* **2010**, *52*, 432–437.
- (42) Tsvetanov, C. B.; Petrova, E. B.; Panayotov, I. M. Polymerization of 1,2-Epoxydes Initiated by Tetraalkyl Aluminates. I. Polymerization of Ethylene Oxide in the Presence of Sodium Tetrabutyl Aluminate. *J. Macromol. Sci., Chem.* **1985**, *22*, 1309–1324.
- (43) Arkhipovich, G. N.; Dubrovskii, S. A.; Kazanskii, K. S.; Shupik, A. N. Complexing of Na<sup>+</sup> Ion with Polyethylene Glycol. *Polym. Sci. U.S.S.R.* **1981**, *23*, 1827–1841.
- (44) Ptitsyna, N. V.; Ovsyannikova, S. V.; Gelfer, T. M.; Kazanskii, K. S. Synthesis of Polyethylene Glycols of Molecular Weight above 10,000 by Anionic Polymerization. *Polym. Sci. U.S.S.R.* **1980**, *22*, 2779–2786.
- (45) Kazanskii, K. Donor-Acceptor and Solvation Interactions in Anionic Polymerization of Some Heterocycles. *Pure Appl. Chem.* **1981**, *53*, 1645–1661.
- (46) Sigwalt, P.; Boileau, S. Reactivities of Ions and Ion-Pairs in Anionic Polymerizations of Epoxides and Episulfides. *J. Polym. Sci. C Polym. Symp.* **1978**, *62*, 51–64.
- (47) Boileau, S. *Anionic Polymerization: Kinetics, Mechanisms and Synthesis*; American Chemical Society: Washington DC, 1981.
- (48) Berlinova, I. V.; Panayotov, I. M.; Tsvetanov, C. B. Ionic Equilibria in Living Polymer-Solutions of Ethylene-Oxide with Cesium. *Vysokomol. Soedin. B* **1978**, *20*, 839–342.
- (49) Berlinova, I. V.; Panayotov, I. M.; Tsvetanov, C. B. Influence of the Polyether Chain on the Dissociation of “Living” Polymers Obtained in the Anionic Polymerization of Ethylene Oxide. *Eur. Polym. J.* **1977**, *13*, 757–760.
- (50) Szwarc, M. *Carbanions, Living Polymers, and Electron Transfer Processes*; Interscience Publishers: New York, 1968.
- (51) Szwarc, M. *Ionic Polymerization Fundamentals*; Hanser, 1996.
- (52) Chang, C.; Kiesel, R.; Hogen-Esch, T. Specific Cation Participation in Alkali-Carbanion Initiated Epoxide Cleavage Reactions. *J. Am. Chem. Soc.* **1973**, *95*, 8446–8448.
- (53) Vinogradova, L. V.; Zgonnik, V. N.; Ilina, A. A.; Docheva, D.; Tsvetanov, C. Anionic Polymerization in Oxiranes. Polymerization of Methyl Methacrylate and 2-Vinylpyridine in Ethylene Oxide. *Macromolecules* **1992**, *25*, 6733–6738.
- (54) Price, C.; Carmelit, D. Reactions of Epoxides in Dimethyl Sulfoxide Catalyzed by Potassium t-Butoxide. *J. Am. Chem. Soc.* **1966**, *88*, 4039.
- (55) Gagnon, S. D. *Encyclopedia of Polymer Science and Engineering*; 2nd ed.; Wiley-Interscience: New York, 1985; Vol. 6.
- (56) Wegener, G.; Brandt, M.; Duda, L.; Hofmann, J.; Kleczewski, B.; Koch, D.; Kumpf, R.-J.; Orzesek, H.; Pirkel, H.-G.; Six, C. Trends in Industrial Catalysis in the Polyurethane Industry. *Appl. Catal., A* **2001**, *221*, 303–335.
- (57) Price, C. Polyethers. *Acc. Chem. Res.* **1974**, *7*, 294–301.
- (58) Sloop, S. E.; Lerner, M. M.; Stephens, T. S.; Tipton, A. L.; Paull, D. G.; Stenger-Smith, J. D. Cross-Linking Poly(ethylene oxide) and Poly[oxymethylene-oligo (oxyethylene)] with Ultraviolet Radiation. *J. Appl. Polym. Sci.* **1994**, *53*, 1563–1572.
- (59) Doytcheva, M.; Dotcheva, D.; Stamenova, R.; Orahovats, A.; Tsvetanov, C.; Leder, J. Ultraviolet-Induced Crosslinking of Solid Poly(ethylene oxide). *J. Appl. Polym. Sci.* **1997**, *64*, 2299–2307.
- (60) Tsvetanov, C. B.; Stamenova, R.; Riess, G.; Ferrand, M.; Limal, D. U.S. Patent 20050043429 A1, 2003.
- (61) Doytcheva, M.; Petrova, E.; Stamenova, R.; Tsvetanov, C.; Riess, G. UV-Induced Cross-Linking of Poly(ethylene oxide) in Aqueous Solution. *Macromol. Mater. Eng.* **2004**, *289*, 676–680.
- (62) Hill, F. N.; Fitzpatrick, J. T.; Bailey, J. F. E.; Union Carbide Corp: U.S. Patent 2,969,402, 1961.
- (63) Miller, R. A.; Price, C. C. Polyethers. VII. Aluminum Catalysts for Polymerization of Ethylene Oxide. *J. Polym. Sci.* **1959**, *34*, 161–163.
- (64) Vandenberg, E. Organometallic Catalysts for Polymerizing Monosubstituted Epoxides. *J. Polym. Sci.* **1960**, *47*, 486–489.
- (65) Osgan, M.; Teyssie, P. Polymerization of Heterocyclic Monomers. *J. Polym. Sci., Part B: Polym. Lett.* **1967**, *5*, 789.
- (66) Hsieh, H. Polymerization of Alkylene Oxides with Trialkylaluminum, Metal Acetylacetonates, and Water. *J. Appl. Polym. Sci.* **1971**, *15*, 2425–2438.
- (67) Zhang, Y.; Shen, Z. *Acta Polym. Sin.* **1998**, *6*, 469.
- (68) Dimitrov, P.; Hasan, E.; Rangelov, S.; Trzebicka, B.; Dworak, A.; Tsvetanov, C. B. High Molecular Weight Functionalized Poly(ethylene oxide). *Polymer* **2002**, *43*, 7171–7178.
- (69) Goeke, G. L.; Karol, F. J.; Union Carbide Corporation: U.S. Patent 4193892 A, 1980.
- (70) Kazanskii, K.; Tarasov, A.; Paleyeva, I. Y.; Dubrovskii, S. High Molecular Suspension Polymerization of Ethylene Oxide under the Action of Diphenylcalcium. *Polym. Sci. U.S.S.R.* **1978**, *20*, 442–452.
- (71) (a) Berlinova, I. V.; Panayotov, I. M.; Tsvetanov, K. B. Ionic Equilibria in Living Polymer-Solutions of Ethylene-Oxide with Cesium Anion. *Vysokomol. Soedin. B* **1978**, *20*, 839–842. (b) Bulgarian Patent 25,142, 1978.
- (72) Billouard, C.; Carlotti, S.; Desbois, P.; Deffieux, A. “Controlled” High-Speed Anionic Polymerization of Propylene Oxide Initiated by Alkali Metal Alkoxide/Trialkylaluminum Systems. *Macromolecules* **2004**, *37*, 4038–4043.
- (73) Brocas, A.-L.; Mantzaridis, C.; Tunc, D.; Carlotti, S. Polyether Synthesis: From Activated or Metal-Free Anionic Ring-Opening Polymerization of Epoxides to Functionalization. *Prog. Polym. Sci.* **2013**, *38*, 845–873.
- (74) Aida, T.; Inoue, S. Living Polymerization of Epoxides with Metalloporphyrin and Synthesis of Block Copolymers with Controlled Chain Lengths. *Macromolecules* **1981**, *14*, 1162–1166.
- (75) Aida, T.; Mizuta, R.; Yoshida, Y.; Inoue, S. Polymerization of Epoxides Catalyzed by Metalloporphine. *Makromol. Chem.* **1981**, *182*, 1073–1079.
- (76) Sugimoto, H.; Kawamura, C.; Kuroki, M.; Aida, T.; Inoue, S. Lewis Acid-Assisted Anionic Ring-Opening Polymerization of Epoxide by the Aluminum Complexes of Porphyrin, Phthalocyanine, Tetraazaannulene, and Schiff Base as Initiators. *Macromolecules* **1994**, *27*, 2013–2018.
- (77) Akatsuka, M.; Aida, T.; Inoue, S. High-Speed “Immortal” Polymerization of Epoxides Initiated with Aluminum Porphyrin. Acceleration of Propagation and Chain-Transfer Reactions by a Lewis Acid. *Macromolecules* **1994**, *27*, 2820–2825.
- (78) Aida, T.; Inoue, S. Metalloporphyrins as Initiators for Living and Immortal Polymerizations. *Acc. Chem. Res.* **1996**, *29*, 39–48.
- (79) Braune, W.; Okuda, J. An Efficient Method for Controlled Propylene Oxide Polymerization: The Significance of Bimetallic Activation in Aluminum Lewis Acids. *Angew. Chem., Int. Ed.* **2003**, *42*, 64–68.
- (80) Labbé, A.; Carlotti, S.; Billouard, C.; Desbois, P.; Deffieux, A. Controlled High-Speed Anionic Polymerization of Propylene Oxide Initiated by Onium Salts in the Presence of Triisobutylaluminum. *Macromolecules* **2007**, *40*, 7842–7847.
- (81) Deffieux, A.; Carlotti, S.; Desbois, P. New Perspectives in Living/Controlled Anionic Polymerization. *Macromol. Symp.* **2005**, *229*, 24–31.
- (82) Carlotti, S.; Desbois, P.; Billouard, C.; Deffieux, A. Reactivity Control in Anionic Polymerization of Ethylenic and Heterocyclic Monomers through Formation of ‘Ate’ Complexes. *Polym. Int.* **2006**, *55*, 1126–1131.
- (83) Gervais, M.; Labbé, A. L.; Carlotti, S.; Deffieux, A. Direct Synthesis of  $\alpha$ -Azido, $\omega$ -Hydroxypolyethers by Monomer-Activated Anionic Polymerization. *Macromolecules* **2009**, *42*, 2395–2400.

- (84) Sakakibara, K.; Nakano, K.; Nozaki, K. Regio-Controlled Ring-Opening Polymerization of Perfluoroalkyl-Substituted Epoxides. *Chem. Commun.* **2006**, 3334–3336.
- (85) Sakakibara, K.; Nakano, K.; Nozaki, K. Regioregular Polymerization of Fluorine-Containing Epoxides. *Macromolecules* **2007**, *40*, 6136–6142.
- (86) Roos, K.; Carlotti, S. Grignard-Based Anionic Ring-Opening Polymerization of Propylene Oxide Activated by Triisobutylaluminum. *Eur. Polym. J.* **2015**, *70*, 240–246.
- (87) Herzberger, J.; Frey, H. Epicyanohydrin: Polymerization by Monomer Activation Gives Access to Nitrile-, Amino-, and Carboxyl-Functional Poly(ethylene glycol). *Macromolecules* **2015**, *48*, 8144–8153.
- (88) Rejsek, V.; Sauvanier, D.; Billouard, C.; Desbois, P.; Deffieux, A.; Carlotti, S. Controlled Anionic Homo- and Copolymerization of Ethylene Oxide and Propylene Oxide by Monomer Activation. *Macromolecules* **2007**, *40*, 6510–6514.
- (89) Gervais, M.; Brocas, A.-L.; Cendejas, G.; Deffieux, A.; Carlotti, S. Synthesis of Linear High Molar Mass Glycidol-Based Polymers by Monomer-Activated Anionic Polymerization. *Macromolecules* **2010**, *43*, 1778–1784.
- (90) Brocas, A.-L.; Deffieux, A.; Le Malicot, N.; Carlotti, S. Combination of Phosphazene Base and Triisobutylaluminum for the Rapid Synthesis of Polyhydroxy Telechelic Poly(propylene oxide). *Polym. Chem.* **2012**, *3*, 1189–1195.
- (91) Pierre, L. E. S.; Price, C. C. The Room Temperature Polymerization of Propylene Oxide. *J. Am. Chem. Soc.* **1956**, *78*, 3432–3436.
- (92) Quirk, R. P.; Lizarraga, G. M. Anionic Synthesis of Well-Defined, Poly[(styrene)-block-(propylene oxide)] Block Copolymers. *Macromol. Chem. Phys.* **2000**, *201*, 1395–1404.
- (93) Grobelny, Z.; Matlengiewicz, M.; Jurek, J.; Michalak, M.; Kwapińska, D.; Swinarew, A.; Schab-Balcerzak, E. The Influence of Macrocyclic Ligands and Water on Propylene Oxide Polymerization Initiated with Anhydrous Potassium Hydroxide in Tetrahydrofuran. *Eur. Polym. J.* **2013**, *49*, 3277–3288.
- (94) Osterwinter, C.; Schubert, C.; Tonhauser, C.; Wilms, D.; Frey, H.; Friedrich, C. Rheological Consequences of Hydrogen Bonding: Linear Viscoelastic Response of Linear Polyglycerol and Its Permethylated Analogues as a General Model for Hydroxyl-Functional Polymers. *Macromolecules* **2015**, *48*, 119–130.
- (95) Brocas, A.-L.; Gervais, M.; Carlotti, S.; Pispas, S. Amphiphilic Diblock Copolymers Based on Ethylene Oxide and Epoxides Bearing Aliphatic Side Chains. *Polym. Chem.* **2012**, *3*, 2148.
- (96) Gervais, M.; Brocas, A.-L.; Deffieux, A.; Ibarboure, E.; Carlotti, S. Rapid and Controlled Synthesis of Hydrophobic Polyethers by Monomer Activation. *Pure Appl. Chem.* **2012**, *84*, 2103–2111.
- (97) Müller, S. S.; Moers, C.; Frey, H. A Challenging Comonomer Pair: Copolymerization of Ethylene Oxide and Glycidyl Methyl Ether to Thermoresponsive Polyethers. *Macromolecules* **2014**, *47*, 5492–5500.
- (98) Labbé, A. I.; Brocas, A.-L.; Ibarboure, E.; Ishizone, T.; Hirao, A.; Deffieux, A.; Carlotti, S. Selective Ring-Opening Polymerization of Glycidyl Methacrylate: Toward the Synthesis of Cross-Linked (Co)-polyethers with Thermoresponsive Properties. *Macromolecules* **2011**, *44*, 6356–6364.
- (99) Labbé, A.; Carlotti, S.; Deffieux, A.; Hirao, A. Controlled Polymerization of Glycidyl Methyl Ether Initiated by Onium Salt/Triisobutylaluminum and Investigation of the Polymer LCST. *Macromol. Symp.* **2007**, *249–250*, 392–397.
- (100) Carlotti, S.; Labbé, A. I.; Rejsek, V.; Doutaz, S. p.; Gervais, M.; Deffieux, A. Living/Controlled Anionic Polymerization and Copolymerization of Epichlorohydrin with Tetraoctylammonium Bromide–Triisobutylaluminum Initiating Systems. *Macromolecules* **2008**, *41*, 7058–7062.
- (101) Lundberg, P.; Lee, B. F.; van den Berg, S. A.; Pressly, E. D.; Lee, A.; Hawker, C. J.; Lynd, N. A. Poly[(ethylene oxide)-co-(methylene ethylene oxide)]: A Hydrolytically Degradable Poly(ethylene oxide) Platform. *ACS Macro Lett.* **2012**, *1*, 1240–1243.
- (102) Meyer, J.; Keul, H.; Möller, M. Poly(glycidyl amine) and Copolymers with Glycidol and Glycidyl Amine Repeating Units: Synthesis and Characterization. *Macromolecules* **2011**, *44*, 4082–4091.
- (103) Hu, H.; Yuan, W.; Lu, L.; Zhao, H.; Jia, Z.; Baker, G. L. Low Glass Transition Temperature Polymer Electrolyte Prepared from Ionic Liquid Grafted Polyethylene Oxide. *J. Polym. Sci., Part A: Polym. Chem.* **2014**, *52*, 2104–2110.
- (104) Brocas, A.-L.; Cendejas, G.; Caillol, S.; Deffieux, A.; Carlotti, S. Controlled Synthesis of Polyepichlorohydrin with Pendant Cyclic Carbonate Functions for Isocyanate-Free Polyurethane Networks. *J. Polym. Sci., Part A: Polym. Chem.* **2011**, *49*, 2677–2684.
- (105) Rejsek, V.; Desbois, P.; Deffieux, A.; Carlotti, S. Polymerization of Ethylene Oxide Initiated by Lithium Derivatives Via the Monomer-Activated Approach: Application to the Direct Synthesis of PS-*b*-PEO and PI-*b*-PEO Diblock Copolymers. *Polymer* **2010**, *51*, 5674–5679.
- (106) Babu, H. V.; Muralidharan, K. Polyethers with Phosphate Pendant Groups by Monomer Activated Anionic Ring Opening Polymerization: Syntheses, Characterization and Their Lithium-Ion Conductivities. *Polymer* **2014**, *55*, 83–94.
- (107) Hahn, F. E. Heterocyclic Carbenes. *Angew. Chem., Int. Ed.* **2006**, *45*, 1348–1352.
- (108) Herrmann, W. A. *N*-Heterocyclic Carbenes: A New Concept in Organometallic Catalysis. *Angew. Chem., Int. Ed.* **2002**, *41*, 1290–1309.
- (109) Enders, D.; Niemeier, O.; Henseler, A. Organocatalysis by *N*-Heterocyclic Carbenes. *Chem. Rev.* **2007**, *107*, 5606–5655.
- (110) Marion, N.; Díez-González, S.; Nolan, S. P. *N*-Heterocyclic Carbenes as Organocatalysts. *Angew. Chem., Int. Ed.* **2007**, *46*, 2988–3000.
- (111) Flanagan, D. M.; Romanov-Michailidis, F.; White, N. A.; Rovis, T. Organocatalytic Reactions Enabled by *N*-Heterocyclic Carbenes. *Chem. Rev.* **2015**, *115*, 9307–9387.
- (112) Fèvre, M.; Pinaud, J.; Gnanou, Y.; Vignolle, J.; Taton, D. *N*-Heterocyclic Carbenes (NHCs) as Organocatalysts and Structural Components in Metal-Free Polymer Synthesis. *Chem. Soc. Rev.* **2013**, *42*, 2142–2172.
- (113) Fèvre, M.; Vignolle, J.; Gnanou, Y.; Taton, D. in *Polymer Science: A Comprehensive Reference*; Penczek, S., Grubbs, R. H., Eds.; Elsevier: Amsterdam, 2012; Vol. 4, pp 67–115.
- (114) Naumann, S.; Dove, A. P. *N*-Heterocyclic Carbenes as Organocatalysts for Polymerizations: Trends and Frontiers. *Polym. Chem.* **2015**, *6*, 3185–3200.
- (115) Naumann, S.; Dove, A. P. *N*-Heterocyclic Carbenes for Metal-Free Polymerization Catalysis: An Update. *Polym. Int.* **2015**, DOI: 10.1002/pi.5034.
- (116) Arduengo, A. J.; Harlow, R. L.; Kline, M. A. Stable Crystalline Carbene. *J. Am. Chem. Soc.* **1991**, *113*, 361–363.
- (117) Jones, R. A.; Karatza, M.; Voro, T. N.; Civeir, P. U.; Franck, A.; Ozturk, O.; Seaman, J. P.; Whitmore, A. P.; Williamson, D. J. Extended Heterocyclic Systems 1. The Synthesis and Characterisation of Pyrrolylpyridines, Alternating Pyrrole: Pyridine Oligomers and Polymers, and Related Systems. *Tetrahedron* **1996**, *52*, 8707–8724.
- (118) Jones, R. A.; Civeir, P. U. Extended Heterocyclic Systems 2. The Synthesis and Characterisation of (2-Furyl)pyridines, (2-Thienyl)pyridines, and Furan-Pyridine and Thiophene-Pyridine Oligomers. *Tetrahedron* **1997**, *53*, 11529–11540.
- (119) Raynaud, J.; Absalon, C.; Gnanou, Y.; Taton, D. *N*-Heterocyclic Carbene-Induced Zwitterionic Ring-Opening Polymerization of Ethylene Oxide and Direct Synthesis of  $\alpha,\omega$ -Difunctionalized Poly(ethylene oxide)s and Poly(ethylene oxide)-*b*-Poly(*ε*-caprolactone) Block Copolymers. *J. Am. Chem. Soc.* **2009**, *131*, 3201–3209.
- (120) Raynaud, J.; Absalon, C.; Gnanou, Y.; Taton, D. *N*-Heterocyclic Carbene-Organocatalyzed Ring-Opening Polymerization of Ethylene Oxide in the Presence of Alcohols or Trimethylsilyl Nucleophiles as Chain Moderators for the Synthesis of  $\alpha,\omega$ -Heterodifunctionalized Poly(ethylene oxide)s. *Macromolecules* **2010**, *43*, 2814–2823.
- (121) Raynaud, J.; Ottou, W. N.; Gnanou, Y.; Taton, D. Metal-Free and Solvent-Free Access to  $\alpha,\omega$ -Heterodifunctionalized Poly(propylene oxide)s by *N*-Heterocyclic Carbene-Induced Ring Opening Polymerization. *Chem. Commun.* **2010**, *46*, 3203–3205.

- (122) Lindner, R.; Lejkowski, M. L.; Lavy, S.; Deglmann, P.; Wiss, K. T.; Zorbakhsh, S.; Meyer, L.; Limbach, M. Ring-Opening Polymerization and Copolymerization of Propylene Oxide Catalyzed by *N*-Heterocyclic Carbenes. *ChemCatChem* **2014**, *6*, 618–625.
- (123) Naumann, S.; Buchmeiser, M. R. Liberation of *N*-Heterocyclic Carbenes (NHCs) from Thermally Labile Progenitors: Protected NHCs as Versatile Tools in Organo- and Polymerization Catalysis. *Catal. Sci. Technol.* **2014**, *4*, 2466.
- (124) Fèvre, M.; Vignolle, J.; Taton, D. Azolium Hydrogen Carbonates and Azolium Carboxylates as Organic Pre-Catalysts for *N*-Heterocyclic Carbene-Catalyzed Group Transfer and Ring-Opening Polymerisations. *Polym. Chem.* **2013**, *4*, 1995–2003.
- (125) Naumann, S.; Thomas, A. W.; Dove, A. P. *N*-Heterocyclic Olefins as Organocatalysts for Polymerization: Preparation of Well-Defined Poly(propylene oxide). *Angew. Chem., Int. Ed.* **2015**, *54*, 9550–9554.
- (126) Kuhn, N.; Bohnen, H.; Kreutzberg, J.; Blaser, D.; Boese, R. 1,3,4,5-Tetramethyl-2-Methyleneimidazole-an Ylidic Olefin. *J. Chem. Soc., Chem. Commun.* **1993**, 1136–1137.
- (127) Kronig, S.; Jones, P. G.; Tamm, M. Preparation of 2-Alkylidene-Substituted 1,3,4,5-Tetramethylimidazolines and Their Reactivity Towards Rh<sup>I</sup> Complexes and B(C<sub>6</sub>F<sub>5</sub>)<sub>3</sub>. *Eur. J. Inorg. Chem.* **2013**, *2013*, 2301–2314.
- (128) Fürstner, A.; Alcarazo, M.; Goddard, R.; Lehmann, C. W. Coordination Chemistry of Ene-1,1-Diamines and a Prototype “Carbodicarbene”. *Angew. Chem., Int. Ed.* **2008**, *47*, 3210–3214.
- (129) Boileau, S.; Illy, N. Activation in Anionic Polymerization: Why Phosphazene Bases Are Very Exciting Promoters. *Prog. Polym. Sci.* **2011**, *36*, 1132–1151.
- (130) Zhao, J.; Hadjichristidis, N. A.; Gnanou, Y. Phosphazene-Promoted Anionic Polymerization. *Polimery* **2014**, *59*, 49–59.
- (131) Hirao, A.; Goseki, R.; Ishizone, T. Advances in Living Anionic Polymerization: From Functional Monomers, Polymerization Systems, to Macromolecular Architectures. *Macromolecules* **2014**, *47*, 1883–1905.
- (132) Zhao, J.; Hadjichristidis, N. A.; Schlaad, H. In *Anionic Polymerization*; Hadjichristidis, N., Hirao, A., Eds.; Springer: Japan, 2015; pp 429–449.
- (133) Schwesinger, R.; Schlemper, H. Peralkylated Polyaminophosphazenes—Extremely Strong, Neutral Nitrogen Bases. *Angew. Chem., Int. Ed. Engl.* **1987**, *26*, 1167–1169.
- (134) Schwesinger, R.; Hasenfratz, C.; Schlemper, H.; Walz, L.; Peters, E.-M.; Peters, K.; von Schnering, H. G. How Strong and How Hindered Can Uncharged Phosphazene Bases Be? *Angew. Chem., Int. Ed. Engl.* **1993**, *32*, 1361–1363.
- (135) Schwesinger, R.; Schlemper, H.; Hasenfratz, C.; Willaredt, J.; Dambacher, T.; Breuer, T.; Ottaway, C.; Flutschinger, M.; Boele, J.; Fritz, H.; et al. Extremely Strong, Uncharged Auxiliary Bases; Monomeric and Polymer-Supported Polyaminophosphazenes (P<sub>2</sub>–P<sub>3</sub>). *Liebigs Ann. Chem.* **1996**, *1996*, 1055–1081.
- (136) Solladié-Cavallo, A.; Liptaj, T.; Schmitt, M.; Solgadi, A. Iso-Propyl Phenylacetate: Formation of a Single Enolate with *t*-BuP<sub>4</sub> as Base. *Tetrahedron Lett.* **2002**, *43*, 415–418.
- (137) Eßwein, B.; Steidl, N. M.; Möller, M. Anionic Polymerization of Oxirane in the Presence of the Polyiminophosphazene Base *t*-BuP<sub>4</sub>. *Macromol. Rapid Commun.* **1996**, *17*, 143–148.
- (138) Rexin, O.; Müllhaupt, R. Anionic Ring-Opening Polymerization of Propylene Oxide in the Presence of Phosphonium Catalysts. *J. Polym. Sci., Part A: Polym. Chem.* **2002**, *40*, 864–873.
- (139) Rexin, O.; Müllhaupt, R. Anionic Ring-Opening Polymerization of Propylene Oxide in the Presence of Phosphonium Catalysts at Various Temperatures. *Macromol. Chem. Phys.* **2003**, *204*, 1102–1109.
- (140) Zhao, J.; Pahovnik, D.; Gnanou, Y.; Hadjichristidis, N. Sequential Polymerization of Ethylene Oxide,  $\epsilon$ -Caprolactone and L-Lactide: A One-Pot Metal-Free Route to Tri- and Pentablock Terpolymers. *Polym. Chem.* **2014**, *5*, 3750–3753.
- (141) Misaka, H.; Tamura, E.; Makiguchi, K.; Kamoshida, K.; Sakai, R.; Satoh, T.; Kakuchi, T. Synthesis of End-Functionalized Polyethers by Phosphazene Base-Catalyzed Ring-Opening Polymerization of 1,2-Butylene Oxide and Glycidyl Ether. *J. Polym. Sci., Part A: Polym. Chem.* **2012**, *50*, 1941–1952.
- (142) Keul, H.; Möller, M. Synthesis and Degradation of Biomedical Materials Based on Linear and Star Shaped Polyglycidols. *J. Polym. Sci., Part A: Polym. Chem.* **2009**, *47*, 3209–3231.
- (143) Kwon, W.; Rho, Y.; Kamoshida, K.; Kwon, K. H.; Jeong, Y. C.; Kim, J.; Misaka, H.; Shin, T. J.; Kim, J.; Kim, K.-W.; et al. Well-Defined Functional Linear Aliphatic Diblock Copolyethers: A Versatile Linear Aliphatic Polyether Platform for Selective Functionalizations and Various Nanostructures. *Adv. Funct. Mater.* **2012**, *22*, 5194–5208.
- (144) Reinicke, S.; Schmelz, J.; Lapp, A.; Karg, M.; Hellweg, T.; Schmalz, H. Smart Hydrogels Based on Double Responsive Triblock Terpolymers. *Soft Matter* **2009**, *5*, 2648–2657.
- (145) Zhao, J.; Pahovnik, D.; Gnanou, Y.; Hadjichristidis, N. Catalyst “Switch” Strategy for the Sequential Metal-Free Polymerization of Epoxides and Cyclic Esters/Carbonate. *Macromolecules* **2014**, *47*, 3814–3822.
- (146) Zhao, J.; Pahovnik, D.; Gnanou, Y.; Hadjichristidis, N. One-Pot Synthesis of Linear- and Three-Arm Star-Tetrablock Quarterpolymers Via Sequential Metal-Free Ring-Opening Polymerization Using a “Catalyst Switch” Strategy. *J. Polym. Sci., Part A: Polym. Chem.* **2015**, *53*, 304–312.
- (147) Zhao, J.; Pahovnik, D.; Gnanou, Y.; Hadjichristidis, N. Phosphazene-Promoted Metal-Free Ring-Opening Polymerization of Ethylene Oxide Initiated by Carboxylic Acid. *Macromolecules* **2014**, *47*, 1693–1698.
- (148) Esswein, B.; Möller, M. Polymerization of Ethylene Oxide with Alkylolithium Compounds and the Phosphazene Base “*t*-BuP<sub>4</sub>”. *Angew. Chem., Int. Ed. Engl.* **1996**, *35*, 623–625.
- (149) Zhao, J.; Schlaad, H.; Weidner, S.; Antonietti, M. Synthesis of Terpene-Poly(ethylene oxide)S by *t*-BuP<sub>4</sub>-Promoted Anionic Ring-Opening Polymerization. *Polym. Chem.* **2012**, *3*, 1763–1768.
- (150) Misaka, H.; Sakai, R.; Satoh, T.; Kakuchi, T. Synthesis of High Molecular Weight and End-Functionalized Poly(Styrene Oxide) by Living Ring-Opening Polymerization of Styrene Oxide Using the Alcohol/Phosphazene Base Initiating System. *Macromolecules* **2011**, *44*, 9099–9107.
- (151) Isono, T.; Asai, S.; Satoh, Y.; Takaoka, T.; Tajima, K.; Kakuchi, T.; Satoh, T. Controlled/Living Ring-Opening Polymerization of Glycidylamine Derivatives Using *t*-BuP<sub>4</sub>/Alcohol Initiating System Leading to Polyethers with Pendant Primary, Secondary, and Tertiary Amino Groups. *Macromolecules* **2015**, *48*, 3217–3229.
- (152) Zhao, J.; Alamri, H.; Hadjichristidis, N. A Facile Metal-Free “Grafting-from” Route from Acrylamide-Based Substrate toward Complex Macromolecular Combs. *Chem. Commun.* **2013**, *49*, 7079–7081.
- (153) Dentzer, L.; Bray, C.; Noinville, S.; Illy, N.; Guégan, P. Phosphazene-Promoted Metal-Free Ring-Opening Polymerization of 1,2-Epoxybutane Initiated by Secondary Amides. *Macromolecules* **2015**, *48*, 7755–7764.
- (154) Isono, T.; Kamoshida, K.; Satoh, Y.; Takaoka, T.; Sato, S.-i.; Satoh, T.; Kakuchi, T. Synthesis of Star- and Figure-Eight-Shaped Polyethers by *t*-BuP<sub>4</sub>-Catalyzed Ring-Opening Polymerization of Butylene Oxide. *Macromolecules* **2013**, *46*, 3841–3849.
- (155) Isono, T.; Satoh, Y.; Miyachi, K.; Chen, Y.; Sato, S.-i.; Tajima, K.; Satoh, T.; Kakuchi, T. Synthesis of Linear, Cyclic, Figure-Eight-Shaped, and Tadpole-Shaped Amphiphilic Block Copolyethers via *t*-BuP<sub>4</sub> Catalyzed Ring-Opening Polymerization of Hydrophilic and Hydrophobic Glycidyl Ethers. *Macromolecules* **2014**, *47*, 2853–2863.
- (156) Schmalz, H.; Lanzendörfer, M. G.; Abetz, V.; Müller, A. H. E. Anionic Polymerization of Ethylene Oxide in the Presence of the Phosphazene Base *t*-BuP<sub>4</sub> – Kinetic Investigations Using In-Situ FT-NIR Spectroscopy and MALDI-ToF MS. *Macromol. Chem. Phys.* **2003**, *204*, 1056–1071.
- (157) Toy, A. A.; Reinicke, S.; Müller, A. H. E.; Schmalz, H. One-Pot Synthesis of Polyglycidol-Containing Block Copolymers with Alkyl-lithium Initiators Using the Phosphazene Base *t*-BuP<sub>4</sub>. *Macromolecules* **2007**, *40*, 5241–5244.

- (158) Förster, S.; Krämer, E. Synthesis of PB-PEO and PI-PEO Block Copolymers with Alkylolithium Initiators and the Phosphazene Base *t*-BuP<sub>4</sub>. *Macromolecules* **1999**, *32*, 2783–2785.
- (159) Pispas, S.; Hadjichristidis, N. Aggregation Behavior of Poly(butadiene-*b*-ethylene oxide) Block Copolymers in Dilute Aqueous Solutions: Effect of Concentration, Temperature, Ionic Strength, and Type of Surfactant. *Langmuir* **2003**, *19*, 48–54.
- (160) Justynska, J.; Hordyjewicz, Z.; Schlaad, H. Toward a Toolbox of Functional Block Copolymers Via Free-Radical Addition of Mercaptans. *Polymer* **2005**, *46*, 12057–12064.
- (161) Floudas, G.; Vazaioni, B.; Schipper, F.; Ulrich, R.; Wiesner, U.; Iatrou, H.; Hadjichristidis, N. Poly(ethylene oxide-*b*-isoprene) Diblock Copolymer Phase Diagram. *Macromolecules* **2001**, *34*, 2947–2957.
- (162) Schmalz, H.; Knoll, A.; Müller, A. J.; Abetz, V. Synthesis and Characterization of ABC Triblock Copolymers with Two Different Crystalline End Blocks: Influence of Confinement on Crystallization Behavior and Morphology. *Macromolecules* **2002**, *35*, 10004–10013.
- (163) Siebert, M.; Albrecht, K.; Spiertz, R.; Keul, H.; Moller, M. Reactive Amphiphilic Block Copolymers for the Preparation of Hybrid Organic/Inorganic Materials with Covalent Interactions. *Soft Matter* **2011**, *7*, 587–594.
- (164) Zhao, J.; Mountrichas, G.; Zhang, G.; Pispas, S. Amphiphilic Polystyrene-*b*-Poly(p-hydroxystyrene-*g*-ethylene oxide) Block-Graft Copolymers via a Combination of Conventional and Metal-Free Anionic Polymerization. *Macromolecules* **2009**, *42*, 8661–8668.
- (165) Schacher, F.; Müllner, M.; Schmalz, H.; Müller, A. H. E. New Block Copolymers with Poly(*N,N*-dimethylaminoethyl methacrylate) as a Double Stimuli-Responsive Block. *Macromol. Chem. Phys.* **2009**, *210*, 256–262.
- (166) Zhang, L.; Nederberg, F.; Messman, J. M.; Pratt, R. C.; Hedrick, J. L.; Wade, C. G. Organocatalytic Stereoselective Ring-Opening Polymerization of Lactide with Dimeric Phosphazene Bases. *J. Am. Chem. Soc.* **2007**, *129*, 12610–12611.
- (167) Zhang, L.; Nederberg, F.; Pratt, R. C.; Waymouth, R. M.; Hedrick, J. L.; Wade, C. G. Phosphazene Bases: A New Category of Organocatalysts for the Living Ring-Opening Polymerization of Cyclic Esters. *Macromolecules* **2007**, *40*, 4154–4158.
- (168) Yang, H.; Xu, J.; Pispas, S.; Zhang, G. Hybrid Copolymerization of  $\epsilon$ -Caprolactone and Methyl Methacrylate. *Macromolecules* **2012**, *45*, 3312–3317.
- (169) Xu, J.; Yang, J.; Ye, X.; Ma, C.; Zhang, G.; Pispas, S. Synthesis and Properties of Amphiphilic and Biodegradable Poly( $\epsilon$ -Caprolactone-*co*-glycidol) Copolymers. *J. Polym. Sci., Part A: Polym. Chem.* **2015**, *53*, 846–853.
- (170) Zhao, J.; Hadjichristidis, N. Polymerization of 5-Alkyl  $\delta$ -Lactones Catalyzed by Diphenyl Phosphate and Their Sequential Organocatalytic Polymerization with Monosubstituted Epoxides. *Polym. Chem.* **2015**, *6*, 2659–2668.
- (171) Penelle, J. *unpublished results* **2015**.
- (172) Chen, S.; Xu, N.; Shi, J. Structure and Properties of Polyether Polyols Catalyzed by Fe/Zn Double Metal Cyanide Complex Catalyst. *Prog. Org. Coat.* **2004**, *49*, 125–129.
- (173) Johnston, H. R.; Gen Tire & Rubber Co. U.S. Patent 3,278,459, 1966.
- (174) Kim, I.; Ahn, J.-T.; Ha, C. S.; Yang, C. S.; Park, I. Polymerization of Propylene Oxide by Using Double Metal Cyanide Catalysts and the Application to Polyurethane Elastomer. *Polymer* **2003**, *44*, 3417–3428.
- (175) Ehlers, S.; Bayer Aktiengesellschaft: U.S. Patent 6,486,361, 2002.
- (176) Ostrowski, T.; BASF Aktiengesellschaft: U.S. Patent 7,968,754, 2005.
- (177) Eleveld, M. B.; Shell Oil Company: U.S. Patent 6,977,236, 2005.
- (178) Buckley, B. J.; Dow Global Technologies LLC: U.S. Patent 20140094534 A1, 2012.
- (179) Ionescu, M. *Chemistry and Technology of Polyols for Polyurethanes*; Rapra Technology, 2005.
- (180) Huang, Y.-J.; Qi, G. R.; Chen, L. S. Effects of Morphology and Composition on Catalytic Performance of Double Metal Cyanide Complex Catalyst. *Appl. Catal., A* **2003**, *240*, 263–271.
- (181) Huang, Y.-J.; Zhang, X.-H.; Hua, Z.-J.; Chen, S.-L.; Qi, G.-R. Ring-Opening Polymerization of Propylene Oxide Catalyzed by a Calcium-Chloride-Modified Zinc-Cobalt Double Metal-Cyanide Complex. *Macromol. Chem. Phys.* **2010**, *211*, 1229–1237.
- (182) Wei, R.-J.; Zhang, Y.-Y.; Zhang, X.-H.; Du, B.-Y.; Fan, Z.-Q. Regio-Selective Synthesis of Polyepichlorohydrin Diol Using Zn-Co(III) Double Metal Cyanide Complex. *RSC Adv.* **2014**, *4*, 21765–21771.
- (183) Zhang, X.-H.; Hua, Z.-J.; Chen, S.; Liu, F.; Sun, X.-K.; Qi, G.-R. Role of Zinc Chloride and Complexing Agents in Highly Active Double Metal Cyanide Catalysts for Ring-Opening Polymerization of Propylene Oxide. *Appl. Catal., A* **2007**, *325*, 91–98.
- (184) Chen, S.; Zhang, P.; Chen, L. Fe/Zn Double Metal Cyanide (DMC) Catalyzed Ring-Opening Polymerization of Propylene Oxide: Part 3. Synthesis of DMC Catalysts. *Prog. Org. Coat.* **2004**, *50*, 269–272.
- (185) Yoon, J. H.; Lee, I. K.; Choi, H. Y.; Choi, E. J.; Yoon, J. H.; Shim, S. E.; Kim, I. Double Metal Cyanide Catalysts Bearing Lactate Esters as eco-Friendly Complexing Agents for the Synthesis of Highly Pure Polyols. *Green Chem.* **2011**, *13*, 631–639.
- (186) Kim, I.; Anas, K.; Lee, S.; Ha, C.-S.; Park, D.-W. Tuning of the Activity and Induction Period of Double Metal Cyanide Catalyzed Ring-Opening Polymerizations of Propylene Oxide by Using Ionic Liquids. *Catal. Today* **2008**, *131*, 541–547.
- (187) Huang, Y. J.; Zhang, X. H.; Hua, Z. J.; Qi, G. R. Calcium Chloride Doped Zinc-Cobalt Metal-Cyanide Complex: Unexpected Highly Activity Towards Ring-Opening Polymerization of Propylene Oxide. *Chin. Chem. Lett.* **2010**, *21*, 897–901.
- (188) Lee, S. H.; Lee, I. K.; Ha, J. Y.; Jo, J. K.; Park, I.; Ha, C.-S.; Suh, H.; Kim, I. Tuning of the Activity and Induction Period of the Polymerization of Propylene Oxide Catalyzed by Double Metal Cyanide Complexes Bearing  $\beta$ -Alkoxy Alcohols as Complexing Agents. *Ind. Eng. Chem. Res.* **2010**, *49*, 4107–4116.
- (189) Lee, S.; Baek, S. T.; Anas, K.; Ha, C.-S.; Park, D.-W.; Lee, J. W.; Kim, I. Tuning of Activity, Induction Period and Polymer Properties of Double Metal Cyanide Catalyzed Ring-Opening Polymerizations of Propylene Oxide by Using Quaternary Ammonium Salts. *Polymer* **2007**, *48*, 4361–4367.
- (190) Ooms, P.; Bayer Aktiengesellschaft: U.S. Patent 6,376,420, 2002.
- (191) Ooms, P.; Bayer Aktiengesellschaft: U.S. Patent 6,953,765, 2005.
- (192) Kim, I.; Ahn, J.-T.; Lee, S.-H.; Ha, C.-S.; Park, D.-W. Preparation of Multi-Metal Cyanide Catalysts and Ring-Opening Polymerization of Propylene Oxide. *Catal. Today* **2004**, *93–95*, 511–516.
- (193) Lee, S. H.; Byun, S. H.; Baek, S. T.; Seo, H. S.; Park, D.-W.; Ha, C.-S.; Kim, I. Multi-Metal Cyanide Catalysts for Ring-Opening Polymerization of Propylene Oxide. *Catal. Today* **2008**, *132*, 170–177.
- (194) Byun, S.; Seo, H.; Lee, S.; Ha, C.-S.; Kim, I. Zn(II)-Co(III)-Fe(III) Multi-Metal Cyanide Complexes as Highly Active Catalysts for Ring-Opening Polymerization of Propylene Oxide. *Macromol. Res.* **2007**, *15*, 393–395.
- (195) Yu, S. J.; Liu, Y.; Byeon, S. J.; Park, D. W.; Kim, I. Ring-Opening Polymerization of Propylene Oxide by Double Metal Cyanide Catalysts Prepared by Reacting CoCl<sub>2</sub> with Various Metal Cyanide Salts. *Catal. Today* **2014**, *232*, 75–81.
- (196) Huang, Y.-J.; Qi, G.-R.; Wang, Y.-H. Controlled Ring-Opening Polymerization of Propylene Oxide Catalyzed by Double Metal-Cyanide Complex. *J. Polym. Sci., Part A: Polym. Chem.* **2002**, *40*, 1142–1150.
- (197) Wu, L.-C.; Yu, A.-F.; Zhang, M.; Liu, B.-H.; Chen, L.-B. DMC Catalyzed Epoxide Polymerization: Induction Period, Kinetics, and Mechanism. *J. Appl. Polym. Sci.* **2004**, *92*, 1302–1309.
- (198) Televantos, Y.; Le-Khac, Bi. ARCO Chemical Technology; U.S. Patent 5,767,323, 1998.
- (199) Hayes, J. E. Bayer Antwerp; U.S. Patent 6,835,801, 2004.
- (200) Kaushiva, B. D. Bayer Materialscience Llc; U.S. Patent 7,005,552 B2, 2006.
- (201) Pazos, J. F. Arco Chemical Technology; U.S. Patent 5,777,177, 1998.
- (202) McDaniel, K. G.; Combs, G. G. Bayer Materialscience, Llc; U.S. Patent 20140275632 A1, 2014.

## Chemical Reviews

## Review

- (203) Laitar, D. S.; Babb, D. A.; Villa, C. M.; Keaton, R.; Masy, J.-P. U.S. Patent 2,013,028,9236, 2013.
- (204) Clement, K. S. Dow Global Technologies, Inc.; U.S. Patent 6,642,423, 2002.
- (205) Darensbourg, D. J.; Adams, M. J.; Yarbrough, J. C. Toward the Design of Double Metal Cyanides for the Copolymerization of CO<sub>2</sub> and Epoxides. *Inorg. Chem.* **2001**, *40*, 6543–6544.
- (206) Chen, S.; Hua, Z.; Fang, Z.; Qi, G. Copolymerization of Carbon Dioxide and Propylene Oxide with Highly Effective Zinc Hexacyanocobaltate(III)-Based Coordination Catalyst. *Polymer* **2004**, *45*, 6519–6524.
- (207) Robertson, N. J.; Qin, Z.; Dallinger, G. C.; Lobkovsky, E. B.; Lee, S.; Coates, G. W. Two-Dimensional Double Metal Cyanide Complexes: Highly Active Catalysts for the Homopolymerization of Propylene Oxide and Copolymerization of Propylene Oxide and Carbon Dioxide. *Dalton Transactions* **2006**, 5390–5395.
- (208) Sun, X.-K.; Zhang, X.-H.; Chen, S.; Du, B.-Y.; Wang, Q.; Fan, Z.-Q.; Qi, G.-R. One-Pot Terpolymerization of CO<sub>2</sub>, Cyclohexene Oxide and Maleic Anhydride Using a Highly Active Heterogeneous Double Metal Cyanide Complex Catalyst. *Polymer* **2010**, *51*, 5719–5725.
- (209) Sun, X.-K.; Zhang, X.-H.; Wei, R.-J.; Du, B.-Y.; Wang, Q.; Fan, Z.-Q.; Qi, G.-R. Mechanistic Insight into Initiation and Chain Transfer Reaction of CO<sub>2</sub>/Cyclohexene Oxide Copolymerization Catalyzed by Zinc-Cobalt Double Metal Cyanide Complex Catalysts. *J. Polym. Sci., Part A: Polym. Chem.* **2012**, *50*, 2924–2934.
- (210) Wei, R.-J.; Zhang, X.-H.; Du, B.-Y.; Fan, Z.-Q.; Qi, G.-R. Selective Production of Poly(carbonate-co-ether) over Cyclic Carbonate for Epichlorohydrin and CO<sub>2</sub> Copolymerization Via Heterogeneous Catalysis of Zn–Co (III) Double Metal Cyanide Complex. *Polymer* **2013**, *54*, 6357–6362.
- (211) Wei, R.-J.; Zhang, X.-H.; Du, B.-Y.; Sun, X.-K.; Fan, Z.-Q.; Qi, G.-R. Highly Regioselective and Alternating Copolymerization of Racemic Styrene Oxide and Carbon Dioxide Via Heterogeneous Double Metal Cyanide Complex Catalyst. *Macromolecules* **2013**, *46*, 3693–3697.
- (212) Wei, R.-J.; Zhang, X.-H.; Zhang, Y.-Y.; Du, B.-Y.; Fan, Z.-Q.; Qi, G.-R. Functional Poly(carbonate-co-ether) Synthesis from Glycidyl Methacrylate/CO<sub>2</sub> Copolymerization Catalyzed by Zn-Co(III) Double Metal Cyanide Complex Catalyst. *RSC Adv.* **2014**, *4*, 3188–3194.
- (213) Sebastian, J.; Srinivas, D. Effects of Method of Preparation on Catalytic Activity of Co–Zn Double-Metal Cyanide Catalysts for Copolymerization of CO<sub>2</sub> and Epoxide. *Appl. Catal., A* **2014**, *482*, 300–308.
- (214) Yi-jun, H.; Guo-rong, Q.; Guan-xi, C. Random Copolymer of Propylene Oxide and Ethylene Oxide Prepared by Double Metal Cyanide Complex Catalyst. *Chin. J. Polym. Sci.* **2002**, *20*, 453–459.
- (215) Gu, Y.; Dong, X.; Sun, D. X. Synthesis of Novel Polyether Polyol by Using Double Metal Cyanide. *J. Macromol. Sci., Part A: Pure Appl. Chem.* **2012**, *49*, 586–590.
- (216) Langanke, J.; Hofmann, J.; Gürtler, C.; Wolf, A. Facile Synthesis of Formaldehyde-Based Polyether(-Carbonate) Polyols. *J. Polym. Sci., Part A: Polym. Chem.* **2015**, *53*, 2071–2074.
- (217) Hager S. L.; Reese, M. M. N.; Neal, B. L. Bayer Material Science Llc.; U.S. Patent 20130210951 A1, 2013.
- (218) Kunst, A.; Löffler, A.; Lutter, H.-D.; Han, W.; Müller, J. BASF SE; U.S. Patent 20110269863 A1, 2011.
- (219) Desroches, M.; Escouvois, M.; Auvergne, R.; Caillol, S.; Boutevin, B. From Vegetable Oils to Polyurethanes: Synthetic Routes to Polyols and Main Industrial Products. *Polym. Rev.* **2012**, *52*, 38–79.
- (220) Hua, Z.; Qi, G.; Chen, S. Ring-Opening Copolymerization of Maleic Anhydride with Propylene Oxide by Double-Metal Cyanide. *J. Appl. Polym. Sci.* **2004**, *93*, 1788–1792.
- (221) Suh, H. S.; Ha, J. Y.; Yoon, J. H.; Ha, C.-S.; Suh, H.; Kim, I. Polyester Polyol Synthesis by Alternating Copolymerization of Propylene Oxide with Cyclic Acid Anhydrides by Using Double Metal Cyanide Catalyst. *React. Funct. Polym.* **2010**, *70*, 288–293.
- (222) Dreyfuss, P. *Poly (tetrahydrofuran)*; CRC Press: New York, 1982; Vol. 8.
- (223) Penczek, S.; Kubisa, P.; Matyjaszewski, K. *Cationic Ring-Opening Polymerization*; Springer-Verlag: Berlin, 1985; Vol. I, II.
- (224) Penczek, S. Cationic Ring-Opening Polymerization (CROP) Major Mechanistic Phenomena. *J. Polym. Sci., Part A: Polym. Chem.* **2000**, *38*, 1919–1933.
- (225) Kubisa, P. In *Polymer Science: A Comprehensive Reference*; Penczek, S., Grubbs, R. H., Eds.; Elsevier: Amsterdam, 2012; Vol. 4, pp 141–163.
- (226) Hoogenboom, R. *Handbook of Ring-Opening Polymerization*; Wiley Online Library: Weinheim, 2009; Vol. 6.
- (227) Kobayashi, S.; Morikawa, K.; Saegusa, T. Superacids and Their Derivatives. X. Mechanistic Studies of Selective Cyclodimerization of Ethylene Oxide by Superacid Ester Catalysts. *Polym. J.* **1979**, *11*, 405–412.
- (228) Kern, R. J. Twelve-membered Polyether Rings. Cyclic Tetramers of some Olefin Oxides. *J. Org. Chem.* **1968**, *33*, 388–390.
- (229) Penczek, S.; Kubisa, P.; Szymański, R. Activated Monomer Propagation in Cationic Polymerizations. *Makromol. Chem., Macromol. Symp.* **1986**, *3*, 203–220.
- (230) Kubisa, P.; Penczek, S. Cationic Activated Monomer Polymerization of Heterocyclic Monomers. *Prog. Polym. Sci.* **1999**, *24*, 1409–1437.
- (231) Goethals, E. J. Cationic Polymerization and Related Processes: Proceedings of 6th International Symposium Held in Ghent, Belgium, 30. Aug. 02. Sept. 1983, Acad. Pr.: London, 1984.
- (232) Brzezińska, K.; Szymański, R.; Kubisa, P.; Penczek, S. Activated Monomer Mechanism in Cationic Polymerization, 1. Ethylene Oxide, Formulation of Mechanism. *Makromol. Chem., Rapid Commun.* **1986**, *7*, 1–4.
- (233) Kubisa, P.; Bednarek, M.; Biedroń, T.; Biela, T.; Penczek, S. Progress in Activated Monomer Polymerization. Kinetics of AM Polymerization. *Macromol. Symp.* **2000**, *153*, 217–226.
- (234) Biedron, T.; Brzezinska, K.; Kubisa, P.; Penczek, S. Macromonomers by Activated Polymerization of Oxiranes. Synthesis and Polymerization. *Polym. Int.* **1995**, *36*, 73–80.
- (235) Huang, W.; Zhou, Y.; Yan, D. Direct Synthesis of Amphiphilic Block Copolymers from Glycidyl Methacrylate and Poly(ethylene glycol) by Cationic Ring-Opening Polymerization and Supramolecular Self-Assembly thereof. *J. Polym. Sci., Part A: Polym. Chem.* **2005**, *43*, 2038–2047.
- (236) Bednarek, M.; Kubisa, P.; Penczek, S. Coexistence of Activated Monomer and Active Chain End Mechanisms in Cationic Copolymerization of Tetrahydrofuran with Ethylene Oxide. *Macromolecules* **1999**, *32*, 5257–5263.
- (237) Yahiaoui, A.; Hachemaoui, A.; Belbachir, M. Cationic Polymerization of Ethylene Oxide with Maghnite-H as a Clay Catalyst in the Presence of Ethylene Glycol. *J. Appl. Polym. Sci.* **2009**, *113*, 535–540.
- (238) Kubisa, P. *Cationic Polymerization of Heterocyclics, in Cationic Polymerizations*; Marcel Dekker: New York, 1996.
- (239) Thompson, M. S.; Vadala, T. P.; Vadala, M. L.; Lin, Y.; Riffle, J. S. Synthesis and Applications of Heterobifunctional Poly(ethylene oxide) Oligomers. *Polymer* **2008**, *49*, 345–373.
- (240) Tasdelen, M. A.; Kahveci, M. U.; Yagci, Y. Telechelic Polymers by Living and Controlled/Living Polymerization Methods. *Prog. Polym. Sci.* **2011**, *36*, 455–567.
- (241) Obermeier, B.; Wurm, F.; Mangold, C.; Frey, H. Multifunctional Poly(ethylene glycol)s. *Angew. Chem., Int. Ed.* **2011**, *50*, 7988–7997.
- (242) Barthel, M. J.; Schacher, F. H.; Schubert, U. S. Poly(ethylene oxide) (PEO)-Based ABC Triblock Terpolymers – Synthetic Complexity vs. Application Benefits. *Polym. Chem.* **2014**, *5*, 2647–2662.
- (243) Yang, S.; Kim, Y.; Kim, H. C.; Siddique, A. B.; Youn, G.; Kim, H. J.; Park, H. J.; Lee, J. Y.; Kim, S.; Kim, J. Azide-Based Heterobifunctional Poly(ethylene oxide)s: Na<sub>2</sub>-Initiated “Living” Polymerization of Ethylene Oxide and Chain End Functionalizations. *Polym. Chem.* **2016**, DOI: 10.1039/C5PY01444A.
- (244) Odian, G. *Principles of Polymerization*; John Wiley & Sons, Inc.: New York, 2004; pp 544–618.
- (245) Cammas, S.; Nagasaki, Y.; Kataoka, K. Heterobifunctional Poly(ethylene oxide): Synthesis Of Alpha-Methoxy-Omega-Amino and Alpha-Hydroxy-Omega-Amino PEOs with the same Molecular Weights. *Bioconjugate Chem.* **1995**, *6*, 226–230.

- (246) Yue, J.; Li, X.; Mo, G.; Wang, R.; Huang, Y.; Jing, X. Modular Functionalization of Amphiphilic Block Copolymers via Radical-mediated Thiol-ene Reaction. *Macromolecules* **2010**, *43*, 9645–9654.
- (247) Studer, P.; Breton, P.; Riess, G. Allyl End-functionalized Poly(ethylene oxide)-block-Poly(methylene malonate 2.1.2) Block Copolymers: Synthesis, Characterization, and Chemical Modification. *Macromol. Chem. Phys.* **2005**, *206*, 2461–2469.
- (248) Pozza, G. M. E.; Barthel, M. J.; Crotty, S.; Vitz, J.; Schacher, F. H.; Lutz, P. J.; Schubert, U. S. Precise Synthesis of Undecenyl Poly(ethylene oxide) Macromonomers as Heterofunctional Building Blocks for the Synthesis of Linear Diblocks or of Branched Materials. *Eur. Polym. J.* **2014**, *57*, 221–236.
- (249) Wilms, V. S.; Bauer, H.; Tonhauser, C.; Schilman, A. M.; Müller, M. C.; Tremel, W.; Frey, H. Catechol-initiated Polyethers: Multifunctional Hydrophilic Ligands for PEGylation and Functionalization of Metal Oxide Nanoparticles. *Biomacromolecules* **2013**, *14*, 193–199.
- (250) Thomas, A.; Bauer, H.; Schilman, A.-M.; Fischer, K.; Tremel, W.; Frey, H. The “Needle in the Haystack” makes the Difference: Linear and Hyperbranched Polyglycerols with a Single Catechol Moiety for Metal Oxide Nanoparticle Coating. *Macromolecules* **2014**, *47*, 4557–4566.
- (251) Hofmann, A. M.; Wurm, F.; Frey, H. Rapid Access to Polyfunctional Lipids with Complex Architecture via Oxyanionic Ring-Opening Polymerization. *Macromolecules* **2011**, *44*, 4648–4657.
- (252) Hofmann, A. M.; Wurm, F.; Hühn, E.; Nawroth, T.; Langguth, P.; Frey, H. Hyperbranched Polyglycerol-Based Lipids via Oxyanionic Polymerization: Toward Multifunctional Stealth Liposomes. *Biomacromolecules* **2010**, *11*, 568–574.
- (253) Fritz, T.; Hirsch, M.; Richter, F. C.; Müller, S. S.; Hofmann, A. M.; Rusitzka, K. A. K.; Markl, J.; Massing, U.; Frey, H.; Helm, M. Click Modification of Multifunctional Liposomes Bearing Hyperbranched Polyether Chains. *Biomacromolecules* **2014**, *15*, 2440–2448.
- (254) Mohr, K.; Müller, S. S.; Müller, L. K.; Rusitzka, K.; Gietzen, S.; Frey, H.; Schmidt, M. Evaluation of Multifunctional Liposomes in Human Blood Serum by Light Scattering. *Langmuir* **2014**, *30*, 14954–14962.
- (255) Bakardzhiev, P.; Rangelov, S.; Trzebicka, B.; Momekova, D.; Lalev, G.; Garamus, V. M. Nanostructures by Self-Assembly of Polyglycidol-Derivatized Lipids. *RSC Adv.* **2014**, *4*, 37208–37219.
- (256) Mosquet, M.; Chevalier, Y.; Le Perchec, P.; Guicquero, J.-P. Synthesis of Poly(ethylene oxide) with a Terminal Amino Group by Anionic Polymerization of Ethylene Oxide Initiated by Amino-alcoholates. *Macromol. Chem. Phys.* **1997**, *198*, 2457–2474.
- (257) Mangold, C.; Wurm, F.; Obermeier, B.; Frey, H. Hetero-Multifunctional Poly(ethylene glycol) Copolymers with Multiple Hydroxyl Groups and a Single Terminal Functionality. *Macromol. Rapid Commun.* **2010**, *31*, 258–264.
- (258) Wurm, F.; Klos, J.; Räder, H. J.; Frey, H. Synthesis and Noncovalent Protein Conjugation of Linear-Hyperbranched PEG-Poly(glycerol)  $\alpha,\omega_n$ -Telechelics. *J. Am. Chem. Soc.* **2009**, *131*, 7954–7955.
- (259) Li, Z.; Chau, Y. Synthesis of X(Y)-(EO)(N)-OCH(3) Type Heterobifunctional and X(Y)-(EO)(N)-Z Type Heterotrifunctional Poly(ethylene glycol)s. *Bioconjugate Chem.* **2011**, *22*, 518–522.
- (260) Dingels, C.; Müller, S. S.; Steinbach, T.; Tonhauser, C.; Frey, H. Universal Concept for the Implementation of a Single Cleavable Unit at Tunable Position in Functional Poly(ethylene glycol)s. *Biomacromolecules* **2013**, *14*, 448–459.
- (261) Li, Z.; Chau, Y. Synthesis of Heterobifunctional Poly(ethylene glycol)s by an Acetal Protection Method. *Polym. Chem.* **2010**, *1*, 1599.
- (262) Hiki, S.; Kataoka, K. Versatile and Selective Synthesis of “Click Chemistry” Compatible Heterobifunctional Poly(ethylene glycol)s Possessing Azide and Alkyne Functionalities. *Bioconjugate Chem.* **2010**, *21*, 248–254.
- (263) Otsuka, H.; Nagasaki, Y.; Kataoka, K. Characterization of Aldehyde-PEG Tethered Surfaces: Influence of PEG Chain Length on the Specific Biorecognition. *Langmuir* **2004**, *20*, 11285–11287.
- (264) Xie, Y.; Duan, S.; Forrest, M. L. Alkyne- and 1,6-Elimination-Succinimidyl Carbonate - Terminated Heterobifunctional Poly(ethylene glycol) for Reversible “Click” PEGylation. *Drug Discovery Ther.* **2010**, *4*, 240–245.
- (265) Thomas, A.; Niederer, K.; Wurm, F.; Frey, H. Combining Oxyanionic Polymerization and Click-Chemistry: A General Strategy for the Synthesis of Polyether Polyol Macromonomers. *Polym. Chem.* **2014**, *5*, 899–909.
- (266) Ishii, T.; Yamada, M.; Hirase, T.; Nagasaki, Y. New Synthesis of Heterobifunctional Poly(ethylene glycol) Possessing a Pyridyl Disulfide at one End and a Carboxylic Acid at the other End. *Polym. J.* **2005**, *37*, 221–228.
- (267) Hayashi, H.; Iijima, M.; Kataoka, K.; Nagasaki, Y. pH-Sensitive Nanogel Possessing Reactive PEG Tethered Chains on the Surface. *Macromolecules* **2004**, *37*, 5389–5396.
- (268) Yagci, Y.; Ito, K. Macromolecular Architecture Based on Anionically Prepared Poly(ethylene oxide) Macromonomers. *Macromol. Symp.* **2005**, *226*, 87–96.
- (269) Obermeier, B.; Wurm, F.; Frey, H. Amino Functional Poly(ethylene glycol) Copolymers via Protected Amino Glycidol. *Macromolecules* **2010**, *43*, 2244–2251.
- (270) Lee, B. F.; Kade, M. J.; Chute, J. A.; Gupta, N.; Campos, L. M.; Fredrickson, G. H.; Kramer, E. J.; Lynd, N. A.; Hawker, C. J. Poly(allyl glycidyl ether) - a Versatile and Functional Polyether Platform. *J. Polym. Sci., Part A: Polym. Chem.* **2011**, *49*, 4498–4504.
- (271) Lee, B. F.; Wolffs, M.; Delaney, K. T.; Sprafke, J. K.; Leibfarth, F. A.; Hawker, C. J.; Lynd, N. A. Reactivity Ratios, and Mechanistic Insight for Anionic Ring-Opening Copolymerization of Epoxides. *Macromolecules* **2012**, *45*, 3722–3731.
- (272) Koyama, Y.; Umehara, M.; Mizuno, A.; Itaba, M.; Yasukouchi, T.; Natsume, K.; Suginaka, A. Synthesis of Novel Poly(ethylene glycol) Derivatives having Pendant Amino Groups and Aggregating Behavior of its Mixture with Fatty Acid in Water. *Bioconjugate Chem.* **1996**, *7*, 298–301.
- (273) Obermeier, B.; Frey, H. Poly(ethylene glycol-co-allyl glycidyl ether)s: A PEG-based Modular Synthetic Platform for Multiple Bioconjugation. *Bioconjugate Chem.* **2011**, *22*, 436–444.
- (274) Mangold, C.; Dingels, C.; Obermeier, B.; Frey, H.; Wurm, F. PEG-based Multifunctional Polyethers with Highly Reactive Vinyl-Ether Side Chains for Click-Type Functionalization. *Macromolecules* **2011**, *44*, 6326–6334.
- (275) Mangold, C.; Obermeier, B.; Wurm, F.; Frey, H. From an Epoxide Monomer Toolkit to Functional PEG Copolymers with Adjustable LCST Behavior. *Macromol. Rapid Commun.* **2011**, *32*, 1930–1934.
- (276) Sokolovskaya, E.; Yoon, J.; Misra, A. C.; Bräse, S.; Lahann, J. Controlled Microstructuring of Janus Particles Based on a Multifunctional Poly(ethylene glycol). *Macromol. Rapid Commun.* **2013**, *34*, 1554–1559.
- (277) Barthel, M. J.; Mansfeld, U.; Hoepfener, S.; Czaplowska, J. A.; Schacher, F. H.; Schubert, U. S. Understanding and Tuning the Self-Assembly of Polyether-Based Triblock Terpolymers in Aqueous Solution. *Soft Matter* **2013**, *9*, 3509–3520.
- (278) Hrubý, M.; Koňák, Č.; Ulbrich, K. Poly(allyl glycidyl ether)-Block-Poly(ethylene oxide): A Novel Promising Polymeric Intermediate for the Preparation of Micellar Drug Delivery Systems. *J. Appl. Polym. Sci.* **2005**, *95*, 201–211.
- (279) Vetrík, D.; Hrubý, M.; Hovorka, O.; Etrych, T.; Vetrík, M.; Kovar, L.; Kovar, M.; Ulbrich, K.; Rihova, B. Biological Evaluation of Polymeric Micelles with Covalently Bound Doxorubicin. *Bioconjugate Chem.* **2009**, *20*, 2090–2097.
- (280) Huang, J.; Li, Z.; Xu, X.; Ren, Y.; Huang, J. Preparation of Novel Poly(ethylene oxide-co-glycidol)-graft-Poly( $\epsilon$ -caprolactone) Copolymers and Inclusion Complexation of the Grafted Chains with  $\alpha$ -Cyclodextrin. *J. Polym. Sci., Part A: Polym. Chem.* **2006**, *44*, 3684–3691.
- (281) Southan, A.; Hoch, E.; Schönhaar, V.; Borchers, K.; Schuh, C.; Müller, M.; Bach, M.; Tovar, G. E. M. Side Chain Thiol-Functionalized Poly(ethylene glycol) by Post-Polymerization Modification of Hydroxyl

- Groups: Synthesis, Crosslinking and Inkjet Printing. *Polym. Chem.* **2014**, *5*, 5350–5359.
- (282) Mangold, C.; Wurm, F.; Obermeier, B.; Frey, H. Functional Poly(ethylene glycol)<sup>+</sup>: PEG-Based Random Copolymers with 1,2-Diol Side Chains and Terminal Amino Functionality. *Macromolecules* **2010**, *43*, 8511–8518.
- (283) Wurm, F.; Nieberle, J.; Frey, H. Synthesis and Characterization of Poly (glyceryl glycerol) Block Copolymers. *Macromolecules* **2008**, *41*, 1909–1911.
- (284) Rangelov, S.; Almgren, M.; Tsvetanov, C.; Edwards, K. Synthesis, Characterization, and Aggregation Behavior of Block Copolymers Bearing Blocks of Lipid-Mimetic Aliphatic Double Chain Units. *Macromolecules* **2002**, *35*, 4770–4778.
- (285) Rangelov, S.; Almgren, M.; Edwards, K.; Tsvetanov, C. Formation of Normal and Reverse Bilayer Structures by Self-Assembly of Nonionic Block Copolymers Bearing Lipid-Mimetic Units. *J. Phys. Chem. B* **2004**, *108*, 7542–7552.
- (286) Rangelov, S.; Petrova, E.; Berlinova, L. V.; Tsvetanov, C. Synthesis and Polymerization of Novel Oxirane Bearing an Aliphatic Double Chain Moiety. *Polymer* **2001**, *42*, 4483–4491.
- (287) Tonhauser, C.; Schill, C.; Dingels, C.; Frey, H. Branched Acid-Degradable, Biocompatible Polyether Copolymers via Anionic Ring-Opening Polymerization Using an Epoxide Inimer. *ACS Macro Lett.* **2012**, *1*, 1094–1097.
- (288) Sheno, R. A.; Lai, B. F.; Imran ul-haq, M.; Brooks, D. E.; Kizhakkedathu, J. N. Biodegradable Polyglycerols with Randomly Distributed Ketal Groups as Multi-Functional Drug Delivery Systems. *Biomaterials* **2013**, *34*, 6068–6081.
- (289) Sheno, R. A.; Narayanannair, J. K.; Hamilton, J. L.; Lai, B. F.; Horte, S.; Kainthan, R. K.; Varghese, J. P.; Rajeev, K. G.; Manoharan, M.; Kizhakkedathu, J. N. Branched Multifunctional Polyether Polyketals: Variation of Ketal Group Structure Enables Unprecedented Control over Polymer Degradation in Solution and within Cells. *J. Am. Chem. Soc.* **2012**, *134*, 14945–14957.
- (290) Son, S.; Shin, E.; Kim, B. S. Redox-Degradable Biocompatible Hyperbranched Polyglycerols: Synthesis, Copolymerization Kinetics, Degradation, and Biocompatibility. *Macromolecules* **2015**, *48*, 600–609.
- (291) Elbert, J.; Didzoleit, H.; Fasel, C.; Ionescu, E.; Riedel, R.; Stihl, B.; Gallei, M. Surface-Initiated Anionic Polymerization of [1]-Silaferrrocenophanes for the Preparation of Colloidal Preceramic Materials. *Macromol. Rapid Commun.* **2015**, *36*, 597–603.
- (292) Tonhauser, C.; Alkan, A.; Schömer, M.; Dingels, C.; Ritz, S.; Mailänder, V.; Frey, H.; Wurm, F. R. Ferrocenyl Glycidyl Ether: A Versatile Ferrocene Monomer for Copolymerization with Ethylene Oxide to Water-Soluble, Thermoresponsive Copolymers. *Macromolecules* **2013**, *46*, 647–655.
- (293) Alkan, A.; Natalello, A.; Wagner, M.; Frey, H.; Wurm, F. R. Ferrocene-Containing Multifunctional Polyethers: Monomer Sequence Monitoring via Quantitative <sup>13</sup>C NMR Spectroscopy in Bulk. *Macromolecules* **2014**, *47*, 2242–2249.
- (294) Alkan, A.; Thomi, L.; Gleede, T.; Wurm, F. R. Vinyl Ferrocenyl Glycidyl Ether: An Unprotected Orthogonal Ferrocene Monomer for Anionic and Radical Polymerization. *Polym. Chem.* **2015**, *6*, 3617–3624.
- (295) Lee, A.; Lundberg, P.; Klinger, D.; Lee, B. F.; Hawker, C. J.; Lynd, N. A. Physiologically Relevant, pH-Responsive PEG-Based Block and Statistical Copolymers with *N,N*-Diisopropylamine Units. *Polym. Chem.* **2013**, *4*, 5735–5742.
- (296) Barthel, M. J.; Rudolph, T.; Crotty, S.; Schacher, F. H.; Schubert, U. S. Homo- and Diblock Copolymers of Poly(furfuryl glycidyl ether) by Living Anionic Polymerization: Toward Reversibly Core-Crosslinked Micelles. *J. Polym. Sci., Part A: Polym. Chem.* **2012**, *50*, 4958–4965.
- (297) Barthel, M. J.; Rudolph, T.; Teichler, A.; Paulus, R. M.; Vitz, J.; Hoepfner, S.; Hager, M. D.; Schacher, F. H.; Schubert, U. S. Self-Healing Materials Via Reversible Crosslinking of Poly(ethylene oxide)-*block*-Poly(furfuryl glycidyl ether) (PEO-*b*-PFGE) Block Copolymer Films. *Adv. Funct. Mater.* **2013**, *23*, 4921–4932.
- (298) Hörenz, C.; Rudolph, T.; Barthel, M. J.; Günther, U.; Schacher, F. H. Amphiphilic Polyether-Based Block Copolymers as Crosslinkable Ligands for Au-Nanoparticles. *Polym. Chem.* **2015**, *6*, 5633–5642.
- (299) Wagner, M.; Barthel, M. J.; Freund, R. R. A.; Hoepfner, S.; Traeger, A.; Schacher, F. H.; Schubert, U. S. Solution Self-Assembly of Poly(ethylene oxide)-*block*-Poly(furfuryl glycidyl ether)-*Block*-Poly(allyl glycidyl ether) Based Triblock Terpolymers: A Field-Flow Fractionation Study. *Polym. Chem.* **2014**, *5*, 6943–6956.
- (300) Moers, C.; Wrazidlo, R.; Natalello, A.; Netz, I.; Mondeshki, M.; Frey, H. 1-Adamantyl)Methyl Glycidyl Ether: A Versatile Building Block for Living Polymerization. *Macromol. Rapid Commun.* **2014**, *35*, 1075–1080.
- (301) Moers, C.; Nuhn, L.; Wissel, M.; Stangenberg, R.; Mondeshki, M.; Berger-Nicoletti, E.; Thomas, A.; Schaeffel, D.; Koynov, K.; Klapper, M.; et al. Supramolecular Linear-*g*-Hyperbranched Graft Polymers: Topology and Binding Strength of Hyperbranched Side Chains. *Macromolecules* **2013**, *46*, 9544–9553.
- (302) Niederer, K.; Schuell, C.; Leibig, D.; Johann, T.; Frey, H. *Catechol-Acetonide Glycidyl Ether (CAGE): A Functional Epoxide Monomer for Linear and Hyperbranched Multi-Catechol Functional Polyether Architectures*; 2015, submitted.
- (303) Liu, Y.; Wei, W.; Xiong, H. Polyether Based Side-Chain Liquid Crystalline Polymers: Anionic Polymerization and Phase Structures. *Polymer* **2013**, *54*, 6572–6579.
- (304) Peris, S.; Tylkowski, B.; Carles Ronda, J.; Garcia-Valls, R.; Reina, J. A.; Giamberini, M. Synthesis, Characterization, and Photoresponsive Behavior of New Azobenzene-Containing Polyethers. *J. Polym. Sci., Part A: Polym. Chem.* **2009**, *47*, 5426–5436.
- (305) Ramirez, S. M.; Layman, J. M.; Bissel, P.; Long, T. E. Ring-Opening Polymerization of Imidazole Epoxides for the Synthesis of Imidazole-Substituted Poly(ethylene oxides). *Macromolecules* **2009**, *42*, 8010–8012.
- (306) Benhabbour, S.; Chapman, R.; Scharfenberger, G.; Meyer, W. H.; Goward, G. Study of Imidazole-Based Proton-Conducting Composite Materials Using Solid-State NMR. *Chem. Mater.* **2005**, *17*, 1605–1612.
- (307) Zhou, Z.-h.; Yang, H.-j.; Chen, M.; Lou, C.-f.; Zhang, Y.-z.; Chen, K.-p.; Wang, Y.; Yu, M.-l.; Yu, F.; Li, J.-y. Comparative Proteomic Analysis between the Domesticated Silkworm (*Bombyx Mori*) Reared on Fresh Mulberry Leaves and on Artificial Diet. *J. Proteome Res.* **2008**, *7*, 5103–5111.
- (308) xxDallas, A.; Vlassov, A. V. nai: A Novel Antisense Technology and its Therapeutic Potential. *Medical Science Monitor* **2006**, *12*, RA67–RA74.
- (309) Sokolovskaya, E.; Barner, L.; Bräse, S.; Lahann, J. Synthesis and on-Demand Gelation of Multifunctional Poly(ethylene glycol)-Based Polymers. *Macromol. Rapid Commun.* **2014**, *35*, 780–786.
- (310) Hagiwara, T.; Terasaki, Y.; Hamana, H.; Narita, T.; Umezawa, J.; Furuhashi, K. Polymerization of 3,3,3-Trifluoro-1,2-Epoxypropane with Organozinc Compounds and Alkali Metal Alkoxides. *Makromol. Chem., Rapid Commun.* **1992**, *13*, 363–370.
- (311) Umezawa, J.; Hagiwara, T.; Hamana, H.; Narita, T.; Furuhashi, K.; Nohira, H. Copolymerization of 3,3,3-Trifluoro-1,2-Epoxypropane with 1,2-Epoxypropane Using Organozinc Compounds. *Macromolecules* **1995**, *28*, 833–837.
- (312) Wilms, V. S.; Frey, H. Aminofunctional Polyethers: Smart Materials for Applications in Solution and on Surfaces. *Polym. Int.* **2013**, *62*, 849–859.
- (313) Reuss, V. S.; Werre, M.; Frey, H. Thermoresponsive Copolymers of Ethylene Oxide and *N,N*-Diethyl Glycidyl Amine: Polyether Polyelectrolytes and PEGylated Gold Nanoparticle Formation. *Macromol. Rapid Commun.* **2012**, *33*, 1556–1561.
- (314) Kurzbach, D.; Wilms, V. S.; Frey, H.; Hinderberger, D. Impact of Amino-Functionalization on the Response of Poly(ethylene glycol) (PEG) to External Stimuli. *ACS Macro Lett.* **2013**, *2*, 128–131.
- (315) Herzberger, J.; Kurzbach, D.; Werre, M.; Fischer, K.; Hinderberger, D.; Frey, H. Stimuli-Responsive Tertiary Amine Functional PEGs Based On *N,N*-Dialkylglycidylamines. *Macromolecules* **2014**, *47*, 7679–7690.

- (316) Xu, F. J.; Yang, W. T. Polymer Vectors via Controlled/Living Radical Polymerization for Gene Delivery. *Prog. Polym. Sci.* **2011**, *36*, 1099–1131.
- (317) Yoshikawa, K.; Yoshikawa, Y.; Koyama, Y.; Kanbe, T. Highly Effective Compaction of Long Duplex DNA Induced by Polyethylene Glycol with Pendant Amino Groups. *J. Am. Chem. Soc.* **1997**, *119*, 6473–6477.
- (318) Li, Z.; Chau, Y. Synthesis of Linear Polyether Polyol Derivatives as New Materials for Bioconjugation. *Bioconjugate Chem.* **2009**, *20*, 780–789.
- (319) Reuss, V. S.; Obermeier, B.; Dingels, C.; Frey, H. *N,N*-Diallylglycidylamine: A Key Monomer for Amino-Functional Poly(ethylene glycol) Architectures. *Macromolecules* **2012**, *45*, 4581–4589.
- (320) Hans, M.; Keul, H.; Möller, M. Chain Transfer Reactions Limit the Molecular Weight of Polyglycidol Prepared via Alkali Metal Based Initiating Systems. *Polymer* **2009**, *50*, 1103–1108.
- (321) Ponomarenko, V. A.; Khomutov, A. M.; Il'chenko, S. I.; Ignatenko, A. V. The Effect of Substituents of the Anionic Polymerization of *A*-Oxides. *Polym. Sci. U.S.S.R.* **1971**, *13*, 1735–1740.
- (322) Wei, P. E.; Butler, P. E. Synthesis and Polymerization Studies of Several Chloro and Cyano Epoxides. *J. Polym. Sci., Part A-1: Polym. Chem.* **1968**, *6*, 2461–2475.
- (323) Cantor, S. E.; Brindell, G. D.; Brett, T. J. Synthesis and Polymerization Studies of Cyano Epoxides. *J. Macromol. Sci., Chem.* **1973**, *7*, 1483–1508.
- (324) Burness, D. M.; Bayer, H. O. Synthesis and Reactions of Quaternary Salts of Glycidyl Amines. *J. Org. Chem.* **1963**, *28*, 2283–2288.
- (325) Huval, C.; Bailey, M.; Holmes-Farley, S. R.; Mandeville, W. H.; Miller-Gilmore, K.; Sacchiero, R.; Dhal, P. Amine Functionalized Polyethers as Bile Acid Sequestrants: Synthesis and Biological Evaluation. *J. Macromol. Sci., Part A: Pure Appl. Chem.* **2001**, *38*, 1559–1574.
- (326) Thavanesan, T.; Herbert, C.; Plamper, F. A. Insight in the Phase Separation Peculiarities of Poly(dialkylaminoethyl methacrylate)s. *Langmuir* **2014**, *30*, 5609–5619.
- (327) Kurzbach, D.; Schömer, M.; Wilms, V. S.; Frey, H.; Hinderberger, D. How Structure-Related Collapse Mechanisms Determine Nanoscale Inhomogeneities in Thermoresponsive Polymers. *Macromolecules* **2012**, *45*, 7535–7548.
- (328) Rangelov, S.; Tsvetanov, C. Towards the Synthesis of Amino-Substituted Epoxides: Synthesis and Characterization of Glycidylidido-dicylamine. *Des. Monomers Polym.* **2001**, *4*, 39–43.
- (329) Mecerreyes, D. Polymeric Ionic Liquids: Broadening the Properties and Applications of Polyelectrolytes. *Prog. Polym. Sci.* **2011**, *36*, 1629–1648.
- (330) Hu, H.; Yuan, W.; Jia, Z.; Baker, G. L. Ionic Liquid-Based Random Copolymers: A New Type of Polymer Electrolyte with Low Glass Transition Temperature. *RSC Adv.* **2015**, *5*, 3135–3140.
- (331) Lundberg, P.; Lynd, N. A.; Zhang, Y.; Zeng, X.; Krogstad, D. V.; Paffen, T.; Malkoch, M.; Nyström, A. M.; Hawker, C. J. pH-Triggered Self-Assembly of Biocompatible Histamine-Functionalized Triblock Copolymers. *Soft Matter* **2013**, *9*, 82–89.
- (332) Hrubý, M.; Koňák, Č.; Ulbrich, K. Polymeric Micellar pH-Sensitive Drug Delivery System for Doxorubicin. *J. Controlled Release* **2005**, *103*, 137–148.
- (333) Zhou, L.; Cheng, R.; Tao, H.; Ma, S.; Guo, W.; Meng, F.; Liu, H.; Liu, Z.; Zhong, Z. Endosomal pH-Activatable Poly(ethylene oxide)-*graft*-Doxorubicin Prodrugs: Synthesis, Drug Release, and Biodistribution in Tumor-Bearing Mice. *Biomacromolecules* **2011**, *12*, 1460–1467.
- (334) Fox, T. G. Influence of Diluents and of Copolymer Composition on the Glass Temperature of a Polymer System. *Bull. Am. Phys. Soc.* **1956**, *1*, 123–132.
- (335) Zhang, W.; Allgaier, J.; Zorn, R.; Willbold, S. Determination of the Compositional Profile for Tapered Copolymers of Ethylene Oxide and 1,2-Butylene Oxide by in-Situ-NMR. *Macromolecules* **2013**, *46*, 3931–3938.
- (336) Bailey, F. E.; Koleske, J. V. *Alkylene Oxides and Their Polymers*; Surfactant Science Ser. Vol. 35; CRC Press: Boca Raton, FL, 1990.
- (337) Cracknell, R. Oil Soluble Polyethers in Automotive Crankcase Lubricants. *Lubr. Eng.* **1993**, *49*, 129–136.
- (338) Thio, Y.; Wu, J.; Bates, F. Epoxy Toughening Using Low Molecular Weight Poly(hexylene oxide)-Poly(ethylene oxide) Diblock Copolymers. *Macromolecules* **2006**, *39*, 7187–7189.
- (339) Hamley, I.; O'Driscoll, B.; Lotze, G.; Moulton, C.; Allgaier, J.; Frielinghaus, H. Highly Asymmetric Phase Diagram of a Poly(1,2-octylene oxide)-Poly(ethylene oxide) Diblock Copolymer System Comprising a Brush-Like Poly(1,2-octylene oxide) Block. *Macromol. Rapid Commun.* **2009**, *30*, 2141–2146.
- (340) Gerstl, C.; Schneider, G.; Pyckhout-Hintzen, W.; Allgaier, J.; Richter, D.; Alegria, A.; Colmenero, J. Segmental and Normal Mode Relaxation of Poly(alkylene oxide)s Studied by Dielectric Spectroscopy and Rheology. *Macromolecules* **2010**, *43*, 4968–4977.
- (341) Ponomarenko, V. A.; Khomutov, A. M.; Ilchenko, S. I.; Ignatenk, A. V. Influence of Substituted Groups on Anionic Polymerization of Alpha-Oxides. *Vysokomol. Soedin. A* **1971**, *13*, 1546–1556.
- (342) Ponomarenko, V. A.; Khomutov, A. M.; Ilchenko, S. I.; Ignatenk, A. V.; Khomutov, N. M. Influence of Substituted Groups on Reactivity of Monosubstituted Ethylene Oxide During Coordination-Anionic Copolymerization. *Vysokomol. Soedin. A* **1971**, *13*, 1551–1561.
- (343) Stolarzewicz, A.; Neugebauer, D. Influence of Substituent on the Polymerization of Oxiranes by Potassium Hydride. *Macromol. Chem. Phys.* **1999**, *200*, 2467–2470.
- (344) Oguni, N.; Lee, K.; Tani, H. Microstructure Analysis of Poly(propylene oxide) by <sup>13</sup>C Nuclear Magnetic Resonance Spectroscopy. *Macromolecules* **1972**, *5*, 819–820.
- (345) Schilling, F.; Tonelli, A. Carbon-13 NMR Determination of Poly(propylene oxide) Microstructure. *Macromolecules* **1986**, *19*, 1337–1343.
- (346) Chisholm, M. H.; Navarro-Llobet, D. NMR Assignments of Regioregular Poly(propylene oxide) at the Triad and Tetrad Level. *Macromolecules* **2002**, *35*, 2389–2392.
- (347) Childers, M.; Longo, J.; Van Zee, N.; LaPointe, A.; Coates, G. Stereoselective Epoxide Polymerization and Copolymerization. *Chem. Rev.* **2014**, *114*, 8129–8152.
- (348) Allgaier, J.; Willbold, S.; Chang, T. Synthesis of Hydrophobic Poly(alkylene oxide)s and Amphiphilic Poly(alkylene oxide) Block Copolymers. *Macromolecules* **2007**, *40*, 518–525.
- (349) Gerstl, C.; Schneider, G.; Pyckhout-Hintzen, W.; Allgaier, J.; Willbold, S.; Hofmann, D.; Disko, U.; Frielinghaus, H.; Richter, D. Chain Conformation of Poly(alkylene oxide)s Studied by Small-Angle Neutron Scattering. *Macromolecules* **2011**, *44*, 6077–6084.
- (350) Gerstl, C.; Schneider, G.; Fuxman, A.; Zamponi, M.; Frick, B.; Seydel, T.; Koza, M.; Genix, A.; Allgaier, J.; Richter, D.; et al. Quasielastic Neutron Scattering Study on the Dynamics of Poly(alkylene oxide)s. *Macromolecules* **2012**, *45*, 4394–4405.
- (351) Liu, Y.; Wei, W.; Xiong, H. Gradient and Block Side-Chain Liquid Crystalline Polyethers. *Polym. Chem.* **2015**, *6*, 583–590.
- (352) Malik, M.; Trathnigg, B.; Kappe, C. Selectivity of PEO-*block*-PPO Diblock Copolymers Non the Microwave-Accelerated, Anionic Ring-Opening Polymerization of Propylene Oxide with PEG as Initiator. *Macromol. Chem. Phys.* **2007**, *208*, 2510–2524.
- (353) Malik, M.; Trathnigg, B.; Kappe, C. Microwave Assisted Synthesis and Characterization of End Functionalized Poly(propylene oxide) as Model Compounds. *Eur. Polym. J.* **2008**, *44*, 144–154.
- (354) Malik, M.; Trathnigg, B.; Kappe, C. Microwave-Assisted Polymerization of Higher Alkylene Oxides. *Eur. Polym. J.* **2009**, *45*, 899–910.
- (355) Dulle, M.; Malik, M.; Trathnigg, B.; Glatter, O. Self-Assembly and Structural Analysis of Multiblock Poly(oxyalkylene) Copolymers. *Macromolecules* **2010**, *43*, 7868–7871.
- (356) Petrov, P.; Berlinova, I. V.; Tsvetanov, C.; Rosselli, S.; Schmid, A.; Zilaei, A.; Miteva, T.; Durr, M.; Yasuda, A.; Nelles, G. High-Molecular-Weight Polyoxirane Copolymers and Their Use in High-Performance Dye-Sensitized Solar Cells. *Macromol. Mater. Eng.* **2008**, *293*, 598–604.
- (357) Sun, W.; Ding, J.; Mobbs, R.; Heatley, F.; Attwood, D.; Booth, C. Preparation of a Diblock Copoly(oxybutylene oxyethylene) and Study



- of Its Micellisation and Surface-Properties in Dilute Aqueous-Solution. *Colloids Surf.* **1991**, *54*, 103–111.
- (358) Luo, Y.; Nicholas, C.; Attwood, D.; Collett, J.; Price, C.; Booth, C. Micellization and Gelation of Block-Copoly(oxethylene oxybutylene oxyethylene)  $E_{58}B_{17}E_{58}$ . *Colloid Polym. Sci.* **1992**, *270*, 1094–1105.
- (359) Yan, Z.; Yang, Z.; Price, C.; Booth, C. Cyclization of Poly(ethylene glycol)s and Related Block-Copolymers. *Makromol. Chem., Rapid Commun.* **1993**, *14*, 725–732.
- (360) Dickson, S.; Yu, G.; Heatley, F.; Booth, C. Reactivity Ratios for the Anionic Copolymerization of Ethylene-Oxide and Butylene Oxide in Bulk. *Eur. Polym. J.* **1993**, *29*, 281–286.
- (361) Booth, C.; Attwood, D. Effects of Block Architecture and Composition on the Association Properties of Poly(oxyalkylene) Copolymers in Aqueous Solution. *Macromol. Rapid Commun.* **2000**, *21*, 501–527.
- (362) Booth, C.; Attwood, D.; Price, C. Self-Association of Block Copoly(oxyalkylene)s in Aqueous Solution. Effects of Composition, Block Length and Block Architecture. *Phys. Chem. Chem. Phys.* **2006**, *8*, 3612–3622.
- (363) Liang, G.-D.; Xu, J.-T.; Fan, Z.-Q.; Mai, S.-M.; Ryan, A. J. Effect of Substrate and Molecular Weight on the Stability of Thin Films of Semicrystalline Block Copolymers. *Langmuir* **2007**, *23*, 3673–3679.
- (364) Ribeiro, M. E. N. P.; de Oliveira, S. A.; Ricardo, N. M. P. S.; Mai, S.-M.; Attwood, D.; Yeates, S. G.; Booth, C. Diblock Copolymers of Ethylene Oxide and 1,2-Butylene Oxide in Aqueous Solution: Formation of Unimolecular Micelles. *Int. J. Pharm.* **2008**, *362*, 193–196.
- (365) Kelarakis, A.; Chaibundit, C.; Krysmann, M. J.; Havredaki, V.; Viras, K.; Hamley, I. W. Interactions of an Anionic Surfactant with Poly(oxyalkylene) Copolymers in Aqueous Solution. *J. Colloid Interface Sci.* **2009**, *330*, 67–72.
- (366) Smart, T. P.; Ryan, A. J.; Howse, J. R.; Battaglia, G. Homopolymer Induced Aggregation of Poly(ethylene oxide) $_n$ -*b*-Poly(Butylene Oxide) $_m$  Polymersomes. *Langmuir* **2010**, *26*, 7425–7430.
- (367) Cambón, A.; Rey-Rico, A.; Mistry, D.; Brea, J.; Loza, M. I.; Attwood, D.; Barbosa, S.; Alvarez-Lorenzo, C.; Concheiro, A.; Taboada, P.; et al. Doxorubicin-Loaded Micelles of Reverse Poly(butylene oxide)-Poly(ethylene oxide)-Poly(butylene oxide) Block Copolymers as Efficient “Active” Chemotherapeutic Agents. *Int. J. Pharm.* **2013**, *445*, 47–57.
- (368) Cambón, A.; Figueroa-Ochoa, E.; Juárez, J.; Villar-Álvarez, E.; Pardo, A.; Barbosa, S.; Soltero, J. F. A.; Taboada, P.; Mosquera, V. Complex Self-Assembly of Reverse Poly(butylene oxide)-Poly(ethylene oxide)-Poly(butylene oxide) Triblock Copolymers with Long Hydrophobic and Extremely Lengthy Hydrophilic Blocks. *J. Phys. Chem. B* **2014**, *118*, 5258–5269.
- (369) Mortensen, K.; Schwahn, D.; Janssen, S. Pressure-Induced Melting of Micellar Crystal. *Phys. Rev. Lett.* **1993**, *71*, 1728–1731.
- (370) Schild, H. G.; Tirrell, D. A. Microcalorimetric Detection of Lower Critical Solution Temperatures in Aqueous Polymer Solutions. *J. Phys. Chem.* **1990**, *94*, 4352–4356.
- (371) Wu, J.; Thio, Y.; Bates, F. Structure and Properties of PBO-PEO Diblock Copolymer Modified Epoxy. *J. Polym. Sci., Part B: Polym. Phys.* **2005**, *43*, 1950–1965.
- (372) Thio, Y.; Wu, J.; Bates, F. The Role of Inclusion Size in Toughening of Epoxy Resins by Spherical Micelles. *J. Polym. Sci., Part B: Polym. Phys.* **2009**, *47*, 1125–1129.
- (373) Istratov, V.; Kautz, H.; Kim, Y.-K.; Schubert, R.; Frey, H. Linear-Dendritic Nonionic Poly(propylene oxide)-Polyglycerol Surfactants. *Tetrahedron* **2003**, *59*, 4017–4024.
- (374) Dimitrov, P.; Rangelov, S.; Dworak, A.; Tsvetanov, C. Synthesis and Associating Properties of Poly(ethoxyethyl glycidyl ether)/Poly(propylene oxide) Triblock Copolymers. *Macromolecules* **2004**, *37*, 1000–1008.
- (375) Halacheva, S.; Rangelov, S.; Tsvetanov, C. Poly(glycidol)-Based Analogues to Pluronic Block Copolymers. Synthesis and Aqueous Solution Properties. *Macromolecules* **2006**, *39*, 6845–6852.
- (376) Halacheva, S.; Rangelov, S.; Tsvetanov, C.; Garamus, V. Aqueous Solution Properties of Polyglycidol-Based Analogues of Pluronic Copolymers. Influence of the Poly(propylene oxide) Block Molar Mass. *Macromolecules* **2010**, *43*, 772–781.
- (377) Schömer, M.; Frey, H. Water-Soluble “Poly(propylene oxide)” by Random Copolymerization of Propylene Oxide with a Protected Glycidol Monomer. *Macromolecules* **2012**, *45*, 3039–3046.
- (378) Matlock, P. L.; Brown, W. L.; Clinton, N. A. In *Synthetic Lubricants and High-Performance Functional Fluids, Revised and Expanded*, 2nd ed.; Rudnick, L. R., Shubkin, R. L., Eds.; CRC Press: Boca Raton, FL, 1999.
- (379) Louai, A.; Sarazin, D.; Pollet, G.; Francois, J.; Moreaux, F. Properties of Ethylene-Oxide Propylene-Oxide Statistical Copolymers in Aqueous-Solution. *Polymer* **1991**, *32*, 703–712.
- (380) Lin, J.; Wu, J.; Ho, Y. Synthesis and in Situ Transformation of Poly(oxybutylene) Amides by Butoxylation. *J. Appl. Polym. Sci.* **2001**, *82*, 435–445.
- (381) Greaves, M.; Zaugg-Hoozemans, E.; Khelidj, N.; van Voorst, R.; Meertens, R. Performance Properties of Oil-Soluble Synthetic Polyalkylene Glycols. *Lubr. Sci.* **2012**, *24*, 251–262.
- (382) Zhou, N.; Lodge, T.; Bates, F. Phase Behavior of Polyisoprene-Poly(butylene oxide) and Poly(ethylene-*alt*-propylene)-Poly(butylene oxide) Block Copolymers. *Soft Matter* **2010**, *6*, 1281–1290.
- (383) Cho, B.-S.; Kim, J.-S.; Lee, J.-M.; Kweon, J.-O.; Noh, S.-T. Synthesis and Characterization of Poly(ferrocenyl glycidyl ether)-1,2-Butylene Oxide Copolymers. *Macromol. Res.* **2014**, *22*, 826–831.
- (384) Sugimoto, H.; Inoue, S. Copolymerization of Carbon Dioxide and Epoxide. *J. Polym. Sci., Part A: Polym. Chem.* **2004**, *42*, 5561–5573.
- (385) Darensbourg, D. Making Plastics from Carbon Dioxide: Salen Metal Complexes as Catalysts for the Production of Polycarbonates from Epoxides and CO<sub>2</sub>. *Chem. Rev.* **2007**, *107*, 2388–2410.
- (386) Luinstra, G. Poly(propylene carbonate), Old Copolymers of Propylene Oxide and Carbon Dioxide with New Interests: Catalysis and Material Properties. *Polym. Rev.* **2008**, *48*, 192–219.
- (387) Qin, Y.; Wang, X. Carbon Dioxide-Based Copolymers: Environmental Benefits of PPC, an Industrially Viable Catalyst. *Biotechnol. J.* **2010**, *5*, 1164–1180.
- (388) Kember, M.; Buchard, A.; Williams, C. Catalysts for CO<sub>2</sub>/Epoxide Copolymerisation. *Chem. Commun.* **2011**, *47*, 141–163.
- (389) Lu, X.; Ren, W.; Wu, G. CO<sub>2</sub> Copolymers from Epoxides: Catalyst Activity, Product Selectivity, and Stereochemistry Control. *Acc. Chem. Res.* **2012**, *45*, 1721–1735.
- (390) Darensbourg, D.; Wilson, S. What’s New with CO<sub>2</sub>? Recent Advances in Its Copolymerization with Oxiranes. *Green Chem.* **2012**, *14*, 2665–2671.
- (391) Lu, X.; Darensbourg, D. Cobalt Catalysts for the Coupling of CO<sub>2</sub> and Epoxides to Provide Polycarbonates and Cyclic Carbonates. *Chem. Soc. Rev.* **2012**, *41*, 1462–1484.
- (392) Taherimehr, M.; Pescarmona, P. Green Polycarbonates Prepared by the Copolymerization of CO<sub>2</sub> with Epoxides. *J. Appl. Polym. Sci.* **2014**, *131*, 41141.
- (393) Paul, S.; Zhu, Y.; Romain, C.; Brooks, R.; Saini, P.; Williams, C. Ring-Opening Copolymerization (ROCOP): Synthesis and Properties of Polyesters and Polycarbonates. *Chem. Commun.* **2015**, *51*, 6459–6479.
- (394) Fusco, S.; Borzacchiello, A.; Netti, P. A. Perspectives On: PEO-PPPO-PEO Triblock Copolymers and Their Biomedical Applications. *J. Biocat. Compat. Polym.* **2006**, *21*, 149–164.
- (395) Chiappetta, D. A.; Sosnik, A. Poly(ethylene oxide)-Poly(propylene oxide) Block Copolymer Micelles as Drug Delivery Agents: Improved Hydrosolubility, Stability and Bioavailability of Drugs. *Eur. J. Pharm. Biopharm.* **2007**, *66*, 303–317.
- (396) Mortensen, K.; Pedersen, J. S. Structural Study on the Micelle Formation of Poly(ethylene oxide)-Poly(propylene oxide)-Poly(ethylene oxide) Triblock Copolymer in Aqueous Solution. *Macromolecules* **1993**, *26*, 805–812.
- (397) Schmolka, I. R. A Review of Block Polymer Surfactants. *J. Am. Oil Chem. Soc.* **1977**, *54*, 110–116.

- (398) Kabanov, A. V.; Batrakova, E. V.; Alakhov, V. Y. Pluronic® Block Copolymers as Novel Polymer Therapeutics for Drug and Gene Delivery. *J. Controlled Release* **2002**, *82*, 189–212.
- (399) Torcello-Gómez, A.; Wulff-Pérez, M.; Gálvez-Ruiz, M. J.; Martín-Rodríguez, A.; Cabrerizo-Vílchez, M.; Maldonado-Valderrama, J. Block Copolymers at Interfaces: Interactions with Physiological Media. *Adv. Colloid Interface Sci.* **2014**, *206*, 414–427.
- (400) Stolnik, S.; Illum, L.; Davis, S. S. Long Circulating Micro-particulate Drug Carriers. *Adv. Drug Delivery Rev.* **2012**, *64* (Supplement), 290–301.
- (401) Durand, A.; Marie, E. Macromolecular Surfactants for Miniemulsion Polymerization. *Adv. Colloid Interface Sci.* **2009**, *150*, 90–105.
- (402) Nagarajan, R. Solubilization of Hydrocarbons and Resulting Aggregate Shape Transitions in Aqueous Solutions of Pluronic (PEO–PPO–PEO) Block Copolymers. *Colloids Surf., B* **1999**, *16*, 55–72.
- (403) Alexandridis, P.; Holzwarth, J. F.; Hattton, T. A. Micellization of Poly(ethylene oxide)-Poly(propylene oxide)-Poly(ethylene oxide) Triblock Copolymers in Aqueous Solutions: Thermodynamics of Copolymer Association. *Macromolecules* **1994**, *27*, 2414–2425.
- (404) Alexandridis, P.; Alan Hattton, T. Poly(ethylene oxide) Poly(propylene oxide) Poly(ethylene oxide) Block Copolymer Surfactants in Aqueous Solutions and at Interfaces: Thermodynamics, Structure, Dynamics, and Modeling. *Colloids Surf., A* **1995**, *96*, 1–46.
- (405) Kozlov, M. Y.; Melik-Nubarov, N. S.; Batrakova, E. V.; Kabanov, A. V. Relationship between Pluronic Block Copolymer Structure, Critical Micellization Concentration and Partitioning Coefficients of Low Molecular Mass Solutes. *Macromolecules* **2000**, *33*, 3305–3313.
- (406) Hecht, E.; Hoffmann, H. Interaction of ABA Block Copolymers with Ionic Surfactants in Aqueous Solution. *Langmuir* **1994**, *10*, 86–91.
- (407) Batrakova, E.; Lee, S.; Li, S.; Venne, A.; Alakhov, V.; Kabanov, A. Fundamental Relationships between the Composition of Pluronic Block Copolymers and Their Hypersensitization Effect in MDR Cancer Cells. *Pharm. Res.* **1999**, *16*, 1373–1379.
- (408) Alexandridis, P. Poly(ethylene oxide)/Poly(propylene oxide) Block Copolymer Surfactants. *Curr. Opin. Colloid Interface Sci.* **1997**, *2*, 478–489.
- (409) Alakhov, D. Y.; Kabanov, A. V. Pluronics and MDR Reversal: An Update. *Mol. Pharmaceutics* **2014**, *11*, 2566–2578.
- (410) Alakhov, V. Y.; Moskaleva, E. Y.; Batrakova, E. V.; Kabanov, A. V. Hypersensitization of Multidrug Resistant Human Ovarian Carcinoma Cells by Pluronic P85 Block Copolymer. *Bioconjugate Chem.* **1996**, *7*, 209–216.
- (411) Pitto-Barry, A.; Barry, N. P. E. Pluronic® Block-Copolymers in Medicine: From Chemical and Biological Versatility to Rationalisation and Clinical Advances. *Polym. Chem.* **2014**, *5*, 3291–3297.
- (412) Yoncheva, K.; Calleja, P.; Agüeros, M.; Petrov, P.; Miladinova, I.; Tsvetanov, C.; Irache, J. M. Stabilized Micelles as Delivery Vehicles for Paclitaxel. *Int. J. Pharm.* **2012**, *436*, 258–264.
- (413) Kabanov, A. V.; Batrakova, E. V.; Miller, D. W. Pluronic® Block Copolymers as Modulators of Drug Efflux Transporter Activity in the Blood–Brain Barrier. *Adv. Drug Delivery Rev.* **2003**, *55*, 151–164.
- (414) Yang, T.-F.; Chen, C.-N.; Chen, M.-C.; Lai, C.-H.; Liang, H.-F.; Sung, H.-W. Shell-Crosslinked Pluronic L121 Micelles as a Drug Delivery Vehicle. *Biomaterials* **2007**, *28*, 725–734.
- (415) Petrov, P.; Bozakov, M.; Tsvetanov, C. B. Innovative Approach for Stabilizing Poly(ethylene oxide)-*b*-Poly(propylene oxide)-*b*-Poly(ethylene oxide) Micelles by Forming Nano-Sized Networks in the Micelle. *J. Mater. Chem.* **2005**, *15*, 1481–1486.
- (416) Ruel-Gariépy, E.; Leroux, J.-C. In Situ-Forming Hydrogels—Review of Temperature-Sensitive Systems. *Eur. J. Pharm. Biopharm.* **2004**, *58*, 409–426.
- (417) Gutowska, A.; Jeong, B.; Jasonowski, M. Injectable Gels for Tissue Engineering. *Anat. Rec.* **2001**, *263*, 342–349.
- (418) Frisman, L.; Seliktar, D.; Bianco-Peled, H. Nanostructuring PEG-Fibrinogen Hydrogels to Control Cellular Morphogenesis. *Biomaterials* **2011**, *32*, 7839–7846.
- (419) Frisman, L.; Seliktar, D.; Bianco-Peled, H. Nanostructuring Biosynthetic Hydrogels for Tissue Engineering: A Cellular and Structural Analysis. *Acta Biomater.* **2012**, *8*, 51–60.
- (420) Bromberg, L. Intelligent Hydrogels for the Oral Delivery of Chemotherapeutics. *Expert Opin. Drug Delivery* **2005**, *2*, 1003–1013.
- (421) Huang, K.; Lee, B. P.; Ingram, D. R.; Messersmith, P. B. Synthesis and Characterization of Self-Assembling Block Copolymers Containing Bioadhesive End Groups. *Biomacromolecules* **2002**, *3*, 397–406.
- (422) Lee, Y.; Park, S. Y.; Mok, H.; Park, T. G. Synthesis, Characterization, Antitumor Activity of Pluronic Mimicking Copolymer Micelles Conjugated with Doxorubicin Via Acid-Cleavable Linkage. *Bioconjugate Chem.* **2008**, *19*, 525–531.
- (423) Halacheva, S.; Rangelov, S.; Tsvetanov, C. Synthesis of Polyglycidol-Based Analogues to Pluronic L121–F127 Copolymers. Self-Assembly, Thermodynamics, Turbidimetric, and Rheological Studies. *Macromolecules* **2008**, *41*, 7699–7705.
- (424) D’Errico, G.; Paduano, L.; Khan, A. Temperature and Concentration Effects on Supramolecular Aggregation and Phase Behavior for Poly(propylene oxide)-*b*-Poly(ethylene oxide)-*b*-Poly(propylene oxide) Copolymers of Different Composition in Aqueous Mixtures. *J. Colloid Interface Sci.* **2004**, *279*, 379–390.
- (425) Zhou, Z.; Chu, B. Phase Behavior and Association Properties of Poly(oxypropylene)-Poly(oxyethylene)-Poly(oxypropylene) Triblock Copolymer in Aqueous Solution. *Macromolecules* **1994**, *27*, 2025–2033.
- (426) Naskar, B.; Ghosh, S.; Moulik, S. P. Solution Behavior of Normal and Reverse Triblock Copolymers (Pluronic L44 and 10S) Individually and in Binary Mixture. *Langmuir* **2012**, *28*, 7134–7146.
- (427) Huff, A.; Patton, K.; Odhner, H.; Jacobs, D. T.; Clover, B. C.; Greer, S. C. Micellization and Phase Separation for Triblock Copolymer 17R4 in H<sub>2</sub>O and in D<sub>2</sub>O. *Langmuir* **2011**, *27*, 1707–1712.
- (428) Jiang, R.; Jin, Q.; Li, B.; Ding, D.; Shi, A.-C. Phase Diagram of Poly(ethylene oxide) and Poly(propylene oxide) Triblock Copolymers in Aqueous Solutions. *Macromolecules* **2006**, *39*, 5891–5896.
- (429) Larrañeta, E.; Isasi, J. R. Phase Behavior of Reverse Poloxamers and Poloxamines in Water. *Langmuir* **2013**, *29*, 1045–1053.
- (430) Wang, Q.; Li, L.; Jiang, S. Effects of a PPO–PEO–PPO Triblock Copolymer on Micellization and Gelation of a PEO–PPO–PEO Triblock Copolymer in Aqueous Solution. *Langmuir* **2005**, *21*, 9068–9075.
- (431) Xie, Y.; Tang, J.; Lu, Z.; Sun, Z.; An, L. Effects of Poly(propylene oxide)–Poly(ethylene oxide)–Poly(propylene oxide) Triblock Copolymer on the Gelation of Poly(ethylene oxide)–Poly(propylene oxide)–Poly(ethylene oxide) Aqueous Solutions. *J. Macromol. Sci., Part B: Phys.* **2013**, *52*, 1183–1197.
- (432) Guiraud, S.; Alimi-Guez, D.; van Wittenbergh, L.; Scherman, D.; Kichler, A. The Reverse Block Copolymer Pluronic 25R2 Promotes DNA Transfection of Skeletal Muscle. *Macromol. Biosci.* **2011**, *11*, 590–594.
- (433) Sosnik, A.; Sefton, M. V. Methylation of Poloxamine for Enhanced Cell Adhesion. *Biomacromolecules* **2006**, *7*, 331–338.
- (434) Cho, E.; Lee, J. S.; Webb, K. Formulation and Characterization of Poloxamine-Based Hydrogels as Tissue Sealants. *Acta Biomater.* **2012**, *8*, 2223–2232.
- (435) Gonzalez-Lopez, J.; Sandez-Macho, I.; Concheiro, A.; Alvarez-Lorenzo, C. Poloxamines and Poloxamers as Polymeric Micellar Carriers for Simvastatin: Interactions at the Air–Water Interface and in Bulk Solution. *J. Phys. Chem. C* **2010**, *114*, 1181–1189.
- (436) Dong, J.; Chowdhry, B. Z.; Leharne, S. A. Surface Activity of Poloxamines at the Interfaces between Air–Water and Hexane–Water. *Colloids Surf., A* **2003**, *212*, 9–17.
- (437) Pitard, B.; Bello-Roufai, M.; Lambert, O.; Richard, P.; Desigaux, L.; Fernandes, S.; Lanctin, C.; Pollard, H.; Zeghal, M.; Rescan, P.-Y.; et al. Negatively Charged Self-Assembling DNA/Poloxamine Nanospheres for in Vivo Gene Transfer. *Nucleic Acids Res.* **2004**, *32*, e159.
- (438) Moghimi, S. M.; Hunter, A. C. Poloxamers and Poloxamines in Nanoparticle Engineering and Experimental Medicine. *Trends Biotechnol.* **2000**, *18*, 412–420.

- (439) Cuestas, M. L.; Sosnik, A.; Mathet, V. L. Poloxamines Display a Multiple Inhibitory Activity of ATP-Binding Cassette (ABC) Transporters in Cancer Cell Lines. *Mol. Pharmaceutics* **2011**, *8*, 1152–1164.
- (440) Gonzalez-Lopez, J.; Alvarez-Lorenzo, C.; Taboada, P.; Sosnik, A.; Sanchez-Macho, I.; Concheiro, A. Self-Associative Behavior and Drug-Solubilizing Ability of Poloxamine (Tetronic) Block Copolymers. *Langmuir* **2008**, *24*, 10688–10697.
- (441) Fairclough, J. P. A.; Yu, G.-E.; Mai, S.-M.; Crothers, M.; Mortensen, K.; Ryan, A. J.; Booth, C. First Observation of an Ordered Microphase in Melts of Poly(oxyethylene)-Poly(oxypropylene) Block Copolymers. *Phys. Chem. Chem. Phys.* **2000**, *2*, 1503–1507.
- (442) Mansur, C. R. E.; Oliveira, C. M. F.; González, G.; Lucas, E. F. Phase Behavior of Aqueous Systems Containing Block Copolymers of Poly(ethylene oxide) and Poly(propylene oxide). *J. Appl. Polym. Sci.* **1997**, *66*, 1767–1772.
- (443) Mansur, C. R. E.; Benzi, M. R.; Lucas, E. F. Study of Adsorption of Nonionic Surfactants at the Liquid–Solid Interface by FTIR/CIR. *J. Appl. Polym. Sci.* **2001**, *82*, 1668–1676.
- (444) Takahashi, M.; Kubo, W.; Miyata, H. PEO-*b*-PPO Diblock Copolymers for the Preparation of 2D Hexagonal Mesoporous Silica Films with Extremely Large Structural Periods. *Chem. Lett.* **2013**, *42*, 909–911.
- (445) Nagarajan, R.; Bradley, R. A.; Nair, B. R. Thermodynamically Stable, Size Selective Solubilization of Carbon Nanotubes in Aqueous Solutions of Amphiphilic Block Copolymers. *J. Chem. Phys.* **2009**, *131*, 104906.
- (446) Steinschulte, A. A.; Xu, W.; Draber, F.; Hebbeker, P.; Jung, A.; Bogdanovski, D.; Schneider, S.; Tsukruk, V. V.; Plamper, F. A. Interface-Enforced Complexation between Copolymer Blocks. *Soft Matter* **2015**, *11*, 3559–3565.
- (447) Deschênes, L.; Saint-Germain, F.; Lyklema, J. Langmuir Monolayers of Non-Ionic Polymers: Equilibrium or Metastability? Case Study of PEO and its PPO–PEO Diblock Copolymers. *J. Colloid Interface Sci.* **2015**, *449*, 494–505.
- (448) Firestone, M. A.; Seifert, S. Interaction of Nonionic PEO–PPO Diblock Copolymers with Lipid Bilayers. *Biomacromolecules* **2005**, *6*, 2678–2687.
- (449) Lapienis, G. Star-Shaped Polymers Having PEO Arms. *Prog. Polym. Sci.* **2009**, *34*, 852–892.
- (450) Doycheva, M.; Berger-Nicoletti, E.; Wurm, F.; Frey, H. Rapid Synthesis and MALDI-ToF Characterization of Poly(ethylene oxide) Multiarm Star Polymers. *Macromol. Chem. Phys.* **2010**, *211*, 35–44.
- (451) Huin, C.; Eskandani, Z.; Badi, N.; Farcas, A.; Bennevault-Celton, V.; Guégan, P. Anionic Ring-Opening Polymerization of Ethylene Oxide in DMF with Cyclodextrin Derivatives as new Initiators. *Carbohydr. Polym.* **2013**, *94*, 323–331.
- (452) Tonhauser, C.; Mazurowski, M.; Rehahn, M.; Gallei, M.; Frey, H. Water-Soluble Poly(vinylferrocene)-*b*-Poly(ethylene oxide) Diblock and Miktoarm Star Polymers. *Macromolecules* **2012**, *45*, 3409–3418.
- (453) Wang, G.; Fan, X.; Huang, J. Synthesis of 4 $\mu$ -PS<sub>2</sub>PEO<sub>2</sub>, 4 $\mu$ -PS<sub>2</sub>PCL<sub>2</sub>, 4 $\mu$ -PI<sub>2</sub>PEO<sub>2</sub>, and 4 $\mu$ -PI<sub>2</sub>PCL<sub>2</sub> Star-Shaped Copolymers by the Combination of Glaser Coupling with Living Anionic Polymerization and Ring-Opening Polymerization. *J. Polym. Sci., Part A: Polym. Chem.* **2010**, *48*, 5313–5321.
- (454) Guo, Q.; Liu, C.; Tang, T.; Huang, J.; Zhang, X.; Wang, G. Synthesis of Amphiphilic A<sub>2</sub>B<sub>3</sub> Star-Shaped Copolymers by Mechanisms Transformation Combining with Thiol-ene Reaction. *J. Polym. Sci., Part A: Polym. Chem.* **2013**, *51*, 4572–4583.
- (455) Jiang, G.; Xu, H. Synthesis and Evaluation of a Star Amphiphilic Block Copolymer from Poly( $\epsilon$ -Caprolactone) and Poly(ethylene oxide) as Load and Release Carriers for Guest Molecules. *J. Appl. Polym. Sci.* **2010**, *118*, 1372–1379.
- (456) Li, Y.; Zhang, B.; Hoskins, J. N.; Grayson, S. M. Synthesis, Purification, and Characterization of “Perfect” Star Polymers via “Click” Coupling. *J. Polym. Sci., Part A: Polym. Chem.* **2012**, *50*, 1086–1101.
- (457) Li, N.; Echeverría, M.; Moya, S.; Ruiz, J.; Astruc, D. “Click” Synthesis of Nona-PEG-Branched Triazole Dendrimers and Stabilization of Gold Nanoparticles That Efficiently Catalyze p-Nitrophenol Reduction. *Inorg. Chem.* **2014**, *53*, 6954–6961.
- (458) Chang, X.; Liu, L.; Guan, Y.; Dong, C.-M. Disulfide-Centered Star-Shaped Polypeptide-PEO Block Copolymers for Reduction-Triggered Drug Release. *J. Polym. Sci., Part A: Polym. Chem.* **2014**, *52*, 2000–2010.
- (459) Durmaz, H.; Dag, A.; Erdogan, E.; Demirel, A. L.; Hizal, G.; Tunca, U. Multiarm Star Block and Multiarm Star Mixed-Block Copolymers via Azide-Alkyne Click Reaction. *J. Polym. Sci., Part A: Polym. Chem.* **2010**, *48*, 99–108.
- (460) Durmaz, H.; Dag, A.; Gursoy, D.; Demirel, A. L.; Hizal, G.; Tunca, U. Multiarm Star Triblock Terpolymers Via Sequential Double Click Reactions. *J. Polym. Sci., Part A: Polym. Chem.* **2010**, *48*, 1557–1564.
- (461) Kulis, J.; Jia, Z.; Monteiro, M. J. One-Pot Synthesis of Mikto Three-Arm AB<sub>2</sub> Stars Constructed from Linear and Macrocyclic Polymer Chains. *Macromolecules* **2012**, *45*, 5956–5966.
- (462) Bahadori, F.; Dag, A.; Durmaz, H.; Cakir, N.; Onyüksel, H.; Tunca, U.; Topcu, G.; Hizal, G. Synthesis and Characterization of Biodegradable Amphiphilic Star and Y-Shaped Block Copolymers as Potential Carriers for Vinorelbine. *Polymers* **2014**, *6*, 214–242.
- (463) Doganci, E.; Gorur, M.; Uyanik, C.; Yilmaz, F. Synthesis of AB<sub>3</sub>-Type Miktoarm Star Polymers with Steroid Core via a Combination of “Click” Chemistry and Ring Opening Polymerization Techniques. *J. Polym. Sci., Part A: Polym. Chem.* **2014**, *52*, 3390–3399.
- (464) Blasco, E.; Schmidt, B.; Barner-Kowollik, C.; Pinol, M.; Oriol, L. A Novel Photoresponsive Azobenzene-Containing Miktoarm Star Polymer: Self-Assembly and Photoresponse Properties. *Macromolecules* **2014**, *47*, 3693–3700.
- (465) Liu, R.; Li, Z. Y.; Wang, W. J.; Yuan, D.; Meng, C. F.; Wu, Q.; Zhu, F. M. Synthesis and Self-Assembly of Amphiphilic Star-Block Copolymers Consisting of Polyethylene and Poly(ethylene glycol) Segments. *J. Appl. Polym. Sci.* **2013**, *129*, 2216–2223.
- (466) Gou, P.-F.; Zhu, W.-P.; Shen, Z.-Q. Calixarene-Centered Amphiphilic A<sub>2</sub>B<sub>2</sub> Miktoarm Star Copolymers Based on Poly( $\epsilon$ -Caprolactone) and Poly(ethylene glycol): Synthesis and Self-Assembly Behaviors in Water. *J. Polym. Sci., Part A: Polym. Chem.* **2010**, *48*, 5643–5651.
- (467) Gou, P.-F.; Zhu, W.-P.; Shen, Z.-Q. Synthesis, Self-Assembly, and Drug-Loading Capacity of Well-Defined Cyclodextrin-Centered Drug-Conjugated Amphiphilic A<sub>14</sub>B<sub>7</sub> Miktoarm Star Copolymers Based on Poly( $\epsilon$ -caprolactone) and Poly(ethylene glycol). *Biomacromolecules* **2010**, *11*, 934–943.
- (468) Gao, C.; Wang, Y.; Gou, P.; Cai, X.; Li, X.; Zhu, W.; Shen, Z. Synthesis and Characterization of Resorcinarene-Centered Amphiphilic A<sub>6</sub>B<sub>3</sub> Miktoarm Star Copolymers Based on Poly( $\epsilon$ -caprolactone) and Poly(ethylene glycol) by Combination of Click and “Click” Chemistry. *J. Polym. Sci., Part A: Polym. Chem.* **2013**, *51*, 2824–2833.
- (469) Khanna, K.; Varshney, S.; Kakkar, A. Designing Miktoarm Polymers Using a Combination of “Click” Reactions in Sequence with Ring-Opening Polymerization. *Macromolecules* **2010**, *43*, 5688–5698.
- (470) Iskin, B.; Yilmaz, G.; Yagci, Y. Synthesis of ABC Type Miktoarm Star Copolymers by Triple Click Chemistry. *Polym. Chem.* **2011**, *2*, 2865–2871.
- (471) Huan, X.; Wang, D.; Dong, R.; Tu, C.; Zhu, B.; Yan, D.; Zhu, X. Supramolecular ABC Miktoarm Star Terpolymer Based on Host–Guest Inclusion Complexation. *Macromolecules* **2012**, *45*, 5941–5947.
- (472) Sun, W.; He, X.; Gao, C.; Liao, X.; Xie, M.; Lin, S.; Yan, D. Novel Amphiphilic and Photo-Responsive ABC<sub>2</sub>-Miktoarm Star Terpolymers: Synthesis, Self-Assembly and Photo-Responsive Behavior. *Polym. Chem.* **2013**, *4*, 1939–1949.
- (473) Liu, H.; Miao, K.; Zhao, G.; Li, C.; Zhao, Y. Synthesis of an Amphiphilic PEG-PCL-PSt-PLLA-PAA Star Quintopolymer and its Self-Assembly for pH-Sensitive Drug Delivery. *Polym. Chem.* **2014**, *5*, 3071–3080.
- (474) Li, W.; Matyjaszewski, K. Uniform PEO Star Polymers Synthesized in Water via Free Radical Polymerization or Atom Transfer Radical Polymerization. *Macromol. Rapid Commun.* **2011**, *32*, 74–81.
- (475) Cho, H. Y.; Srinivasan, A.; Hong, J.; Hsu, E.; Liu, S.; Shrivats, A.; Kwak, D.; Bohaty, A. K.; Paik, H.-J.; Hollinger, J. O.; et al. Synthesis of

- Biocompatible PEG-Based Star Polymers with Cationic and Degradable Core for siRNA Delivery. *Biomacromolecules* **2011**, *12*, 3478–3486.
- (476) Fukae, K.; Terashima, T.; Sawamoto, M. Cation-Condensed Microgel-Core Star Polymers as Polycationic Nanocapsules for Molecular Capture and Release in Water. *Macromolecules* **2012**, *45*, 3377–3386.
- (477) Koda, Y.; Terashima, T.; Sawamoto, M. Fluorous Microgel Star Polymers: Selective Recognition and Separation of Polyfluorinated Surfactants and Compounds in Water. *J. Am. Chem. Soc.* **2014**, *136*, 15742–15748.
- (478) Terashima, T.; Nishioka, S.; Koda, Y.; Takenaka, M.; Sawamoto, M. Arm-Cleavable Microgel Star Polymers: A Versatile Strategy for Direct Core Analysis and Functionalization. *J. Am. Chem. Soc.* **2014**, *136*, 10254–10257.
- (479) Park, S.; Cho, H. Y.; Wegner, K. B.; Burdynska, J.; Magenau, A. J. D.; Paik, H.-J.; Jurga, S.; Matyjaszewski, K. Star Synthesis Using Macroinitiators Via Electrochemically Mediated Atom Transfer Radical Polymerization. *Macromolecules* **2013**, *46*, 5856–5860.
- (480) McKenzie, T. G.; Wong, E. H. H.; Fu, Q.; Lam, S. J.; Dunstan, D. E.; Qiao, G. G. Highly Efficient and Versatile Formation of Biocompatible Star Polymers in Pure Water and Their Stimuli-Responsive Self-Assembly. *Macromolecules* **2014**, *47*, 7869–7877.
- (481) Syrett, J. A.; Haddleton, D. M.; Whittaker, M. R.; Davis, T. P.; Boyer, C. Functional, Star Polymeric Molecular Carriers, Built from Biodegradable Microgel/Nanogel Cores. *Chem. Commun.* **2011**, *47*, 1449–1451.
- (482) Gao, A. X.; Liao, L.; Johnson, J. A. Synthesis of Acid-Labile PEG and PEG-Doxorubicin-Conjugate Nanoparticles via Brush-First ROMP. *ACS Macro Lett.* **2014**, *3*, 854–857.
- (483) Feng, Z.; Zhi-Ming, W.; Ya-Fei, H.; Xiao-Hui, D.; Yan-Ru, G.; Jian-Ming, P.; Yong-Sheng, Y.; Sun, L. Synthesis, Self-Assembly, and Drug Release Behavior of Star-Shaped Poly( $\epsilon$ -caprolactone)-*b*-Poly(ethylene oxide) Block Copolymer with Porphyrin Core. *J. Appl. Polym. Sci.* **2014**, *131*, 40996.
- (484) Lim, H. J.; Lee, H.; Kim, K. H.; Huh, J.; Ahn, C.-H.; Kim, J. W. Effect of Molecular Architecture on Micellization, Drug Loading and Releasing of Multi-Armed Poly(ethylene glycol)-*b*-Poly( $\epsilon$ -caprolactone) Star Polymers. *Colloid Polym. Sci.* **2013**, *291*, 1817–1827.
- (485) Gou, P.-F.; Zhu, W.-P.; Shen, Z.-Q. Drug-Grafted Seven-Arm Amphiphilic Star Poly( $\epsilon$ -caprolactone-co-carbonate)-*b*-Poly(ethylene glycol)s Based on a Cyclodextrin Core: Synthesis and Self-Assembly Behavior in Water. *Polym. Chem.* **2010**, *1*, 1205.
- (486) Nabil, M. R.; Tabatabaei Rezaei, S. J.; Sedghi, R.; Niknejad, H.; Entezami, A. A.; Oskooie, H. A.; Heravi, M. M. Self-Assembled Micelles of Well-Defined Pentaerythritol-Centered Amphiphilic A<sub>4</sub>B<sub>5</sub> Star-Block Copolymers Based on PCL and PEG for Hydrophobic Drug Delivery. *Polymer* **2011**, *52*, 2799–2809.
- (487) Pu, Y.; Zhang, L.; Zheng, H.; He, B.; Gu, Z. Synthesis and Drug Release of Star-Shaped Poly(benzyl L-aspartate)-*block*-Poly(ethylene glycol) Copolymers with POSS Cores. *Macromol. Biosci.* **2014**, *14*, 289–297.
- (488) Lam, S. J.; Sulistio, A.; Ladewig, K.; Wong, E. H. H.; Blencowe, A.; Qiao, G. G. Peptide-Based Star Polymers as Potential siRNA Carriers. *Aust. J. Chem.* **2014**, *67*, 592.
- (489) Yan, Y.; Wei, D.; Li, J.; Zheng, J.; Shi, G.; Luo, W.; Pan, Y.; Wang, J.; Zhang, L.; He, X.; et al. A Poly(L-lysine)-Based Hydrophilic Star Block Copolymer as a Protein Nanocarrier with Facile Encapsulation and pH-Responsive Release. *Acta Biomater.* **2012**, *8*, 2113–2120.
- (490) Chen, G.; Wang, L.; Cordie, T.; Vokoun, C.; Eliceiri, K. W.; Gong, S. Multi-Functional Self-Fluorescent Unimolecular Micelles for Tumor-Targeted Drug Delivery and Bioimaging. *Biomaterials* **2015**, *47*, 41–50.
- (491) Dai, X.-H.; Wang, Z.-M.; Gao, L.-Y.; Pan, J.-M.; Wang, X.-H.; Yan, Y.-S.; Liu, D.-M. Star-Shaped Poly(L-lactide)-*b*-Poly(ethylene glycol) with Porphyrin Core: Synthesis, Self-Assembly, Drug-Release Behavior and Singlet Oxygen Research. *New J. Chem.* **2014**, *38*, 3569.
- (492) Gu, D.; Ladewig, K.; Klimak, M.; Haylock, D.; McLean, K. M.; O'Connor, A. J.; Qiao, G. G. Amphiphilic Core Cross-Linked Star Polymers as Water-Soluble, Biocompatible and Biodegradable Unimolecular Carriers for Hydrophobic Drugs. *Polym. Chem.* **2015**, *6*, 6475–6487.
- (493) Rodionov, V.; Gao, H.; Scroggins, S.; Unruh, D. A.; Avestro, A.-J.; Fréchet, J. M. J. Easy Access to a Family of Polymer Catalysts from Modular Star Polymers. *J. Am. Chem. Soc.* **2010**, *132*, 2570–2572.
- (494) Qiu, F.; Tu, C.; Chen, Y.; Shi, Y.; Song, L.; Wang, R.; Zhu, X.; Zhu, B.; Yan, D.; Han, T. Control of the Optical Properties of a Star Copolymer with a Hyperbranched Conjugated Polymer Core and Poly(ethylene glycol) Arms by Self-Assembly. *Chem. - Eur. J.* **2010**, *16*, 12710–12717.
- (495) Qiu, F.; Wang, D.; Zhu, Q.; Zhu, L.; Tong, G.; Lu, Y.; Yan, D.; Zhu, X. Real-Time Monitoring of Anticancer Drug Release with Highly Fluorescent Star-Conjugated Copolymer as a Drug Carrier. *Biomacromolecules* **2014**, *15*, 1355–1364.
- (496) Chen, R.; Wang, L. Synthesis of an Amphiphilic Hyperbranched Polymer as a Novel pH-Sensitive Drug Carrier. *RSC Adv.* **2015**, *5*, 20155–20159.
- (497) Whitton, G.; Gauthier, M. Arborescent Micelles: Dendritic Poly( $\gamma$ -benzyl L-glutamate) Cores Grafted with Hydrophilic Chain Segments. *J. Polym. Sci., Part A: Polym. Chem.* **2015**, DOI: 10.1002/pola.27943.
- (498) Xie, Z.; He, H.; Deng, Y.; Wang, X.; Liu, C. Three-Arm Star Compounds Composed of 1,3,5-Tri(azobenzeneethynyl)Benzene Cores and Flexible PEO Arms: Synthesis, Optical Functions, Hybrid Ormosil Gel Glasses. *J. Mater. Chem. C* **2013**, *1*, 1791.
- (499) Lee, D.-I.; Kim, C.-J.; Lee, C.-H.; Ahn, L.-S. Synthesis of a Fluorescent and Star-Shaped 4-Arm PEG with Different Functional Groups at its Ends. *J. Ind. Eng. Chem.* **2012**, *18*, 1186–1190.
- (500) Mineo, P.; Alicata, R.; Micali, N.; Villari, V.; Scamporrino, E. Water-Soluble Star Polymers with a Phthalocyanine as the Core and Poly(ethylene glycol) Chains as Branches. *J. Appl. Polym. Sci.* **2012**, *126*, 1359–1368.
- (501) Pozza, G. M. E.; Harris, H.; Barthel, M. J.; Vitz, J.; Schubert, U. S.; Lutz, P. J. Macromonomers as Well-Defined Building Blocks in the Synthesis of Hybrid Octafunctional Star-Shaped Poly(ethylene oxide)s. *Macromol. Chem. Phys.* **2012**, *213*, 2181–2191.
- (502) Rother, M.; Barqawi, H.; Pfefferkorn, D.; Kressler, J.; Binder, W. H. Synthesis and Organization of Three-Arm-Star PIB-PEO Block Copolymers at the Air/Water Interface: Langmuir- and Langmuir-Blodgett Film Investigations. *Macromol. Chem. Phys.* **2010**, *211*, 204–214.
- (503) de Espinosa, L. M.; Winkler, M.; Meier, M. A. R. Acyclic Diene Metathesis Polymerization and Heck Polymer-Polymer Conjugation for the Synthesis of Star-Shaped Block Copolymers. *Macromol. Rapid Commun.* **2013**, *34*, 1381–1386.
- (504) Zhang, Y.; Zhao, Q.; Shao, H.; Zhang, S.; Han, X. Synthesis and Characterization of Star-Shaped Block Copolymer sPCL-*b*-PEG-GA. *Adv. Mater. Sci. Eng.* **2014**, *2014*, 1–6.
- (505) Lin, Y.; Zhang, A. Synthesis and Characterization of Star-Shaped Poly(D,L-lactide)-*block*-Poly(ethylene glycol) Copolymers. *Polym. Bull.* **2010**, *65*, 883–892.
- (506) Durmaz, H.; Dag, A.; Tunca, U.; Hizal, G. Synthesis and Characterization of Pyrene Bearing Amphiphilic Miktoarm Star Polymer and its Noncovalent Interactions with Multiwalled Carbon Nanotubes. *J. Polym. Sci., Part A: Polym. Chem.* **2012**, *50*, 2406–2414.
- (507) Lagunas, C.; Fernandez-Franco, X.; Ferrando, F.; Flores, M.; Serra, A.; Morancho, J.; Salla, J.; Ramis, X. New Epoxy Thermosets Modified with Amphiphilic Multiarm Star Polymers as Toughness Enhancer. *React. Funct. Polym.* **2014**, *83*, 132–143.
- (508) Zhu, W.; Ling, J.; Shen, Z. Synthesis and Characterization of Amphiphilic Star-Shaped Polymers with Calix[6]Arene Cores. *Macromol. Chem. Phys.* **2006**, *207*, 844–849.
- (509) Sunder, A.; Müllhaupt, R.; Frey, H. Hyperbranched Polyether-Polyols Based on Polyglycerol: Polarity Design by Block Copolymerization with Propylene Oxide. *Macromolecules* **2000**, *33*, 309–314.
- (510) Knischka, R.; Lutz, P. J.; Sunder, A.; Müllhaupt, R.; Frey, H. Functional Poly(ethylene oxide) Multiarm Star Polymers: Core-First Synthesis Using Hyperbranched Polyglycerol Initiators. *Macromolecules* **2000**, *33*, 315–320.

- (511) Flory, P. J. Molecular Size Distribution in Three Dimensional Polymers 0.6. Branched Polymers Containing A-R-B<sub>n</sub> Type Units. *J. Am. Chem. Soc.* **1952**, *74*, 2718–2723.
- (512) Hawker, C.; Lee, R.; Frechet, J. One-Step Synthesis of Hyperbranched Dendritic Polyesters. *J. Am. Chem. Soc.* **1991**, *113*, 4583–4588.
- (513) Hölter, D.; Burgath, A.; Frey, H. Degree of Branching in Hyperbranched Polymers. *Acta Polym.* **1997**, *48*, 30–35.
- (514) Schömer, M.; Schüll, C.; Frey, H. Hyperbranched Aliphatic Polyether Polyols. *J. Polym. Sci., Part A: Polym. Chem.* **2013**, *51*, 995–1019.
- (515) Schüll, C.; Wilms, D.; Frey, H.; Matyjaszewski, K.; Möller, M. *Polymer Science: A Comprehensive Reference* **2012**, *4*, 571–596.
- (516) Smeets, N. Amphiphilic Hyperbranched Polymers from the Copolymerization of a Vinyl and Divinyl Monomer: The Potential of Catalytic Chain Transfer Polymerization. *Eur. Polym. J.* **2013**, *49*, 2528–2544.
- (517) Zhao, T.; Zhang, H.; Zhou, D.; Gao, Y.; Dong, Y.; Greiser, U.; Tai, H.; Wang, W. Water-Soluble Hyperbranched Polymers from Controlled Radical Homopolymerization of PEG Diacrylate. *RSC Adv.* **2015**, *5*, 33823–33830.
- (518) Hawker, C. J.; Chu, F.; Pomery, P. J.; Hill, D. J. T. Hyperbranched Poly(ethylene glycol)s: A New Class of Ion-Conducting Materials. *Macromolecules* **1996**, *29*, 3831–3838.
- (519) Unal, S.; Lin, Q.; Mourey, T. H.; Long, T. E. Tailoring the Degree of Branching: Preparation of Poly(ether ester)s via Copolymerization of Poly(ethylene glycol) Oligomers (A2) and 1,3,5-Benzenetricarbonyl Trichloride (B3). *Macromolecules* **2005**, *38*, 3246–3254.
- (520) Patel, R. H.; Patel, K. S. Synthesis and Characterization of Flame Retardant Hyperbranched Polyurethanes for Nano-Composite and Nano-Coating Applications. *Prog. Org. Coat.* **2015**, *88*, 283–292.
- (521) Masukawa, S.; Kikkawa, T.; Fujimori, A.; Oishi, Y.; Shibasaki, Y. Synthesis of A<sub>2</sub>B<sub>3</sub>-Type Hyperbranched Copolymers Based on a 3-Armed Unimolecular 4-N-Methylbenzamide Pentamer and Poly(propylene oxide). *Chem. Lett.* **2015**, *44*, 536–538.
- (522) Feng, X.-S.; Taton, D.; Chaikof, E. L.; Gnanou, Y. Toward an Easy Access to Dendrimer-Like Poly(ethylene oxide)s. *J. Am. Chem. Soc.* **2005**, *127*, 10956–10966.
- (523) Dworak, A.; Walach, W. Synthesis, Characterization and Properties of Functional Star and Dendritic Block Copolymers of Ethylene Oxide and Glycidol with Oligoglycidol Branching Units. *Polymer* **2009**, *50*, 3440–3447.
- (524) Wirotni, A.-L.; Ibarboure, E.; Scarpantonio, L.; Schappacher, M.; McClenaghan, N. D.; Deffieux, A. Hydro-soluble Dendritic Poly(ethylene oxide)s with Zinc Tetraphenylporphyrin Branching Points as Photosensitizers. *Polym. Chem.* **2013**, *4*, 1903–1912.
- (525) Walach, W.; Trzebicka, B.; Justynska, J.; Dworak, A. High Molecular Arborescent Poly(oxyethylene) with Hydroxyl Containing Shell. *Polymer* **2004**, *45*, 1755–1762.
- (526) Feng, X.; Taton, D.; Chaikof, E. L.; Gnanou, Y. Fast Access to Dendrimer-Like Poly(ethylene oxide)s through Anionic Ring-Opening Polymerization of Ethylene Oxide and Use of Nonprotected Glycidol as Branching Agent. *Macromolecules* **2009**, *42*, 7292–7298.
- (527) Wilms, D.; Schömer, M.; Wurm, F.; Hermanns, M. I.; Kirkpatrick, C. J.; Frey, H. Hyperbranched PEG by Random Copolymerization of Ethylene Oxide and Glycidol. *Macromol. Rapid Commun.* **2010**, *31*, 1811–1815.
- (528) Perevyazko, I.; Seiwert, J.; Schömer, M.; Frey, H.; Schubert, U. S.; Pavlov, G. M. Hyperbranched Poly(ethylene glycol) Copolymers: Absolute Values of the Molar Mass, Properties in Dilute Solution, and Hydrodynamic Homology. *Macromolecules* **2015**, *48*, 5887–5898.
- (529) Schömer, M.; Seiwert, J.; Frey, H. Hyperbranched Poly(propylene oxide): A Multifunctional Backbone-Thermoresponsive Polyether Polyol Copolymer. *ACS Macro Lett.* **2012**, *1*, 888–891.
- (530) Seiwert, J.; Leibig, D.; Kemmer-Jonas, U.; Bauer, M.; Perevyazko, I.; Preis, J.; Frey, H. Hyperbranched Polyols via Copolymerization of 1,2-Butylene Oxide and Glycidol: Comparison of Batch Synthesis and Slow Monomer Addition. *Macromolecules* **2015**, DOI: 10.1021/acs.macromol.5b02402.
- (531) Royappa, A.; Dalal, N.; Giese, M. Amphiphilic Copolymers of Glycidol with Nonpolar Epoxide Comonomers. *J. Appl. Polym. Sci.* **2001**, *82*, 2290–2299.
- (532) Pang, Y.; Liu, J.; Wu, J.; Li, G.; Wang, R.; Su, Y.; He, P.; Zhu, X.; Yan, D.; Zhu, B. Synthesis, Characterization, and *in vitro* Evaluation of Long-Chain Hyperbranched Poly(ethylene glycol) as Drug Carrier. *Bioconjugate Chem.* **2010**, *21*, 2093–2102.
- (533) Hamley, I. W. PEG-Peptide Conjugates. *Biomacromolecules* **2014**, *15*, 1543–1559.
- (534) Immordino, M. L.; Dosio, F.; Cattel, L. Stealth Liposomes: Review of the Basic Science, Rationale, and Clinical Applications, Existing and Potential. *Int. J. Nanomedicine* **2006**, *1*, 297–315.
- (535) Hatakeyama, H.; Akita, H.; Harashima, H. The Poly(ethylene glycol) Dilemma: Advantage and Disadvantage of PEGylation of Liposomes for Systemic Genes and Nucleic Acids Delivery to Tumors. *Biol. Pharm. Bull.* **2013**, *36*, 892–899.
- (536) He, Z.-Y.; Chu, B.-Y.; Wei, X.-W.; Li, J.; Edwards III, C. K.; Song, X.-R.; He, G.; Xie, Y.-M.; Wei, Y.-Q.; Qian, Z.-Y. Recent Development of Poly(ethylene glycol)-Cholesterol Conjugates as Drug Delivery Systems. *Int. J. Pharm.* **2014**, *469*, 168–178.
- (537) Gabizon, A.; Shmeeda, H.; Horowitz, A. T.; Zalipsky, S. Tumor Cell Targeting of Liposome-Entrapped Drugs with Phospholipid-Anchored Folic Acid-PEG Conjugates. *Adv. Drug Delivery Rev.* **2004**, *56*, 1177–1192.
- (538) Zalipsky, S.; Mullah, N.; Dibble, A.; Flaherty, T. New Chemoenzymatic Approach to Glyco-Lipopolymers: Practical Preparation of Functionally Active Galactose-Poly(ethylene glycol)-Distearoylphosphatidic Acid (GAL-PEG-DSPA) Conjugate. *Chem. Commun.* **1999**, 653–654.
- (539) Storchak, E. P.; Summerton, J. E.; Weller, D. D. Uncharged Stereoregular Nucleic Acid Analogs: 2. Morpholino Nucleoside Oligomers with Carbamate Internucleoside Linkages. *Nucleic Acids Res.* **1989**, *17*, 6129–6141.
- (540) Bonora, G. M.; Zaramella, S.; Veronese, F. M. Synthesis by High-Efficiency Liquid-Phase (HELP) Method of Oligonucleotides Conjugated with High-Molecular Weight Poly(ethylene glycol)s (PEGs). *Biol. Proced. Online* **1998**, *1*, 59–69.
- (541) Shokrzadeh, N.; Winkler, A. M.; Dirin, M.; Winkler, J. Oligonucleotides Conjugated with Short Chemically Defined Poly(ethylene glycol) Chains Are Efficient Antisense Agents. *Bioorg. Med. Chem. Lett.* **2014**, *24*, 5758–5761.
- (542) Vllasaliu, D.; Fowler, R.; Stolnik, S. Pegylated Nanomedicines: Recent Progress and Remaining Concerns. *Expert Opin. Drug Delivery* **2014**, *11*, 139–154.
- (543) Suk, J. S.; Xu, Q.; Kim, N.; Hanes, J.; Ensign, L. M. PEGylation as a Strategy for Improving Nanoparticle-Based Drug and Gene Delivery. *Adv. Drug Delivery Rev.* **2015**, DOI: 10.1016/j.addr.2015.09.012.
- (544) Walter, H.; Johansson, G.; Brooks, D. E. Partitioning in Aqueous Two-Phase Systems: Recent Results. *Anal. Biochem.* **1991**, *197*, 1–18.
- (545) Azevedo, A. M.; Rosa, P. A.; Ferreira, I. F.; Aires-Barros, M. R. Chromatography-Free Recovery of Biopharmaceuticals through Aqueous Two-Phase Processing. *Trends Biotechnol.* **2009**, *27*, 240–247.
- (546) Matsushima, A.; Kadera, Y.; Hiroto, M.; Nishimura, H.; Inada, Y. Bioconjugates of Proteins and Poly(ethylene glycol): Potent Tools in Biotechnological Processes. *J. Mol. Catal. B: Enzym.* **1996**, *2*, 1–17.
- (547) Kishimoto, T.; Itami, M.; Yomo, T.; Urabe, I.; Yamada, Y.; Okada, H. Improved Methods for the Preparation of N6-(2-Carboxyethyl)-NAD and Poly(ethylene glycol)-Bound NAD(H). *J. Ferment. Bioeng.* **1991**, *71*, 447–449.
- (548) Khandare, J.; Minko, T. Polymer-Drug Conjugates: Progress in Polymeric Prodrugs. *Prog. Polym. Sci.* **2006**, *31*, 359–397.
- (549) Harris, J. M.; Chess, R. B. Effect of PEGylation on Pharmaceuticals. *Nat. Rev. Drug Discovery* **2003**, *2*, 214–221.
- (550) Giorgi, M. E.; Agusti, R.; de Lederkremer, R. M. Carbohydrate PEGylation, an Approach to Improve Pharmacological Potency. *Beilstein J. Org. Chem.* **2014**, *10*, 1433–1444.

- (551) Abuchowski, A.; McCoy, J. R.; Palczuk, N. C.; van Es, T.; Davis, F. F. Effect of Covalent Attachment of Poly(ethylene glycol) on Immunogenicity and Circulating Life of Bovine Liver Catalase. *J. Biol. Chem.* **1977**, *252*, 3582–3586.
- (552) Abuchowski, A.; van Es, T.; Palczuk, N. C.; Davis, F. F. Alteration of Immunological Properties of Bovine Serum Albumin by Covalent Attachment of Poly(ethylene glycol). *J. Biol. Chem.* **1977**, *252*, 3578–3581.
- (553) Roberts, M. J.; Bentley, M. D.; Harris, J. M. Chemistry for Peptide and Protein PEGylation. *Adv. Drug Delivery Rev.* **2012**, *64*, 116–127.
- (554) Ryan, S. M.; Mantovani, G.; Wang, X.; Haddleton, D. M.; Brayden, D. J. Advances in PEGylation of Important Biotech Molecules: Delivery Aspects. *Expert Opin. Drug Delivery* **2008**, *5*, 371–383.
- (555) Bailon, P.; Won, C. Y. PEG-Modified Biopharmaceuticals. *Expert Opin. Drug Delivery* **2009**, *6*, 1–16.
- (556) Alconcel, S. N. S.; Baas, A. S.; Maynard, H. D. FDA-Approved Poly(ethylene glycol)-Protein Conjugate Drugs. *Polym. Chem.* **2011**, *2*, 1442–1448.
- (557) Caliceti, P.; Veronese, F. M. Pharmacokinetic and Biodistribution Properties of Poly(ethylene glycol)-Protein Conjugates. *Adv. Drug Delivery Rev.* **2003**, *55*, 1261–1277.
- (558) Kang, B.; Okwieka, P.; Schottler, S.; Seifert, O.; Kontermann, R. E.; Pfizenmaier, K.; Musyanovych, A.; Meyer, R.; Diken, M.; Sahin, U.; et al. Tailoring the Stealth Properties of Biocompatible Polysaccharide Nanocontainers. *Biomaterials* **2015**, *49*, 125–134.
- (559) Müller, S. S.; Dingels, C.; Hofmann, A. M.; Frey, H. In *Tailored Polymer Architectures for Pharmaceutical and Biomedical Applications*; Scholz, C., Kressler, J., Eds.; ACS Symposium Series; ACS: Washington, DC, 2013; Vol. 1135, pp 11–25.
- (560) Pasut, G.; Veronese, F. M. Polymer–Drug Conjugation, Recent Achievements and General Strategies. *Prog. Polym. Sci.* **2007**, *32*, 933–961.
- (561) Damodaran, V. B.; Fee, C. J. Protein PEGylation: An Overview of Chemistry and Process Considerations. *Eur. Pharm. Rev.* **2010**, *1*, 18–36.
- (562) Canalle, L. A.; Lowik, D. W.; van Hest, J. C. Polypeptide-Polymer Bioconjugates. *Chem. Soc. Rev.* **2010**, *39*, 329–353.
- (563) de Graaf, A. J.; Kooijman, M.; Hennink, W. E.; Mastrobattista, E. Nonnatural Amino Acids for Site-Specific Protein Conjugation. *Bioconjugate Chem.* **2009**, *20*, 1281–1295.
- (564) Gauthier, M. A.; Klok, H. A. Peptide/Protein-Polymer Conjugates: Synthetic Strategies and Design Concepts. *Chem. Commun.* **2008**, *23*, 2591–2611.
- (565) Pfister, D.; Morbidelli, M. Process for Protein PEGylation. *J. Controlled Release* **2014**, *180*, 134–149.
- (566) Ivens, I. A.; Achanzar, W.; Baumann, A.; Brändli-Baiocco, A.; Cavagnaro, J.; Dempster, M.; Depelchin, B. O.; Irizarry Rovira, A. R.; Dill-Morton, L.; Lane, J. H.; et al. PEGylated Biopharmaceuticals: Current Experience and Considerations for Nonclinical Development. *Toxicol. Pathol.* **2015**, *43*, 959–983.
- (567) Ginn, C.; Khalili, H.; Lever, R.; Brocchini, S. PEGylation and its Impact on the Design of New Protein-Based Medicines. *Future Med. Chem.* **2014**, *6*, 1829–1846.
- (568) Brocchini, S.; Godwin, A.; Balan, S.; Choi, J. W.; Zloh, M.; Shaunak, S. Disulfide Bridge Based PEGylation of Proteins. *Adv. Drug Delivery Rev.* **2008**, *60*, 3–12.
- (569) Fee, C. J. Size Comparison between Proteins PEGylated with Branched and Linear Poly(ethylene glycol) Molecules. *Biotechnol. Bioeng.* **2007**, *98*, 725–731.
- (570) Zalipsky, S. Chemistry of Poly(ethylene glycol) Conjugates with Biologically-Active Molecules. *Adv. Drug Delivery Rev.* **1995**, *16*, 157–182.
- (571) Boutoureira, O.; Bernardes, G. J. Advances in Chemical Protein Modification. *Chem. Rev.* **2015**, *115*, 2174–2195.
- (572) Nischan, N.; Hackenberger, C. P. Site-Specific PEGylation of Proteins: Recent Developments. *J. Org. Chem.* **2014**, *79*, 10727–10733.
- (573) Zhang, C.; Yang, X. L.; Yuan, Y. H.; Pu, J.; Liao, F. Site-Specific PEGylation of Therapeutic Proteins Via Optimization of Both Accessible Reactive Amino Acid Residues and PEG Derivatives. *BioDrugs* **2012**, *26*, 209–215.
- (574) Dozier, J.; Distefano, M. Site-Specific PEGylation of Therapeutic Proteins. *Int. J. Mol. Sci.* **2015**, *16*, 25831.
- (575) Fee, C. J.; Van Alstine, J. M. Purification of PEGylated Proteins. *Methods Biochem. Anal.* **2011**, *54*, 339–362.
- (576) Gonzalez-Valdez, J.; Rito-Palomares, M.; Benavides, J. Advances and Trends in the Design, Analysis, and Characterization of Polymer-Protein Conjugates for “PEGylated” Bioprocesses. *Anal. Bioanal. Chem.* **2012**, *403*, 2225–2235.
- (577) Becker, R.; Dembek, C.; White, L. A.; Garrison, L. P. The Cost Offsets and Cost-Effectiveness Associated with PEGylated Drugs: A Review of the Literature. *Expert Rev. Pharmacoecon Outcomes Res.* **2012**, *12*, 775–793.
- (578) Schellekens, H.; Hennink, W. E.; Brinks, V. The Immunogenicity of Poly(ethylene glycol): Facts and Fiction. *Pharm. Res.* **2013**, *30*, 1729–1734.
- (579) Zhang, F.; Liu, M. R.; Wan, H. T. Discussion About Several Potential Drawbacks of PEGylated Therapeutic Proteins. *Biol. Pharm. Bull.* **2014**, *37*, 335–339.
- (580) Fishburn, C. S. The Pharmacology of PEGylation: Balancing PD with PK to Generate Novel Therapeutics. *J. Pharm. Sci.* **2008**, *97*, 4167–4183.
- (581) Dust, J. M.; Fang, Z. H.; Harris, J. M. Proton Nmr Characterization of Poly(ethylene glycol)s and Derivatives. *Macromolecules* **1990**, *23*, 3742–3746.
- (582) Chan, B.; Wara, D.; Bastian, J.; Hershfield, M. S.; Bohnsack, J.; Azen, C. G.; Parkman, R.; Weinberg, K.; Kohn, D. B. Long-Term Efficacy of Enzyme Replacement Therapy for Adenosine Deaminase (Ada)-Deficient Severe Combined Immunodeficiency (Scid). *Clin. Immunol.* **2005**, *117*, 133–143.
- (583) Hauser, G.; Awad, T.; Brok, J.; Thorlund, K.; Stimac, D.; Mabrouk, M.; Gluud, C.; Gluud, L. L. PEGinterferon Plus Ribavirin Versus Interferon Plus Ribavirin for Chronic Hepatitis C. *Cochrane Database Syst. Rev.* **2014**, *2*, CD005441.
- (584) Tong, W. H.; Pieters, R.; Kaspers, G. J.; te Loo, D. M.; Bierings, M. B.; van den Bos, C.; Kollen, W. J.; Hop, W. C.; Lanvers-Kaminsky, C.; Relling, M. V.; et al. A Prospective Study on Drug Monitoring of PEGasparaginase and Erwinia Asparaginase and Asparaginase Antibodies in Pediatric Acute Lymphoblastic Leukemia. *Blood* **2014**, *123*, 2026–2033.
- (585) Kozłowski, A.; Harris, J. M. Improvements in Protein PEGylation: PEGylated Interferons for Treatment of Hepatitis C. *J. Controlled Release* **2001**, *72*, 217–224.
- (586) Veronese, F. M.; Caliceti, P.; Schiavon, O. Branched and Linear Poly(ethylene glycol): Influence of the Polymer Structure on Enzymological, Pharmacokinetic, and Immunological Properties of Protein Conjugates. *J. Bioact. Compat. Polym.* **1997**, *12*, 196–207.
- (587) Caliceti, P.; Schiavon, O.; Sartore, L.; Monfardini, C.; Veronese, F. M. Active-Site Protection of Proteolytic-Enzymes by Poly(ethylene glycol) Surface Modification. *J. Bioact. Compat. Polym.* **1993**, *8*, 41–50.
- (588) Salmaso, S.; Semenzato, A.; Bersania, S.; Chinol, M.; Paganelli, G.; Caliceti, P. Preparation and Characterization of Active Site Protected Poly(ethylene glycol)-Avidin Bioconjugates. *Biochim. Biophys. Acta, Gen. Subj.* **2005**, *1726*, 57–66.
- (589) Schiavon, O.; Caliceti, P.; Ferruti, P.; Veronese, F. M. Therapeutic Proteins: A Comparison of Chemical and Biological Properties of Uricase Conjugated to Linear or Branched Poly(ethylene glycol) and Poly(*N*-acryloylmorpholine). *Farmacol.* **2000**, *55*, 264–269.
- (590) Kunstelj, M.; Fidler, K.; Škrajnar, Š.; Kenig, V.; Smilović, V.; Kusterle, M.; Caserman, S.; Zore, I.; Porekar, V. G.; Jevševar, S. Cysteine-Specific PEGylation of rhG-CSF via Selenylsulfide Bond. *Bioconjugate Chem.* **2013**, *24*, 889–896.
- (591) Hinds, K.; Koh, J. J.; Joss, L.; Liu, F.; Baudys, M.; Kim, S. W. Synthesis and Characterization of Poly(ethylene glycol)-Insulin Conjugates. *Bioconjugate Chem.* **2000**, *11*, 195–201.
- (592) Youn, Y. S.; Chae, S. Y.; Lee, S.; Jeon, J. E.; Shin, H. G.; Lee, K. C. Evaluation of Therapeutic Potentials of Site-Specific PEGylated Glucagon-Like Peptide-1 Isomers as a Type 2 Anti-Diabetic Treatment:

## Chemical Reviews

## Review

- Insulinotropic Activity, Glucose-Stabilizing Capability, and Proteolytic Stability. *Biochem. Pharmacol.* **2007**, *73*, 84–93.
- (593) Youn, Y. S.; Kwon, M. J.; Na, D. H.; Chae, S. Y.; Lee, S.; Lee, K. C. Improved Intrapulmonary Delivery of Site-Specific PEGylated Salmon Calcitonin: Optimization by PEG Size Selection. *J. Controlled Release* **2008**, *125*, 68–75.
- (594) Yamamoto, Y.; Tsutsumi, Y.; Yoshioka, Y.; Nishibata, T.; Kobayashi, K.; Okamoto, T.; Mukai, Y.; Shimizu, T.; Nakagawa, S.; Nagata, S.; et al. Site-Specific PEGylation of a Lysine-Deficient Tnf-Alpha with Full Bioactivity. *Nat. Biotechnol.* **2003**, *21*, 546–552.
- (595) Cho, H.; Daniel, T.; Buechler, Y. J.; Litzinger, D. C.; Maio, Z.; Putnam, A. M.; Kraynov, V. S.; Sim, B. C.; Bussell, S.; Javahishvili, T.; et al. Optimized Clinical Performance of Growth Hormone with an Expanded Genetic Code. *Proc. Natl. Acad. Sci. U. S. A.* **2011**, *108*, 9060–9065.
- (596) Pechar, M.; Kopeckova, P.; Joss, L.; Kopecek, J. Associative Diblock Copolymers of Poly(ethylene glycol) and Coiled-Coil Peptides. *Macromol. Biosci.* **2002**, *2*, 199–206.
- (597) Sharp, K. A.; Yalpani, M.; Howard, S. J.; Brooks, D. E. Synthesis and Application of a Poly(ethylene glycol)-Antibody Affinity Ligand for Cell Separations in Aqueous Polymer Two-Phase Systems. *Anal. Biochem.* **1986**, *154*, 110–117.
- (598) Gais, H. J.; Ruppert, S. Modification and Immobilization of Proteins with Poly(ethylene glycol) Tressylates and Polysaccharide Tressylates - Evidence Suggesting a Revision of the Coupling Mechanism and the Structure of the Polymer-Polymer Linkage. *Tetrahedron Lett.* **1995**, *36*, 3837–3838.
- (599) Treetharnmathurot, B.; Ovarlarnporn, C.; Wungsintaweekul, J.; Duncan, R.; Wiwattanapatapee, R. Effect of PEG Molecular Weight and Linking Chemistry on the Biological Activity and Thermal Stability of Pegylated Trypsin. *Int. J. Pharm.* **2008**, *357*, 252–259.
- (600) Obermeyer, A. C.; Jarman, J. B.; Francis, M. B. N-Terminal Modification of Proteins with O-Aminophenols. *J. Am. Chem. Soc.* **2014**, *136*, 9572–9579.
- (601) Cong, Y.; Pawlisz, E.; Bryant, P.; Balan, S.; Laurine, E.; Tommasi, R.; Singh, R.; Dubey, S.; Peciak, K.; Bird, M.; et al. Site-Specific PEGylation at Histidine Tags. *Bioconjugate Chem.* **2012**, *23*, 248–263.
- (602) Chamow, S. M.; Kogan, T. P.; Venuti, M.; Gadek, T.; Harris, R. J.; Peers, D. H.; Mordenti, J.; Shak, S.; Ashkenazi, A. Modification of Cd4 Immunoadhesin with Monomethoxypoly(ethylene glycol) Aldehyde via Reductive Alkylation. *Bioconjugate Chem.* **1994**, *5*, 133–140.
- (603) Wirth, P.; Soupe, J.; Tritsch, D.; Biellmann, J.-F. Chemical Modification of Horseradish Peroxidase with Ethanal-Methoxypoly(ethylene glycol): Solubility in Organic Solvents, Activity, and Properties. *Bioorg. Chem.* **1991**, *19*, 133–142.
- (604) McFarland, J. M.; Francis, M. B. Reductive Alkylation of Proteins Using Iridium Catalyzed Transfer Hydrogenation. *J. Am. Chem. Soc.* **2005**, *127*, 13490–13491.
- (605) Bentley, M. D.; Roberts, M. J.; Harris, J. M. Reductive Amination Using Poly(ethylene glycol) Acetaldehyde Hydrate Generated in Situ: Applications to Chitosan and Lysozyme. *J. Pharm. Sci.* **1998**, *87*, 1446–1449.
- (606) Kinstler, O. B.; Brems, D. N.; Lauren, S. L.; Paige, A. G.; Hamburger, J. B.; Treuheit, M. J. Characterization and Stability of N-Terminally PEGylated rhG-CSF. *Pharm. Res.* **1996**, *13*, 996–1002.
- (607) Lee, H.; Jang, I. H.; Ryu, S. H.; Park, T. G. N-Terminal Site-Specific Mono-PEGylation of Epidermal Growth Factor. *Pharm. Res.* **2003**, *20*, 818–825.
- (608) Baker, D. P.; Lin, E. Y.; Lin, K.; Pellegrini, M.; Petter, R. C.; Chen, L. L.; Arduini, R. M.; Brickelmaier, M.; Wen, D.; Hess, D. M.; et al. N-Terminally PEGylated Human Interferon-Beta-1a with Improved Pharmacokinetic Properties and in Vivo Efficacy in a Melanoma Angiogenesis Model. *Bioconjugate Chem.* **2006**, *17*, 179–188.
- (609) Basu, A.; Yang, K.; Wang, M.; Liu, S.; Chintala, R.; Palm, T.; Zhao, H.; Peng, P.; Wu, D.; Zhang, Z.; et al. Structure-Function Engineering of Interferon-Beta-1b for Improving Stability, Solubility, Potency, Immunogenicity, and Pharmacokinetic Properties by Site-Selective Mono-PEGylation. *Bioconjugate Chem.* **2006**, *17*, 618–630.
- (610) Huang, Z.; Lu, M.; Zhu, G.; Gao, H.; Xie, L.; Zhang, X.; Ye, C.; Wang, Y.; Sun, C.; Li, X. Acceleration of Diabetic-Wound Healing with PEGylated RhaFGF in Healing-Impaired Streptozocin Diabetic Rats. *Wound Repair Regen.* **2011**, *19*, 633–644.
- (611) Ikeeda, Y.; Katamachi, J.; Kawasaki, H.; Nagasaki, Y. Novel Protein PEGylation Chemistry via Glutalaldehyde-Functionalized Peg. *Bioconjugate Chem.* **2013**, *24*, 1824–1827.
- (612) Miron, T.; Wilchek, M. A Simplified Method for the Preparation of Succinimidyl Carbonate Poly(ethylene glycol) for Coupling to Proteins. *Bioconjugate Chem.* **1993**, *4*, 568–569.
- (613) Lee, S.; Greenwald, R. B.; McGuire, J.; Yang, K.; Shi, C. Drug Delivery Systems Employing 1,6-Elimination: Releasable Poly(ethylene glycol) Conjugates of Proteins. *Bioconjugate Chem.* **2001**, *12*, 163–169.
- (614) Greenwald, R. B.; Pendri, A.; Martinez, A.; Gilbert, C.; Bradley, P. Peg Thiazolidine-2-Thione, a Novel Reagent for Facile Protein Modification: Conjugation of Bovine Hemoglobin. *Bioconjugate Chem.* **1996**, *7*, 638–641.
- (615) Veronese, F. M.; Largajolli, R.; Boccu, E.; Benassi, C. A.; Schiavon, O. Surface Modification of Proteins. Activation of Monomethoxy-Polyethylene Glycols by Phenylchloroformates and Modification of Ribonuclease and Superoxide Dismutase. *Appl. Biochem. Biotechnol.* **1985**, *11*, 141–152.
- (616) Beauchamp, C. O.; Gonias, S. L.; Menapace, D. P.; Pizzo, S. V. A New Procedure for the Synthesis of Polyethylene Glycol-Protein Adducts; Effects on Function, Receptor Recognition, and Clearance of Superoxide Dismutase, Lactoferrin, and Alpha 2-Macroglobulin. *Anal. Biochem.* **1983**, *131*, 25–33.
- (617) González, M.; Ceaglio, N. A.; de los Milagros Bürgi, M.; Etcheverrigaray, M.; Kratje, R. B.; Vaillard, S. E. Novel Reactive PEG for Amino Group Conjugation. *RSC Adv.* **2015**, *5*, 14002–14009.
- (618) Atassi, M. Z.; Manshour, T. Synthesis of Tolerogenic Monomethoxypolyethylene Glycol and Polyvinyl Alcohol Conjugates of Peptides. *J. Protein Chem.* **1991**, *10*, 623–627.
- (619) Kozlowski, A. Shearwater Corporation; U.S. Patent 6376604 B2, 2002.
- (620) Zalipsky, S.; Mullah, N.; Engbers, C.; Hutchins, M. U.; Kiwan, R. Thiolytically Cleavable Dithiobenzyl Urethane-Linked Polymer-Protein Conjugates as Macromolecular Prodrugs: Reversible PEGylation of Proteins. *Bioconjugate Chem.* **2007**, *18*, 1869–1878.
- (621) Dingels, C.; Wurm, F.; Wagner, M.; Klok, H. A.; Frey, H. Squaric Acid Mediated Chemospecific PEGylation of Proteins: Reactivity of Single-Step-Activated Alpha-Amino Poly(ethylene glycol)s. *Chem. - Eur. J.* **2012**, *18*, 16828–16835.
- (622) Kwok, K. Y.; McKenzie, D. L.; Evers, D. L.; Rice, K. G. Formulation of Highly Soluble Poly(ethylene glycol)-Peptide DNA Condensates. *J. Pharm. Sci.* **1999**, *88*, 996–1003.
- (623) Kuan, C. T.; Wang, Q. C.; Pastan, I. Pseudomonas Exotoxin-a Mutants - Replacement of Surface-Exposed Residues in Domain-II with Cysteine Residues That Can Be Modified with Polyethylene-Glycol in a Site-Specific Manner. *J. Biol. Chem.* **1994**, *269*, 7610–7616.
- (624) Howorka, S.; Movileanu, L.; Lu, X. F.; Magnon, M.; Cheley, S.; Braha, O.; Bayley, H. A Protein Pore with a Single Polymer Chain Tethered within the Lumen. *J. Am. Chem. Soc.* **2000**, *122*, 2411–2416.
- (625) Woghiren, C.; Sharma, B.; Stein, S. Protected Thiol-Polyethylene Glycol: A New Activated Polymer for Reversible Protein Modification. *Bioconjugate Chem.* **1993**, *4*, 314–318.
- (626) Jones, M. W.; Mantovani, G.; Ryan, S. M.; Wang, X.; Brayden, D. J.; Haddleton, D. M. Phosphine-Mediated One-Pot Thiol-Ene "Click" Approach to Polymer-Protein Conjugates. *Chem. Commun.* **2009**, 5272–5274.
- (627) Morpurgo, M.; Veronese, F. M.; Kachensky, D.; Harris, J. M. Preparation and Characterization of Poly(ethylene glycol) Vinyl Sulfone. *Bioconjugate Chem.* **1996**, *7*, 363–368.
- (628) Goodson, R. J.; Katre, N. V. Site-Directed PEGylation of Recombinant Interleukin-2 at its Glycosylation Site. *Bio/Technology* **1990**, *8*, 343–346.
- (629) Badescu, G.; Bryant, P.; Swierkosz, J.; Khayrabad, F.; Pawlisz, E.; Farys, M.; Cong, Y.; Muroi, M.; Rumpf, N.; Brocchini, S.; et al. A New

- Reagent for Stable Thiol-Specific Conjugation. *Bioconjugate Chem.* **2014**, *25*, 460–469.
- (630) Shaunak, S.; Godwin, A.; Choi, J. W.; Balan, S.; Pedone, E.; Vijayarangam, D.; Heidelberger, S.; Teo, I.; Zloh, M.; Brocchini, S. Site-Specific PEGylation of Native Disulfide Bonds in Therapeutic Proteins. *Nat. Chem. Biol.* **2006**, *2*, 312–313.
- (631) Jones, M. W.; Strickland, R. A.; Schumacher, F. F.; Caddick, S.; Baker, J. R.; Gibson, M. I.; Haddleton, D. M. Polymeric Dibromomaleimides as Extremely Efficient Disulfide Bridging Bioconjugation and PEGylation Agents. *J. Am. Chem. Soc.* **2012**, *134*, 1847–1852.
- (632) Schumacher, F. F.; Nobles, M.; Ryan, C. P.; Smith, M. E.; Tinker, A.; Caddick, S.; Baker, J. R. In Situ Maleimide Bridging of Disulfides and a New Approach to Protein PEGylation. *Bioconjugate Chem.* **2011**, *22*, 132–136.
- (633) Toda, N.; Asano, S.; Barbas, C. F., 3rd. Rapid, Stable, Chemoselective Labeling of Thiols with Julia-Kocienski-Like Reagents: A Serum-Stable Alternative to Maleimide-Based Protein Conjugation. *Angew. Chem., Int. Ed.* **2013**, *52*, 12592–12596.
- (634) Lin, Y. A.; Chalker, J. M.; Floyd, N.; Bernardes, G. J.; Davis, B. G. Allyl Sulfides Are Privileged Substrates in Aqueous Cross-Metathesis: Application to Site-Selective Protein Modification. *J. Am. Chem. Soc.* **2008**, *130*, 9642–9643.
- (635) Engler, A. C.; Lee, H. I.; Hammond, P. T. Highly Efficient “Grafting onto” a Polypeptide Backbone Using Click Chemistry. *Angew. Chem., Int. Ed.* **2009**, *48*, 9334–9338.
- (636) Deiters, A.; Cropp, T. A.; Summerer, D.; Mukherji, M.; Schultz, P. G. Site-Specific PEGylation of Proteins Containing Unnatural Amino Acids. *Bioorg. Med. Chem. Lett.* **2004**, *14*, 5743–5745.
- (637) Schoffelen, S.; Lambermon, M. H.; van Eldijk, M. B.; van Hest, J. C. Site-Specific Modification of *Candida Antarctica* Lipase B via Residue-Specific Incorporation of a Non-Canonical Amino Acid. *Bioconjugate Chem.* **2008**, *19*, 1127–1131.
- (638) Debets, M. F.; van Berkel, S. S.; Schoffelen, S.; Rutjes, F. P.; van Hest, J. C.; van Delft, F. L. Aza-Dibenzocyclooctynes for Fast and Efficient Enzyme PEGylation Via Copper-Free (3 + 2) Cycloaddition. *Chem. Commun.* **2010**, *46*, 97–99.
- (639) Schneider, S.; Gattner, M. J.; Vrabel, M.; Flugel, V.; Lopez-Carrillo, V.; Prill, S.; Carell, T. Structural Insights into Incorporation of Norbornene Amino Acids for Click Modification of Proteins. *ChemBioChem* **2013**, *14*, 2114–2118.
- (640) Carrico, I. S.; Carlson, B. L.; Bertozzi, C. R. Introducing Genetically Encoded Aldehydes into Proteins. *Nat. Chem. Biol.* **2007**, *3*, 321–322.
- (641) Gaertner, H. F.; Offord, R. E. Site-Specific Attachment of Functionalized Poly(ethylene glycol) to the Amino Terminus of Proteins. *Bioconjugate Chem.* **1996**, *7*, 38–44.
- (642) Nojima, Y.; Iguchi, K.; Suzuki, Y.; Sato, A. The pH-Dependent Formation of Pegylated Bovine Lactoferrin by Branched Polyethylene Glycol (PEG)-*N*-Hydroxysuccinimide (NHS) Active Esters. *Biol. Pharm. Bull.* **2009**, *32*, 523–526.
- (643) Zhang, C.; Yang, X.; Gao, A.; Hu, X.; Pu, J.; Liu, H.; Feng, J.; Liao, J.; Li, Y.; Liao, F. Comparison of Modification of a Bacterial Uricase with *N*-Hydroxysuccinimide Esters of Succinate and Carbonate of Monomethoxyl Poly(ethylene glycol). *Biotechnol. Appl. Biochem.* **2014**, *61*, 683–690.
- (644) Wylie, D. C.; Voloch, M.; Lee, S.; Liu, Y. H.; Cannon-Carlson, S.; Cutler, C.; Pramanik, B. Carboxyalkylated Histidine Is a pH-Dependent Product of PEGylation with SC-PEG. *Pharm. Res.* **2001**, *18*, 1354–1360.
- (645) Katre, N. V.; Knauf, M. J.; Laird, W. J. Chemical Modification of Recombinant Interleukin 2 by Polyethylene Glycol Increases its Potency in the Murine Meth Sarcoma Model. *Proc. Natl. Acad. Sci. U. S. A.* **1987**, *84*, 1487–1491.
- (646) Boccu, E.; Largajolli, R.; Veronese, F. M. Coupling of Monomethoxypolyethyleneglycols to Proteins Via Active Esters. *Z. Naturforsch. C* **1983**, *38*, 94–99.
- (647) Levine, P. M.; Craven, T. W.; Bonneau, R.; Kirshenbaum, K. Intrinsic Bioconjugation for Site-Specific Protein PEGylation at *N*-Terminal Serine. *Chem. Commun.* **2014**, *50*, 6909–6912.
- (648) Zhang, X.; Li, F.; Lu, X. W.; Liu, C. F. Protein C-Terminal Modification through Thioacid/Azide Amidation. *Bioconjugate Chem.* **2009**, *20*, 197–200.
- (649) Garman, A. J.; Kalindjian, S. B. The Preparation and Properties of Novel Reversible Polymer-Protein Conjugates. 2-Omega-Methoxy-polyethylene (5000) Glycoxymethylene-3-Methylmaleyl Conjugates of Plasminogen Activators. *FEBS Lett.* **1987**, *223*, 361–365.
- (650) Kim, T. H.; Swierczewska, M.; Oh, Y.; Kim, A.; Jo, D. G.; Park, J. H.; Byun, Y.; Sadegh-Nasseri, S.; Pomper, M. G.; Lee, K. C.; et al. Mix to Validate: A Facile, Reversible PEGylation for Fast Screening of Potential Therapeutic Proteins in Vivo. *Angew. Chem., Int. Ed.* **2013**, *52*, 6880–6884.
- (651) Yamaguchi, N.; Zhang, L.; Chae, B. S.; Palla, C. S.; Furst, E. M.; Kiick, K. L. Growth Factor Mediated Assembly of Cell Receptor-Responsive Hydrogels. *J. Am. Chem. Soc.* **2007**, *129*, 3040–3041.
- (652) Yamaguchi, N.; Kiick, K. L. Polysaccharide-Poly(ethylene glycol) Star Copolymer as a Scaffold for the Production of Bioactive Hydrogels. *Biomacromolecules* **2005**, *6*, 1921–1930.
- (653) Gonzalez-Gonzalez, M.; Mayolo-Deloya, K.; Rito-Palomares, M. PEGylation, Detection and Chromatographic Purification of Site-Specific Pegylated CD133-Biotin Antibody in Route to Stem Cell Separation. *J. Chromatogr. B: Anal. Technol. Biomed. Life Sci.* **2012**, *893–894*, 182–186.
- (654) Wei, K.; Li, J.; Chen, G.; Jiang, M. Dual Molecular Recognition Leading to a Protein-Polymer Conjugate and Further Self-Assembly. *ACS Macro Lett.* **2013**, *2*, 278–283.
- (655) Kogan, T. P. The Synthesis of Substituted Methoxy-Poly(ethyleneglycol) Derivatives Suitable for Selective Protein Modification. *Synth. Commun.* **1992**, *22*, 2417–2424.
- (656) Zhou, Z.; Zhang, J.; Sun, L.; Ma, G.; Su, Z. Comparison of Site-Specific PEGylations of the *N*-Terminus of Interferon Beta-1b: Selectivity, Efficiency, and in Vivo/Vitro Activity. *Bioconjugate Chem.* **2014**, *25*, 138–146.
- (657) King, D.; Chapman, A. U.S. Patent 20040121415 A1, 2004.
- (658) Jones, M. W.; Mantovani, G.; Blindauer, C. A.; Ryan, S. M.; Wang, X.; Brayden, D. J.; Haddleton, D. M. Direct Peptide Bioconjugation/PEGylation at Tyrosine with Linear and Branched Polymeric Diazonium Salts. *J. Am. Chem. Soc.* **2012**, *134*, 7406–7413.
- (659) Lonshakov, D. V.; Sheremet'ev, S. V.; Belosludtseva, E. M.; Korovkin, S. A.; Semchenko, A. V.; Katlinskij, A. V. Synthesis of 4-Aminobenzoic Acid Esters of Polyethylene Glycol and Their Use for PEGylation of Therapeutic Proteins. *RSC Adv.* **2015**, *5*, 42903–42909.
- (660) Ban, H.; Nagano, M.; Gavrilyuk, J.; Hakamata, W.; Inokuma, T.; Barbas, C. F., 3rd. Facile and Stable Linkages through Tyrosine: Bioconjugation Strategies with the Tyrosine-Click Reaction. *Bioconjugate Chem.* **2013**, *24*, 520–532.
- (661) Sato, H. Enzymatic Procedure for Site-Specific PEGylation of Proteins. *Adv. Drug Delivery Rev.* **2002**, *54*, 487–504.
- (662) Mero, A.; Schiavon, M.; Veronese, F. M.; Pasut, G. A New Method to Increase Selectivity of Transglutaminase Mediated PEGylation of Salmon Calcitonin and Human Growth Hormone. *J. Controlled Release* **2011**, *154*, 27–34.
- (663) DeFrees, S.; Wang, Z. G.; Xing, R.; Scott, A. E.; Wang, J.; Zopf, D.; Gouty, D. L.; Sjoberg, E. R.; Panneerselvam, K.; Brinkman-Van der Linden, E. C.; et al. GlycoPEGylation of Recombinant Therapeutic Proteins Produced in *Escherichia Coli*. *Glycobiology* **2006**, *16*, 833–843.
- (664) Stennicke, H. R.; Ostergaard, H.; Bayer, R. J.; Kalo, M. S.; Kinealy, K.; Holm, P. K.; Sorensen, B. B.; Zopf, D.; Bjorn, S. E. Generation and Biochemical Characterization of GlycoPEGylated Factor VIIa Derivatives. *Thromb. Haemostasis* **2008**, *100*, 920–928.
- (665) Cazalis, C. S.; Haller, C. A.; Sease-Cargo, L.; Chaikof, E. L. C-Terminal Site-Specific PEGylation of a Truncated Thrombomodulin Mutant with Retention of Full Bioactivity. *Bioconjugate Chem.* **2004**, *15*, 1005–1009.
- (666) Serwa, R.; Majkut, P.; Horstmann, B.; Swiecicki, J. M.; Gerrits, M.; Krause, E.; Hackenberger, C. P. R. Site-Specific PEGylation of Proteins by a Staudinger-Phosphite Reaction. *Chem. Sci.* **2010**, *1*, 596–602.



- (667) Li, N.; Lim, R. K.; Edwardraja, S.; Lin, Q. Copper-Free Sonogashira Cross-Coupling for Functionalization of Alkyne-Encoded Proteins in Aqueous Medium and in Bacterial Cells. *J. Am. Chem. Soc.* **2011**, *133*, 15316–15319.
- (668) Dumas, A.; Spicer, C. D.; Gao, Z.; Takehana, T.; Lin, Y. A.; Yasukohchi, T.; Davis, B. G. Self-Liganded Suzuki-Miyaura Coupling for Site-Selective Protein PEGylation. *Angew. Chem., Int. Ed.* **2013**, *52*, 3916–3921.
- (669) Berberich, J. A.; Yang, L. W.; Madura, J.; Bahar, I.; Russell, A. J. A Stable Three-Enzyme Creatinine Biosensor. I. Impact of Structure, Function and Environment on PEGylated and Immobilized Sarcosine Oxidase. *Acta Biomater.* **2005**, *1*, 173–181.
- (670) Meng, F.; Manjula, B. N.; Smith, P. K.; Acharya, S. A. PEGylation of Human Serum Albumin: Reaction of PEG-Phenyl-Isothiocyanate with Protein. *Bioconjugate Chem.* **2008**, *19*, 1352–1360.
- (671) Zhu, L.; Kemple, M. D.; Yuan, P.; Prendergast, F. G. N-Terminus and Lysine Side Chain  $pK_a$  Values of Melittin in Aqueous Solutions and Micellar Dispersions Measured by  $^{15}N$  NMR. *Biochemistry* **1995**, *34*, 13196–13202.
- (672) Hiki, S.; Kataoka, K. A Facile Synthesis of Azido-Terminated Heterobifunctional Poly(ethylene glycol)s for “Click” Conjugation. *Bioconjugate Chem.* **2007**, *18*, 2191–2196.
- (673) Hermanson, G. T. *Bioconjugate Techniques*, 3rd ed.; Elsevier Science: Burlington, 2013.
- (674) Joppich, M.; Luisi, P. L. Peptides Flanked by Two Polymer Chains: I. Synthesis of Glycyl-L-Tryptophylglycine Substituted by Poly(ethylene oxide) at Both the Carboxy and the Amino End Groups. *Makromol. Chem.* **1979**, *180*, 1381–1384.
- (675) Zhang, Y.; Wang, G.; Huang, J. A New Strategy for Synthesis of “Umbrella-Like” Poly(ethylene glycol) with Monofunctional End Group for Bioconjugation. *J. Polym. Sci., Part A: Polym. Chem.* **2010**, *48*, 5974–5981.
- (676) Siddique, A.; Cho, Y.; Kim, Y.; Bahng, S. H.; Kim, S. W.; Lee, J. Y.; Kang, H. J.; Kim, S.; Bae, Y. H.; Kim, J. pH-Sensitive Drug-Conjugates on Water-Soluble Polymer Frameworks. *Macromol. Chem. Phys.* **2015**, *216*, 265–276.
- (677) Oishi, M.; Sasaki, S.; Nagasaki, Y.; Kataoka, K. pH-Responsive Oligodeoxynucleotide (ODN)-Poly(ethylene glycol) Conjugate through Acid-Labile Beta-Thiopropionate Linkage: Preparation and Polyion Complex Micelle Formation. *Biomacromolecules* **2003**, *4*, 1426–1432.
- (678) Oishi, M.; Nagasaki, Y.; Itaka, K.; Nishiyama, N.; Kataoka, K. Lactosylated Poly(ethylene glycol)-SiRNA Conjugate through Acid-Labile Beta-Thiopropionate Linkage to Construct pH-Sensitive Polyion Complex Micelles Achieving Enhanced Gene Silencing in Hepatoma Cells. *J. Am. Chem. Soc.* **2005**, *127*, 1624–1625.
- (679) Tao, L.; Mantovani, G.; Lecolley, F.; Haddleton, D. M. Alpha-Aldehyde Terminally Functional Methacrylic Polymers from Living Radical Polymerization: Application in Protein Conjugation “PEGylation”. *J. Am. Chem. Soc.* **2004**, *126*, 13220–13221.
- (680) Ryan, S. M.; Wang, X.; Mantovani, G.; Sayers, C. T.; Haddleton, D. M.; Brayden, D. J. Conjugation of Salmon Calcitonin to a Combed-Shaped End Functionalized Poly(Poly(ethylene glycol) Methyl Ether Methacrylate) Yields a Bioactive Stable Conjugate. *J. Controlled Release* **2009**, *135*, 51–59.
- (681) Sayers, C. T.; Mantovani, G.; Ryan, S. M.; Randev, R. K.; Keiper, O.; Leszczyszyn, O. I.; Blindauer, C.; Brayden, D. J.; Haddleton, D. M. Site-Specific N-Terminus Conjugation of Poly(mPEG1100) Methacrylates to Salmon Calcitonin: Synthesis and Preliminary Biological Evaluation. *Soft Matter* **2009**, *5*, 3038.
- (682) Broyer, R. M.; Grover, G. N.; Maynard, H. D. Emerging Synthetic Approaches for Protein-Polymer Conjugations. *Chem. Commun.* **2011**, *47*, 2212–2226.
- (683) Le Droumaguet, B.; Nicolas, J. Recent Advances in the Design of Bioconjugates from Controlled/Living Radical Polymerization. *Polym. Chem.* **2010**, *1*, 563.
- (684) Cate, M. G. J. T.; Rettig, H.; Bernhardt, K.; Börner, H. G. Sequence-Defined Polypeptide-Polymer Conjugates Utilizing Reversible Addition Fragmentation Transfer Radical Polymerization. *Macromolecules* **2005**, *38*, 10643–10649.
- (685) Mantovani, G.; Lecolley, F.; Tao, L.; Haddleton, D. M.; Clerx, J.; Cornelissen, J. J.; Velonia, K. Design and Synthesis of N-Maleimido-Functionalized Hydrophilic Polymers Via Copper-Mediated Living Radical Polymerization: A Suitable Alternative to PEGylation Chemistry. *J. Am. Chem. Soc.* **2005**, *127*, 2966–2973.
- (686) French, A. C.; Thompson, A. L.; Davis, B. G. High-Purity Discrete PEG-Oligomer Crystals Allow Structural Insight. *Angew. Chem., Int. Ed.* **2009**, *48*, 1248–1252.
- (687) Harada, A.; Li, J.; Kamachi, M. Formation of Inclusion Complexes of Monodisperse Oligo(ethylene glycol)s With Alpha-Cyclodextrin. *Macromolecules* **1994**, *27*, 4538–4543.
- (688) Davis, P. D.; Crapps, E. C. Quanta Biodesign, Ltd.; U.S. patent 7,888,536, 2011.
- (689) Davis, P. D.; Wilbur, D. S. University of Washington, Quanta Biodesign, Ltd.; U.S. patent 20,130,052,130, 2013.
- (690) Davis, P. D. Equip, Llc; U.S. patent 20,150,065,711, 2015.
- (691) Perry, S. Z.; Hibbert, H. Studies on Reactions Relating to Carbohydrates and Polysaccharides: XLVIII. Ethylene Oxide and Related Compounds: Synthesis of the Polyethylene Glycols. *Can. J. Res.* **1936**, *14b*, 77–83.
- (692) Fordyce, R.; Lovell, E. L.; Hibbert, H. Studies on Reactions Relating to Carbohydrates and Polysaccharides. LVI. The Synthesis of the Higher Polyoxyethylene Glycols. *J. Am. Chem. Soc.* **1939**, *61*, 1905–1910.
- (693) Ahmed, S. A.; Tanaka, M. Synthesis of Oligo(ethylene glycol) toward 44-mer. *J. Org. Chem.* **2006**, *71*, 9884–9886.
- (694) Lumpi, D.; Braunshier, C.; Hametner, C.; Horkel, E.; Zachhuber, B.; Lendl, B.; Fröhlich, J. Convenient Multigram Synthesis of Monodisperse Oligo(ethylene glycol)s: Effective Reaction Monitoring by Infrared Spectroscopy Using an Attenuated Total Reflection Fibre Optic Probe. *Tetrahedron Lett.* **2009**, *50*, 6469–6471.
- (695) Szekeley, G.; Schaepertoens, M.; Gaffney, P. R. J.; Livingston, A. G. Iterative Synthesis of Monodisperse PEG Homostars and Linear Heterobifunctional PEG. *Polym. Chem.* **2014**, *5*, 694–697.
- (696) Berna, M.; Dalzoppo, D.; Pasut, G.; Manunta, M.; Izzo, L.; Jones, A. T.; Duncan, R.; Veronese, F. M. Novel Monodisperse PEG-Dendrons as New Tools for Targeted Drug Delivery: Synthesis, Characterization and Cellular Uptake. *Biomacromolecules* **2006**, *7*, 146–153.
- (697) Xia, G.; Li, Y.; Yang, Z.; Jiang, Z.-X. Development of a Scalable Process for  $\alpha$ -Amino- $\omega$ -Methoxyl-Dodecaethylene Glycol. *Org. Process Res. Dev.* **2015**, *19*, 1769.
- (698) Li, Y.; Qiu, X.; Jiang, Z.-X. Macrocylic Sulfates as Versatile Building Blocks in the Synthesis of Monodisperse Poly(ethylene glycol)s and Monofunctionalized Derivatives. *Org. Process Res. Dev.* **2015**, *19*, 800–805.
- (699) Bailon, P.; Palleroni, A.; Schaffer, C. A.; Spence, C. L.; Fung, W. J.; Porter, J. E.; Ehrlich, G. K.; Pan, W.; Xu, Z. X.; Modi, M. W.; et al. Rational Design of a Potent, Long-Lasting Form of Interferon: A 40 kDa Branched Polyethylene Glycol-Conjugated Interferon Alpha-2a for the Treatment of Hepatitis C. *Bioconjugate Chem.* **2001**, *12*, 195–202.
- (700) Podobnik, B.; Helk, B.; Smilovic, V.; Skrajnar, S.; Fidler, K.; Jevsevar, S.; Godwin, A.; Williams, P. Conjugation of PolyPEG to Interferon Alpha Extends Serum Half-Life While Maintaining Low Viscosity of the Conjugate. *Bioconjugate Chem.* **2015**, *26*, 452–459.
- (701) Lutz, J. F.; Hoth, A. Preparation of Ideal Peg Analogues with a Tunable Thermosensitivity by Controlled Radical Copolymerization of 2-(2-Methoxyethoxy)Ethyl Methacrylate and Oligo(ethylene glycol) Methacrylate. *Macromolecules* **2006**, *39*, 893–896.
- (702) Gao, W.; Liu, W.; Mackay, J. A.; Zalutsky, M. R.; Toone, E. J.; Chilkoti, A. In Situ Growth of a Stoichiometric PEG-Like Conjugate at a Protein's N-Terminus with Significantly Improved Pharmacokinetics. *Proc. Natl. Acad. Sci. U. S. A.* **2009**, *106*, 15231–15236.
- (703) Veronese, F. M.; Mero, A.; Caboi, F.; Sergi, M.; Marongiu, C.; Pasut, G. Site-Specific PEGylation of G-CSF by Reversible Denaturation. *Bioconjugate Chem.* **2007**, *18*, 1824–1830.

- (704) Gao, M.; Tian, H.; Ma, C.; Gao, X.; Guo, W.; Yao, W. Expression, Purification, and C-Terminal Site-Specific PEGylation of Cysteine-Mutated Glucagon-Like Peptide-1. *Appl. Biochem. Biotechnol.* **2010**, *162*, 155–165.
- (705) Sridhar, B. V.; Brock, J. L.; Silver, J. S.; Leight, J. L.; Randolph, M. A.; Anseth, K. S. Tissue Engineering: Development of a Cellularly Degradable PEG Hydrogel to Promote Articular Cartilage Extracellular Matrix Deposition. *Adv. Healthcare Mater.* **2015**, *4*, 702–713.
- (706) Filpula, D.; Zhao, H. Releasable PEGylation of Proteins with Customized Linkers. *Adv. Drug Delivery Rev.* **2008**, *60*, 29–49.
- (707) Georgianna, W. E.; Lusic, H.; McIver, A. L.; Deiters, A. Photodegradable Polyethylene Glycol for the Light-Regulation of Protein Function. *Bioconjugate Chem.* **2010**, *21*, 1404–1407.
- (708) Barz, M.; Luxenhofer, R.; Zentel, R.; Vicent, M. J. Overcoming the PEG-Addiction: Well-Defined Alternatives to PEG, from Structure–Property Relationships to Better Defined Therapeutics. *Polym. Chem.* **2011**, *2*, 1900.
- (709) Qi, Y.; Chilkoti, A. Protein–Polymer Conjugation — Moving Beyond PEGylation. *Curr. Opin. Chem. Biol.* **2015**, *28*, 181–193.
- (710) Wurm, F.; Dingels, C.; Frey, H.; Klok, H. A. Squaric Acid Mediated Synthesis and Biological Activity of a Library of Linear and Hyperbranched Poly(glycerol)-Protein Conjugates. *Biomacromolecules* **2012**, *13*, 1161–1171.
- (711) Braunecker, W. A.; Matyjaszewski, K. Controlled/Living Radical Polymerization: Features, Developments, and Perspectives. *Prog. Polym. Sci.* **2007**, *32*, 93–146.
- (712) Duncan, R.; Vicent, M. J. Polymer Therapeutics-Prospects for 21st Century: The End of the Beginning. *Adv. Drug Delivery Rev.* **2013**, *65*, 60–70.
- (713) Duncan, R. Polymer Conjugates as Anticancer Nanomedicines. *Nat. Rev. Cancer* **2006**, *6*, 688–701.
- (714) Hardwicke, J.; Moseley, R.; Stephens, P.; Harding, K.; Duncan, R.; Thomas, D. W. Bioresponsive Dextrin-rhEGF Conjugates: In Vitro Evaluation in Models Relevant to its Proposed Use as a Treatment for Chronic Wounds. *Mol. Pharmaceutics* **2010**, *7*, 699–707.
- (715) Tao, L.; Liu, J.; Xu, J.; Davis, T. P. Synthesis and Bioactivity of Poly(HPMA)-Lysozyme Conjugates: The Use of Novel Thiazolidine-2-Thione Coupling Chemistry. *Org. Biomol. Chem.* **2009**, *7*, 3481–3485.
- (716) Besheer, A.; Hertel, T. C.; Kressler, J.; Mäder, K.; Pietzsch, M. Enzymatically Catalyzed HES Conjugation Using Microbial Transglutaminase: Proof of Feasibility. *J. Pharm. Sci.* **2009**, *98*, 4420–4428.
- (717) Mero, A.; Pasut, G.; Dalla Via, L.; Fijten, M. W.; Schubert, U. S.; Hoogenboom, R.; Veronese, F. M. Synthesis and Characterization of Poly(2-ethyl-2-oxazoline)-Conjugates with Proteins and Drugs: Suitable Alternatives to PEG-Conjugates? *J. Controlled Release* **2008**, *125*, 87–95.
- (718) Steinbach, T.; Wurm, F. R. Poly(Phosphoester)s: A New Platform for Degradable Polymers. *Angew. Chem., Int. Ed.* **2015**, *54*, 6098–6108.
- (719) Ulbricht, J.; Jordan, R.; Luxenhofer, R. On the Biodegradability of Polyethylene Glycol, Polypeptoids and Poly(2-oxazoline)s. *Biomaterials* **2014**, *35*, 4848–4861.
- (720) Yang, Q.; Lai, S. K. Anti-PEG Immunity: Emergence, Characteristics, and Unaddressed Questions. *WIREs Nanomed. Nanobiotechnol.* **2015**, *7*, 655–677.
- (721) Harding, J. R.; Amanchukwu, C. V.; Hammond, P. T.; Shao-Horn, Y. Instability of Poly(ethylene oxide) Upon Oxidation in Lithium–Air Batteries. *J. Phys. Chem. C* **2015**, *119*, 6947–6955.
- (722) de Sainte Claire, P. Degradation of PEO in the Solid State: A Theoretical Kinetic Model. *Macromolecules* **2009**, *42*, 3469–3482.
- (723) Kawasaki, H.; Takeda, Y.; Arakawa, R. Mass Spectrometric Analysis for High Molecular Weight Synthetic Polymers Using Ultrasonic Degradation and the Mechanism of Degradation. *Anal. Chem.* **2007**, *79*, 4182–4187.
- (724) Hassouna, F.; Morlat-Thérias, S.; Mailhot, G.; Gardette, J. L. Influence of Water on the Photodegradation of Poly(ethylene oxide). *Polym. Degrad. Stab.* **2007**, *92*, 2042–2050.
- (725) Jayakannan, M.; Ramakrishnan, S. Recent Developments in Polyether Synthesis. *Macromol. Rapid Commun.* **2001**, *22*, 1463.
- (726) Yamaoka, T.; Tabata, Y.; Ikada, Y. Distribution and Tissue Uptake of Poly(ethylene glycol) with Different Molecular Weights after Intravenous Administration to Mice. *J. Pharm. Sci.* **1994**, *83*, 601–606.
- (727) Yamahira, S.; Yamaguchi, S.; Kawahara, M.; Nagamune, T. Collagen Surfaces Modified with Photo-Cleavable Polyethylene Glycol-Lipid Support Versatile Single-Cell Arrays of Both Non-Adherent and Adherent Cells. *Macromol. Biosci.* **2014**, *14*, 1670–1676.
- (728) Knorr, V.; Allmendinger, L.; Walker, G. F.; Paintner, F. F.; Wagner, E. An Acetal-Based PEGylation Reagent for pH-Sensitive Shielding of DNA Polyplexes. *Bioconjugate Chem.* **2007**, *18*, 1218–1225.
- (729) Cui, W.; Qi, M.; Li, X.; Huang, S.; Zhou, S.; Weng, J. Electrospun Fibers of Acid-Labile Biodegradable Polymers with Acetal Groups as Potential Drug Carriers. *Int. J. Pharm.* **2008**, *361*, 47–55.
- (730) Pohlitz, H.; Bellinghausen, L.; Schömer, M.; Heydenreich, B.; Saloga, J.; Frey, H. Biodegradable pH-Sensitive Poly(ethylene glycol) Nanocarriers for Allergen Encapsulation and Controlled Release. *Biomacromolecules* **2015**, *16*, 3103–3111.
- (731) Schröder, R.; Pohlitz, H.; Schüler, T.; Panthöfer, M.; Unger, R. E.; Frey, H.; Tremel, W. Transformation of Vaterite Nanoparticles to Hydroxycarbonate Apatite in a Hydrogel Scaffold: Relevance to Bone Formation. *J. Mater. Chem. B* **2015**, *3*, 7079–7089.
- (732) Feng, X.; Chaikof, E. L.; Absalon, C.; Drummond, C.; Taton, D.; Gnanou, Y. Dendritic Carrier Based on PEG: Design and Degradation of Acid-Sensitive Dendrimer-Like Poly(ethylene oxide)s. *Macromol. Rapid Commun.* **2011**, *32*, 1722–1728.
- (733) DuBois Clochard, M.-C.; Rankin, S.; Brocchini, S. Synthesis of Soluble Polymers for Medicine that Degrade by Intramolecular Acid Catalysis. *Macromol. Rapid Commun.* **2000**, *21*, 853–859.
- (734) Lai, J.; Wang, L.-Q.; Tu, K.; Zhao, C.; Sun, W. Linear Azo Polymer Containing Conjugated 5,5'-Azodisalicyclic Acid Segments in the Main Chain: Synthesis, Characterization, and Degradation. *Macromol. Rapid Commun.* **2005**, *26*, 1572–1577.
- (735) Lai, J.; Tu, K.; Wang, H.; Chen, Z.; Wang, L.-Q. Degradability of the Linear Azo Polymer Conjugated 5,5'-Azodisalicyclic Acid Segment in the Main Chain for Colon-Specific Drug Delivery. *J. Appl. Polym. Sci.* **2008**, *108*, 3305–3312.
- (736) Tziampazis, E.; Kohn, J.; Moghe, P. V. PEG-Variant Biomaterials as Selectively Adhesive Protein Templates: Model Surfaces for Controlled Cell Adhesion and Migration. *Biomaterials* **2000**, *21*, 511–520.
- (737) Sharma, R. I.; Kohn, J.; Moghe, P. V. Poly(ethylene glycol) Enhances Cell Motility on Protein-Based Poly(ethylene glycol)-Polycarbonate Substrates: A Mechanism for Cell-Guided Ligand Remodeling. *J. Biomed. Mater. Res.* **2004**, *69A*, 114–123.
- (738) d'Acunz, F.; Kohn, J. Alternating Multiblock Amphiphilic Copolymers of PEG and Tyrosine-Derived Diphenols. I. Synthesis and Characterization. *Macromolecules* **2002**, *35*, 9360–9365.
- (739) Lee, Y.; Koo, H.; Jin, G.-w.; Mo, H.; Cho, M. Y.; Park, J.-Y.; Choi, J. S.; Park, J. S. Poly(ethylene oxide sulfide): New Poly(ethylene glycol) Derivatives Degradable in Reductive Conditions. *Biomacromolecules* **2005**, *6*, 24–26.
- (740) Lee, J.; Joo, M. K.; Kim, J.; Park, J. S.; Yoon, M.-Y.; Jeong, B. Temperature-Sensitive Biodegradable Poly(ethylene glycol). *J. Biomater. Sci., Polym. Ed.* **2009**, *20*, 957–965.
- (741) Reid, B.; Tzeng, S.; Warren, A.; Kozielski, K.; Elisseff, J. Development of a PEG Derivative Containing Hydrolytically Degradable Hemiacetals. *Macromolecules* **2010**, *43*, 9588–9590.
- (742) Qi, M.; Li, X.; Yang, Y.; Zhou, S. Electrospun Fibers of Acid-Labile Biodegradable Polymers Containing Ortho Ester Groups for Controlled Release of Paracetamol. *Eur. J. Pharm. Biopharm.* **2008**, *70*, 445–452.
- (743) Ulbrich, K.; Strohalm, J.; Kopeček, J. Poly(ethylene glycol)s Containing Enzymatically Degradable Bonds. *Makromol. Chem.* **1986**, *187*, 1131–1144.
- (744) Pechar, M.; Ulbrich, K.; Šubr, V.; Seymour, L. W.; Schacht, E. H. Poly(ethylene glycol) Multiblock Copolymer as a Carrier of Anti-Cancer Drug Doxorubicin. *Bioconjugate Chem.* **2000**, *11*, 131–139.

## Chemical Reviews

Review

(745) Gitsov, I.; Johnson, F. E. Synthesis and Hydrolytic Stability of Poly(oxyethylene-H-phosphonate)s. *J. Polym. Sci., Part A: Polym. Chem.* **2008**, *46*, 4130–4139.

(746) Wang, D.-A.; Williams, C. G.; Li, Q.; Sharma, B.; Elisseff, J. H. Synthesis and Characterization of a Novel Degradable Phosphate-Containing Hydrogel. *Biomaterials* **2003**, *24*, 3969–3980.

(747) Fu, H.; Gao, H.; Wu, G.; Wang, Y.; Fan, Y.; Ma, J. Preparation and Tunable Temperature Sensitivity of Biodegradable Polyurethane Nanoassemblies from Diisocyanate and Poly(ethylene glycol). *Soft Matter* **2011**, *7*, 3546–3552.

(748) Liu, X.-M.; Quan, L.-d.; Tian, J.; Laquer, F. C.; Ciborowski, P.; Wang, D. Syntheses of Click PEG–Dexamethasone Conjugates for the Treatment of Rheumatoid Arthritis. *Biomacromolecules* **2010**, *11*, 2621–2628.

(749) Pattni, B. S.; Chupin, V. V.; Torchilin, V. P. New Developments in Liposomal Drug Delivery. *Chem. Rev.* **2015**, *115*, 10938–10966.



---

 Resume (CV)
**Curriculum Vitae**

Hannah Sarah Pohlit (née Köhring) Dipl.-Chem.

born 16.12.1985

Institute of Organic Chemistry

University Mainz

Duesbergweg 10-14, 55128 Mainz, Germany

Phone: +49 6131 3925700

Email: h.pohlit@uni-mainz.de

**University Education**

- |                   |  |
|-------------------|--|
| 10/2012 – present | PhD thesis: “Degradable poly(ethylene glycol) nanocarriers for allergen encapsulation, targeted transport and controlled release”, Johannes Gutenberg-University Mainz (JGU), in the group of Prof. Frey (Institute of Organic Chemistry) and in the group of Prof. Saloga (Department of Dermatology) |
| 03/2012           | Diploma in Biomedical Chemistry (Overall result: very good, Ø 1,2)   |
| 07/2011 – 03/2012 | Diploma thesis: “Encapsulation of allergen into degradable poly(ethylene glycol) nanoparticles”, JGU, in the group of Prof. Frey (Institute of Organic Chemistry) and the group of Prof. Saloga (Department of Dermatology), Ø 1,0   |
| 04/2010 – 08/2010 | Research stay at Marine Biodiscovery Centre, Prof. Jaspars, University of Aberdeen, UK   |
| 10/2006 – 04/2012 | Studies of “Biomedical Chemistry” at the JGU   |

**Stipends / Awards**

- |                   |   |
|-------------------|---|
| 10/2015           | ALK Award: “ALK Förderpreis Allergologie”   |
| 10/2014           | Junior members poster award of DGAKI (German Society for Allergology and Clinical Immunology) |
| 04/2014 – 04/2016 | Junior member of the Gutenberg Akademie   |
| 03/2013 – present | Member at Max Planck Graduate Center (MPGC)   |
| 03/2013 – 03/2016 | PhD member and scholarship at Materials Science in Mainz Graduate School (MAINZ)              |

- 08/2011 – 12/2011           Scholarship “Förderungsstipendium“ of the Studienstiftung Rheinland-Pfalz
- 03/2008 – 03/2012           Student scholarship of the „Evangelisches Studienwerk Villigst“

### **Internships / Practical Experiences**

- 04/2013 – present           Teaching assistant at the Institute of Organic Chemistry, JGU
- 01/2013 – present           Training of two laboratory technicians
- 06/2012 – 08/2012           “Explore together” internship, BASF, Tarrytown, NY, USA
- 10/2010 – 10/2010           Department of Dermatology, University Hospital Mainz
- 09/2008 – 10/2008           Leeds Institute for Molecular Medicine, Leeds, UK

### **Summerschools and Soft Skill Courses**

- 02/2015                       13th EAACI Winter School, Les Arcs, France
- 08/2013                       Participant of “Roche Continents 2013”
- 05/2013                       ACS Workshop “Sustainable Polymers”, Safety Harbor, USA
- 2013 – 2015                  Soft skill courses within the graduate schools, i.e. time- and project management, leadership, business administration for chemists, science communication and scientific data management

### **Commitment**

- 2001 – present               Social commitment towards the scout association “Heliand Pfadfinderinnenschaft”
- 2001 – 2002 training as a group leader,
- 2002 – 2010 group leader,
- 2004 – 2014 administration of finances,
- 2005 – 2014 voluntary engagement in the steering committee,
- 2012 – present training of new group leaders
- 09/2009 – 08/2011       Participant at the course of lecture “Immunology and Infectology” of the “German National Academic Foundation”
- 10/2006 – 07/2009       Training as a chorister at the Johannes Gutenberg-University Mainz
- 08/2005 – 07/2006       European voluntary service: Olaus-Petri-Parish, Örebro, Sweden

## Publications

**Pohlit, H.**, Frey, H., Saloga, J., "Could allergen-specific immunotherapy benefit from the use of nanocarriers?", *Nanomedicine*, **2016**, 11, 1329-1331.

Herzberger, J., Niederer, K., **Pohlit, H.**, Seiwert, J., Worm, M., Wurm, F., Frey, H., "Polymerization of Ethylene Oxide, Propylene Oxide and Other Alkylene Oxides: Synthesis, Novel Polymer Architectures and Bioconjugation", *Chem. Rev.*, **2016**, 116, 2170–2243.

**Pohlit, H.**, „Polyethylenglykol-(PEG)-Nanopartikel zur Verkapselung und pH-abhängigen intrazellulären Freisetzung von Allergenen“, *Lebendige Wissenschaft Medizin*, **2015**.

**Pohlit, H.**, Bellinghausen, I., Schömer, M., Heydenreich, B., Saloga, J., Frey, H., "Biodegradable pH-Sensitive Poly(ethylene glycol) Nanocarriers for Allergen Encapsulation and Controlled Release", *Biomacromolecules*, **2015**, 16, 3103–3111.

Schröder, R., **Pohlit, H.**, Schüler, T., Panthöfer, M., Unger, R. E., Frey, H., Tremel, W., „Transformation of vaterite nanoparticles to hydroxycarbonate apatite in a hydrogel scaffold: relevance to bone formation“, *J. Mater. Chem. B*, **2015**, 3, 7079-7089.

Frey, H., **Köhring, H.**, Saloga, J., „Spaltbare Polyethylenglykol-(PEG)-Makromoleküle zum Einschluss von (Glyko-)Proteinen/Antigenen/Allergenen in abbaubaren Poly(ethylenglykol-(PEG)-Nanopartikeln sowie Verfahren zu ihrer Herstellung“, German Patent DE102013015112 A1, **2015**.

## Conference Contributions

**Pohlit, H.**, "Degradable poly(ethylene glycol) (PEG)-nanocarriers for encapsulation of therapeutic proteins, directed transport and controlled release", 10. Deutscher Allergiekongress, Köln, Germany, **2015**, oral presentation, invited.

**Pohlit, H.**, Bellinghausen, I., Saloga, J., Frey, H., "Biodegradable PEG Nanocarriers Build from PEG-Acetal- Dimethacrylates for Specific Immunotherapy", NanoDDS, Seattle, USA, **2015**, poster presentation.

**Köhring, H.** Bellinghausen, I., Saloga, J., Frey, H., „Allergen-loaded pH-Sensitive Poly(ethylene glycol) Nanogels for Specific Immunotherapy“, NanoBioMater, Bad Herrenalb, **2015**, poster presentation.

**Köhring, H.**, Bellinghausen, I., Frey, H., Saloga, J., "Analysis of basophilic activation and T cell responses by allergens encapsulated into degradable PEG-nanocarriers", ADF, Ulm, **2015**, poster presentation.

**Köhring, H.**, Bellinghausen, I., Frey, H., Saloga, "Acid-labile PEG-Nanocarriers for Allergen Encapsulation, Targeted Transport and Controlled Release", 13th EAACI Winter School, Les Arcs, France, **2015**, poster presentation.

**Köhring, H.**, Bellinghausen, I., Saloga, J., Frey, H., "Degradable PEG-Acetal-Dimethacrylates as Building Block for PEG Nanocarriers: Allergen Encapsulation and Controlled Release", Freiburg Polymer Symposium, Freiburg, Germany, **2015**, poster presentation.

**Köhring, H.**, Bellinghausen, I., Frey, H., Saloga, J., "Proliferative responses and shielding of allergens encapsulated into degradable PEG-nanocarriers" 9. Deutscher Allergiekongress, Wiesbaden, Germany, **2014**, poster presentation.

**Köhring, H.**, Bellinghausen, I., Frey, H., Saloga, J., "Encapsulation of Allergens into degradable nanocarriers", EAACI Copenhagen, Copenhagen, Denmark, **2014**, oral presentation.

**Köhring, H.;** Bellinghausen, I.; Saloga, J.; Frey, H., “Acid-degradable PEG nanocarriers for allergen encapsulation and controlled release”, 247th ACS National Meeting, Dallas, United States, **2014**, poster presentation.

**Köhring, H.;** Bellinghausen, I., Frey, H., Saloga, J., “Acid-labile poly(ethylene glycol) nanocarriers for allergen encapsulation and controlled release for specific immunotherapy”, Mainzer Allergieworkshop, Frühjahrstagung der DGAKI, Mainz, Germany, **2014**, oral presentation.

**Köhring, H.;** Bellinghausen, I.; Saloga, J.; Frey, H., “Degradable PEG-nanocarriers for allergen encapsulation and controlled release”, Bayreuth Polymer Symposium, Germany, **2013**, poster presentation.



## Declaration

I hereby declare that I wrote the dissertation submitted without any unauthorized external assistance and used only sources acknowledged in the work. All textual passages which are appropriated verbatim or paraphrased from published and unpublished texts as well as all information obtained from oral sources are duly indicated and listed in accordance with bibliographical rules. In carrying out this research, I complied with the rules of standard scientific practice as formulated in the statutes of Johannes Gutenberg-University Mainz to insure standard scientific practice.